THE GEOCHEMISTRY AND MAGNETIC MINERALOGY OF HOLOCENE STRATA IN ACID BASINS:

CASE-STUDIES OF GRANITIC CATCHMENTS IN THE GALLOWAY AND RANNOCHMOOR REGIONS OF SCOTLAND.

BY

THOMAS MARTIN WILLIAMS

A thesis presented in partial fulfillment of the requirements for the degree of DOCTOR OF PHILOSOPHY.

UNIVERSITY OF EDINBURGH

JANUARY 1988

ABSTRACT OF THESIS (Regulation 7.9)

The enrichment of trace metals and magnetic oxides in the surficial sediments of poorly buffered basins is frequently cited to implicate atmospheric pollution in the acidification of lake systems. In establishing such linkages, the possible role of natural enrichment mechanisms has often been ignored.

In this study, the acid Loch Dee basin in Galloway and Loch Ba, Rannochmoor are used to test two approaches which may yield more reliable "pollution chronologies". The first involves the evaluation of the "bulk" geochemical and magnetic stratigraphy of sediments by reference to physical, sequential chemical and pore-water data, thus allowing for the differentiation of anomalies of lithospheric, diagenetic and anthropogenic origin. The second examines the idea that ombrotrophic peats within, or near the study catchments may hold a superior pollution record on account of their isolation from lithospheric influences.

Geochemical and magnetic data show that the uppermost 1m of the Loch Dee sediment reservoir is characterised by lithological homogeneity. Excepting the co-precipitation of authigenic Mn, Co and Fe oxides at the sediment/water interface, diagenetic alteration of the palaeo-geochemical record is limited. The Pb, Zn, Cu and SIRM gradients through the uppermost 20cm of these sediments directly mirror the history of hydrocarbon pollutant deposition. 210Pb data show the major increments to Pb, Zn, Cu and Fe304 incorporation rates to occur after 1850 with post-1967 anthropogenic fluxes exceeding "natural" lithospheric supplies by factors of 3 - 17.

At Loch Ba, anthropogenic pollution only exerts a predominant control on the concentration gradients of Pb, Zn and Cu through the uppermost 15cm of sediment in the southern sub-basin. In the central sub-basin, associated Cu/Zn, REE and magnetically conspicuous Fe203 enrichment occurs at 60cm - 80cm depth as a consequence of a granitic sediment influx. Major geochemical changes in strata deposited between 1850 and 1986 result from the precipitation of Zn, Cu, Co, Ni, Fe and Mn from the oxic, surficial pore-waters. Scavenging by hydrous Fe/Mn oxides is likely to be of primary significance to this enrichment mechanism. The oxidation-sensitivity, geochemical fractionation and morphology of magnetic mineral assemblages in the uppermost 20cm of the Loch Ba sediments suggests that ferrimagnetic enrichment reflects the increased presence of detrital Fe304 and the authigenesis of Fe3S4. There is no evidence that anthropogenic pollutants influence the mineral magnetic record.

Geochemical and magnetic data show that the loading of heavy metals and ferrimagnetic minerals to peatland sites in the Galloway and Rannochmoor regions is directly related to the proximity of industrial pollutant sources. However, the chemical and magnetic stratigraphy of sample cores is strongly influenced by the prevailing redox regime. All analysed elements are depleted in the permanently anoxic core sectors and Pb, Zn, Cu, Cd, Fe, Cr, Al and Ti undergo secondary enrichment across the sub-oxic/oxic threshold. Inverse linkages between SIRM and the redox-sensitive parameters, Fe/Mn and Cu/Zn, indicate the dissolution of anthropogenic magnetites where eH falls below -300mV. Because the onset of severe anoxia is associated with water inundation, sample cores from "hummock" topography provide the most faithful atmospheric deposition records.

It is concluded that sediment-based pollution studies should universally incorporate methods for appraising the influence of hydogenous phases on chemical and magnetic stratigraphy. In lithologically complex sediments, the independence of trace metal gradients from ignition loss and lithophile element profiles should also be established. The re-examination of Fe304 persistence in acid, anoxic environments must be a major research priority.

DECLARATION

The work presented in this thesis is entirely my own. All experimental work and thesis construction has been conducted independently, in accordance with the regulations set out by the University of Edinburgh. No material within this thesis has previously been published or submitted as part of a degree programme. Sources of documented information are cited in all instances.

T.M WILLIAMS.

ACKNOWLEDGEMENTS

The research leading to the production of this thesis was initiated at the University of Reading in October 1984. I am grateful to all staff in Reading who provided advice during the period October 1984 - September 1985. Since October 1985, all work has been carried out at the University of Edinburgh under the supervision of Dr P.A Furley (Department of Geography) and Dr R. Thompson (Department of Geophysics), to whom I am deeply grateful for their advice and encouragement.

I would also like to thank Prof F. Oldfield (University of Liverpool) and Dr A.G Mackenzie (SURRC) for granting access to facilities for mineral magnetic and gamma spectrometric analysis at their institutions. Valuable assistance was also provided by the technical staff of the Edinburgh University Geophysics department during the collection of sediment-cores. I am thankful to D.A. Gray for help with the manipulation of the GIMMS software used for the generation of the data-graphics presented in this thesis.

All research presented in this thesis was carried out under NERC funding.

CONTENTS

CHAPTER 3.

LOCH DEE AND LOCH BA SEDIMENTS: GEOCHEMISTRY.

CHAPTER 4.

LOCH DEE AND LOCH BA SEDIMENTS: MAGNETIC MINERALOGY.

SECTION 2.

CHAPTER 5.

GEOCHEMICAL STUDIES OF OMBROTROPHIC PEAT CORES FROM GALLOWAY AND RANNOCHMOOR.

CHAPTER 6.

MINERAL MAGNETIC STUDIES OF OMBROTROPHIC PEAT CORES FROM GALLOWAY AND RANNOCHMOOR.

CHAPTER 7.

SUMMARY OF PRINCIPAL OBSERVATIONS, CONCLUSIONS AND WIDER IMPLICATIONS

LIST OF FIGURES

ADJ. PAGE

CHAPTER 2.

CHAPTER 3.

CHAPTER 4.

CHAPTER 5.

CHAPTER 6.

LIST OF TABLES

CHAPTER 4.

CHAPTER 5.

CHAPTER 6.

LIST OF ACRONYMS.

1) Geochemical acronyms.

AAS - Atomic absorption spectrophotometry.
AVS - Acid-volatile sulphide.
BP - Before present.
CRS - Constant rate of supply.
eH - Conceptually the negative log of the e^- activity. (pE : 2.3RT/F)
INAA - Instrumental neutron activation analysis.
KeV - Kilo electron volts.
LOI - Loss on ignition.
NVS - Non-volatile sulphide.
PAH - Polycyclic aromatic hydrocarbon.
pH - Log of H ion concentration.
ppm - Parts per million.
REE - Rare earth element group or lanthanide group running from La (57) to Lu (71) in the periodic table.
SEF - Sedimentary enrichment factor.
SEM - Scanning electron microscopy.

2) Magnetic acronyms.

AF - Alternating field.
ARM - Anhysteretic remanent magnetisation.
BOCR - Coercivity of remanence.
HIRM - High-field isothermal remanence (>0.1T).
IRM - Isothermal remanent magnetisation.
K - Volume magnetic susceptibility.
LIRM - Low-field isothermal remanence (<0.1T).
MD - Multi-domain.
MDF - Median demagnetising field.
mAm^{2}kg^{-1} milli-Ampere ^{2} / kg $^{-1}$
mT - milli-Tesla.
Oe - Oersted.
PSD - Pseudo-single domain.
SIRM - Saturation isothermal remanent magnetisation.
SP - Superparamagnetic.
SSD - Stable single domain.
Xlf - Low frequency specific magnetic susceptibility.

CHAPTER ONE

Introduction

1.1: Basis for the study of the geochemistry and magnetic mineralogy of Holocene strata in acid lake basins.

During the past decade, the acidification of poorly buffered surface waters has promoted intense research activity. Throughout this work, the lack of suitably extensive monitoring programmes has constituted a major problem and consequently, reconstructive methods have been fundamental to the provision of data. In particular, micropalaeontologists have used sedimentary diatom assemblages to characterise the past pH conditions of acid lakes (Berge 1976, Battarbee 1983-86, Charles 1985, Norton et al 1981) by relating downcore variations in fossil spectra to the pH-based classifications of diatom taxa established by Hustedt (1937-1939) and Nygaard (1956). Through the use of such methods, it has become apparent that lake waters generally underwent minimal pH adjustment during mid-Flandrian episodes of soil acidification and peat accumulation (eg. Jones et al 1986). Yet numerous catchments in Britain, Scandinavia and North America have been shown to have acidified rapidly during the past 150 years (Battarbee et al 1983-1986, Huttunen et al 1983, Berge 1976, Charles 1985, Norton et al 1981). Because these trends have been observed in both afforested and unafforested catchments (Flower and Battarbee 1983), land

use modifications and soil leaching processes of the nature outlined by Rosenquist et al (1977, 1978, 1980), Krug and Frink (1983), Dobson et al (1987) and Pennington (1984) cannot constitute the principal cause. Instead, the deposition of mineral acids deriving from hydrocarbon combustion appears to provide the most plausible explanation (Drablos and Tollan 1980, Battarbee 1985, Renberg 1985).

In previous attempts to test the above hypothesis, the temporal synchroneity of increasing atmospheric pollutant deposition and the onset of acidification in poorly buffered catchments has been subject to considerable scrutiny (eg. Battarbee et al 1985, Norton et al 1981). Because existing monitoring programmes (eg Warren Spring rep. ISBN 085624 323X, 1983) cannot provide information concerning atmospheric pollutant loadings over the required time period, such information has again been deciphered from the sedimentary record. Specifically, lake sediments are known to chronicle the history of geochemical fluxes to lake basins (Mackereth 1965, Renberg 1976) and the downcore concentration gradients of pollutant phases which emanate from fossil fuel combustion processes have been considered to analogue temporal trends of acidic deposition (Norton et al 1981, Davis et al 1983, Battarbee et al 1985, Renberg 1985). The anthropogenic peturbation of lake-water acidity has, therefore, been diagnosed in instances where the

uppermost 10cm - 50cm of sediment cores from acidified catchments exhibit enrichment with trace metals (Battarbee et al 1985, Norton et al 1981, Tolonen and Jaakkola 1983, Davis et al 1983, Andersson 1985, Oullet and Jones 1983), magnetic oxides (Oldfield et al 1983), 32S (Nriagu and Coker 1983), PAH or PCB compounds (Stumm and Baccini 1978), soot particles (Renberg 1985) and mineral cenospheres (Goldberg et al 1981).

However, upon examining the literature cited above it is apparent that the increased utilization of sediment-based methods for appraising anthropogenic pollutant loadings has been accompanied by a tendency to interpret downcore geochemical profiles without sufficient regard for their true complexity. Lake sediments, in fact, constitute a sink for an assemblage of lithogenic and biogenic materials of diffuse origin (Jones and Bowser 1978, Mackereth 1965). Consequently, the isolation of anthropogenically-derived phases within sediments may be highly problematic, irrespective of the geochemical or mineralogical methods adopted for appraising lithogeochemical fluxes to lake basins (Henshaw 1978, Price 1977, Karlin 1984, Ochsenbein et al 1983). Furthermore, because recent cultural modifications to catchment surfaces, for example afforestation, typically produce concomitant modifications to both the volume and the lithogeochemistry of sediment fluxes, downcore lithological variations are frequently most pronounced in the surficial sectors of basin sediments

(eg. Dearing 1979). In such instances, the lithological complexity of sediments will, therefore, be maximised in those strata which are of most interest to workers attempting to decipher the history of atmospherically derived elemental fluxes.

More importantly, many workers have adopted the oversimplified view that sediments constitute an inert repository for lithogenic, atmospheric and biogenic inputs. In reality, diagenetic processes may cause profound geochemical modifications during sediment burial, therefore destroying any palaeo-geochemical record held within the sediment column. In particular, the well documented mechanisms of iron alteration in both marine and lacustrine sediments (Berner 1969, 1970, 1981, Presley et al 1972, Price 1977, Davison et al 1985, Hilton et al 1986) are instigated by oxidative decomposition processes which also mobilize trace elements. Consequently, some mobilized metals, for example Cr, V and U, may be leached from the surficial strata and will accumulate in the underlying, anoxic sediments by virtue of the relative insolubility of their lower valency phases. Alternatively, metals which exhibit increased mobility under reducing conditions may be subject to migration through anoxic pore-waters and may subsequently precipitate as authigenic mineral phases or become adsorbed to silicate complexes in strata other than those of their origin (Presley et al 1972, Henshaw

1978, Pedersen et al 1986, Cornwell 1986, Farmer and Lovell 1986, Cline and Chambers 1977). Significantly, precipitation and adsorption processes involving the removal of Mn, Fe, Cu, Zn, As, La, Ce, Ni, Co and P from anoxic pore-waters are typically operative either in discrete centres characterised by ferro-manganese nodules, or within the least reducing levels of the sediment column. In many instances, oxic conditions only prevail near the sediment/water interface and hence, the precipitation of trace metals from pore-waters will be most prolific in strata of post-industrial age. Accordingly, Cornwell (1986) has suggested that diagenetically controlled metal profiles may frequently have been incorrectly interpreted as being reflective of temporally changing atmospheric loadings.

In instances where mineral magnetic methods have been used for appraising anthropogenic pollutant fluxes to lake basins, previous workers again appear to have adopted an oversimplistic approach to the interpretation of data. Most notably, downcore magnetic variations in lake sediment cores have frequently been considered to reflect only temporal fluctuations in the loading of magnetic minerals from the atmosphere and the lithosphere (Dearing 1979, Thompson et al 1980, Oldfield et al 1983). This interpretive framework has, therefore, shown neglect for processes promoting both the dissolution and the authigenic formation of ferrimagnetic minerals, as observed by Karlin (1984),

Karlin and Levi (1983, 1985), Anderson (1986), Canfield and Berner (1987) and Hilton et al (1986). Yet upon examination of the typical effects of such diagenetic processes, it is apparent that they may produce downcore magnetic profiles which analogue those commonly attributed to atmospheric deposition. For example, Hilton et al (1986) and Brown (1982) have shown the formation of crystalline monosulphides (eg Fe3S4) to occur specifically in sediments which are rich in organic C and which contain a supply of free elemental S. In lake sediments, elemental S is yielded upon the oxidation of bisulphide and hence, is most available where conditions fluctuate between aerobia and anoxia. In many lake basins, such conditions characterise the strata lying immediately beneath the sediment/water interface. Consequently, the formation of ferrimagnetic sulphides may be most prevalent within surficial strata, leading to enhanced SIRM and X signals in those sedimentary levels which are studied most closely by workers attempting to identify anthropogenerated magnetic minerals.

1.2: Aims of the present study.

In the light of the above uncertainties, it is apparent that the credibility of sediment-based pollution chronologies requires qualification. Furthermore, the need for such qualification is evidently most critical in instances where downcore geochemical or mineral magnetic

variations have been used to implicate anthropogenic pollution in the acidification of surface waters. Within a British context, the acidified lochs in the Galloway region of SW Scotland have, to date, formed the focus of most research of this nature (Battarbee et al 1985, Burns et al 1984, Brown et al 1986). However, with the expansion of the Royal Society Surface Water Acidification Programme (SWAP), sediment-based methods are also being utilized to provide information regarding the history of atmospheric deposition in other acid catchments, such as those within the Rannochmoor National Nature Reserve. Accordingly, acid basins within these regions provide the most logical locations in which to fulfill the aims of the present study. These aims are: -

1) To analyse and interpret the downcore geochemical and mineral magnetic characteristics of lake sediment cores from the acidified Loch Dee catchment in Galloway and from Loch Ba on Rannochmoor. In interpreting any geochemical or magnetic anomalies occurring within strata of post-industrial age, the possible significance of anthropogenic, lithogenic and diagenetic processes will all be examined.

2) To investigate the possibility that alternative, potentially superior methods can be developed for obtaining records of the history of atmospheric deposition within the Loch Dee and Loch Ba catchments.

1.3: Methodology

Section 1 of the present study is concerned with the first defined aim. In this section, the downcore geochemical variability of sediment cores from Loch Dee and Loch Ba will initially be appraised through the use of bulk elemental methods (AAS and INAA). In analogous fashion, the total concentration and mineralogy of magnetic components will be evaluated for all levels of sample cores by collating Xlf, SIRM, ARM and demagnetisation data. In interpreting this bulk elemental and magnetic data, it is anticipated that "lithogenically- derived" downcore geochemical/mineralogical anomalies will be conspicuous by the dis-proportionate alteration of the profiles of parameters which are specifically responsive to changing sediment sources. It is also proposed that diagenetically produced geochemical or magnetic mineral anomalies will be stratigraphically coincident with major redox adjustments. Strata undergoing diagenetic enrichment or depletion should, in turn, be characterised by anomalous pore-water constituencies and anomalous geochemical partitioning between lithogenous and hydrogenous phases.

By considering the above variables, it should be possible to isolate certain downcore geochemical or mineral magnetic variations which are independent of lithogenic and diagenetic controls and hence, can only be reflective of

temporally changing atmospheric pollutant loadings. By placing these "reliable" historical indicators of atmospheric deposition within a geochronological framework, quantitative estimates can then be made of pollutant influx rates throughout the post-industrial period.

Section 2 of the present study deals specifically with the second defined aim. This section is based upon the premise that potentially unrivalled chronological records of atmospheric pollutant deposition could be derived from temporally accumulating materials which receive solely atmospheric inputs and are not subject to diagenetic alteration. Conditions within ombrotrophic peats meet the first of these criteria and preliminary studies have provided evidence to suggest that Pb, Cu and Zn are chronologically retained upon burial by virtue of the slow decomposition rates which characterise such environments (Livett et al 1979, Pakarinen and Tolonen 1977). In addition, a rapidly growing field of mineral magnetic research has produced empirical evidence to show that the downcore concentration gradients of ferrimagnetic minerals may reflect the deposition of anthropogenically mobilized particulates within the essentially non-magnetic matrix of peat materials (Thompson et al 1980, Oldfield et al 1978, 1979, 1984).

In the light of the above information, the present study serves to test the hypothesis that temporal trends in

atmospheric deposition may have been chronicled within peat accumulations in the Loch Dee and Loch Ba catchment areas. Conceptually, this hypothesis will be evaluated in two stages. Firstly, AAS and magnetic methods will be utilized to assess the correlation between the downcore geochemical or magnetic trends within dated sample cores and documented records relating to the anthropogenic mobilization of elements and magnetic oxides over time. Secondly, consideration will be given to the possibility that the downcore trends observed within sample cores do not reflect temporally changing geochemical loadings as argued by Livett et al (1979), Schell (1986) and Pakarinen et al (1977), but have resulted from post-depositional processes.

In appraising the significance of post-depositional processes within peatlands, it is anticipated that mechanisms promoting elemental mobilization will primarily effect reducible or soluble metal phases upon burial, leaving the distributions of residual, silicate fractions relatively unaltered. Consequently, sequential chemical analyses may illuminate the reliability of downcore elemental profiles for use in the determination of temporal trends in atmospheric deposition. Because several elements, for example Fe and Mn, display increasing mobility upon reduction, it is also proposed that diagenetically produced elemental distributions will be conspicuous by their correlation with downcore eH variations.

With reference to the fate of magnetic oxides upon burial within anoxic peats, considerable attention will be afforded to determining the post-depositional stability of the partially reduced oxide, Fe3O4. While Krauskopf (1979) has provided thermodynamic data to suggest the persistence of Fe3O4 under most natural environmental conditions, recent empirical studies illustrating the operation of dissolutionary processes in sediments (Henshaw 1978, Canfield and Berner 1987, Karlin 1984) may also have implications for magnetic studies of peatlands. The possible dissolution of magnetite upon burial in peatlands may, therefore, usefully be examined by assessing the strength of any correlation between SIRM or Xlf profiles and downcore redox variations. In addition, it is anticipated that, should dissolutionary processes be operative, they will produce downcore variations in the physical and mineralogical characteristics of magnetic mineral assemblages which should be optically conspicuous upon the examination of magnetic mineral extracts by scanning electron microscopy.

In summary, it is proposed that by combining geochronological, magnetic and geochemical data, it should be possible to determine the controls upon downcore elemental and magnetic variations within sedimentary and ombrotrophic strata. It should then be possible to assess the degree to which records of atmospheric loadings with

time have been chronicled within the respective environments. By obtaining such information, the present study aims both to qualify the reliability of existing sediment-based pollution records for the Galloway and Rannochmoor regions and to improve present levels of understanding with regard to the post-depositional behaviour of trace metals and magnetic minerals within lake sediments and peats.

CHAPTER TWO

Lake sediment analyses: Rationale and Methodology.

2.1 Introduction.

The following chapter is concerned with the development of a geochemically and magnetically based methodology for appraising the temporal variability of atmospheric pollutant fluxes to Holocene sediments. From Fig 2/1, which outlines the pathways by which elements and magnetic mineral phases may be incorporated into sedimentary strata, it is apparent that any viable methodology must yield four forms of information. Firstly, it is necessary to determine the downcore concentration gradients of elements and magnetic minerals which are intrinsically associated with anthropogenic pollution. Secondly, it is necessary to quantify the "background" supply of these phases from the lithosphere, thus facilitating the differentiation of detrital and anthropogenic fluxes. Thirdly, it is necessary to establish the degree to which individual elements or magnetic minerals have been subject to processes of sedimentary alteration, diffusion or dissolution. Finally, a geochronological framework is required to facilitate the quantification of the influx of atmospherically derived elements and magnetic minerals throughout the period of sediment accumulation. It is with the above needs in mind that a methodology has been developed for utilization

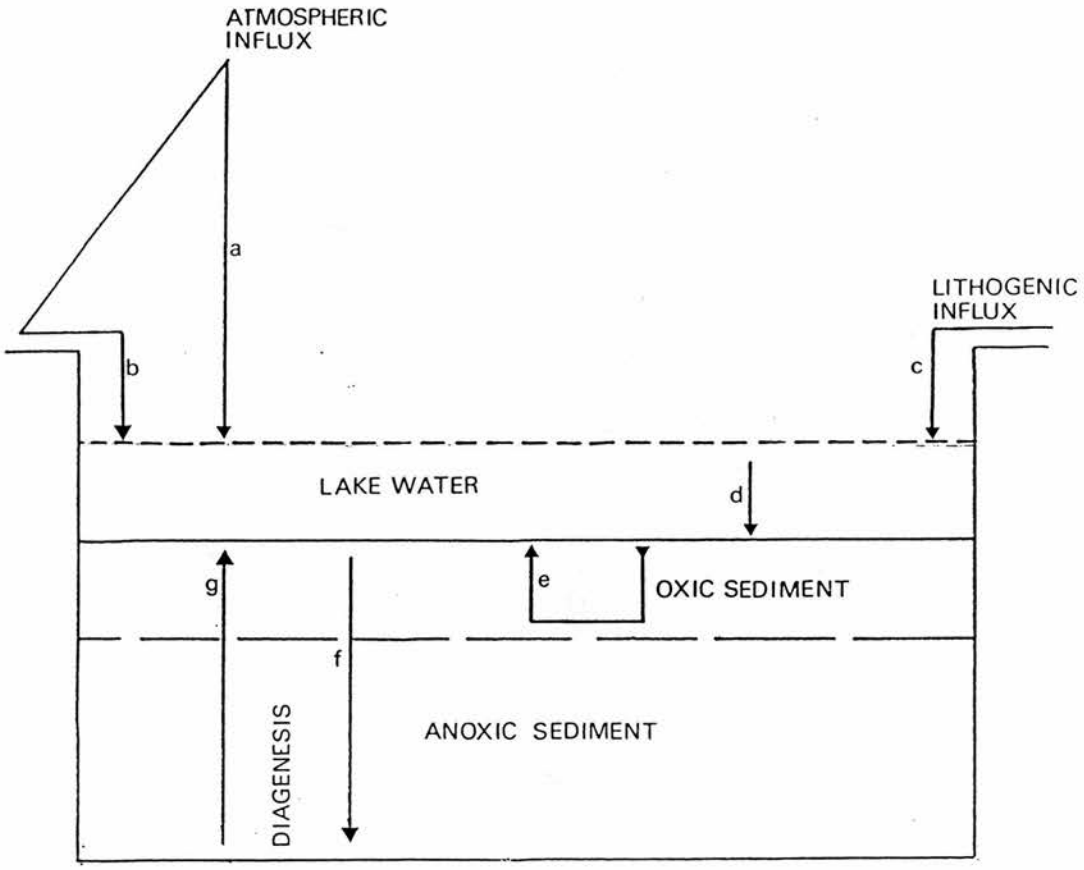

FIG 2/1: Schematic representation of the pathways by which elements and magnetic minerals are incorporated into sedimentary sinks. On a simplistic level, the model has three distinct components. Firstly, an allogenic component is identifiable and includes all fluxes from outwith the lake itself. Lithospherically (c) and atmospherically (a + b) supplied elements and minerals are both, therefore, allogenic. In turn, the atmospheric fraction, deriving from anthropogenic, deflationary and volcanic activity, may be deposited either through direct fallout onto the lake surface (a) or via the catchment (b). Secondly, an autogenic influx of elements and mineral phases is supplied by organic matter in the lake water column (d). All phases emanating from allogenic and autogenic pathways may subsequently by subject to sedimentary mixing by processes of bioturbation (e). Thirdly, diagenetic components may occur in the sediment column, resulting from pore-water diffusion and sulphide precipitation in anoxic strata (f) or pore-water migration+oxide precipitation/adsorption in aerobic strata (g).

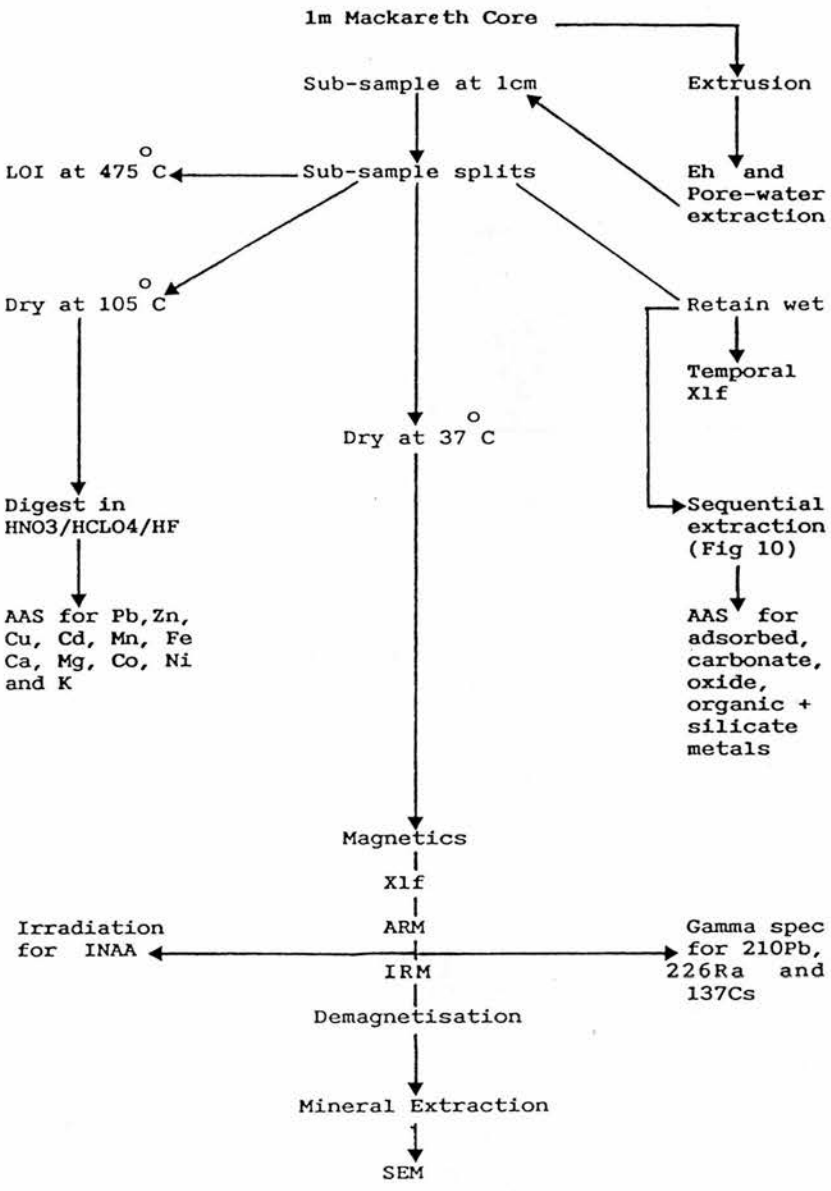

FIG 2/2: Summary of the methodological approach used during the present study for the analysis of lake sediment cores from Loch Dee and Loch Ba. It is important to note that while no individual core was subjected to the full range of analyses, sub-samples of 1cm thickness were typically split into three sections. The first section was dried at 105°C for use in bulk geochemical analyses. The second section was dried at 37°C for use in non-destructive magnetic, gamma spectrometric and neutron activation analyses. The third section was retained wet in an anoxic environment for subsequent use in sequential chemical analyses. All eH measurements and pore-water extracts were obtained from un-oxidized sediments during the core extrusion process.

during the present study. This methodology is summarised in Fig 2/2 and, taking the geochemical, mineral magnetic and radiometric components in turn, the rationale underlying its' development is discussed below.

2.2 Geochemical analyses of lake sediments: Rationale.

2.2.1 The appraisal of atmospheric deposition.

From the studies published to date, it is apparent that the downcore concentration gradients of over 60 elements may be subject to modification through the incorporation of anthropogenic pollutants into lacustrine sediments (Shapiro et al 1972, Brugam 1978, Oullet and Jones 1982, 1983, Shrimp et al 1970, Aston 1973, Cline and Chambers 1977, Forstner 1976, Oldfield et al 1983, Galloway and Likens 1979). In selecting a smaller elemental group for use in characterising pollutant influxes to remote basins, three criteria appear to have particular applicability. Firstly, Lantzy (1979) has observed that elements which are mobilized by hydrocarbon combustion (Table 1) fall into two discrete groups, each having a different impact upon the geochemical budgets of sediment reservoirs (Tables 2 - 3). "Atmophilic" elements (eg. Hg, V, Se, Br, Cd and Pb) are currently mobilized through hydrocarbon combustion at rates which are analogous to those of natural denudational processes. Consequently, temporal inconsistencies in their atmospheric

Table 1: Selected elemental abundances in natural and refined hydrocarbon materials (ppm). Data of Lantzy (1979).

Element	Soils	Andesites	Oil	Coal
Al	71300	88500	0.5	10000
Ti	4600	8000	0.1	500
Sm	6	6	-	1.6
Fe	38000	58000	2.5	10000
Mn	850	1200	0.1	50
Cr	100	56	0.3	18
V	100	100	50	25
Ni	40	55	10	15
Cu	20	62	0.1	15
Cd	0.5	0.29	0.01	0.5
Zn	50	72	0.25	50
As	5	1.5	0.01	5
Hg	0.05	0.07	0.022	2
Pb	10	5.8	136	25

Table 2 : Lithospheric (hydrological) vs atmospheric fluxes of elements to global sedimentary sinks (10^8 g/yr). Elemental characteristics are as defined by Lantzy (1979).

Element	Atmospheric flux	Fluvial flux	Character
Al	33000	170000000	Lithophile
Ti	2700	840000	Liphophile
Sm	3	890	Lithophile
Fe	49000	9900000	Lithophile
Mn	3000	160000	Lithophile
Co	62	3500	Lithophile
Cr	720	17000	Lithophile
Ni	1200	13000	Lithophile
Cu	2600	11000	Atmophile
Cd	510	1200	Atmophile
Zn	10000	25000	Atmophile
As	2900	3000	Atmophile
Se	200	180	Atmophile
Sb	340	1000	Atmophile
Mo	310	700	Atmophile
Hg	410	52	Atmophile
Pb	5700	4700	Atmophile

Table 3: Natural and anthropogenic fluxes of elements to the atmosphere (10^8 g/yr). Data is derived from Lantzy (1979), Klein et al (1975), Bertine and Goldberg (1971) and Hart et al (1981).

Element	Continental dust flux	Volcanic dust flux	Anthropogenic flux
Al	356500	132000	72000
Ti	23000	12000	5200
Sm	32	9	12
Fe	190000	87500	107000
Mn	4250	1800	3160
Co	40	30	44
Cr	500	84	940
V	500	150	2100
Ni	200	83	980
Cu	100	93	2600
Cd	2.5	0.4	55
Zn	250	108	8500
As	25	3	780
Se	3	1	140
Mo	10	1.4	510
Ag	0.5	0.1	50
Hg	0.3	0.1	110
Pb	50	8.7	20300

influx are sensitively chronicled within the sediment column. In contrast, temporal variations in the anthropogenic flux of "lithophilic" elements (eg. Fe, Mn, K, Ca, Mg, Ni, Si, Al, Ti, P) exert a less conspicuous impact upon downcore geochemical trends in sediments on account of the far greater influxes of these elements deriving from natural lithospheric processes. Accordingly, the profiles of "atmophilic" elements may be considered to be best suited for use in the characterisation of atmospheric pollutant loadings to lake basins over time.

Secondly, observations made during studies of the combustion chemistry of fossil fuels indicate that elements which display thermal volatility provide universally applicable parameters for use in the development of sediment-based pollution chronologies. In most instances, surface re-adsorption processes lead to the disproportionate enrichment of such elements in the finest available particulates on account of their high surface area/volume ratios (Raask et al 1981, Hart 1981, Klein et al 1975, Allen et al 1984, Goldberg et al 1981, Natusch et al 1974). Alternatively, volatization may lead to the formation of low temperature vapour phases which are not subject to re-adsorption. In either case, volatile elements, therefore, become associated with phases of low mass and are inefficiently retained by the electrostatic-precipitation units typically installed in combustion plant. Consequently, they are subject to considerable atmospheric dispersal. Predictably, most atmophilic elements volatize at below 1500 ^{o}K and Klein et al (1975) have observed that Se, Cl, Hg,Br, Cr, Cu, Zn, Ga, As, Mo and Pb all behave in this manner. Conversely, elements within the "lithophilic" group do not volatise at typical combustion temperatures of around 2000 ^{o}K (Allen et al 1984) and hence, show no preferential enrichment within the smallest, most widely dispersed particulate emissions.

Thirdly, downcore elemental profiles can only yield

valid paleo-environmental information in instances where processes of post-depositional mobilization are not operative. The potential mobility of elements within sedimentary systems is, therefore, of fundamental significance to the selection of geochemical parameters for use in the derivation of sediment-based pollution chronologies. The suitability of particular elements may best be qualified by reference to empirical studies in which geochemical trends in dated sediment cores have unequivocally been shown to analogue documented historical records of anthropogenic elemental mobilization. Examples are provided by Rippey (1982) who has correlated an eight-fold increase in Cu concentrations towards the surface of Lough Neagh sediments (from 50µg/g at 11cm - 90cm to 400µg/g within the uppermost 10cm) with temporal trends in the discharge of organic waste to the lake basin. In the Sudbury region of Ontario, Carignan and Nriagu (1985) have observed a ten-fold increase of both Cu and Ni concentrations in the surficial 20cm of lake sediments. In accordance with Hutchinson et al (1974) and Conroy (1975), Carignan and Nriagu (1985) have attributed such trends to the growth of nickel smelting activities in the Sudbury area. Sheider et al (1981) have confirmed the above conclusions by using radiometric methods to show that anomalously low Ni concentrations within cores from Muskoka occur only in strata deposited during shutdown periods of the Inco Ltd smelter. In addition, Goldberg et al (1981) and Andersson (1985) have noted that concentrations of Ni have

declined in strata deposited during the past 15 years in the Lake Michigan and Lake Gardsjon basins in accordance with the recently declining levels of fossil fuel combustion throughout Europe and the USA.

With respect to the correlation between documented anthropogenic activities and the downcore sedimentary profiles of other elements, it is notable that Aston (1973) and Kennedy et al (1970) have found anomalously high concentrations of the atmophilic element, Hg, to be confined to the post-industrial strata of sediment reservoirs in the UK and USA. Forstner (1976) and Crecelius et al (1975) have made similar observations in studies of the distribution of Hg within sediments from Lake Saoseo, Switzerland and Puget Sound, USA. In both of these instances, the upward accumulation patterns of Hg also show synchroneity with the development of proximal chloro-alkali plant. Sedimentary Pb profiles have been found to reflect anthropogenic influx patterns with equal consistency. The progressive enrichment of Pb in strata which have been deposited since 1750 AD in numerous lake basins in the UK and USA appears to show synchroneity with the initiation of smelting activities throughout Europe and North America (Wong et al 1984, Ochsenbein et al 1983, Galloway 1979, Hamilton-Taylor 1979, Rippey 1982). While the greatest Pb enrichment has generally been observed in sediments which have accumulated during the 20th century, several workers have been able to

correlate such trends with increasing vehicular emissions during this period (Chow 1970, Farmer 1978, Brown 1986). With respect to Zn, studies of sediment cores from the British Lake District have shown concentrations to increase in strata deposited since 1860 in accordance with the onset of industrialisation in the region (Ochsenbein et al 1983). The persistence of such trends within numerous sample cores from Blelham Tarn and Puget Sound has also facilitated the use of Zn profiles in a geochronological capacity (Crecelius et al 1975, Ochsenbein et al 1983, Capuzzo 1973).

In summary, the evidence presented above allows for the identification of an elemental group whose members are characterised by atmophilic transportation within the environment, thermal volatility and a degree of immobility in sedimentary sinks. This elemental group, possibly comprising Pb, Hg, Mo, Sb, Se, As, Zn, Cd, Cu, Ga, Cl, Br and Cr, may be considered to contain the best diagnostic parameters for use in the construction of sediment based pollution chronologies.

2.2.2 The determination of sediment lithology.

From examining the pathways by which elements are incorporated into sediments (Fig 2/1), it is apparent that total allogenic fluxes reflect the sum of anthropogenic and lithospheric components. Consequently, some knowledge of the lithogeochemical constituency of sediments may be

considered fundamental to the accurate appraisal of atmospheric loadings with time.

In previous studies, the trace metal influx to post-industrial strata, over and above that which is attributable to lithogenous inputs, has most frequently been evaluated through the determination of "sedimentary enrichment factors" (SEFs). To calculate SEFs, the elemental abundances occurring in deeply buried strata have typically been used for data normalization and have, therefore, been considered to indicate the likely "lithogenically derived" concentration of elements at all stratigraphic levels (Oullet and Jones 1982, 1983, Tolonen et al 1983, Skei and Paus 1979, Wong et al 1984, Davis et al 1983). However, in adopting this premise Oullet and Jones (1982), Davis et al (1983) and Tolonen et al (1983) have all assumed lithogeochemical fluxes to remain constant with time. In reality such premises are frequently inapplicable; particularly in catchments which have been subject to recent land use modifications with concomitant adjustments to their sedimentological regime (Dearing 1979, Brugam 1978). Consequently, SEF data of the nature outlined above may be indicative of the impact of atmospheric deposition upon the total sedimentary budgets of particular elements, but they do not facilitate the complete isolation of anthropogenic and lithogenic inputs.

Alternative methods of appraising lithological influences on downcore geochemical trends have frequently been based upon the assumption that the profiles of "major lithophile" elements are directly reflective of the temporal consistency of detrital fluxes to the sediment reservoir. For example, Mack reth (1965) proposed that the downcore profiles of K, Na, Mg and Ca are primarily lithogenically governed. In similar fashion, Tolonen et al (1983) and Norton et al (1981) have used Ti and Al profiles to determine the downcore variability of inorganic constituents in lake sediments. These profiles have, in turn, been used by Tolonen et al (1983) to appraise the respective controls exerted by anthropogenic and lithogenic processes upon downcore geochemical trends in acidified Scandinavian basins. However, on account of the relative abundance of these major elements within most geological materials, their downcore variability may simply be diagnostic of total mineral content, rather than of discrete lithogeochemical changes. Accordingly, the profiles of major elements alone, cannot be considered to provide definitive evidence of the lithogeochemical consistency of sediment cores.

Two additional sources of geochemical information may depict lithological consistency less equivocally. Firstly, calculations of the ratios of Al/Si, Ca/Mg, Fe/K, Zr/Rb and La/Sc prevailing throughout sample cores have been successfully used to identify lithogeochemical changes in

both marine and lacustrine systems (Jones and Bowser 1978, Calvert 1977, Henshaw 1978). Secondly, sediment lithology may plausibly be characterised by analysing the downcore variability of rare earth element (REE) spectra. This method has obvious advantages because, in contrast to other elements, REEs occur in stable oxidation states (Higgo 1987) and hence exhibit limited sedimentary mobility. In addition, rare earth elements are essentially lithophilic and accordingly, their profiles provide lithogeochemical data which are free from atmospheric interference (Schell 1986).

The basis of the REE approach to appraising sediment lithology is illustrated by Figs 2/3 and 2/4, outlining the ease with which igneous materials can be differentiated through examination of their REE spectra. By using the REE concentrations of sedimentary shales for normalization, basic igneous materials appear to be characterised by their depletion of "light rare earths" (notably La and Ce). In contrast, acid igneous materials (eg. granites, diorites and quartz monzonites) exhibit enrichment of La and Ce but are typically depleted of "heavy rare earths", notably Tm, Yb and Lu. In addition, Gordon et al (1969) and Krouskopf (1979) found the Sc concentrations of both basic materials and shales to exceed those of granites and rhyolites by 1000%, with andesites forming an intermediary catagory. Given this knowledge of the characteristic REE spectra of

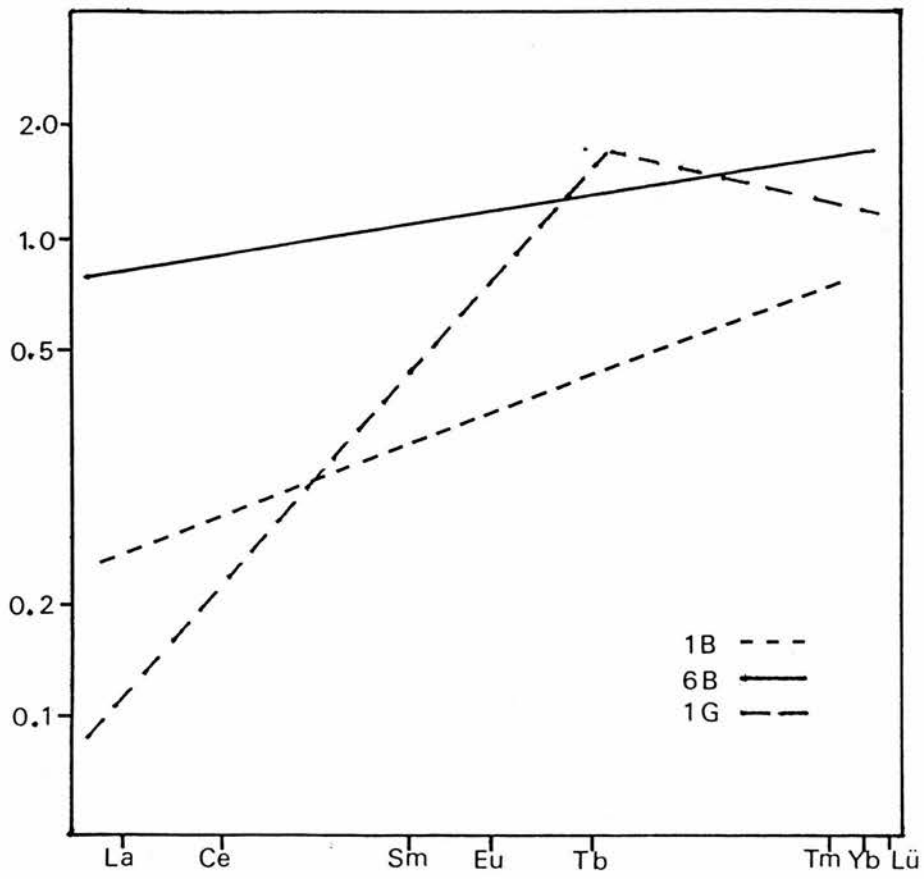

FIG 2/3: Rare earth element composition of basic igneous rocks, normalised against REE concentrations observed in sedimentary shales (after Gordon et al 1969). Sample 1G represents a USA INAA "standard gabbro". Other samples represent basalts. It is particularly notable that all samples are characterised by their depletion of La, Ce and Sm.

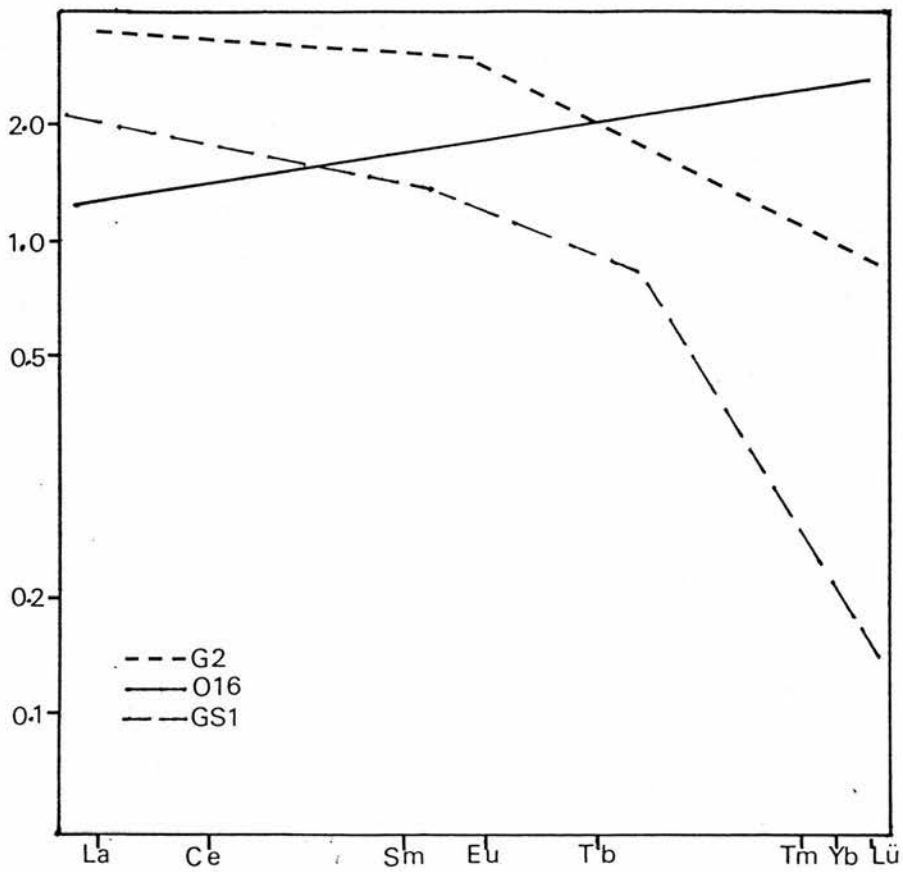

FIG 2/4: Rare earth element composition of silicic igneous rocks, normalized against REE concentrations observed in sedimentary shales (after Gordon et al 1969). Samples G2 and GS1 represent USA INAA "standard granites" which display a notable enrichment of La and Ce, but are depleted of Tb, Tm, Yb and Lu.

selected detrital materials, the downcore fluctuations of Hf, La, Ce, Sc, Tm, Yb, Lu, Eu and Sm can be utilized to diagnose both sediment-source linkages and lithogeochemical anomalies within sedimentary basins. To exemplify, Thompson and Bradshaw (1986) found silicic tephra layers within Icelandic sediments to be conspicuous by their tendency to produce Ce, La and Hf anomalies. In contrast, basaltic ash layers in these sediments were found to be characterised by the occurrence of low La concentrations relative to those observed in the tephra-free strata (Fig 2/5).

2.2.3 The appraisal of organic fluxes.

Downcore variations in the organic constituency of lacustrine sediments may, in two respects, exert a considerable influence on trace metal concentration gradients. Firstly, close associations between the concentrations of Cu, Ni, Mo, Zn, Pb, U and Hg and the amount of organic C have been observed in many sediments, particularly within anoxic systems (Price 1977, Baturin et al 1967, Price and Calvert 1972, Rosental et al 1986). Crude relationships have also been observed between the downcore profiles of Hg, Cr, Zn and Cu and the total combustable fractions of lake sediments (Presley et al 1972, Filipek et al 1979, Cline and Chambers 1977, Nriagu et al 1979, Copeland and Ayers 1972). While the significance of co-existing sulphides to the accumulation of trace metals within anoxic, organic sediments has been poorly appraised

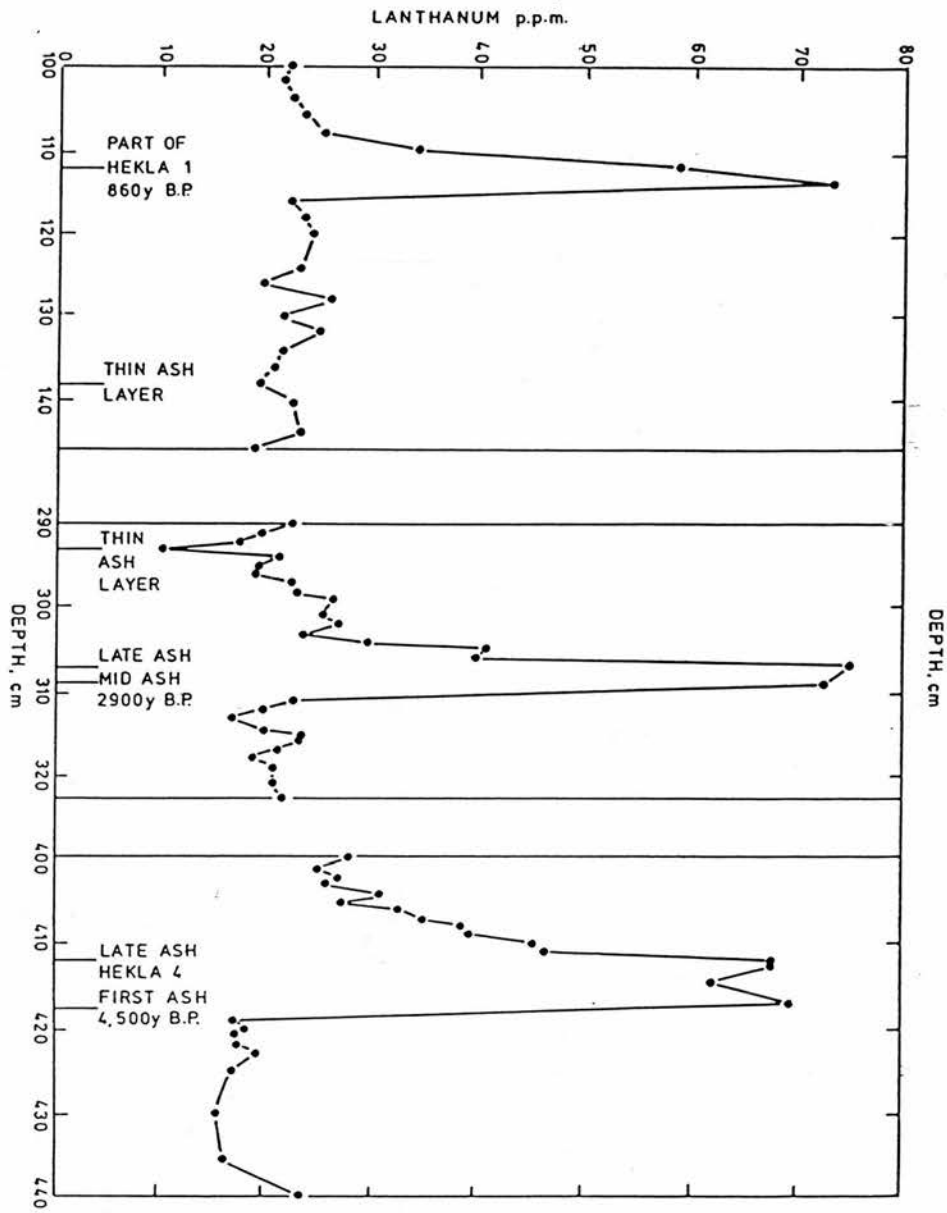

FIG 25 Downcore variations in La concentration within tephra banded Icelandic lake sediments (Thompson and Bradshaw 1986). La appears considerably enriched within acid ash layers of sediment at 110, 310 and 410cm depth. In contrast, the deposition of basic volcanic material is characterised by the depletion of La within the sediment at 295cm depth.

(Price 1977), such trends are widely considered to be diagnostic of the immobilization and preferential enrichment of trace metals in sedimentary sequences which hold complexing organic matter (Jackson 1980). Subsequently, organically bound metals may be released through the processes of oxidative decomposition which characterise anaerobic sediments and hence, where sulphidization is not prolific, elemental mobilities can be directly controlled by rates of organic breakdown. In turn, the complexation of Cu and actinide elements with humic acids, amino-acids and soluble ligands has been found to reduce the sorption potential of these elements following their release from solid phases (Higgo 1987). Consequently, the organic constituency of sedimentary pore-waters may also be considered to mediate rates of elemental diffusion (Stumm and Baccini 1978, Stumm and Morgan 1981).

Secondly, studies at Blelham Tarn (Ochsenbein et al 1983) have shown that, in contrast to the findings of Dillan and Evans (1982), the loading of pollutant trace metals to sedimentary strata cannot always be equated with direct fluxes of metals onto the lake surface. For pollutant metals which rapidly become bound within organo-metallic complexes, the flux delivered to sediments via the catchment surface may, therefore, co-vary with fluxes of allochthonous organic matter.

In the light of the above evidence, several workers have seen the need to interpret sedimentary trace metal profiles by reference to additional parameters which are diagnostic of the downcore variability of organic content. Most frequently, simple organic C or LOI profiles are used for this purpose. For example, Tolonen et al (1983) have normalized the Cu variations observed in cores from Scandinavian sediments against downcore trends of LOI, thus providing a more realistic impression of temporal trends in the deposition of Cu from the atmosphere. Alternatively, the profiles of such elements as Br, I and Mo which are held almost solely in organic phases (Price and Calvert 1972, Shishkina 1965, Swanson et al 1966), or ratios of organically/inorganically supplied elements (eg. Ba/Si and Zr/Si) can be used to diagnose organically controlled geochemical anomalies.

2.2.4 The appraisal of diagenetic processes.

Throughout the preceding sections, the methods proposed for the appraisal of atmospheric, lithogenic and organic fluxes to lake basins incorporate an inherent assumption that elements may remain immobile upon burial. While the validity of this assumption has to some extent been qualified by observations of the synchroneity of downcore geochemical adjustments and the history of the anthropogenic peturbation of the environment (eg Renberg 1985, Shrimp et al 1970, Oullet and Jones 1983, Aston 1973),

the true post-depositional behaviour of many trace metals remains poorly known. To maximise the credibility of any conclusions drawn from sediment-based studies it is, therefore, necessary to ascertain the extent of diagenetic activity within the sediment reservoir. This information may, in turn, be derived from examining the geochemical conditions prevailing in the sedimentary pore-waters, the downcore redox gradient and the geochemical partitioning of elements throughout the sediment column.

a) Sedimentary pore-waters.

Chemical variations in the pore-waters of lake sediments are known to be diagnostic of the operation of diagenetic processes, irrespective of whether geochemical modifications are discernible in the sediments themselves (Jones and Bowser 1978). However, in instances where geochemical anomalies are observable within both pore-waters and sedimentary solids, they are typically inversely related. Such relationships have most frequently been identified with respect to Fe and Mn, which become depleted from sediments and enriched in the interstitial waters through the dissolution of Fe^{3+} and Mn^{4+} bearing phases as they enter the anoxic zone of the sediment column (Lynn and Bonatti 1965, Filipek et al 1981, Mortimer 1971, Presley et al 1972). Divalent Fe and Mn species can then migrate in solution and commonly precipitate as authigenic oxides near the oxic sediment/water interface (Farmer and Lovell 1986,

Cornwell 1986). Alternatively, Fe and Mn may precipitate as oxides in discrete ferro-manganese nodules (Price 1977, Broecker 1974) or may form authigenic siderite ($FeCO_3$), vivianite ($FePO_4$), Fe-monosulphides and rhodochrosite ($MnCO_3$) upon reaching pore-water saturation as determined by the prevailing pH/eH regime (Berner 1970, 1981). In all instances, strata undergoing diagenetic enrichment through the precipitation of hydrogenous phases are characterised either by locally depressed pore-water loadings or by dissolved Fe and Mn concentrations at saturation with respect to the authigenesis of thermodynamically stable carbonate or sulphide minerals.

Recent studies have shown that several trace metals can be subject to redistributional mechanisms of the nature outlined for Fe and Mn. Under such circumstances, the stratigraphic locations of trace metal mobilization and precipitation may again be conspicuous by the occurrence of geochemical anomalies in the interstitial waters. For example, Farmer and Lovell (1986) observed that the enrichment of As in the surficial 5cm of sample cores from Loch Lomond correlated closely with the depletion of Mn, Fe and As from the sedimentary pore-waters. Consequently, Farmer and Lovell (1986) have deduced that the principal mechanism of As enrichment is the upward migration of As(111) through the anoxic pore-water column, with the subsequent precipitation of As(V) under oxidizing conditions at the sediment/water interface (Fig 2/6). Similar processes

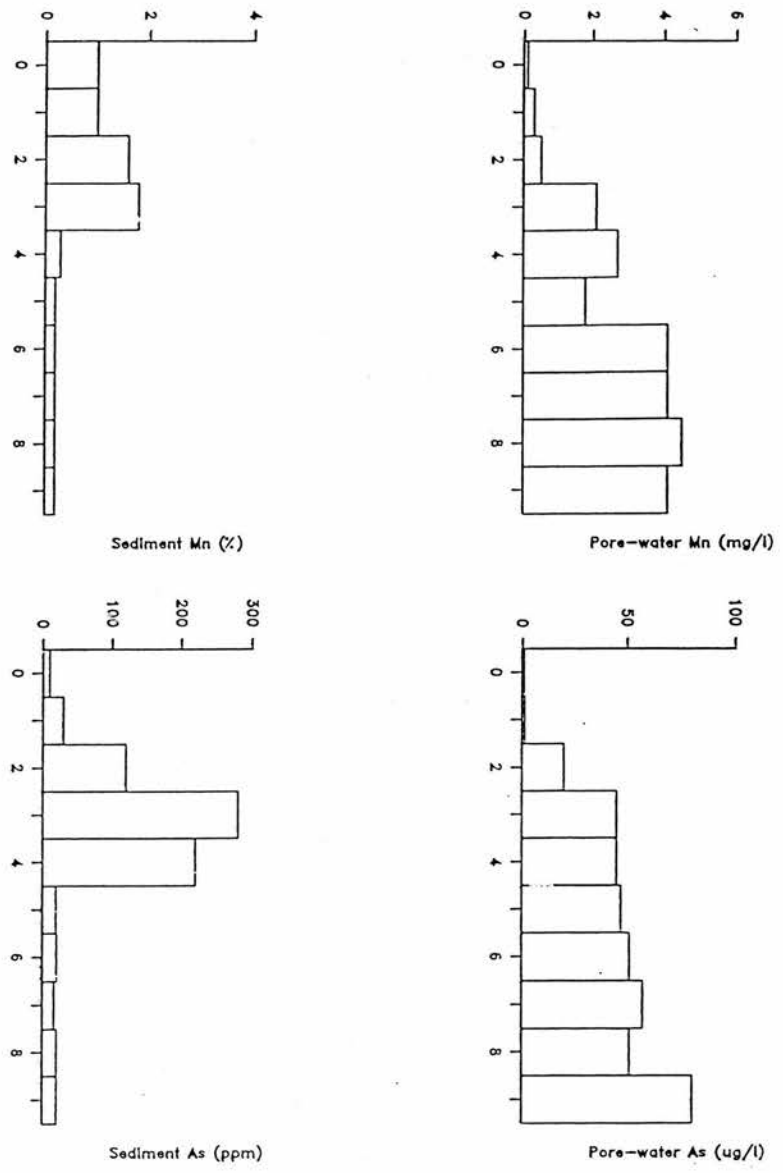

FIG 2/6: Solid phase and pore-water concentrations of Mn and As in the Loch Lomond basin (after Farmer and Lovell 1986). Both elements appear to undergo depletion from interstitial water in the uppermost 5cm, in conjunction with the Mn/As enrichment of solid sedimentary material. The oxidative precipitation of dissolved Mn2+ and As3 as immobile Mn4+ and As5 near the sediment/water interface provides the most plausible explanation for these trends.

have also been cited by Cornwell (1986) to explain the occurrence of anomalously high concentrations of Mo and Ba in the uppermost 5cm of unpolluted arctic lake sediments. In addition, observations have been made of the depression of Cu (Pedersen et al 1986) and actinide element concentrations (Higgo 1987) in the pore-waters of surficial sediments, suggesting that these elements are also subject to accumulation through the direct precipitation of authigenic phases within oxic strata.

While the operation of direct, redox controlled Fe-Mn-Cu mineral dissolution and precipitation processes can be diagnosed by changes in their pore-water concentrations, the dissolved loadings of Co, Pb, Ce, Eu, La and Zn also frequently co-vary with Mn (Ballistrieri et al 1986, Graybeal and Heath 1984, Broecker 1974, Henshaw 1978, Price 1977, Presley et al 1972). Yet for the rare earth elements, such trends cannot be attributed to redox mediated precipitation processes as most exist in stable oxidation states. Accordingly, it is apparent that the precipitation of Fe^{3+} and Mn^{4+} under oxic conditions dramatically increases the adsorption capacity of sedimentary materials, leading to the scavenging of Co, Ce, Cu, La and other trace metals from solution (Robinson 1981). By illuminating strata whose pore-waters display depleted concentrations of these elements it may, therefore, be possible to identify sediments undergoing diagenetic enrichment through trace element adsorption to Mn oxides. Conversely, deeply buried

strata whose pore-waters are characterised both by high Mn concentrations and anomalously high Co, Cu, Ce and La concentrations may plausibly be undergoing diagenetic depletion through the dissolution of ferro-manganese nodules.

It is important to note that dissolved elemental concentrations are subject to both pH and eH controls which, in combination, govern the prevailing thermo-dynamically stable mineral phases with which pore-waters must maintain equilibrium. While the pore-water concentrations of Fe and Mn have frequently been found to be controlled in this manner through the precipitation of MnCO3, FeCO3, FePO4 and FeS (Berner 1981, Mackareth 1965, Henshaw 1978), dissolved concentrations of Cu, Ni and Al may be subject to similar mediatory processes. For example, on account of the strongly acidic surface waters of Clearwater and MacFarlane Lakes, Ontario, Carignan et al (1985) found Cu and Ni to undergo downward diffusion through the interstitial waters of the basin sediments. Yet increased pH levels at 5cm depth, coinciding with the reduction of dissolved SO4, were found to reduce the equilibrated pore-water loading of Cu and Ni, thus leading to CuS (covellite) and NiS (millerite) authigenesis.

b) Geochemical partitioning in lake sediments.

Sequential chemical methods are particularly assistive in

deciphering the controls upon downcore geochemical trends in sedimentary systems on account of their ability to distinguish between elemental phases of differing origin. In oxidizing basins in which diagenetic activity is impeded, lithogenically and biogenically supplied elements are predominantly retained in the organic and silicate fractions of the sediment. Under such circumstances, adjustments to the fractionation of elements in post-industrial strata may be a conspicuous consequence of anthropogenic pollution. For example, Filipek et al (1979) found atmospherically derived Zn phases to be geochemically distinct from lithogenous Zn fractions in the surficial levels of Lake Michigan sediments on account of their residence in NaOAc-soluble carbonates. In similar fashion, Farmer (1978) has observed the strong affinity of hydrocarbon-derived Pb phases to reducible oxides, hence allowing their differentiation from lithogenous, organic/silicate dominated Pb components.

In sediment reservoirs which comprise a two layer oxidizing-reducing system, the partitioning of elements is indicative of both the nature and the stratigraphic focus of diagenetic processes. Enrichment anomalies which result from the precipitation of labile elements from interstitial pore-waters at the sediment/water interface are typically characterised by the dis-proportionate significance of adsorbed and reducible oxide phases (Presley et al 1972, Rosental et al 1986). In anoxic strata,

diagenetically produced enrichment anomalies are equally discernible, but generally result from the immobilization of elements through the precipitation of metal carbonates, phosphates or sulphides (Presley et al 1972, Filipek et al 1979). Because these hydrogenous components can be extracted individually, diagenetic enrichment anomalies can easily be distinguished from those which are attributable to temporally inconsistent allogenic fluxes of elements, as the latter generally produce no concomitant modification of fractionation patterns.

Although the profiles of elements which predominantly reside in "residual" or poorly reactive phases constitute the best palaeo-geochemical parameters (being least subject to alteration or mobilization), it is notable that silicate-bound elements are not totally immune to diagenesis in Holocene sediments. To exemplify, Filipek et al (1979) have shown Zn and Cr to undergo progressive alteration upon burial in the Lake Michigan basin, being slowly transferred between the silicate and sulphide fractions of the sediment column. Accordingly, by facilitating the construction of downcore H2O2 extractable/residual metal ratios, sequential chemical methods may aid in identifying the most slowly operative processes of diagenetic alteration in sedimentary systems.

2.2.5: Geochemical methodology.

On the basis of the evidence presented above, it is apparent that any geochemically based methodology for use in appraising the temporal variability of atmospheric pollutant loadings to lake sediments should comprise techniques for the provision of bulk geochemical, sequential chemical, eH, pore-water and LOI data. For purposes of the present study, the following methods have been utilized to acquire such information from sediment cores from Loch Dee, Galloway and Loch Ba, Rannochmoor.

a) Bulk elemental analyses by atomic absorption spectrophotometry.

Of all currently available analytical methods, atomic absorption spectrophotometry has been most frequently utilized for the determination of total elemental concentrations within organic rich sediments (eg. Oullet and Jones 1982, 1983, Tolonen et al 1983, Norton et al 1981, Mackereth 1966, Ochsenbein et al 1983). Simple air/acetylene flame methods have been found to be eminently suitable for the analysis of many atmophilic pollutants, including Co, Ni, Pb, Cu, Zn, Cr and Cd (Price 1972) and accordingly, such methods have been used extensively during the present study. Several of the previously discussed lithophilic elements (Fe, Mn, Na, K, Mg and Ca) have also been analysed in similar fashion.

All AAS analyses were carried out using 1.0g of homogenised sediment, air dried at 105°C. Although sample cores were sub-sectioned at 1cm intervals, bulk chemical analyses were restricted to 45 levels of core Dee(3), 29 levels of core Dee(4), 69 levels of core Ba(2) and 45 levels of core Ba(3). Core locations are given in section 3.3. The downcore frequencies of analyses were, in all instances, governed by the observed downcore variability of results.

Sample digestion procedures were primarily chosen to ensure the complete dissolution of both organic and mineralogenic sediment fractions. Dry ashing procedures were avoided, thus precluding any possible loss of elements through volatization (Allen et al 1974). Of the most widely used "wet chemical" preparation methods, those utilizing HNO3/HClO4/HCl (Nriagu et al 1979, Wong et al 1984, Skei and Paus 1979) and those involving HNO3/HClO4/H2SO4 have been considered unsuitable on account of their failure to dissolve silicate minerals. Consequently, all bulk elemental analyses carried out during the present study utilized digestion methods described by Ochsenbein et al (1983). These methods are described fully in Appendix 1(a).

"Blank" solutions were prepared for analysis by using the reagents described in Appendix 1(a). Their elemental constituencies then provided an indication of the contaminant metal concentration introduced to each sediment

sample during the digestion process against which, all data have been normalized. Flame AAS analyses for Pb, Zn, Cu, Fe, Mn, Ca, K, Cd, Na, Mg, Co and Ni were carried out on a Unicam SP9 spectrophotometer. The most sensitive analytical lines were used in all instances. ANALAR standards of 100, 50, 25, 10, 8, 6, 4, 3, 2, 1 and 0.5 ppm concentration were used in the calibration of all AAS data. The respective AAS detection limits of all analysed elements are given in Table 4.

Table 4: AAS analyses: Analytical absorption frequencies and analytical detection limits (ppm).

	Pb	Zn	Cu	Cd	Fe	Mn	Cr	Ni
Freq.nm	217	214	324	229	248	279	357	232
Det.limit	1.2	1.2	1.0	0.1	2.0	1.5	0.5	1.0

	Co	Ca	Na	K	Mg
Freq.nm	241	423	589	766	285
Det.limit	1.5	2.0	1.5	0.5	0.5

b) Instrumental neutron activation analysis.

On account of both the difficulties in separating the X-ray spectra of rare earth elements and of their poor suitability for analysis by AAS, INAA methods have been utilized for the determination of lanthanide and actinide element concentrations (Ce, La, Sc, Eu, Sm, Hf, Nb, Yb and Np). All INAA procedures followed those described by

Gordon et al (1969).

INAA analyses were carried out on 12 samples, taken from 2cm, 4cm, 6cm, 10cm, 20cm, 30cm, 40cm, 50cm, 60cm, 70cm, 80cm and 85cm levels of core Ba(3). No other cores were subjected to INAA as their lithogeochemical variability could be established by use of more basic, geochemical and magnetic techniques. The number of core Ba(3) samples subjected to INAA was also restricted by the limited availability of analytical facilities at the Scottish Universities Research and Reactor Centre (SURRC) and by the inherently lengthy nature of INAA methods.

All samples used in INAA were dried at $37^{o}C$, homogenised and packed into polythene vials, each containing approximately 0.1g of sediment. Each vial was then wrapped in Al foil alongside an Fe wire flux of 2cm length. The Ba(3) samples and three internationally certified calibration standards (SL1, IS5 and IS6 from IAEA, Vienna) were then simultaneously irradiated for 6 hours in a flux of 3.6×10^{12} ncm-2s-1 in the core of the SURRC nuclear reactor. To account for the neutron flux variation between samples caused by their differing orientations within the reactor core, the pure Fe wires attached to each sample were analysed by gamma spectrometry 72 hours after irradiation. The resultant data, showing the variations between the 55Fe photopeaks produced per 1g of Fe by each flux

monitor, were then used as normalization factors for the gamma spectra which were derived from the samples themselves.

All Ba(3) and IAEA samples were stored for 72 hours following irradiation, thus allowing the decay of short-lived nuclides of Mn, Al, Ti, Na and Mg which otherwise produce interference accross REE photopeaks. Samples were then analysed by gamma spectrometry, using an 80cm3 Ge(Li) detector with a resolution of 2.2KeV at 1333 KeV. All samples were placed 10cm above the Ge(Li) detector during analysis and gamma spectra were stored automatically on an EGG-ORTEC data acquisition system.

The elemental constituencies of the Ba(3) samples were calculated from their respective gamma spectra by use of a three stage procedure. Firstly, activated elements were identified by matching the energy frequency of their photopeaks to a computer library of nuclide activation energies. For exemplification, Table 5 provides a summary of target elements, activation energies and half lives of the nuclides typically identified during INAA and may be considered to be analogous to the computer library. In addition, the gamma spectrum derived from INA analysis of the 85cm Ba(3) sample is illustrated in Fig 2/7,with the obviously identifiable peaks labelled. Nuclide photopeaks of below 100KeV were not considered to provide reliable geochemical information on account of the poor resolution of

Table 5: Elemental analyses by INAA: Target isotopes, product nuclides and principal observable photopeaks.

Element	Target	Product	Half-life	Photopeaks (KeV)
Na	23Na	24Na	15.0 hr	1369, 1732
K	41K	42K	12.4 hr	1524
Rb	85Rb	86Rb	18.6 day	1077
Cs	133Cs	134Cs	2.05 yr	605, 795
Ba	130Ba	131Ba	12.0 day	216, 373, 496
La	139La	140La	40.2 hr	487, 816, 1596
Ce	140Ce	141Ce	33.0 day	145
Nd	146Nd	147Nd	11.1 day	91, 531
Sm	152Sm	153Sm	47.0 hr	103
Eu	151Eu	152Eu	9.2 hr	122, 842
	153Eu	154Eu	16.0 yr	724, 1277
Gd	152Gd	153Gd	242 day	97, 103
Tb	159Tb	160Tb	72 day	299, 963
Dy	164Dy	165Dy	2.32 hr	95
Tm	169Tm	170Tm	130 day	84
Yb	174Yb	175Yb	4.2 day	283, 396
Lu	176Lu	177Lu	6.7 day	208
Th	232Th	233Th	22 m	
		233Pa	27 day	94, 98, 312, 416
Hf	180Hf	181Hf	42 day	133, 482
Ta	182Ta	183Ta	115 day	68, 100, 1122
Mn	55Mn	56Mn	2.58 hr	847, 1811
Co	59Co	60Co	35 day	1173
Fe	58Fe	59Fe	45 day	1100, 1291
Sc	45Sc	46Sc	83 day	889, 1120
Cr	50Cr	51Cr	27 day	320

the Ge(Li) detector at low energies. Any photopeaks which were matched to activation products with half lives of less than 6 hours were also considered spurious as such nuclides should have decayed substantially during the 72 hour sample storage period.

The second stage of the INAA data interpretation procedure involved the calculation of the original

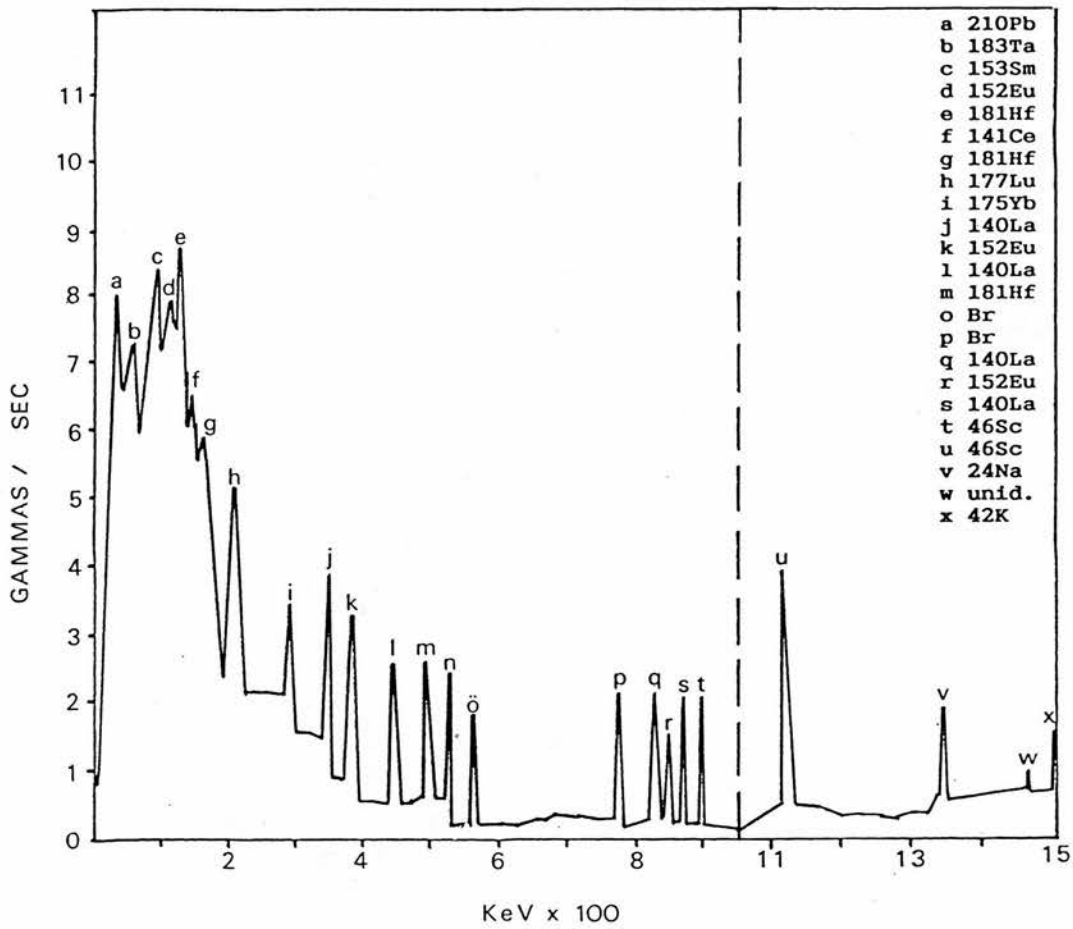

FIG 2/7: Gamma spectra obtained from sedimentary material taken from 85cm depth at coring station Ba(3) following activation in a neutron flux of 3.6 x 10^{12} ncm/sec for 6 hours. Counts reflect the gamma activity remaining after a 72 hour post-irradiation storage period.

magnitudes of all identifiable photopeaks at the time of activation. Such calculations were made by assuming all photopeaks to have declined exponentially during the 72 hour sample storage period at a rate governed by the half lives of the nuclides producing them (Faure 1977).

Finally, by determining the initial magnitudes of photopeaks produced per gram of IAEA standard material (for which elemental concentrations had formerly been established), calculations were made of the concentrations of target elements required to produce the photopeaks observed during analyses of the Ba(3) samples, thus facilitating the derivation of elemental data in ppm.

c) Sequential chemical analyses by AAS.

Sequential chemical data were only acquired for Pb, Zn, Cu, Cd, Mn, Co, Ni, Fe, Ca and K and hence, the analysis of sample solutions followed the AAS procedures outlined earlier (section 2.2.5a). However, to obtain sample solutions containing only certain, defined geochemical fractions of the above elements, the digestion methods adopted for sequential chemical analyses differed markedly.

Several experimental procedures, varying in manipulative complexity, have been proposed for determining the partitioning of elements within sedimentary materials. For purposes of the present study it has been considered

particularly important to distinguish between adsorbed, carbonate and oxide phases, thus facilitating the full characterisation of any diagenetic processes operating within sample cores. Consequently, sequential methods merely designed to distinguish between residual (silicate and non-volatile sulphide) and reducible fractions (Skei and Paus 1979, Rosental et al 1986, Malo 1977, Presley et al 1972) were not considered suitable. Instead, a methodology based upon that outlined by Tessier et al (1979, 1986) was adopted. An illustration of this method is provided in Fig 2/8 and a full description of the procedure is provided in Appendix 1(b).

d) Pore-water analyses by AAS.

The suite of elements selected for analysis within pore-water samples was such that previously described AAS methods of analysis were considered eminently suitable (section 2.2.5a). During the extraction of pore-water samples emphasis was placed upon the maintenance of anoxic conditions, thus avoiding any change in the speciation of dissolved metals. On account of the unavailability of conventional nitrogen operated extruders (Presley et al 1967) or glove box facilities (Hesslein 1976), pore-water samples were obtained by use of methods described by Davison et al (1982). Such methods principally involved the extraction of 5-10ml of interstitial water from the required

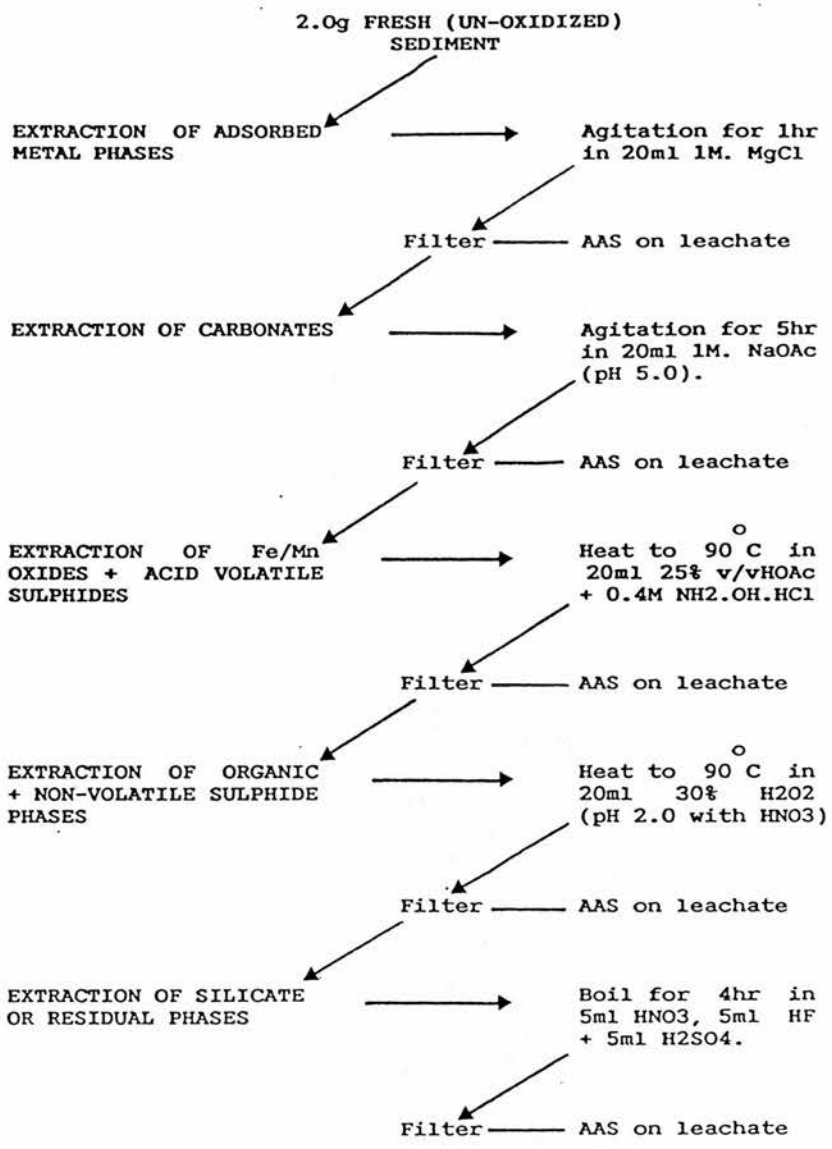

FIG 2/8: Five stage chemical procedure for the sequential extraction of adsorbed, carbonate, Fe/Mn oxide, organic/NVS and silicate mineral phases from sedimentary solids (after Tessier et al 1979).

stratigraphic levels of sample cores during core extrusion (within 48 hours of collection), using an air free hypodermic syringe. The extracted samples were then passed through a 30um filter into nitogen filled vials. All samples were analysed by AAS within 48 hours of extraction from their respective cores.

e) Redox analyses.

Measurements of eH were carried out during core extrusion, using an AGB-50 mV meter (with a range -2000 - +2000mV) and a Pt electrode. For the calibration of electrode data, standard solutions were used in accordance with methods outlined by Zobell (1963). Following each insertion of the Pt electrode into the previously un-oxidised sediment, an equilibration period of 20 minutes was allowed to elapse, thus allowing the mV readings to stablize.

f) Loss on Ignition (LOI) determinations.

The LOI procedure used for determining the organic content of sediment samples followed that outlined by Allen et al (1974). The method essentially involved the ignition of pre-weighed, 0.25g samples at 475 ^{o}C in a muffle furnace. Samples were left at this temperature for 12 hours, after which they were removed and re-weighed to determine the weight loss attributable to the combustion of organic matter and the removal of inter-lattice water. All LOI data

presented during the present study simply express the percentage weight loss which occurred during combustion.

2.3: Mineral magnetic studies of lake sediments: Rationale.

2.3.1: The appraisal of atmospheric deposition.

On account of the oxidation of pyrite and the subsequent formation of ferrimagnetic oxides, many particulates which emanate from hydrocarbon combustion processes contain a strongly magnetic fraction (Hunt et al 1984, Raask et al 1981). Accordingly, mineral magnetic methods exhibit considerable potential for the identification and characterisation of these particulates. Ferrimagnetic minerals can be magnetically diagnosed at concentrations of around 1ppm by use of essentially non-destructive techniques. Hence, magnetic analyses do not preclude the subjection of small samples to subsequent geochemical or optical examination and may be considered to be well suited for use in the characterisation of aquatic (eg. Scoullos et al 1979), atmospheric (eg. Hunt et al 1984) and sedimentary pollutants.

NOTE: Full definitions of all of the mineral magnetic parameters utilized during the present study are provided in Appendix 2.

The utility of magnetic methods for distinguishing between anthropogenic and detrital particulates is founded in their distinctive mineralogical and granulometric properties. For example, ferrimagnets which form during rapid post-combustion cooling within power plant are typically of MD structure. Accordingly, these mineral phases are characterised by their strong response to weak magnetizing fields, "soft" demagnetisation behaviour (BOCR < 40mT), low SIRM/X ratios (<10kAm-1), high SIRM/ARM ratios (>30) and low frequency dependent susceptibilities (Hunt et al 1984, Oldfield et al 1983, Scoullos et al 1979). In contrast, particulates emanating from sectors of the lithosphere which lack primary ferrimagnets (eg. granites and limestones) characteristically display SSD or SP magnetic behaviour (Mullins 1977, Longworth et al 1979). Hence, their demagnetisation profiles are relatively hard (BOCR > 40mT), their susceptibities display up to 50% frequency dependence and the proportion of ARM discriminated phases is high (Mullins and Tite 1973, Maher 1984, Hunt et al 1984, Scoullos et al 1979).

Mineralogical distinctions between anthropogenic magnetites of differing origin can, in turn, be made magnetically. For example, from Table 6 it is apparent that a significant magnetically "hard" (probably haematite) component is present in most fly ash samples, producing coercivities of around 40mT and S ratios of below 0.7. In contrast, the essentially pure spinels derived from

vehicle combustion processes typically exhibit coercivities of around 35mT (Hunt et al 1984).

Table 6: Mineral magnetic properties of selected hydrocarbon residues (Williams unpub. data, Hunt et al 1984).

Sample Source	Size	BOCR	S	SIRM/ARMx	Xfd
Mersey tunnel auto exhaust	7um	35mT	0.74	-	-
Merey tunnel auto exhaust	3.3um	41mT	0.71	-	-
Hams Hall PFA	7um	40mT	0.63	263	-
Hams Hall PFA	1.1um	42mT	0.52	169	-
Ratcliffe PFA	1.5um	42mT	0.63	145	9%

Given conducive sedimentary conditions, mineral magnetic methods may, therefore, be utilized to diagnose the presence of hydrocarbon-derived particulates both through their ability to identify anomalous zones of ferrimagnetic enhancement and through their sensitivity to downcore mineralogical or granulometric variations. To date, such methods have been most successfully applied by Oldfield et al (1983), who found the post-industrial levels of sediment cores from Newton Mere to be characterised by upwardly increasing SIRM and X values which correlated closely with sedimentary concentration gradients of Pb, Zn and Cu. Surficial samples from these sediments were also found to display anomalously low SIRM/X ratios (<10.0KAm-1) and SIRM

coercivities of below 40mT, indicating the declining significance of detrital ferrimagnets and the increased predominance of hydrocarbon-derived particulates. However, it must be emphasised that in most sedimentary basins diagnoses of the presence of particulates from particular anthropogenic processes are less simplistic. In this respect, it is notable that the above-mentioned sediments of Newton Mere are particularly conducive to the identification of atmospherically deposited magnetic minerals on account of their organic nature and hence, the low "background" ferrimagnetic mineral concentrations within the sediment column. Yet in instances where sediment reservoirs are fed with material from magnetite bearing strata (eg basalt), or where the sediments are simply predominantly inorganic, any pollutant flux of magnetic phases may not noticably modify the "natural" mineral assemblage. Furthermore, Oldfield (1984) has noted that rapid sedimentation rates may reduce the mass specific concentration of atmospherically supplied magnetic minerals within lake sediments, thus making their presence less discernible.

Recent alterations to the detrital flux of magnetic minerals to sediments may further complicate attempts to decipher the historical loading of hydrocarbon - derived particulates. For example, Dearing (1979) has identified ferrimagnetically enhanced strata near the surface of sediment cores from North Wales which are solely attributable to catchment afforestation. In similar fashion,

Dearing and Flower (1982) have related enhanced Xlf signals within sediment cores from Lough Neagh to increased fluxes of fine detrital material resulting from agrarian activities. Thompson et al (1980) have also shown that the burning of catchment vegetation may create reducing conditions conducive to the formation of magnetite which may subsequently accumulate in lake basins. Accordingly, basins in which atmospherically derived magnetic particulates are most likely to be conspicuous are those which are free from catchment disturbance, contain slowly accumulating, organic rich sediments and lie on predominantly anti-ferromagnetic bedrock.

2.3.2 Mineral magnetic methods of determining sediment lithology.

In section 2.2.2 it was intimated that the isolation of pollutant elements or hydrocarbon-derived particulates within sediments requires some knowledge of downcore lithological variability. While major element profiles (Karlin 1984, Mackereth 1966, Ochsenbein et al 1983), elemental ratios (Henshaw 1978, Calvert 1977) and REE spectra (Thompson and Bradshaw 1986) have been shown to yield valuable information of this nature, the mineral magnetic characteristics of sediments may also provide a detailed impression of sedimentological consistency. For example, studies of the Jackmoor Brook catchment (Oldfield

et al 1979, Walling et al 1979, Oldfield 1983) have illustrated that magnetic parameters can be used to differentiate between suspended sediments of diverse origin (see Table 7). By applying similar methods to sediment cores, Oldfield et al (1983) and Thompson et al (1975) have been able to decipher the sedimentological history of the Rhode River, Jackmoor Brook and Lough Neagh catchments through the establishment of magnetically based sediment-source linkages for samples from all stratigraphic levels of the sediment column.

Table 7: Magnetic distinctions between source materials for sediments within the Jackmoor Brook (JB) and Rhode River (RR) catchments, N. America (after Oldfield et al 1983, Walling et al 1979).

Source material	X (um3Kg)	SIRM (mAm2kg)	SIRM/X (kAm-1)	BOCR (mT)
Woodland topsoil (JB)	2.5	10	4	20
Cultivated soil (JB)	0.8	<10	5 - 7	24 - 41
Gleyed soil (JB)	0.2	5	>10	30
Bedrock (JB)	0.1	1	>10	>200
Beach sands (RR)	8	2	10	
Coarse topsoil (RR)	6	4	40	
Fine topsoil (RR)	20	10	60	

2.3.3 Mineral magnetic methods of core correlation.

While palaeomagnetic data have long been used for the stratigraphic correlation of sample cores (Thompson 1978, 1979, Clark and Thompson 1978, Mackereth 1971), mineral

magnetic correlation methods also constitute a rapid mechanism for deriving such information. For example, Thompson et al (1975) have demonstrated that recurrent features within the Xlf profiles of several cores from Lough Neagh reflect stratigraphic levels of temporally sychronous origin. By correlating these magnetically synchronous horizons it is, therefore, possible to calculate total sediment influx rates for lake basins (Bloemendal et al 1979) and to extrapolate radiometric or biostratigraphic data between cores (Oldfield 1983).

2.3.4 Sedimentary magnetism and mineral authigenesis.

Several workers have noted the operation of sedimentary processes involving the formation of authigenic iron phases, including siderite (Calvert 1977, Mackereth 1965), vivianite (Mackereth 1965), hydrotroilite, mackinavite, greigite (Berner 1970, Berner 1981, Calvert 1977, Price 1977, Howarth and Teal 1979, Karlin 1984, Hilton et al 1986) and pyrite (Berner 1970, 1981). Yet although the authigenesis of the ferrimagnetic minerals pyrrhotite (Kobayashi and Nomura 1972, 1974) and titanomagnetite (Johnson et al 1975) has been observed in deep sea sediments, magnetists studying Holocene sediments have until recently, given little consideration to the possible effects of authigenesis upon remanent and mineral magnetic properties. Instead, it has been assumed that because the

iron sulphides, carbonates and phosphates which typically form in lacustrine sediments are predominantly paramagnetic, detrital oxides and hydroxides must control the magnetic mineralogy of such sediments.

However, Karlin (1984) and Hilton et al (1986) have recently observed marked temporal losses in the magnetic susceptibility of surficial sediments during storage (Fig 2/9). Karlin (1984) has postulated that the progressive oxidation of Fe_3S_4, an inverse spinel structure and sulphide analogue to magnetite, may be responsible for these losses. This appears a plausible explanation, given the widespread occurrence of Fe_3S_4 in both marine and lacustrine sediments (Price 1977, Berner 1981, Jones and Bowser 1978). Should this be the case, core correlations based upon Xlf or SIRM peaks may be erroneous. Furthermore, monosulphide formation may be most prolific in strata which alternate between oxic and anoxic conditions, thus generating the elemental S required for Fe_3S_4 authigenesis (Brown 1982). These conditions typically occur near the sediment/water interface and accordingly, the authigenic formation of greigite may create Xlf profiles analogous to those produced by recently increased anthropogenic magnetite fluxes.

In the light of the above evidence, it may be considered justifiable to incorporate methods which can establish the presence or absence of authigenic monosulphides in any sediment cores used for appraising atmospheric fluxes of

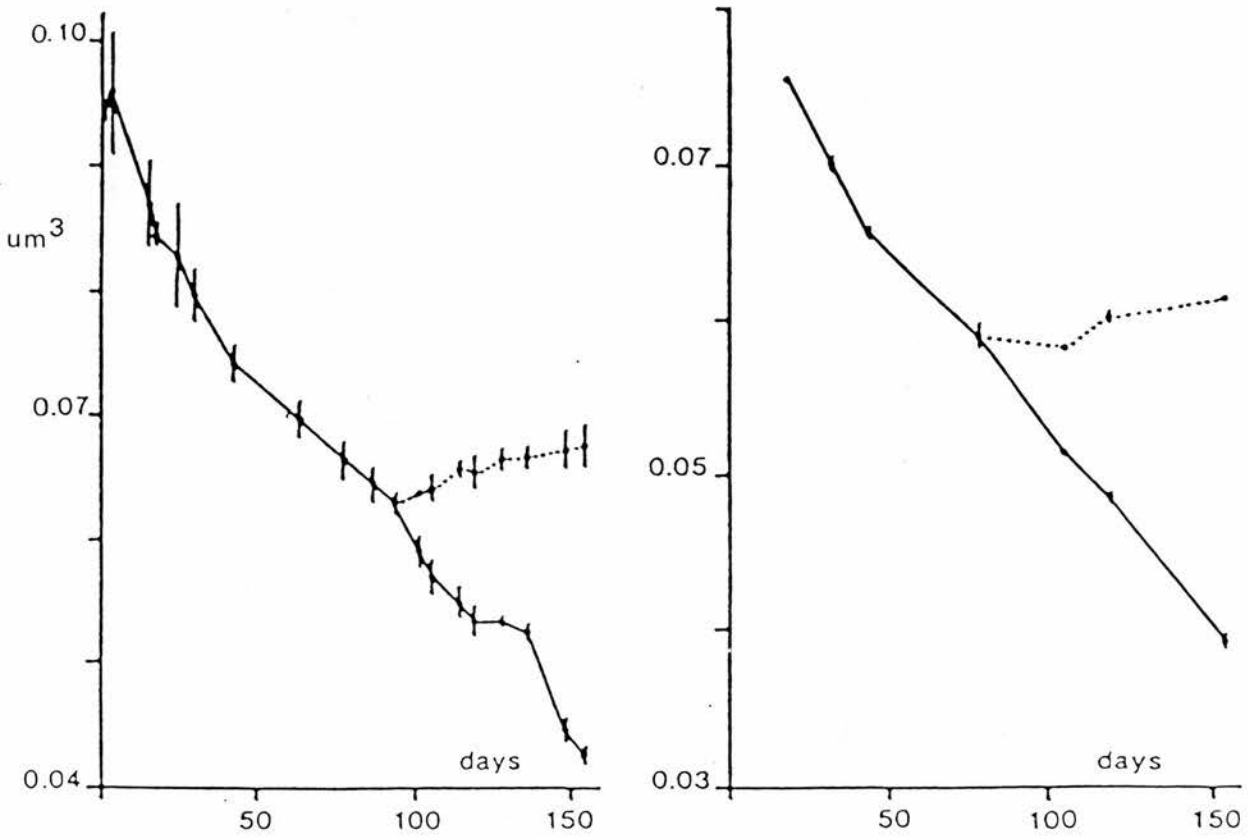

FIG 2/9: Adjustments to low frequency (left) and high frequency (right) magnetic susceptibility during the progressive oxidation of surficial lake sediment samples from the British Lake District (after Hilton et al 1986). In both instances, the prolonged exposure of fresh sediments to atmospheric conditions promotes the loss of 80% of original susceptibilities, suggesting the prevalence of redox-sensitive ferrimagnets within the sediment reservoir. Such conclusions are, in turn, consistent with the stablization of susceptibility signals (dotted lines) following the placement of samples in an anaerobic environment.

magnetic minerals over time. However, thermomagnetic methods of diagnosing sedimentary greigite (Rickard 1975, Karlin 1984), based upon observations of greigite/pyrrhotite conversion at 180°C in a reducing environment with the subsequent loss of susceptibility at 310 °C (the Curie point of pyrrhotite), are generally unsuitable for the analysis of organic sediments on account of their combustability. Methods involving magnetic mineral separation are also generally inappropriate as they tend to involve the exposure of samples to oxidizing conditions with the concomitant loss of monosulphides. Accordingly, sequential chemical and temporal magnetic methods of the nature outlined by Hilton et al (1986) appear to be best suited for use in the characterisation of magnetic sulphides. These methods are described fully in section 2.3.6.

2.3.5 Morphological analyses of magnetic minerals.

Previous workers have noted that a knowledge of the morphological characteristics of magnetic particulates may, in two respects, assist in the interpretation of mineral magnetic data. Firstly, Hunt et al (1984), Raask et al (1981) and Goldberg et al (1981) have shown that anthropogenic magnetites are characterised by their residence within cenospheric particulates and hence, are morphologically distinct from detrital phases. By correlating trends of upward ferrimagnetic enrichment with

the increased presence of cenospheric particulates in the surficial strata of sediment cores it may, therefore, be possible to unequivocally demonstrate associations between mineral magnetic profiles and historical variations in hydrocarbon pollutant deposition. Secondly, Karlin (1984), Karlin and Levi (1985) and Canfield and Berner (1987) have utilized SEM micrographs to demonstrate that Fe3O4 can be subject to dissolution under the eH/pH conditions of anoxic sedimentary pore-waters. Should such processes be widely operative, they may have considerable ramifications with respect to the interpretation of magnetic data. Accordingly, SEM evidence may aid in the correct interpretation of downcore magnetic trends by removing the possibility that ferrimagnetic concentration gradients reflect dissolutionary processes, rather than temporally changing allogenic particulate fluxes.

2.3.6 Mineral magnetic methodology.

From the evidence outlined above, it is apparent that a magnetically-based methodology for use in the appraisal of atmospheric influxes to lake sediments with time should ideally incorporate both "concentration dependent" and mineralogically biased magnetic parameters. In addition, methods of distinguishing between primary and secondary minerals in sediments, alongside methods which facilitate optical mineralogical analysis can be considered advantageous. On the basis of the rationale presented, the

following analytical procedures have been adopted for use during the present study.

a) Bulk magnetic analyses.

All magnetic measurements made during the present study have followed an analytical sequence designed to provide maximum precision. On account of the need to make all "in field" measurements prior to the induction of any artificial remanent magnetization, low frequency susceptibility measurements (Xlf) were made first, with anhysteretic remanent magnetisation (ARM), saturation isothermal remanent magnetisation (SIRM) and demagnetisation analyses being made subsequently (see Appendix 2 for full definitions and explanations of parameters).

With the exception of core Ba(1), from which samples were removed at 2cm intervals, all magnetic analyses were carried out on sub-samples taken at 1cm resolution. Samples were dried at 37°C, thus precluding any thermal enhancement of ferrimagnetic components (Thompson 1983) and were packed into 10cc polythene containers. All sample containers were cleaned in an ultrasonic bath prior to use and had SIRM values of below .001mAm2kg-1. Samples were all weighed prior to analysis, thus allowing results to be expressed on a mass-specific basis.

Magnetic susceptibilities (Xlf) were measured using two cross-calibrated coil sensors, the first linked to a Digico processing system and the second using a Bartington Instruments low frequency bridge and meter. All results are expressed in um3kg-1. No frequency dependent (Xfd) or high frequency measurements were made on sediment samples.

Anhysteretic remanent magnetizations (ARM) were produced within selected samples from cores Dee(3) and Ba(2) by their placement in a custom-built AC demagnetisation unit, producing an AC field which decayed from 100mT to 0.1mT in the presence of a DC field of 0.1mT (1oe). ARM values were acquired for sub-samples from core Ba(3) through their placement in an AC demagnetisation unit supplied by Molspin Ltd. This unit produced an AC field which decayed from 100mT to 0.1mT in the presence of a 0.05mT (0.5oe) DC field. Following their acquisition, sample ARMs were measured using a portable fluxgate magnetometer supplied by Molspin Ltd. All ARM data are presented on a mass - specific basis (mAm2 kg-1).

Saturation isothermal remanent magnetization (SIRM) measurements were made following the induction of remanence in a field of 1.0T. This field was produced using a conventional electromagnet. Values were determined using a Molspin fluxgate magnetometer. All presented data are expressed on a mass-specific basis (mAm2kg-1).

The SIRM coercivities of sediment samples, along with their stepwise demagnetisation profiles, were determined by subjecting all previously "saturated" samples to progressively increasing fields of reversed polarity. The electromagnet previously used for SIRM acquisition was used to generate reversed fields of -15, -30, -40, -60, -80, -100, -200 and -300mT. Remanence measurements were made after the subjection of samples to each of the demagnetizing fields.

The coercive values (BOCR) of samples have been calculated graphically. These values represent the reversed field strength required to reduce each formerly acquired SIRM to zero.

b) Determination of authigenic mineral phases.

The possible presence of the spinel sulphide, Fe3S4 or other authigenic magnetic mineral components was determined for sub-samples from 8 levels of core Dee(4) and 10 levels of core Ba(1) in accordance with two methods outlined by Hilton et al (1986). The first involved the repeated measurement of the volume susceptibilities (K) of fresh samples over a period of four months. By exposing samples to oxidizing conditions during this period, greigite which may have formed in the sediment column should progressively oxidize, producing some temporal loss of K. For purposes of the present study, the measurement of K at

14 day intervals (using a Bartington meter) was considered sufficient. It is important to note that while samples were stored in an oxidizing (atmospheric) environment, their moisture loss was minimised by covering them with polythene.

The second adopted method entailed the application of a series of leachates to sediment samples, each intended to remove a specific mineral phase from the sediment (Hilton et al 1986). The likely contribution of adsorbed, carbonate, AVS and NVS phases to magnetic signals was then evaluated by measuring K after each stage of the under-mentioned leaching sequence (Fig 2/10).

Selected wet sediment samples from core Ba(1) were subjected to a leaching sequence involving MgCl for the removal of adsorbed phases,NaOAc (pH 5.0) for the removal of carbonates, HOAc for the removal of AVS phases and acidified H2O2 for the removal of organic and non-volatile sulphide fractions. The actual application of these leachates was similar to that decribed in Appendix 1 (b), except that the solid phases rather than the leachates were retained for analysis.

c) Optical analyses of magnetic mineral assemblages.

Sub-samples from 1cm, 25cm and 80cm levels of core Ba(3) and from 1cm, 4cm, 25cm and 80cm levels of core Dee(3) were selected for use in optical mineral analyses. Extraction

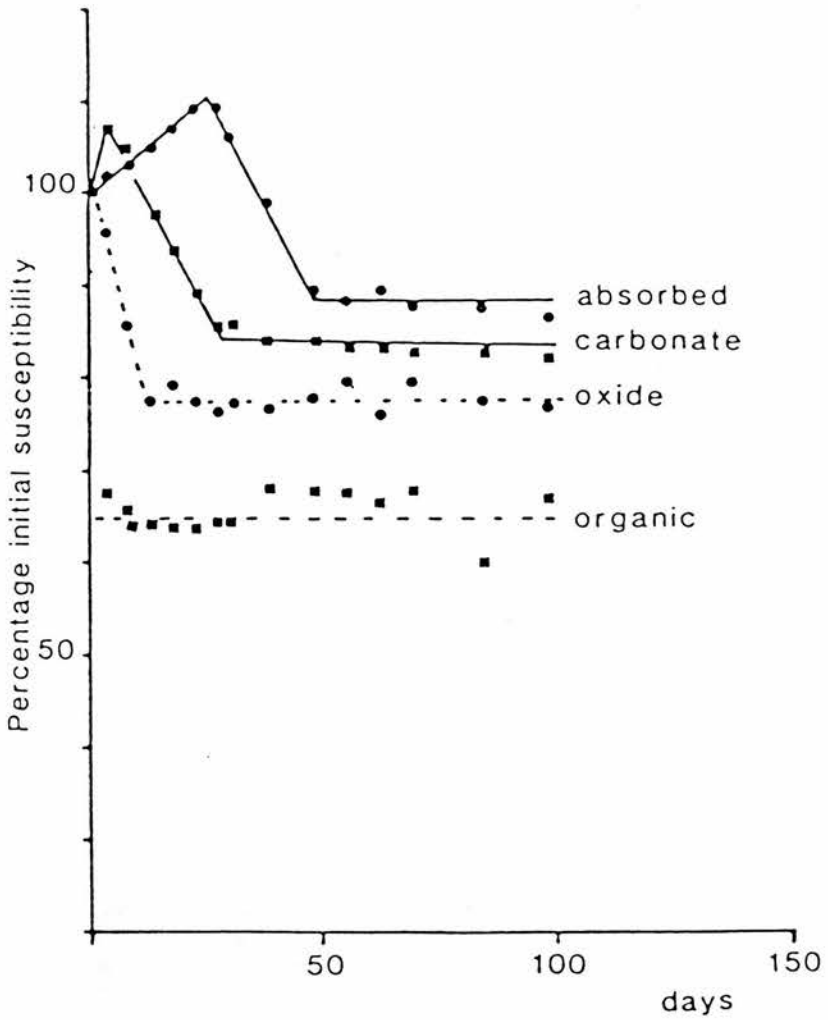

FIG 2/10: Geochemical speciation of oxidation-sensitive ferrimagnets in surficial sediment samples from the British Lake District as determined by sequential chemical methods (after Hilton et al 1986). The continuation of temporal magnetic susceptibility adjustments following the subjection of samples to leaching with MgCl, NaOAc and HOAc suggests that adsorbed, carbonate and acid-volatile sulphide phases do not constitute the redox-sensitive magnetic fraction. In contrast, the stablization of susceptibity signals following the application of H2O2 indicates that a non-volatile sulphide influences the ferrimagnetic properties of pristine sediments.

experiments were initially carried out using several systems to identify a method which removed the largest possible fraction of the magnetic component from the sediment (as defined by sediment SIRM/extract SIRM ratios). Of the methods tested, peristaltic pump or continual flow systems of the type decribed by Karlin (1984) were found to exhibit failings associated with the blockage of the circulation tube by organic sediment fractions. In turn, the removal of organic matter with H2O2 prior to the extraction of magnetic minerals was considered unsatisfactory as the thermal regime created by H2O2 oxidation is adequate for the formation of magnetite. The mineralogy of magnetic extracts yielded by "peristaltic pump" extraction systems was also found to vary in accordance with the type of collection magnet utilized. In particular, high field/low gradient REE magnets showed a bias towards multi-domain magnetites but yielded only low concentrations of haematite.

In contrast, a system described by Canfield and Berner (1987) consistently removed 60% of the total sedimentary fraction which made a contribution to SIRM and displayed none of the problems previously discussed. Accordingly, Canfield and Berner's extraction system was adopted for use and simply entailed the placement of a high flux REE magnet, covered in a latex sheath, within a suspension of sediment. After 24 hours of persistent agitation the sheath was removed from the sample solution and the

magnetic fractions deposited upon it evaporated to dryness for subsequent analysis.

All optical analyses of magnetic extracts were carried out by coating samples with a conductive Au film and examining them on a Cambridge Instruments S90B scanning electron microscope.

2.4.1 Geochronological analyses of sediments: Rationale.

It has previously been intimated that to interpret downcore geochemical or magnetic fluctuations in sediment cores, some prior knowledge of sedimentation rates is required. Most notably, geochronological methods facilitate the identification of correlations between trace metal enrichment patterns in the sediment column and documented variations in the anthropogenic mobilization of pollutants. In addition, geochronological data can be used to normalize trace metal profiles against sedimentation rate anomalies, thus allowing for the calculation of annual pollutant influx data.

While sedimentary sequences have been dated by use of a wide range of biostratigraphic and radiometric methods, palynological, 14C, 40K/40Ar (Allegre 1974) Sm/Nd (Faure 1977) and equilibrated U/Th series methods (Hansen et al 1971, Faure 1977) are generally poorly suited for the development of chronologies on a 10 - 150 year time-scale.

Consequently, a range of short-lived nuclides, including the 238U series members 210Pb and 226Ra, the fission products 55Fe, 239Pu and 137Cs and the cosmogenic nuclide 32Si have been considered to constitute the principal chronometers for post-industrial sediments (Krishnaswami et al 1971, 1978, Oldfield et al 1978, 1979, 1983, 1984, Koide et al 1973). For simplicity, the utility of just two of these nuclides, 210Pb and 137Cs, is examined below.

2.4.2: Geochronology with 210Pb.

Lead 210, with a half-life of 22.26 years, has been found to exhibit particular potential for the dating of lacustrine sediments (Oldfield et al 1979, 1983, 1984, Koide et al 1973, Robbins et al 1975, 1977, Battarbee et al 1984, Krishnaswami et al 1971, 1978), marine sediments (Koide et al 1972, Helz et al 1985) and ice accumulations (Goldberg 1963, Crozaz 1964) on a 10 - 150 year time-scale. In addition to its' favourable decay rate, 210Pb displays suitability with respect to its' environmental behaviour, being subject to continuous atmospheric fallout (Turekian et al 1977) and undergoing rapid translocation between the water column and the sediment reservoir (Rama et al 1961, Carpenter et al 1982, Helz et al 1985). This rapid translocation, through sorption to both organic and inorganic particulates, precludes any significant 210Pb decay prior to its' incorporation within the sediment, thus making geochronological determinations relatively

uncomplicated. Oldfield et al (1978, 1984) have also provided evidence to show that 210Pb is not typically subject to diagenetic mobilization in the sediment column and only Koide et al (1973), who observed the co-precipitation of 210Pb with Mn in marine sediments, have produced contradictory data.

210Pb geochronologies are most commonly established through assessing the downcore activity gradient of the 210Pb fraction which derives from the atmosphere via the decay of 222Rn. This flux (0.2 - 1.0pCi/cm2/yr-1) creates a 210Pb component within the sediment reservoir which is "unsupported" or isolated from its parent nuclide. Hence, this component can easily be used for sedimentary age determinations, given a knowledge of its initial concentration and its temporal decay constant (T 1/2 = 22.26yr).

To isolate the "unsupported" 210Pb fraction from that which is "supported" by the in-situ decay of 226Ra in the sediment column, prior assessment of the 226Ra assay is required (see Fig 2/11). By assuming that in-situ 210Pb generation in a given sample is equilibrated to the disintegration of 226Ra, the "supported 210Pb activity can be calculated and subtracted from the total 210Pb assay to yield the activity of the "unsupported" component. While it is widely acknowledged that the intermediate nuclide, 222Rn

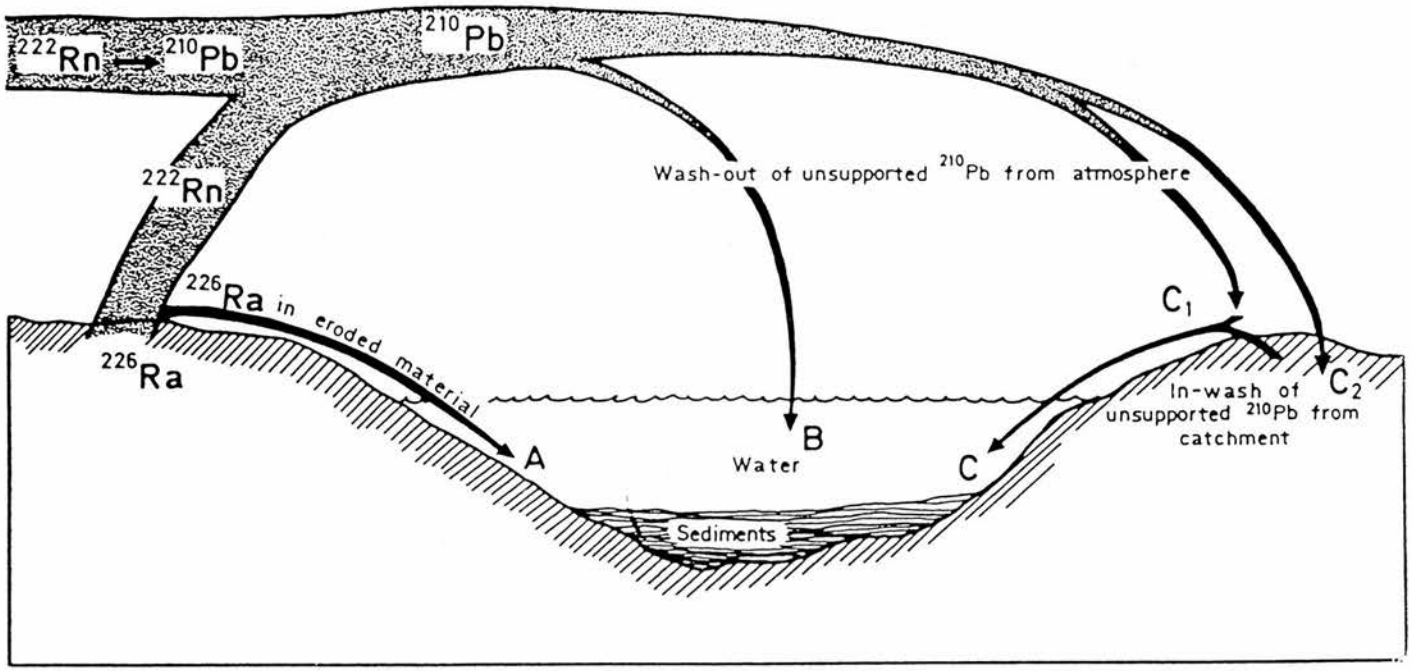

FIG 2/11: Pathways of 210Pb to sedimentary sinks (after Oldfield et al 1983). Two major components of the total flux are identifiable. An "unsupported" component is delivered to the sediment, via the catchment (C) or via the water column (B) following the fallout of 210Pb (derived from 222Rn) from the atmosphere. A "supported" component is supplied to the sediment reservoir through the influx of detrital material which contains the grand-parent nuclide, 226Ra (A).

may be subject to some diffusion through the sediment column, thus leading to disequilibrium between 226Ra and supported 210Pb, such discrepencies have not generally been considered to effect geochronological calculations (Oldfield and Appleby 1984).

2.4.3 Methods of determining 210Pb assays.

In most published studies to date, the total 210Pb activities of sediment samples have been determined by use of one of three methods. These methods entail either the direct derivation of 210Pb assays by beta spectrometry (Faure 1977), the calculation of 210Pb activities from the activity of the grandaughter product, 210Bi (Krishnaswami et al 1971) or the calculation of 210Pb activities from the assay of the grandaughter product, 210Po (Robbins and Edgington 1975, Buesseler et al 1985, Helz et al 1985, Davis et al 1984). However, all of these methods are inherently problematic. For example, analyses by alpha or beta spectrometry require elaborate, ion exchange-based recovery procedures to attain an analytically suitable concentration of 210Pb. In addition, direct 210Pb beta counts are subject to high error margins on account of the low (0.02MeV) beta energies produced by the 210Pb disintegration process.

In the light of the shortcomings of the above methods, gamma spectrometric techniques, utilizing recently developed

high resolution Ge(Li) crystals, may be considered to provide the most practical form of 210Pb analysis. Such techniques require no radiochemical extraction of 210Pb and are based upon the detection of any 46.3KeV gamma activity within bulk sediment samples. Analyses by gamma spectrometry also facilitate the simultaneous acquisition of assays for 226Ra, 137Cs, 134Cs, 241Am and a wide range of other nuclides of use in geochronological work.

2.4.4 Calculation of sedimentation rates from 210Pb data.

Because the atmospheric flux of 210Pb can be considered to be constant over periods of 1 - 10 years (Turekian 1977), 210Pb dating models are universally based on the premise that sedimentary 210Pb incorporation rates are unvariable with time (Krishnaswami et al 1971, Robbins et al 1975, 1977, Koide et al 1973, Goldberg 1963). In instances where such assumptions can be coupled with constant dry mass accumulation rates within the sediment reservoir, the unsupported 210Pb concentration (C) will, therefore, vary exponentially with the cumulative dry mass of the sediment (m) in the manner outlined by Krishnaswami (1971):-

$$C = C(o)e^{-km/r}$$

where C(o) is the unsupported 210Pb concentration at the sediment/water interface, r is the dry mass accumulation

rate and:-

$$k = \frac{Ln2}{22.26} = 0.03114yr\text{-}1$$

On account of its' simplicity, this model has been subject to widespread use for the determination of sediment chronologies (eg. Krishnaswami et al 1971, Robbins and Edgington 1973, Koide et al 1973), with minor inflections in the 210Pb gradient being explained by reference to sediment compaction (Robbins and Edgington 1975), bioturbation (Robbins et al 1977), sediment slumping (Edgington et al 1976) or 210Pb diagenesis (Koide et al 1973). However, observations of non-monotonic 210Pb behaviour at depths of 6cm - 30cm in sediment cores from New Guinea, Lake Huron and Lake Michigan (Oldfield et al 1978, 1979, 1983) have highlighted the inapplicability of the "constant sedimentation rate" assumption to 210Pb studies of many lake basins. A more realistic, although more complex model may, therefore, be developed to explain downcore 210Pb activity variations by perceiving a constant rate of 210Pb supply to a sediment column which is characterised by temporally variable dry mass accumulation. This "constant rate of supply" (CRS) approach was initially developed by Goldberg (1963) and has been subject to refinement by Oldfield and Appleby (1983). Mathematically, the CRS model can be

described as follows:-

1) If $A = F\,Cdm$

$= F\,pCdx$

where A is the cumulative unsupported 210Pb concentration in sediments of below depth x or dry mass m (and p = dm/dx or the dry wt/wet volume ratio) then the age (t) of sediments at depth (x) satisfies the equation:-

2) $A = A(o)e^{-kt}$

where A(o) is the total unsupported 210Pb within the sediment column and kt is the decay constant. A and A(o) are calculated by direct numerical integration of the 210Pb gradient.

The age of sediments of depth x is then given by:-

3) $t = (1/k)\,\mathrm{Ln}\,\frac{A(o)}{A}$

The sedimentation rate (r) at any point is given by

4) $r = \frac{kA}{C}$

The mean 210Pb supply (P) is

5) $P = k A(o)$

2.4.5 Geochronology with 137Cs.

137Cs has been injected into the environment as a result of artificially instigated fission reactions occurring during the last four decades. Consequently the nuclide is present only within sediments deposited during this period, except in instances where downward 137Cs diffusion has taken place. Because 137Cs has a half life of 30 years, downcore activity variations caused by radioactive decay are negligible in comparison to those which are attributable to changing 137Cs loadings with time. Under favourable conditions, geochronological information may, therefore, be attained by simply correlating downcore 137Cs profiles with documented historical records of the nuclides fallout in the northern hemisphere (Oldfield et al 1979, Krishnaswami and Lal 1978, Robbins and Edgington 1975). An example of the use of this method for the dating of sediments from Lake Windermere is provided in Fig 2/12.

However, while Krishnaswami et al (1971) have found good accordance between 137Cs and 210Pb-derived chronologies for Indian sediments, a number of behavioural problems may potentially reduce the utility of 137Cs dating methods. For

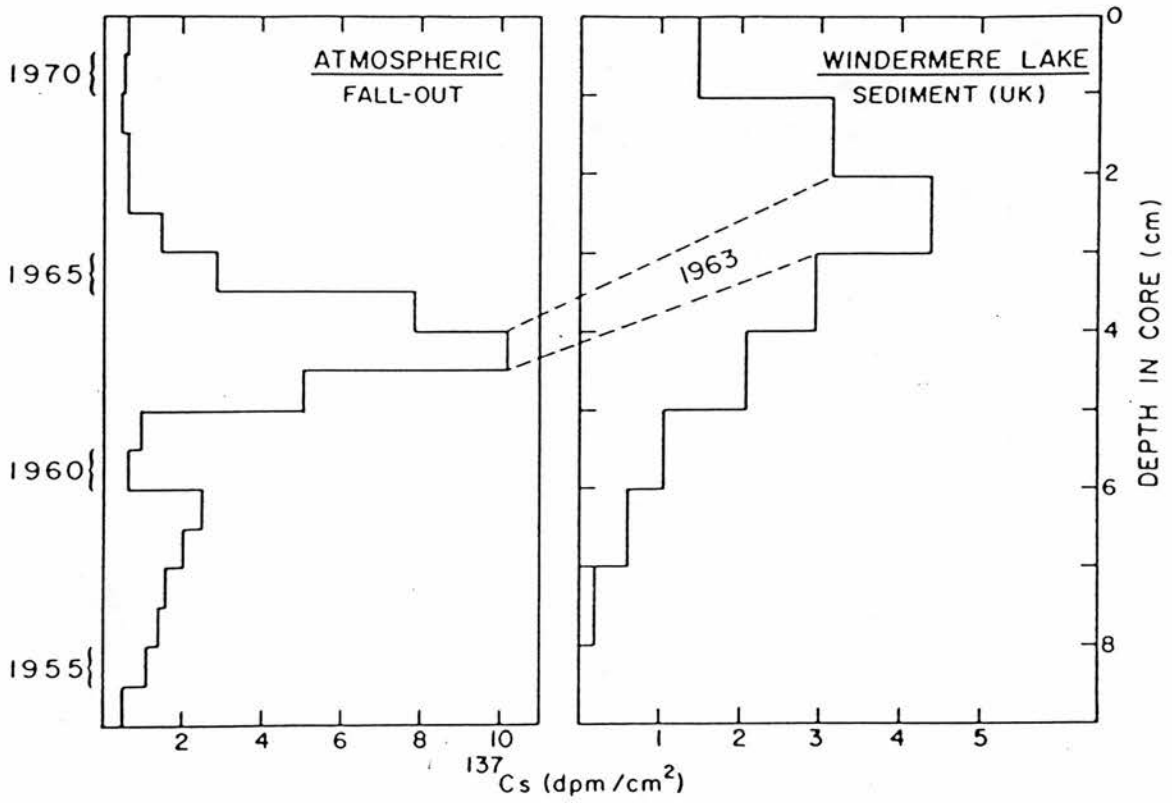

FIG 2/12: Exemplification of the application of 137Cs dating methods to Lake Windermere sediments (after Pennington 1971). The initial "take-off" of 137Cs activities at 8cm depth reflects the first major injection of the nuclide into the atmosphere at around 1950. The stratigraphic level at which maximum 137Cs activities are observable (2cm - 3cm) is also datable, corresponding to the atmospheric "fallout" peak in 1963.

example, McCall et al (1984) have observed that the sedimentary 137Cs budgets of many lake basins cannot be accounted for by a direct 137Cs flux to the lake surface. Consequently, 137Cs which becomes adsorbed to clay minerals (Tamura and Jacobs 1960) or forms organic complexes in the catchment must also contribute to the 137Cs budget of lake sediments. This fraction may reside in the catchment for long periods prior to incorporation within the sediment column, thus creating discordance between atmospheric fallout records and downcore 137Cs profiles. In addition, Davis et al (1984) have identified problems relating to the diffusion of 137Cs through the sediments of soft-water lakes. In a study of catchments in New England and Scandinavia, 137Cs activities consistently appeared to be accentuated in the surficial sediments, while detectable 137Cs concentrations were also apparent in 19th century strata. Several other workers (Norton and Hess 1980, Galloway and Likens 1979, Oullet and Jones 1983) have noted similar 137Cs anomalies in the sediments of acid lakes and have attributed them to the pH dependent solubility of the nuclide, as decribed by Higgo (1987). Diffusive processes of this nature appear to be most prevalent in organic sediments which lack clay mineral adsorption sites, while the common accumulation of 137Cs at the sediment/water interface reflects the affinity of the nuclide to active organic matter.

2.4.6: Geochronological methodology.

All 210Pb and 137Cs data presented during the present study have been acquired through gamma spectrometry, using facilities made available at SURRC and Liverpool University. Samples for analysis were taken at 1cm intervals from the surficial 16cm of cores Dee(3) and Ba(3). All samples were dried at 37C (thus precluding any nuclide volatization) and were packed into shallow cylindrical containers of uniform geometry. The geometric form of samples was designed both to ensure that each sample exposed an equal surface area to the Ge(Li) detector and to produce the maximum possible surface area/volume ratio. By adopting this geometric form, any self absorption of 46.3 KeV gammas passing through the sample was minimised. Respective counts of 400,000 seconds and 80,000 seconds were acquired for the Ba(3) and Dee(3) samples, using an 80cm3 Ge(Li) gamma detector housed within a radiometrically inert Pb well. Background interference was further reduced by the placement of additional Pb shielding around the counting well.

Simultaneously produced 226Ra and 210Pb assays were used in the determination of unsupported 210Pb fractions, by calculating and subtracting the 226Ra supported 210Pb fraction in the manner discussed previously. Unsupported 210Pb data were then used to calculate sediment

accumulation rates for cores Dee(3) and Ba(3) in accordance with the CRS model (Oldfield and Appleby 1978, 1983, 1984).

Sedimentary 137Cs assays were determined from the 661KeV gamma photopeaks produced during the formerly discussed 80,000 sec. and 400,000 sec. counts.

2.5.1 Summary.

The preceding discussion has outlined the major contols upon downcore geochemical and mineral magnetic variations in lake sediments. It is apparent that while atmospherically deposited pollutant phases may produce enhanced trace element and magnetic mineral concentrations within some post-industrial strata, lithogenic and diagenetic processes may also produce similar downcore changes. Selective geochemical, magnetic and radiometric methods have, therefore, been described and evaluated with a view to constructing an analytical approach suitable for use in differentiating lithologically, diagenetically and anthropogenically produced anomalies in lake sediment cores. In the following chapters, the adopted approach (as summarised in Fig 2/2) will be tested with particular emphasis being placed upon its' ability to illuminate temporal variations in the deposition of hydrocarbon derived pollutants within the Loch Dee and Loch Ba basins.

CHAPTER THREE

Loch Dee and Loch Ba sediments: Geochemistry.

3.1 Introduction

In this chapter, attention is focused upon the geochemical characterisation of the upper-Holocene sediment sequences within the Loch Dee basin, Galloway and the Loch Ba basin, Rannochmoor. The chapter comprises four sections. The first provides descriptions of the physical characteristics of the two study catchments and of the methods utilized for sample core extraction (3.2 - 3.3). The second incorporates data which illustrate the downcore variability of geochemical conditions in the solid fractions and the interstitial pore-waters of the sediment reservoirs (3.4 - 3.5). In the third section, radiometric data are presented to facilitate an evaluation of the temporal variability of sedimentation rates in the two basins (3.6). Finally, an attempt is made to determine the extent to which geochemical anomalies within sample cores are reflective of temporal variations in the geochemical constituency of lithospheric inputs, sedimentary diagenesis or temporal changes in the elemental influx from the atmosphere (3.8 - 3.9). In instances where variable atmospheric fluxes exert a significant influence upon the palaeo-geochemical record, attempts are made to date and quantify these changes through the incorporation of radiometric data into the interpretive framework.

3.2: Site descriptions.

3.2.1: The Loch Dee catchment.

Loch Dee lies within a remote area of the Galloway hills (NG ref NX 470790) and comprises three discrete sub-basins, the Dargill Lane to the west, White Laggan to the south and Green Burn to the south-east (Fig 3/1). The loch surface covers approximately 1 km2 at an altitude of 225m. The catchment bedrock is primarily composed of biotite-rich granite (Fig 3/2) and is characteristic of much of the southern sector of the Loch Doon plutonic complex (Gardiner and Reynolds 1932). While acid, silicic bedrock is common to all acidified basins in Galloway, it is notable that limited drainage derives from the metamorphosed Ordovician strata which form the aureole to the south of the igneous intrusion. Gardiner and Reynolds (1932) have noted the predominance of hornfels in the metamorphosed bedrock, while the outlying strata comprise Ordovician/Silurian shales and greywackes.

The natural vegetation of the Loch Dee catchment has been described by Burns et al (1984) and Boatman (1983) as belonging to the Trichophoreto-Eriophoretum and Molinieto-Callunetum associations of McVean and Ratcliffe (1962). However, around 25% of the Loch Dee catchment has been afforested since 1962 and Picea sitchensis now covers the

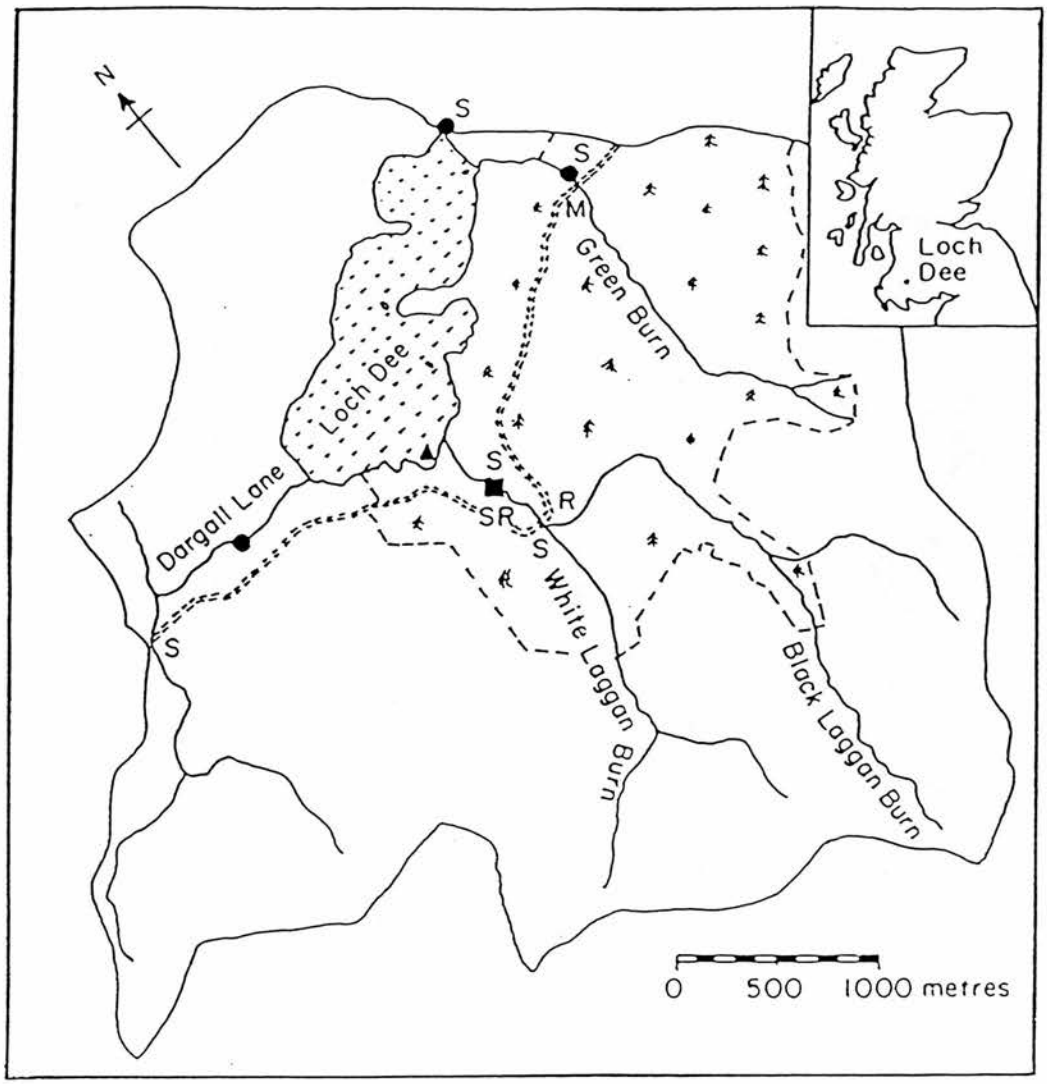

FIG 3/1: Outline and location of the Loch Dee catchment. The area under afforestation is demarked by the broken line.

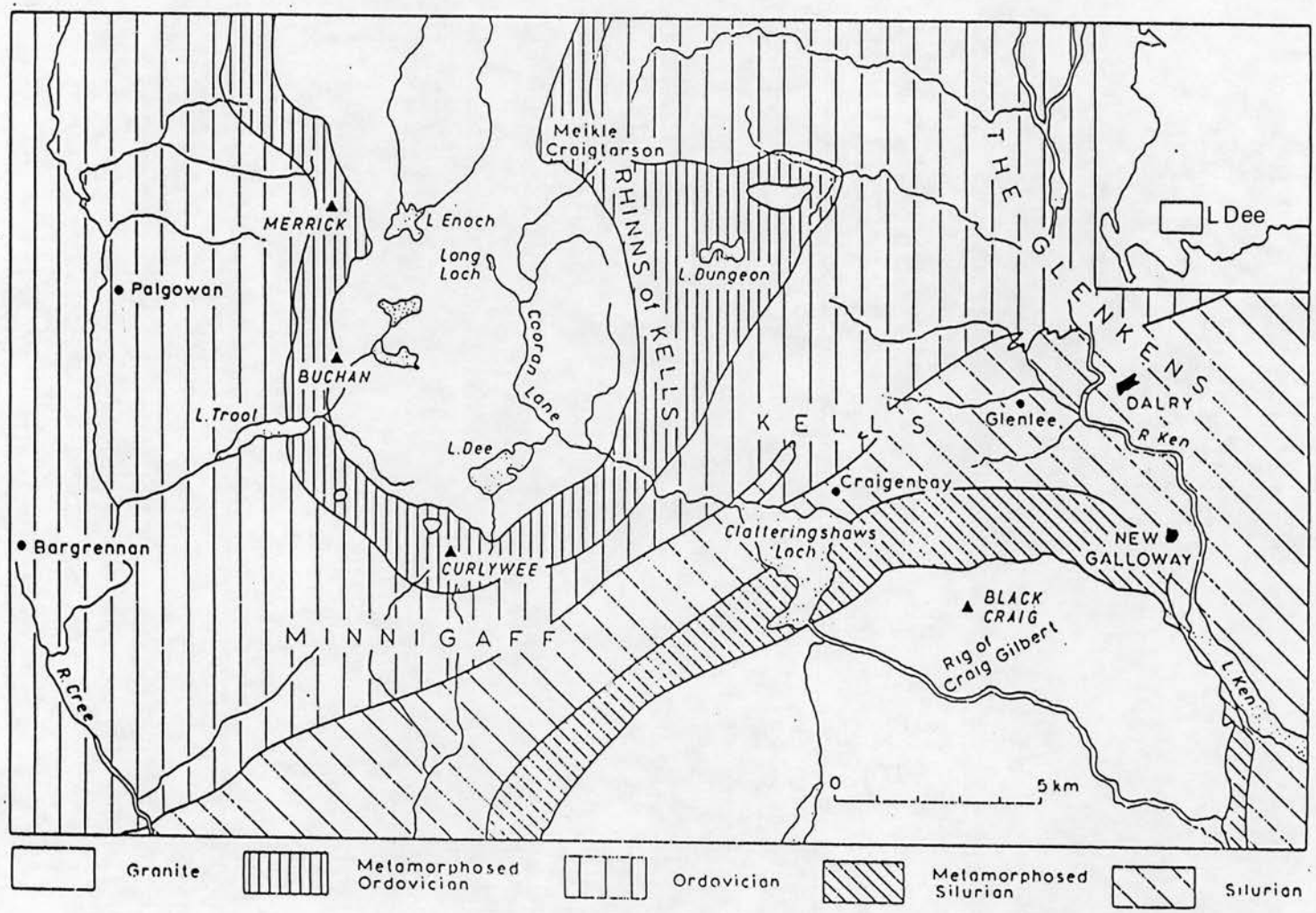

FIG3/2 : 'Geology of Loch Dee and surrounding environs.

southern and eastern flanks of the loch, extending along the Green Burn and White Laggan tributaries (see Fig 3/1).

High annual precipitation levels (2200mm/yr) are a notable characteristic of the entire Galloway area and constitute the principal cause of the 98kg/ha SO4 loading reported within the Loch Dee catchment (Burns et al 1984). As a consequence of this high SO4 input, low bedrock erosion rates and the peat dominated overburden, the surface waters of Loch Dee are inherently acidic, with pH minima of 4.8 occurring during periods of peak streamflow (Burns et al 1984). The Loch is poorly buffered, yielding mean HCO3 alkalinity values of 8ueq/l (Burns et al 1984).

3.2.2: The Loch Ba catchment:

Loch Ba (NG ref. NN 320505) comprises three sub-basins, forming a poorly defined catchment at 275m altitude to the south-west Loch Laidon (Fig 3/3). The loch is confined within a grano-diorite complex which typifies the Rannochmoor/Cruachan plutonic masses. Limited drainage also derives from the Moinian quartzites, granulites and mica-schists which form the strata to the south of the catchment (Fig 3/4). The vegetation of the catchment can be ascribed to the Trichophoreto-Eriophoretum nodum of McVean and Ratcliffe (1962), with Calluna, Narthecium, Trichophorum, Eriophorum and Sphagnum displaying dominance.

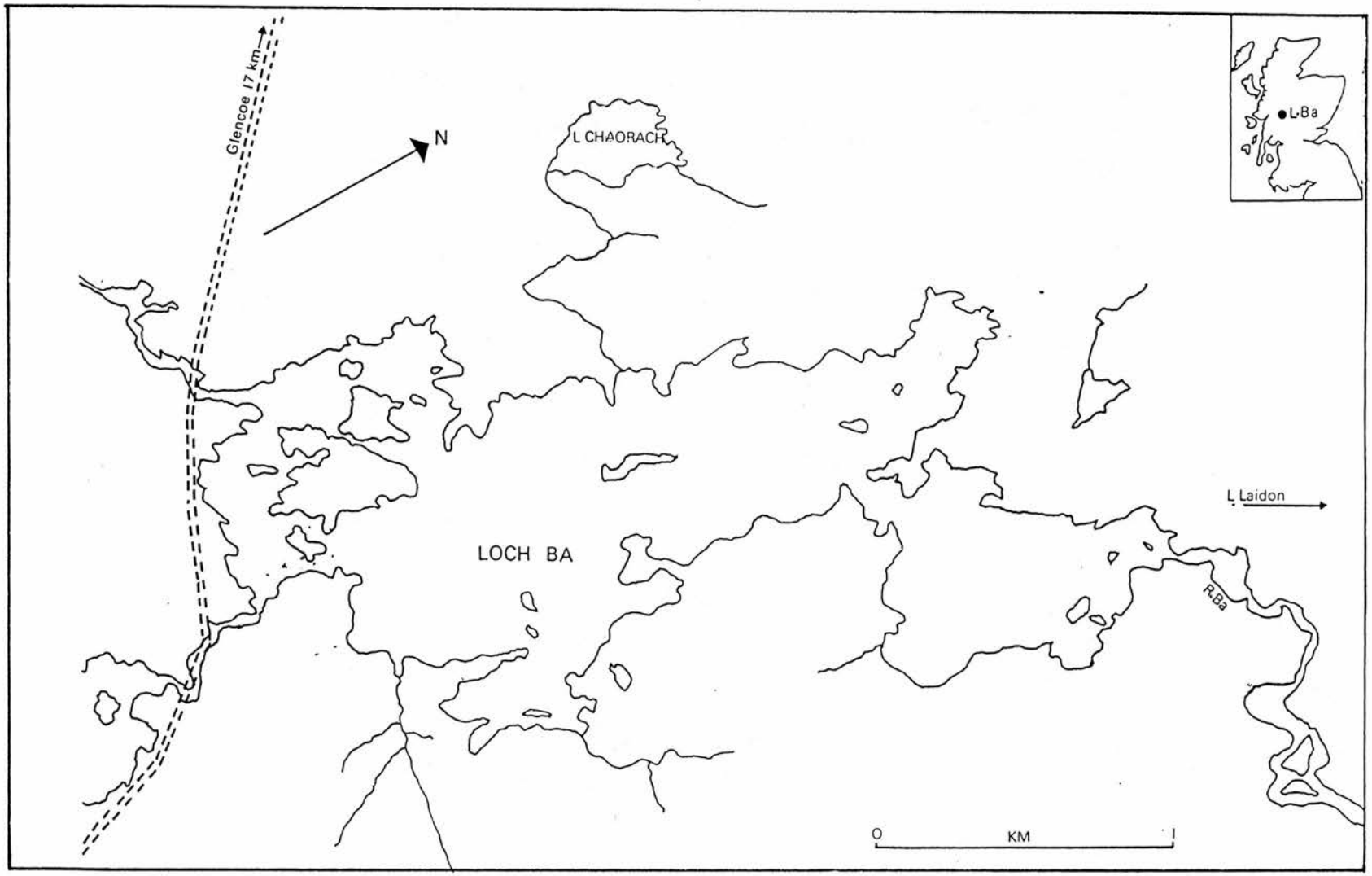

FIG 3/3: Outline and location of the Loch Ba catchment.

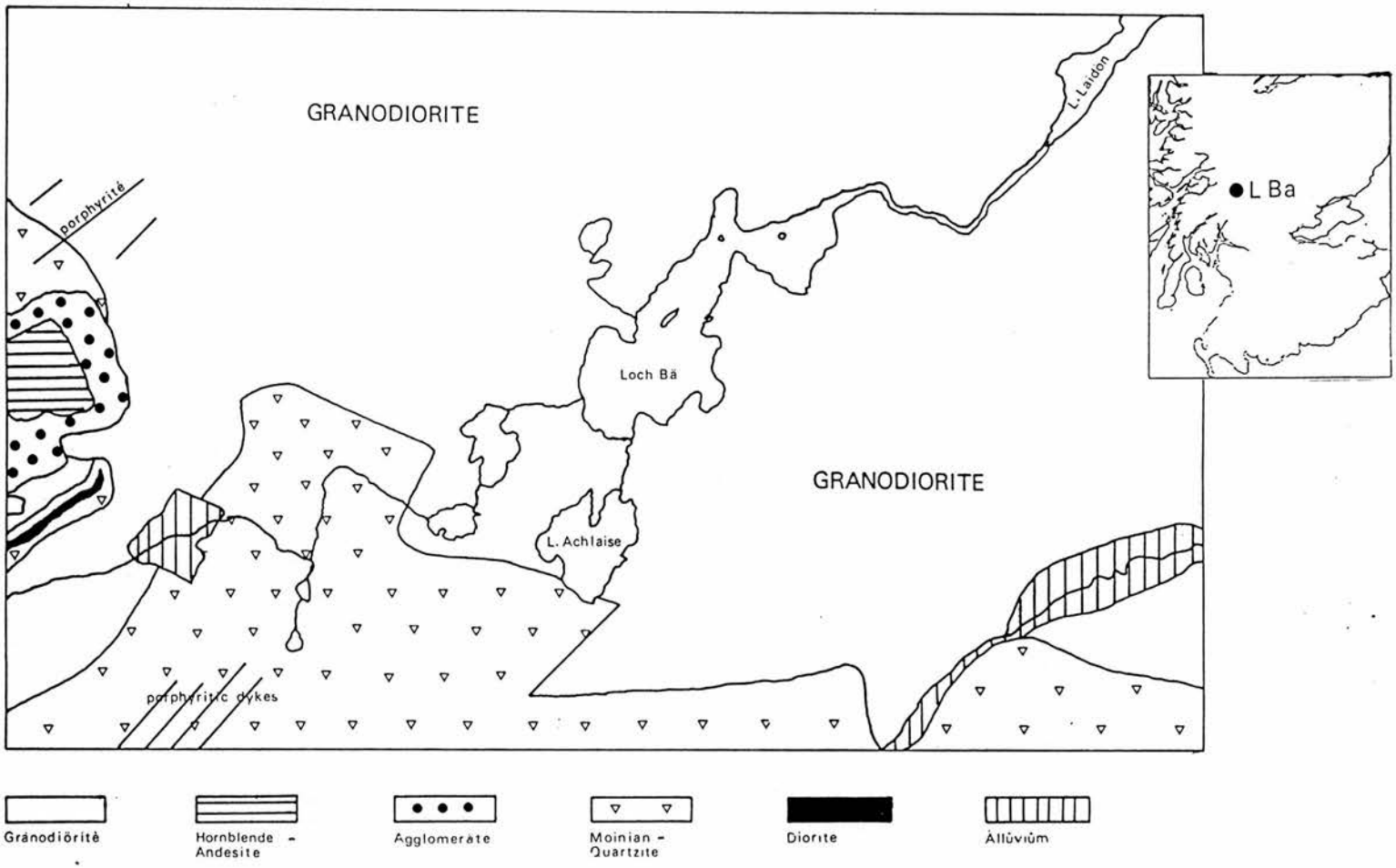

FIG 3/4: Geology of Loch Ba and surrounding environs.

Conditions within the surface waters of Loch Ba fluctuate between oligotrophy and dystrophy (NCC 1979) and accordingly, are inherently acidic. At the time of sample core collection, pH values of 4.9 were recorded and HCO3 alkalinity fell within the range 2 - 5ueq/l.

3.3: Sample collection and core extrusion.

Three 1m cores were collected from Loch Ba on 1.7.86 by use of a 1m pneumatic piston corer (Mackereth 1969). Five 1m cores were collected from Loch Dee on 1.9.86 by use of identical methods. For purposes of the provision of geochemical records which are least likely to have been influenced by lake level changes, sediment slumping or post-depositional redistribution, analyses have only been carried out on cores taken from the deepest available coring locations within the catchment sub-basins. Cores Dee(3) and Dee(4) represent the sedimentary sequence at the deepest point within Loch Dee (14m). Core Ba(2) was extracted from the deepest point in the southern sub-basin of Loch Ba (9m). Core Ba(3) represents the sedimentary sequence at the deepest point in the central sub-basin of Loch Ba (14m). The locations of these coring stations are illustrated in Figs 3/5a - b.

Following extraction, all sample cores were retained in an upright position in sealed plastic tubes during

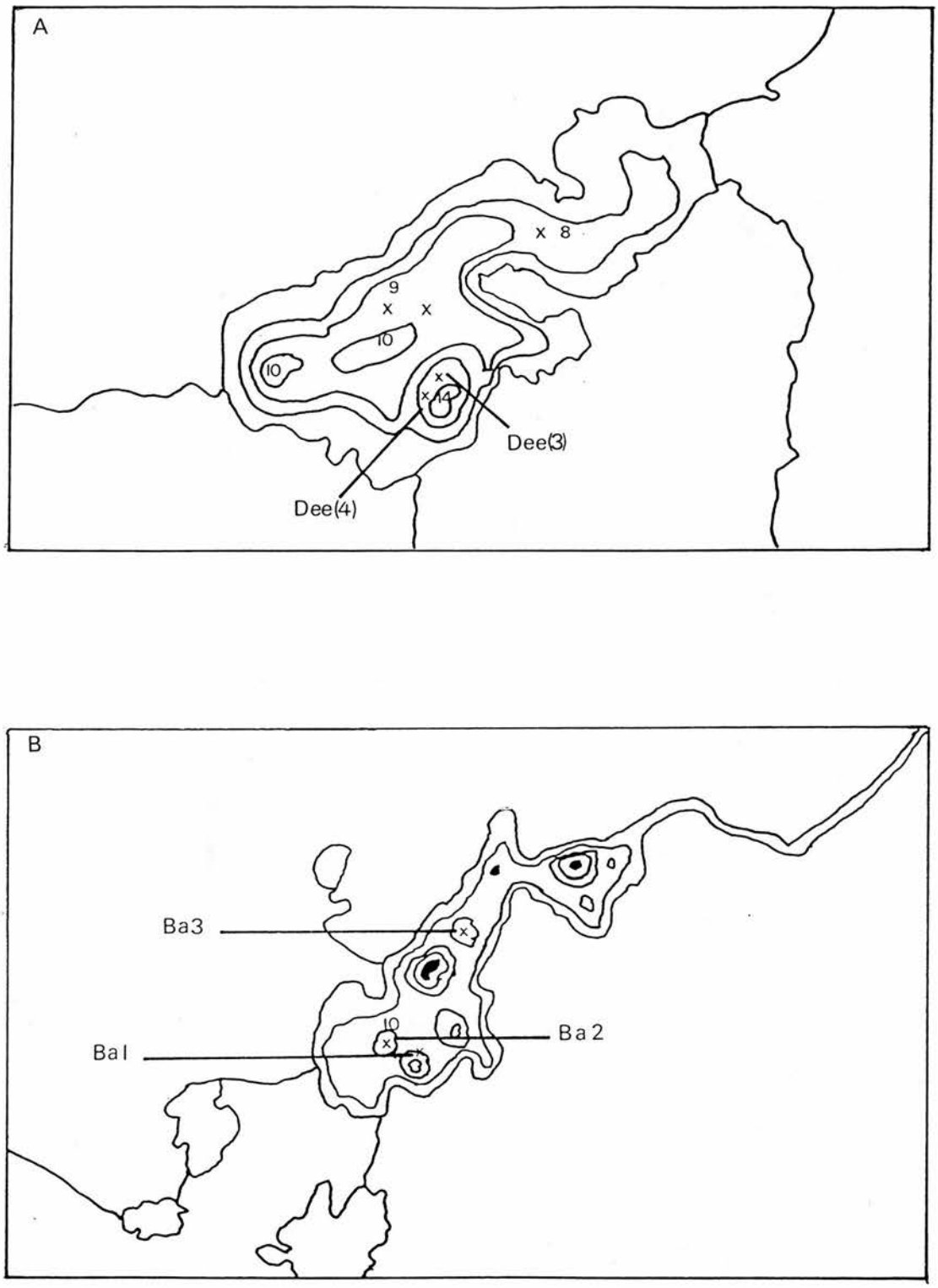

FIG 3/5: Locations of coring stations at Loch Dee (A) and Loch Ba (B).

transportation to the laboratory. Cores used for redox, pore-water or sequential chemical analyses were extruded within 24 hours of collection by passing a hydraulically pressurised piston through the core tube. Sub-samples were removed following each 1cm progression of the piston.

3.4.1 Loch Dee cores: sediment geochemistry.

a) "Bulk" elemental data.

AAS-determined Pb, Zn, Cu, Cd, Mn, Fe, Co, Ni, Ca and Mg concentrations within sub-samples from 42 stratigraphic levels of core Dee(3) and 29 levels of core Dee(4) indicate considerable accordance between the geochemical characteristics of sediments at the respective coring stations. Descriptive statistical data show the mean concentrations of Pb, Cu, Cd, Fe, Co and Ni to vary by less than 20% between cores (Tables 8 - 9). Excepting a major Mg anomaly at 1cm depth in core Dee(4) and minor differences in Zn and Mn accumulation patterns in the surficial 5cm of sediment, similar comparability is apparent with respect to the downcore concentration gradients of Pb, Zn, Cu, Cd, Mn, Cd, Ni and Mg (Figs 3/6 - 3/9). For the profiles of Pb, Zn and Cu, between-core correlation coefficients exceed 0.7. Consequently, elemental enrichment patterns in cores Dee(3) and Dee(4) may conveniently be evaluated simultaneously.

Table 8: Core Dee(3) - Descriptive statistics for elemental data (µg/g).

	Pb	Zn	Cu	Cd	Mn	Fe	Co	Ni	Ca	Mg
MEAN	134	241	50	11	3845	56K	32	84	199	1133
MED	121	197	44	12	3691	57K	32	86	176	1153
MIN	69	111	31	8	2666	50K	24	64	46	833
MAX	287	586	100	15	5533	82K	48	107	415	1222

Table 9: Core Dee(4) - Descriptive statistics for elemental data (µg/g)

	Pb	Zn	Cu	Cd	Mn	Fe	Co	Ni	Ca	Mg
MEAN	128	328	50	9	2467	67K	36	72	1601	1095
MED	180	399	61	7	1700	67K	34	100	1600	1300
MIN	70	290	54	0.5	1400	40K	28	85	1200	1000
MAX	300	830	110	10	8700	137K	72	137	1980	7000

From Figs 3/6 - 3/9 it is apparent that strata extending from 20cm - 90cm depth are effectively homogeneous in both sample cores, with all elements except Ca fluctuating between their "whole core" minimum and median concentrations. However, the enrichment patterns of individual elements differ markedly in the surficial 20cm of sediment, facilitating the identification of three discrete behavioural groups. Specifically:-

1) Pb, Zn and Cu display progressive upward enhancement throughout the uppermost 20cm of the sediment column (Figs 3/6a - c and 3/8a - c). In core Dee(3) the Pb gradient

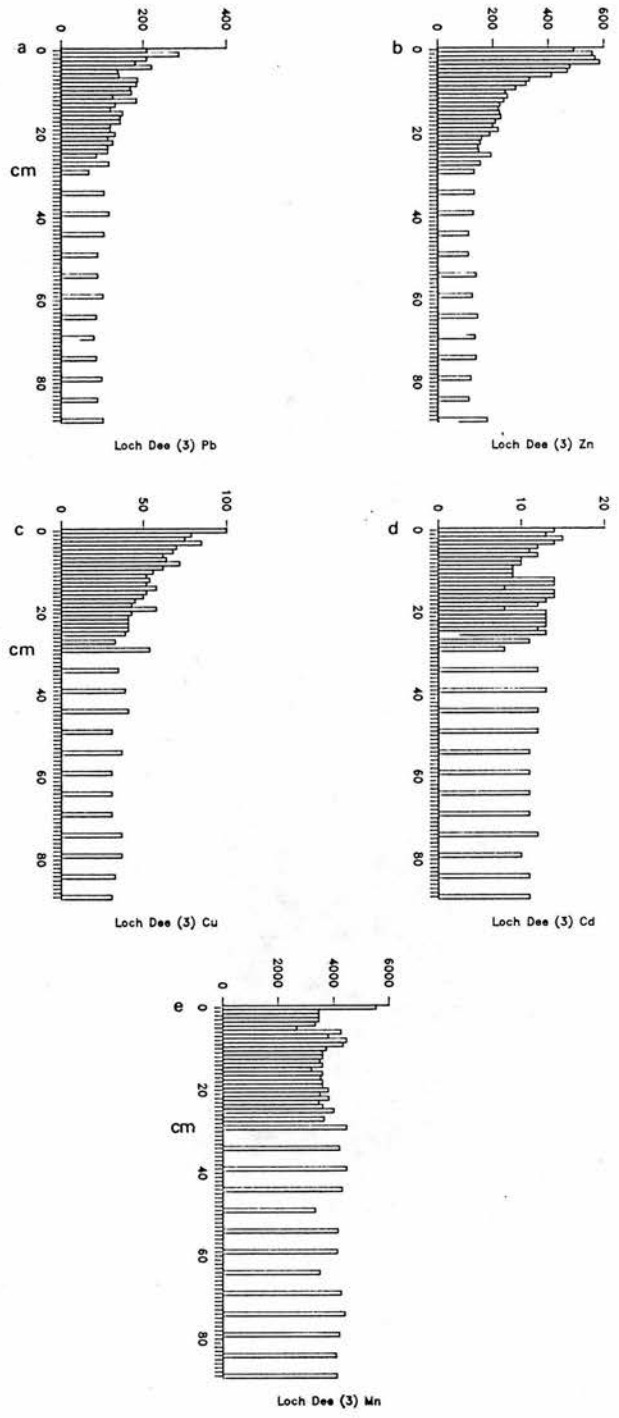

FIG 3/6: Total concentrations of Pb, Zn, Cu, Cd and Mn (µg/g dry weight) in sub-samples from 42 stratigraphic levels of core Dee(3).

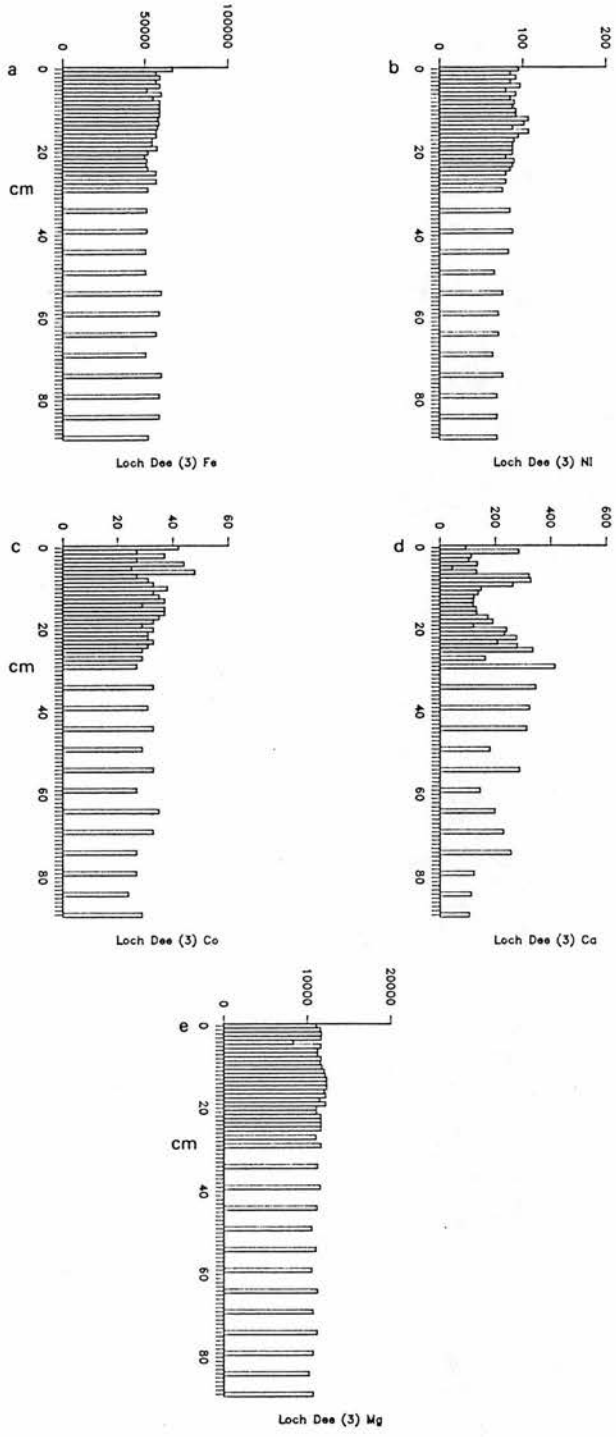

FIG 3/7: Total concentrations of Fe, Ni, Co, Ca and Mg (µg/g dry weight) in sub-samples from 42 stratigraphic levels of core Dee(3).

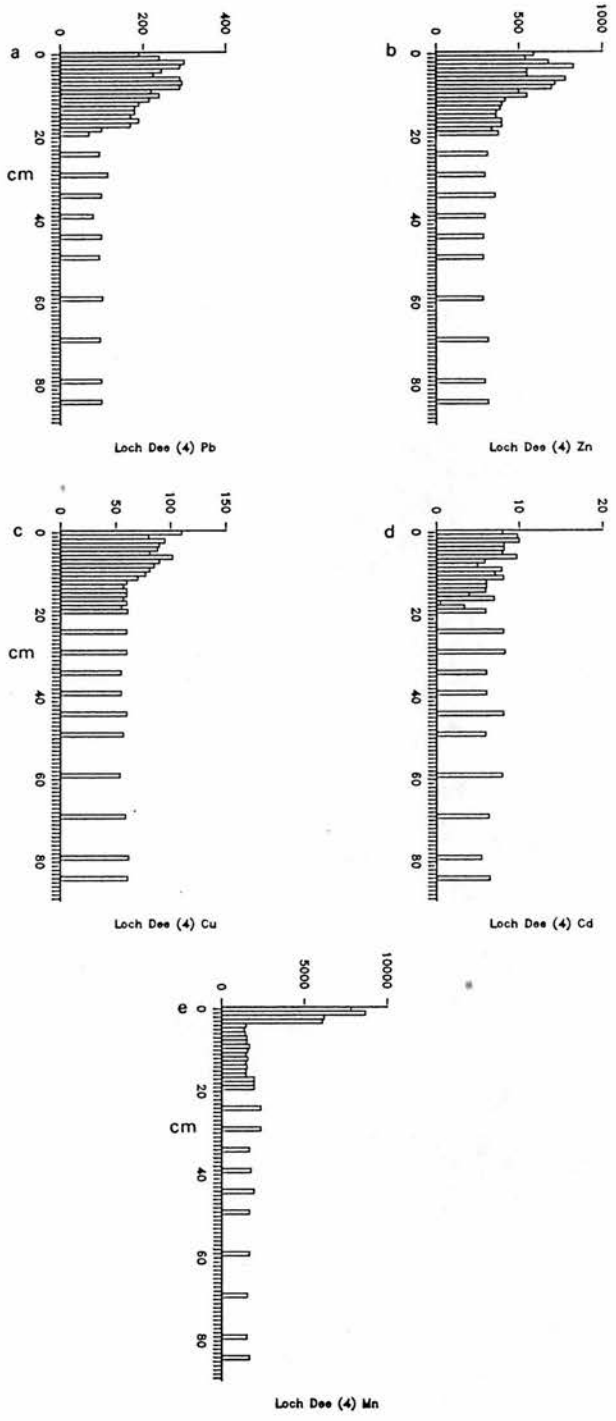

FIG 3/8: Total concentrations of Pb, Zn, Cu, Cd and Mn (µg/g dry weight) in sub-samples from 29 stratigraphic levels of core Dee(4).

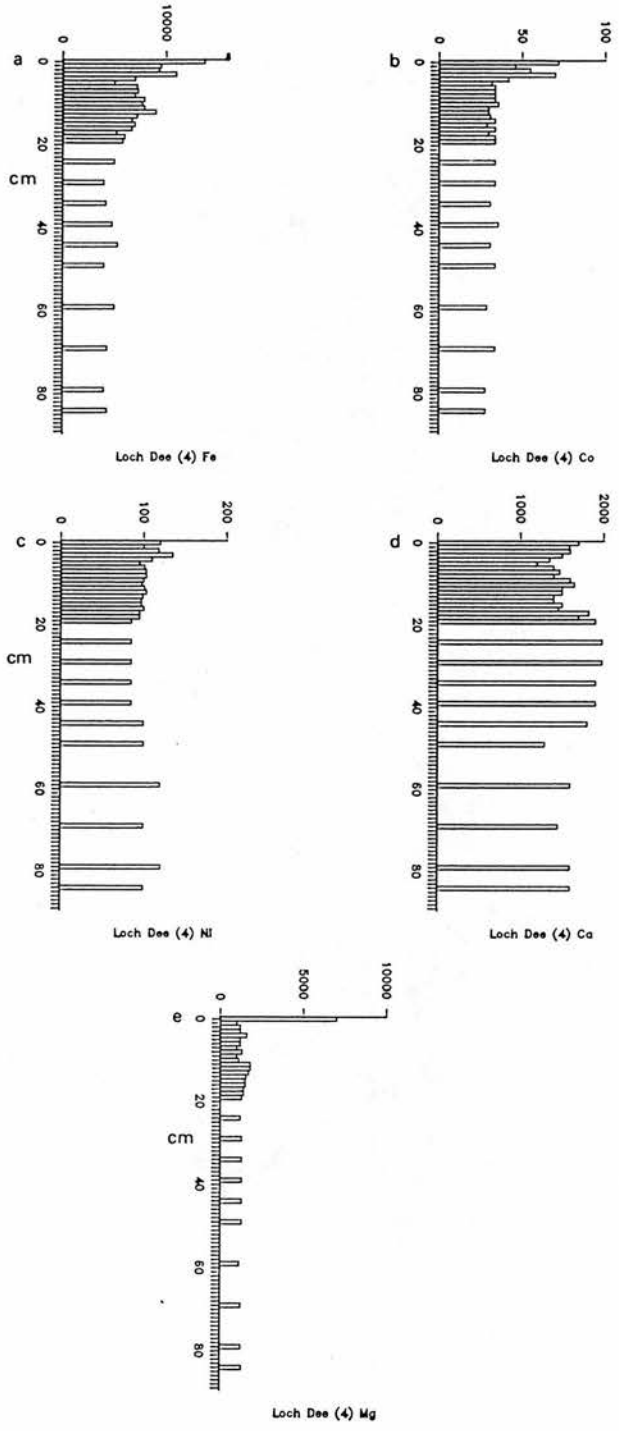

FIG 3/9: Total concentrations of Fe, Co, Ni, Ca and Mg (µg/g dry weight) in sub-samples from 29 stratigraphic levels of core Dee(4).

depicts steadily increasing concentrations from around 120µg/g at 25cm depth to a peak of 287µg/g at 2cm depth (Fig 3/6a). Pb enrichment patterns only differ in core Dee(4) to the extent that initial enhancement (to above 150ug/g) is evident at 20cm depth, with concentrations declining upward of 3cm depth (Fig 3/8a). Zn concentrations increase progressively upward of 18cm depth in both sample cores (Fig 3/6b and 3/8b), attaining maxima of 600µg/g at 4cm depth in core Dee(3) and 830µg/g at 4cm depth in core Dee(4). The Cu gradients through cores Dee(3) and Dee(4) are most closely analogous, with concentrations increasing from around 55µg/g upward of 17cm depth to maxima of 100 - 110µg/g at the sediment/water interface (Figs 3/6c and 3/8c). Statistical verification of the related enrichment patterns of Pb, Zn and Cu is provided by their correlation coefficients, which exceed 0.78 in all instances (Tables 10 - 11).

2) Mn, Fe and Co form a second distributional group, characterised by the confinement of enrichment to the surficial 2cm - 5cm of sediment. Such trends are most pronounced at coring station Dee(4) where concentrations rise from below 2000µg/g Mn, 40µg/g Co and 50000µg/g Fe at 5cm - 90cm depth to 8700µg/g Mn, 72µg/g Co and 137000µg/g Fe in the uppermost 4cm of sediment (Figs 3/8e, 3/9a and 3/9b). Correlations coefficients for Fe, Mn and Co exceed 0.7 in this core (Table 11).

	DEPTH	Pb	Zn	Cu	Cd	Mn	Fe	Ni
Pb	-0.698							
Zn	-0.662	0.836						
Cu	-0.750	0.815	0.900					
Cd	-0.193	0.296	0.271	0.124				
Mn	0.284	-0.140	-0.168	0.040	-0.135			
Fe	-0.181	0.387	0.404	0.484	-0.039	0.310		
Ni	-0.772	0.587	0.403	0.532	0.364	-0.184	0.303	
Co	-0.400	0.326	0.285	0.293	0.329	0.101	0.348	0.586
Ca	0.065	-0.195	-0.340	-0.228	-0.138	0.360	-0.386	-0.178
Mg	-0.396	0.038	0.003	0.160	0.042	-0.167	-0.009	0.442

	Co	Ca
Ca	-0.226	
Mg	-0.064	0.019

Table 10: Correlation coefficients (R) depicting the co-variability of elements through core Dee(3).

	Depth	Pb	Zn	Cu	Cd	Mn	Fe	Co
Pb	-0.712							
Zn	-0.647	0.908						
Cu	-0.568	0.789	0.887					
Cd	-0.164	0.161	0.158	0.192				
Mn	-0.338	0.300	0.402	0.518	-0.039			
Fe	-0.672	0.635	0.646	0.706	-0.096	0.700		
Co	-0.436	0.419	0.590	0.677	-0.019	0.835	0.791	
Ni	-0.023	0.442	0.477	0.502	-0.058	0.439	0.552	0.589
Ca	0.245	-0.616	-0.460	-0.366	-0.390	0.115	-0.266	-0.016
Mg	-0.198	0.006	0.096	0.395	-0.048	0.444	0.591	0.565

Table 11: Correlation coefficients (R) depicting the co-variability of elements through core Dee(4).

3) Ni, Mg, and Cd show no marked enrichment in the surficial 25cm of cores Dee(3) and Dee(4). Excepting the 7000µg/g Mg anomaly at 1cm depth in core Dee(4), concentrations of around 90µg/g Ni, (Figs 3/7b and 3/9c), 10µg/g Cd (Figs 3/6d and 3/8d) and 1100µg/g Mg (Figs 3/7e and 3/9e) prevail throughout all analysed levels of the sediment reservoir.

b) Elemental partitioning.

Elemental fractionation data for sub-samples from 19 stratigraphic levels of core Dee(4) confirm the previously noted geochemical homogeneity of strata extending from 25cm - 90cm depth (Figs 3/10 - 3/19). Throughout this sequence, the partitioning of elements between mineral phases shows limited variability, with 100% Cu, 100% Cd and at least 87% Fe, 70% Ni, 67% Pb, 56% Mg and 54% Co residing in poorly reactive, H2O2 extractable or silicate complexes. Zn (62% NaOAc extractable), Ca (72% MgCl + NaOAc extractable) and Mn (81% MgCl + NaOAc + NH2.OH.HCl extractable) display equally consistent fractionation patterns but are predominantly held in hydrogenous phases. Notably, elements which are not subject to marked enrichment in the surficial 20cm of sediment (Ca, Ni and Mg) maintain consistent geochemical partitioning throughout the entire core (see Figs 3/17 - 3/19).

Upon examining the sequential chemical data presented for

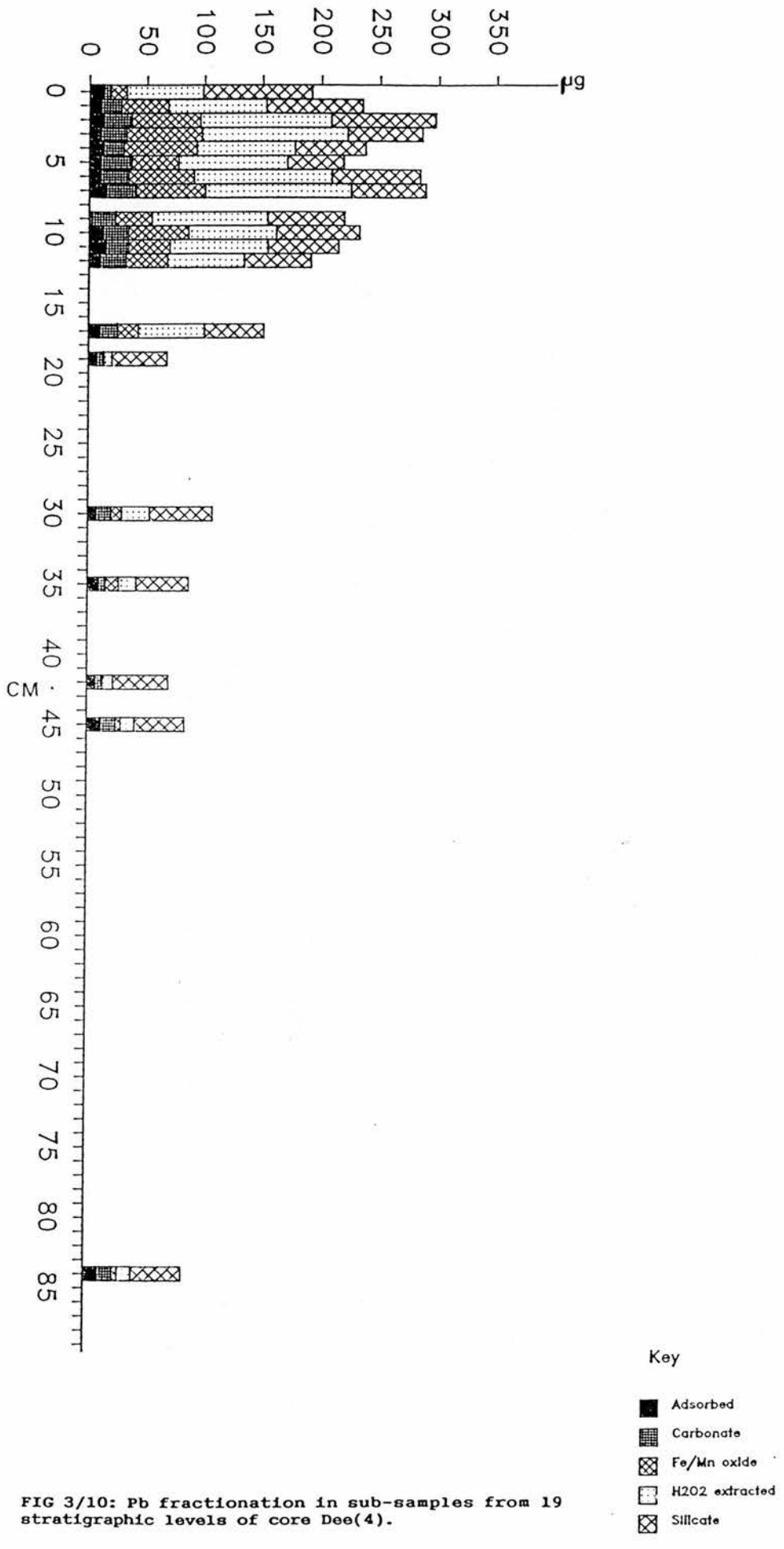

FIG 3/10: Pb fractionation in sub-samples from 19 stratigraphic levels of core Dee(4).

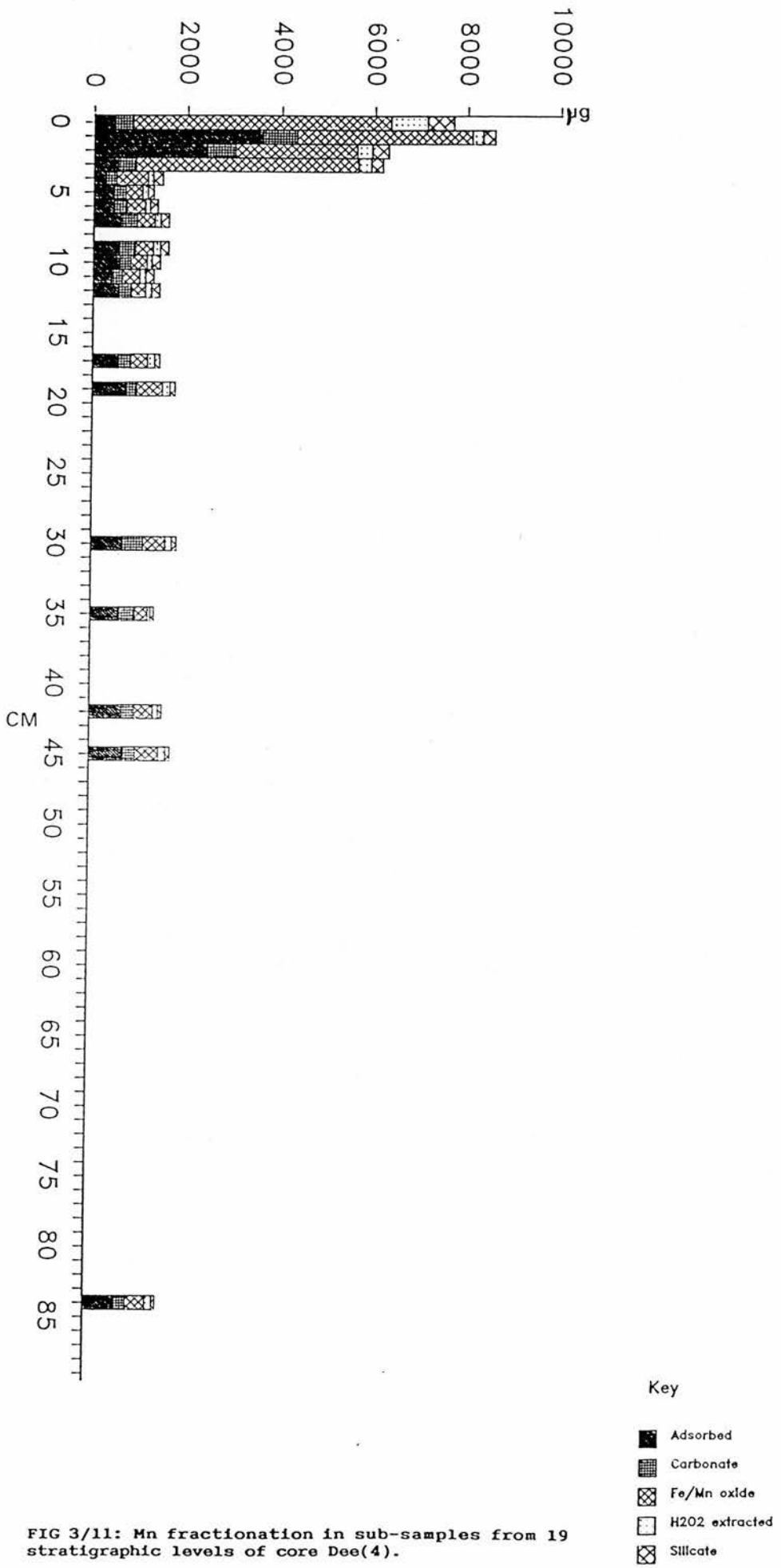

FIG 3/11: Mn fractionation in sub-samples from 19 stratigraphic levels of core Dee(4).

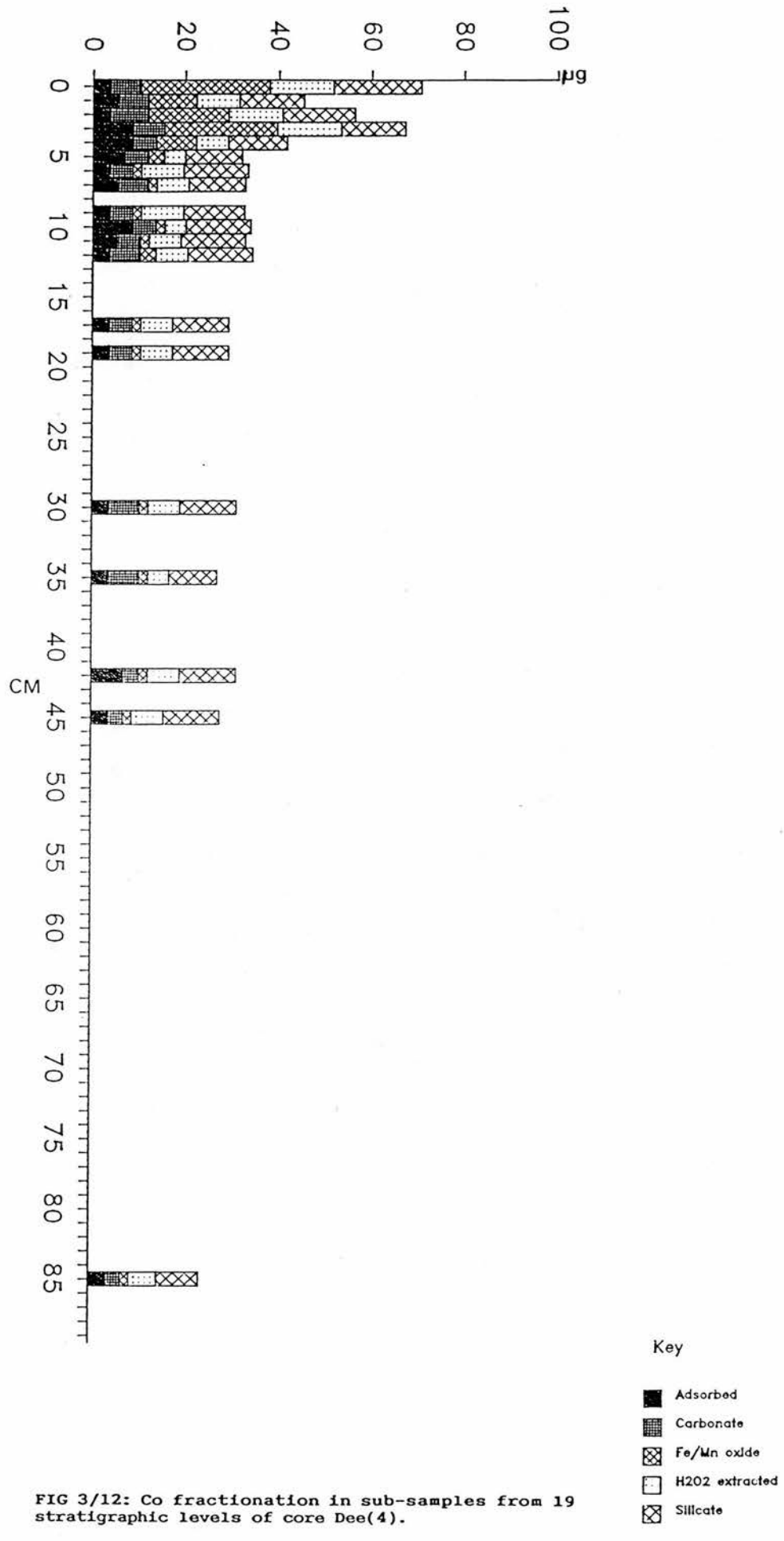

FIG 3/12: Co fractionation in sub-samples from 19 stratigraphic levels of core Dee(4).

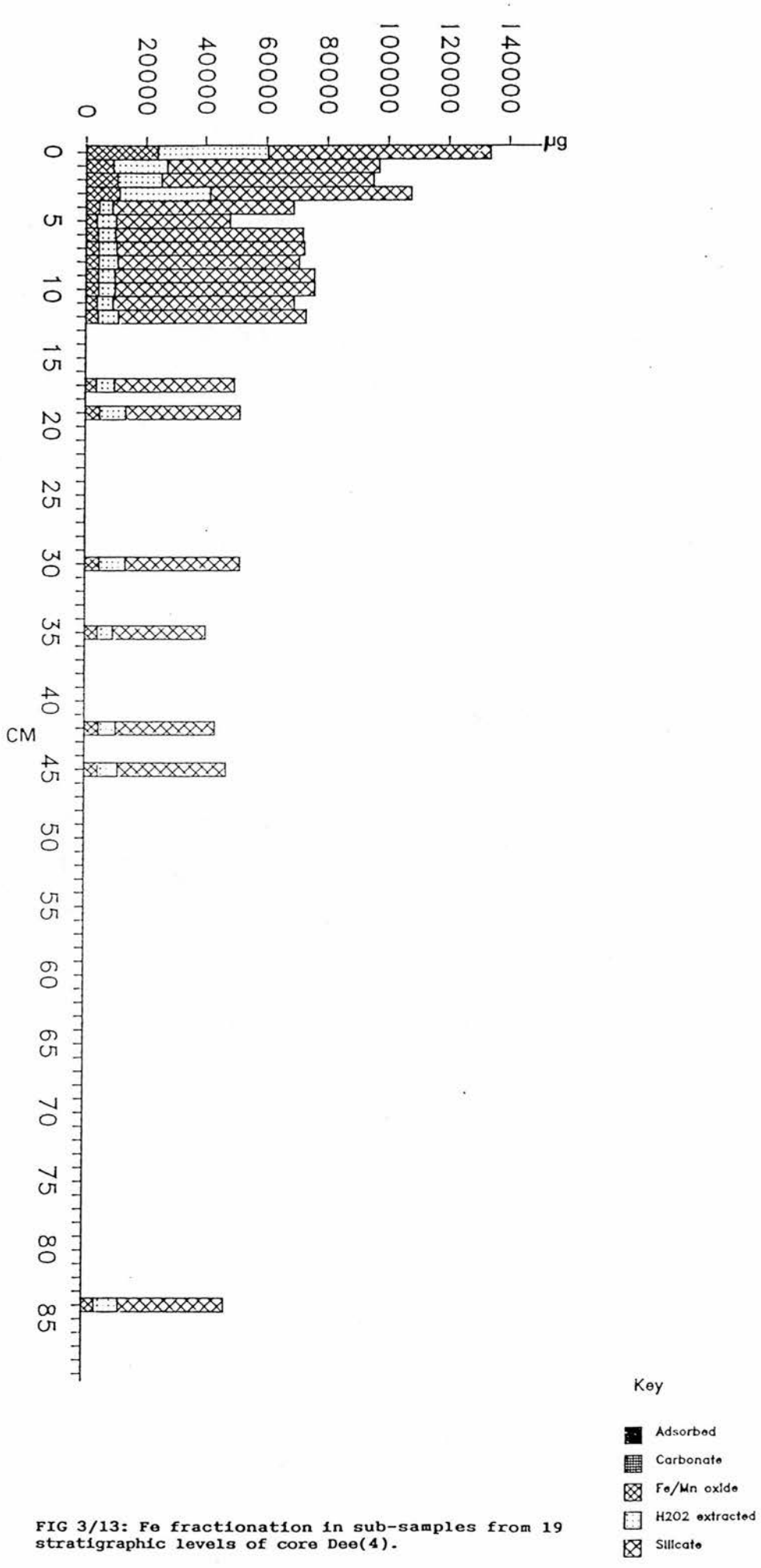

FIG 3/13: Fe fractionation in sub-samples from 19 stratigraphic levels of core Dee(4).

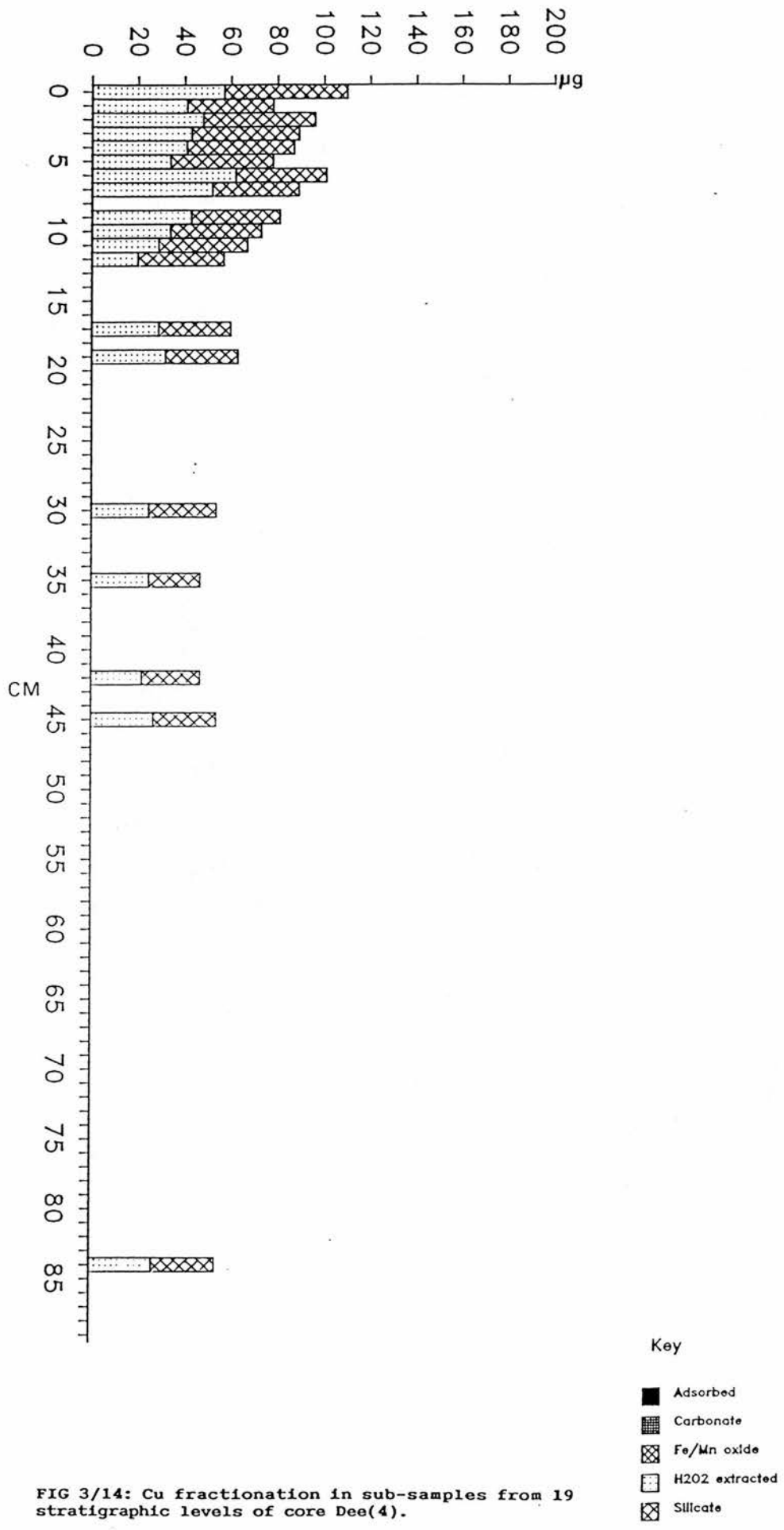

FIG 3/14: Cu fractionation in sub-samples from 19 stratigraphic levels of core Dee(4).

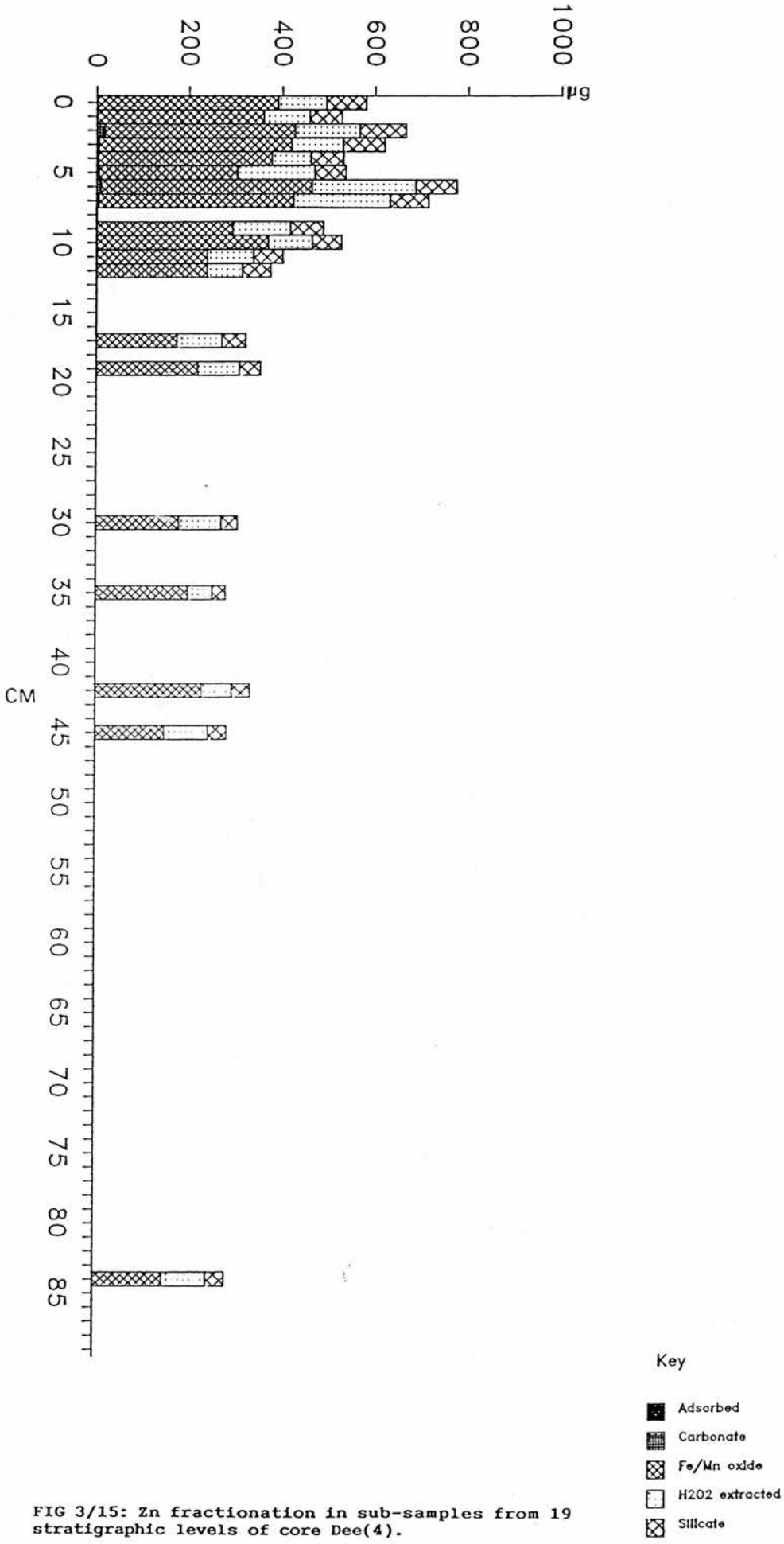

FIG 3/15: Zn fractionation in sub-samples from 19 stratigraphic levels of core Dee(4).

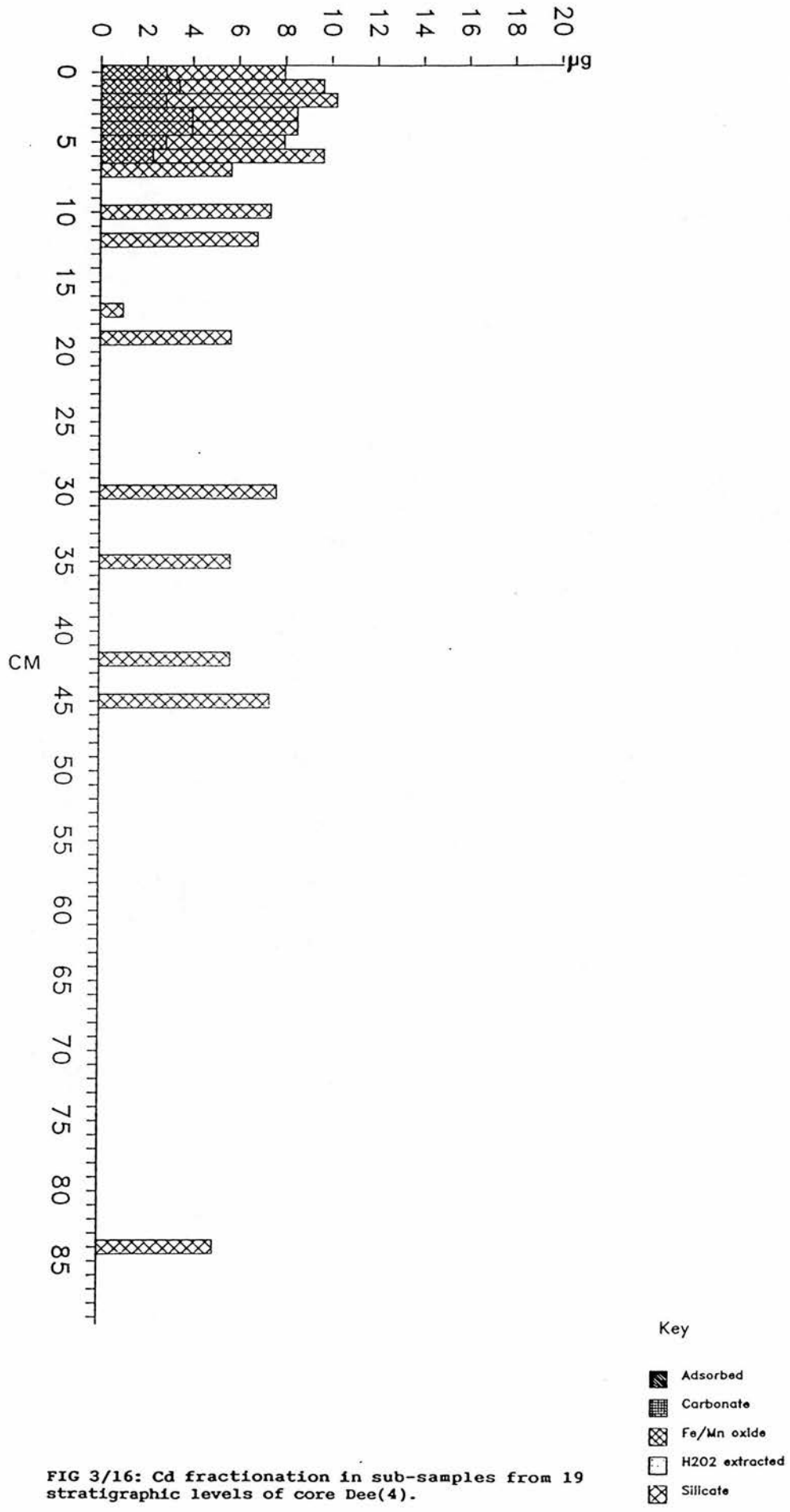

FIG 3/16: Cd fractionation in sub-samples from 19 stratigraphic levels of core Dee(4).

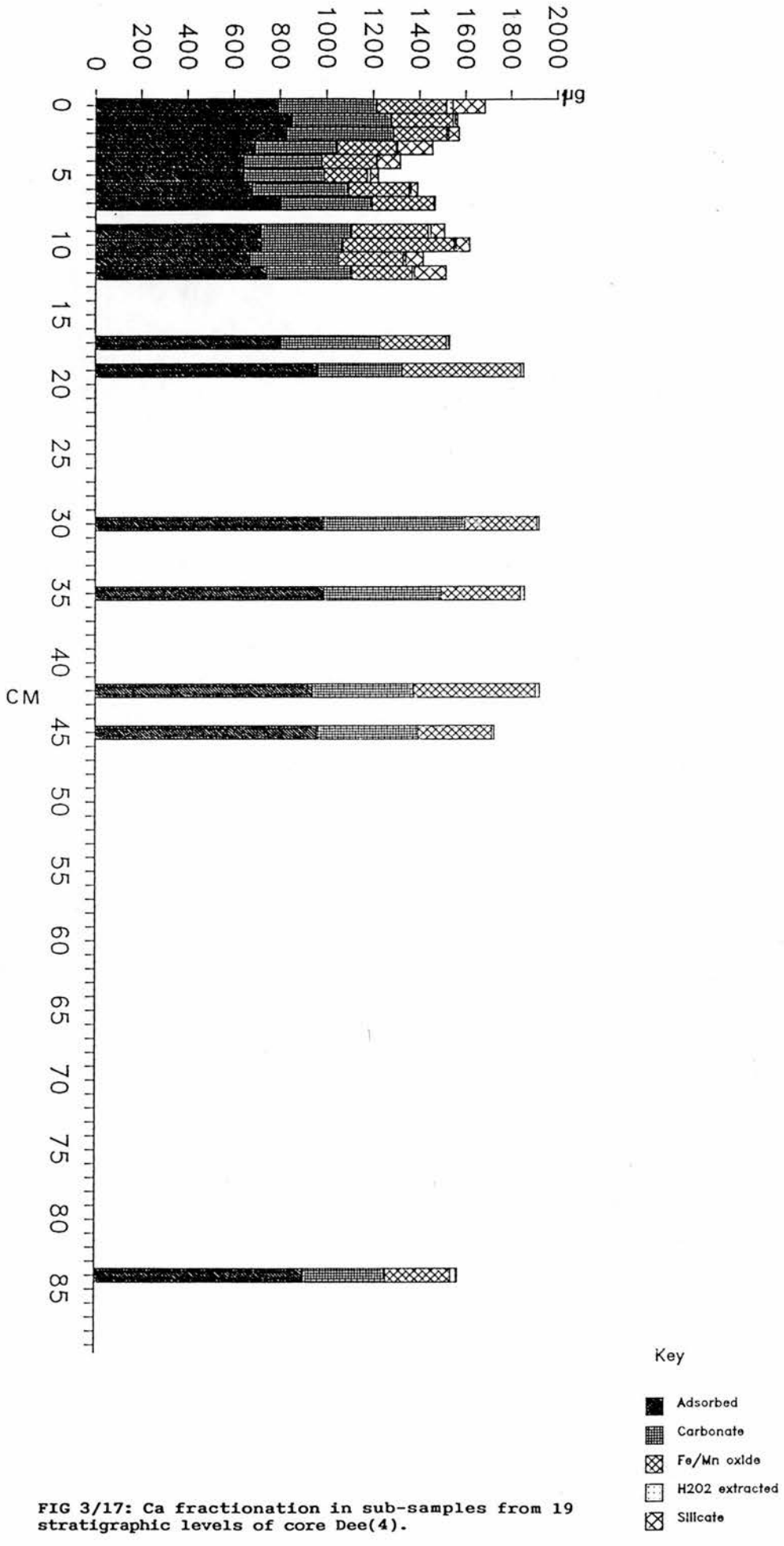

FIG 3/17: Ca fractionation in sub-samples from 19 stratigraphic levels of core Dee(4).

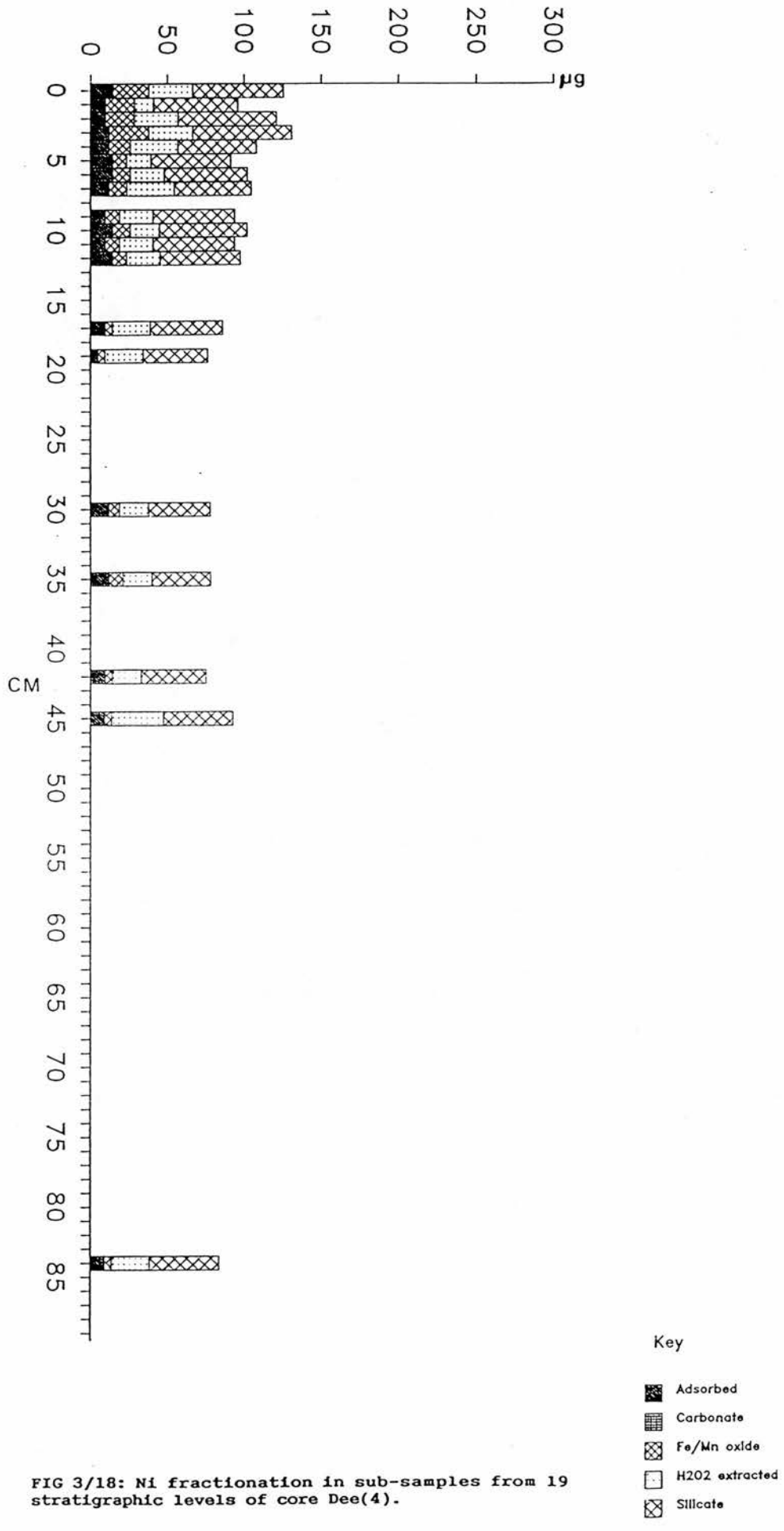

FIG 3/18: Ni fractionation in sub-samples from 19 stratigraphic levels of core Dee(4).

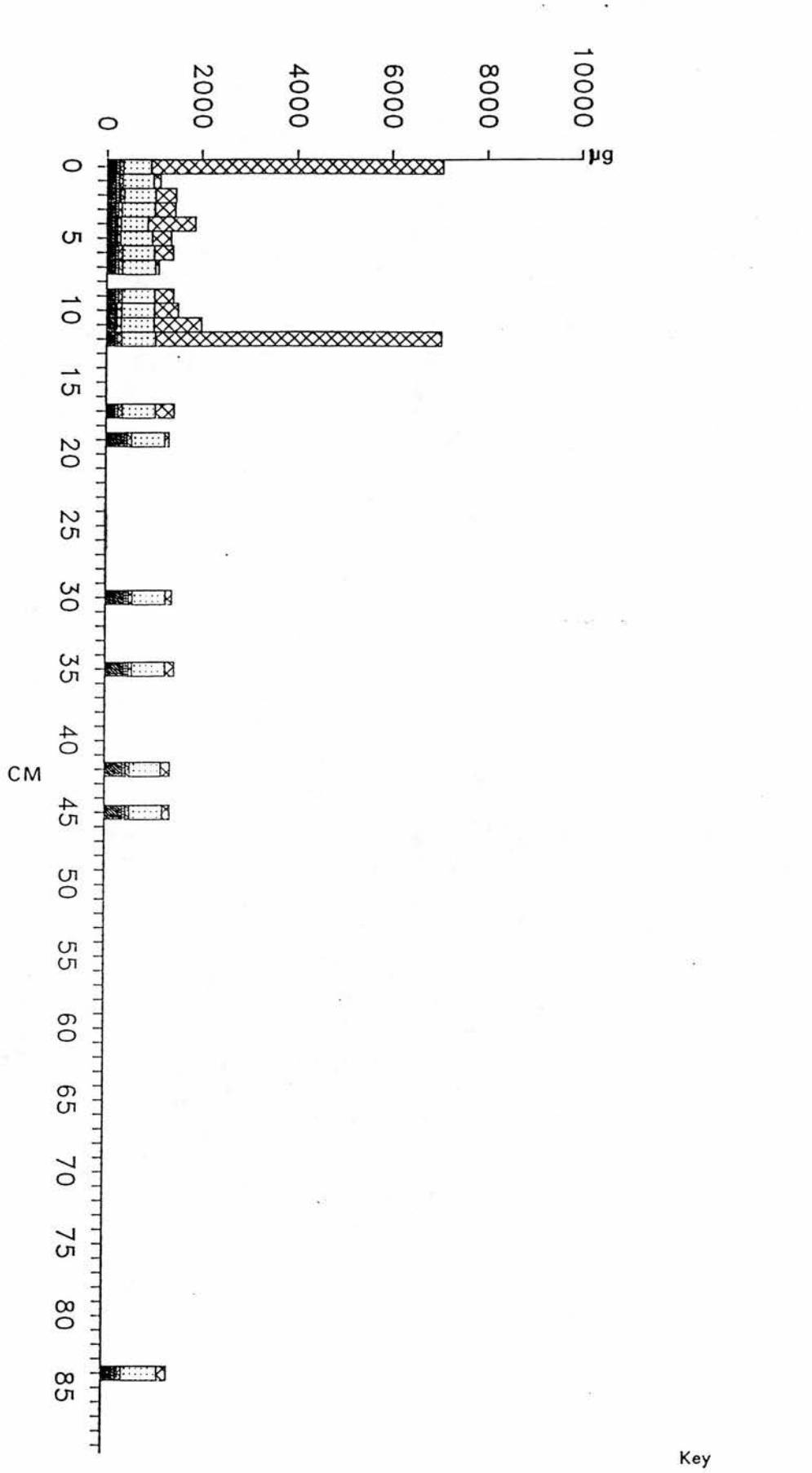

FIG 3/19: Mg fractionation in sub-samples from 19 stratigraphic levels of core Dee(4).

sub-samples from the surficial 20cm of core Dee(4), the differing relationships between elemental enrichment and geochemical partitioning facilitate the identification of two elemental groups. The first group comprises Pb, Mn, Co and Fe which all become enhanced as a consequence of the dis-proportionate accumulation of specific geochemical or mineralogical fractions upward of 18cm, 4cm, 4cm and 4cm respectively. In the case of Pb (Fig 3/10), increments to total concentrations upward of 18cm are attributable to the enrichment of H2O2 extractable (organic and NVS) phases by factors of 2.5 - 12, with the NH2.OH.HCl + HOAc extractable component also increasing dis-proportionately. This latter fraction constitutes 20% (60µg/g) of total Pb at 4cm depth compared with only 7% at 20cm depth, suggesting the increased prevalence of either reducible Pb oxides or acid-volatile Pb sulphides within the surficial strata.

With respect to Mn and Co, enrichment from below 2000µg/g and 40µg/g respectively at 6cm - 85cm depth to maxima of 8300µg/g Mn and 72µg/g Co at 1cm - 4cm depth solely reflects the accumulation of hydrogenous phases (Figs 3/11 and 3/12). NH2.OH.HCl + HOAc extractable fractions (probably reducible Mn/Co oxides) appear particularly significant, constituting 73% (5500µg/g) of total Mn and 37% (28µg/g) of total Co at 1cm depth.

In the case of Fe, two-fold enrichment in the uppermost 4cm relative to the concentrations prevailing at 20cm - 90cm

depth is associated with the dis-proportionate accumulation of NH2.OH.HCl/HOAc and H2O2 extractable components (Fig 3/13). These fractions hold 60,000µg/g Fe (45% total Fe) at 1cm depth and, given the co-existence of Mn oxides, can be assumed to constitute reducible Fe oxides and organic Fe complexes.

Zn and Cu are clearly distinguishable from the above elements, showing progressive enrichment upward of 12cm depth in core Dee(4) without any marked digression from the geochemical fractionation patterns occurring at 25cm - 90cm depth (Figs 3/14 and 3/15). In the case of Cu, progressively increasing total concentrations (from around 60ug/g at 13cm to a maximum of 110µg/g at the sediment/water interface) occur with H2O2 extractable/silicate Cu ratios remaining within the narrow range 0.63 - 1.66 (Fig 3/14). Adsorbed, carbonate and NH2.OH.HCl + HOAc extractable Cu phases are absent throughout the entire sediment column. With respect to Zn, enrichment beyond a mean of 320µg/g at 18cm - 90cm depth to a mean of 570µg/g at 1cm - 13cm depth is primarily a product of the proportionate accumulation of acid-volatile phases (around 65% of total Zn) and Zn silicates (around 10% of total Zn). Significant deviations from this fractionation pattern are only identifiable at 7cm - 8cm depth, where Zn concentrations exceed 700µg/g in association with the presence of anomalous concentrations (> 200µg/g) of H2O2 extractable (organic or non-volatile sulphide) components (Fig 3/15).

3.4.2 Loch Ba cores: sediment geochemistry.

a) "Bulk" elemental data.

Elemental concentration data for 69 sub-samples from core Ba(2) and 45 sub-samples from core Ba(3) illuminate marked inconsistencies in the geochemical characteristics of sediments at the respective coring stations. Of the elements analysed in both cores, only Pb, Cd and Mn yield mean and peak abundance values with less than 20% between-core variability. In the cases of Zn, Ni, Cu and Co, peak concentrations in the Ba(3) sediment column exceed those prevailing at station Ba(2) by factors of 1.8 - 2.6 (Tables 12 - 13). Because these distinctions are coupled with major variations in the stratigraphic locations of elemental enrichment, downcore geochemical trends in cores Ba(2) and Ba(3) can best be evaluated independently.

Table 12: Core Ba(2) - Descriptive statistics for elemental data (µg/g).

	MEAN	MED.	MIN	MAX
Pb	53	45	28	125
Zn	80	65	39	180
Cu	30	31	16	61
Cd	5.4	4.1	3.7	6.0
Mn	298	275	195	553
Fe	42000	37000	21000	70000
Co	49	55	21	79
Ni	79	81	61	122
K	422	441	380	650

Table 13: Core Ba(3) - Descriptive statistics for elemental data (µg/g).

	MEAN	MED	MIN	MAX
Pb	58	50	31	152
Zn	132	115	44	450
Cu	48	41	27	108
Cd	4.9	4.7	2.5	7.0
Mn	342	332	186	670
Fe	47000	49000	41000	51500
Co	69	70	28	200
Ni	141	150	39	210
Mg	2485	2275	350	9500
Sm	3.4	2.5	1.6	9.5
Hf	0.9	0.7	0	2.1
Eu	2.0	1.6	0	5.6
Ce	0.17	0	0	2.0
La	4.4	2.9	2.3	11.9
Br	6.5	6.5	1.2	11.2
Nb	0.25	0	0	1.14
Yb	0.37	0	0	1.3
Sc	0.6	0	0	1.6
Na	1223	1090	675	1994
K	128	106	86	230

Core Ba(2).

Elemental enrichment patterns in the sediment column at coring station Ba(2) are essentially analogous to those prevailing in the Loch Dee sediment reservoir. Hence, strata extending from 20cm - 90cm depth display considerable geochemical homogeneity and elements fall into three discrete groups on account of their variable enrichment trends in the overlying sediments. Specifically:-

1) Pb, Zn and Cu are all subject to progressive enrichment upward of 15cm depth, attaining concentration maxima of

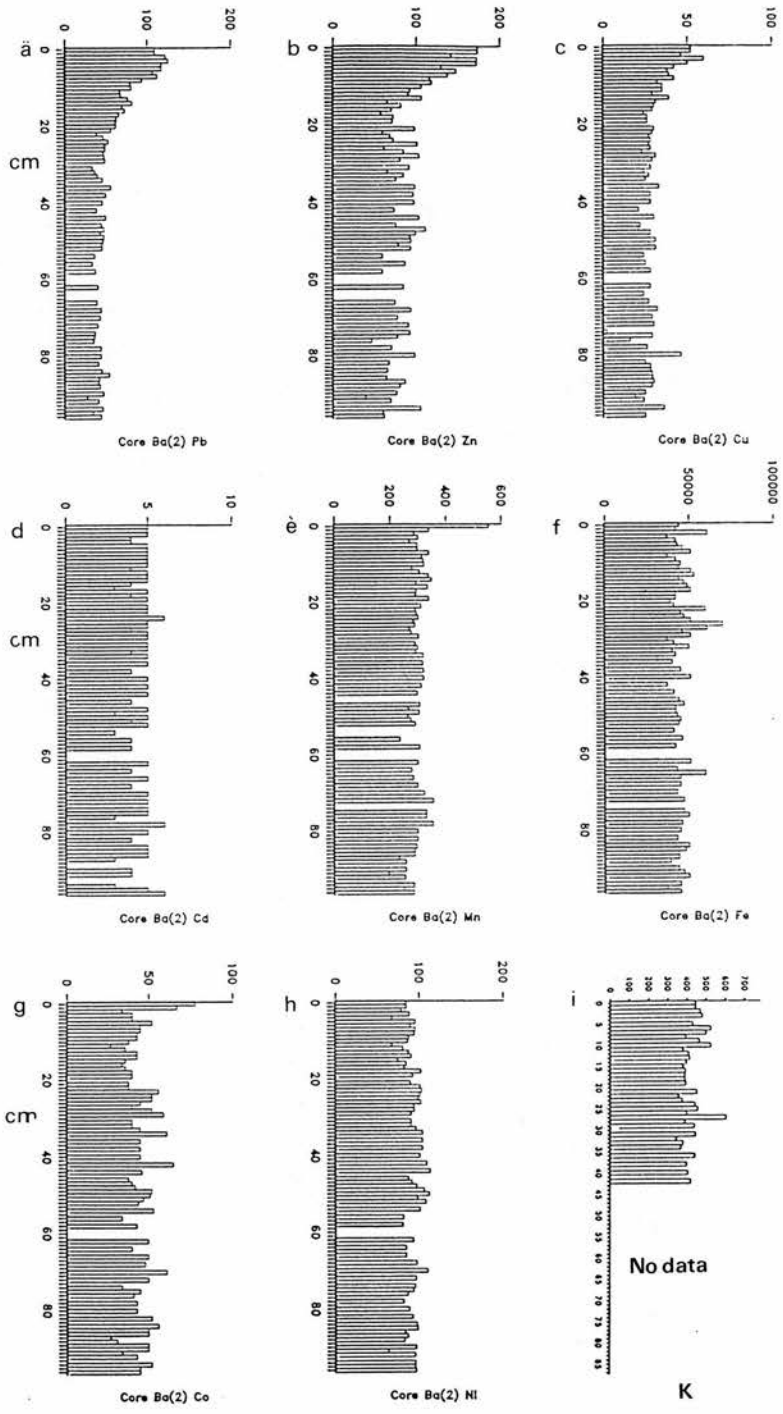

FIG 3/20: Total concentrations of Pb, Zn, Cu, Cd, Mn, Fe, Co, Ni and K (µg/g dry weight) in sub-samples from 69 stratigraphic levels of core Ba(2).

	Depth	Pb	Zn	Cu	Cd	Mn	Fe	Co
Pb	-0.706							
Zn	-0.557	0.779						
Cu	-0.523	0.748	0.711					
Cd	-0.265	0.160	0.057	0.133				
Mn	-0.293	0.331	0.261	0.462	0.201			
Fe	-0.175	0.055	-0.118	0.207	0.018	0.365		
Co	-0.002	0.089	0.187	0.223	0.274	0.350	0.027	
Ni	0.118	-0.238	-0.111	-0.184	0.136	-0.013	-0.054	0.435

Table 14: Correlation coefficients (R) depicting the co-variability of elements through core Ba(2).

125µg/g, 180µg/g and 61µg/g respectively in the uppermost 4cm (Figs 3/20a - c). The profiles of these elements are statistically correlatable, yielding R coefficients in excess of 0.70 (Table 14).

2) Mn and Co maintain consistent concentrations of around 320µg/g and 50µg/g respectively throughout the 3cm - 95cm core sectors, but are markedly enriched at the sediment/water interface. Concentrations of 553µg/g Mn and 79µg/g Co are observable within this zone (Figs 3/20e and g).

3) Concentrations of Ni, Fe, Cd and K fluctuate around their respective "whole core" mean values of 79µg/g, 42000µg/g, 5.4µg/g and 422µg/g throughout the entire sediment column (Figs 3/20d, f, h and i).

Core Ba(3).

The AAS and INAA data acquired for core Ba(3) show downcore elemental enrichment patterns to be distinct from those occurring in core Ba(2) in two respects. Firstly, elemental anomalies in the upper sectors of the sediment are confined to a narrow stratigraphic zone extending from the sediment/water interface to 3cm depth. Secondly, 11 of the 21 analysed elements are subject to greatest enrichment at depths of 40cm - 80cm. The behavioural groupings established on the basis of elemental co-variability in core Ba(2) are

also largely inapplicable. Instead, visual and statistical evidence can be invoked to place 18 of the 21 analysed elements into the following three groups:-

1) Pb, Zn, Mn, Co and Np exhibit greatest enrichment at 1cm - 3cm depth, where respective concentrations of 152ug/g, 450µg/g, 670µg/g, 200µg/g and 0.8µg/g exceed "whole core" mean values by at least a factor of two (Figs 3/21a, b, e and g, 3/22a).

2) Sm, Hf, Eu, Ce, La, Yb, Nb, Sc, Na and K exhibit greatest enrichment in strata extending from 40cm - 80cm depth. Of these elements Sm, Eu, La and Sc are particularly closely correlated (R = 0.63 - 0.95) and exceed their "whole core" mean values by at least a factor of 2 at 60cm - 70cm depth (Figs 3/22b, d and f, 3/23a). Nb and Yb correlate less strongly with the remainder of the "rare earth suite" (see Table 16), but still attain concentration maxima of 1.1µg/g and 1.3µg/g respectively at 50cm - 60cm depth (Figs 3/23c and 3/23d).

3) Concentrations of Fe, Ni and Cd fluctuate around their respective "whole core" means (47000µg/g, 141µg/g and 4.9µg/g) at all stratigraphic levels (Figs 3/21d, f and h). While Mn and Co have formerly been assigned to an elemental group which is characterised by enrichment at the sediment/water interface, it is notable that correlation

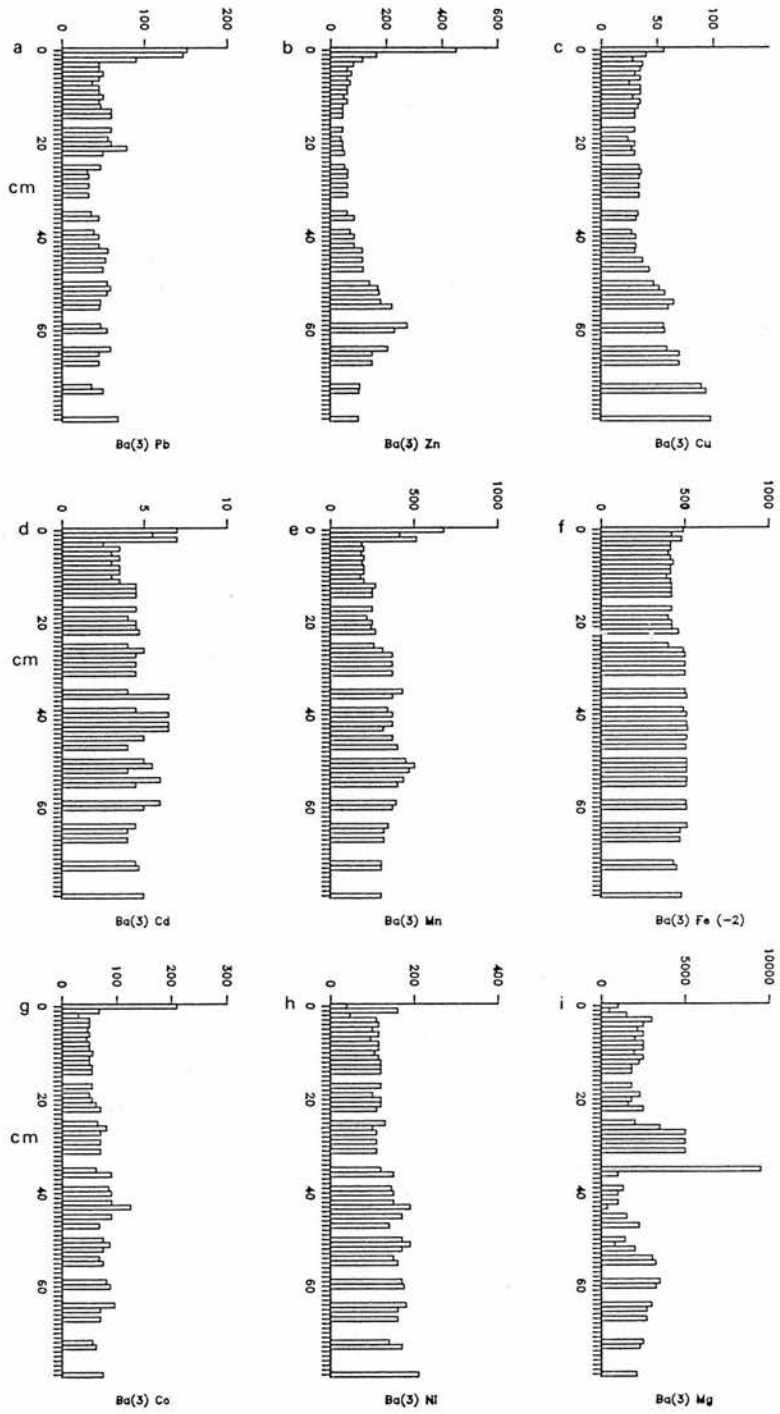

FIG 3/21: AAS determined total concentrations of Pb, Zn, Cu, Cd, Mn, Fe, Co, Ni and Mg in sub-samples from 45 stratigraphic levels of core Ba(3). All data are expressed in µg/g dry weight except Fe, for which data are presented in µg/g x 10-2.

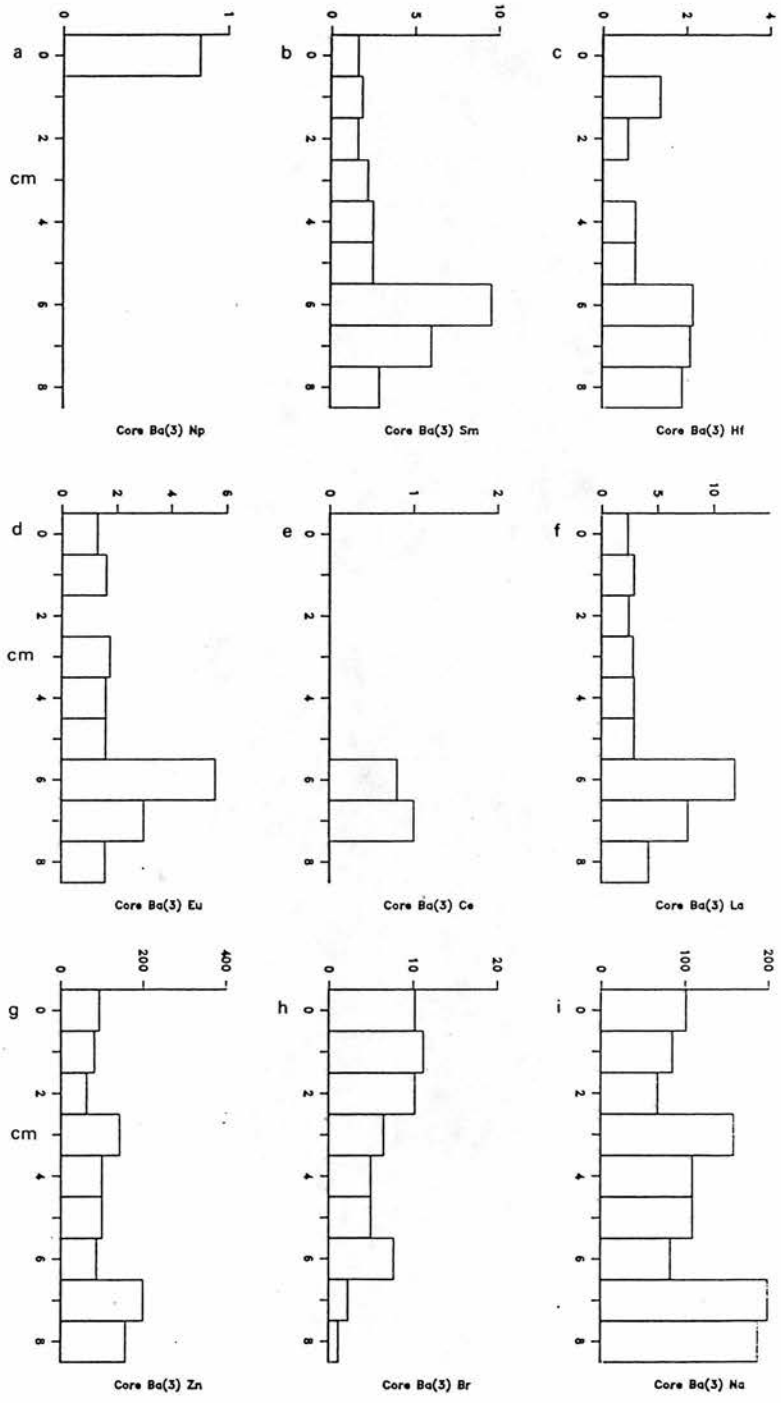

FIG 3/22: INAA determined total concentrations of Np, Sm, Hf, Eu, Ce, La, Zn, Br and Na (µg/g dry weight) in sub-samples from 2cm, 10cm, 20cm, 30cm, 40cm, 50cm, 60cm, 70cm and 80cm levels of core Ba(3).

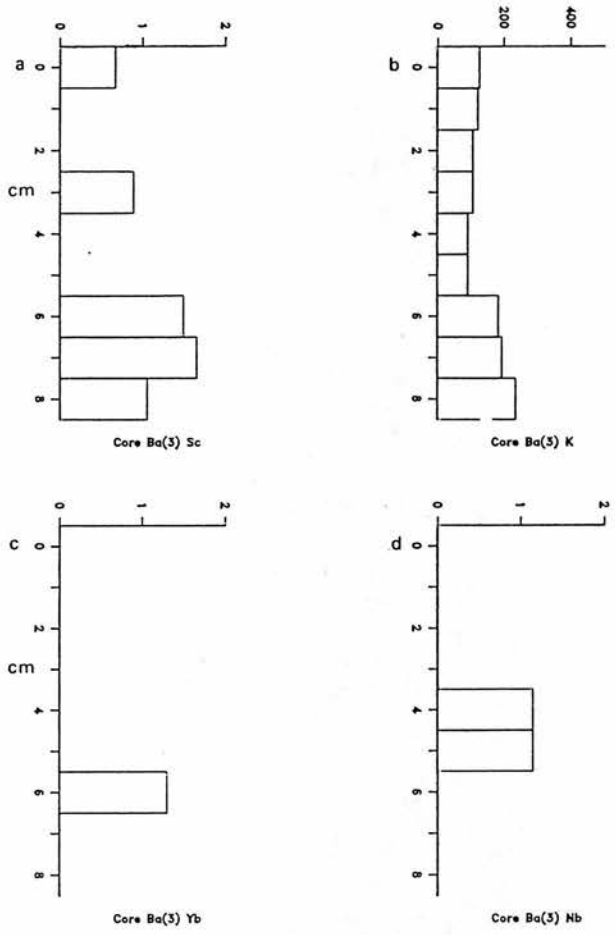

FIG 3/23: INAA determined concentrations of Sc, K, Yb and Nb (µg/g dry weight) in sub-samples from 2cm, 10cm, 20cm, 30cm, 40cm, 50cm, 60cm, 70cm and 80cm levels of core Ba(3).

	DEPTH	Mn	Fe	Cu	Zn	Pb	Ni	Co
Mn	0.415							
Fe	0.448	0.819						
Cu	0.761	0.178	0.082					
Zn	0.124	0.450	0.423	0.333				
Pb	-0.450	-0.034	-0.172	-0.041	0.534			
Ni	0.758	0.330	0.323	0.457	-0.008	-0.283		
Co	0.513	0.326	0.563	0.010	-0.041	-0.340	0.763	
Mg	0.110	0.135	0.133	-0.019	-0.180	-0.465	-0.131	-0.097
Cd	-0.070	0.322	0.414	-0.040	0.455	0.472	-0.109	0.117
LOI	-0.843	-0.298	-0.383	-0.702	0.049	0.546	-0.509	-0.391

Table 15: Correlation coefficients (R) depicting the co-variability of AAS-determined elements through core Ba(3).

	Depth	Np	Sm	Hf	Eu	Ce	La	Zn
Np	-0.526							
Sm	0.580	-0.255						
Hf	0.600	-0.438	0.799					
Eu	0.486	-0.224	0.954	0.713				
Ce	-0.304	0.596	-0.289	-0.436	-0.206			
La	0.569	-0.250	0.996	0.812	0.947	-0.317		
Zn	0.643	-0.134	0.215	0.254	0.193	-0.223	0.205	
Br	-0.893	0.349	-0.254	-0.287	-0.198	0.164	-0.227	-0.801
Na	0.644	-0.146	0.100	0.140	0.089	-0.206	0.095	0.980
Sc	0.583	0.038	0.666	0.455	0.631	-0.247	0.680	0.745
K	0.532	0.001	0.004	0.244	-0.071	-0.221	0.048	0.732
Yb	0.274	-0.187	0.865	0.557	0.870	-0.189	0.873	-0.234
Nb	0.102	-0.166	-0.193	-0.151	-0.148	0.357	-0.266	-0.181

	Br	Na	Sc	K	Yb
Na	-0.834				
Sc	-0.504	0.681			
K	-0.617	0.782	0.554		
Yb	0.110	-0.306	0.371	-0.308	
Nb	-0.248	-0.158	-0.544	-0.413	-0.189

Table 16: Correlation coefficients depicting the co-variability of INAA-determined elements through core Ba(3).

coefficients for Mn v Fe and Co v Ni exceed 0.7 (Table 15). Consequently, Mn and Co can be considered to display affinities to the Fe, Cd, Ni group in all but the uppermost 2cm of sediment.

The assignment of Cu (Fig 3/21c) to a specific elemental grouping is problematic. Despite the synchronous enrichment of Cu and Pb at the sediment/water interface, whole core correlations are negative on account of the progressive enrichment of Cu downward of 50cm depth (to a maximum of 108µg/g at 80cm). Consequently, it appears that the Cu profile is related to the Pb, Zn, Mn, Co grouping through the upper half of the core sequence, but shows greater affinity to K, Na and the REE's in the basal sector.

Mg (Fig 3/21i) and Br (Fig 3/22h) display individualistic downcore profiles, with the former being subject to greatest enrichment (5500 - 9500µg/g) at 27cm - 37cm depth and Br concentrations increasing progressively from 1.2µg/g at 80cm to around 10µg/g in the uppermost 20cm.

b) Elemental partitioning.

The Pb, Zn, Cu, Cd, Fe, Mn, Co and Ni fractionation data acquired for sub-samples from 69 stratigraphic levels of core Ba(2) indicate that the non-enriched levels of the Loch Ba sediment reservoir are characterised by consistent elemental partitioning patterns (Figs 3/24 - 3/31). In the 20cm - 90cm core sequence, the geochemical fractionation of

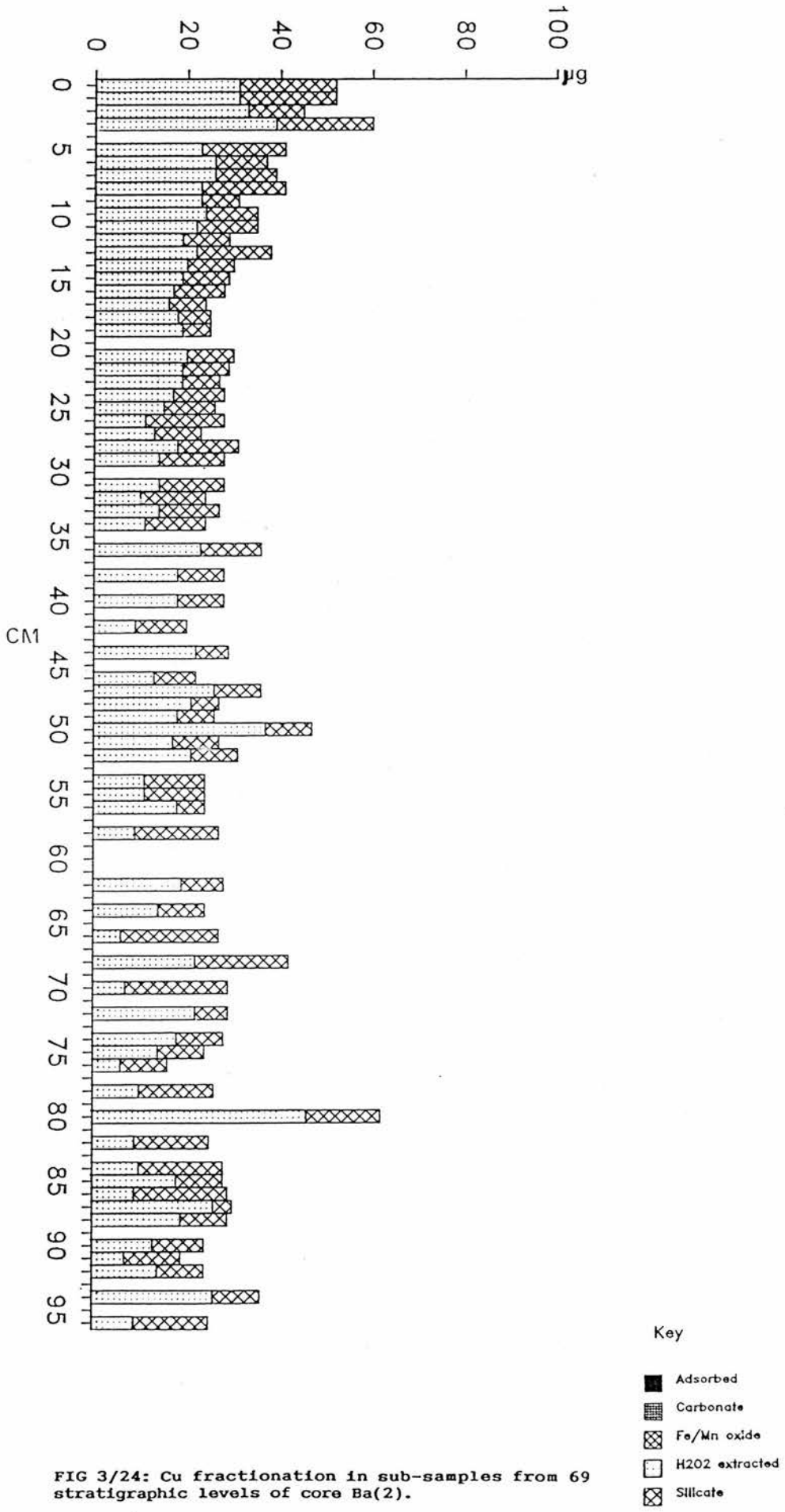

FIG 3/24: Cu fractionation in sub-samples from 69 stratigraphic levels of core Ba(2).

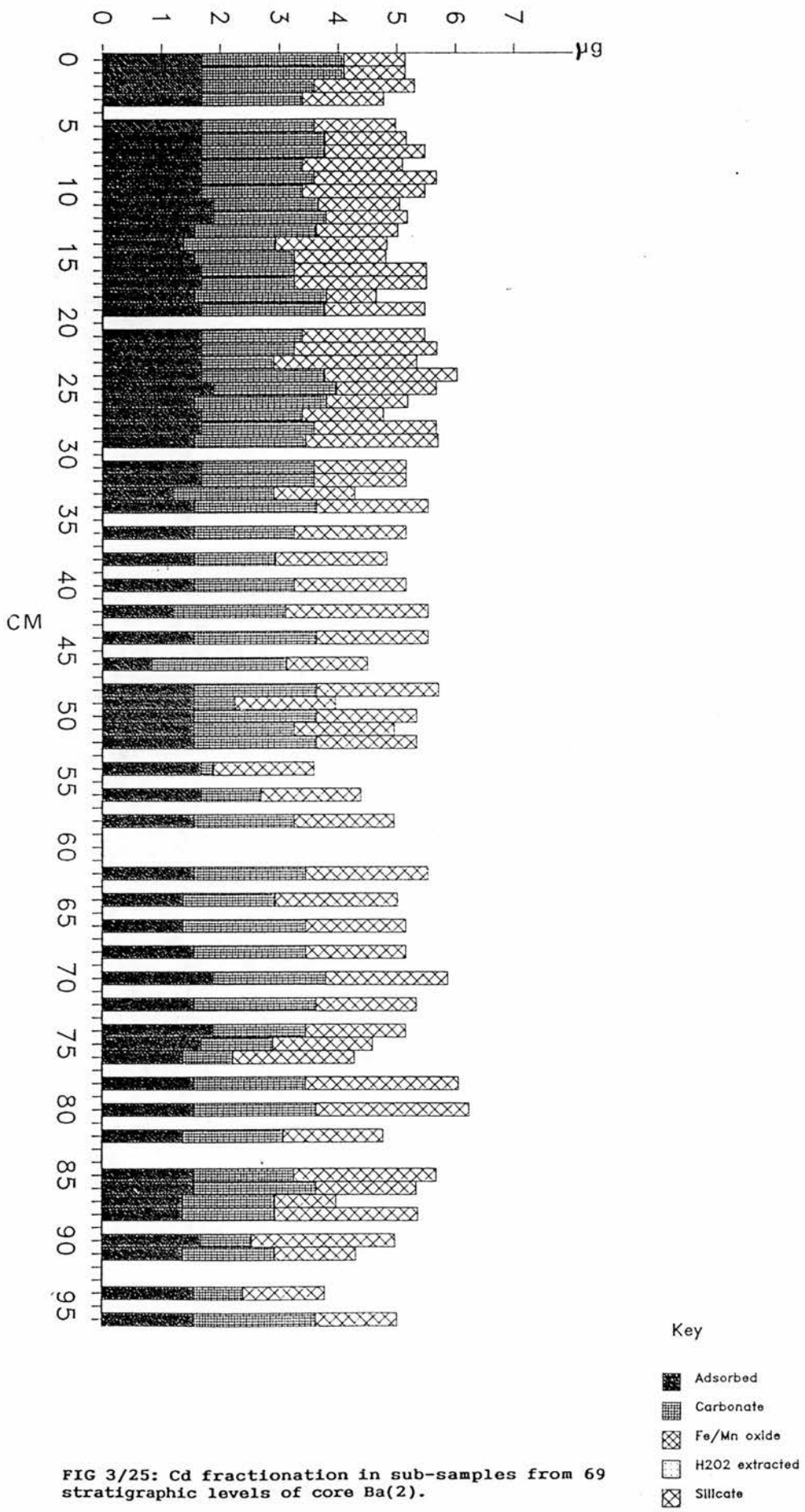

FIG 3/25: Cd fractionation in sub-samples from 69 stratigraphic levels of core Ba(2).

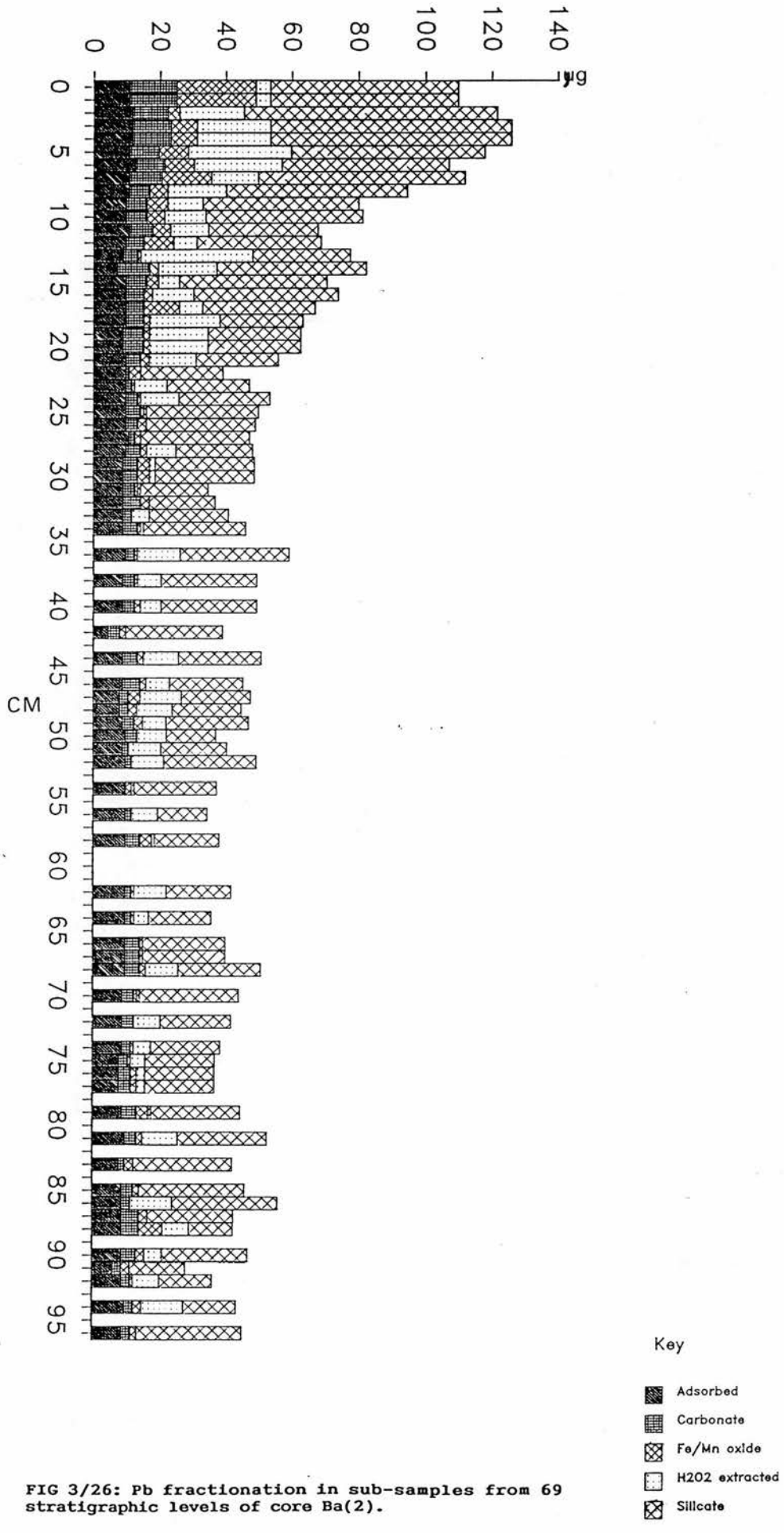

FIG 3/26: Pb fractionation in sub-samples from 69 stratigraphic levels of core Ba(2).

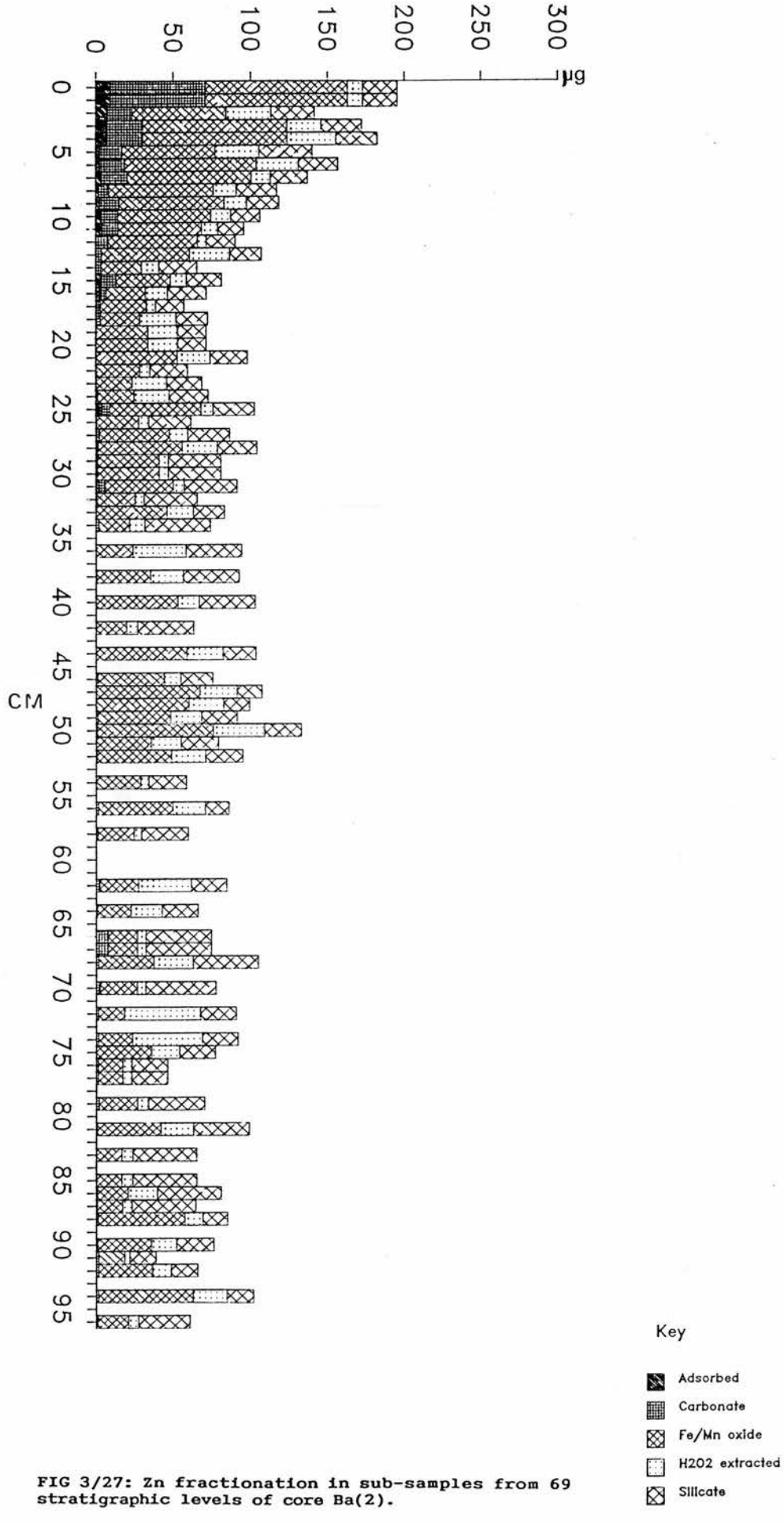

FIG 3/27: Zn fractionation in sub-samples from 69 stratigraphic levels of core Ba(2).

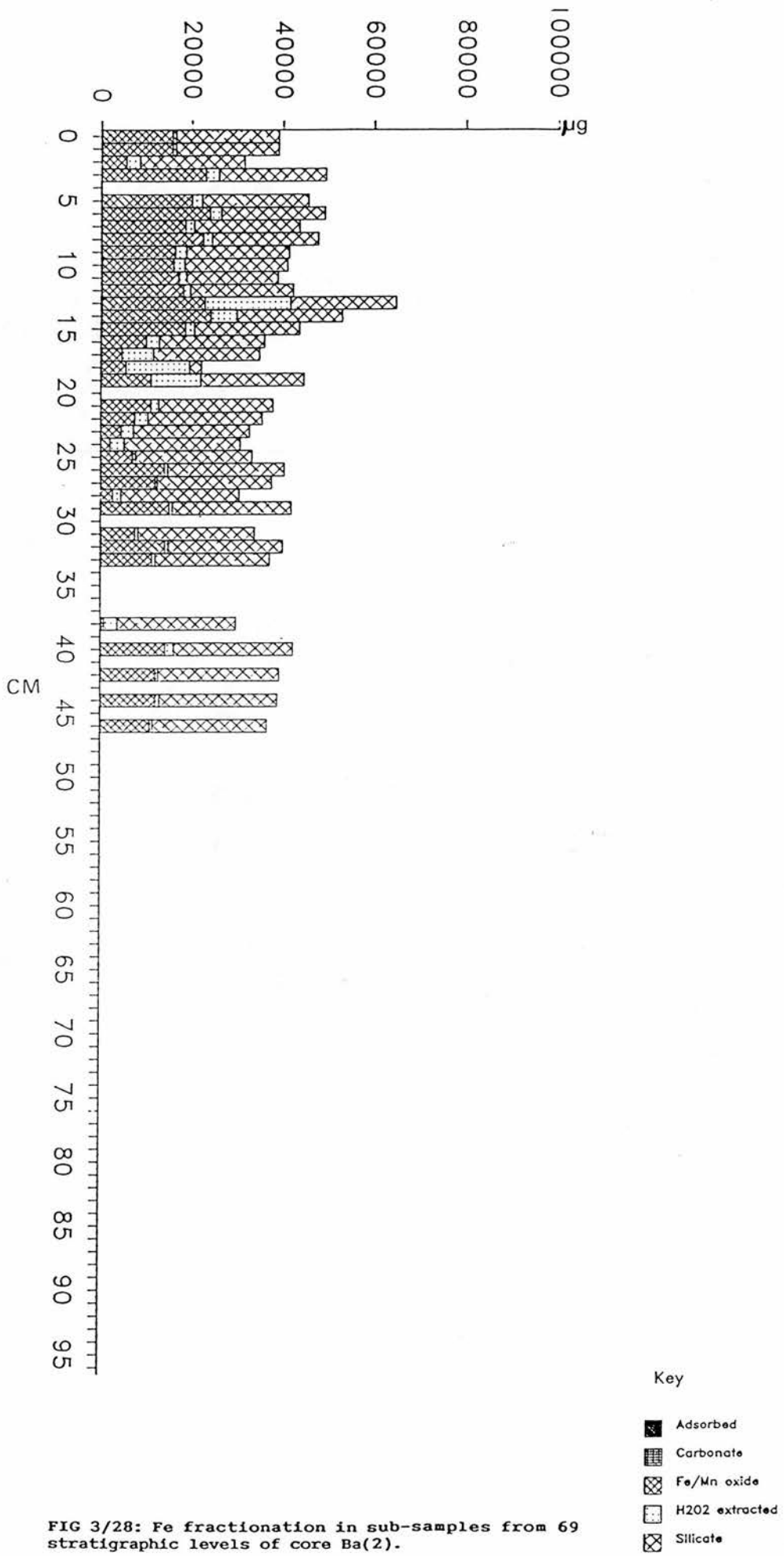

FIG 3/28: Fe fractionation in sub-samples from 69 stratigraphic levels of core Ba(2).

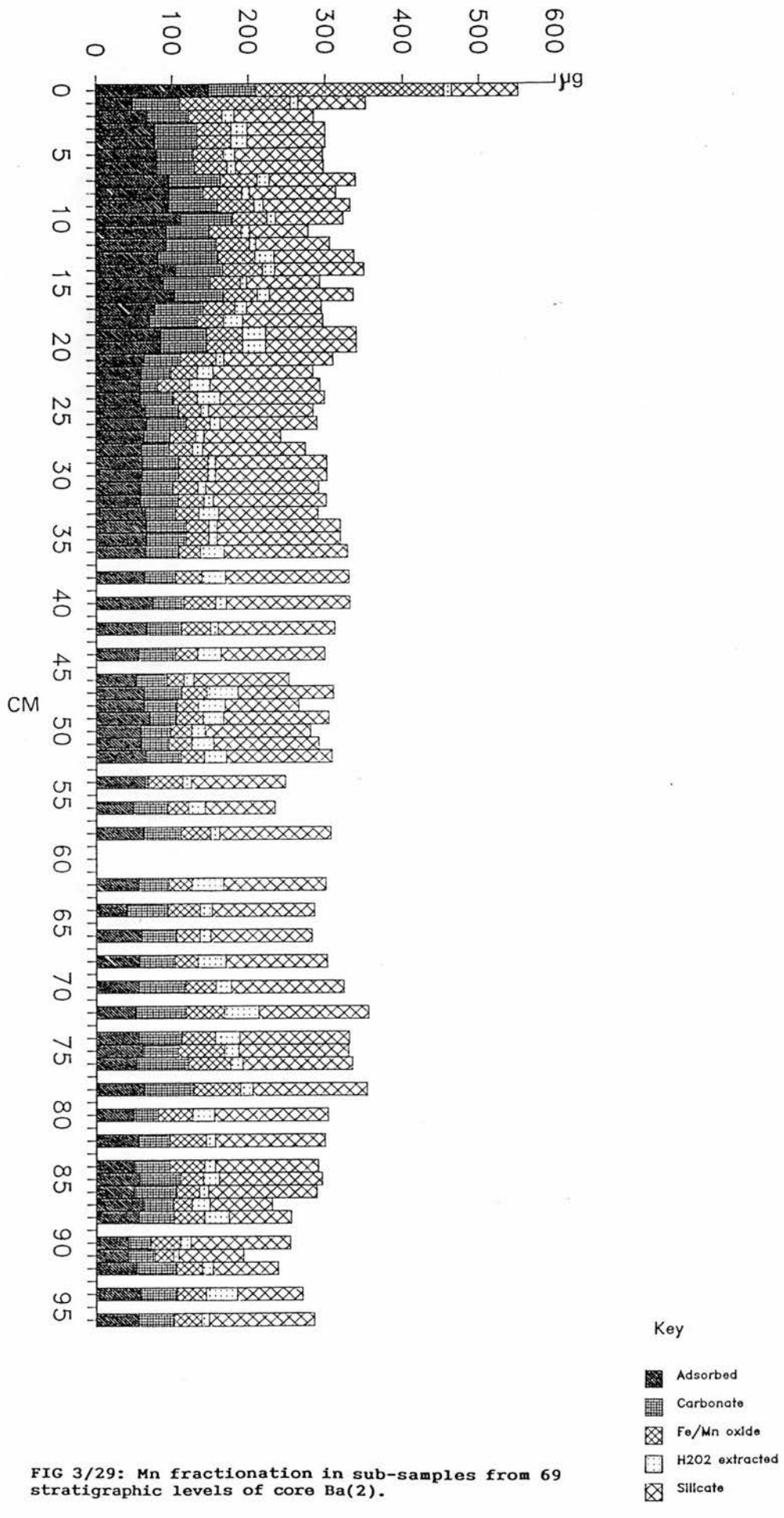

FIG 3/29: Mn fractionation in sub-samples from 69 stratigraphic levels of core Ba(2).

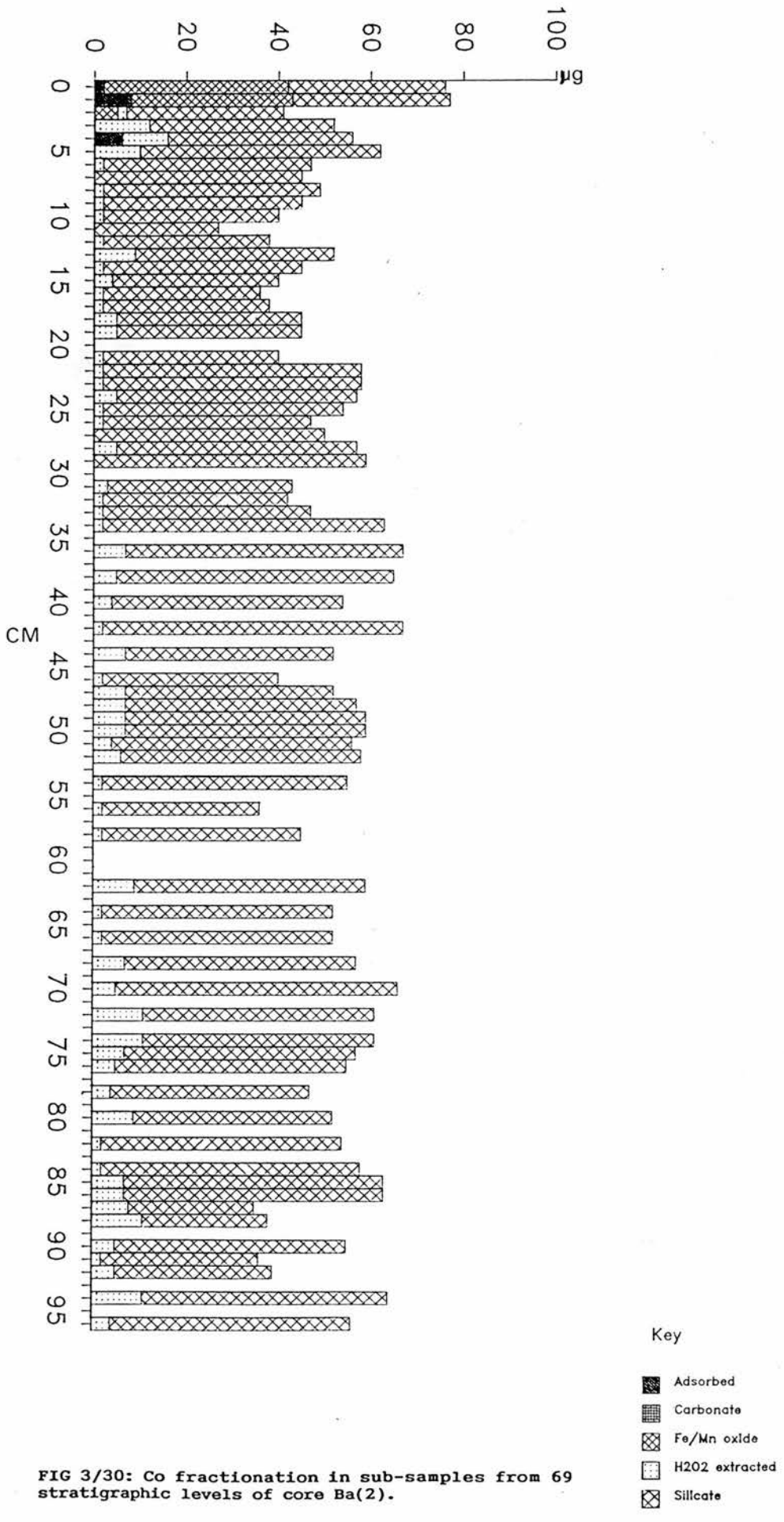

FIG 3/30: Co fractionation in sub-samples from 69 stratigraphic levels of core Ba(2).

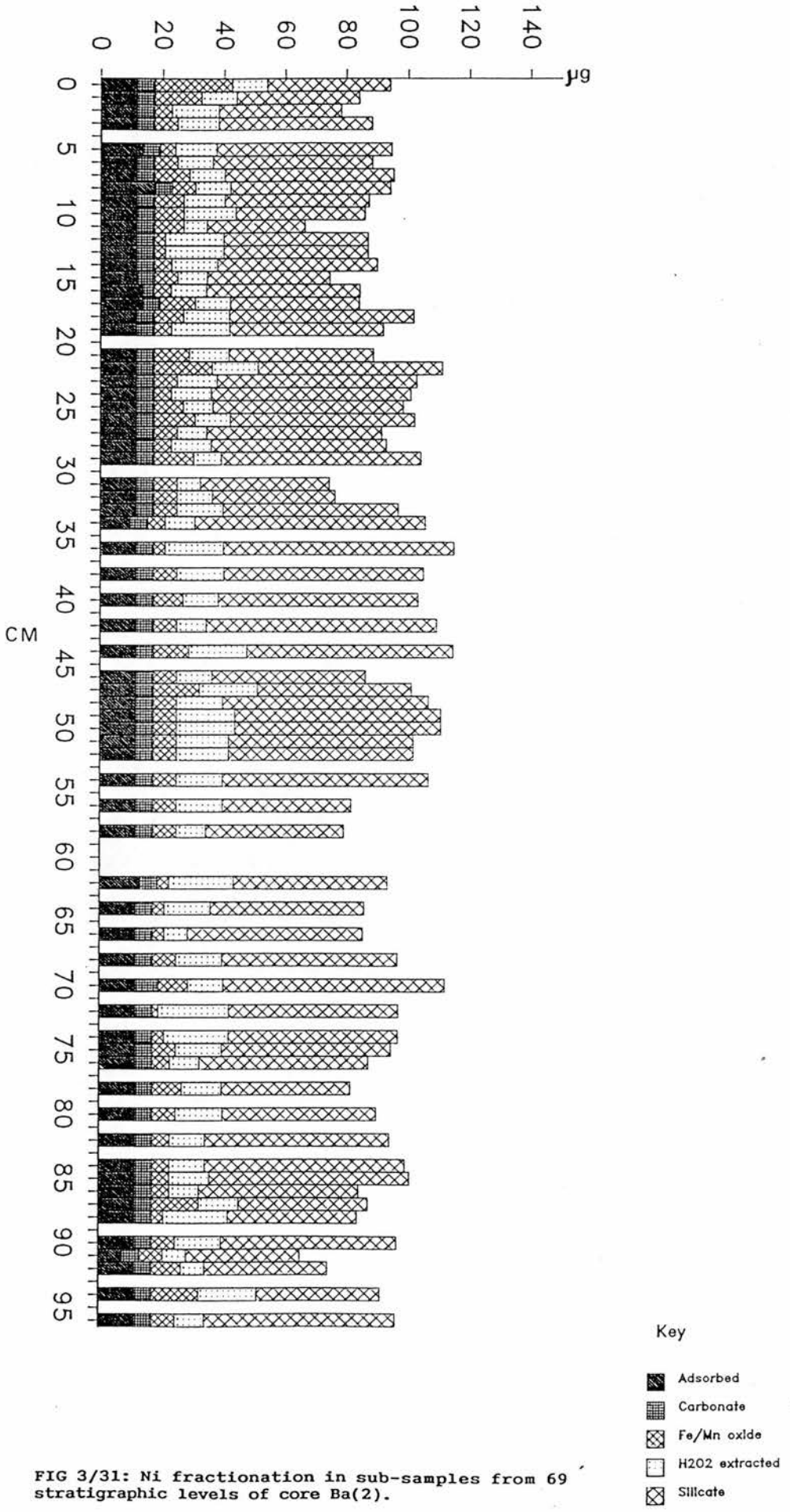

FIG 3/31: Ni fractionation in sub-samples from 69 stratigraphic levels of core Ba(2).

Cu (56% H2O2 extractable, 44% silicate), Fe (67% silicate), Pb (52% silicate) and Ni (57% silicate) is similar to that occurring in the non-enriched levels of the Loch Dee sediments (section 3.4.1). In the cases of Cd, Zn, Co and Mn, partitioning patterns are less analogous. Instead, Cd predominantly resides in hydrogenous, MgCl + NaOAc extractable phases, while Zn (45% H2O2 extractable + silicate), Co (91% silicate) and Mn (51% H2O2 extractable + silicate) are increasingly held in poorly reactive fractions.

With the exceptions of Cu and Cd (Figs 3/24 - 3/25) all elements exhibit geochemical alteration in the upper 2cm - 20cm of core Ba(2). Of the elements which are subject to progressive upward enrichment, initial increments to total Pb concentrations are associated with the dis-proportionate accumulation of H2O2 extractable (organic or NVS) phases from a mean of 7µg/g at 22cm - 95cm depth to a mean of 14.6µg/g in strata extending from 11cm - 21cm depth (Fig 3/26). In the uppermost 10cm, the proportion of total Pb held in the H2O2 extractable fraction declines once more, but NaOAc extractable (carbonate) and NH2.OH.HCl/HOAc extractable (AVS or reducible oxide) components become increasingly significant. The total concentration of Pb held in these phases is maximised at the sediment/water interface, where 49µg/g (44% total) Pb is extractable with MgCl, NaOAc and NH2.OH.HCl/HOAc. In the case of Zn, a

progressive increase of total concentrations from a mean of 67µg/g at 16cm - 95cm depth to a maximum of 197µg/g at 1cm depth occurs without any notable variation of H2O2 extractable or silicate-bound concentrations (Fig 3/27). Instead, the downcore Zn gradient is primarily controlled by hydrogenous phases. Zn carbonates increase in concentration from a mean of 0.1µg/g at 20cm - 95cm depth to a maximum of 61µg/g at 1cm depth. Accompanying upward enrichment of NH2.OH.HCl + HOAc extractable (AVS or reducible oxide) fractions is also apparent, to a maximum concentration of 92µg/g at the sediment/water interface.

Although Fe displays no consistent enrichment pattern in the uppermost 20cm of core Ba(2), fractionation adjustments in this zone are, in many respects, analogous to those described for Pb. A deviation from the 94% silicate + NH2.OH.HCl/HOAc extractable Fe partitioning pattern which characterises the 20cm - 47cm core sequence is initially identifiable at 17cm - 19cm depth, where H2O2 extractable (organic or NVS) fractions hold 12 - 63% of total Fe (Fig 3/28). However, upward of 12cm depth H2O2 extractible components appear to be replaced by NH2.OH.HCl + HOAc extractable (oxide or AVS) phases, leading to the production of mean AVS + oxide/silicate Fe ratios of 0.9, compared to mean ratios of 0.42 at 21cm - 47cm depth.

Variations in the partitioning of Mn, Co and Ni are confined to the uppermost 2cm of sediment. In the cases of

Mn and Co (Figs 3/29 - 3/30), enrichment to concentrations of 550µg/g and 78µg/g respectively at the sediment/water interface is attributable to the dis-proportionate accumulation of NH2.OH.HCl + HOAc extractable (oxide ar AVS) phases and, to a lesser extent, MgCl extractable (adsorbed) phases. Consequently, ratios of silicate/non-silicate-bound concentrations decline to only 0.19 for Mn and 0.94 for Co in the surficial 2cm, with values at 5cm - 90cm being at least a factor of 4 higher.

Alterations to the partitioning of Ni in the uppermost 2cm of sediment are less conspicuous than those described for Mn and Co and do not promote any enhancement of total concentrations. However, from Fig 3/31 it is apparent that NH2.OH.HCl + HOAc extractable Ni concentrations rise to a "whole core" maximum of 24µg/g at the sediment/water interface, constituting 23% of total Ni at this level. In contrast, the mean fraction of total Ni held within these AVS or reducible oxide phases in strata extending from 3cm - 97cm depth is only 7%.

3.5: Pore-water geochemistry.

3.5.1: Loch Dee sediments.

An insight into the pore-water geochemistry of the Loch Dee sediment reservoir is provided by Figs 3/32 - 3/33,

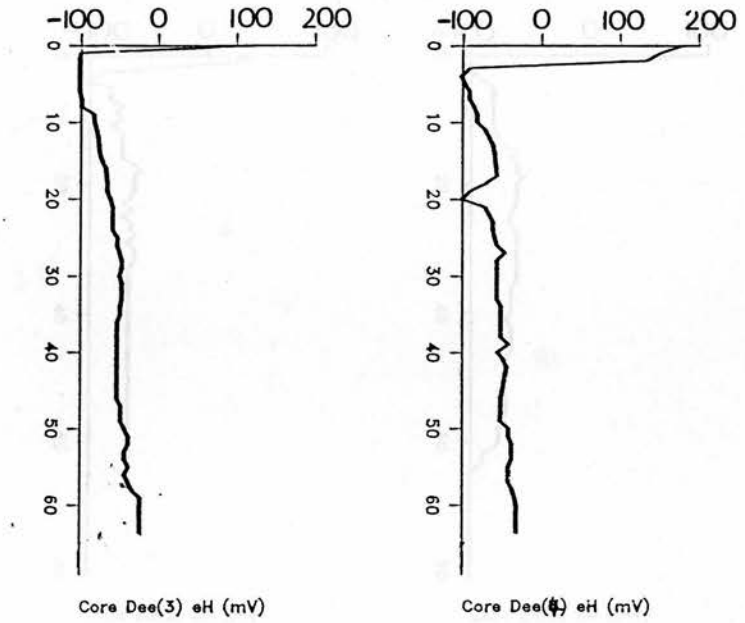

FIG 3/32: Redox gradients through the uppermost 65cm of cores Dee(3) and Dee(4).

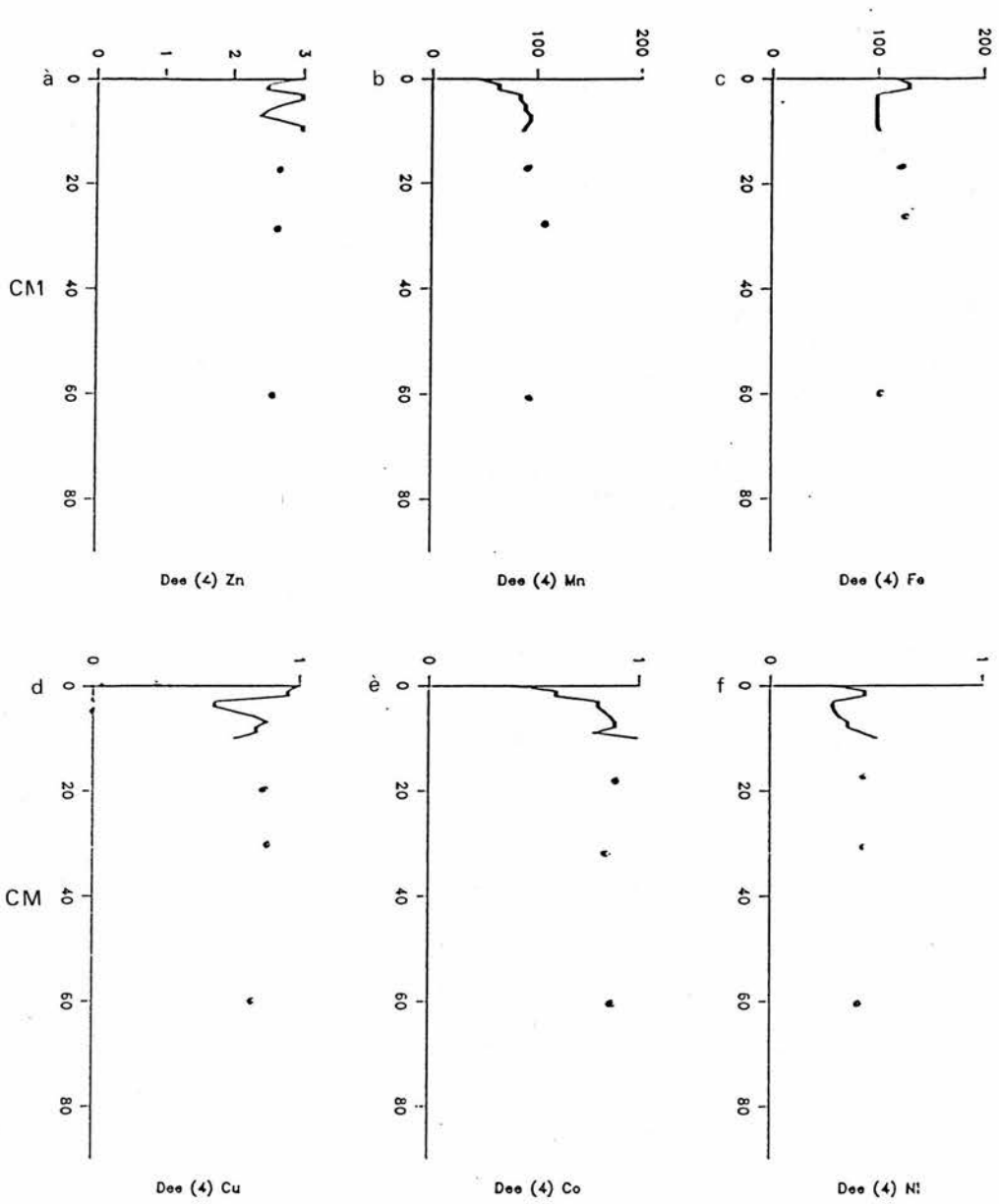

FIG 3/33: Pore-water concentrations of Zn, Mn, Fe, Cu, Co and Ni (µmol/l) at 1cm, 2cm, 3cm, 4cm, 5cm, 6cm, 7cm, 8cm, 9cm, 10cm, 11cm, 12cm, 18cm, 29cm and 60cm levels of core Dee(4).

illustrating the eH gradients through sediments at stations Dee(3) and Dee(4), along with the downcore variability of dissolved Zn, Mn, Fe, Cu, Co and Ni concentrations at station Dee(4).

On the basis of these data, the sediment column can be sub-divided into three stratigraphic sections. In the uppermost section comprising the surficial 1cm of core Dee(3) and sediments at 1cm - 3cm depth in core Dee(4), the prevalence of oxic conditions is coincident with the presence of dissolved Mn and Co concentrations which are at least a factor of 2 lower than those of all underlying strata (Figs 3/33b and e). The second section, extending from 3cm - 8cm depth in core Dee(3) and 4cm - 6cm depth in core Dee(4), is characterised by conditions of severe anoxia (eH -100mV). Pore-water Mn and Co concentrations increase progressively with depth throughout this sequence, but Cu and Ni appear to undergo depletion. In core Dee(4), "whole core" minima of 0.67µmol/l Cu and 0.26µmol/l Ni occur simultaneously at 4cm depth (Figs 3/33d and f). Dissolved Fe loadings also fall markedly downward of 3cm depth, but remain constant at around 98µmol/l to a depth of 9cm. The third stratigraphic sequence, comprising all strata of below 8cm depth, is characterised by the prevalence of less strongly anoxic conditions, with eH values increasing progressively to around -35mV at 65cm depth. Throughout these strata, the elemental constituency of the interstitial water shows limited variability, holding concentrations of

around 2.8µmol/l Zn, 100µmol/l Mn, 110µmol/l Fe, 0.85µmol/l Cu, 0.9µmol/l Co and 0.4µmol/l Ni.

In addition to the pore-water data presented in Fig 3/33, AAS analyses of 12 water samples have been used to ascertain the presence of mean concentrations of 0.08µmol/l Zn, 8.1µmol/l Fe, 1.2µmol/l Mn and 0.1µm/l Pb in the lake water column. Zn, Fe and Mn, therefore, display enrichment in the interstitial pore-waters of the sediment relative to concentrations in the lake water. In contrast, only the 1cm level of core Dee(4) holds detectable dissolved Pb concentrations (0.09µmol/l). Accordingly, Pb can be considered to be depleted throughout the pore-waters of the entire sediment column.

3.5.2: Loch Ba sediments.

Geochemical conditions in the pore-waters of the Loch Ba sediment reservoir are illustrated by Figs 3/34 - 3/36, showing the downcore eH gradients and dissolved concentrations of Zn, Cu, Ni, Mn, Fe and Co at stations Ba(2) and Ba(3). The redox profiles of the respective cores are essentially analogous, indicating the prevalence of oxic conditions (eH +30 - +90mV) in the uppermost 2cm of sediment and strongly reducing conditions at 3cm - 7cm depth (Fig 3/34).

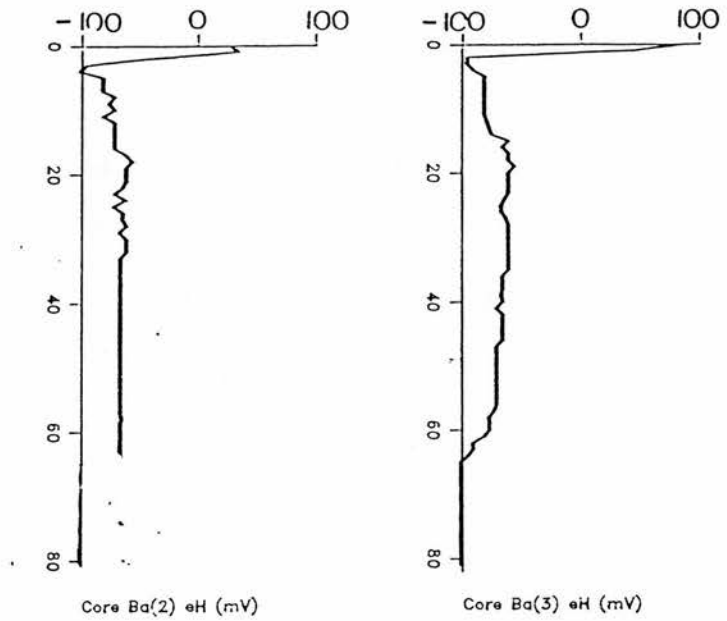

FIG 3/34: Redox gradients through the uppermost 63cm of core Ba(2) and throughout core Ba(3).

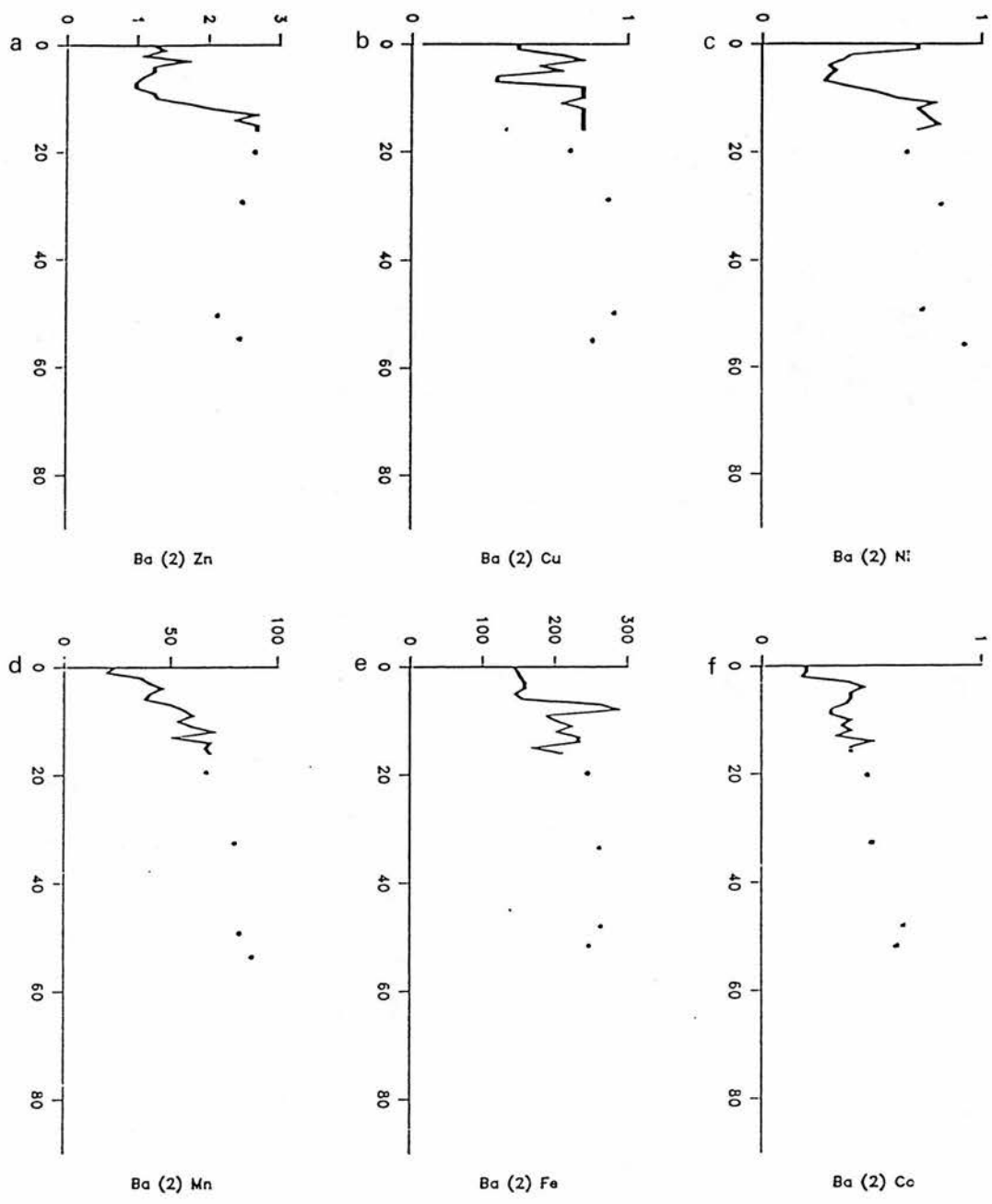

FIG 3/35: Pore-water concentrations of Zn, Cu, Ni, Mn, Fe and Co (μmol/l) at 1cm, 2cm, 3cm, 4cm, 5cm, 6cm, 7cm, 8cm, 9cm, 10cm, 11cm, 12cm, 13cm, 14cm, 15cm, 16cm, 17cm, 20cm, 32cm, 49cm and 54cm levels of core Ba(2).

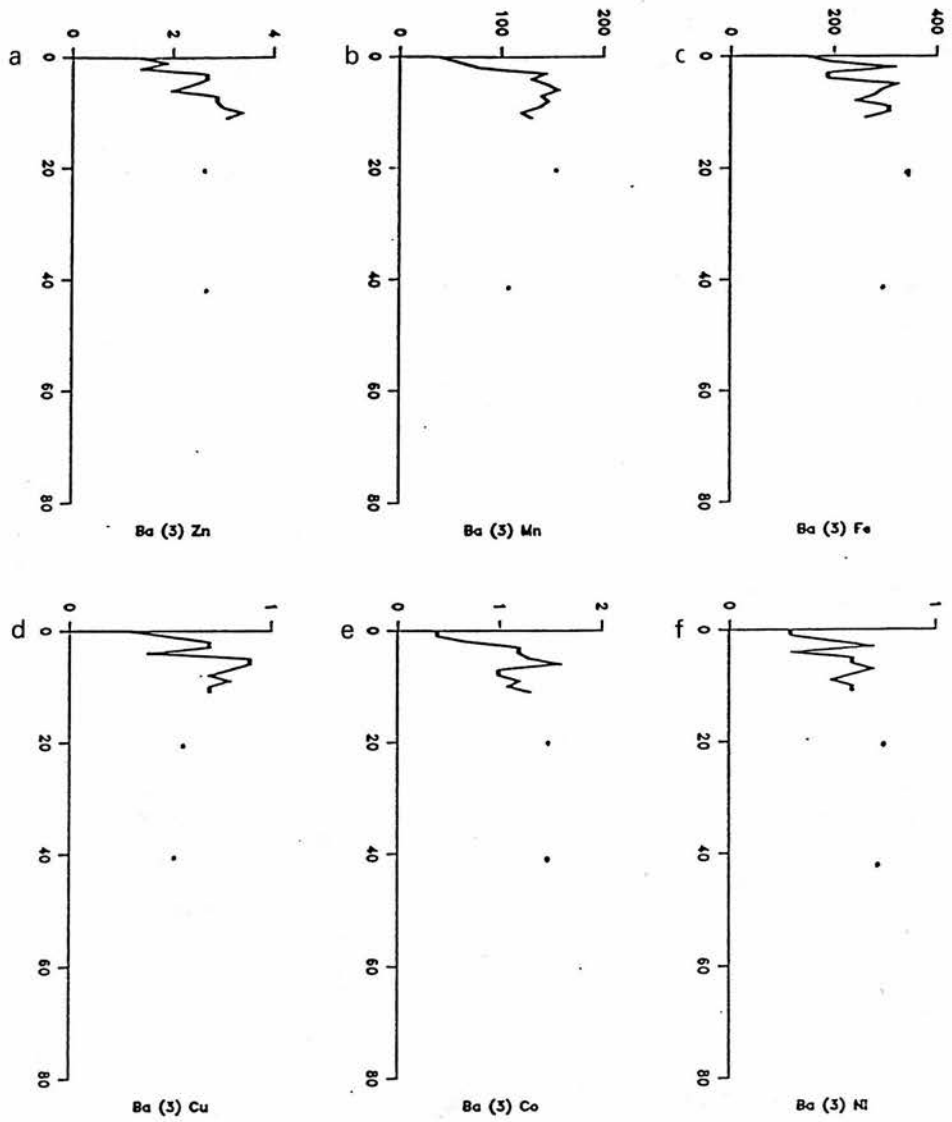

FIG 3/36: Pore-water concentrations of Zn, Mn, Fe, Cu, Co and Ni (µmol/l) at 1cm, 2cm, 3cm, 4cm, 5cm, 6cm, 7cm, 8cm, 9cm, 10cm, 11cm, 12cm, 13cm, 14cm, 20cm and 40cm levels of core Ba(3).

Notably, the relationship between eH and the elemental loading of the interstitial pore-waters varies markedly between cores Ba(2) and Ba(3). In the former, Zn, Cu, Ni and Fe attain concentration minima of 1μmol/l, 0.4μmol/l, 0.3μmol/l and 138μmol/l respectively in the strongly anoxic, 5cm - 7cm core levels (Fig 3/35). In the case of Ni (Fig 3/35c), dissolved concentrations rise progressively through the uppermost 5cm of sediment to 0.79μmol/l at the sediment/water interface. Pore-water Zn and Cu concentrations also increase at 5cm - 3cm depth, but fall once again to 1.2μmol/l and 0.51μmol/l respectively at the sediment surface (Figs 3/35a - b).

Major adjustments to the concentrations of Mn and Co occur independently of those of the other analysed elements in the Ba(2) pore-waters. In the case of Mn, progressive depletion is evident upward of 15cm depth, with concentrations falling from a mean of 74μmol/l at 16cm - 55cm depth to a minimum of 22μmol/l at 1cm - 2cm depth (Fig 3/35d). Co concentrations fluctuate between 0.4 - 0.7μmol/l at 5cm - 55cm depth, but fall sharply to 0.09μmol/l in the surficial 3cm (Fig 3/35f).

In core Ba(3), dissolved elemental concentrations undergo most marked alteration in the oxic, surficial 2cm of sediment, where Zn, Mn, Fe, Cu, Co and Ni attain concentration minima of 1.8μmol/l, 37μmol/l, 178μmol/l, 0.3μmol/l, 0.31μmol/l and 0.3μmol/l respectively (Fig 3/36). Downward of 5cm depth, the mean pore-water concentrations of

all analysed elements exceed those occurring at the sediment/water interface by factors of 2 - 3.4.

3.6: Radiometric data.

3.6.1: Loch Dee sediments.

Figs 3/37 and 3/38 illustrate the downcore gamma activity gradients of "unsupported" 210Pb (determined from 226Ra and total 210Pb gamma assays), 137Cs and 241Am in the sediment column at coring station Dee(3). The 210Pb profile, depicting a non-linear, non-exponential decline from peak activities of 31pCi/g at the sediment/water interface to 0pCi/g downward of 7cm depth, suggests that sediment influx rates are temporally inconsistent. In turn, the acute reduction of 210Pb activity from 31pCi/g to 23pCi/g through the surficial 1cm of sediment is indicative of the limited downward translocation of 210Pb by processes of bioturbation.

Through the placement of the 210Pb profile for core Dee(3) into the interpretive framework of the CRS model (see section 2.4.4), it is possible to ascertain that 7.5cm of sediment has been deposited since 146yrs BP (Table 17). Prior to 1960, these post-industrial sediments accumulated at rates which fell within the narrow range 0.031cm/yr-1 - 0.053cm/yr-1. After 1960, markedly more rapid rates of

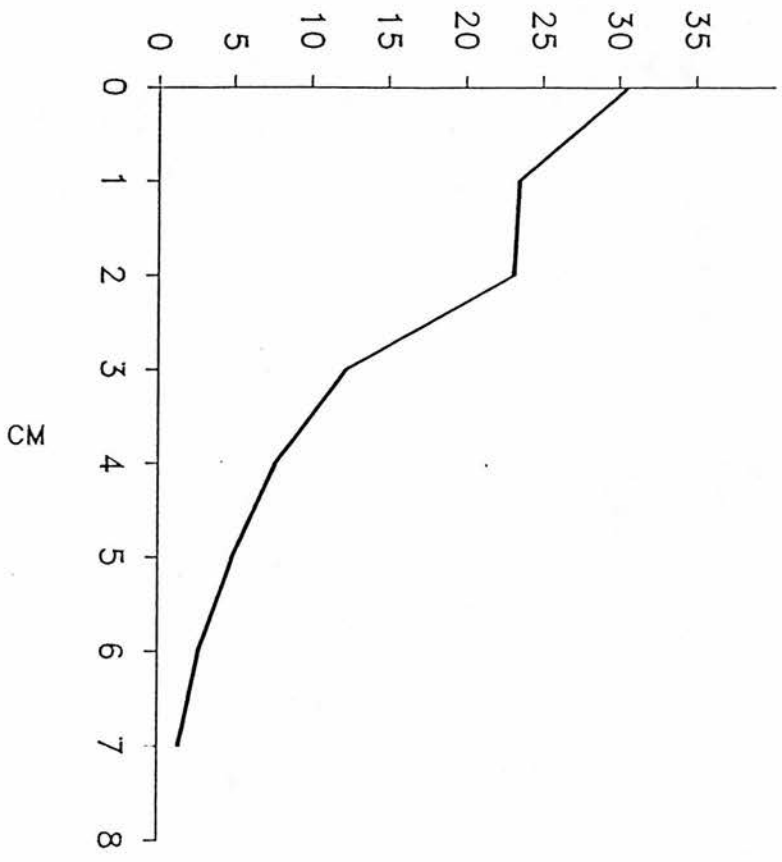

FIG 3/37: Unsupported 210Pb activity (pCi/g) through the surficial sector of core Dee(3).

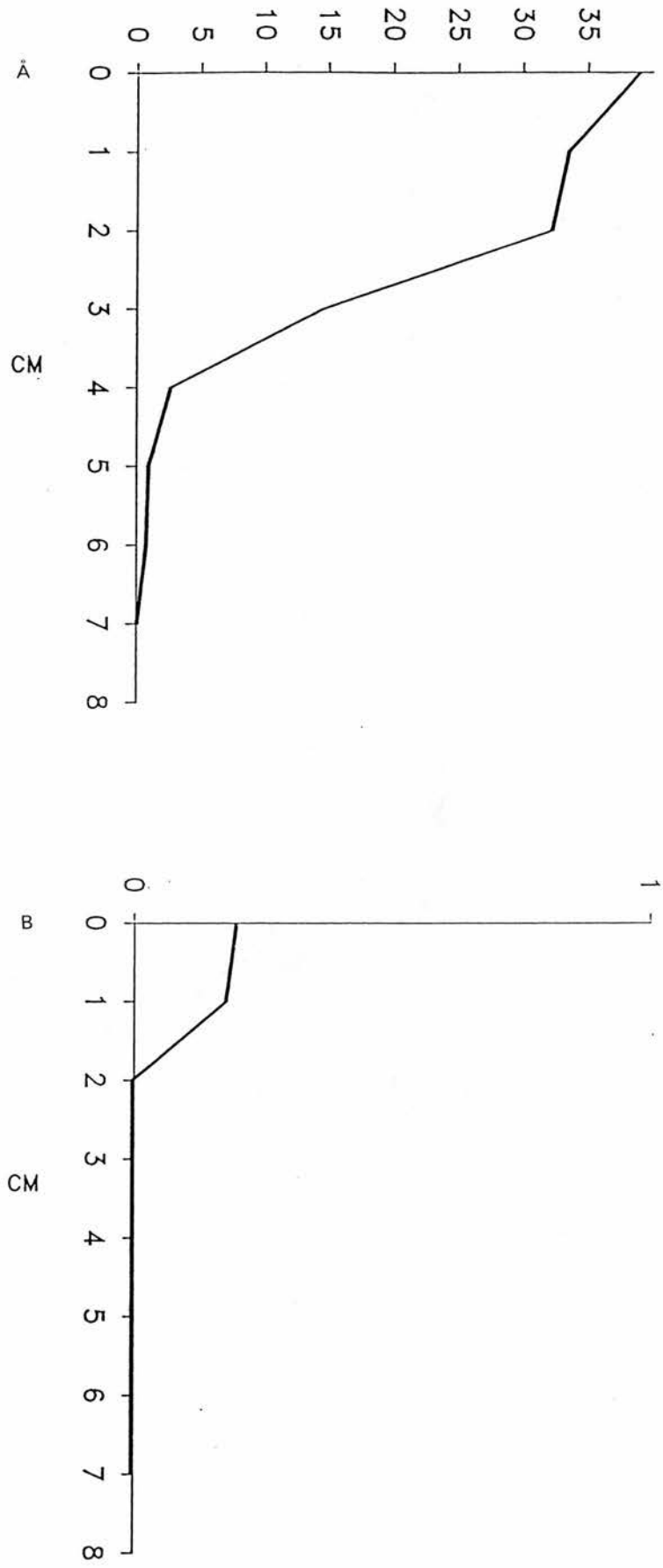

FIG 3/38: 137Cs (a) and 241Am (b) activities (pCi/g) through the surficial sector of core Dee(3)

Table 17: 210Pb derived sedimentation rates at coring station Dee(3) as determined by the CRS model.

Depth (cm)	Date	Age	Accum. rate (cm/yr)	%St.Error
0	1986	0		
0.5	1983	3	0.131	4.0
1.0	1979	7	0.116	4.5
1.5	1975	11	0.101	4.5
2.0	1967	19	0.077	4.8
2.5	1960	26	0.053	5.2
3.0	1950	36	0.052	5.3
3.5	1940	46	0.051	5.5
4.0	1930	56	0.049	6.6
4.5	1920	66	0.046	7.6
5.0	1908	78	0.043	9.7
5.5	1986	90	0.039	11.9
6.0	1883	103	0.037	16.4
6.5	1869	117	0.036	20.8
7.0	1855	131	0.033	22.8
7.5	1840	146	0.031	24.8

sedimentation prevailed, falling within the range 0.077cm/yr-1 - 0.131cm/yr-1. This adjustment is essentially synchronous with the initiation of the afforestation programme in the Loch Dee catchment and hence, can be considered to reflect the influence of pre-afforestation ploughing.

On examining the 137Cs activity gradient through the Dee(3) sediment column (Fig 3/38a), three features are inconsistent with documented 137Cs "fallout" records (eg. Krishnaswami and Lal 1978) and hence, detract from the nuclides utility as a geochronometer. Firstly, maximum 137Cs activities of 39pCi/g occur at the sediment/water interface,

while maximum "bomb fallout" rates prevailed in 1963. Although the assimilation of 137Cs by active organic matter at the sediment surface may contribute to the production of this anomaly, the influx of 137Cs deriving from the Chernobyl reactor emission in 1986 provides the most plausible explanation. This explanation is, in turn, consistent with the occurrence of maximum 241Am activities (0.1pCi/g) in the uppermost 1cm of sediment (Fig 3/38b). Secondly, 137Cs activities of 33pCi/g in sediments which accumulated between 1967 - 1979 (1cm - 2cm) exceed those prevailing within sediments which were deposited during the 1950 - 1967 period, when atmospheric 137Cs fluxes were factors of 2 - 5 greater. In accordance with the observations of Davis et al (1984), such trends are diagnostic of the diffusion of "Chernobyl-derived" 137Cs through the sediment column, prompted by pore-water acidity and the dearth of inorganic sorption sites in the uppermost 1cm of sediment. The diffusion of nuclides deposited following the Chernobyl emission is also indicated by the occurrence of measurable 241Am activities (0.09pCi/g) at 1cm - 2cm depth (Fig 3/38b). Finally, the diffusion of 137Cs into lower stratigraphic levels of core Dee(3) is signified by the occurrence of activities of 15pCi/g at 3cm - 4cm depth. Sediments at this depth have been assigned 210Pb origins of 36yrs - 56yrs BP and hence, precede the first major injections of 137Cs into the atmosphere.

3.6.2: Loch Ba sediments.

The downcore gamma activity gradients of "unsupported" 210Pb (derived from 226Ra and total 210Pb assays) and 137Cs through the uppermost 10cm of sediment at coring station Ba(3) are illustrated in Fig 3/39. The 210Pb profile, depicting a non-linear decline of activity from 28pCi/g at the sediment/water interface to 0pCi/g at 3cm - 4cm depth, is diagnostic of the prevalence of unusually low sedimentation rates, with the less acute gradient through the uppermost 1cm being attributable to sediment bioturbation. For purposes of geochronological calculations, the apparent recurrence of detectable "unsupported" 210Pb activities (1pCi) at 5cm - 6cm depth can be ignored, but probably reflects the downward diffusion of 222Rn from the overlying strata.

Quantitative sediment accumulation data, acquired through the integration of the 210Pb profile into the CRS model, suggest that only 3cm of sediment has been deposited since 146yrs BP (Table 18). For the 1840 - 1926 period, annual sediment influxes can reliably be calculated to be 0.016 - 0.020cm/yr-1. CRS-based determinations of sedimentation rates for the surficial 1cm are far higher (0.100 - 0.125cm/yr-1), but include an undefined error factor on account of the influence of bioturbation on the 210Pb gradient through this stratigraphic level.

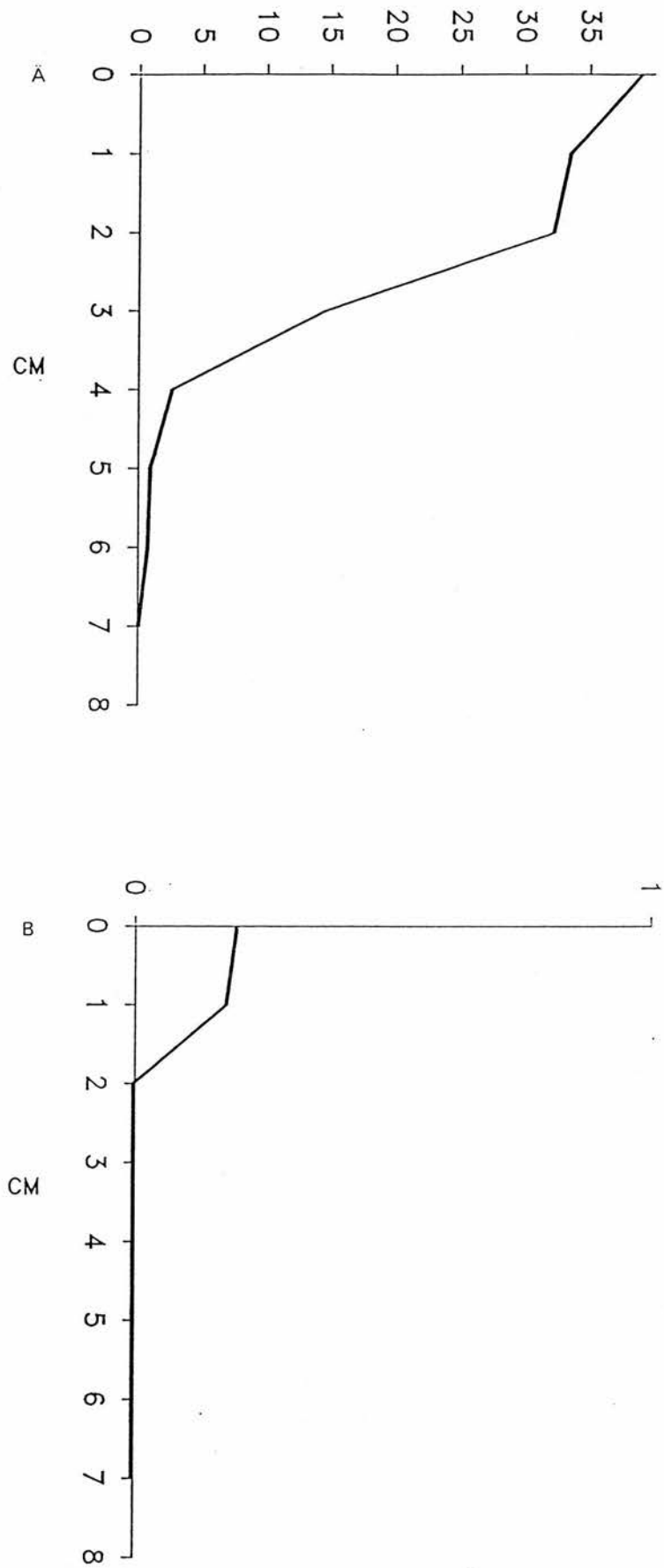

FIG 3/38: 137Cs (a) and 241Am (b) activities (pCi/g) through the surficial sector of core Dee(3)

Table 18: 210Pb based sedimentation rates at coring station Ba(3) as determined by the CRS model.

Depth (cm)	Date	Age	Acc. Rate (cm/yr)	%St.Error
0	1986	0		
0.5	1982	4	0.125	5.1
1.0	1976	10	0.085	5.2
1.5	1956	30	0.058	8.0
2.0	1926	50	0.020	11.0
2.5	1888	98	0.017	14.7
3.0	1840	146	0.016	21.0

The 137Cs data acquired for core Ba(3) provide no reliable geochronological information, with the occurrence of 12pCi/g activities in sediments which contain no unsupported 210Pb (6cm - 7cm) being diagnostic of extensive diffusion (Fig 3/39). However, both the 137Cs data presented and additional 134Cs assays for the uppermost 10 sub-samples from core Ba(3) are of value in confirming that the unusually low 210Pb-based sedimentation rate values are not a consequence of the loss of the surficial strata during core extraction. Specifically, maximum 137Cs activities of 82pCi/g at 0cm - 1cm depth in core Ba(3) are diagnostic of the presence of contaminants emitted from the Chernobyl reactor in 1986. In addition,134Cs from the same source is detectable in the uppermost 1cm of the core, where activites of 0.09pCi/g prevail. Consequently, the 0 - 1cm sub-sample must contain material which lay at the sediment/water interface at station Ba(3) in 1986.

3.7: Summary of geochemical data.

3.7.1: Loch Dee cores.

Bulk geochemical data for cores Dee(3) and Dee(4) indicate that major enrichment anomalies are confined to the uppermost 20cm of the sediment reservoir. Within this stratigraphic zone, Pb, Zn and Cu concentrations exhibit progressive upward enhancement, while Mn, Co and less consistently, Fe undergo 2 - 4 fold enricnment in the surficial 4cm. Ni and Mg concentrations are essentially unvariable throughout the entire sediment column.

A quantitative summary of elemental accumulation patterns is provided by the sedimentary enrichment factors presented in Tables 19 - 20. These tables express the elemental concentrations of sub-samples from the uppermost 23cm of core Dee(3) and the surficial 20cm of core Dee(4), normalized against the mean elemental abundances of 6 non-mineralized granite/norite samples from the Loch Doon and Cairnsmore plutonic complexes. The use of normalization factors derived from bedrock rather than from the deeply buried, non-enriched sectors of the respective cores (eg Oullet and Jones 1982) is intended to maximise the "between-core" comparability of SEF data. However, it is notable that the lowermost stratigraphic levels for which SEF data are

presented reflect the points at which elemental concentrations yield values of 0.9 - 1.1 when normalized against the mean abundances prevailing at 40cm - 80cm depth in each core.

Table 19: Core Dee (3) - Sedimentary enrichment factors for sub-samples from 1cm - 23cm depth. Normalization values derive from the mean elemental abundances in non-mineralized igneous bedrock (ppm).

	Pb	Zn	Cu	Cd	Fe	Mn	Co	Ni	Mg	Ca
Norm value	26	51	12	0.5	27K	900	3	4	4K	12K
1cm	8.0	9.4	8.3	26.4	2.4	5.9	13.5	23.7	.27	.02
2cm	10.9	11.0	6.4	24.2	2.0	3.6	8.7	20.0	.28	.07
3cm	8.0	11.0	6.1	28.6	2.2	3.6	11.6	21.9	.28	.02
4cm	6.9	11.4	6.7	26.4	2.0	3.6	8.7	20.0	.28	.02
5cm	8.4	8.8	5.8	24.2	2.2	3.6	14.5	23.7	.20	.05
6cm	5.1	9.2	5.5	22.0	1.8	2.7	7.7	18.2	.28	.01
7cm	5.1	7.9	4.9	24.2	2.2	5.0	15.4	21.9	.27	.03
8cm	6.9	6.1	5.2	19.8	2.0	4.0	8.7	20.0	.28	.08
9cm	6.9	6.1	5.8	19.8	2.2	5.0	10.6	21.9	.28	.08
10cm	6.2	5.3	4.9	17.6	2.2	5.0	10.6	21.9	.29	.07
11cm	6.5	4.6	4.6	17.6	2.2	4.0	12.5	21.9	.30	.04
12cm	4.9	4.8	4.3	17.6	2.2	3.6	10.6	21.9	.30	.03
13cm	6.9	4.6	4.3	26.4	2.2	3.6	11.7	25.5	.31	.03
14cm	5.1	4.3	4.3	26.4	2.2	3.6	11.7	23.7	.32	.03
15cm	4.3	4.1	4.6	15.4	2.0	3.6	9.6	21.9	.32	.03
16cm	5.4	4.3	4.3	26.4	2.0	3.1	11.7	25.5	.31	.03
17cm	5.4	4.3	4.0	26.4	2.0	3.6	11.7	23.7	.30	.04
18cm	5.4	4.1	3.7	24.2	1.8	3.6	11.7	21.9	.28	.04
19cm	4.3	3.8	3.3	24.2	1.8	3.6	11.7	21.9	.29	.05
20cm	4.3	4.1	4.6	15.4	1.8	3.6	10.6	21.9	.28	.03
21cm	5.1	3.5	3.3	24.2	2.2	4.0	9.6	20.0	.29	.05
22cm	4.3	3.0	3.3	24.2	2.0	4.0	9.6	21.9	.29	.05
23cm	4.9	2.8	3.3	24.2	2.0	3.6	10.6	21.9	.29	.06

Table 20: Core Dee (4) - Sedimentary enrichment factors for sub-samples from 1cm - 20cm depth. Normalization values derive from the mean elemental abundances in non-mineralized igneous bedrock (ppm).

	Pb	Zn	Cu	Cd	Fe	Mn	Co	Ni	Mg	Ca
Norm Val.	26	51	12	0.5	27K	900	3	4	4K	12K
1cm	7.2	11.8	9.1	15.6	5.0	8.6	23.4	29.9	1.7	.15
2cm	9.1	10.5	6.7	18.4	3.4	9.5	14.9	23.0	.25	.14
3cm	12.1	13.0	7.7	19.8	3.3	6.7	18.1	27.6	.27	.14
4cm	11.8	11.8	7.2	15.6	4.0	6.7	22.4	32.2	.27	.13
5cm	9.1	10.5	7.2	15.6	2.6	1.4	13.8	25.3	.30	.10
6cm	8.3	10.5	6.2	15.6	1.9	1.4	10.6	23.0	.25	.09
7cm	11.8	15.5	8.7	18.4	2.6	1.4	10.6	25.3	.25	.12
8cm	11.8	13.6	7.2	11.3	2.6	1.6	10.6	25.3	.24	.13
9cm	11.4	13.6	7.2	14.2	2.0	1.6	10.6	25.3	.27	.12
10cm	8.3	9.3	6.2	14.2	2.7	1.9	10.6	25.3	.24	.14
11cm	9.1	10.5	6.2	14.2	2.6	1.6	11.7	23.0	.25	.15
12cm	7.9	8.0	5.8	14.2	2.6	1.4	9.6	25.3	.33	.13
13cm	7.2	7.4	4.8	11.3	2.4	2.3	9.6	25.3	.32	.13
14cm	6.4	8.0	4.8	12.8	2.4	2.1	9.6	23.0	.32	.12
15cm	6.0	7.4	5.3	12.8	2.2	1.9	9.6	20.7	.31	.12
16cm	6.0	6.8	4.3	13.0	2.2	2.3	10.6	20.7	.31	.13
17cm	6.4	6.8	5.8	13.0	2.0	2.1	10.6	20.7	.31	.13
18cm	6.4	7.4	5.8	1.4	1.9	2.3	9.6	23.0	.30	.16
19cm	3.8	6.8	5.8	12.8	2.0	2.6	11.7	20.7	.20	.15
20cm	2.6	6.8	5.8	11.3	1.9	2.6	11.7	20.7	.30	.17

Excepting Mg and Ca, all analysed elements are characterised by enrichment (relative to bedrock) throughout the sediment reservoir, with "whole-core" SEF values following the pattern Ni > Cd > Co > Zn > Pb > Cu > Mn > Mg > Ca. At station Dee(3), downcore variability factors of sedimentary enrichment (reflecting the magnitude of elemental enrichment anomalies) follow the pattern Zn (3.8)

> Pb (2.5) > Cu (2.5) > Mn (1.9) > Cd (1.8) > Co (1.7) > Ni (1.3) > Mg (1.1). In core Dee(4), the pattern is Mn (6.7) > Pb (4.6) > Fe (2.6) > Co (2.5) > Zn (2.2) > Cu (1.9) > Cd (1.6) > Ni (1.6) > Mg (1.3 excluding the 1cm sub-sample).

Geochemical fractionation data for core Dee(4) show Cu, Cd, Fe, Ni, Pb, Mg and Co to be most closely associated with poorly reactive, organic/silicate complexes, while Zn, Ca and Mn are predominantly held in reducible fractions. However, the accumulation of hydrogenous phases appears to be responsible for the production of enrichment anomalies of all elements except Cu and to a lesser extent, Zn.

Pore-water and redox data show the enrichment of solid phases of Fe, Cu, Mn and Co near the sediment/water interface to be coincident with adjustments to the geochemistry of the interstitial waters. Cu is depleted from the pore-waters of the most anoxic, 4cm - 7cm levels of the sediment column and Mn and Co both undergo depletion at the oxic, sediment surface.

Unsupported 210Pb activities at station Dee(3) indicate that 7.5cm of sediment has accumulated since 146yrs BP. 137Cs distributions are of little geochronological value, being dominated by "Chernobyl" Cs which has been subject to considerable downward diffusion.

3.7.2: Loch Ba cores.

Bulk geochemical data for cores Ba(2) and Ba(3) highlight inconsistencies with respect to the downcore constituency of sediments in different sectors of the basin. At station Ba(2), elemental enrichment is confined to the uppermost 20cm of sediment. Pb, Zn and Cu show progressive upward accumulation throughout this zone, while Mn and Co concentrations increase by a factor of 2 at the sediment/water interface. Ni, K, Cd and Fe concentrations exhibit limited variability throughout the entire sediment column.

SEF data (derived from the normalization of the elemental concentrations in the uppermost 25 Ba(2) sub-samples against the mean elemental abundances in 4 non-mineralized samples of catchment granite) show all elements except Mn and K to be characterised by relative enrichment throughout the sediment reservoir (Table 21). Whole-core SEF values follow the pattern - Ni > Co > Cd > Pb > Zn > Cu > Mn > K. The downcore variability of SEFs (signifying the magnitude of elemental anomalies) is greatest for Pb (factor of 3.3), then Zn (3.1) > Cu (2.7) > Co (2.0) > Mn (1.7) > Fe (1.6) > Ni (1.5) > Cd (1.5) > K (1.4).

At station Ba (3), Pb, Zn, Cd, Cu, Mn and Co are all enriched in the uppermost 3cm of sediment and display acute downcore concentration gradients. Sm, Hf, Eu, Ce, La, Na, Sc

Table 21: Core Ba(2): Sedimentary enrichment factors for sub-samples from 1cm - 25cm depth. Normalization values are derived from the mean elemental abundances in non-mineralized bedrock samples (ppm).

	Pb	Zn	Cu	Cd	Fe	Mn	Co	Ni	K
Norm. Values	24	55	24	1	24K	740	5	2	
1cm	4.5	3.1	2.1	5.1	1.64	0.7	15.6	42.0	.01
2cm	4.5	3.1	2.1	5.1	1.64	0.6	15.4	42.0	.01
3cm	5.0	2.5	1.9	5.3	1.37	0.3	7.2	39.0	.01
4cm	5.2	3.1	2.5	4.7	2.08	0.4	8.0	44.0	.01
5cm	4.8	3.1	2.7	4.8	-	0.4	10.4	45.0	.01
6cm	4.8	2.3	1.7	4.9	1.87	0.4	9.0	47.0	.01
7cm	4.4	2.7	1.5	5.1	2.08	0.4	9.0	47.5	.01
8cm	4.6	2.4	1.6	5.4	1.70	0.4	9.0	47.7	.01
9cm	3.9	2.1	1.7	5.9	2.00	0.4	8.6	47.5	.01
10cm	3.3	2.1	1.3	5.6	1.70	0.4	8.6	43.5	.01
11cm	3.3	1.9	1.4	5.4	1.71	0.4	7.6	43.3	.01
12cm	2.7	1.6	1.4	4.9	1.61	0.4	5.4	33.5	.01
13cm	2.8	1.6	1.2	5.1	1.75	0.4	7.2	40.0	.01
14cm	3.2	1.9	1.6	5.0	2.75	0.4	8.6	43.1	.01
15cm	3.4	1.1	1.2	5.0	2.33	0.4	8.6	45.4	.01
16cm	2.9	1.4	1.2	4.8	1.75	0.4	7.2	37.5	.01
17cm	3.0	1.2	1.2	3.9	1.63	0.4	7.2	41.0	.01
18cm	2.7	1.0	1.0	5.5	1.60	0.4	7.2	41.0	.01
19cm	2.6	1.3	1.0	4.6	0.87	0.4	8.0	51.0	.01
20cm	2.6	1.2	1.0	5.4	1.75	0.4	8.0	46.0	.01
21cm	2.6	1.2	1.2	5.4	1.64	0.4	8.2	45.0	.01
22cm	2.3	1.7	1.2	5.4	1.60	0.4	7.8	44.0	.01
23cm	1.6	1.0	1.2	5.2	1.51	0.4	7.8	50.5	.01
24cm	1.9	1.2	1.1	5.3	1.57	0.4	11.2	51.5	.01
25cm	2.2	1.3	1.1	6.0	1.61	0.4	10.1	50.5	.01

and K accumulate at 60cm - 80cm depth in association with a secondary zone of Zn/Cu enrichment. Bedrock-normalized SEF data for selected samples from 1cm - 83cm depth show Pb, Zn, Cu, Cd, Fe, Ni, Co and Br to be characterised by relative enrichment throughout the sediment,while Mn, Mg,

Tables 22 - 23 Core Ba (3): Sedimentary enrichment factors for AAS and INAA determined elements in selected sub-samples from 1cm - 80cm depth. Normalization values derive from the mean elemental abundances in non-mineralised bedrock samples (ppm).

	Pb	Zn	Cu	Cd	Mn	Fe	Ni	Co	Mg
Norm values	24	55	24	1	740	24K	2	5	4000
1cm	6.3	8.1	2.3	7.0	0.9	2.0	20.0	40.0	0.2
2cm	6.1	3.0	1.6	5.5	0.5	1.7	80.0	13.7	0.1
3cm	3.7	2.0	1.1	7.0	0.6	2.0	23.0	6.0	0.3
4cm	1.8	1.4	1.5	3.5	0.2	1.7	55.0	10.0	0.7
13cm	1.9	0.8	1.3	4.5	0.3	1.7	60.0	10.0	0.5
22cm	3.2	0.8	1.1	4.5	0.3	1.7	60.0	12.5	0.4
27cm	1.2	2.4	1.5	5.0	0.4	2.0	50.0	16.2	0.8
36cm	1.5	1.0	1.3	4.0	0.5	2.1	60.0	12.5	2.3
44cm	2.3	2.0	1.2	6.5	0.4	2.1	85.0	25.0	0.1
48cm	2.0	2.1	1.7	4.0	0.5	2.1	70.0	13.5	0.5
52cm	2.4	3.0	2.1	5.5	0.6	2.1	85.0	17.4	0.2
60cm	1.9	5.0	2.7	6.0	0.5	2.1	85.0	16.2	0.7
65cm	2.4	3.9	2.8	4.5	0.4	2.1	90.0	19.2	0.7
73cm	1.5	1.9	3.7	4.5	0.4	1.7	70.0	11.2	0.6

	Sm	Ce	Eu	La	Br	Sc	Yb	Hf
Norm Values	11	65	2	50	0.4	4	5	7
2cm	0.19	0.001	0.84	0.06	25.0	0.22	0.001	0.001
10cm	0.19	0.001	0.91	0.04	27.5	0.22	0.001	0.22
20cm	0.16	0.001	0.001	0.04	25.0	0.001	0.001	0.10
30cm	0.20	0.001	0.85	0.04	14.3	0.001	0.001	0.001
40cm	0.30	0.001	1.07	0.06	12.0	0.001	0.001	0.15
50cm	0.30	0.001	1.07	0.06	12.0	0.001	0.001	0.15
60cm	0.92	0.03	3.0	0.21	20.0	0.44	0.26	0.32
70cm	0.88	0.04	2.69	0.21	8.26	0.74	0.001	0.30
80cm	0.55	0.001	1.66	0.14	4.75	0.54	0.001	0.20

Sm, Eu, La, Sc, Yb and Hf are depleted (Tables 22 - 23). For the enriched elements, whole-core SEFs follow the pattern Ni > Co > Cd > Zn > Pb > Fe > Cu. The downcore variability of SEFs for AAS-determined elements is greatest for Mg (factor of 23), then Zn (10.1) > Co (9) > Mn (4.5) > Ni (4.5) > Fe (4.5) > Pb (4.2) > Cu (3.3) > Cd (1.5).

Sequential chemical data for the Loch Ba sediments show Cu, Fe, Pb, Mn, Ni and Co to be most strongly associated with poorly reactive, organic/silicate complexes. In contrast, over 50% of Cd and Zn is typically held in reducible phases. Excepting Cu, elemental enrichment near the sediment/water interface is attributable to the disproportionate accumulation of specific geochemical fractions. These include H2O2 extractable and carbonate Pb, Zn carbonates, Mn oxides and Co oxides.

Geochemical conditions in the pore-waters of the Loch Ba sediments vary markedly between coring stations. In core Ba(2), maximum depletion of dissolved Zn, Fe, Cu and Ni occurs in association with the prevalence of severely reducing conditions at 5cm - 7cm depth, while Mn and Co undergo depletion at the sediment surface. At station Ba(3), greatest depletion of all elements from the interstitial waters is apparent at the oxic, sediment/water interface.

Unsupported 210Pb data for core Ba(3) indicate the occurrence of unusually low sedimentation rates, with only

3cm of material having been deposited since 146yrs BP. 137Cs diffusion is apparent from the detection of 661KeV gamma activity in strata which hold no unsupported 210Pb. Consequently, 137Cs profiles are of little geochronological utility in the Loch Ba basin.

3.8: Interpretation of geochemical data.

3.8.1: Loch Dee sediments.

a) Lithospheric controls.

In section 3.1 it was proposed that any conspicuous geochemical anomalies in sample cores should be examined by reference to the potential influence of lithospheric, diagenetic and anthropogenic processes. However, with respect to the enrichment of Pb, Zn and Cu upward of 20cm depth and the accumulation of Mn, Co and Fe at the surface of the Loch Dee sediment reservoir, the insignificance of lithospheric influences can easily be established. Three sources of evidence may be invoked. Firstly, upward enhancement of these elements occurs without any concomitant variation in the total concentrations of Mg, Ca and Ni, which are known to be derived predominantly from lithospheric origins (Ochsenbein et al 1983, Mackereth 1965, Lantzy 1979, Bertine and Goldberg 1971). Downward of 4cm, all other analysed lithophilic elements (Fe, Mn and Co) also display profiles which are characteristic of lithological

homogeneity.

In turn, the ratios of the silicate-bound fractions of elements which exhibit greatest sedimentary enrichment relative to bedrock (and hence should be most sensitive to lithogeochemical change) display considerable downcore consistency. As an illustration of this; ratios of silicate Ni/silicate Co remain within the narrow range 3.7 - 5.1, thus signifying the prevalence of a temporally stable lithogeochemical flux.

Secondary confirmation that surficial Pb, Zn, Cu, Co, Mn and Fe anomalies have developed independently of lithospheric influences can be obtained by examining the geochemical fractionation patterns prevailing throughout the upper core sectors. These elements accumulate in association with either the dis-proportionate enrichment of non-detrital phases (eg. $NH_2OH.HCl/HOAc + H_2O_2$ extractable Pb, adsorbed/oxide Mn and Co, organic/oxide Fe) or with only limited deviation from the elemental partitioning patterns occurring in non-enriched strata (Cu and Zn). In all cases, the ratios of detrital (silicate)/hydrogenous concentrations decline towards the sediment surface (Table 24). In instances where trace element enrichment in sediments is lithospherically controlled, a reversal of such trends would occur (Henshaw 1978). Accordingly, alternative mechanisms can confidently be assumed to be responsible.

Table 24: Ratios of detrital/non-silicate Pb, Zn, Cu, Co, Mn and Fe in non-enriched and enriched strata at coring station Dee(4).

	Sample level	Ratio	Sample level	Ratio
Pb	30cm	1.01	3cm	0.41
Zn	30cm	0.15	7cm	0.12
Cu	30cm	1.20	1cm	0.95
Co	30cm	0.66	1cm	0.35
Mn	30cm	0.07	2cm	0.03
Fe	30cm	2.81	1cm	1.30

Finally, the possibility that the organic content of sediments exerts some control upon the accumulation patterns of Pb, Zn, Cu, Fe, Co and Mn (as observed by Price 1977, Rosental et al 1986, Baturin 1967, Nriagu et al 1979) appears to be precluded by the poor consistency of relationships between these elements and LOI. In core Dee(3) LOI values decrease from 53% at 25cm depth to 31% at 18cm depth, indicating that the onset of Pb, Zn and Cu enrichment is, in fact, coincident with an increase in the minerogenic fraction (Fig 3/40a). LOI values also remain relatively stable upward of 17cm depth and hence, do not correlate significantly with elemental variations. In core Dee(4) major adjustments to LOI occur at 58cm - 65cm depth, where values fall from 52% to 36%. Values also increase abruptly at between 32cm and 28cm depth, but fluctuate at around 41% upward of this level (Fig 40b). Neither of these changes are associated with the alteration of elemental profiles, thus suggesting that the minerogenic/organic

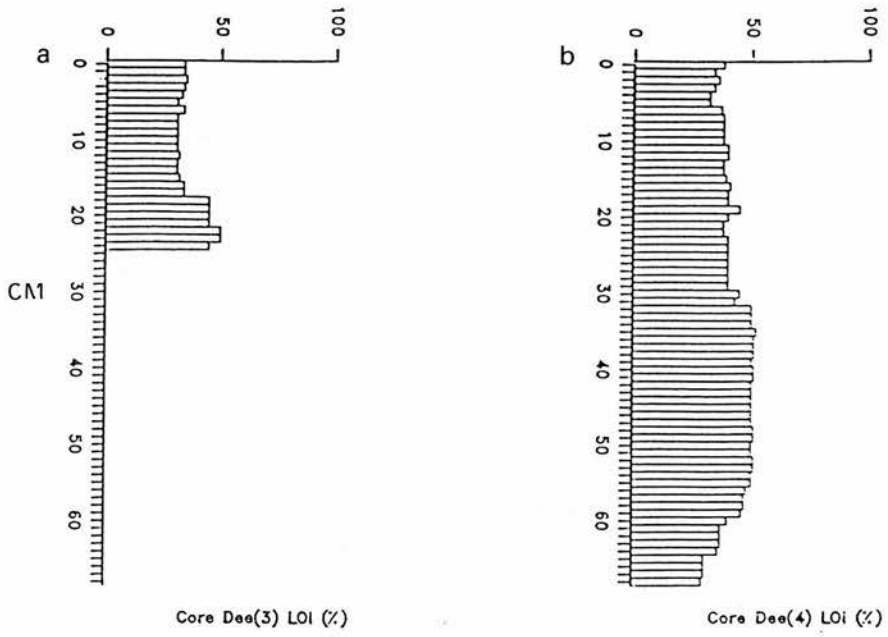

FIG 3/40: Loss on ignition profiles through the uppermost 25cm of core Dee(3) and throughout core Dee(4).

composition of the sediment is of little geochemical significance.

b) Diagenetic controls.

In section 2.2.4 it was noted that the formation of authigenic mineral phases of Fe, Mn, Co, Ni and Cu (amorphous FeS, mackinavite, siderite, rhodochrosite, covellite, millerite) has frequently been invoked to explain geochemical anomalies in sediments. In the Loch Dee basin, pore-water chemistry and geochemical fractionation patterns suggest that such processes constitute the principal cause of Mn and Co enrichment (by factors of 1.5 - 4.5) at the sediment/water interface, but cannot account for the accumulation patterns of Fe, Cu, Pb or Zn.

With respect to Mn, the two-fold depletion of pore-water concentrations in the uppermost 4cm of core Dee(4) is coincident with the occurrence of 5500 - 7600μg/g Mn in adsorbed and reducible oxide phases. Such inverse aqueous/solid phase gradients are attributable to the operation of well documented Mn4+ precipitation processes across the anoxic/oxic threshold (Llyn and Bonatti 1965, Presley et al 1972, Calvert 1977, Broecker 1974, Carignan and Nriagu 1985, Mortimer 1971, Farmer and Lovell 1986, Pedersen et al 1986). Sediments at station Dee(4) display analogous Co depletion in the pore-waters of the oxic, surficial 4cm of sediment, with concentrations of reducible

Co oxides increasing by factors of 5 - 10 at this level. The co-precipitation of Co with Mn has been widely observed in recent sediments (Henshaw 1978, Broecker 1974) and accordingly, enrichment upward of 7cm in core Dee(3) and in the uppermost 4cm of core Dee(4) can be attributed to Co^{2+} - Co^{3+} redox cycling.

The reduction of pore-water Fe concentrations at the sediment/water interface at station Dee(4) is diagnostic of the precipitation of dissolved Fe^{2+} as insoluble Fe^{3+} oxides on account of the oxic conditions prevailing. These reducible oxides are, in turn, conspicuous by the occurrence of concentrations of 22000µg/g Fe in $NH_2.OH.HCl$ extractable fractions at 1cm depth. However, the precipitation of labile phases does not fully account for the enrichment of Fe to concentrations of 137000µg/g in the uppermost 4cm of sediment, as it has previously been noted that H_2O_2 extractable fractions show the most marked increments in these strata (see section 3.4.1). Authigenic NVS fractions are also unlikely be responsible, given the oxic conditions and the co-existence of thermodynamically stable Fe^{3+}, Mn^{4+} and Co^{3+} oxides. Instead, in-situ processes of Fe complexation by active organic matter of the nature observed by Andersson (1985) can be considered to exert a more significant influence on surficial Fe retention than inorganic precipitation processes.

Processes of Cu, Ni and Zn diagenesis primarily involve the precipitation of the authigenic sulphides, covellite (CuS), millerite (NiS) and sphalerite (ZnS) in the most severely reducing, 4cm - 7cm levels of the Loch Dee sediments. Such processes are conspicuous by the localized depletion of Cu, Ni and Zn from the pore-waters of core Dee(4) and, on the basis of evidence provided by Carignan and Nriagu (1985), probably result from both eH and pH adjustments downward of 4cm depth. Pore-water pH values are likely to be elevated at this level as a consequence of the reduction of dissolved SO4. Hence, the equilibrated dissolved loading of Ni, Cu and Zn will be depressed. However, it must be emphasised that the effects of Cu/Ni sulphide precipitation are not conspicuous in either the bulk elemental or the geochemical fractionation profiles obtained through analyses of Loch Dee sediment cores. Instead, downcore variations in the concentrations of Cu and Ni occur without any deviation from their predominantly "poorly reactive" (H2O2 extractable + silicate) geochemical partitioning. In the case of Zn, minimum pore-water concentrations of 2.4µmol/l at 7cm depth in core Dee(4) do coincide with the occurrence of maximum solid phase concentrations in which the H2O2 extractable (NVS) component is dis-proportionately large. Yet NH2.OH.HCl + HOAc extractable fractions still dominate the overall Zn concentration gradient. Consequently, sulphide authigenesis cannot be invoked to explain the progressive upward enrichment of either Cu or Zn through the surficial 20cm of

sediment.

The increasing dissolved Cu and Ni concentrations prevailing upward of 4cm depth suggest that their well documented accumulation through redox-cycling with Mn at the oxic sediment surface (Ochsenbein et al 1983, Pedersen et al 1986, Cornwell 1986) is inhibited in the Loch Dee basin. Instead, labile phases appear to be free to diffuse downward of the sediment surface to the stratigraphic locus of sulphide precipitation. Explanation of such trends may be derived from the observations of Carignan and Nriagu (1985) who found the solubility potentials of Cu and Ni to be enhanced in the uppermost levels of lake sediments with inherently acidic (< pH 5.0) surface waters.

The presence of dissolved Pb at concentrations which fall below analytical detection limits downward of 1cm depth in core Dee(4) suggests that Pb enrichment does not occur through aqueous/solid phase transformations in the buried sediment. Furthermore, the enhancement of dissolved Pb concentrations upward of 1cm depth in the sediment and in the lake water, is diagnostic of the net loss of Pb across the sediment/water interface. The solubility of Pb increases markedly at below pH 5.0 (Andersson 1985, Krouskopf 1979). Hence, the acidity of the Loch Dee surface waters provides a likely explanation for this loss. A downcore increase of pH (resulting from SO4 reduction) could, in turn, account for the immobilization of Pb downward of 1cm depth.

c) Anthropogenic controls.

Given the minor importance of lithogeochemical and diagenetic processes with respect to the upward accumulation of the "atmophile" elements, Pb, Zn and Cu, atmospheric deposition is likely to be the predominant influence. The applicability of this hypothesis can best be qualified by examining the chronology of Pb, Zn and Cu enrichment patterns and their relationship with technological growth. The age of strata showing the first signs of enhancement and the shape of the accumulation curves through the overlying strata warrant particular scrutiny.

In core Dee(3), the locus of initial Pb, Zn and Cu enrichment (16cm - 18cm) can be dated to around 1600AD, assuming that sediments at 8cm - 18cm depth accumulated at a constant rate of 0.03cm/yr (ie. at the same rate as the oldest 210Pb-dated strata at this coring station). With respect to the dating of geochemical changes in core Dee(4), the analogy between the downcore mineral magnetic record and that prevailing at station Dee(3) indicates a comparability of sedimentation rates at the respective stations (see chapter 4). Through the extrapolation of the 210Pb - based chronology from core Dee(3), origins in excess of 350yrs BP can, therefore, be assigned to strata showing initial Pb, Zn and Cu enhancement in core Dee(4).

On referring to preceding studies of sediments which show

evidence of Pb, Zn and Cu enhancement as a consequence of atmospheric deposition, the "take-off" date of 1600AD at Loch Dee seems unusually early. The base of Pb anomalies have more frequently been dated to between 1830 and 1930 in the sediments of basins in New England (Davis et al 1983), the Great Lakes, USA (Goldberg et al 1981), Canada (Oullet and Jones 1982, Dillon and Evans 1982, Wong et al 1984), Norway (Skei and Paus 1979) and Britain (Hamilton-Taylor 1979, Rippey 1982, Ochsenbein et al 1983). Increased Cu pollution levels generally accompany Pb in the above instances, with enhanced Zn fluxes usually occurring after 1890. In Lake Gardsjon, Sweden and Lake Laflamme, Quebec, signs of atmospheric Pb, Zn and Cu deposition are only evident in sediments which have accumulated since 1940 on account of the remoteness of these catchments from localized pollutant sources (Andersson 1985, Oullet and Jones 1982). These increments to the pollutant loading of post-war strata probably result from the construction of "tall-stack" thermal combustion plant (Oullet and Jones 1982) which serve to increase the dispersal of hydrocarbon-derived emissions.

However, the apparent deviation of the Pb, Zn and Cu deposition chronologies in cores Dee(3) and Dee(4) from those of most other sediments need not cast doubt upon the validity of the former. Evidence derived from peats (Livett et al 1979), ice accumulations (Murozumi et al 1969) and Norwegian lake sediments (Davis et al 1983) suggests that atmospheric Pb concentrations did increase

significantly during the 1550 - 1750 period. Furthermore, this early increase would have been likely in S.W Scotland on account of the initiation of Pb extraction/smelting activities after 1650 (Drakeford 1979). The apparent confinement of atmophilic element enrichment to the post-1800 levels of the Galloway sediment cores studied by Battarbee and Flower (1985) is, therefore, probably a reflection of the more rapid (c. 0.1cm/yr) sedimentation rates prevailing at their coring stations than is the case at stations Dee(3) and Dee(4). Such conditions of rapid sedimentation reduce the mass-specific concentration of elements in the sediment column and serve to make the effects of minor fluctuations of atmospheric deposition less discernible.

The adjustments to mass-specific Pb, Zn and Cu incorporation rates occurring during the sedimentation period 146ys BP - present in the Loch Dee basin are closely analogous to those observed in most other polluted catchments (eg. Skei and Paus 1979, Norton et al 1981, Battarbee and Flower 1985, Ochsenbein et al 1983). At station Dee(3), the bulk Zn profile depicts markedly increased rates of deposition after 1855 (7cm depth). In core Dee(4) the Pb, Zn and Cu gradients all become more acute in post - 1840 sediments (8 - 9cm depth). At both sampling sites, peak concentrations of Pb and Zn prevail in sediments deposited between 1930 and 1979 (1cm - 4cm depth).

These trends are similar to those observed in Galloway sediments by Battarbee and Flower (1985) who, in turn, correlated the Pb, Zn and Cu gradients with temporal variations in the consumption of fossil fuels throughout the UK. By reference to the data of Renberg (1985) regarding European hydrocarbon combustion rates, this interpretation appears fully applicable to the Pb, Zn and Cu profiles of cores Dee(3) and Dee(4). Specifically, the onset of mass coal and oil combustion (>100 x 10^6 tons/yr) at around 1840 is synchronous with the increased loading of Pb, Zn and Cu in sediments at 7cm - 9cm depth. At this time, regional (fossil fuel-derived) pollutant fluxes appear to have replaced local (mineral extraction/smelting derived) fluxes as the principal source of non-lithogenic Pb, Zn and Cu. Fossil fuel consumption rose from 700 x 10^6 tons/yr to 1600 x 10^6 tons/yr between 1940 and 1970, thus accounting for the occurrence of Pb and Zn maxima at 2 - 4cm depth in the Loch Dee sediments. During the past decade, hydrocarbon combustion rates have fallen to around 1200 x 10^6 tons/yr and hence, equate with the falling mass-specific concentrations of Pb and Zn in the uppermost 1cm of sediment.

d) Quantification of total elemental fluxes.

It must be emphasised that the dry-mass concentration profiles of all elements are not the simple product of metal influx variations, but also respond to mass sedimentation rates(AR), the sediment density (WSD) and the fractional dry

weight (FDW) of sub-samples. By interchanging the unknown "elemental influx" parameter for the known "dry mass elemental concentration" parameter, the downcore concentration gradients of atmophilic elements in the dated sediments at station Dee(3) can be used to decipher the temporal variability of elemental fluxes by applying the following equation:-

Elemental flux (µg/cm2/yr) to sediments of depth D or age A

= FDW(g/cm3) x WSD(g/cm3) x AR(cm/yr) x Dry mass elemental conc.(µg/g)

The resultant Pb, Zn, Cu, Cd and Ni flux data for the period 1456 - present (Table 25) highlight two significant points. Firstly, it is possible to confirm the conclusions drawn from bulk elemental profiles regarding temporal variations in the total fluxes of Pb, Zn and Cu to the sediment. Enrichment upward of 7cm depth is directly equatable with the enhancement of fluxes by factors of 4 - 6 between 1855 and 1979. Post-1979 Pb, Zn and Cu fluxes were also at least 36% lower than those prevailing during the 1950 - 1979 period, with such changes being accurately chronicled by downcore variations of their mass-specific concentrations. Post-war flux estimates of 1.56 - 3.15µg/cm2/yr Pb, 3.97 - 6.15µg/cm2/yr Zn and 0.69 - 0.80µg/cm2/yr Cu to the Loch Dee sediments fall within the range established for other polluted basins. For example, Goldberg et al (1981) have determined the total present-day

Pb flux to Lake Michigan to be 1.4µg/cm2/yr, while values for Lake Washington are 3.4µg/cm2/yr. In both of these instances, Pb fluxes exceed those of Cu but fall 100% below those of Zn.

Table 25: Total annual fluxes of Pb, Zn, Cu, Cd and Ni (µg/cm2/yr) to sediments at station Dee(3) during the period 1455 - present.

Depth cm	Age span yrs	AR	FDW	WD	Pb	Zn	Cu	Ni	Cd
0 - 1	1979 - 86	0.13	0.07	0.88	1.68	3.97	0.80	0.79	0.11
1 - 2	1967 - 79	0.10	0.11	0.99	3.15	6.15	0.86	0.98	0.14
2 - 3	1950 - 67	0.05	0.16	1.09	1.93	5.26	0.69	0.89	0.14
3 - 4	1930 - 50	0.05	0.16	1.09	1.56	5.21	0.75	0.89	0.12
4 - 5	1908 - 30	0.04	0.14	1.03	1.46	3.85	0.46	0.56	0.07
5 - 6	1883 - 08	0.04	0.14	1.08	0.81	2.77	0.40	0.49	0.07
6 - 7	1855 - 83	0.03	0.10	0.88	0.44	1.30	0.19	0.28	0.03
7 - 8	1840 - 55	0.03	0.11	0.99	0.63	1.12	0.21	0.30	0.03
8 - 9	1808 - 40	0.03	0.12	1.04	0.67	1.18	0.28	0.35	0.02
9 -10	1776 - 08	0.03	0.11	1.03	0.62	0.98	0.22	0.34	0.02
10-11	1744 - 76	0.03	0.10	1.03	0.54	0.73	0.16	0.30	0.03
11-12	1712 - 46	0.03	0.12	0.97	0.49	0.88	0.18	0.34	0.05
12-13	1680 - 12	0.03	0.13	1.12	0.57	1.08	0.23	0.43	0.03
13-14	1648 - 80	0.03	0.12	1.07	0.50	0.85	0.19	0.41	0.06
14-15	1616 - 48	0.03	0.14	0.93	0.49	0.89	0.23	0.34	0.03
15-16	1584 - 16	0.03	0.10	1.08	0.53	0.75	0.17	0.35	0.05
16-17	1552 - 84	0.03	0.10	1.03	0.47	0.75	0.15	0.31	0.04
17-18	1520 - 52	0.03	0.10	1.03	0.47	0.68	0.17	0.28	0.05
18-19	1488 - 20	0.03	0.12	1.07	0.51	0.83	0.17	0.34	0.04
19-20	1456 - 88	0.03	0.13	0.97	0.50	0.77	0.22	0.29	0.03

AR = sediment accumulation rate (cm/yr-1), FDW = fractional dry weight (g/cm3), WD = wet density (g/cm3).

A second point to note from the flux data presented in Table 25 is the adjustment of the annual Ni and Cd supply to

the Loch Dee sediments during the 1855 - 1979 period. Although these elements display no mass-specific accumulation in the post-industrial strata (1cm - 7cm), they maintain stable concentrations through increasingly rapidly deposited sediments at 1cm - 3cm depth. Flux calculations show this consistency to be the product of a 3-fold increase in the annual Cd and Ni input. On the basis of conclusions drawn from earlier published studies of Cd and Ni enriched sediments (Carignan and Nriagu 1985, Wong et al 1984, Goldberg et al 1981), these increased fluxes can most plausibly be related to hydrocarbon combustion activities during the post-1850 period.

e) Isolation of the anthropogenic flux.

Whilst the effects of industrial activity on the geochemistry of the Loch Dee sediments are apparent from the downcore concentration gradients and the total influx variations of pollutant elements, these parameters comprise both lithogenic and anthropogenic components. On account of the lithological consistency of the basin sediments, the lithospherically-derived concentration of atmophile elements should be analogous at all levels. For core Dee(3), the anthropogenic flux of elements to post-industrial strata can, therefore, be deduced by subtracting a value approximating that of the total flux to the deeply buried, non-enriched core sectors. For purposes of calculation,

the mean annual Pb, Zn, Cu, Ni and Cd flux values for sediments at 40cm - 80cm provide ideal normalization factors.

Table 26: Post-industrial anthropogenic fluxes of Pb, Zn, Cu, Cd and Ni (µg/cm2/yr) to sediments at coring station Dee(3).

Depth cm	Time-span	Pb	Zn	Cu	Ni	Cd
0 - 1	1979 - 86	1.21	3.24	0.62	0.46	0.06
1 - 2	1967 - 79	2.68	5.42	0.68	0.65	0.09
2 - 3	1950 - 67	1.46	4.53	0.51	0.56	0.09
3 - 4	1930 - 50	1.09	4.48	0.57	0.56	0.07
4 - 5	1908 - 30	0.99	3.12	0.28	0.23	0.02
5 - 6	1883 - 08	0.34	2.04	0.22	0.16	0.02
6 - 7	1855 - 83	0	0.57	0.01	0	0
7 - 8	1840 - 55	0.16	0.39	0.03	0	0
8 - 9	1808 - 40	0.20	0.45	0.10	0.02	0
9 -10	1776 - 08	0.15	0.25	0.04	0.01	0
10-11	1744 - 76	0.07	0	0	0	0
11-12	1712 - 44	0.02	0.15	0	0.01	0
12-13	1680 - 12	0.10	0.35	0.05	0.10	0
13-14	1648 - 80	0.03	0.12	0.01	0.08	0.01
14-15	1616 - 48	0.02	0.16	0.05	0.01	0
15-16	1584 - 16	0.06	0.02	0	0.02	0
16-17	1552 - 84	0	0.02	0	0	0
17-18	1520 - 52	0	0	0	0	0
18-19	1488 - 20	0.04	0.10	0	0	0
19-20	1456 - 88	0.03	0.04	0.04	0	0
LITHOSPHERIC FLUXES		0.47	0.73	0.18	0.33	0.03

Anthropogenic flux data, based upon the above mode of normalization, are presented in Table 26 and allow the following conclusions to be drawn:-

1) By 1908, the anthropogenic fluxes of Pb, Zn, Cu and Cd to the Loch Dee sediments had risen to exceed their

lithospheric counterparts. At the time of peak pollutant deposition (1967 - 1979), fluxes from the respective sources differed by factors of 7.4 for Zn, 5.8 for Pb, 3.7 for Cu and 3.0 for Cd.

2) Regression of the anthropogenic Pb, Zn and Cu flux data for the period 1840 - present against the crude downcore profiles of these elements shows 71% of the variability of mass-specific Pb, Zn and Cu concentrations through the uppermost 8cm of core Dee(3) to be a consequence of human peturbation.

3) The post-1850 anthropogenic flux values for Pb, Zn, Cu and Ni fall within the range established for present-day atmospheric fallout at Blelham Tarn (Ochsenbein et al 1983), the S. Pennines (Pierson et al 1973, Livett et al 1979) and most North American sites (Goldberg et al 1981, Dillon and Evans 1982, Jeffries and Snyder 1981). In contrast to the findings of Ochsenbein et al (1983) at Blelham Tarn, the entire anthropogenic flux of these elements to the Loch Dee sediments can, therefore, confidently be equated with direct atmospheric fallout onto the lake surface. There is no evidence that non-atmospheric pollutant fluxes are significant.

3.8.2: Loch Ba sediments.

a) Lithospheric controls.

From the data presented in section 3.4.2, the significance of sediment lithology to elemental enrichment patterns appears to differ markedly between sample cores from the southern (Ba2) and central (Ba3) sub-basins. At station Ba(2), concentrations of total Ni, K and Fe and silicate-bound Cd, Zn, Fe, Mn, Co and Ni show limited downcore variability. As in the Loch Dee basin, these trends are diagnostic of lithological homogeneity. From Table 27, the enrichment of Pb, Zn and Cu upward of 20cm depth and the production of Mn and Co anomalies at the sediment surface can also be seen to be associated with the accumulation of hydrogenous phases. Consequently, these elements appear to undergo enrichment independently of any alteration to the geochemistry of the detrital influx.

Table 27: Ratios of detrital/non-silicate Pb, Zn, Cu, Mn and Co in non-enriched and enriched strata at station Ba(2).

	Sample level	Ratio	Sample level	Ratio
Pb	30cm	1.46	4cm	1.26
Zn	30cm	0.65	4cm	0.21
Cu	30cm	1.00	4cm	0.65
Mn	30cm	0.98	1cm	0.19
Co	30cm	100% detrital	1cm	0.94

In contrast to core Ba(2), sediments at station Ba(3) display a zone of marked Cu and Zn enrichment at 60cm - 80cm depth. Given the palynologically-derived origin of 9500yrs BP for the 70cm sub-sample (section 4.5.2), such enrichment cannot reflect cultural disturbance. Downward of 70cm, Cu accumulation also occurs in increasingly minerogenic sediments (LOI < 10%), thus precluding enrichment through complexation with organic matter. The clearly "lithospheric" nature of such anomalies, therefore, raises the question as to whether similar mechanisms are responsible for the enrichment of Cu and Zn in the uppermost 3cm of sediment. This question can best be resolved by characterising the geochemical changes which accompany Cu and Zn enrichment at 60cm - 60cm depth; and then examining the extent to which these changes are recurrent towards the sediment surface.

In the basal sector of core Ba(3), the rare earth elements which have affinities to silicic materials (La, Ce, Sm, Eu, Hf) display two-fold enrichment. The ratios of elements which indicate the relative proportions of sediment from silicic/basic sources or silicic/non-igneous sources (K/Mg, La/Ni, Sm/Sc) also increase at 60cm - 80cm depth (Table 28). Lanthanum enrichment is known to be greatest in granite (Krauskopf 1979, Gordon et al 1969). Hence, its increased concentration in the sediment, relative to REE's which are more universally enriched in silicic rocks (eg. Eu), suggests that the unusually high concentrations of Zn and Cu

at 60cm - 80cm depth are attributable to the presence of sediments derived directly from the catchment bedrock.

Table 28: Elemental ratios for the differentiation of sediment sources to station Ba(3). For purposes of interpretation, K, La and Sm are associated with silicic source materials, with La having particular affinities to granite. Mg, Ni and Sc all occur at higher concentrations in shales and basic igneous rocks.

Depth cm	K/Mg	La/Ni	Sm/Sc	La/Eu	Hf/Sm
10	0.048	0.02	-	1.5	0.80
20	0.060	0.017	-	-	0.41
30	0.020	0.022	2.78	1.00	-
40	0.080	0.016	-	1.5	0.39
50	0.040	0.015	-	1.5	0.39
60	0.060	0.057	6.81	2.16	0.21
70	0.090	0.045	3.68	3.10	0.30
80	0.121	0.022	2.79	2.21	0.71

On account of the depletion of both the "silicic" REE's and Sc upward of 40cm depth, the reduction of the Cu and Zn flux can be attributed to a shift away from an igneous sediment source. The K/Mg ratios of only 0.02 - 0.06 at 10cm - 30cm depth are consistent with the prevalence of glacial drift as the replacement source material. Significantly, K, Sm, Hf, Eu, Ce, La and Sc do not show enrichment at any point through the uppermost 20cm of the sediment column. Given the relationship between Cu, Zn, K and the REE's in the "lithospherically " enhanced core sectors, the accumulation of atmophilic elements at the sediment surface

can, therefore, be considered to occur independently of lithological adjustments.

The significance of organic content to the enrichment of trace elements varies considerably between sediments at stations Ba(2) and Ba(3). In the former, LOI increases progressively from 20% at 32cm depth to 57% at the sediment surface (Fig 3/41a) and hence, correlates significantly with the profiles of Pb, Zn and Cu ($R > 0.55$). With respect to Zn, this relationship must be non-causal, as sequential chemical data show that inorganic (carbonate and $NH_2.OH.HCl/HOAc$ extractable) phases control the concentration gradient. In the cases of Pb and Cu, LOI also co-varies with the concentration of H_2O_2 extractable phases ($R > 0.5$) which, in turn, exert a major influence on the total Pb and Cu profiles. Consequently, there is reason to assume that some enrichment of Pb and Cu in the upper core sector has resulted from either an increased influx of metal-carrying organic matter, or through complexation (at rates controlled by the availability of organic matter) in the sediment column.

At station Ba(3), the influence of organic content on the downcore geochemical constituency of sediments is only conspicuous with respect to the distribution of Br. In accordance with the observations of Shishkina (1965) and Swanson (1966), the downcore Br and LOI profiles are strongly co-variable ($R = 0.91$), thus suggesting that Br

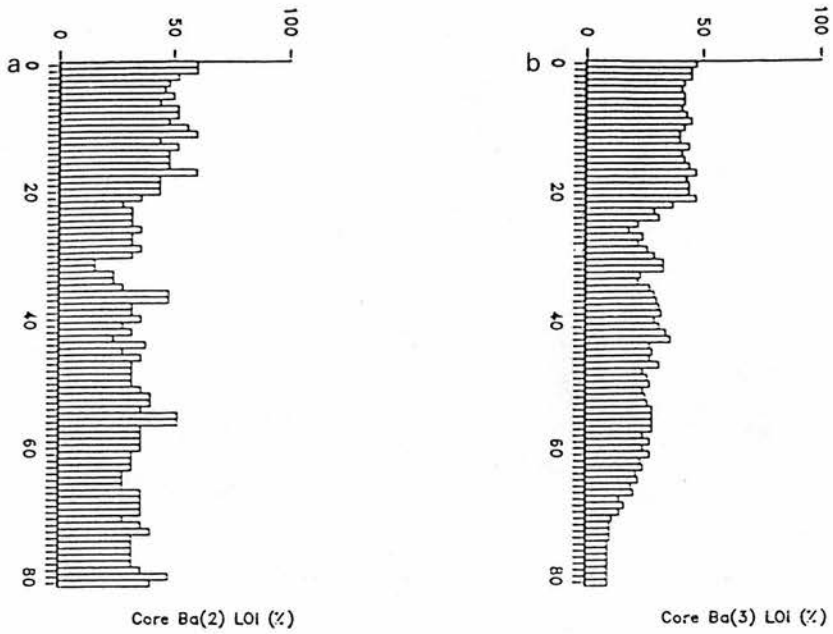

FIG 3/41: Loss on ignition profiles throughout cores Ba(2) and Ba(3).

is wholely supplied to the sediment in organic complexes. A ratio of 1.5 - 2.0ppm Br/10% organic matter prevails throughout the core. Hence, strata holding less than 10% organic matter at 70cm - 80cm depth (Fig 3/41b) contain only 1 - 2ppm Br, while the increasingly organic, uppermost 20cm of sediments (LOI = 45 - 50%) contain 10 - 11ppm Br.

b) Diagenetic controls.

In section 3.4.2, it was noted that the profiles of Pb, Zn and Cu differ markedly between the upper sectors of cores Ba(2) and Ba(3). In the latter, enrichment is restricted to strata at 1cm - 3cm depth which, on the basis of 210Pb data, can be assigned an origin of 0 - 146yrs BP. For core Ba(2), synchronous magnetic horizons can be used to extrapolate the 210Pb chronology from core Ba(3) and allows the locus of initial Pb enrichment (15cm) to be tentatively dated to in excess of 400yrs BP (see footnote).

NOTE Magneto-stratigraphic linkages between cores Ba(2) and Ba(3) are outlined in section 4.5.2. These linkages indicate that strata at 7cm depth in core Ba(3) are synchronous with those at 12cm depth in core Ba(2). By assuming that the 4cm - 7cm levels of core Ba(3) accumulated at a constant rate of 0.016cm/yr (the rate of accumulation ascertained for the oldest 210Pb dated sample), these synchronous horizons can be assigned origins of 380yrs BP.

On examining the pore-water profiles through the respective cores, the above discrepancies appear to reflect the operation of contrasting diagenetic mechanisms at stations Ba(2) and Ba(3). In core Ba(2), the precipitation of sulphides in the strongly anoxic strata at 4cm - 8cm depth is signified by the 2 - 5 fold reduction of dissolved Cu, Ni, Fe and Zn concentrations. In studies of sediments with similar pore-water profiles, Carignan and Nriagu (1985) considered that this process served to limit both the diffusion of labile phases through the anoxic strata and the upward migration of dissolved Cu, Zn, Fe and Ni to the oxic/anoxic boundary. However, in contrast to the assumptions of Carignan and Nriagu (1985), geochemical fractionation data show that sulphidization does not, in itself, cause any major alteration to the total metal loading of the 4cm - 8cm core sequence. Instead, the Zn concentration gradient is predominantly controlled by oxides and carbonates, while LOI and sequential chemical analyses suggest that organic and silicate phases dominate the profiles of Cu and Pb. Diagenetic alteration of the geochemical constituency of core Ba(2) is, therefore, only evident with respect to the distributions of Mn and Co, which precipitate as authigenic oxides at the sediment/water interface.

In core Ba(3), the diagenetic cycling of elements differs in two respects. Firstly, sulphide precipitation is not prolific, being evident only from the inflection of

dissolved Fe, Cu and Ni profiles at 4cm depth. Consequently, metals which are liberated through the reduction of labile phases or the decomposition of organic matter upon burial are not immobilized, but are free to migrate across the anoxic/oxic boundary in solution. This process provides adequate explanation of the depletion of pollutant elements in sediments which accumulated between 150 - 380yrs BP. Secondly, the dissolved loadings of all analysed trace metals decline in association with the precipitation of hydrogenous Fe/Mn phases in the oxic strata. The resultant profiles are analogous to those observed by Cornwell (1986) for Ni, Mo, Ba, Zn, Co and Cu in Toolik lake, Alaska and are diagnostic of the scavenging of dissolved metals by hydrous Fe/Mn oxides.

Although the surfaces of authigenic Fe/Mn oxides are known to be important sites for the removal of trace metals from natural waters (Cornwell 1983, Robinson 1981, Ballistrieri and Jones 1986), the differing pore-water trends at the surface of cores Ba(2) and Ba(3) suggests that eH is the critical rate-limiting control. In core Ba(2), the trace metals which are least soluble under oxic conditions (Cu and Co) are removed in association with Mn oxide formation, but low pH and eH values of only 30mV inhibit the precipitation of Zn and Ni. At station Ba(3), mean dissolved concentrations of Ni, Zn and Cu are analogous to those in core Ba(2), but surficial eH values of 80mV produce

conditions of saturation with respect to the more soluble metals. Consequently, Ni and Zn precipitate with Mn despite their low sorption potentials in acid waters, thus leading to the assimilation of dis-proportionately high solid phase concentrations at 1cm depth.

c) Anthropogenic controls.

On account of the poor resolution and the extensive diagenetic alteration of the recent palaeo-geochemical record, the significance of temporally varying anthropogenic pollutant fluxes to the chemical stratigraphy of core Ba(3) is limited. For core Ba(2), it is also acknowledged that partitioning into the increasingly organic, uppermost 20cm of sediment may have influenced the profiles of Pb and Cu. However, because H2O2 extractable fractions do not hold more than 30% of total Pb at any stratigraphic level and downcore LOI variations are less than 100%, the role of organic matter cannot be of primary importance. In the absence of any lithogenic or diagenetic explanation, the two-fold enhancement of Pb, Zn and Cu concentrations upward of 20cm can, therefore, be assumed to reflect anthropogenic controls. This interpretation is supported by the following lines of evidence:-

1) The profiles of Pb, Zn and Cu are, in most respects, analogous to those which are unequivocally reflective of anthropogenic pollution at Loch Dee (section 3.8.1) and in

other polluted UK basins (eg. Battarbee and Flower 1985, Rippey 1982, Ochsenbein et al 1983). The magnetically extrapolated date of 380yrs BP (see page 125) for the 12cm sub-sample suggests that 20% increments to Pb deposition occurred in response to the initial anthropogenic release of Pb into the atmosphere at around 1600 (Murozumi et al 1969, Davis et al 1983, Lee and Tallis 1973). The predominance of regional smelting activities over fossil fuel combustion as a source of atmospheric metal pollution at this time has been established from the sediments of Loch Dee (section 3.8.1). This source also appears responsible for the early influx of anthropogenic Pb to Loch Ba, given that no other elements display analogous enrichment at 10cm - 12cm depth.

2) The trends of rapidly increased Pb incorporation, with associated two-fold Zn and Cu enrichment between 8cm and 4cm depth have, where previously observed, been universally related to the onset of mass hydrocarbon combustion (Wong et al 1984, Skei and Paus 1979, Davis et al 1983, Oullet and Jones 1983). On the basis of the data of Renberg (1985), the 8cm core level can, therefore, be tentatively dated to 1850.

3) Although increased sedimentation rates are likely to be significant, the lower concentrations of Pb and Cu upward of 3cm depth typify the trends which occur in most other polluted UK sediments. These trends result from the declining rates of hydrocarbon consumption over the past 10 - 15 years (eg. Battarbee and Flower 1985).

4) The speciation patterns of atmophilic elements in the upper core sectors analogue those formerly attributed to anthropogenic pollution in Lake Michigan (Filipek et al 1979) and Lake Gardsjon (Andersson 1985). For example, the affinity of pollutant Zn to carbonate phases is well known (Filipek et al 1979). Hence, the absence of NaOAc extractable Zn downward of 17cm depth and the attainment of concentrations of 61ug/g in this fraction at the sediment surface, can be considered diagnostic of the increased significance of hydrocarbon-derived Zn. The increased residence of Cu and Pb in H2O2 extractable phases is also typical of polluted sediments (Andersson 1985) and reflects the rapid partitioning of these elements into organic matter.

d) Quantification of the flux of "atmophilic" elements.

In the absence of radiometric data, conventional methods of flux calculation (see page 116) have limited applicability to the Ba(2) sediment sequence. However, estimates of the total and anthropogenic fluxes of Pb, Zn and Cu to these sediments can be made, by incorporating the following assumptions into calculations:-

1) The 12cm core level dates to 380yrs BP and the initial locus of increased rates of Pb, Zn and Cu incorporation (8cm) dates to approximately 1850.

2) Sedimentation rates were constant at 0.017cm/yr during the period 380 - 146yrs BP and 0.054cm/yr during the period 146yrs BP - present.

3) On account of the apparent lithological homogeneity of the sediment, the "lithospherically-derived" concentrations of Pb, Zn and Cu are constant throughout the core. The anthropogenic flux to the uppermost 12cm of sediment, therefore, corresponds to the total flux minus the mean flux value for strata at 20cm - 97cm depth.

4) The mean sediment accumulation rate of the 20cm - 97cm core sequence is analogous to that of the 9cm - 12cm sequence.

Table 29: Total (T) and anthropogenic (A) fluxes of Pb, Zn and Cu to station Ba(2) during the period 1621 - present (µg/cm2/yr-1). The methods of total flux calculation followed those outlined on page 116. Anthropogenic flux values are derived from deducting the pre-cultural flux from the total flux.

Depth (cm)	Age-span (years)	AR	FDW	WD	TPb	APb	TZn	AZn	TCu	ACu
0 -1	1969-86	.05	.10	0.9	0.57	0.47	0.99	0.84	0.26	0.19
1 -2	1952-69	.05	.07	0.8	0.38	0.28	0.66	0.51	0.18	0.11
2 -3	1935-52	.05	.06	0.8	0.35	0.25	0.40	0.25	0.13	0.06
3 -4	1918-35	.05	.05	0.8	0.29	0.19	0.41	0.26	0.14	0.07
4 -5	1901-18	.05	.06	0.9	0.37	0.27	0.52	0.37	0.15	0.08
5 -6	1884-01	.05	.07	0.9	0.41	0.31	0.50	0.35	0.15	0.08
6 -7	1867-84	.05	.09	0.9	0.52	0.42	0.76	0.61	0.18	0.11
7 -8	1850-67	.05	.09	0.9	0.54	0.44	0.65	0.50	0.18	0.11
8 -9	1792-50	.017	.11	0.9	0.17	0.07	0.21	0.06	0.07	0.00
9-10	1735-92	.017	.08	0.8	0.08	0.00	0.15	0.00	0.03	0.00
10-11	1678-35	.017	.08	0.9	0.09	0.00	0.13	0.00	0.04	0.00
11-12	1621-78	.017	.10	1.0	0.11	0.01	0.15	0.00	0.06	0.00
20-97	PRE-IND	.017	.13	1.0	0.10	-	0.15	-	0.07	-

From the data presented in Table 29, the predominance of industrial processes as a source of atmophilic elements to Loch Ba is clear. Despite the likely under-estimation of total present-day deposition (resulting from the adoption of a "constant sedimentation rate" assumption for the surficial 8cm of the core), the anthropogenic loading of Pb, Zn and Cu appears to have exceeded the lithospheric flux by factors of 2.7 - 5.3 during the 1969 - 1986 period. Regression of the anthropogenic flux data against the crude profiles of these elements suggests that 61% of downcore variations in their concentration are attributable to human peturbation.

Given the remote location of the site, it is not suprising that anthropogenic Pb, Zn and Cu fluxes to Loch Ba are at least 300% lower than those prevailing at Loch Dee (section 3.8.1e), Blelham Tarn (Ochsenbein et al 1983) and Ranafjord (Skei and Paus 1979). However, the present anthropogenic Pb flux of 0.47µg/cm2/yr to Loch Ba is 400% greater than the total flux to UK sites which have been classified as receiving only "background" pollutant loadings, for example, Glensheildaig (Livett 1982). The present-day deposition rates of Pb, Zn and Cu at Loch Ba also equal or exceed those prevailing at Alonquin Park, Ontario (Wong et al 1984), throughout New England (Davis et al 1983, Norton et al 1981) and at Holmatvn, Norway (Davis et al 1983). Significantly, these sites have all been found to have undergone lake water adjustments as a consequence of the associated deposition of mineral acids. Because the

principal lake water "buffering component", HCO3 is virtually absent in the Loch Ba basin, hydrocarbon pollutant deposition of the magnitude inferred by the present fluxes of Pb, Zn and Cu may, therefore, be sufficient to induce similar acidification.

3.9: Summary and conclusions.

From the data presented, it is clear that cultural activities have markedly altered the geochemical budgets of the Loch Dee and Loch Ba sediment reservoirs. Most notably, anthropogenic fluxes of Pb, Zn and Cu have increased progressively since 1850 and now exceed natural, lithospheric inputs by factors of 2.7 - 7.4. The impact of this increase in pollutant Pb, Zn and Cu deposition is directly chronicled in the downcore geochemical records of the lithologically homogeneous sediments at coring stations Dee(3), Dee(4) and Ba(3), where two-fold enrichment occurs through the uppermost 15cm. The geochemical data for sample cores from these stations, therefore, confirm previous observations (eg. Aston 1973, Capuzzo 1973, Brugam 1978, Forstner 1976, Norton et al 1981, Oullet and Jones 1983), that heavy metal enrichment can often be indicative of the extent of anthropogenic peturbation in lake systems.

However, the geochemical conditions prevailing in the sediment column at station Ba(3) illustrate that sedimentary

strata can be subject to enrichment with heavy-metals through two natural mechanisms. Firstly, two-fold increments to Zn and Cu concentrations, with associated REE enrichment, occur at 60cm - 80cm depth as a result of a granitic sediment influx. Secondly, Cu, Zn, Co and Ni are enriched in the uppermost 2cm of sediment as a consequence of their co-precipitation with hydrogenous Fe/Mn oxides.

The implications of the geochemical trends observed in core Ba(3) are as follows:-

1) The accumulation of heavy metals in strata of post-industrial age cannot, in itself, be considered diagnostic of anthropogenic pollution, but may plausibly reflect sedimentological or diagenetic influences.

2) The differentiation of diagenetic and anthropogenic enrichment anomalies is only possible, given a knowledge of the relationships between the speciation, dissolved concentrations and solid phase concentrations of elements. For example, the inversely related pore-water and solid phase profiles of Zn, Cu, Ni and Co form the basis of the "diagenetic" interpretation of elemental enrichment at the surface of core Ba(3). In instances where similar profiles have been interpreted by simply dating the locus of enrichment to around 1850, anthropogenic controls have universally been cited (eg. Aston 1973, Forstner 1976).

3) Diagenetic contrasts between cores Ba(2) and Ba(3) suggest that mechanisms of Pb, Zn and Cu enrichment do not only vary between basins but can also vary within basins, should individualistic redox gradients occur in different sectors of the sediment reservoir. Under such circumstances, assumptions that the stratigraphic locations of trace metal enrichment are synchronous across an entire basin will be invalid.

CHAPTER FOUR

Loch Dee and Loch Ba sediments: Magnetic mineralogy.

4.1 Introduction.

In the preceding chapter, geochemical methods were utilized to highlight downcore variations in the constituency of sediment cores from the Loch Dee and Loch Ba basins. Furthermore, most geochemical changes were found to be specifically attributable to lithogenic, diagenetic or anthropogenic components within the sediment reservoirs. On the basis of evidence presented earlier (section 2.3), it may be predicted that such anomalies should also become conspicuous through examination of the downcore mineral magnetic characteristics of sample cores. For example, Dearing et al (1982), Thompson et al (1975), Walling et al (1979) and Oldfield et al (1979) have all noted the sensitivity of mineral magnetic parameters to downcore lithological changes which, in turn, result from temporal variations in the source of sedimentary material. Hilton et al (1986), Karlin (1984), Henshaw (1978) and Canfield and Berner (1987) have demonstrated that certain downcore mineral magnetic fluctuations may constitute a reliable indicator of sedimentary diagenesis. In addition, Oldfield et al (1983) have shown that increased ferrimagnetic mineral concentrations within post-industrial sediments, particularly when associated with trace metal

enrichment, can be diagnostic of the deposition of hydrocarbon-derived pollutants. Consequently, the magnetic data presented in this chapter may be considered to provide a "control" against which all conclusions drawn from geochemical analyses of sample cores from Loch Dee and Loch Ba can be compared.

Bearing the above objectives in mind, magnetic susceptibility (Xlf) and magnetic remanence (SIRM and ARM) data are presented in the foremost sections of this chapter to illustrate the downcore variability of magnetic mineral (notably ferrimagnetic mineral) concentrations within all sample cores previously subjected to geochemical analyses. In addition, data are provided to illustrate the magneto-stratigraphy of sediments at coring station Ba(1). In all cases, data reflecting the concentration of magnetic minerals in sediment samples are supplemented by data which illuminate downcore variations with respect to the precise mineralogy and granulometry of magnetic assemblages.

Following the characterisation of sediment cores through the use of "conventional" magnetic methods, the latter sections of this chapter (sections 4.3 - 4.5) are devoted to determining the extent to which downcore magnetic variations are specifically reflective of lithogenic, diagenetic or anthropogenic influences. In accordance with the previously established rationale (see section 2.3), interpretations are

not only based upon magnetic data, but also draw on evidence concerning the stability of magnetic mineral assemblages upon oxidation, the geochemical partitioning of magnetic phases within sediment samples and the morphology of the signal-carrying components. Finally, in instances where the deposition of anthropogenically mobilized magnetic minerals appears to be discernible in recent sediments, attempts are made to quantify temporal changes in their supply through the calculation of annual fluxes.

4.2 Results of mineral magnetic analyses.

4.2.1 Loch Dee cores.

Previously described methods (section 2.3.6) were used to obtain low frequency magnetic susceptibility (Xlf), saturation isothermal remanent magnetisation (SIRM) and demagnetisation data for sub-samples from 90 stratigraphic levels of core Dee(3) and 60 levels of core Dee(4). Anhysteretic remanent magnetisation (ARM) values were also determined for 54 sub-samples from core Dee(3). In all instances, sub-samples were removed from cores at 1cm intervals.

The results of the above analyses indicate a high degree of similarity between the downcore magnetic characteristics of cores Dee(3) and Dee(4), with major variations in both mineral concentration and magnetic

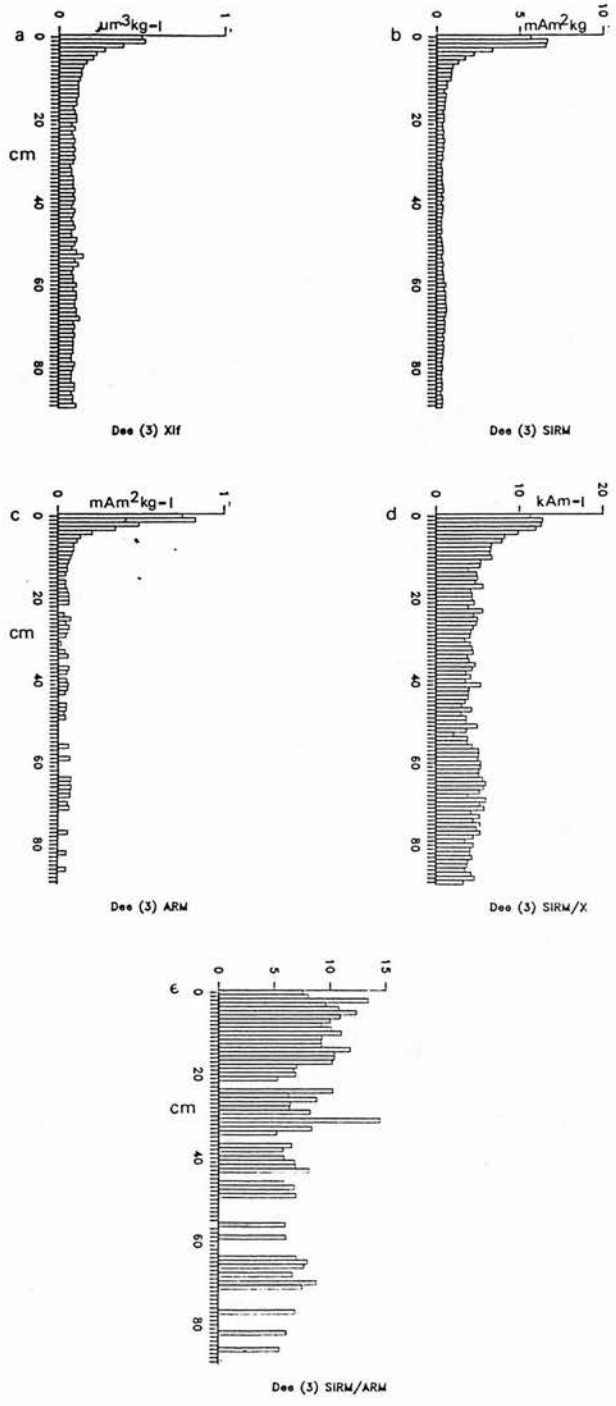

FIG 4/1: Core Dee(3) - concentration dependent (X, SIRM, ARM) and inter-parametic (SIRM/X, SIRM/ARM) magnetic data for sub-samples taken at 1cm resolution. Note: SIRM, X and associated parameters are plotted at 90 stratigraphic levels. ARM data are plotted at 54 stratigraphic levels.

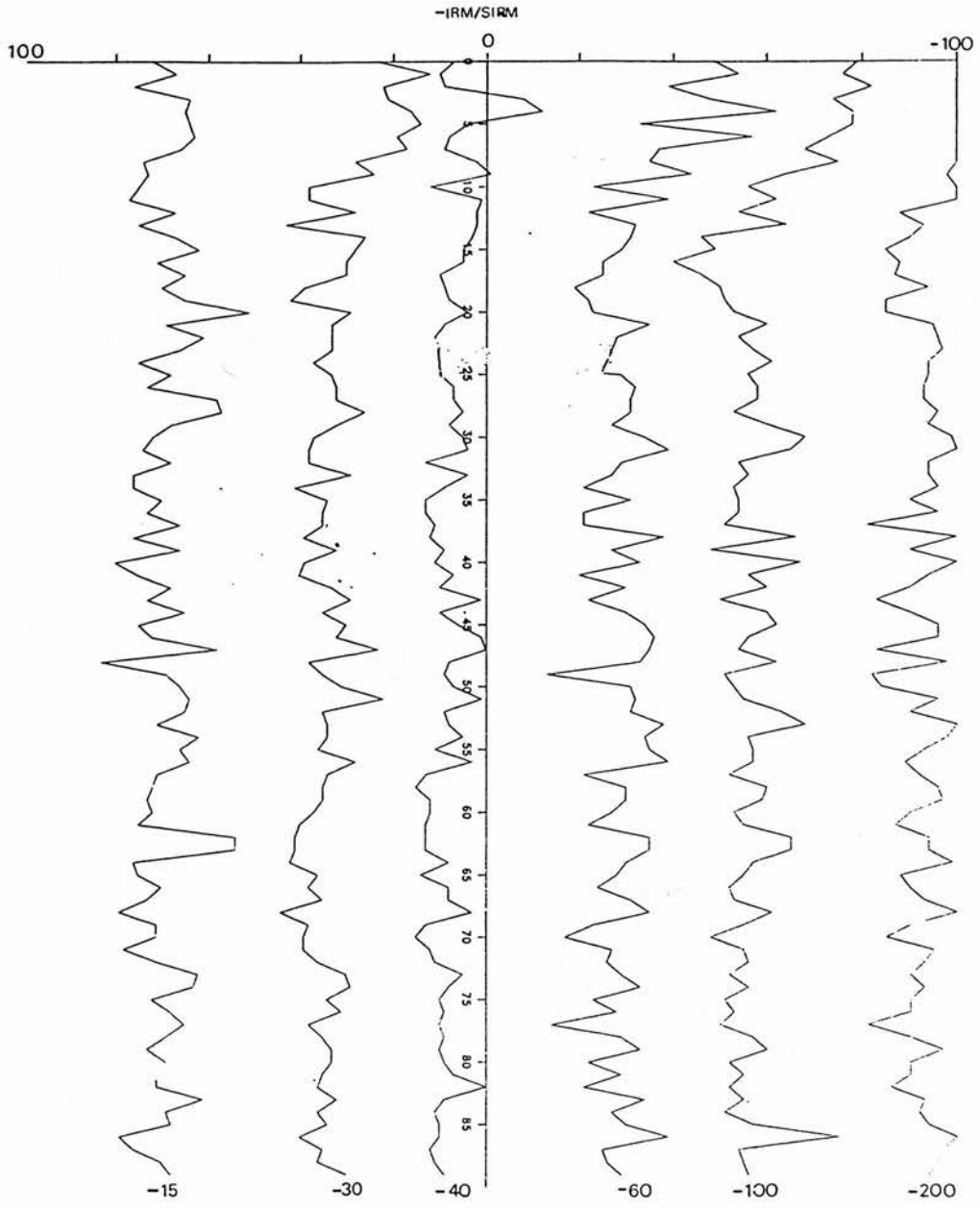

FIG 4/2: Core Dee(3) - downcore variability of SIRM-demagnetisation response, determined through the subjection of saturated samples from 90 stratigraphic levels to reversed fields of 15mT, 30mT, 40mT, 60mT, 100mT and 200mT.

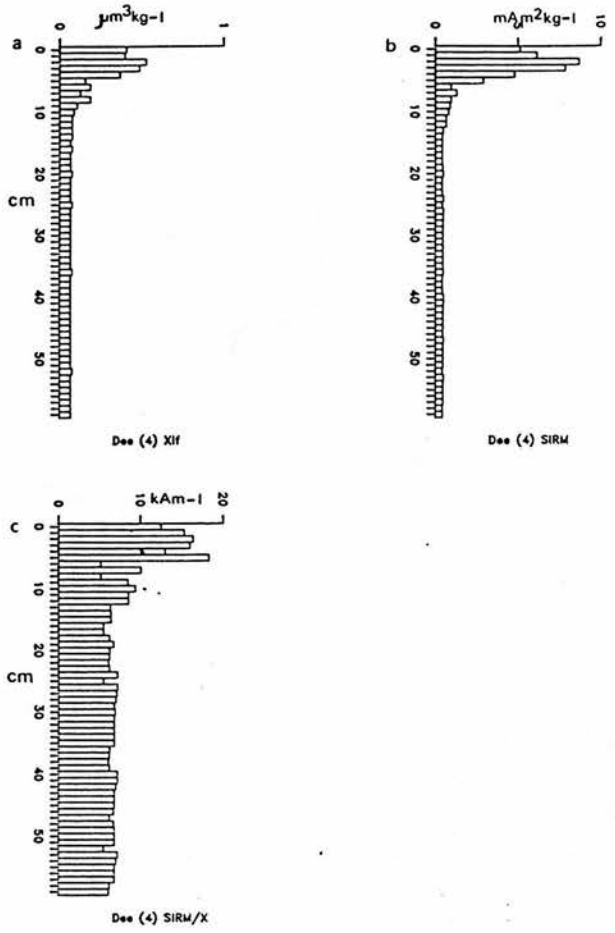

FIG 4/3: Core Dee(4) - concentration dependent (X, SIRM) and inter-parametric (SIRM/X) magnetic data for sub-samples taken at 1cm resolution from the uppermost 60cm of the sediment column.

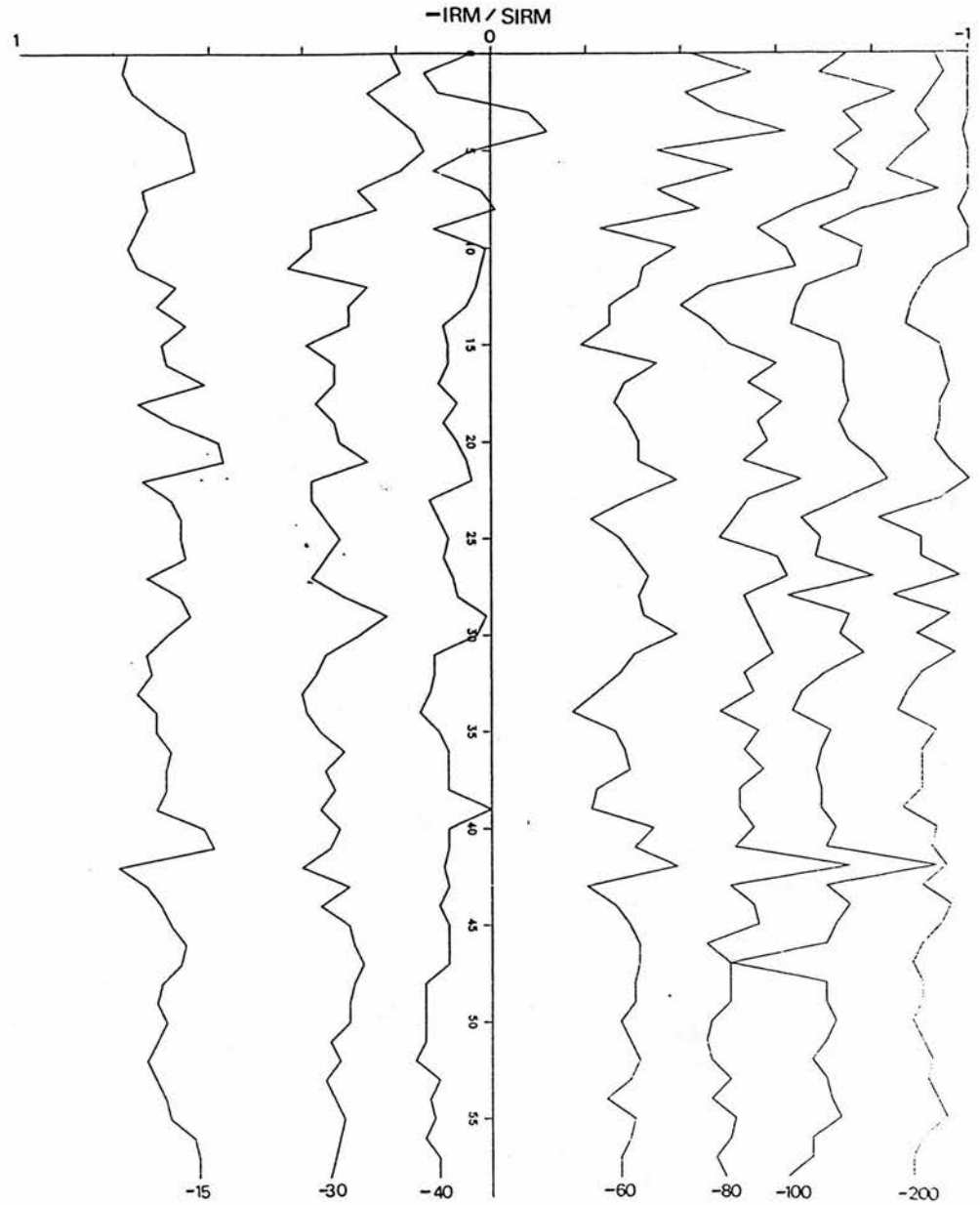

FIG 4/4: Core Dee(4) - downcore variability of SIRM - demagnetisation response, determined through the subjection of saturated samples from 60 stratigraphic levels to reversed fields of 15mT, 30mT, 40mT, 60mT, 80mT, 100mT and 200mT.

mineralogy evident only within the surficial 10cm of sediment (Figs 4/1 - 4/4). The respective SIRM and X1f profiles of cores Dee(3) and Dee(4) are particularly analogous, showing progressively increasing values upward of 8cm depth (Figs 4/1a-b and 4/3a-b). Differentiation between the two analysed cores by reference to SIRM or X1f is, therefore, only possible to the extent that peak values of 7.0mAm2Kg-1 SIRM and 0.52μm3Kg-1 X1f occur at 2cm depth in core Dee(3), while analogous maxima (SIRM = 9.1 mAm2Kg-1, X1f = 0.52 μm3Kg-1) are observable at 3cm depth in core Dee(4). Accordingly, all SIRM and X1f data are diagnostic of the enrichment of ferrimagnetic mineral phases upward of 8cm depth. Furthermore, the concentrations of ferrimagnets which are discriminated by X1f in samples from 1cm - 3cm depth appear to exceed those of samples from between 10cm and 90cm depth by at least a factor of five.

Further magnetic differentiation between samples from 1cm - 8cm depth and those from 10cm - 90cm depth is possible through examining the downcore variability of the ratio of SIRM/X in cores Dee(3) and Dee(4). Notably, progressively increasing values of the "concentration dependent" parameters, SIRM, ARM and X1f, upward of 8cm depth are accompanied by rising ratios of SIRM/X (Figs 4/1d and 4/3c). In core Dee(3) SIRM/X ratios increase from 6.6kAm-1 at 8cm depth to a maximum of 12.8kAm-1 at 2cm depth. In core Dee(4), SIRM/X ratios rise less

consistently, from 5kAm-1 at 9cm depth to over 16kAm-1 in strata at 2cm - 4cm depth. In both instances, adjustments indicate that following the deposition of an 80cm sequence of magnetically homogeneous sediment, an increased influx of ferrimagnets to the uppermost 8cm of sediment occurred with concomitant modifications to either the mineralogy or the granulometry of the signal-carrying phases.

To produce the above changes in the ratio of SIRM/X, one of two downcore mineralogical variations must occur within the Loch Dee sediment reservoir. Firstly, evidence provided by Thompson (1986) showing SIRM/X ratios to be inversely related to mineral grain size (in mono-minerogenic assemblages) could be invoked to suggest that samples from the uppermost 8cm of sediment hold a dis-proportionate fraction of their ferrimagnetic assemblage in the SSD grain size range (see Appendix 2, Fig 7). Conversely, it is plausible that the low SIRM/X ratios observed in strata at 10cm - 90cm depth are not a product of magnetic grain size, but reflect their low ferrimagnetic mineral concentrations (as signified by SIRM or Xlf) alongside high concentrations of paramagnetic Fe. Should this be the case, the contribution of paramagnetic phases to Xlf, but not to SIRM in the 10cm - 90cm sequence would depress the SIRM/X ratios observed for these strata. With the increased concentration of ferrimagnets in the uppermost 8cm, the significance of paramagnetic minerals would decrease, thus leading to higher, granulometrically

controlled SIRM/X ratios for these samples.

For core Dee(3), a more precise diagnosis of the nature of the downcore mineralogical changes demarked by the SIRM/X profile is possible through examining the accompanying variations of SIRM/ARM, as this ratio is independent of paramagnetic influences. Notably, samples containing high ferrimagnetic mineral concentrations at 2cm - 8cm depth also exhibit SIRM/ARM ratios in excess of 9, peaking at 14.0 in the 3cm sub-sample (Fig 4/1e). In contrast, the mean SIRM/ARM ratio for samples from 15cm - 90cm depth is 6.9, with only the 31cm sub-sample yielding a significantly higher SIRM/ARM ratio than those observed in the uppermost 8cm. Accordingly, it can be deduced that the progressive enrichment of ferrimagnets through the surficial 8cm of the Loch Dee sediment reservoir has been accompanied by a reduction in the proportion of smaller, SSD minerals which are preferentially discriminated by ARM. In turn, SIRM/ARM data serve to confirm that the anomalously low SIRM/X ratios calculated for sub-samples from 10cm - 90cm depth are paramagnetically controlled and hence,provide no true indication of mineral granulometry.

The increasing grain size of ferrimagnetic mineral assemblages upward of 8cm depth in the Loch Dee sediment reservoir can be further confirmed through examining the SIRM-demagnetisation data acquired for cores

Dee(3) and Dee(4) (Figs 4/2 and 4/4). These data show that while all samples undergo analogous losses of SIRM upon subjection to a 15mT demagnetising field, those from the uppermost 8cm of sediment sustain anomalously high remanence losses upon placement within stronger reversed fields. Notably, of all sub-samples taken from core Dee(3), only those from 4cm and 5cm depths exhibit coercivities of below 40mT, thus indicating the relatively strong influence of PSD/MD ferrimagnetic grains. Furthermore, samples from 1cm - 8cm depths of core Dee(3) were all found to attain SIRMs of reversed polarity upon placement within a 200mT reverse field, indicating the absence of antiferromagnets in these strata. In contrast, all samples from between 10cm and 85cm depth underwent only 82% - 96% reversal upon subjection to such a field, signifying the increasing downcore significance of HIRM bearing antiferromagnets.

4.2.2 Loch Ba Cores.

The methods outlined in section 2.3.6 were used to obtain Xlf, SIRM and demagnetisation data for 55 sub-samples from core Ba(1), 96 sub-samples from core Ba(2) and 83 sub-samples from core Ba(3). In addition, ARM data were acquired for 47 sub-samples from core Ba(2) and 44 sub-samples from core Ba(3). For cores Ba(2) and Ba(3), sub-sampling intervals of 1cm were adopted. For core Ba(1) sub-sampling was carried out at 2cm intervals.

The results of the above magnetic analyses indicate that the comparability of sample cores is limited and accordingly, each can best be described in turn.

Core Ba(1)

When placed under both visual and statistical scrutiny, downcore magnetic fluctuations in core Ba(1) indicate the presence of 5 discrete magneto-stratigraphic horizons in the uppermost 1.0m of sediment. These horizons are distinguishable with respect to variations in both ferrimagnetic mineral concentration and magnetic mineralogy or granulometry, but can conveniently be defined by reference to "whole core" mean SIRM data in the following manner:-

A) Sub-samples from between 1cm and 18cm depth exhibit considerable ferrimagnetic enrichment, as indicated by their high SIRM and X1f values (peak SIRM = 3.9mAm2kg-1, peak X1f = 0.40μm3kg-1, mean SIRM = 2.7mAm2kg-1) relative to the "whole core" mean (SIRM = 2.4mAm2kg-1). SIRM/X ratios for these strata fall within the range 9kAm-1 to 11kAm-1, indicating the predominance of ferrimagnetic phases of between 0.04μm and 0.1μm in size (Fig 4/5c). Demagnetisation data appear to confirm the presence of PSD/MD ferrimagnets, with up to 80% SIRM loss occurring upon the subjection of samples to a 30mT demagnetising field and SIRM coercivities

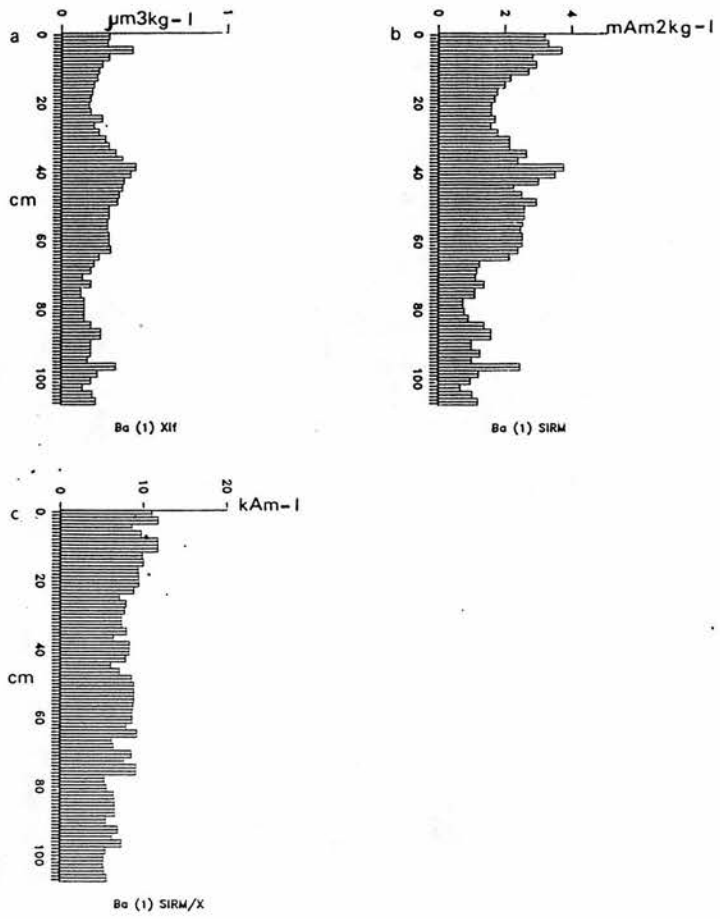

FIG 4/5: Core Ba(1) - Concentration dependent (X, SIRM) and inter-parametric magnetic data (SIRM/X) for sub-samples taken at 2cm resolution.

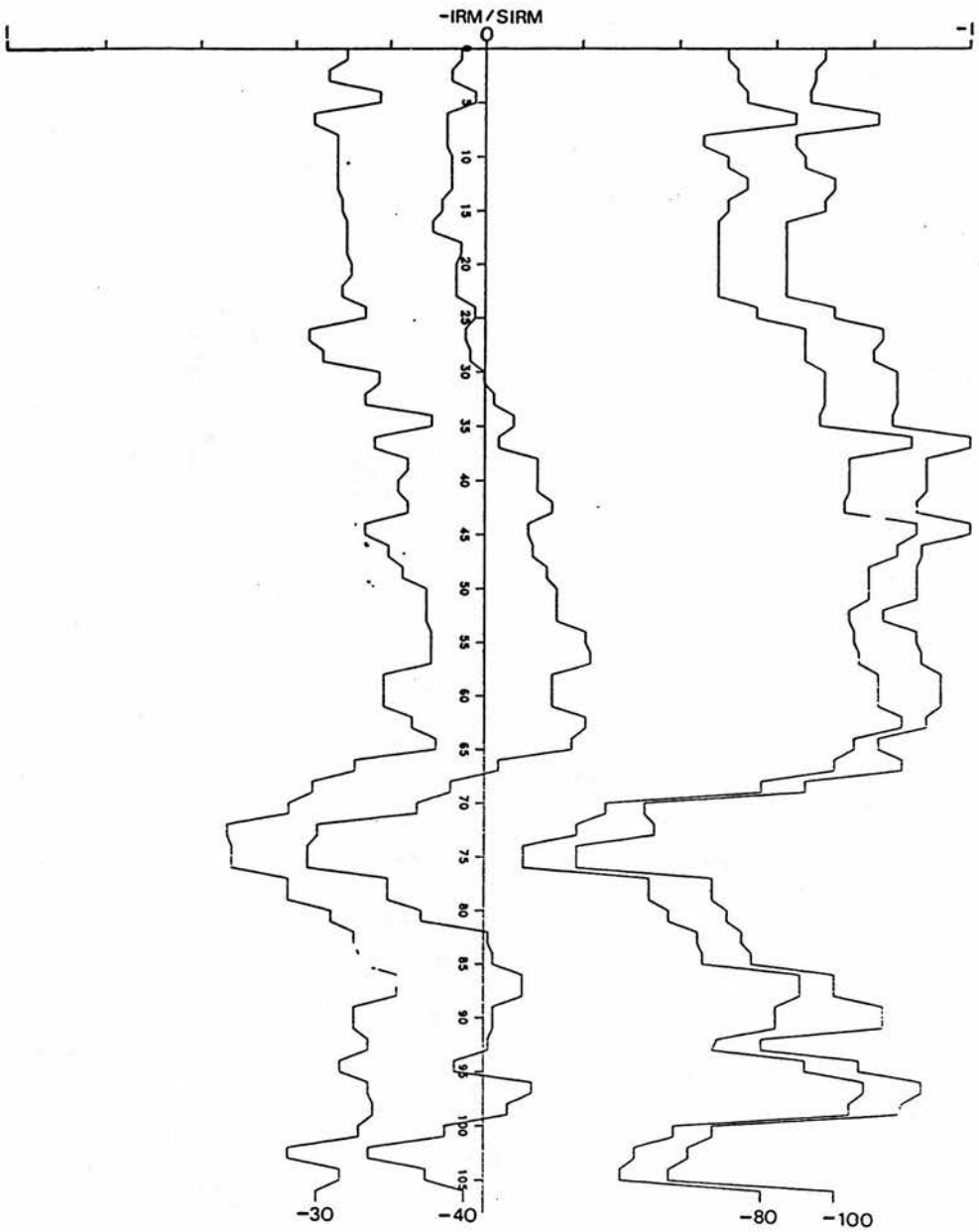

FIG 4/6: Core Ba(1) - Downcore variability of SIRM - demagnetisation response, determined through the subjection of saturated samples from 55 . stratigraphic levels to reversed fields of 30mT, 40mT, 80mT and 100mT.

falling within the range 42mT - 50mT (Fig 4/6). However, following the subjection of samples to a 100mT demagnetising field, reversed IRMs were found to fall 20% - 38% short of original SIRM values, indicating the additional presence of HIRM-bearing SSD magnetites, titanomagnetites or antiferromagnets.

B) At 19cm - 32cm depth, SIRM and Xlf signals decline to below 2mAm2kg-1 and 0.25μm3kg-1 respectively (Figs 4/5a and b). Accordingly, sub-samples from these strata appear to be characterised by ferrimagnetic depletion relative to the "whole core" mean (SIRM = 2.4mAm2kg-1). On account of the dis-proportionate decline of SIRM within these strata, SIRM/X ratios are depressed into the range 6kAm-1 to 9kAm-1 (Fig 4/5c). However, SIRM coercivities (Fig 4/6) are largely indistinguishable from those observed at 1cm to 18cm depth, suggesting that SIRM/X adjustments reflect the increased significance of paramagnetic phases to Xlf, rather than any marked downcore modification of ferrimagnetic mineral grain size.

C) Concentration-dependent signals increase progressively downward of 32cm depth, depicting a zone of ferrimagnetic enrichment which extends through to 68cm depth (Figs 4/5a - b). The extent of enrichment is most apparent upon comparing the peak SIRM value for this horizon (4.1mAm2kg-1) with the "whole core" mean of 2.4mAm2kg-1. In

addition, elevated mean SIRM/X ratios (8.1kAm-1) relative to those observed at 19cm - 32cm depth signify both the depression of paramagnetic influences upon X1f and the predominance of ferrimagnets within a 0.07µm - 0.1µm size range. These PSD/MD grains are, in turn, conspicuous by their effect upon the demagnetisation behaviour of samples, with SIRM coercivities falling within the range 37mT to 41mT and samples from 37cm and 45cm depths attaining SIRMs of reversed polarity following their subjection to a 100mT demagnetising field (Fig 4/6). Accordingly, all data suggest that magnetic assemblages become less granulometrically diverse downward of 18cm depth, with PSD or MD magnetites continuing to control the "concentration dependent" parameters, but with no significant HIRM bearing component in evidence.

D) At 69cm - 82cm depth, SIRM values yield a mean of only 1.0mAm2kg-1, demarking a zone of ferrimagnetic depletion in comparison to mean concentrations throughout the core (SIRM = 2.4mAm2kg-1). Sub-samples from these strata also show evidence of enrichment with antiferromagnetic phases, signified by a BO(CR) value in excess of 70mT at 75cm depth (Fig 4/6). This sample underwent only 20% SIRM reversal upon subjection to a 100mT demagnetising field, suggesting that around 40% of its' SIRM is attributable either to magnetites of below 0.04µm in size, antiferromagnets or titanomagnetites.

E) Downward of 83cm, ferrimagnetic mineral concentrations increase marginally (although remaining markedly below the "whole core" mean) with SIRM values attaining a maximum of 2.6mAm2kg-1 and yielding a mean of 1.1mAm2kg-1 in samples from 83cm - 100cm depth. Mean BO(CR) values of 38mT for these samples are also consistent with the re-emergence of PSD/MD magnetite dominated magnetic assemblages.

Core Ba (2)

Downcore fluctuations of magnetic mineral concentration and mineralogy are diagnostic of the presence of four magnetically discrete horizons in core Ba(2):-

A) Sediments extending from the sediment surface to 13cm depth form an analogous horizon to that described for the uppermost 18cm of core Ba(1), with mean SIRM and Xlf values of 1.9mAm2kg-1 and 0.2µm3kg-1 signifying strong ferrimagnetic mineral presence (Figs 4/7a-b). For comparison, the "whole core" mean SIRM value for core Ba(2) is 1.4mAm2Kg-1. Mean SIRM/X ratios of 9.1kAm-1 (Fig 4/7c) and BO(CR) values within the range 41mT - 47mT (Fig 4/8) are consistent with the predominance of ferrimagnets in excess of 0.045µm in size. However, the failure of samples to undergo more than 83% SIRM reversal upon subjection to a 100mT reverse field indicates the additional presence of haematite or titanomagnetite components.

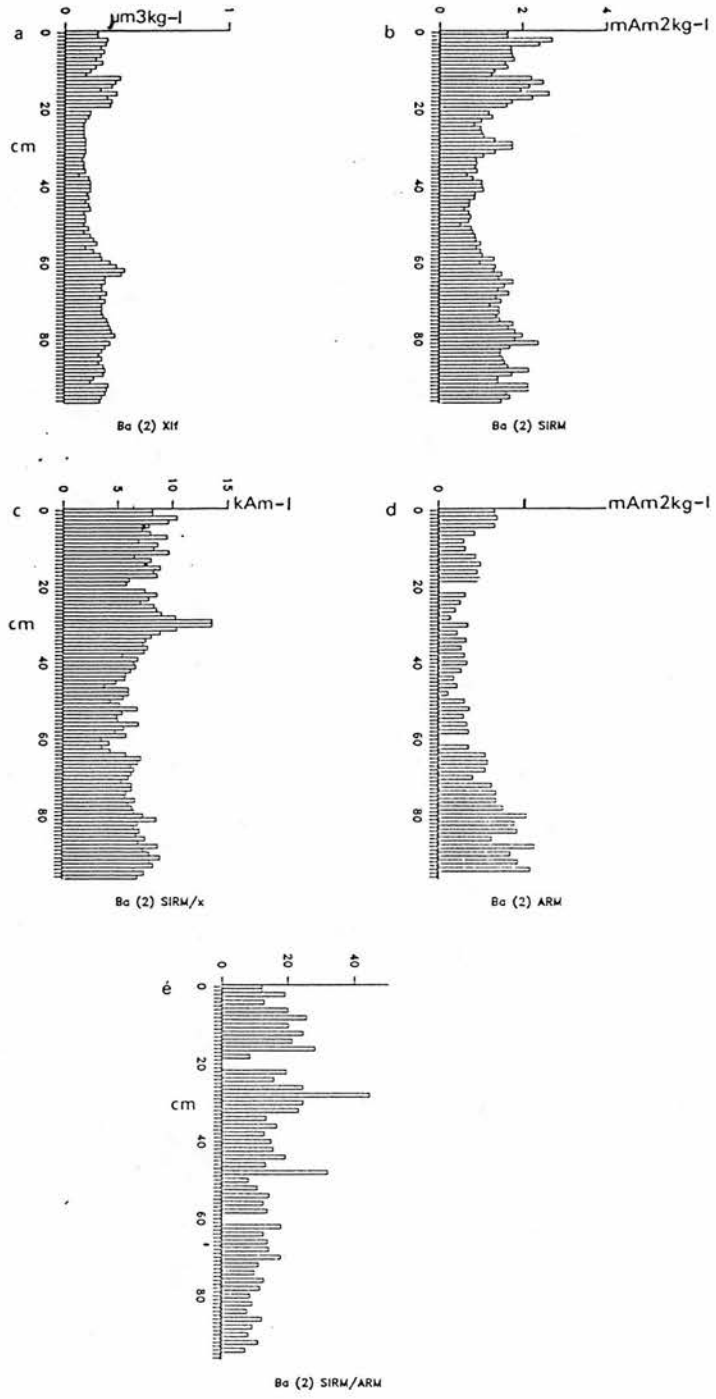

FIG 4/7: Core Ba(2) - concentration dependent (X, SIRM, ARM) and inter-parametric (SIRM/X, SIRM/ARM) magnetic data for sub-samples taken at 1 cm resolution. Note: SIRM/X and associated parameters are plotted at 96 stratigraphic levels. ARM data are plotted at 47 stratigraphic levels.

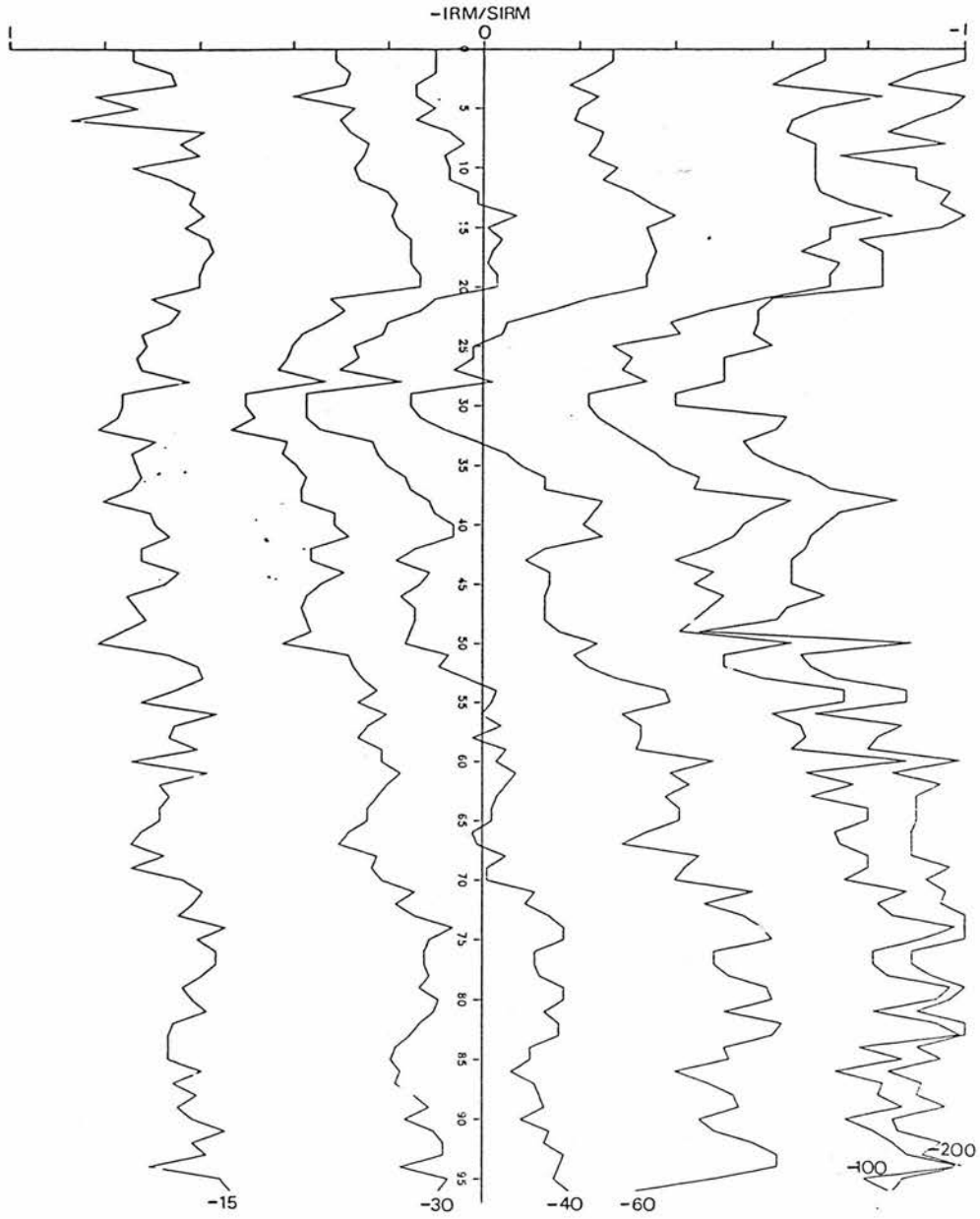

FIG 4/8: Core Ba(2) - Downcore variability of SIRM - demagnetisation response, determined through the subjection of saturated samples from 96 stratigraphic levels to reversed fields of 15mT, 30mT, 40mT, 60mT, 100mT and 200mT.

B) Sub-samples from between 15cm and 20cm depth contain only marginally higher ferrimagnetic mineral concentrations than the overlying strata (signified by mean values of 2.1mAm2kg-1 SIRM and 0.4μm3kg-1 Xlf), but three sources of evidence differentiate them mineralogically. Firstly, ratios of SIRM/X decline to a minimum of 6kAm-1 in strata at 15cm - 20cm depth (Fig 4/7c). These ratios cannot be paramagnetically controlled on account of the strong ferrimagnetic signals prevailing. Accordingly they appear diagnostic of the increasing presence of larger ferrimagnets within the 0.25μm - 1.0μm size range. Secondly, anomalously high SIRM values of 2.6mAm2kg-1 occur without any analogous enhancement of ARM (Fig 4/7d). Consequently, SIRM/ARM ratios increase from a mean of 17.1 at 1cm - 13cm depth to a peak of 32 at 17cm depth (Fig 4/7e) and, in accordance with SIRM/X data, signify a downcore coarsening of ferrimagnetic assemblages between 15cm and 19cm depth. Thirdly, granulometric distinctions between samples from 1cm - 14cm depth and those from 15cm - 20cm depth are apparent from their respective demagnetisation profiles (Fig 4/8). In particular, samples from 15cm - 20cm depth possess anomalously low SIRM coercivities (below 40mT) but are indistinguishable from samples taken from the overlying strata with respect to their behaviour in a 100mT demagnetising field. These data, therefore, indicate that the 14cm - 19cm sequence contains magnetically "hard" SSD components at concentrations which are similar to those

occurring in sub-samples from 1cm - 14cm depth, but with additional contributions to SIRM being attributable to the presence of larger, MD ferrimagnets in the 0.25μm - 1.0μm size range.

C) Sediments extending from 21cm - 54cm depth in core Ba(2) are most clearly characterised by their paucity of ferrimagnetic constituents, as indicated by the depression of Xlf and SIRM signals to respective means of 0.12μm3kg-1 (Fig 4/7a) and 0.9mAm2kg-1 (Fig 4/7b). These values, therefore, fall markedly below the whole "core means" for the concentration dependent parameters (Xlf = 0.20μm3Kg-1, SIRM = 1.4mAm2kg-1). In addition, samples from 31cm - 32cm depth yield elevated SIRM values of 1.8mAm2kg-1 without any concomitant variation of either ARM or Xlf, signifying the presence of a magnetic assemblage of mixed mineralogy, with antiferromagnetic concentrations increasing markedly. Such modifications are further confirmed by demagnetisation data, with samples from 31cm - 32cm depth displaying only 61% SIRM loss upon subjection to a 40mT demagnetising field and yielding BO(CR) values of 75mT (Fig 4/8).

D) Downward of 55cm depth, the elevation of Xlf and SIRM signals to respective maxima of 0.37μm3 g-1 and 2.1mAm2kg-1 is strongly indicative of an increase in ferrimagnetic mineral concentrations (Figs 4/7a - b). Notably, the mean SIRM value for the 55cm - 95cm horizon (1.6mAm2kg-1) is in excess of the "whole core" mean

(1.4mAm2kg-1). However, it is also apparent that while Xlf varies little downward of 65cm depth, SIRM and more significantly, ARM values (Fig 4/7d) show progressive increments with depth, attaining maxima at 80cm - 85cm. Consequently, ratios of SIRM/X increase from 3.7kAm-1 at 60cm depth to 9.6kAm-1 at 92cm depth, with SIRM/ARM ratios falling from 19 at 61cm depth to 5.5 at 95cm depth (Figs 4/7c-e). Interparametric data, therefore, suggest that while ferrimagnetic enhancement characterises the entire 55cm - 97cm sequence, a progressive downcore refinement of ferrimagnetic mineral granulometry also occurs within these strata.

Demagnetisation profiles (Fig 4/8) indicate that, while all samples within the 55cm - 95cm sediment sequence are characterised by "soft" demagnetisation behaviour, BO(CR) values decrease progressively downcore, to a minimum of 31mT at 95cm depth. The extent of IRM reversal upon the placement of samples within a 100mT demagnetising field displays similar downcore variability, with SIRMs of reversed polarity being produced within the sample from 94cm depth. Given the downcore refinement of ferrimagnetic mineral granulometry signified by trends of SIRM/X and SIRM/ARM, this downcore softening of magnetic remanence cannot be attributed to conventionally cited granulometric influences. Accordingly, it can be deduced that while ferrimagnets control the concentration dependent and

interparametric data obtained for samples from 55cm - 97cm depth, HIRM-bearing components also occur in concentrations which increase progressively upward of 97cm depth, causing a concomitant upward increase in SIRM coercivities.

Core Ba (3).

Examination of the "concentration dependent" magnetic data derived from analyses of core Ba(3) facilitates the identification of two magnetically distinct horizons (Figs 4/9a - b):-

A) Samples from 1cm - 22cm depth display respective mean SIRM and Xlf values of 1.7mAm2kg-1 and Xlf = 0.2µm3kg-1, suggesting considerable magnetic enhancement in comparison to mean conditions throughout the core (SIRM = 0.6mAmkg-1). Interparametric data for these samples, showing SIRM/X ratios to fall within the range 5.8kAm-1 - 10.8kAm-1 and SIRM/ARM values to yield a mean of 24, are indicative of the prevalence of magnetites of 0.05µm - 0.25µm in size (Figs 4/9c and e). These PSD/MD mineral phases are, in turn, conspicuous through their influence on the SIRM-demagnetisation behaviour of samples, with BOCR values falling within the range 38mT - 44mT (Fig 4/10). Because samples from 2cm, 5cm, 12cm to 16cm and 18cm to 22cm depths also attain SIRMs of reversed polarity upon their subjection to a 200mT demagnetising field, antiferromagnets can be assumed to be absent.

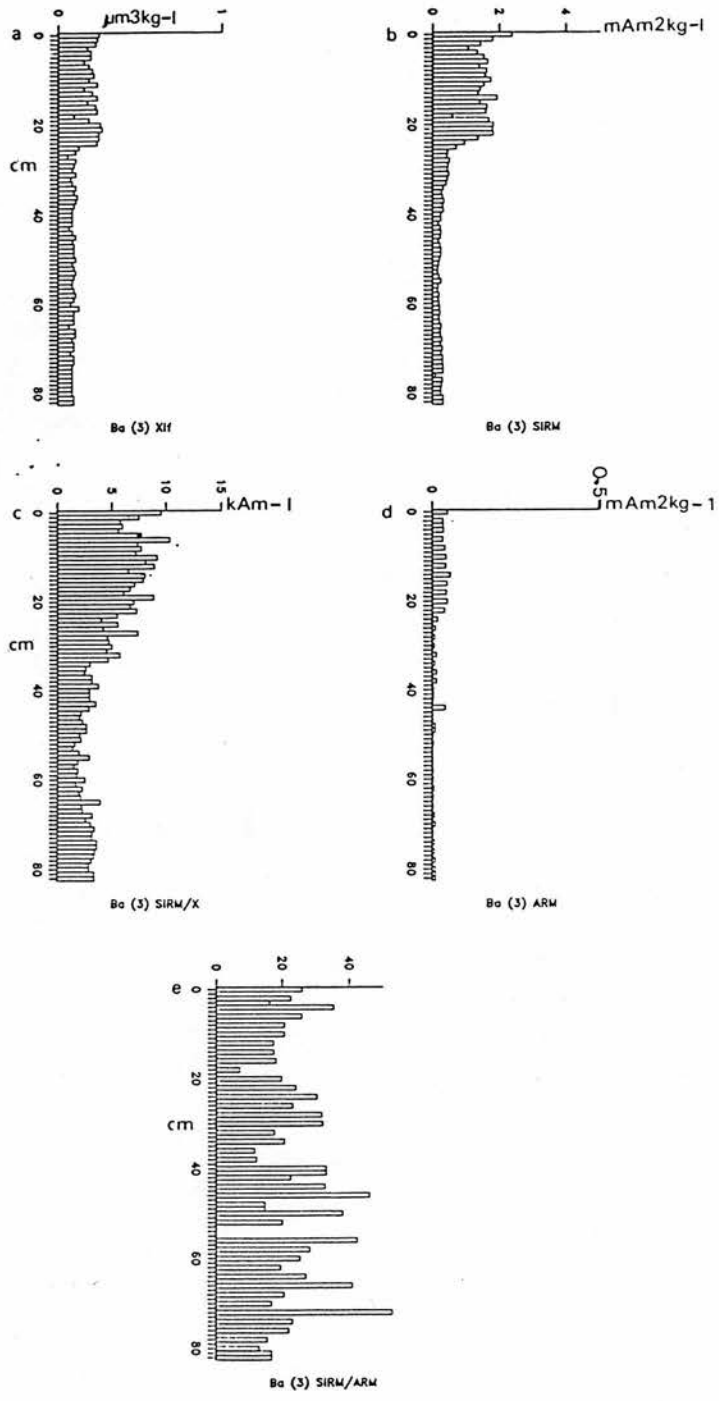

FIG 4/9: Core Ba(3) - Concentration dependent (X, SIRM, ARM) and inter-parametric (SIRM/X, SIRM/ARM) magnetic data for sub-samples taken at 1cm resolution. Note: SIRM, X and associated parameters are plotted at 83 stratigraphic levels. ARM data are plotted at 44 stratigraphic levels.

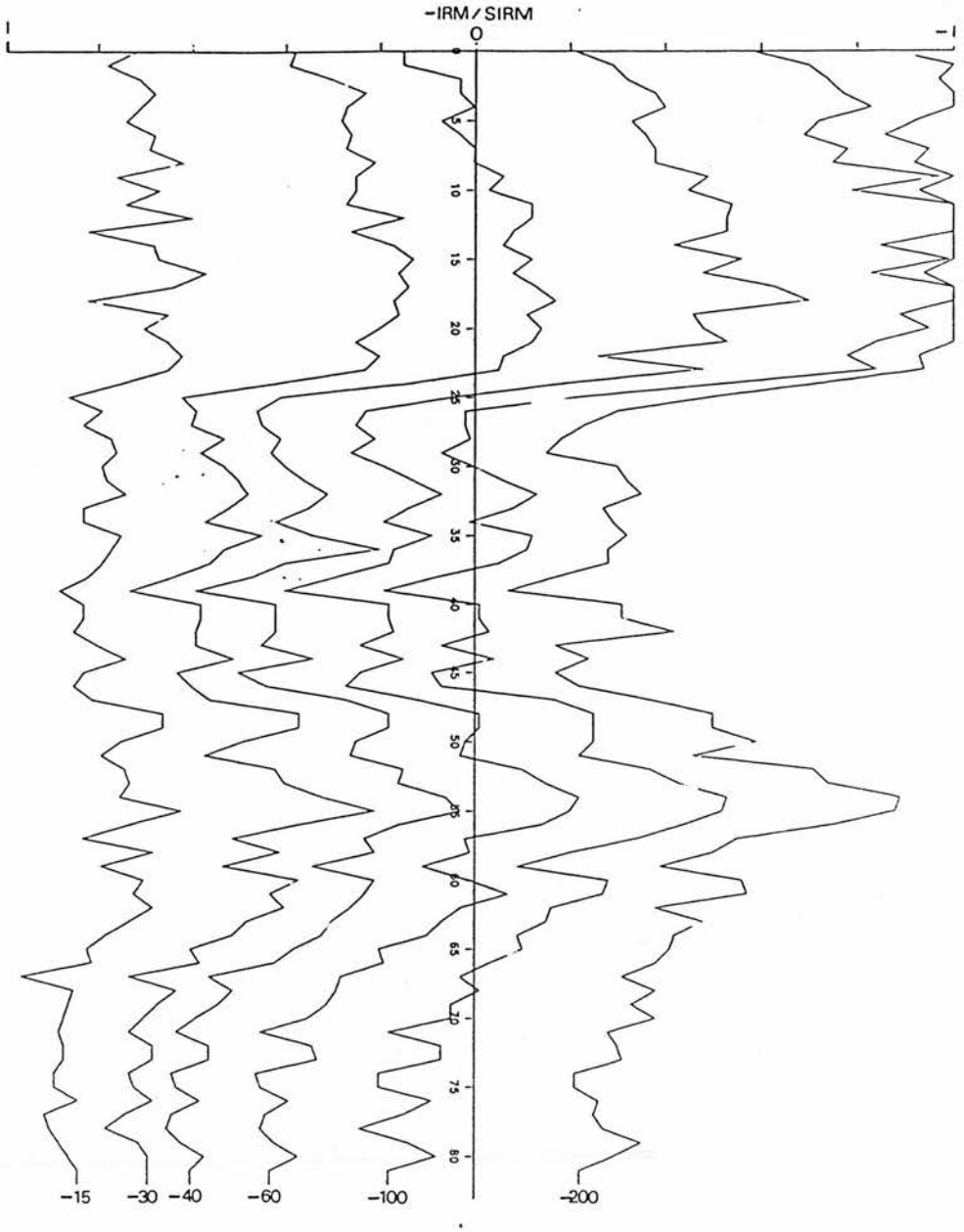

FIG 4/10: Core Ba(3): Downcore variability of SIRM - demagnetisation response, determined through the subjection of samples from 83 stratigraphic levels to reversed fields of 15mT, 30mT, 40mT, 60mT, 100mT and 200mT.

B) Samples from 23cm - 87cm depth are characterised by low ferrimagnetic mineral concentrations, yielding SIRM values of below 0.5mAm2kg-1 throughout (Fig 4/9). On account of the prevalence of such weak signals, interparametric data appear to provide no reliable indication of magnetic mineral granulometry, with SIRM/X ratios of 1.7kAm-1 - 6kAm-1 probably being attributable to the influence of paramagnetic Fe phases (Fig 4/9c). In turn, the elevated SIRM/ARM ratios in these strata appear more reflective of the presence of ARM discriminated ferrimagnets at "noise level" concentrations than of any downcore variation of magnetite grain size (Figs 4/9d and e).

Upon examining the demagnetisation behaviour of samples taken from the 23cm - 83cm sequence (Fig 4/10), several formerly undetected downcore mineralogical variations are identifiable. Specifically, while all samples from these strata contain similarly low ferrimagnetic mineral concentrations, BO(CR) values in the range 89mT - 125mT for the samples from 23cm - 47cm and 65cm - 83cm depths appear diagnostic of the presence of mixed mineral assemblages, within which unusually high haematite or titanomagnetite concentrations occur. In contrast, samples from between 52cm and 58cm depths display SIRM coercivities of less than 60mT, suggesting the return towards a mono-minerogenic, ferrimagnetic assemblage within these strata.

4.3 Results of magnetic analyses following sample oxidation and sequential mineral extraction.

4.3.1 Loch Dee cores.

In accordance with the previously established rationale (section 2.3), the volume magnetic susceptibities (χ) of wet sediment samples from 1cm, 4cm, 7cm, 14cm, 21cm, 28cm, 35cm and 50cm levels of core Dee(4) were measured at 14 day intervals over the period 1.11.86 - 1.3.87. During this period, all samples were stored under atmospheric conditions at room temperature, thus allowing their progressive oxidation.

The results of the above analyses (Table 30) signify a general stability of magnetic signals throughout the four month storage period, with none of the Dee(4) samples undergoing χ losses in excess of 6%. Given that instrumental fluctuations during the measurement period may have been of the order of 10%, such temporal χ changes can be considered insignificant and it may be deduced that the minerals contributing to χ within the Loch Dee sediment reservoir are not highly sensitive to changes of oxidation state. Furthermore, the most notable χ variations actually involve the enhancement of magnetic susceptibilites in samples taken from 1cm, 21cm and 28cm depths. In accordance with the findings of Hilton et al (1986), these increments appear to

be a product of sample shrinkage, thus producing increased ferrimagnetic mineral concentrations per unit volume.

Table 30. Volume magnetic susceptibity (um/10cc) of selected sediment samples from core Dee (4) during storage under atmospheric conditions.

Sample	Original χ 1.11.86	χ on 14.11.86	χ on 1.3.87
1cm	0.45	0.45	0.50
4cm	0.73	0.76	0.72
7cm	0.31	0.29	0.30
14cm	0.14	0.14	0.14
21cm	0.10	0.11	0.13
28cm	0.10	0.11	0.13
35cm	0.09	0.10	0.10
50cm	0.16	0.15	0.15

4.3.2 Loch Ba Cores.

Analyses of χ for wet sediment samples taken from 1cm, 4cm, 7cm, 10cm, 16cm, 20cm, 25cm, 30cm, 40cm and 80cm levels of core Ba(1) were carried out at 14 day intervals during the period 9.9.86 - 10.1.87. During this period, all samples were stored under normal atmospheric conditions at room temperature.

From the results of the above analyses (Table 31) a stratigraphic zone extending from 4cm - 16cm depth in core Ba(1) appears to be conspicuous by the presence of magnetic

assemblages which are highly sensitive to progressive oxidation. Specifically, variations between the initial and post-storage χ signals for samples from 4cm, 7cm, 10cm and 16cm depth fall within the range 28% - 38%, while all other samples underwent χ losses of less than 15% during storage.

Table 31. Volume magnetic susceptibility (um/10cc) of selected sediment samples from core Ba(1) during storage under atmospheric conditions.

Sample	Original χ 9.9.86	χ 23.9.86	χ 7.10.86	χ 10.1.87
1cm	0.26	0.23	0.22	0.22
4cm	0.32	0.24	0.22	0.20
7cm	0.40	0.34	0.31	0.29
10cm	0.28	0.21	0.19	0.18
16cm	0.24	0.20	0.20	0.16
20cm	0.31	0.30	0.30	0.28
25cm	0.31	0.32	0.31	0.30
30cm	0.58	0.57	0.58	0.58
40cm	0.44	0.45	0.46	0.46
80cm	0.20	0.19	0.21	0.21

Data acquired through the subjection of samples from core Ba(1) to SIRM analyses during storage further confirm that the 4cm - 16cm sequence is characterised by the disproportionate presence of oxidation-sensitive ferrimagnets (Table 32). However, it is notable that only the 7cm subsample displays a high SIRM loss (42%) relative to the loss of χ (28%) occurring during storage. In contrast to the findings of Thompson (pers. comm) it may, therefore, be deduced that the oxidation-sensitive magnetic components in

the Loch Ba sediments predominantly yield low SIRM/susceptibility ratios. In turn, these ratios may be considered diagnostic of the residence of oxidation-sensitive minerals within coarse, PSD/MD magnetic grain structures.

Table 32. SIRM (mAm M2) of selected samples from core Ba(1) during storage under atmospheric conditions.

Sample	Original 9.9.86	SIRM on 23.9.86	SIRM on 7.10.86	SIRM on 10.1.87
1cm	0.400	0.395	0.397	0.390
4cm	0.365	0.305	0.300	0.301
7cm	0.340	0.260	0.214	0.198
10cm	0.267	0.210	0.201	0.190
16cm	0.295	0.251	0.227	0.210
20cm	0.184	0.175	0.173	0.173
25cm	0.190	0.189	0.187	0.190
80cm	0.164	0.160	0.157	0.163

In an attempt to fully characterise the mineral phases producing temporal losses of magnetic intensity within the 4cm - 16cm sequence of core Ba(1) during storage, previously described sequential chemical analyses were carried out on sub-samples from 7cm, 9cm and 17cm depths (see section 2.3.6). From the results of these analyses (Table 33), the following trends are particularly significant:-

1) Variations of χ occurring upon the leaching of samples with 1M.MgCl are both minimal (<6.5%) and reversible.

Table 33: Percentage change of volume magnetic susceptibility occurring within selected sub-samples from core Ba (1) following the sequential removal of adsorbed, carbonate, AVS and NVS mineral phases by chemical methods.

Sample	Original χ	%Δ MgCl	%Δ NaOAc	%Δ HOAc	%Δ 30%H2O2
7cm	0.31	-6.5	+6.4	-8.7	-13.0
9cm	0.36	0	+9.1	-11.0	-34.0
17cm	0.32	-3.2	0	-10.0	-25.4

Hence, adsorbed mineral phases cannot constitute the oxidation-sensitive component of the magnetic assemblages within the 4cm - 17cm sediment sequence.

2) The leaching of samples for two hours with 1M.NaOAc (pH 5.0) promoted no depression of χ signals. In accordance with the previously noted dearth of carbonate Fe in the Loch Ba sediments (see Fig 3/28), such stability is indicative of the insignificance of carbonates within the magnetic fraction of the analysed sub-samples.

3) Sub-samples from 7cm, 9cm and 17cm depths of core Ba(1) lost 8.7% - 11% of the mineral phases contributing to their original χ signals following leaching with 1M.HOAc, suggesting that a small, poorly crystalline or AVS component exists within the magnetic assemblage.

4) Losses of χ of the magnitude observed in samples from the 4cm - 16cm sequence of core Ba(1) during storage occurred within the 9cm and 17cm sub-samples following agitation with 30% H_2O_2. It may, therefore, be assumed that a crystalline, non-volatile sulphide mineral comprises the major oxidation-sensitive component of the magnetic assemblage of these samples.

5) The 13% loss of χ observed following the treatment of the 7cm sample with H_2O_2 is clearly not reconcilable with the 28% loss of χ which occurred within sediments from this stratigraphic level during storage. Accordingly, it is likely that while 28% of the minerals contributing to χ in fresh sediments would have been removed by H_2O_2 oxidation, some compensatory ferrimagnetic enhancement has occurred in the sample. Such enhancement plausibly reflects both the reduction of the sample volume resulting from the oxidation of organic matter by H_2O_2 (thus producing increased mass specific ferrimagnetic oxide concentrations within the susceptibility bridge) and the neo-formation of Fe_3O_4 as a consequence of the thermal regime prevailing during the H_2O_2 leaching process.

4.4 Summary of magnetic data.

4.4.1 Loch Dee Cores.

Concentration dependent magnetic data for cores

Dee(3) and Dee(4) show ferrimagnetic minerals to be equally distributed throughout strata at 10cm - 90cm depth, where values of Xlf and SIRM remain below 0.12μm3kg-1 and 1.0mAm2kg-1 respectively. Upward of 8cm depth, ferrimagnetic mineral concentrations increase progressively, producing Xlf and SIRM maxima of 0.52μm3kg-1 and 9.1mAm2kg-1 in the uppermost 3cm. Ferrimagnetic signals appear to be attributable to stable oxide phases rather than to authigenic sulphides at all depths.

The downcore mineralogical variations observed within the Loch Dee sediment reservoir are summarised in Figs 4/11 and 4/12, showing the relationships of SIRM/X and SIRM/ARM with IRM-100mT/SIRM (S) for 60 samples from core Dee(3). Cross-plots of SIRM/X against S clearly differentiate between samples from the uppermost 8cm and those from the underlying strata, with the former falling into the upper left sector of Fig 4/11. These surficial samples fall within an SIRM/X - S range which is typical of mono-mineralogenic assemblages in which magnetites of 0.05μm - 0.25μm dominate (Thompson 1986, Bradshaw and Thompson 1984, Hirons and Thompson 1986).

Samples from between 10cm and 90cm depth contravene accepted, granulometrically controlled relationships between SIRM/X and S for magnetite as they fall below and to the right of those taken from 1cm - 8cm depth (Fig 4/11). The "harder" demagnetisation behaviour of the samples from 10cm

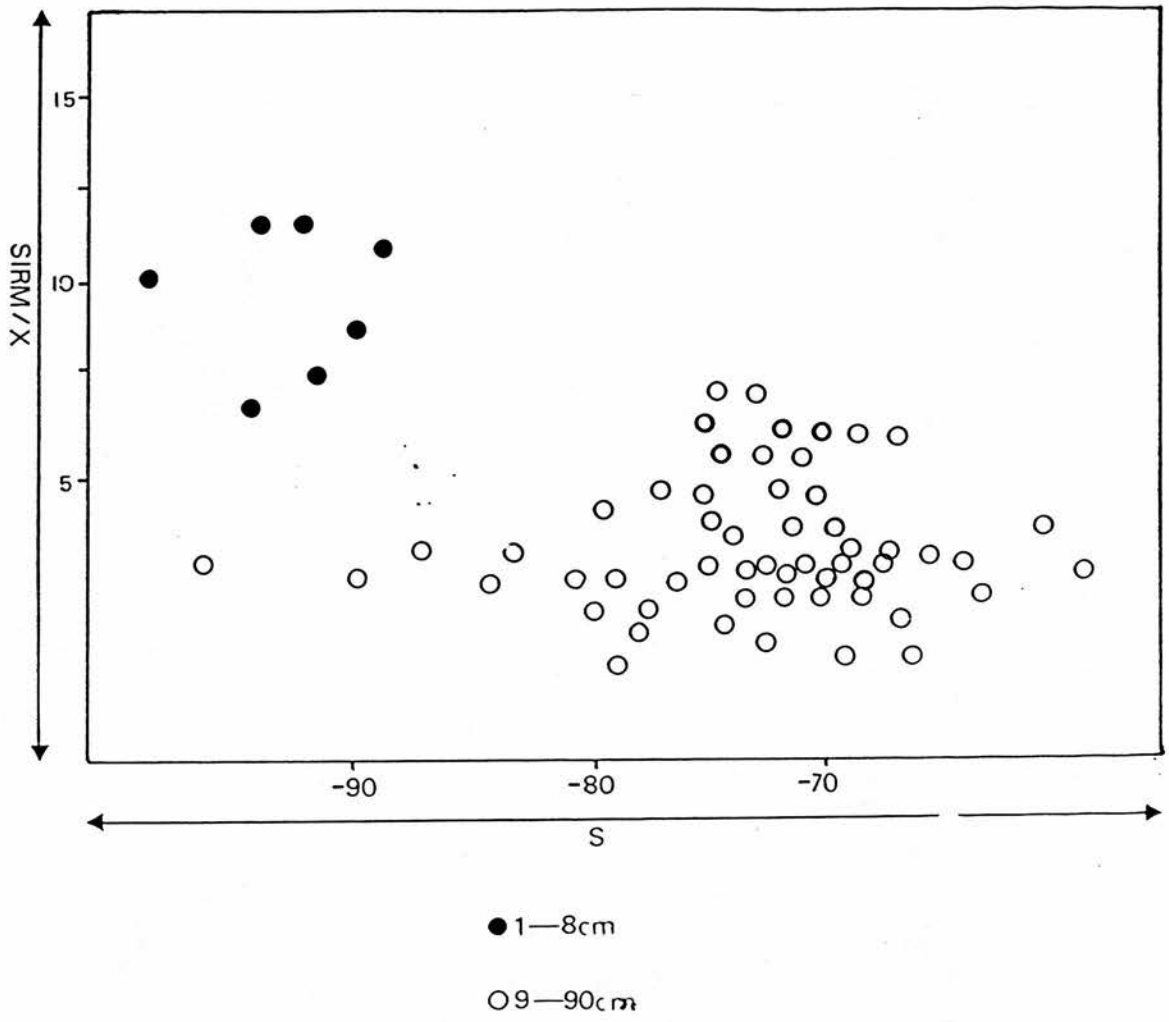

FIG 4/11: Sirm/X vs S (-0.1mT IRM/SIRM) relationships for sub-samples from 60 stratigraphic levels of core Dee(3). Ferrimagnetically enriched samples from the uppermost 8cm of the core are conspicuous by their relatively "soft" demagnetisation behaviour and elevated SIRM/X ratios.

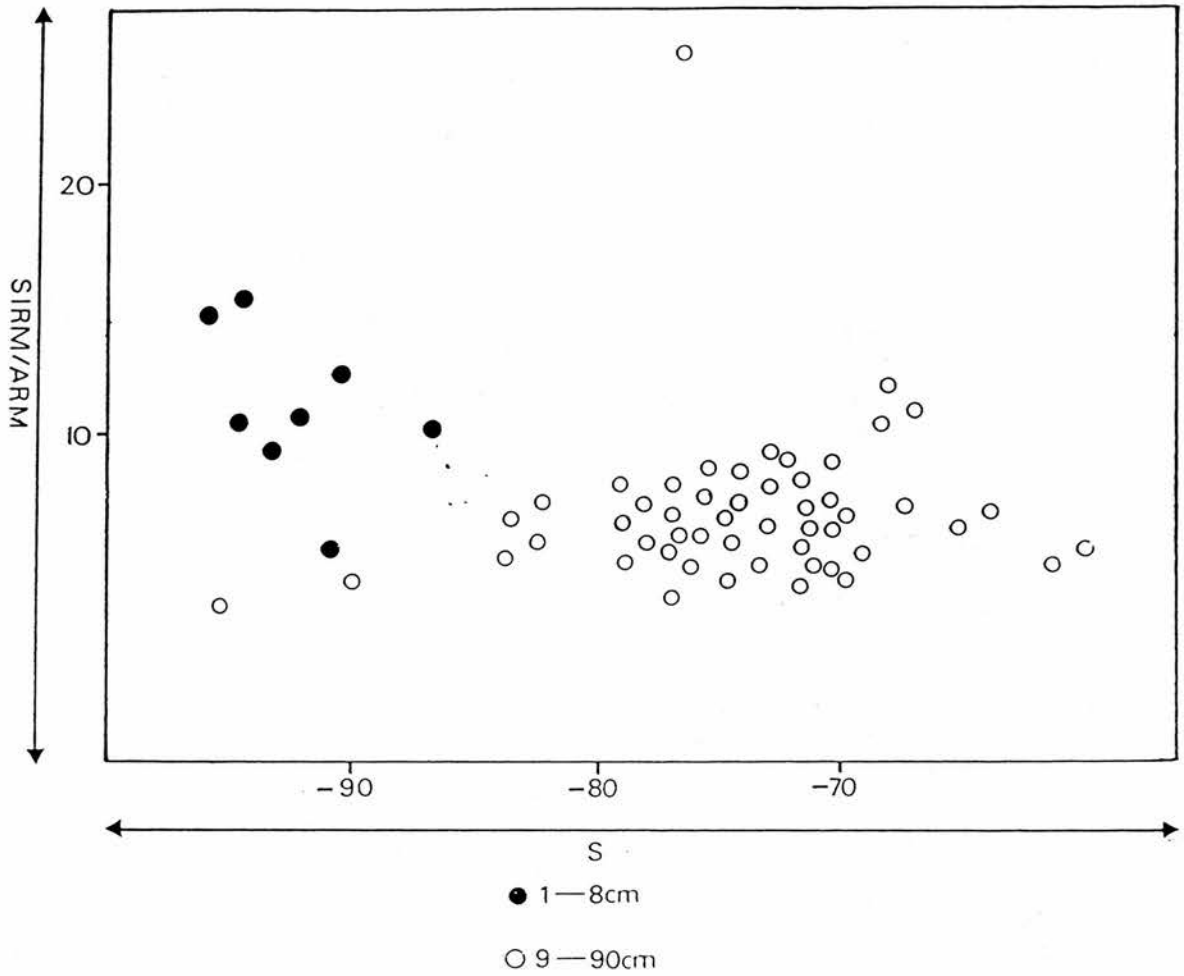

FIG 4/12: SIRM/ARM vs S (-0.1mT IRM/SIRM) relationships for sub-samples from 60 stratigraphic levels of core Dee(3). Ferrimagnetically enriched samples from the uppermost 8cm of the core are conspicuous by their relatively high SIRM/ARM ratios and "soft" demagnetisation behaviour. These trends are diagnostic of a coarsening of ferrimagnetic mineral granulometry towards the sediment surface.

- 90cm depths, in combination with SIRM/X ratios in the range 3.0 - 8.0 must, therefore, be diagnostic of a downcore shift towards an SSD (<0.05um) dominated assemblage, in which both antiferromagnets and paramagnets are significant.

By cross-plotting SIRM/ARM against S for 60 samples from core Dee(3), granulometric distinctions between the ferrimagnetic components of the Loch Dee sediments can be summarised (Fig 4/12). Again, samples from the uppermost 8cm of sediment fall above and to the left of all other samples, in the SIRM/ARM v S range typified by 0.07μm - 0.15μm magnetites. In contrast, underlying samples exhibit "harder" demagnetisation behaviour and higher proportions of ferrimagnets discriminated by ARM rather than by SIRM (0.03um - 0.05um). Hence the samples from 10cm - 90cm depth fall towards the lower right sector of Fig 4/12, reflecting a downcore refinement of ferrimagnetic mineral granulometry.

4.4.2 Loch Ba Cores.

In contrast to the results obtained from analyses of sample cores from Loch Dee, concentration dependent magnetic data (SIRM, ARM and Xlf) for cores Ba(1), Ba(2) and Ba(3) illuminate complex variations in the flux of ferrimagnets to the sediment reservoir. These fluctuations are conspicuous both with sediment depth and across the basin (as reflected by the limited similarity between the Xlf or SIRM profiles

of the respective sample cores). In core Ba(1), high ferrimagnetic mineral concentrations (SIRM >2.0mAm2kg-1) occur within discrete stratigraphic sequences at 1cm - 18cm and 32cm - 68cm depth. In core Ba(2), similarly enhanced strata are observable at 1cm - 20cm depth and 60cm - 100cm depth. In core Ba(3), SIRM values exceed 1.0mAm2kg-1 only in the uppermost 23cm of sediment.

Selected samples from core Ba(1) lost up to 38% of their original χ both during storage under atmospheric conditions and upon subjection to leaching with H2O2. Downcore variations of magnetic mineral concentrations in the Loch Ba sediment reservoir are not, therefore, universally attributable to changing influxes of Fe oxides.

The downcore mineralogical variations within the Loch Ba sample cores are summarised in Fig 4/13, showing the relationship of SIRM/X with IRM-100mT/SIRM (S) for samples from all distinctive magneto-stratigraphic levels of cores Ba(2) and Ba(3). From this figure, it is possible to discern the presence of five mineralogically distinct magnetic assemblages. These are:-

1) Mono-mineralogenic assemblages dominated by magnetites in the size range 0.04µm - 0.1µm, characterising samples from 80cm - 97cm depth in core Ba(2) and from the uppermost 22cm of core Ba(3). A paucity of small (<0.04µm) SSD ferrimagnets, paramagnets and antiferromagnets causes these

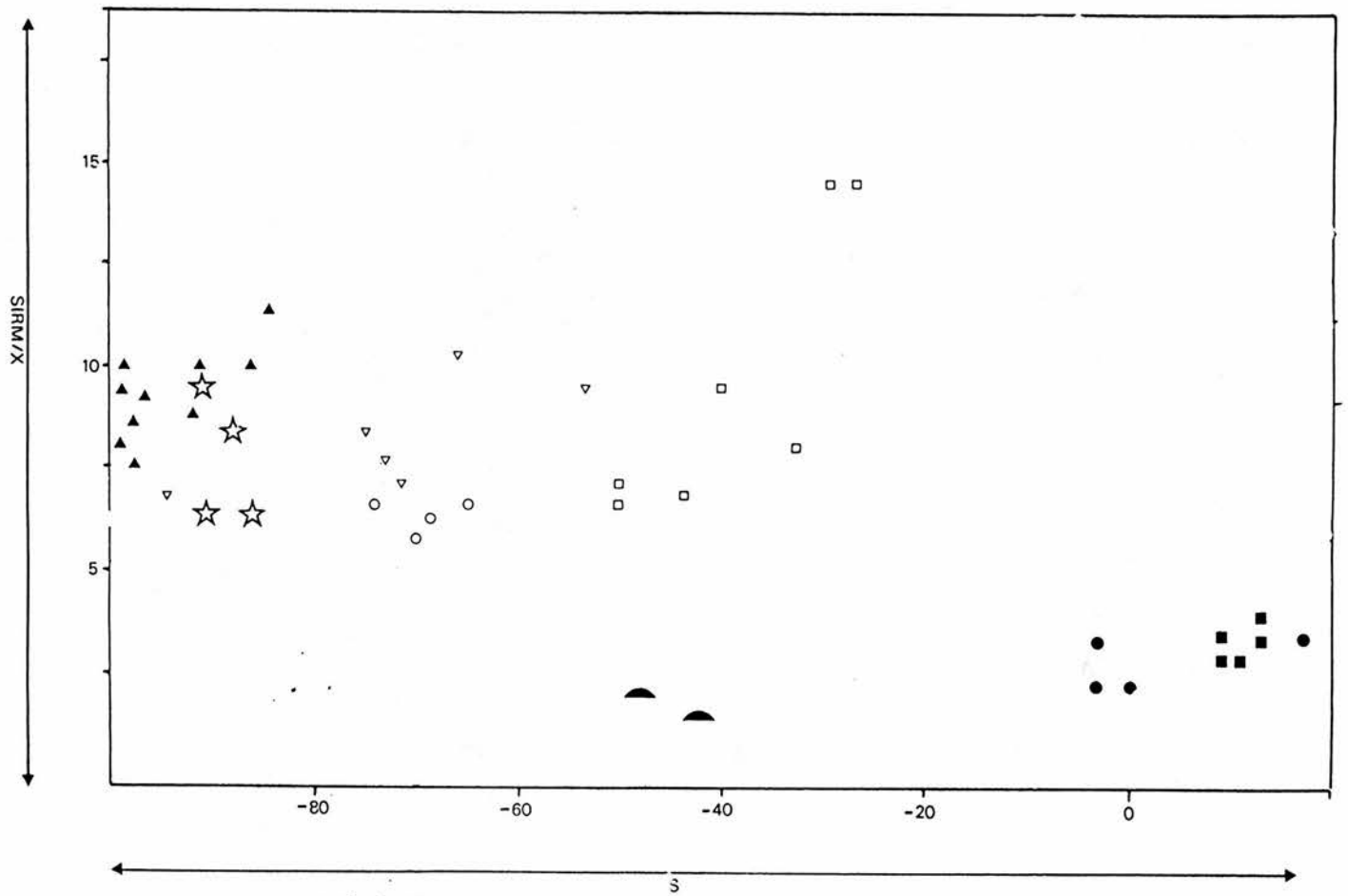

FIG 4/13: SIRM/X vs S (-0.1mT IRM/SIRM) for selected sub-samples from cores Ba(2) and Ba(3). Samples plotting to the left are magnetite dominated, while samples plotting to the right are haematite dominated. For samples with SIRM/X ratios of below 5kAm-1, paramagnetic phases can be assumed to exert a major control.

samples to fall to the left of Fig 4/13, in the SIRM/X range 6kAm-1 - 11kAm-1.

2) Assemblages holding high ferrimagnetic concentrations (thus precluding paramagnetic influences on SIRM/X) alongside significant antiferromagnetic components, typifying samples taken from 1cm to 20cm depths of core Ba(2). While the presence of antiferromagnets causes all these samples to fall within the -60 to -80 S range, the greater presence of MD ferrimagnets (0.1um - 0.25um) in samples from 15cm - 20cm depths of core Ba (2) results in their tendency to fall directly below those from 1cm - 14cm depth.

3) Mixed mineral assemblages containing similar antiferromagnetic mineral concentrations to the samples described above, but containing markedly depleted ferrimagnetic concentrations. Samples taken from 21cm - 54cm depths of core Ba(2) fall most obviously within this category. While SIRM/X ratios for these samples fall in the range 7kAm-1 to 15kAm-1, indicating that "concentration dependent" parameters are controlled by ferrimagnets of up to 0.15μm size, low ferri/antiferromagnetic mineral ratios cause these samples to be plotted to the right of centre on the "S" axis.

4) Assemblages in which low ferrimagnetic mineral concentrations occur alongside significant haematite concentrations. Such assemblages produce similar "S" values to those described above. However, paramagnetic Fe phases strongly influence Xlf on account of the weakness of

ferrimagnetic signals. Accordingly, these assemblages, typifying samples from 52cm - 55cm depths of core Ba(3), lie towards the centre of the "S" axis and at the base of the SIRM/X axis in Fig 4/13, irrespective of ferrimagnetic mineral granulometry.

5) Assemblages dominated by SSD haematite and paramagnets, typifying samples from 65cm - 87cm depths of core Ba(3). While the predominance of anti-ferromagnets causes samples to plot to the right of the "S" axis, paramagnetic controls depress SIRM/X ratios into the lower, 2kAm-1 - 5kAm-1 range, normally associated only with MD magnetites.

4.5 Interpretation of magnetic data.

4.5.1 Loch Dee cores.

Magnetic analyses of cores Dee(3) and Dee(4) indicate that upwardly increasing "concentration dependent" signals are solely attributable to the enrichment of stable Fe oxides within the surficial strata. Hence, of the diagenetic (Hilton et al 1986), lithogenic (Dearing 1979) and anthropogenic (Oldfield et al 1983) mechanisms previously cited in explanation of downcore mineral magnetic variations analogous to those observed in cores Dee(3) and Dee(4), the authigenic formation of Fe3S4 (Karlin 1984, Berner 1981, Price 1977) can be considered insignificant. Excepting the

influence of paramagnetic Fe phases (shown by Fig 3/13 to exclude siderite but plausibly to include amorphous FeS and pyrite), all downcore magnetic fluctuations can, therefore, be interpreted solely by reference to lithospheric or anthropogenic processes.

a) Lithogenic influences:

In the previous chapter, the limited downcore variability of total Mg and Ni, Co, Mn and Fe silicates, Co/Ni ratios and LOI within sample cores was shown to be diagnostic of the lithogeochemical consistency of strata forming the uppermost 20cm of the Loch Dee sediment reservoir. Evidence derived from the downcore mineral magnetic records of cores Dee(3) and Dee(4) may, in turn, be invoked to qualify these geochemically based conclusions. For example, it is inconceivable that the ferrimagnetic enhancement of strata forming the uppermost 10cm of sediment reflects some spontaneous, naturally instigated erosional event, given the known long term consistency of the sedimentological regime within the basin. This point is unequivocally demonstrated by the low variability of SIRM, Xlf, ARM and S throughout the entire 0.1m - 5.0m sectors of a 6m Macker th core (Fig 4/14) taken from coring station Dee(3). Pollen evidence suggests that this core provides a continuous sedimentary record extending to around 4000yrs BP, over which time no ferrimagnetically enhanced sediment fluxes have occurred.

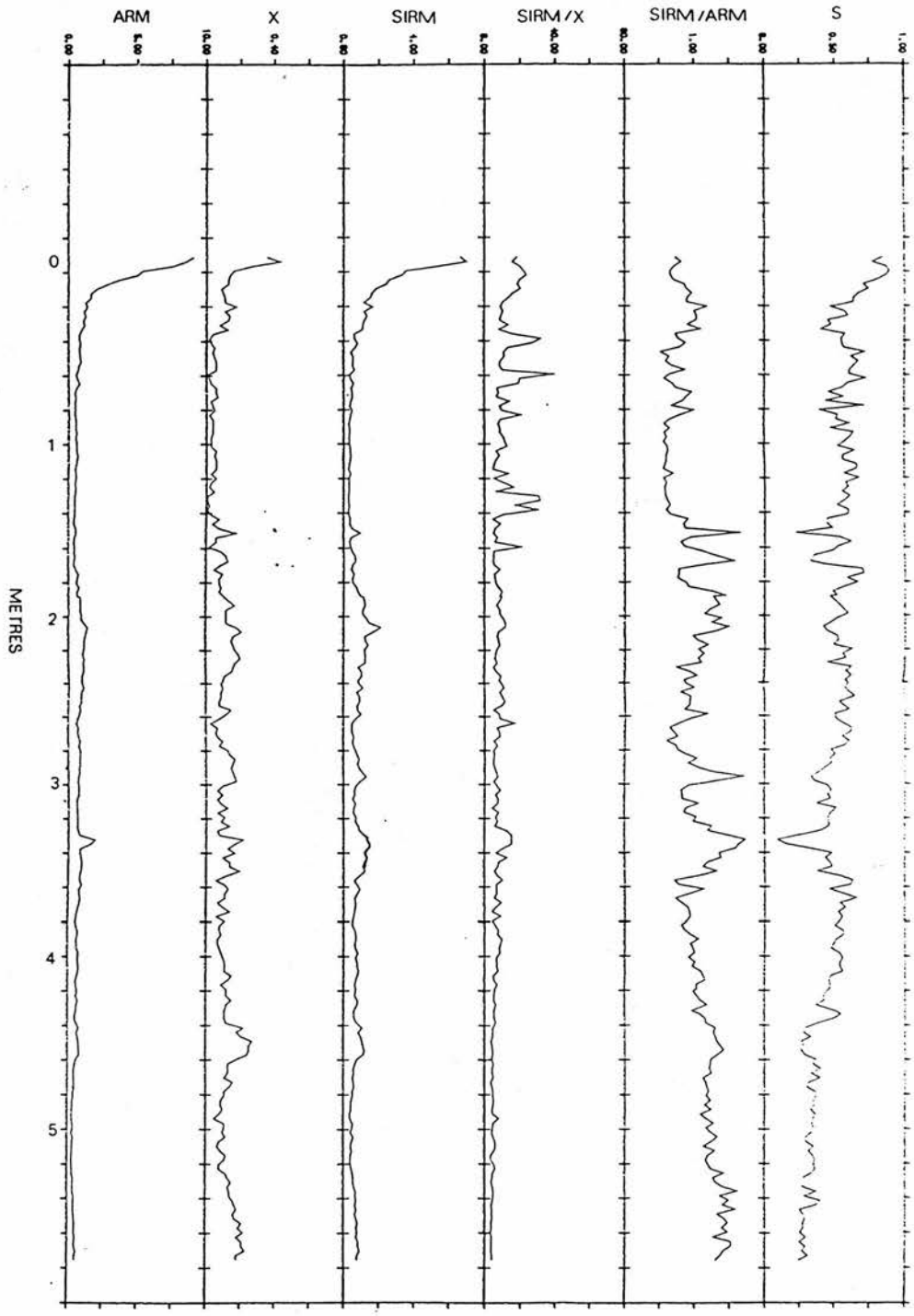

FIG 4/14: Downcore mineral magnetic trends through a 6m Mackereth core from station Dee(3). The consistency of ARM, SIRM and S through the 20cm - 500cm core sectors is indicative of the unvariable mineralogy of detrital magnetic mineral influxes during the sedimentation period.

While previous workers have more frequently identified downcore variations in magnetic mineralogy resulting from the modification of sediment supplies by human activities (Thompson et al 1975, Smith 1986, Higgitt 1982, Worsley 1983, Thompson and Oldfield 1986, Dearing and Flower 1982, Hirons and Thompson 1986), such synchronous cultural catalysts are also unidentifiable in the Loch Dee Basin. More specifically, the palynological data of Moar (1969) and Birks (1972) and documented land use records (Boatman 1983), all indicate an absence of agrarian adjustments in the Loch Dee catchment prior to the 1962 afforestation programme. The progressive enhancement of ferrimagnetic fluxes to sediments deposited throughout the period between 150yrs BP and the present (defined by 210Pb dates for core Dee 3, given in section 3.6.1) cannot, therefore, be attributed to the modification of sediment sources through human activities.

Enhanced influxes of pedogenic magnetites to lake sediments, often resulting from pre-afforestation ploughing, have typically been found to be associated with the increased deposition of 0.03μm - 0.035μm ferrimagnetic grains, falling around the SP/SSD boundary (Hunt et al 1984, Oldfield et al 1983, Maher 1984, Mullins 1977). In granitic catchments such as Loch Dee, magnetic minerals derived from the lithosphere may also be expected to contain significant antiferromagnetic components (as shown by the HIRM-bearing minerals observed in samples from the 10cm - 90cm levels of

core Dee 3). Accordingly, it may be predicted that any ferrimagnetically enriched strata which are a product of increased detrital fluxes of magnetic phases into the Loch Dee basin should display anomalously low SIRM/ARM ratios and SIRM coercivities in excess of 60mT. However, within the uppermost 10cm of cores Dee(3) and Dee(4) a direct reversal of these trends can be identified, with SIRM/ARM ratios rising from a mean of 6.9 at 10cm - 90cm depth to 14 at 3cm and BO(CR) falling to below 40mT at 4cm - 5cm depth. These ferrimagnetically enriched strata, therefore, exhibit mineral magnetic characteristics which are indicative of the decreased influence of detrital magnetites and the increased predominance of ferrimagnets from an alternative source.

b) Anthropogenic influences.

Given that the geochemical and mineral magnetic trends found in cores Dee(3) and Dee(4) are not consistent with the ferrimagnetic enrichment of surficial strata by diagenetic or sedimentological mechanisms, it appears most plausible that atmospherically deposited magnetites are singly responsible. Should this be the case, a number of diagnostic features may be identifiable within cores Dee(3) and Dee(4). Firstly, ferrimagnetically enriched strata should be solely of post-industrial age and the upward accumulation gradient of magnetite should correlate closely with historical changes in the utilization of hydrocarbon fuels.

Secondly, while the mineralogenic or granulometric characteristics of the magnetic assemblages found within surficial strata have been shown to deviate from those of detrital assemblages, they should increasingly approximate those of industrially produced phases, for example, fly ash (PFA). Thirdly, on account of the associated mobilization of magnetic oxides and trace elements during hydrocarbon combustion (Hunt et al 1984, Scoullos 1979, Raask et al 1981, Lantzy 1979), downcore mineral magnetic trends should closely correlate with those of the pollutant trace elements, Pb, Zn and Cu, which have been found in enhanced concentrations towards the surface of the Loch Dee sample cores (see chapter 3). Finally, because hydrocarbon combustion processes produce morphologically unique, magnetite-bearing cenospheres (Goldberg et al 1981, Klein et al 1975, Raask et al 1981), the magnetic mineral assemblages found within the uppermost 8cm of sediment should be optically distinguishable from those of sediments supplied solely with octahedral, detrital magnetites.

To examine the extent to which the mineral magnetic anomalies observed in the uppermost 8cm of core Dee(3) fit the above criteria, the SIRM gradient through the uppermost 12cm of sediment has been placed within the formerly established 210Pb chronology for this core (section 3.6.1). In Fig 4/15a, 210Pb dates signify the origins of strata showing initial ferrimagnetic enhancement (8cm), the steepest ferrimagnetic concentration gradient (3cm - 4cm) and

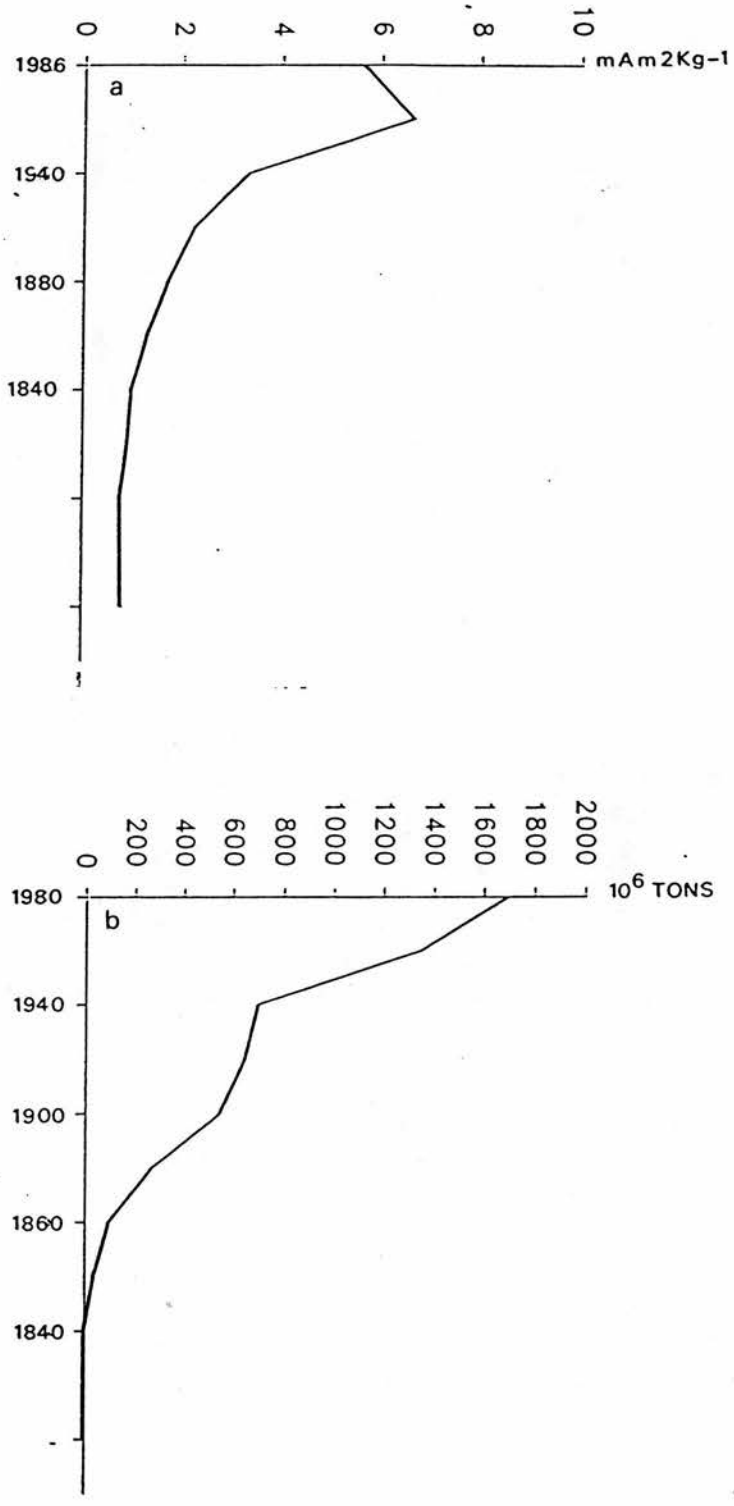

FIG 4/15 : a) Ferrimagnetic accumulation within post-industrial sediments at coring station Dee(3) as defined by SIRM.

b) Temporal variability of fossil fuel consumption throughout Europe during the post-industrial period (after Renberg 1985).

the maximum SIRM value (2cm). From this figure, it is apparent that while ferrimagnetic mineral concentrations first increase within sediments which were deposited at around 1840, markedly accelerated magnetite deposition rates prevailed during the 1940 - 1970 period. Significantly, these trends analogue temporal changes in the levels of fossil fuel combustion throughout Europe (Fig 4/15b), suggesting that patterns of ferrimagnetic enhancement at station Dee(3) have been directly governed by rates of anthropogenic magnetite mobilization. Furthermore, the declining SIRM values observed in the uppermost 1cm of core Dee(3) appear to be consistent with both the stablization of fossil fuel consumption during the last decade and the increased accumulation rates calculated for these strata (Table 17).

Downcore mineralogical and granulometric changes in the surficial 10cm of cores Dee(3) and Dee(4) serve to corroborate the above evidence. For example, Oldfield et al (1983) found anthropogenic magnetites within the surficial strata of cores from Newton Mere to be conspicuous by their tendency to produce untypically coarse, PSD/MD dominated magnetic assemblages. These changes, signified by a softening of magnetic remanence and the elevation of SIRM/ARM ratios, have been confidently identified in the uppermost 8cm of core Dee(3). Furthermore, on comparing the salient mineral magnetic characteristics of samples from the 3cm and 4cm levels of core Dee(3) with those of PFA samples

extracted from the electrostatic precipitation units at Ratcliffe 2000MW generating station and from Hams Hall thermal plant (Hunt et al 1984), distinct similarities are observable (Table 34). These similarities, particularly with respect to the demagnetisation properties and SIRM/X values of the Ratcliffe ash samples and the 3cm sediment sample from core Dee(3) can, therefore, be considered to be indicative of the residence of PFA spherules within the surficial sediments of Loch Dee.

Table 34. Comparative mineral magnetic properties of size graded fly ash from electrostatic precipitation units at Ratcliffe generating station (R), Hams Hall generating station (H) and post-industrial sediments from Loch Dee (D).

Sample	SIRM/x	0.04mTAC SIRM/ARM	-20mT/SIRM	BO(CR)	S
R >20um	9.7	30.3	40	36	-0.74
R <10um	9.7	21.2	40	37	-0.75
R <5um	11.6	23.3	41	38	-0.76
H 7um	-	-	-	40	-0.63
H 1um	-	-	-	42	-0.58
D 3cm	12.1	14.0	45	37	-0.81

The data presented in Table 35 quantify the co-variability of Xlf and SIRM with the concentration gradients of Pb, Zn and Cu in core Dee(3). Post industrial strata in the Loch Dee sediment reservoir have been shown to have become enriched with Pb, Zn and Cu as a consequence of atmospheric deposition (section 3.8.1). Hence, the

persistence of correlation coefficients in excess of 0.70 for SIRM or Xlf and all three pollutant elements suggests that, in accordance with findings of Scoullos et al (1979) and Oldfield et al (1983), these parameters all share common, anthropogenic controls. It is also notable, that SIRM and Xlf are both poorly (or negatively) correlated with the downcore concentration gradients of the lithophilic elements, Ni and Mg at station Dee(3).

Table 35: Correlation coefficients (R) for SIRM, Xlf, atmophilic element concentrations and lithophilic element concentrations within core Dee (3).

	Pb	Zn	Cu	Ni	Mg	Xlf
SIRM	0.71	0.85	0.84	-0.07	-0.23	0.97
Xlf	0.81	0.84	0.79	-0.10	-0.20	

The correlation between historical trends in the mobilization of anthropogenic magnetite and the upward accumulation of ferrimagnets in cores Dee(3) and Dee(4) is unequivocally demonstrated by the results of SEM analyses of magnetic mineral extracts from 1cm, 7cm, 25cm and 80cm depths of core Dee(3). Figs 4/16a - b illustrate the morphology of the ferrimagnetic phases contributing to SIRM and X within the 1cm sample, from which it is evident that cenospheres, falling in the 1um - 20um size range, are prevalent. 127 of these cenospheres, which have no natural terrestrial mode of formation, were observed in the magnetic

A

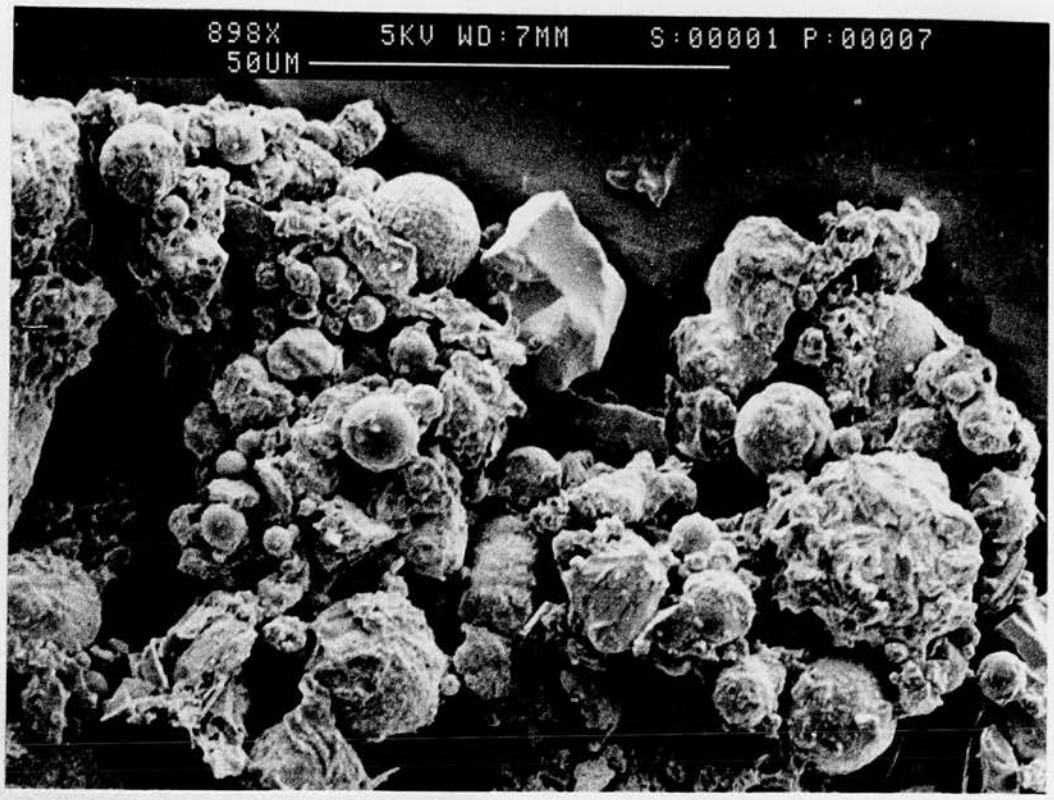
898X 5KV WD:7MM S:00001 P:00007
50UM

FIG 4/16

B

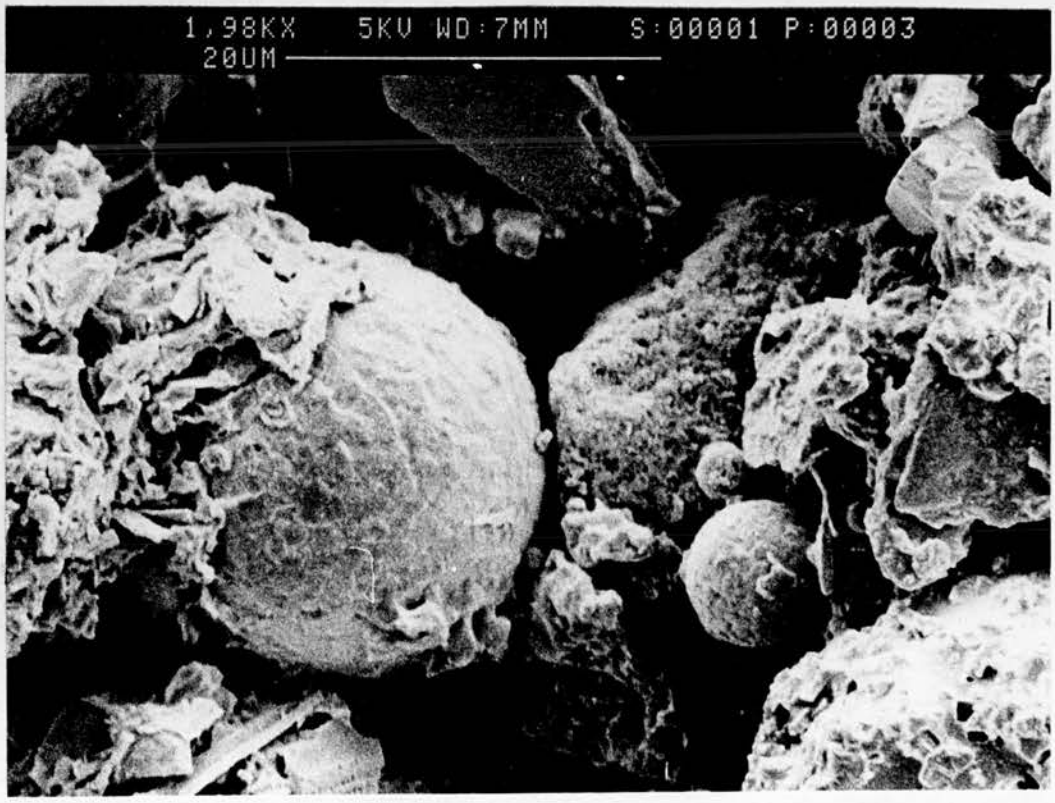
1,98KX 5KV WD:7MM S:00001 P:00003
20UM

extract from the 1cm sample. While Riley and Chester (1971) have attributed the presence of morphologically similar magnetic spherules in deep sea sediments to the deposition of cosmogenic particulates, their occurence at such frequencies can only plausibly reflect the deposition of combustion residues from coal fired generating plant (Raask et al 1981, Goldberg et al 1981). Cenospheric particulates are present in lower concentrations within magnetic extracts from the 4cm sediment sample and are absent in the 25cm and 80cm samples. In combination with the conventional mineral magnetic data emanating from analyses of cores Dee(3) and Dee(4), SEM evidence, therefore, irrefutably confirms the progressively increasing loading of fossil fuel-derived particulates to the Loch Dee catchment during the 1840 - 1979 period.

c) Quantification of the atmospheric magnetic oxide flux.

The above mineral magnetic data and the information derived from SEM analyses provide only qualitative information with respect to temporal variations in the flux of anthropogenically mobilized magnetic oxides. To quantify these temporal changes, magnetic data have been used to calculate the downcore concentration gradients of Fe2O3 and Fe3O4 at station Dee(3). These concentration gradients have, in turn, been normalized against sedimentation rate fluctuations to facilitate the derivation of annual flux

data.

Given that the Xlf value of pure Fe3O4 is 565μm3kg-1 (Maher 1984, Thompson 1986), the Fe3O4 concentrations in samples from core Dee(3) are decipherable through the application of the equation:

$$\text{Fe3O4\%} = \frac{\text{samp. Xlf}}{565} \times 100$$

$$\text{Fe3O4 (ug/g)} = \text{Fe3O4\%} \times 10K$$

The concentrations of Fe2O3 within samples can, in turn, be calculated on the basis of data provided by Thompson (1986), showing the mean SIRM of Fe3O4 grains accross the size range 0.065um to 4.0um to be 10.0kAm2kg-1, while the mean SIRM of Fe2O3 accross a similar size range is 0.25kAm2kg-1. Thompson (1986) and Hirons and Thompson (1986) have also shown that the magnetic phases which contribute to IRMs grown in fields of below 0.1T are principally formed of Fe3O4, while any addition to this IRM grown in fields of 0.1T - 1.0T reflects the presence of Fe2O3. Accordingly the concentration of Fe2O3 within any sample of mixed mineralogy is:

$$\text{Fe2O3\%} = \text{Fe3O4\%} \times \frac{\text{HIRM(0.1 - 1.0T)/SIRM}}{\text{LIRM(<0.1T)/SIRM}} \times \frac{10.0}{0.25}$$

$$\text{Fe2O3 (ug/g)} = \text{Fe2O3\%} \times 10K$$

Quantitative data showing the concentrations of Fe2O3 and Fe3O4 within the uppermost 20 sub-samples from core Dee(3) are provided in Table 36.

Table 36: Mass specific concentrations of Fe2O3 and Fe3O4 (µg/g) within the uppermost 20 sub-samples from core Dee(3).

Depth	Fe2O3(µg/g)	Fe3O4(µg/g)	Fe3O4/Fe2O3
1cm	1300	900	0.69
2cm	2900	920	0.31
3cm	2700	690	0.25
4cm	2100	490	0.23
5cm	1600	400	0.25
6cm	1600	370	0.23
7cm	4000	300	0.07
8cm	1000	260	0.26
9cm	500	240	0.48
10cm	2100	240	0.11
11cm	2800	240	0.08
12cm	1800	210	0.11
13cm	2300	210	0.09
14cm	1900	210	0.11
15cm	2800	210	0.07
16cm	2800	190	0.06
17cm	2700	190	0.07
18cm	2200	150	0.06
19cm	1800	170	0.09
20cm	2100	190	0.09
Background	1600	155	0.09

The annual fluxes of Fe2O3 and Fe3O4 to the Loch Dee basin during the period 1840 - 1986, have been calculated using methods described in section 3.8.1 and are the product of the sedimentation rate (cm/yr-1), the dry mass Fe oxide concentration (µg/g), the wet sediment density (g/cm3) and the fractional dry weight (g/cm3). These data are presented in Table 37, along with calculations of the pre-

1840 magnetic oxide fluxes to sediments at coring station Dee(3). Anthropogenic fluxes have been calculated by subtracting the pre-cultural flux value (BG) from the respective total flux values obtained for all ferrimagnetically enriched samples.

Table 37: Total and anthropogenic fluxes of Fe2O3 and Fe3O4 to sediments at coring station Dee (3) during the period 1840 - 1986.

Period	Depth	AR	WD	FDW	THF	AHF	TMF	AMF
1979-86	0-1cm	.13	.88	.07	10.4	2.9	7.2	6.6
1967-78	1-2cm	.10	.99	.11	31.8	24.3	10.1	9.5
1950-66	2-3cm	.05	1.09	.16	24.9	17.4	6.3	5.7
1930-49	3-4cm	.05	1.09	.15	18.6	11.1	4.3	3.7
1908-29	4-5cm	.04	1.03	.14	10.6	3.1	2.6	2.0
1883-07	5-6cm	.04	1.08	.14	9.4	1.9	2.1	1.5
1855-82	6-7cm	.03	.88	.10	13.5	6.0	0.9	0.3
1840-54	7-8cm	.03	.99	.11	3.7	0	0.8	0.2
BG	(15-90cm)	.03	1.04	.12	7.5		0.6	

AR = sediment accumulation rate (cm/yr-1).
WD = wet sediment density (g/cm3).
FDW = fractional dry weight (g/cm3)
THF = total annual Fe2O3 flux rate (µg/cm2/yr-1)
AHF = annual anthropogenic Fe2O3 flux rate (µg/cm2/yr-1)
TMF = total annual Fe3O4 flux rate (µg/cm2/yr-1)
AMF = annual anthropogenic Fe3O4 flux rate (µg/cm2/yr-1).

A number of features, highlighted through the quantification of annual Fe2O3 and Fe3O4 fluxes, aid in summarising the evident relationship between the history of hydrocarbon-derived pollutant deposition and the downcore magnetic adjustments observed in the surficial strata of the

Loch Dee sediment reservoir:-

1) By regressing the SIRM data acquired through magnetic analyses of the uppermost 12cm of core Dee(3) against variations in the annual anthropogenic flux of Fe_3O_4 at this coring station, it has been possible to ascertain that 96% of the observed downcore SIRM fluctuations are attributable to temporally varying atmospheric inputs. The history of fossil fuel-derived particulate deposition is, therefore, unequivocally chronicled by the sedimentary mineral magnetic record.

2) Throughout the post-industrial period, the anthropogenic flux of Fe_3O_4 to the Loch Dee sediment reservoir has far exceeded the supply of this mineral emanating from natural, denudational processes. During the period of maximum anthropogenic enrichment (1967 - 1979), the deposition rate of hydrocarbon-derived magnetite exceeded that of the lithospheric influx by a factor of 17.

3) Progressively increasing fluxes of Fe_3O_4 to the Loch Dee catchment during the period 1840 - 1979 correlate closely with temporal variations in the fluxes of Cu, Pb and Zn (see section 3.8.1). The persistence of correlation coefficients in excess of 0.75 suggest that these pollutants share a common, hydrocarbon-related origin.

4) Fluctuations in the ratios of Fe_3O_4/Fe_2O_3 throughout the uppermost 9cm of core Dee(3) are consistent with the observations of Oldfield (1984) and Jones (1985) that the Fe oxide constitution of fossil fuel-derived particulates

has changed in accordance with advances in fuel combustion technology. Low Fe_3O_4/Fe_2O_3 ratios at 7cm depth (0.07) plausibly reflect the residence of haematite-rich particulates produced by 19th century Bessemer firing plant. In contrast, the anomalously high Fe_3O_4/Fe_2O_3 ratio (0.69) observed at 1cm depth appears consistent with the documented production of magnetite-rich particulates within modern high temperature, pulverised fuel combustion chambers (Raask 1980, Hart 1981).

5) Despite its' mineralogical significance, the impact of the anthropogenic magnetic mineral flux upon the total sedimentary Fe budget of the Loch Dee catchment has been negligable. At no point within the uppermost 1.0m of the sediment reservoir does Fe_2O_3 + Fe_3O_4 constitute more than 5% of total Fe (see Figs 3/7 and 3/9).

4.5.2 Loch Ba cores.

a) Diagenetic influences.

In section 4.3.2, the results of χ analyses of samples from between 1cm and 80cm depths of core Ba(1) following leaching with MgCl, NaOAc (pH5.0), HOAc and H_2O_2, were shown to be consistent with the influence of ferrimagnetic sulphides upon the mineral magnetic properties of sediments at 4cm - 16cm depth. Additional χ analyses of these samples prior to and following oxidation, also illustrated the limited eH range under which these sulphide phases may

persist, suggesting an authigenic mode of formation. In assessing the overall significance of such authigenic components to the mineral magnetic trends observed in cores Ba(1), Ba(2) and Ba(3), the following questions warrant consideration:-

1) What is the precise geochemical constituency of the formerly identified ferrimagnetic sulphide?

2) Under what conditions may this sulphide precipitate?

3) Do conditions which are conducive to the authigenesis of ferrimagnetic sulphide phases prevail at any stratigraphic levels of cores Ba(2) and Ba(3)?

The precise mineralogy of the authigenic phases contributing to χ at 4cm - 16cm depth in core Ba(1) can be deciphered by reference to Table 38, outlining the structure and magnetic behaviour of the full range of known Fe sulphides. From this information, the plausible identity of the relevant sulphide can immediately be restricted to those exhibiting ferrimagnetic characteristics, thus excluding pyrite, marcasite, mackinavite and hydrotroilite. Pyrrhotite is also unlikely to have influenced the mineral magnetic characteristics of the sulphide-bearing strata, given that its sedimentary authigenesis has, to date, only been observed in deep sea sediments (Johnson 1975, Henshaw 1978, Kobayashi and Nomura 1974, Calvert 1977). Detrital pyrrhotites, derived from the Rannochmoor plutonic complex would, in turn, fail to exhibit the

sensitivity to oxidation observed within the 4cm - 16cm samples from core Ba(1). In contrast, the inverse spinel, Fe3S4 (greigite) has frequently been observed in both marine and lacustrine sediments (Berner 1981, Karlin 1984, Price 1977, Calvert 1977, Henshaw 1978) where it has been found to markedly enhance ferrimagnetic signals (Hilton et al 1986, Karlin 1984). On account of the dearth of alternative mineral phases which could produce such effects and of the known H2O2 solubility of Fe3S4 (Hilton et al 1986), this mineral can be considered to be solely responsible for the eH dependent variability of χ observed within core Ba(1).

Table 38: Mineralogy and magnetic properties of Fe sulphides (after Karlin 1984, Calvert 1977, Rickard 1975).

Mineral		Structure	Magnetism	Formation
Pyrite	FeS2	cubic	para	
Marcasite	FeS2	orthorhombic	para	pseudomorph from pyrite
Greigite	Fe3S4	cubic	ferri	
Smythite	Fe3S4	rhombohedral	para	sulphidized FeCO3
Mackinavite	Fe(1.04)S -Fe(1.07)S	tetragonal	para	
Hydro-troilite	FeS(0.87) -FeS(0.92)	amorphous	para	
Pyrrhotite	Fe(1-x)S	hexagonal-monoclinic	ferri	

In explanation of the apparent restriction of Fe3S4 to the 4cm - 16cm sequence of core Ba(1), two formerly identified characteristics of these strata appear significant. Firstly, organic matter has been shown to constitute over 50% of the uppermost 20cm of the Loch Ba sediment reservoir (Fig 3/41). In accordance with the observations of Berner (1970), the initial oxidative decomposition of this matter by sulphate reducing bacteria has been shown to produce conditions of severe anoxia (eH<-80mV) at 3cm - 7cm depth (Fig 3/34). The rapid reduction of SO4 is likely in these strata, producing a concomitant increase in pore-water pH (Carignan and Nriagu 1985) and the generation of saturation conditions within the pore-waters with respect to the precipitation of metal sulphides. Further downcore, the depletion of pore-water H2S, declining SRB activities and accordingly, increased eH values (Fig 3/34) plausibly elevate equilibrated pore-water loadings, thus creating an environment which is less conducive to sulphide precipitation.

Secondly, empirical and experimental analyses have shown the availability of free elemental S (So) to be a major rate limiting control with regard to the authigenesis of Fe3S4 (Berner 1964, 1970, 1981, Zobell 1964, Brown 1982, Howarth and Teal 1979). In turn, Brown (1982) has shown that because So is yielded through the oxidation of bi-sulphide, concentrations will be maximised at the anoxic/oxic sediment boundary where periodic eH fluctuations occur. Such trends

are, therefore, consistent with the prolific authigenesis of Fe3S4 at around 4cm depth.

The limited persistence of Fe3S4 upon burial is signified by the depressed sensitivity of magnetic signals to sample oxidation downward of 16cm depth in core Ba(1). Such trends can best be interpreted by reference to the data of Berner (1970), showing monosulphides to be subject to progressive pyritization during burial, at rates controlled by the availability of reactive sulphur in the interstitial pore-waters.

Taking all of the above findings into account, it is possible to express diagramatically, the "rate" and "location" controlling factors with respect to Fe3S4 authigenesis at coring station Ba(1). From such a diagram (Fig 4/17), the locations at which conditions conducive to the authigenesis of Fe3S4 occur in cores Ba(2) and Ba(3) can be determined. For example, redox data for these cores (Fig 3/34) indicate the prevalence of conditions which are adequate for Fe3S4 authigenesis ($eH \backsim -100mV$) at 3cm - 7cm depths. Pore-water samples from these strata also exhibit depletion of Fe, Ni and Cu (Figs 3/35 and 3/36), particularly at 5cm - 7cm depth in core Ba(2) and at 4cm depth in core Ba(3). These trends are all consistent with the precipitation of authigenic sulphides and accordingly, the ferrimagnetic enrichment of these strata through the

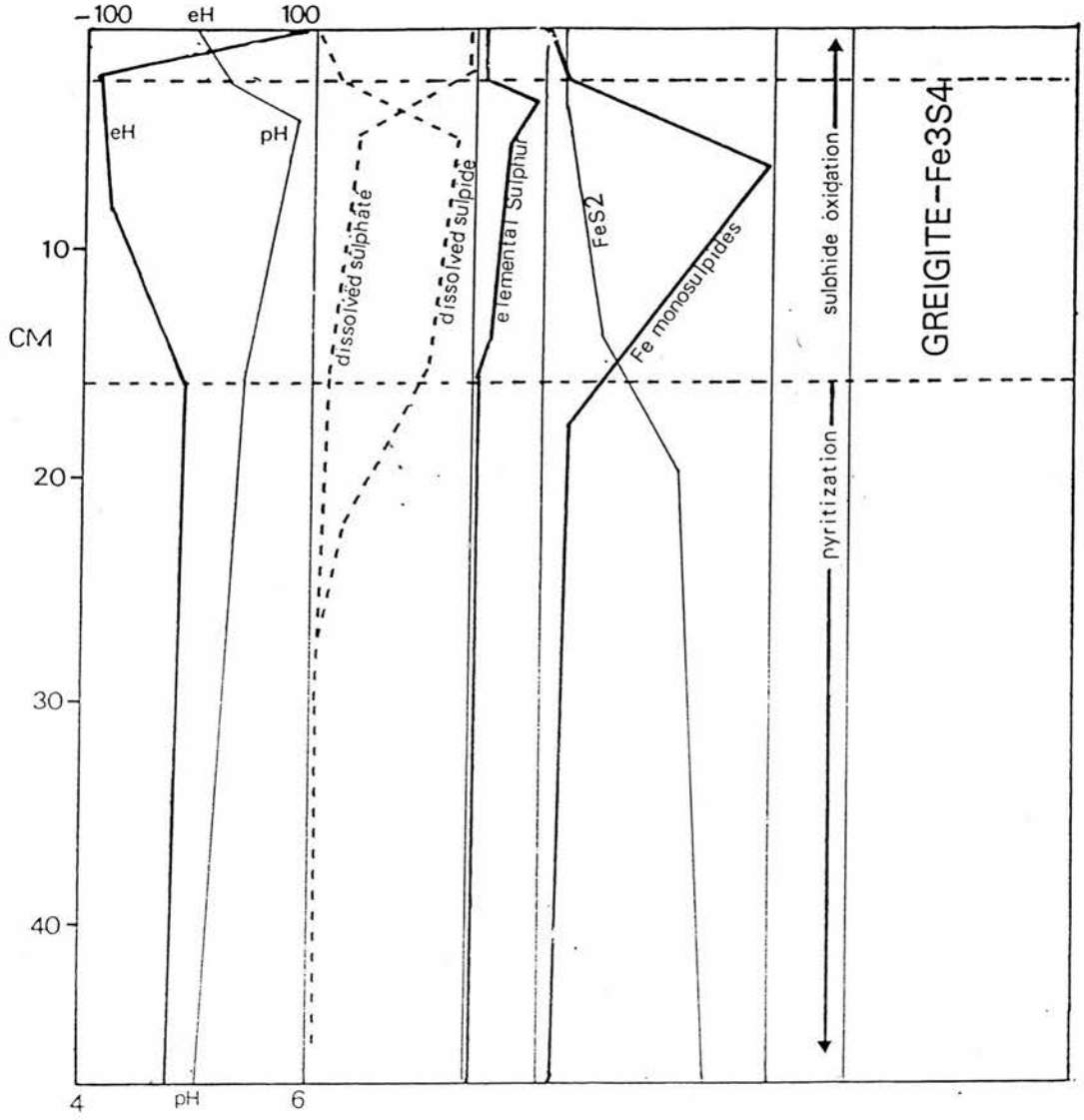

FIG 4/17: A tentative model of the rate controls on Fe3S4 (greigite) authigenesis, based upon observations made in sediments at station Ba(1). The stratigraphic sequence in which greigite is present (within dotted lines) is probably characterised by the following conditions:-
1) Severe anoxia (eH around -100mV), promoting the rapid reduction of dissolved SO4 and hence, elevated pH. These conditions depress the equilibrated pore-water Fe loading and induce precipitation.
2) Available elemental sulphur; as a consequence of the oxidation of sulphide phases at the oxic/anoxic boundary.
The progressive depletion of Fe monosulphides (including Fe3S4) is a consequence of their pyritization upon burial. Because the rate of this process is governed by the availability of dissolved H2S (or SO4), pyrite concentrations increase less markedly with depth as the dissolved H2S supply nears exhaustion.
Sediment organic content is also likely to be a rate-limiting control, given that the accumulation of organic C has a direct bearing on the redox regime.

formation of Fe3S4 is likely.

The implications of the known presence of greigite to the interpretation of the mineral magnetic variations observed within the Loch Ba sample cores are evident from Figs 4/18a-c, in which the formerly established Xlf profiles for the surficial 8cm of all cores (Figs 4/5, 4/7 and 4/9) have been adjusted to exclude any distortions attributable to authigenic components. While it must be emphasised that the adjustments made to the profiles for cores Ba(2) and Ba(3) are tentative (see Fig 4/18 for a description of methods) it is apparent that, should Fe3S4 only contribute to Xlf downward of 3cm depth, ferrimagnetic oxide concentrations must actually increase markedly within the uppermost 3cm. In core Ba(3), these strata have been assigned 210Pb dates which suggest their post-industrial origin (see Table 18). The origins of the magnetic mineral phases within these strata, therefore, warrant particular attention and form the focus of much of the subsequent discussion.

b) Lithogenic vs. anthropogenic influences.

In contrast to the trends observed during analyses of sample cores from the Loch Dee basin, all sediment cores from Loch Ba are characterised by downcore mineral magnetic inconsistencies which are diagnostic of a temporally variable sedimentological regime. Although five

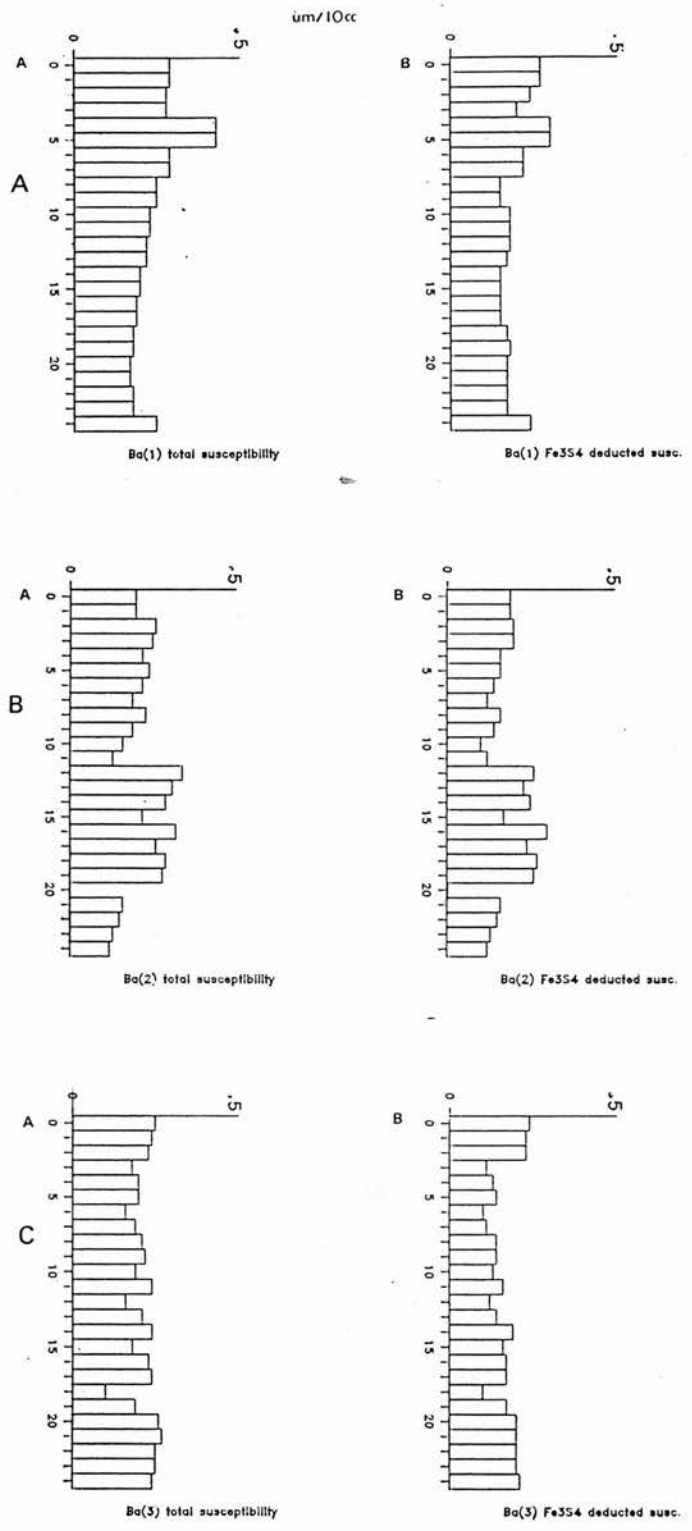

FIG 4/18: Total (A) and Fe3S4 normalised (B) volume susceptibilities through the uppermost 25cm of Loch Ba sample cores. For core Ba(1), the normalised profile simply reflects the total K profile, with the oxidation-sensitive component observed in each of the sub-samples at 4cm - 16cm depth deducted. For cores Ba(2) and Ba(3), deduction of the Fe3S4-produced signal has tentatively been based on the premise that monosulphide distributions are similar to those observed in core Ba(1). Hence, 25% - 30% of total K has been deducted from the 4cm - 7cm sub-samples and 10% - 20% of total K has been deducted from the 8cm - 16cm core levels.

magnetically distinct mineral assemblages have been observed within these cores (see section 4.4.2), influxes of sediment from just two contrasting sources appear responsible. Sediments derived from haematite-rich sources are most conspicuous at 65cm - 87cm depth in core Ba(3) and have formerly been assigned a silicic, igneous origin on account of their enrichment with Cu, Hf, Ce, Sm, Eu, La and K (section 3.8.2). In contrast, the ferrimagnetically dominated mineral assemblages in the surficial 20cm of all sample cores, alongside those at 35cm - 60cm depth in core Ba(1) and at 80cm - 97cm depth in core Ba(2), show no affinity to the granitic catchment bedrock, but are magnetically analogous to the exotic, boulder clay overburden at the southern margin of the basin.

Strata at 25cm - 40cm depths of cores Ba(2) and Ba(3), along with those at 65cm - 80cm depths of core Ba(1) have been found to contain mixed mineral assemblages (see Fig 4/13), suggesting the presence of sediments derived from both of the above sources. Notably, it has not proved possible to distinguish these strata from the ferrimagnetically dominated horizons on geochemical grounds, indicating the superior sensitivity of magnetic parameters for the provision of lithological information.

As a consequence of the lithological complexity of the Loch Ba sediments, the confident determination of the origin

of the ferrimagnetic oxides promoting enhanced SIRM and Xlf signals within the post-industrial, surficial 3cm of sediments is problematic. On the basis of mineral magnetic evidence, two conflicting hypotheses appear to be equally applicable:-

1) Ferrimagnetic oxide assemblages within the surficial 3cm of cores Ba(2) and Ba(3) yield SIRMs in excess of 2mAm2kg-1, SIRM/X ratios within the range 8.0kAm-1 - 11.5kAm-1, SIRM/ARM ratios of 14.1 - 24.3 and BO(CR) values of 41mT - 45mT. These assemblages are analogous both to those observed in the polluted levels of the Loch Dee sediment reservoir and to those produced during hydrocarbon combustion (Table 34). Accordingly, magnetic data could be indicative of the modification of the surficial levels of the Loch Ba sediment reservoir through the deposition of anthropogenerated particulates.

2) Detrital mineral assemblages (probably derived from glacial overburden to the south of the Loch Ba basin) produce SIRMs in excess of 2mAm2kg-1, SIRM/X ratios in the range 7kAm-1 - 9kAm-1, SIRM/ARM ratios of 12 - 22 and BO(CR) values of 37mT - 41mT within samples from 65cm - 75cm depth in core Ba(2). The occurrence of analogous mineral phases at 1cm - 3cm depth in cores Ba(2) and Ba(3) may, therefore, reflect the most recent of several known influxes of sediment derived from glacial overburden.

While conventional mineral magnetic methods are clearly insufficient for ascertaining the true origin of the ferrimagnets promoting enhanced SIRM and Xlf signals in the surficial strata, geochemical methods are equally unhelpful. Most notably, the closely correlated trends of SIRM, Cu, Pb and Zn ($R > 0.66$) through the uppermost 4cm of core Ba(3) cannot be cited as evidence of the co-varying deposition of Fe3O4 and pollutant elements, as Pb, Zn and Cu have been shown to display diagenetically modified profiles (section 3.8.2). In addition, it is not possible to invoke the limited variability of lithophilic elements (K, Fe, Ni) throughout the surficial 10cm of sediments as evidence of the consistency of detrital mineral fluxes, as magnetically distinct lithological anomalies at 65cm - 90cm depth in core Ba(2) are not geochemically conspicuous (see Fig 3/20).

Accordingly, morphological analyses of magnetic mineral extracts from the post-industrial levels of the sediment column provide the best available evidence of the origin of the ferrimagnetic phases producing enhanced SIRM and Xlf signals within these strata. From Fig 4/19, showing an SEM micrograph obtained through the analysis of extracts from 1cm depth in core Ba(3), two features are particularly apparent. Firstly, the magnetic mineral assemblage is dominated by angular/octahedral magnetites which can confidently be assigned lithospheric origins. Secondly, cenospheric particulates of the type considered to be

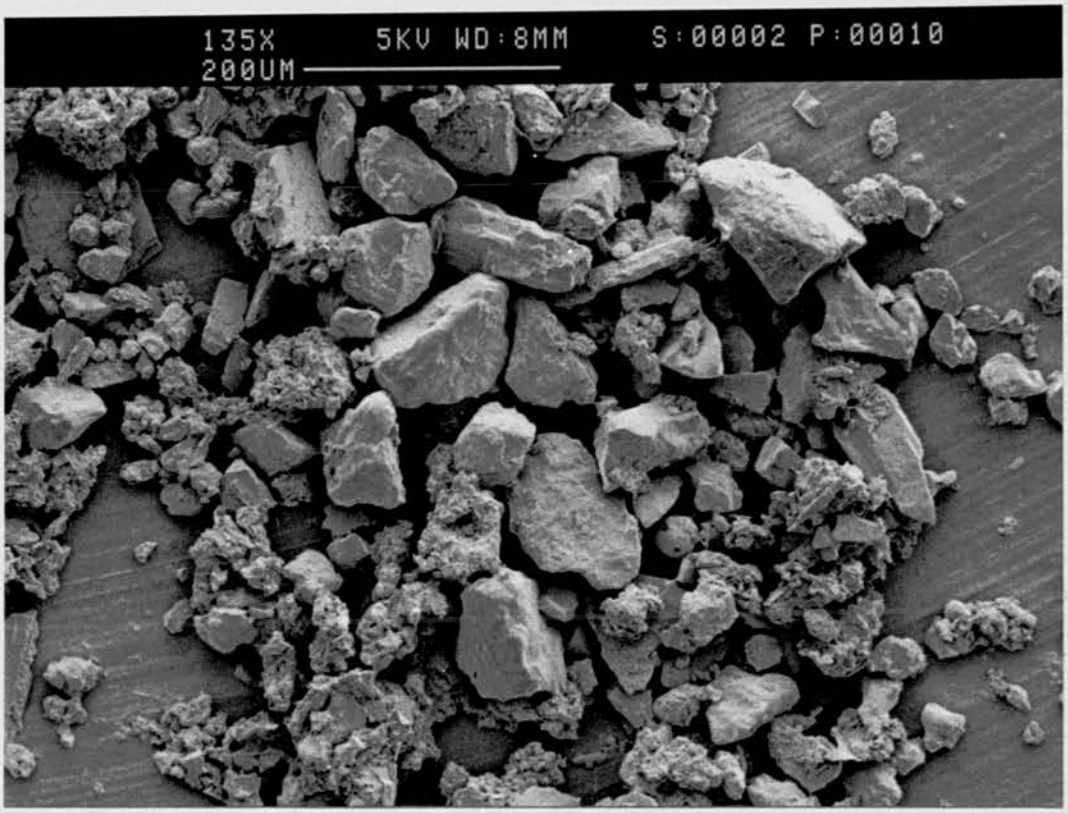

FIG 4/19

diagnostic of the presence of anthropogenerated magnetites in the Loch Dee sediment reservoir are absent. Consequently, SEM evidence unequivocally demonstrates that, while the post-industrial sediments at coring stations Ba(2) and Ba(3) show ferrimagnetic enrichment, atmospheric magnetite fluxes are not responsible.

c) Comparability of the Loch Ba sediment cores.

Although the mineral magnetic trends in the Loch Ba sample cores provide no easily deciphered record relating to the deposition of anthropogenerated particulates they are, in two respects, assistive in the interpretation of the geochemical data for these sediments. Firstly, through the linkage of magnetically analogous horizons within sample cores, the ^{210}Pb dates acquired for core Ba(3) can be extrapolated to core Ba(2). Magnetic correlations, based upon Xlf, SIRM and BO(CR) data for the respective cores (Fig 4/20), suggest that strata at 7cm depth in core Ba(3) are of temporally synchronous origin to those at 12cm in core Ba(2). By assuming that the 0.016cm/yr accumulation rate of sediments at 3cm - 4cm depth in core Ba(3) approximates the rate at which the underlying strata accumulated, sediments at 7cm depth in this core and 12cm depth in core Ba(2) can be assigned an origin of 380yrs BP. Notably, the faster accumulation rate of surficial sediments at coring station Ba(2) is consistent with the presence of

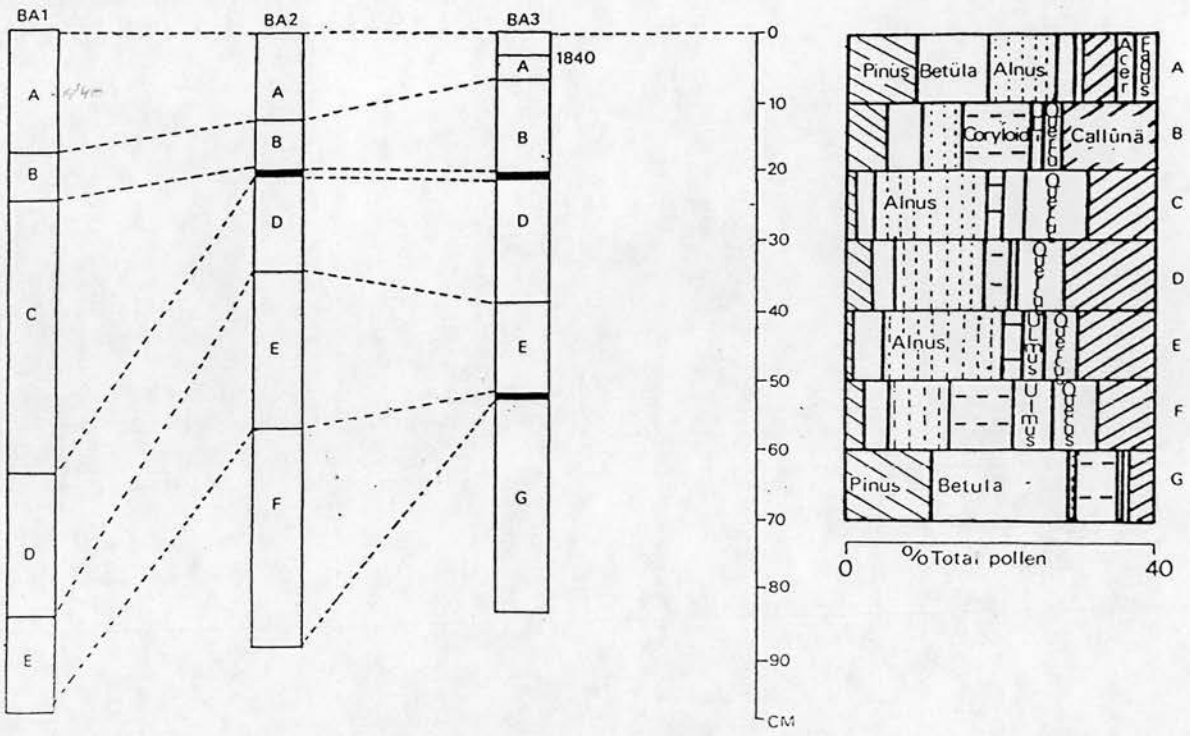

FIG 4/20: LEFT: Magneto-stratigraphic correlation of cores Ba(1), Ba(2) and Ba(3). The characteristic magnetic features of each zone are as follows:

Zone A is characterised by strong ferrimagnetic mineral presence, with BOCr values exceeding 40mT.

Zone B is also characterised by strong ferrimagnetic mineral presence, but the increasing significance of MD magnetites promotes the depression of BOCr to below 40mT.

Zone C is weakly ferrimagnetic, with MD magnetites controlling BOCr and hence, producing values of below 40mT. This zone is absent from cores Ba(2) and Ba(3) as a consequence of sedimentological hiatuses at these stations (depicted by thick black lines).

Zone D is ferrimagnetically depleted and magnetically "hard", yielding BOCR values of up to 80mT. Haematite can be assumed to exert a major control upon the magnetic mineralogy of this zone.

Zone E is ferrimagnetically depleted and magnetically "soft", reflecting the depletion of haematite below the D/E boundary.

Zone F is ferrimagnetically enriched, relative to the overlying sediment. This zone is absent from core Ba(3) as a consequence of a sedimentological hiatus at this coring station (thick black line).

Zone G contains only low magnetite concentrations but yields unusually high BOCR values. Haematite can, therefore, be diagnosed as the predominant magnetic mineral phase.

Confirmation of the occurrence of a sedimentological hiatus at the E/G boundary in core Ba(3) is provided by the mean pollen frequency data for samples from each magnetically distinct zone (RIGHT). At station Ba(3), an abrupt alteration of the palynological record occurs at 50cm - 60cm depth, where Pinus and Betula are replaced by Alnus as the dominant species. This evidence indicates that no sedimentation occurred between 9500 or 10,000yrs BP and 4500yrs BP..

industrially derived Pb, Zn and Cu at greater depths than are evident in core Ba(3) (see section 3.4). Downward of 12cm, the sediments at coring station Ba(2) display less rapid accumulation rates, with what appear to be synchronous reductions to Xlf in evidence at 20cm depth in core Ba(2) and 23cm depth in core Ba(3).

Secondly, the magneto-stratigraphic correlation of the Loch Ba sample cores facilitates the establishment of the locations of hiatuses in the sediment sequences at the respective sampling sites. This procedure has, in turn, been of value in confirming that the post-industrial levels of all cores constitute unbroken sedimentary records. The locations of hiatuses, corroborated by pollen data obtained for four samples from each core, are illustrated in Fig 4/20 and indicate that the sequence extending from 25cm to 65cm depth in core Ba(1) is absent from cores Ba(2) and Ba(3). Haematite-bearing sediments at 65cm - 80cm depth in core Ba(1), therefore, appear to be of temporally synchronous origin to the magnetically analogous strata at 25cm - 40cm depths of cores Ba(2) and Ba(3). In addition, marked palynological contrasts between the sediment samples from 50cm and 70cm depths of core Ba(3) suggest that a section of the Holocene sedimentary record, extending from 9500yrs BP to 4000yrs BP, is absent at this coring station (see Fig 4/20). Haematite-rich strata at 65cm - 87cm depth in core Ba(3) are, therefore, not equatable with any stratigraphic levels of cores Ba(1) and Ba(2).

4.6 Summary and conclusions.

In section 4.1 it was proposed that downcore geochemical variations in the Loch Dee and Loch Ba sediment reservoirs, resulting from lithospheric, diagenetic or anthropogenic influences, should be accompanied by synchronous mineral magnetic adjustments. The data presented in the preceding sections have shown such a hypothesis to be wholely upheld with respect to conditions in the Loch Dee sediments, but to be less applicable to the geochemically and magnetically complex Loch Ba sediments. For the Loch Dee sample cores, the following geochemical/mineral magnetic linkages are evident:-

1) Unvarying downcore profiles of lithophilic elements (notably Ni and Mg), silicate-bound Mn, Co and Fe, Co/Ni ratios and LOI are accompanied by similarly unvariable profiles of SIRM, Xlf, SIRM/ARM and BO(CR) through strata at 10cm - 90cm depth. All geochemical and mineral magnetic data are, therefore, consistent with the lithological homogeneity of sediments in the Loch Dee basin.

2) Upwardly increasing concentrations of Pb, Zn and Cu in the surficial 10cm of sediments, signifying the progressively increased deposition of pollutants from the atmosphere during the post-industrial period, are accompanied by increasing ferrimagnetic mineral concentrations. Within these surficial strata, adjustments

to magnetic mineralogy, granulometry and morphology (involving the increased presence of MD magnetites in cenospheric structures and enhanced Fe3O4/Fe2O3 ratios) suggest that trace metal and magnetic mineral profiles are linked by a common control. This control is solely anthropogenic and has involved the enhancement of annual Pb, Cu, Zn and Fe3O4 fluxes by factors of 7.6, 6.1, 11.3 and 16.8 respectively during the 1840 - 1978 period.

3) The limited post-depositional alteration of Pb, Zn and Cu distributions and the absence of authigenic magnetic minerals suggests that diagenesis does not exert a major influence on the constituency of the Loch Dee sediments. Accordingly, both the downcore elemental and mineral magnetic trends in these sediments serve to provide faithful historical records of the influx of anthropogenic pollutants.

With respect to the conditions prevailing in the Loch Ba sediment reservoir, the less consistent linkages between downcore geochemical and mineral magnetic adjustments can be summarised as follows:-

1) Diagenetic modifications to the sedimentary sequence in the Loch Ba basin are conspicuous upon examination of both the downcore geochemical and mineral magnetic profiles. Conditions promoting the precipitation of Cu, Ni and Fe sulphides within anoxic, sub-surface strata are also

conducive to the authigenesis of ferrimagnetic Fe_3S_4 phases.

2) Lithological changes in the 65cm - 87cm sector of the sediment column at coring station Ba(3) are conspicuous both through the enrichment of Cu, Hf, Sm, La, Ce, Eu, K and Na and through the transgression towards a haematite-dominated magnetic mineral assemblage. However, additional lithological anomalies, signified by the enhancement of ferrimagnetic mineral concentrations at 60cm - 90cm depth in core Ba(2) and 8cm - 20cm depth in core Ba(3) are not discernible from the downcore geochemical record. Accordingly, the sensitivity of mineral magnetic parameters to sediment-source variations can be considered to be superior to that exhibited by lithogeochemical parameters.

3) The closely correlated enrichment patterns of ferrimagnetic oxides and Pb, Zn, Cu, Ni, Co and Mn in the post-industrial levels of core Ba(3) do not reflect a common control. Furthermore, none of these enrichment patterns can be related to anthropogenic activity. Instead, mineral magnetic adjustments result from a lithospheric influx of magnetite-rich sediment since 1840. Enrichment of Pb, Zn, Cu, Co, Ni, Mn and Fe occurs as a consequence of the precipitation of hydrogenous oxides in the surficial 4cm of sediment. The synchronous enhancement of ferrimagnetic mineral and heavy metal concentrations in post-industrial sediments cannot, therefore, be considered to be diagnostic of the deposition of fossil fuel-derived pollutants.

CHAPTER FIVE

Geochemical studies of ombrotrophic peat cores from Galloway and Rannochmoor.

5.1: Introduction.

From the evidence presented in Chapter 3, it is apparent that lithogenic and diagenetic processes can serve to complicate downcore sedimentary records of pollutant loadings with time. Accordingly, the previously noted possibility that more accurate geochemical "pollution chronologies" may be acquired through the analysis of ombrotrophic peat cores (section 1.3) appears to warrant further consideration. In the following chapter this possibility is examined through the collation of data to illustrate the downcore geochemical characteristics of sample cores from the Galloway and Rannochmoor regions.

5.2 Rationale.

Ombrotrophic peats display characteristics which are analogous to those of sediments in that they accumulate material with time and typically retain a high degree of stratification. Yet in contrast to sediments, ombrotrophic peats receive their entire nutrient supply through atmospheric pathways, being isolated from lithogenous or groundwater inputs by virtue of their underlying morphology.

In addition, observations that the ion exchange capacities of Sphagnum species exceed those of clay minerals by at least factor of 10 (Clymo 1963, Livett 1982, Schell 1986) indicate that peatland biota may accumulate trace elements at rates determined primarily by their atmospheric supply. On account of the prevalence of low oxidative decomposition rates within buried strata, it has widely been considered that deposited elements are retained "in situ" upon burial (Witting 1947, Du Reitz 1949, Sjors 1950, Malmer 1955, 1958, Chapman 1964, Bellamy and Reiley 1967, Stewart et al 1968), thus providing a stratified record of chemical loadings with time.

Following observations that the concentrations of Ni, Cr, Pb, Fe, Cu and Zn in surficial peats are typically inversely related to the proximity of industrial complexes (eg. Lee and Tallis 1973, Pakarinen and Tolonen 1976, 1977, Livett, Lee and Tallis 1979, Ylirivokanen 1976), several workers have successfully utilized downcore heavy metal data to construct "peat-based" pollution chronologies. Most notably, results obtained by Livett (1982) showed strata of pre-industrial age to contain 50 - 100µg/g Pb, around 20µg/g Cu and 100µg/g Zn irrespective of their geographical location. Yet while the surficial strata of sample cores from a remote mire at Glensheildaig were found to exhibit only limited enrichment of these metals, peat levels which have accumulated since 1750 at Featherbed

Moss, Moor House, Grassington Moor and Ringinglow were all found to show 4 - 8 fold enhancement of Pb, Zn and Cu concentrations. In the case of the sample cores from Moor House, which lies between the Lancashire and S. Yorkshire industrial areas, concentrations of 800µg/g Pb, 400µg/g Zn and 50µg/g Cu were noted in 20th century strata and the upward accumulation gradient of Pb correlated closely with documented historical records of the metals mobilization within the S. Pennine region. Accordingly, Livett (1982) has concluded that historical variations of atmospheric deposition constitute the principal control upon the downcore heavy metal profiles of most UK peats.

Further evidence that downcore elemental variations within peats analogue temporal trends in their deposition from the atmosphere has been provided through the calculation of annual metal flux rates, based upon both geochronological and geochemical data. Such calculations may be considered to provide a more reliable indication of temporal deposition trends than do simple downcore profiles, as they normalise geochemical data against any variation in rates of peat accumulation. In the most detailed study of this nature to date, Schell (1986) used 137Cs and 210Pb geochronologies to determine the annual rates of deposition for 38 elements at a Pennsylvanian peatland during the 1814 - 1980 period. In the case of Pb, flux estimates for the Pennsylvanian peats range from 2.2µg/cm2/yr-1 for the year 1817 to 13.3µg/cm2/yr-1 in 1978. Significantly, these values are

closely comparable to sediment-based flux estimations. For example, atmospheric Pb flux estimates to Lake Washington range from 3.0µg/cm2/yr for the year 1830 to 18.0µg/cm2/yr in 1980 (Graustein and Turekian 1983). Assuming that the "lake sediment-based" flux calculations are correct, the accordance of Schell's (1986) "peat based" data for Pb, Ce, Eu, Br, Ca, Cu, As and Hg must, therefore, reflect the limited post-depositional mobility of these elements within certain peatlands.

However, several workers have also successfully explained elemental distributions in peat systems by reference to three naturally occurring processes.

1) During studies of peat systems in Norway and Ontario, Braeke (1981) and Gorham et al (1984) observed the occurrence of Zn anomalies at 70cm below the mire surface. Because accumulations of Zn within these pre-industrial strata cannot be attributed to anthropogenic influences, they have been considered to be reflective of the operation of pH-dependent diffusion mechanisms. Conditions of low pH (<5.0) prevail in most ombrotrophic systems and hence, the leaching of Zn is likely to be a universal phenomenon.

2) Gorham et al (1984), Damman (1978) and Clymo (1963) have noted that Cs and K concentrations are typically maximised at the surface of peat cores as a consequence of

their uptake through the roots of active organic matter.

3) In studies of Trannerods Mosse and Storre Mosse, Scandinavia, Damman (1978) has shown that Mn, Fe, Cu, Al, Pb, Zn and P attain distributions which reflect conditions of equilibrium with the prevailing eH gradient. In the case of Mn, such profiles typically involve declining concentrations with depth and are a product of the reduction of Mn to a soluble, divalent state upon burial with the subsequent removal of the element in solution. Fe is also removed from deeply buried strata following its reduction to a divalent state. However, this element may accumulate within the zone of water table fluctuation on account of the periodic precipitation of Fe2+ as insoluble Fe3+. Pb, Cu, Zn and Al all appear to accumulate in analogous fashion to Fe on account of the differing solubilities of their oxide, sulphate and sulphide forms. For example, Pb exhibits greater solubility as PbSO4 than as PbS. Hence Pb may be subject to downward diffusion through the oxic, surficial peat levels but will accumulate at the water table as a consequence of the precipitation of PbS within the inundated zone.

In the light of the likely operation of the above post-depositional mechanisms, it appears plausible that Livett (1982) and Schell (1986) have over-estimated the ability of peats to retain stratified geochemical records. Such over-estimation can, in turn, be seen to derive from the

adoption of several false premises during the interpretation of their data. For instance, Livett (1982) assumed Pb, Zn and Cu to be immobilized principally through the formation of organo-metallic complexes in the peat column. In reality, Gorham et al (1984) have shown that such complexation processes are severely inhibited under the low pH conditions which prevail in most peatlands. Gorham et al's (1984) observations are also consistent with the sequential chemical data obtained by Jones (1985), indicating that Al, Pb, Zn and Ni are not predominantly bound within the H2O2 extractable fractions of peat materials. Furthermore, Higgo (1987) has shown that by reducing rates of sorption, the complexing of trace metals with humic or amino acids may actually increase the diffusive mobility of metals through the peat column.

In addition, Schell (1986) and Livett, Lee and Tallis (1979) appear to have appraised the likely mobility of atmospherically deposited elements without sufficient regard for the naturally prevailing redox regime. For example, by evaluating the solubilities of elements solely on the basis of their behaviour in high valency states, Schell (1986) maintained that Mn, Ce, Sm, Yb, Hf and La should all remain immobile upon burial. In reality the reduction of Mn^{4+} to a soluble, divalent state clearly invalidates such assumptions. In similar fashion, the leaching experiments of Livett et al (1979), showing the

high retention of Pb and Cu within peat samples during agitation with HOAc, H2SO4 and EDTA, do not reflect natural conditions as they were carried out in an oxidizing environment.

5.3 Methodological approach.

From the preceding discussion, it is evident that downcore geochemical trends in peat cores from the Galloway and Rannochmoor regions must be interpreted by reference to two potentially applicable hypotheses. These are:-

1) That geochemical anomalies are a product of temporal variations in the influx of elements to the peat surface and hence, analogue pollutant loadings with time.

2) That elemental distributions within peat systems are essentially reflective of hydrologically or redox mediated mobilization processes.

To examine these hypotheses, "bulk" elemental data are presented in section 5.7 to illustrate the distributions of Pb, Zn, Cu, Cd, Fe, Mn, Cr, Ni, Ca, Hg, K, Na, Mg, Ti, Al, Se and V within sample cores. This suite of elements has been considered suitable on account of its comparability with the elemental suite selected for lake sediment analyses (see chapters 2 and 3) and on account of its' "atmophilic" bias. Where available, hydrological and geochronological

data are presented in conjunction with the bulk elemental profiles for sample cores. This facilitates an evaluation of the extent to which downcore geochemical trends fit either of the hypotheses outlined above. Additional interpretive data, derived from sequential chemical analyses of selected sample cores, are presented in section 5.9.

5.4 Sampling locations.

5.4.1 Brishie Mire, Galloway (NG ref. NX83 472825).

Brishie mire can be considered to constitute an ideal sampling location for use during the present study on account of its' proximity to Loch Dee, from which sediment cores were collected for geochemical analysis (see chapter 3). The mire, lying 3 miles to the north-east of Loch Dee, covers an area of 6.5ha and forms the largest single ombrotrophic facet of the Silver Flowe NNR (Fig 5/1). The bedrock is similar to that described for Loch Dee (section 3.2), with the sampling site extending across a transitional tonalite/granite section of the Loch Doon plutonic complex.

The morphology of the Brishie mire surface has formed the focus of considerable research activity (Boatman 1983, Goode 1970, Boatman, Hulme and Tomlinson 1975) and is most strongly characterised by the prevalence of pool complexes, often in excess of 100m in length. Because the depth of

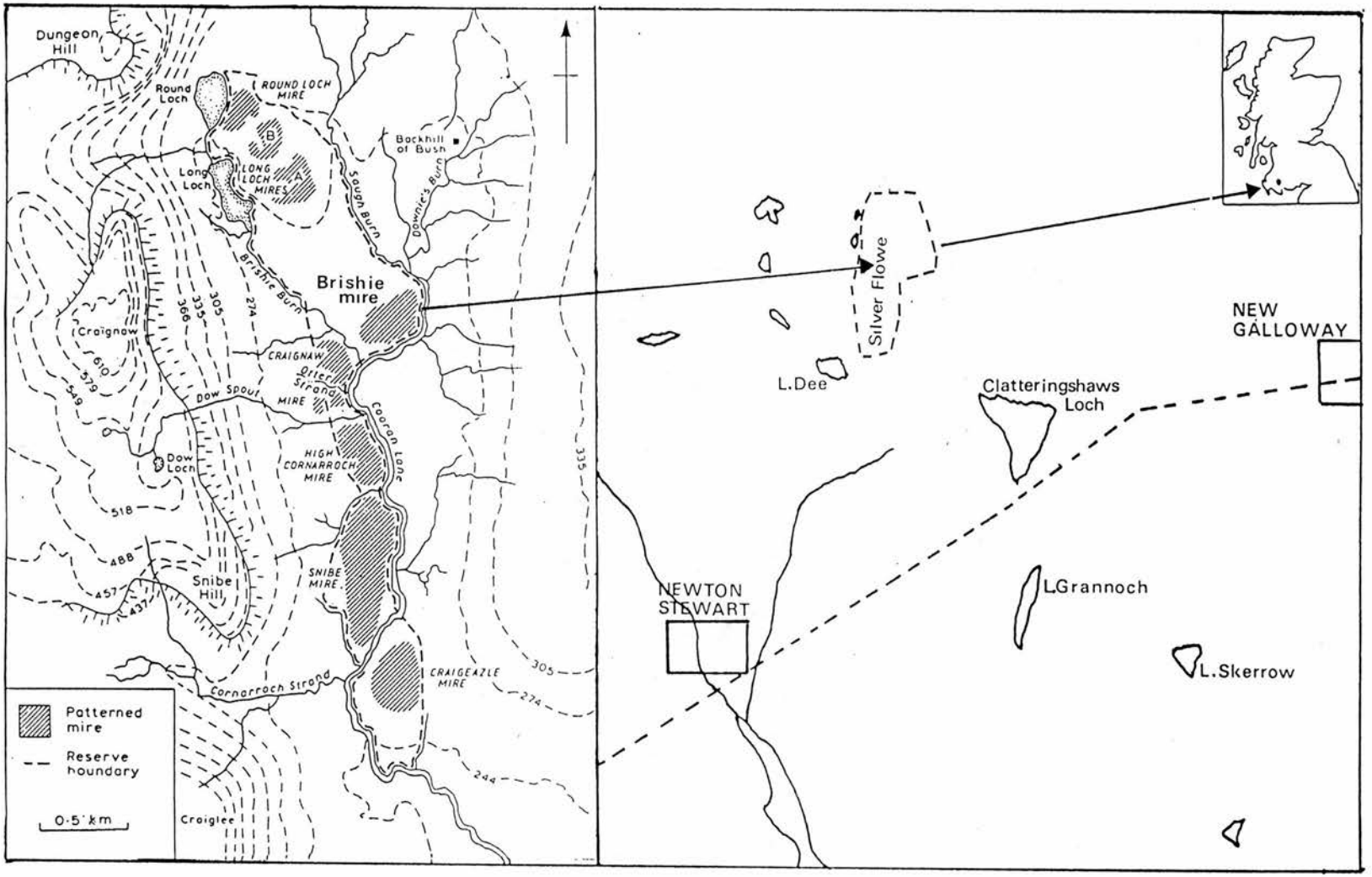

FI3 5/1: Outline and location of Brishie Mire, Galloway.

numerous pools exceeds 1m, a significant proportion of the peat surface is permanently inundated (Boatman 1983).

The vegetation of the Brishie mire complex has been examined in detail by Boatman and Tomlinson (1977) who noted that while species typifying the Trichophoreto-Eriophoretum nodum (McVean and Ratcliffe 1962) are present across the entire peat surface, communities differ markedly in accordance with microtopographic inconsistencies. Pools and hollows are occupied by species which require or tolerate submergence; notably Sphagnum cuspidatum, S.auriculatum, Menyanthes trifoliata and Eriophorum. A more diverse floristic assemblage is evident where the peat surface lies 2cm - 5cm above the water table. At these locations, S.papillosum, S.magellanicum, Rhynchospora alba, Drosera and Narthesium form extensive "carpets". Hummocks, lying up to 50cm above the water table, are principally colonised by Calluna, Eriophorum, Molinea, Erica, Trichophorum and Empetrum.

5.4.2. Craigherron, Galloway (NG ref. NX 525660).

Craigherron mire lies at an altitude of 350m, to the south-west of Loch Grannoch (Fig 5/2). Again this location may be considered to be suitable for the collection of sample cores for use during the present study on account of its proximity to several of Galloways acidified lochs; notably Loch Dee, Loch Fleet and Loch Grannoch. However,

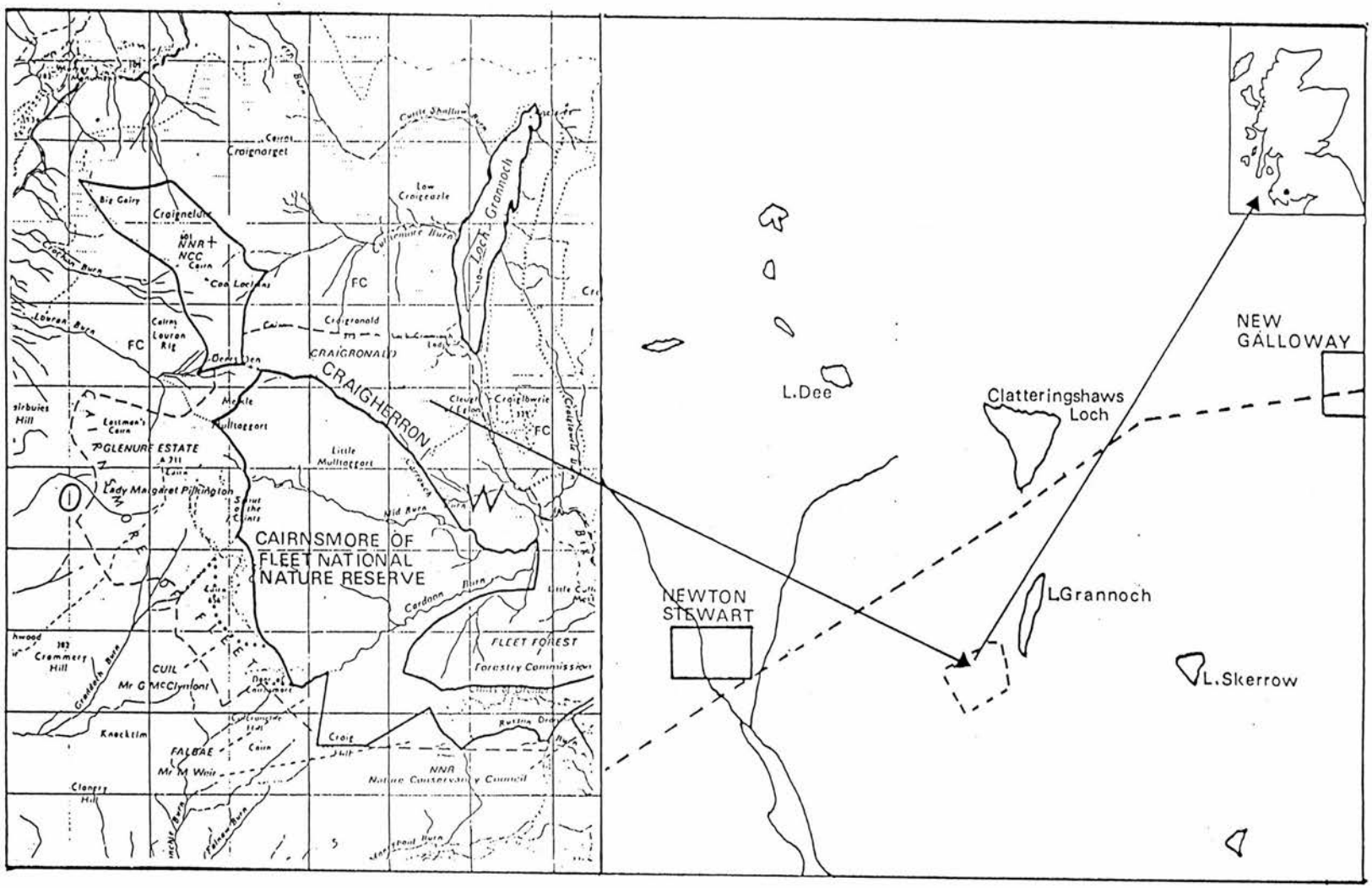

FIG 5/2: Outline and location of Craigherron, Galloway

Craigherron also provides a useful contrast to Brishie mire, being confined within a different, lower Devonian intrusion. This intrusion is entirely granitic, with extensive Cu, Zn and As mineralization in evidence (Drakeford 1979).

The mire surface also contrasts with that of the Silver Flowe peatland, being drier and hence lacking extensive pool systems. Consequently, species which are less tolerent to inundation can dominate, as indicated by the prevalence of Sphagnum papillosum, S.magellanicum, Erica, Calluna, Molinea, Agrostis and Deschampsia. Sphagnum cuspidatum shows restricted presence.

5.4.3 Beinn Chaorach, Rannochmoor (NG ref. NN 293505).

Sample cores were collected from a raised mire system lying 800m east of Beinn Chaorach to facilitate an evaluation of the geochemical characteristics of peat accumulations from within the Loch Ba catchment, Rannochmoor. The location of the sampling site is illustrated in Fig 5/3 and lies entirely upon the previously described Rannochmoor pluton (section 3.2).

The vegetation within the sampling area is characteristic of a relatively dry peat surface, but shows marked variability in accordance with microtopographic inconsistencies. Peat hummocks are principally colonised by

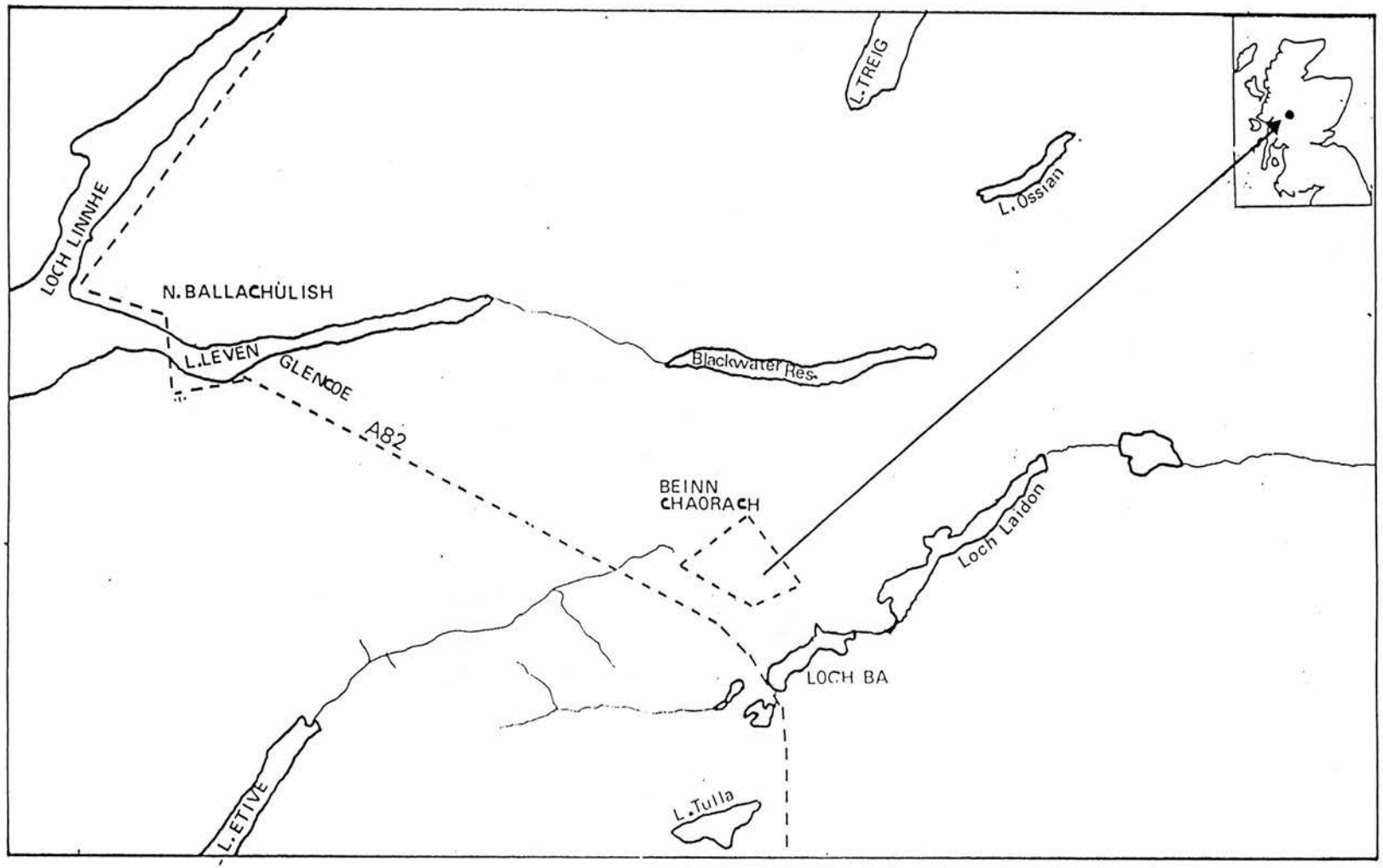

FIG 5/3: Outline and location of Beinn Chaorach, Rannochmoor.

Calluna, Erica and Eriophorum, while periodically inundated "lawns" are formed of Sphagnum magellanicum, S.rubellum and S.papillosum. Juncus and Carex also show strong presence at the margins of the raised mire area.

5.5 Sampling methods and core descriptions.

During the period 1.9.84 - 1.7.86, a total of 22 sample cores were collected from the above field sites. In the following sections, results are presented for just 12 of these cores which, in turn, were collected by use of two methods. Two metre cores, G2M and R2M were extracted by use of a 5.5cm diameter Russian barrel corer. All other cores were collected using a custom built 0.6m tube corer of 22.5cm diameter. The mode of operation for this corer is illustrated in Fig 5/4 from which it is apparent that, following the insertion of the steel "outer core jacket" into the peat, a polythene cylinder (of 22cm diameter) was inserted within it and the outer core tube removed. The peat column which was isolated within the polythene cylinder was then extracted by passing a metal plate beneath the sample core, thus sealing the base of the core and precluding any loss of interstitial water. Finally, the entire column held within the polythene cylinder was dug out, the cylinder capped and stored in an upright position. This procedure was found to facilitate the extraction of cores from "pool" environments without loss of the water overlying the peat surface and hence, can be considered to cause less

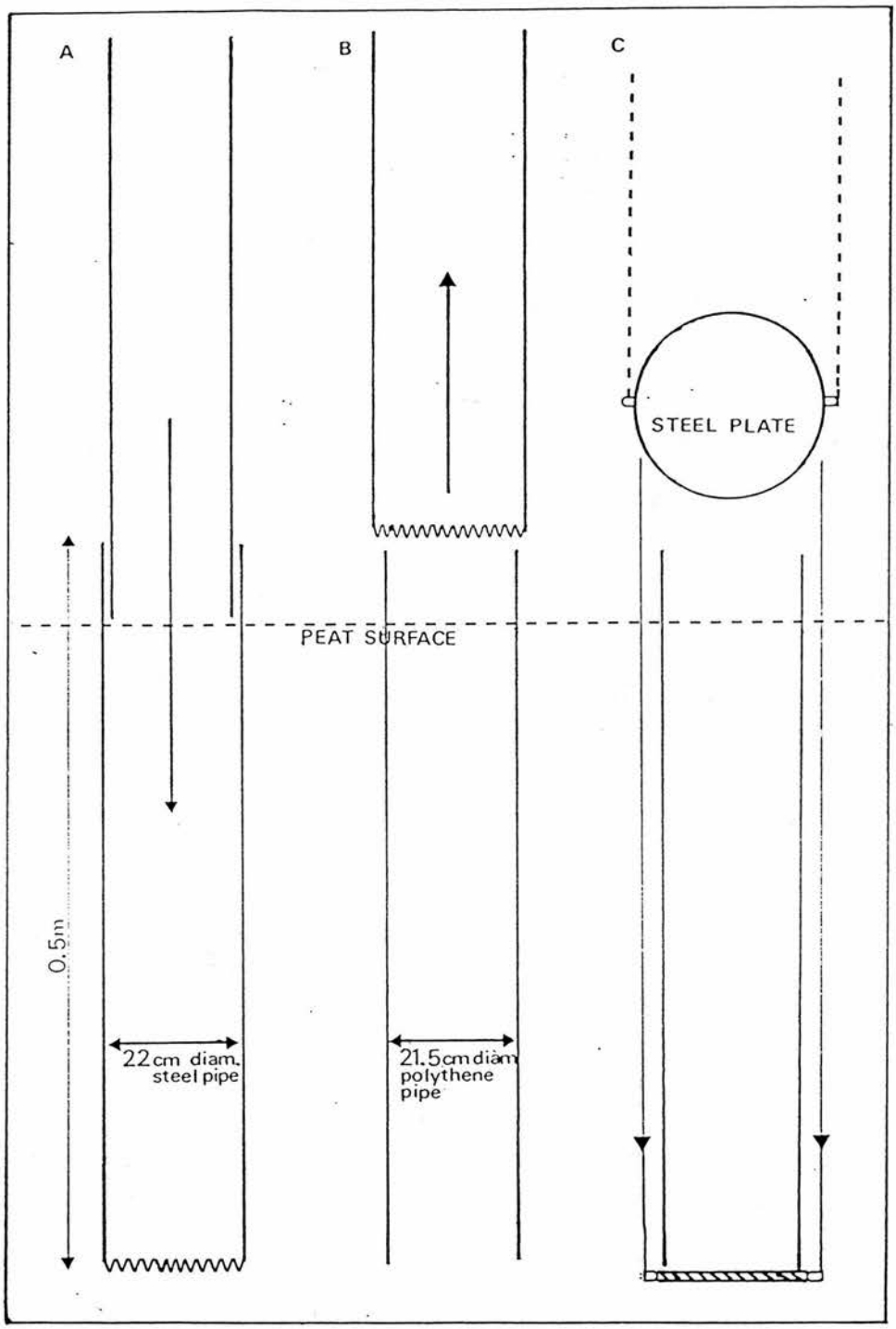

FIG 5/4: Design and operation of the core sampler used for the extraction of 0.5m peat cores from Brishie mire, Craigherron and Beinn Chaorach. The corer comprises a steel barrel which is inserted into the peat, thus cutting a 22cm diameter monolith. Following the placement of a polythene tube inside the corer, a steel plate is pushed down the outside of the corer, guided by two rods. The plate is then pulled underneath the polythene tube to seal the peat column. The enclosed monolith is then dug out and the polythene tube capped and stored in an upright position.

disturbance to samples than any commercially available equipment.

Core descriptions, with respect their microtopography, depth and the range of analyses to which they were subjected, are provided in Table 39.

5.6 Data acquisition.

5.6.1 Bulk elemental data.

All bulk elemental data were acquired by AAS methods, using sub-samples taken from cores at 1cm intervals. In all instances, air dried ($37^{o}C$) samples of 2.00g mass were prepared for analysis by digestion in 15ml HNO3, 5ml HClO4 and 2ml H2SO4 (ARISTAR) in accordance with methods outlined by Allen et al (1974). Digestions were carried out in acid-washed teflon beakers and were considered complete when a clear, particulate free solution had developed. All samples were subsequently diluted to 25ml in 5% HCl and were stored in HCl-washed polythene containers prior to analysis.

Blank solutions and ANALAR standards were utilized in the calibration of all bulk elemental data. These solutions were prepared in accordance with the methods outlined in section 2.2.5.

TABLE 39: Location, description and range of data presented for sample cores from Brishie mire, Craigherron and Beinn Chaorach.

Core	Depth	Location	Topography	Data
G2M	2.0m	Brishie	sphagnum lawn	bulk chemical
G1	44cm	Brishie	calluna hummock	bulk chemical redox, pollen 210Pb
G2	42cm	Brishie	sphagnum lawn	bulk chemical pollen, 210Pb
G3	44cm	Craigherron	S.rubellum hummock	bulk chemical
G4	35cm	Craigherron	sphagnum lawn	bulk chemical redox
G5	35cm	Brishie	sphagnum lawn	seq.chemical redox
G6	30cm	Brishie	sphagnum lawn	bulk chemical redox
R2M	2.0m	Rannoch	sphagnum lawn	bulk chemical
R1	35cm	Rannoch	calluna hummock	bulk chemical 210Pb
R2	22cm	Rannoch	sphagnum lawn	bulk chemical redox, 210Pb
R3	35cm	Rannoch	sphagnum lawn	seq.chemical
R4	35cm	Rannoch	calluna hummock	seq.chemical redox
R5	30cm	Rannoch	sphagnum lawn	bulk chemical redox

Elemental analyses for Pb, Cu, Zn, Cd, Fe, Mn, Ca, Na, Hg, K, Mg, Co, Ni and Cr were made using air/ acetylene flame methods. Measurements of Al, V, Se and Ti were made by AAS using an acetylene/nitrous oxide flame. In all cases, the most sensitive analytical lines were used (Price 1972).

5.6.2 Hydrological data.

Determinations of the water table level at each coring station were made by inserting a 10cm diameter polythene pipe, along which 3cm diameter holes had been drilled at 2cm intervals, into the peat column. Following an equilibration period of 1 hour, the water level within the pipe was considered to be indicative of the stratigraphic level at which inundated conditions prevailed.

5.6.3 Redox data.

Direct redox data were acquired for cores G1, G4, G5, G6, R2 and R5 by use of the Pt electrode methods described in section 2.2.5. All measurements were made at the field sites immediately after the extraction of sample cores. Such a procedure was made possible by collecting sample cores in polythene core tubes, along which 0.75cm diameter holes had been drilled at 3cm intervals. The 0.75cm diameter holes then provided "access points" for the pT electrode, thus allowing redox measurements to be made prior to core extrusion.

5.6.4 Radiometric data.

Previously described gamma spectrometric methods (section 2.4) were used to attain 210Pb, 137Cs and 134Cs assays for a limited number of sub-samples from cores G1, G2, R1 and R2. Of these nuclides, 137Cs and 134Cs are known to display mobility within acid, organic matrices (Oldfield et al 1979, Davis et al 1984) and have not been considered to yield valid geochronological data. In contrast, studies of UK and Scandinavian sample cores (Oldfield et al 1979, El Daoushy et al 1982) have shown 210Pb chronologies to be in accordance with independent, pollen-based chronologies. Hence, 210Pb assays have been considered to be of greatest utility.

Following establishment of the accordance between the 210Pb assays of ashed and fresh sub-samples taken from the peat surface at Beinn Chaorach, all 210Pb counts were made on sub-samples which had previously been ashed at 450 ^{o}C. This preparation procedure facilitated the reduction of 10g - 20g of peat to a volume of suitable size for placement upon a Ge(Li) detector. As a result, counting times were reduced from 500,000 seconds (required to obtain a statistically significant count from 1g of fresh peat) to 80,000 seconds.

5.6.5 Palynological data.

Palynological methods of the nature outlined by Livett et

al (1979) were used to obtain geochronological data for cores G1 and G2. Samples of 1g mass were prepared in accordance with the methods of Moore and Webb (1978) and were spiked with 10,000 lycopodium spores prior to analysis. For each analysed sample, counts of 500 pollen grains were considered sufficient to facilitate the calculation of representative pollen frequency data. Absolute pollen concentrations were calculated for each of the identified taxa by normalizing their spectra against the number of lycopodium spores observed.

5.6.6 Derivation of absolute chronologies.

For the Brishie mire cores, G1 and G2, absolute chronologies were primarily derived from the pollen frequency data presented in Figs 5/5 - 5/6. Information was also derived from the 210Pb assays for samples from 11cm and 30cm depths of core G1 (3.1pCi/g and 0pCi/g respectively) and from 7cm and 30cm depths of core G2 (3.7pCi/g and 0.13pCi/g respectively). In summary, analogous increments to Pinus frequencies upward of 11cm depth in core G1 and 7cm depth in core G2 are associated with the onset of afforestation in the Brishie mire vicinity in 1962. Hence, these strata have been assigned an age of 25yrs BP. In addition, reductions to the ratios of Plantago/Arboreal pollen upward of 29cm in cores G1 and G2

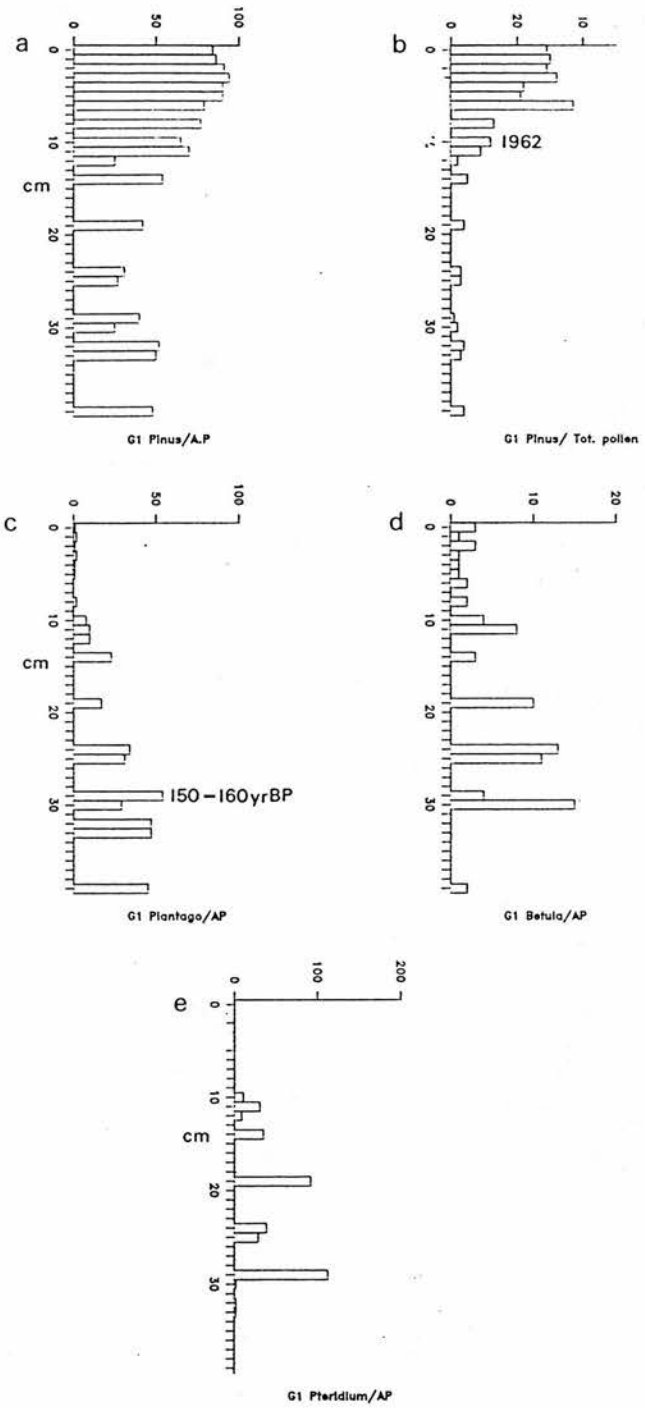

FIG 5/5: Geochronologically significant pollen/spore frequency adjustments in core G1. For each sampling level, spectra for individual taxa are normalised against the total arboreal pollen frequency (AP). Origins of 25yrs BP and 150-160yrs BP have been assigned to strata at 11cm and 29cm depths on the basis of palynological and 210Pb data.

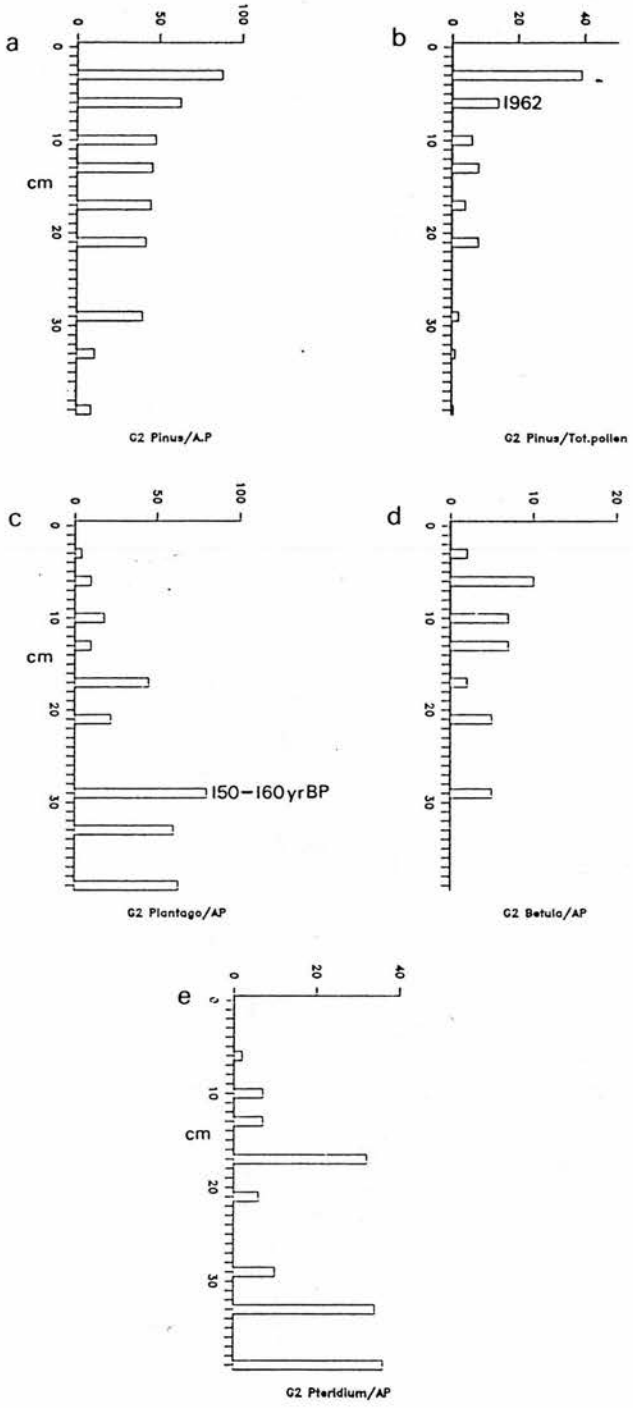

FIG 5/6: Geochronologically significant pollen/spore frequency adjustments in core G2. For each sampling level, spectra for individual taxa are normalised against the total arboreal pollen frequency (AP). Downcore variations of Pinus and Plantago frequencies are correlatable with those occurring in core G1.

suggest that these levels are of synchronous origin. These strata have been assigned an age of 140 - 160yrs BP on account of the negligable 210Pb activity observed within the G1 sample (0.13pCi/g) and the undetectable 210Pb activity observed within the G2 sample. By using the datable horizons of cores G1 and G2 to calculate mean accumulation rates, respective values of 0.44cm/yr-1 and 0.16cm/yr-1 have been assigned to the 1cm - 11cm and 12cm - 29cm sequences of core G1. For core G2, the mean accumulation rate of peats at 1cm - 7cm depth has been calculated as 0.28cm/yr-1, while rates for the 8cm - 29cm strata have determined as 0.20cm/yr-1.

For the Beinn Chaorach cores, R1 and R2, geochronological information has been derived from the 210Pb assays presented in Table 40. With respect to the interpretation of the bulk elemental data for these cores, it is significant that 210Pb activities were found to be undetectable downward of 17cm in core R1 and downward 14cm in core R2. Accordingly, these strata have been assigned origins in excess of 155yrs BP. The CRS-determined accumulation rate of strata upward of 3cm depth in core R2 is 0.21cm/yr-1 and hence, strata at 3cm depth have been assigned an age of 14yrs BP (see footnote). A CRS-based origin of 97yrs BP has also been established for the 11cm sub-sample from this core.

Table 40: Activities of 210Pb, 137Cs (pCi/g) and 134Cs/137Cs ratios within sub-samples from cores R1 and R2.

Sample	210Pb	137Cs	134/137Cs	age yr/acc.rate
R1 3cm	3.5	217.0	0.26	-
R1 17cm	0.02	0.12	-	0.06cm/yr-1
R1 21cm	0	0	-	-
R2 1cm	2.8	283.0	0.33	0
R2 3cm	4.0	7.0	0.22	14
R2 5cm	3.6	2.9	0.12	
R2 9cm	1.4	1.2	0.02	
R2 11cm	0.86	1.1	-	97
R2 13cm	0.26	0.5	-	
R2 14cm	0	0.3	-	155
R2 15cm	0	0.4	-	-
R2 22cm	0	0.2	-	-

NOTE: 210Pb data include 226Ra supported components. Accordingly, any age determinations based upon the CRS model are subject to error.

5.6.7 Sequential chemical data.

Sequential Pb, Zn, Cu, Cr, Cd, Fe and Mn data were obtained for samples taken at 2cm intervals from cores G5 and R3 using the methods of Tessier et al (1979). These methods are described in section 2.2.5 and Appendix 1b.

5.7 Results of bulk geochemical analyses.

5.7.1 Elemental distributions.

On account of the analogous downcore geochemical trends

observed in all sample cores from Brishie mire, Craigherron and Beinn Chaorach (Figs 5/7 - 5/25), the bulk elemental data for these sites can conveniently be evaluated simultaneously. With respect to elemental distributions on a "low resolution" basis, data for 2.0m cores from Brishie mire (G2M) and Beinn Chaorach (R2M) show that, with the exceptions of Na and Ca, all analysed elements are subject to greatest enrichment within the surficial 50cm of the peat column (Figs 5/7 - 5/10). Those elements displaying enrichment towards the peat surface fall into 3 discrete groups. Specifically:-

1) Mn and K are conspicuous as they accumulate only in the surficial 10cm - 20cm of the peat column. In core G2M, Mn and K concentrations of 38µg/g and 1080µg/g respectively at these levels exceed those of all underlying strata by at least a factor of 10 (Figs 5/7f and i). In core R2M analogous trends are apparent, with concentrations of 1000µg/g Mn and 2000µg/g K occurring in the uppermost 10cm and declining to "background" (below 50µg/g) concentrations downward of 20cm (Figs 5/9f and i). Consequently, these elements are strongly characterised by their acute downcore concentration gradients.

2) Pb, Zn, Cd, Cr, Ni and V also attain maximum concentrations within the surficial 20cm of cores G2M and R2M, but can be distinguished from Mn and K on account of

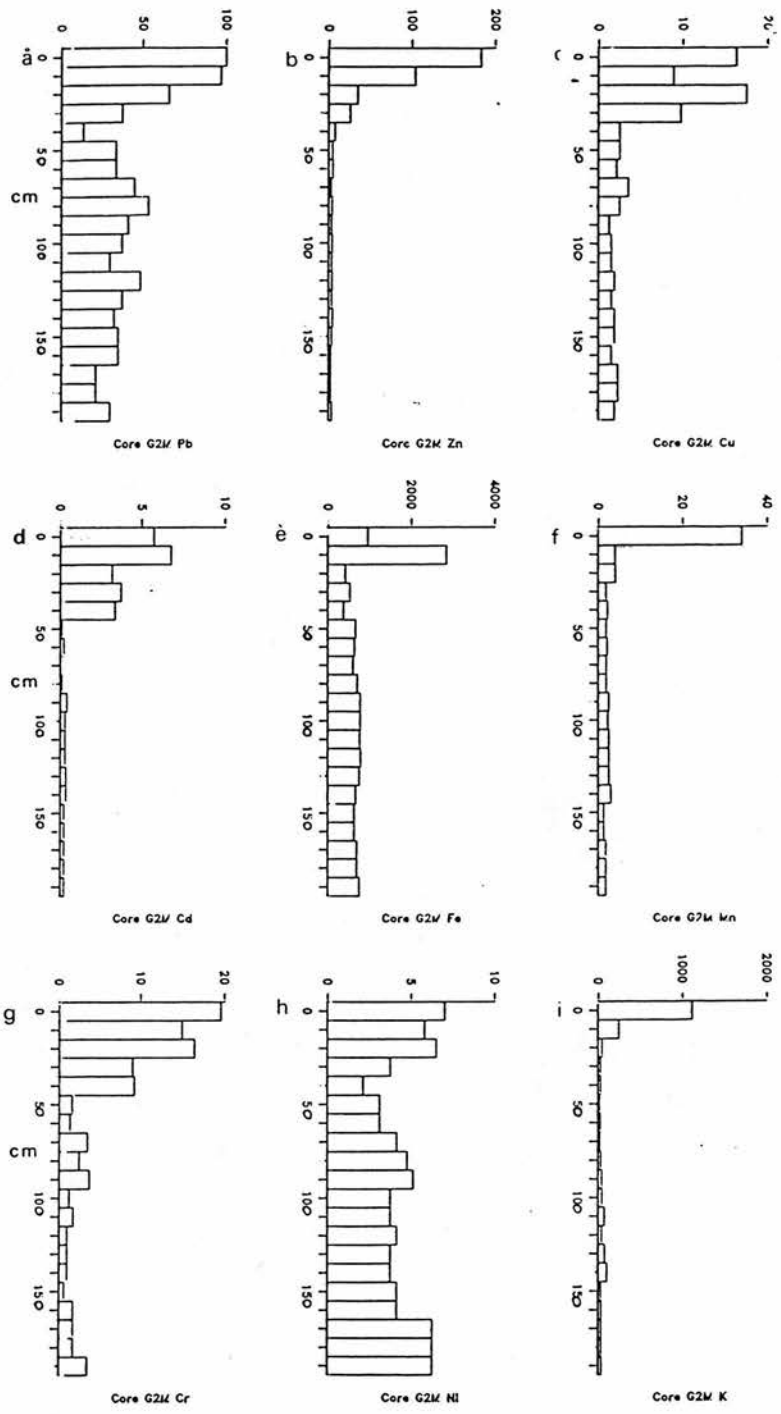

FIG 5/7: Core G2M - Total concentrations of Pb, Zn, Cu, Cd, Fe, Mn, Cr, Ni and K (µg/g dry weight) within sub-samples taken at 10cm resolution.

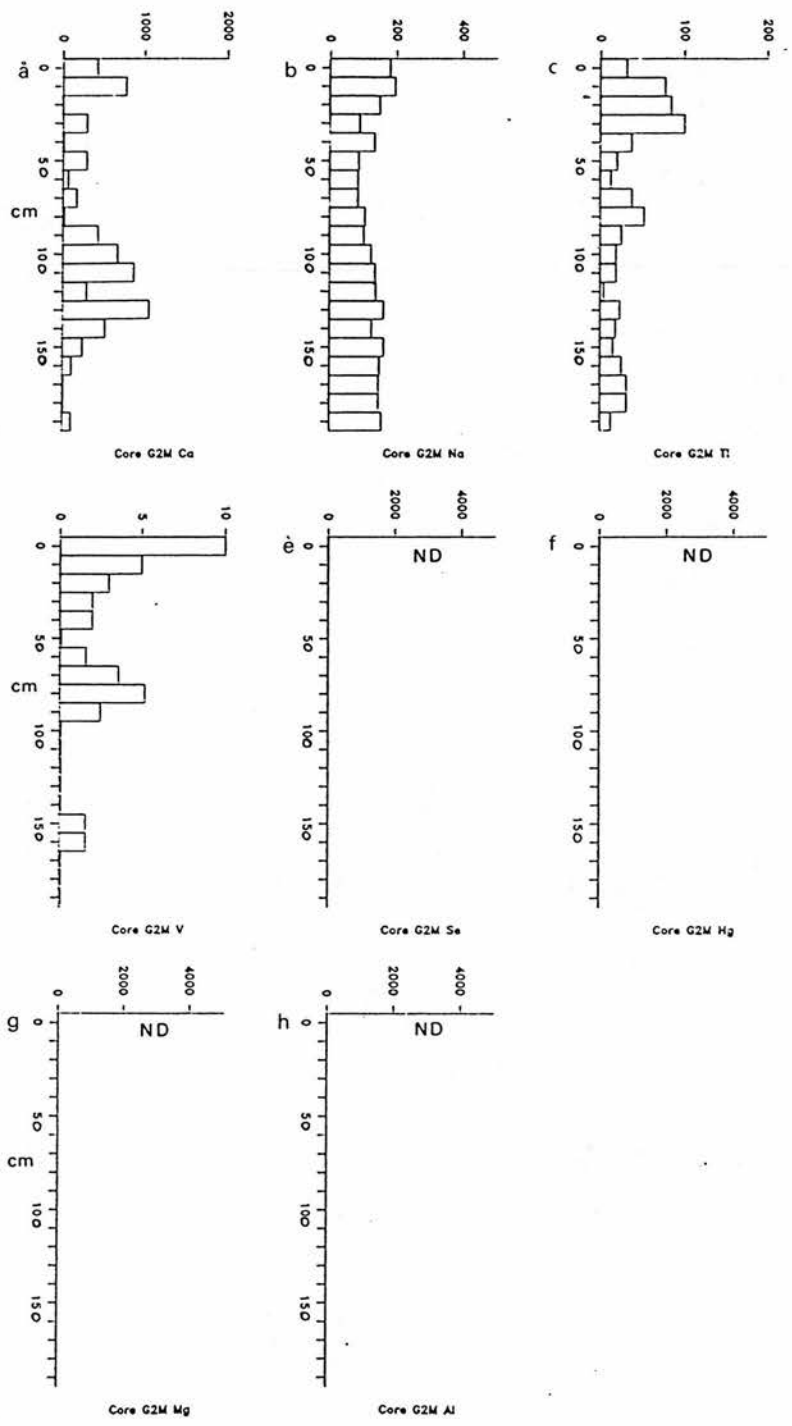

FIG 5/8: Core G2M - Total concentrations of Ca, Na, Ti and V (µg/g dry weight) within sub-samples taken at 10cm resolution. Note: ND signifies that data are not available.

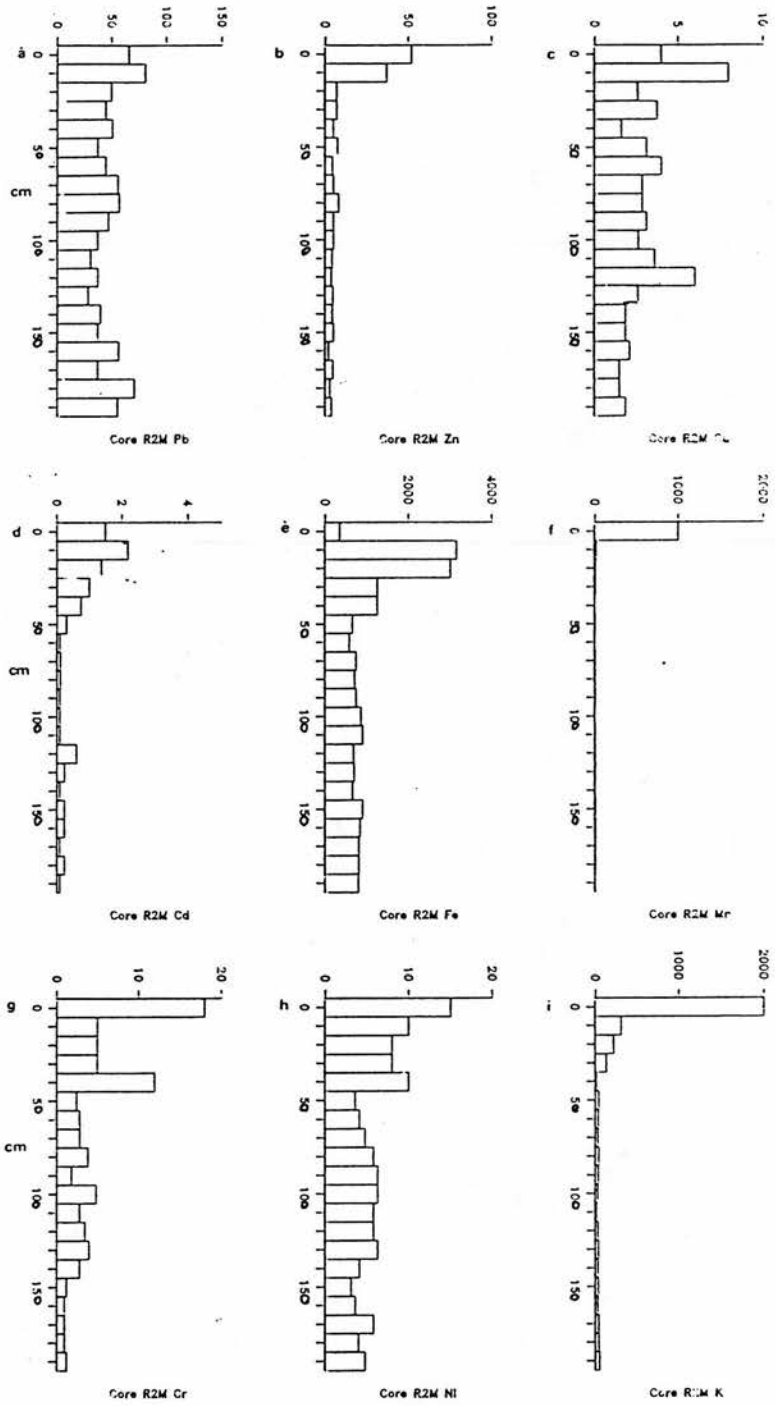

FIG 5/9: Core R2M - Total concentrations of Pb, Zn, Cu, Cd, Fe, Mn, Cr, Ni and K (µg/g dry weight) in sub-samples taken at 10cm resolution.

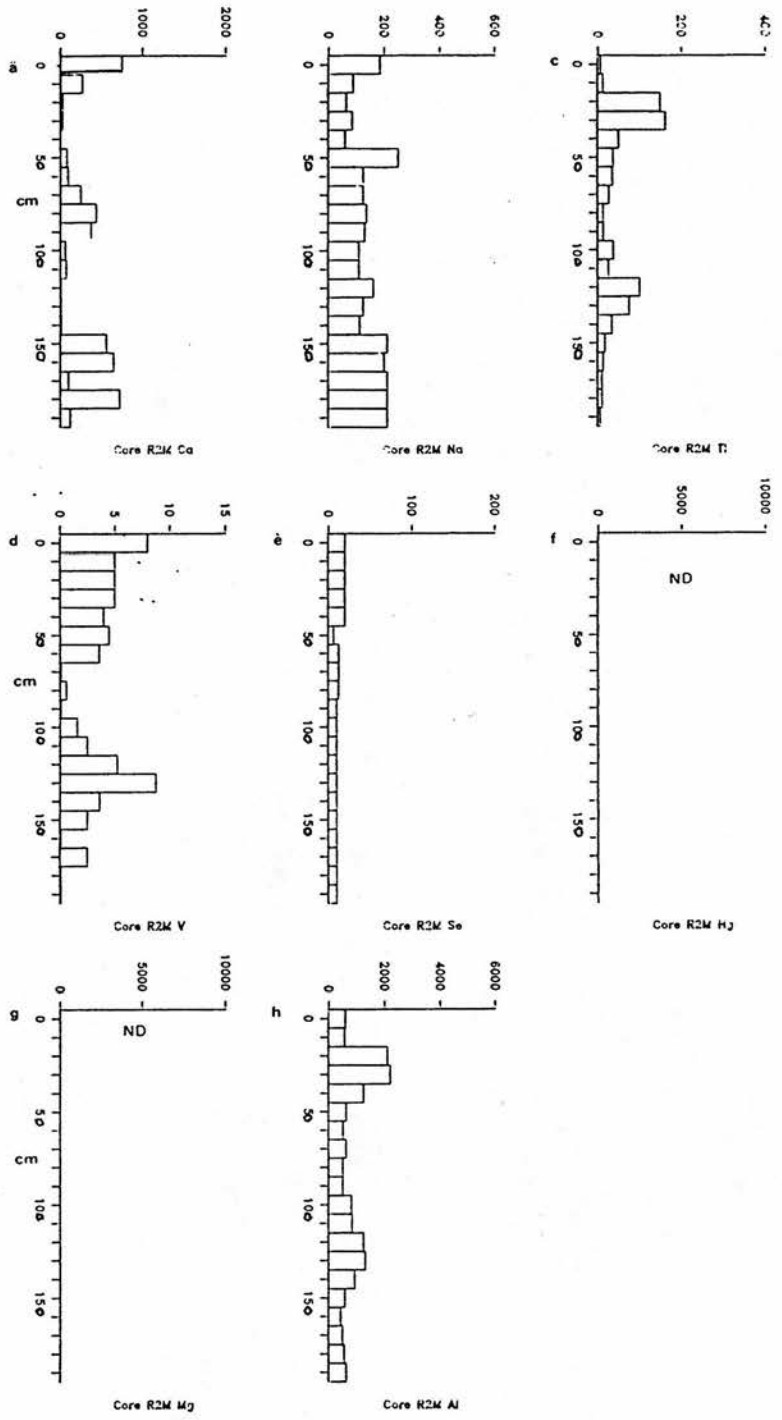

FIG 5/10: Core R2M - Total concentrations of Ca, Na, Ti, V, Se and Al (µg/g dry weight) in sub-samples taken at 10cm resolution.

their more gentle concentration gradients (Figs 5/7a, b, d, g and h, 5/8d, 5/9a, b, d, g and h, 5/10d). "Background" concentrations of these elements are similar in both cores (50µg/g Pb, 5µg/g Zn, 0.5µg/g Cd, 5µg/g Cr, 5µg/g Ni and 5µg/g V) and prevail throughout strata of 50cm - 200cm depth. Upward of 50cm, increments in the concentrations of Cr, V and Ni (by factors of 2 - 10) are also analogous in both cores, but core G2M shows markedly greater surficial enrichment of Pb (to 100µg/g), Zn (to 180µg/g) and Cd (to 7µg/g).

3) Fe, Cu, Al and Ti are distinguishable from the elements described above as they attain peak concentrations (3000µg/g Fe, 19µg/g Cu, 109µg/g Ti in core G2M, 3200µg/g Fe, 9µg/g Cu, 170µg/g Ti and 2100µg/g Al in core R2M) at 20cm - 50cm depth, with concentrations declining both upward and downward of this level (Figs 5/7c and e, 5/8c, 5/9c and e, 5/10c and h).

A more detailed insight into the elemental enrichment patterns within the Galloway and Beinn Chaorach study areas is provided by the "high resolution" data collated for 0.25m - 0.50m cores from Brishie mire (G1, G2 and G6), Craigherron (G3 and G4) and Beinn Chaorach (R1, R2 and R5). Of these cores, G1 - G2, G3 - G4 and R1 - R2 were extracted from adjacent "Calluna hummock" and "Sphagnum lawn" locations. Cores G6 and R5 represent conditions at additional inundated "Sphagnum lawn" sites. Upon examining the downcore

elemental profiles (Figs 5/11 - 5/25) and the correlation matrices (Tables 41 - 48) for these cores, the elemental groupings identified in cores G2M and R2M appear to retain considerable applicability. Specifically, the following trends are apparent:-

1) The profiles of Mn and K in cores G1, G2, G3, G4, G6, R1, R2 and R5 show strong co-variability, as exemplified by the persistence of R coefficients in excess of 0.7. Concentration maxima for these elements occur within the surficial 4cm of all sample cores (Figs 5/11f and i, 5/13f and i, 5/15f and i, 5/17f and i, 5/19f and i, 5/21f and i, 5/23f, 5/24f and i). However, by reference to the geochronological data presented for the paired "hummock" and "lawn" cores G1 and G2, R1 and R2, it is possible to establish that strata showing initial enrichment of Mn and K are not temporally synchronous. Instead, they tend to be older within the former. For example, Mn concentrations increase progressively from 5µg/g to a surficial peak of 249µg/g throughout strata which have accumulated since 1840 at the Brishie mire "hummock" coring site, G1 (Fig 5/11f) while significant Mn enrichment is confined to the 20th century levels of the proximal "lawn" core, G2 (Fig 5/13f). Accordingly, it can be assumed that the downcore Mn gradients observed at sampling sites do not simply reflect temporal variations of the elements atmospheric influx.

	DEPTH	Hg	Cd	Pb	Zn	Cu	Fe	Ca
Hg	-0.200							
Cd	0.220	0.064						
Pb	0.590	-0.096	0.017					
Zn	0.064	0.178	0.039	0.118				
Cu	0.625	-0.081	0.377	0.303	-0.321			
Fe	0.824	-0.399	0.128	0.474	-0.060	0.480		
Ca	0.004	0.252	0.299	0.378	0.072	0.042	0.032	
Mn	-0.761	0.296	0.051	-0.388	-0.148	-0.246	-0.622	0.296
K	-0.943	0.226	-0.146	-0.561	0.106	-0.596	-0.762	0.036
Na	-0.281	-0.055	-0.191	-0.097	0.333	-0.272	-0.100	-0.113
Al	0.604	0.090	0.564	0.119	-0.055	0.807	0.372	-0.030
Ti	0.489	0.118	0.564	0.057	-0.068	0.671	0.344	-0.074
Ni	0.200	0.389	0.221	0.319	0.529	0.040	0.060	0.232
Cr	-0.200	0.091	-0.228	-0.098	-0.134	0.075	-0.270	-0.072
Mg	-0.400	0.108	0.031	-0.215	0.462	-0.420	-0.218	0.234

	Mn	K	Na	Al	Ti	Ni	Cr
K	0.763						
Na	0.066	0.398					
Al	-0.311	-0.545	-0.357				
Ti	-0.271	-0.420	-0.136	0.877			
Ni	-0.044	-0.046	0.196	0.172	0.132		
Cr	0.155	0.113	0.015	0.009	-0.038	-0.117	
Mg	0.390	0.603	0.536	-0.381	-0.236	0.357	-0.244

Table 41: Correlation coefficients (R) illustrating the co-variability of elemental concentrations through core G1.

	DEPTH	Hg	Cd	Pb	Zn	Cu	Fe	Ca
Hg	-0.232							
Cd	-0.346	-0.019						
Pb	-0.414	0.274	0.514					
Zn	-0.782	0.392	0.372	0.290				
Cu	-0.111	0.146	0.285	0.219	-0.025			
Fe	-0.400	0.342	0.697	0.366	0.545	0.198		
Ca	-0.237	-0.012	0.274	0.169	0.128	0.036	0.166	
Mn	-0.709	0.235	0.138	0.213	0.744	-0.112	0.094	0.259
K	-0.768	0.258	0.078	0.133	0.665	-0.096	0.046	0.186
Na	-0.335	0.339	0.296	0.207	0.434	0.142	0.665	0.296
Mg	-0.050	0.468	0.048	0.071	0.313	0.199	0.592	0.050
Al	0.426	-0.200	-0.279	-0.206	-0.463	0.038	-0.284	-0.344
Ti	0.494	-0.114	-0.374	-0.334	-0.471	-0.069	-0.365	-0.278
Ni	-0.471	0.342	0.467	0.345	0.636	0.121	0.437	-0.080
Cr	-0.356	-0.017	0.281	0.268	0.263	0.162	0.166	-0.085

	Mn	K	Na	Mg	Al	Ti	Ni
K	0.800						
Na	0.189	0.305					
Mg	-0.038	0.104	0.781				
Al	-0.418	-0.509	-0.569	-.278			
Ti	-0.410	-0.530	-0.548	-0.266	0.857		
Ni	0.490	0.195	0.255	0.191	-0.117	-0.164	
Cr	0.265	0.116	0.131	-0.036	-0.001	-0.022	0.556

Table 42: Correlation coefficients (R) illustrating the co-variability of elemental concentrations through core G2.

	DEPTH	Pb	Cu	Zn	Ni	Cr	Cd	Mn
Pb	0.422							
Cu	0.863	0.262						
Zn	0.231	-0.015	0.279					
NI	0.078	-0.258	0.118	0.301				
Cr	0.461	-0.025	0.347	0.330	0.348			
Cd	0.495	0.132	0.420	0.697	0.470	0.285		
Mn	-0.682	-0.344	-0.401	-0.378	-0.176	-0.570	-0.520	
Ca	-0.319	0.257	-0.433	-0.456	-0.547	-0.209	-0.550	0.164
Hg	-0.074	-0.327	0.029	0.061	0.692	0.086	0.170	0.037
Fe	-0.131	0.026	-0.320	0.519	0.145	0.190	0.343	-0.432
Mg	-0.236	0.121	-0.353	0.011	-0.081	-0.040	-0.093	-0.060
Na	-0.850	-0.393	-0.701	-0.179	-0.183	-0.344	-0.505	0.656
K	-0.798	-0.431	-0.537	-0.221	-0.142	-0.556	-0.476	0.922
Se	0.363	0.433	0.180	0.044	0.238	0.143	0.162	-0.344
Al	0.695	0.103	0.707	0.468	0.512	0.599	0.641	-0.517
Ti	0.559	-0.033	0.643	0.446	0.676	0.551	0.671	-0.394

	Ca	Hg	Fe	Mg	Na	K	Se	Al
Hg	-0.348							
Fe	0.052	0.060						
Mg	0.405	-0.014	0.608					
Na	0.291	-0.119	0.030	0.178				
K	0.138	0.073	-0.231	0.034	0.782			
Se	0.164	0.176	0.163	0.186	-0.455	-0.371		
Al	-0.559	0.353	0.023	-0.202	-0.672	-0.571	0.257	
Ti	-0.637	0.435	-0.013	-0.250	-0.590	-0.459	0.103	0.896

Table 43: Correlation coefficients (R) illustrating the co-variability of elemental concentrations through core G3.

	DEPTH	Pb	Cu	Zn	Cd	Ni	Cr	Fe
Pb	0.797							
Cu	0.419	0.478						
Zn	.547	-0.384	0.019					
Cd	0.239	0.247	0.675	0.354				
Ni	-0.002	-0.063	0.202	0.194	0.116			
Cr	-0.522	-0.545	0.047	0.632	0.198	0.426		
Fe	-0.266	0.001	-0.188	0.304	0.111	-0.038	-0.094	
Mn	-0.622	-0.507	-0.335	0.081	-0.294	0.015	0.152	0.423
Ca	-0.194	-0.052	-0.089	0.320	0.277	-0.286	0.029	0.135
Na	-0.830	-0.732	-0.486	0.200	-0.412	0.058	0.345	0.192
K	-0.745	-0.644	-0.465	-0.021	-0.500	0.030	0.187	0.169
Se	-0.333	-0.427	-0.049	0.071	-0.098	0.003	0.321	-0.072
Hg	0.525	0.403	0.239	-0.502	-0.135	0.222	-0.434	-0.224
V	-0.693	-0.586	-0.441	0.351	-0.269	0.172	0.289	0.258
Mg	-0.604	-0.549	-0.418	0.470	-0.085	0.144	0.334	0.324
Ti	0.500	0.311	0.517	-0.148	0.186	0.565	0.180	-0.335
Al	-0.391	-0.298	0.235	0.538	0.417	.263	0.387	0.207

	Mn	Ca	Na	K	Se	Hg	V	Mg
Ca	-0.118							
Na	0.810	0.007						
K	0.802	-0.074	0.932					
Se	0.376	-0.381	0.360	0.302				
Hg	-0.158	-0.514	-0.230	-0.133	-0.160			
V	0.527	0.198	0.661	0.628	-0.188	-0.186		
Mg	0.474	0.387	0.667	0.504	-0.113	-0.285	0.680	
Ti	-0.369	-0.545	-0.478	-0.392	-0.048	0.477	-0.350	-0.460
Al	0.188	0.312	0.282	0.170	0.002	-0.265	0.315	0.435

Table 44: Correlation coefficients (R) illustrating the co-variability of elemental concentrations through core G4.

	DEPTH	Pb	Zn	Cd	Cu	Cr	Ni	Hg
Pb	-0.188							
Zn	-0.349	0.673						
Cd	-0.341	0.727	0.834					
Cu	-0.135	0.593	0.448	0.530				
Cr	-0.192	0.749	0.791	0.770	0.592			
Ni	-0.380	0.741	0.673	0.756	0.677	0.842		
Hg	-0.274	-0.134	-0.288	-0.082	-0.313	-0.326	-0.130	
Mn	-0.859	-0.057	-0.022	-0.009	-0.031	-0.095	0.119	0.430
Ti	0.403	0.448	0.193	0.193	0.566	0.389	0.320	-0.325
V	-0.722	0.365	0.469	0.477	0.241	0.435	0.536	0.075
Fe	0.323	0.426	0.443	0.477	0.422	0.615	0.497	-0.342
Na	-0.348	0.120	-0.225	-0.041	0.107	-0.054	0.134	0.575
K	-0.873	0.009	-0.004	0.073	0.049	-0.074	0.151	0.479
Mg	-0.455	0.163	0.188	0.221	-0.172	-0.001	0.131	0.249

	Mn	Ti	V	Fe	Na	K
Ti	-0.459					
V	0.398	-0.056				
Fe	-0.455	0.283	-0.142			
Na	0.545	-0.133	0.138	-0.070		
K	0.921	-0.416	0.499	-0.424	0.664	
Mg	0.424	-0.549	0.115	-0.019	0.346	0.404

Table 45: Correlation coefficients (R) illustrating the co-variability of elemental concentrations through core G6.

	DEPTH	Pb	Zn	Cu	Cd	Mn	Ni	Cr
Pb	-0.560							
Zn	-0.710	0.766						
Cu	-0.534	0.821	0.614					
Cd	-0.545	0.911	0.785	0.859				
Mn	-0.567	0.076	0.001	0.365	0.055			
Ni	-0.162	0.090	0.281	0.051	0.200	-0.024		
Cr	-0.151	-0.024	0.242	-0.187	-0.011	-0.053	0.574	
Ca	-0.683	0.437	0.356	0.502	0.421	0.601	-0.101	-0.198
Fe	0.350	0.323	0.030	0.407	0.339	-0.286	-0.253	-0.397
Na	-0.625	0.144	0.444	0.097	0.081	0.381	0.224	0.316
K	-0.677	0.251	0.283	0.410	0.180	0.790	0.016	0.009
Mg	-0.641	0.257	0.218	0.440	0.260	0.773	0.068	0.018
Hg	0.468	-0.094	-0.273	-0.074	-0.057	-0.276	-0.244	-0.258
Al	0.629	-0.695	-0.720	-0.535	-0.618	-0.155	0.112	0.096
Ti	0.617	-0.636	-0.716	-0.486	-0.598	-0.197	-0.207	-0.247

	Ca	Fe	Na	K	Mg	Hg	Al
Fe	0.021						
Na	0.360	-0.487					
K	0.630	-0.307	0.713				
Mg	0.746	-0.188	0.519	0.866			
Hg	-0.326	0.456	-0.529	-0.320	-0.181		
Al	-0.492	-0.101	-0.257	-0.254	-0.216	0.048	
Ti	-0.425	-0.023	-0.353	-0.269	-0.292	0.154	0.847

Table 46: Correlation coefficients (R) illustrating the co-variability of elemental concentrations through core R1.

	DEPTH	Zn	Pb	Mn	Cd	Cr	Ni	Cu
Zn	-0.911							
Pb	-0.716	0.635						
Mn	-0.854	0.889	0.559					
Cd	-0.795	0.896	0.629	0.742				
Cr	0.049	0.026	0.263	0.042	0.233			
Ni	-0.018	0.047	0.328	0.034	0.284	0.725		
Cu	-0.865	0.959	0.635	0.916	0.886	0.043	0.058	
Hg	-0.119	0.201	0.308	0.043	0.480	0.457	0.666	0.220

Table 47: Correlation coefficients (R) illustrating the co-variability of elemental concentrations through core R2.

	DEPTH	Zn	Cu	Pb	Mn	Cr	Ni	Cd
Zn	-0.852							
Cu	-0.860	0.876						
Pb	-0.805	0.672	0.713					
Mn	-0.740	0.867	0.723	0.676				
Cr	-0.832	0.841	0.818	0.615	0.779			
Ni	-0.650	0.755	0.757	0.601	0.757	0.657		
Cd	-0.810	0.819	0.799	0.745	0.751	0.751	0.780	
Hg	0.141	-0.031	-0.134	-0.091	0.082	-0.181	0.061	0.064
Ti	-0.530	0.418	0.759	0.520	0.314	0.519	0.471	0.473
V	-0.658	0.771	0.552	0.574	0.873	0.693	0.600	0.538
Se	0.111	-0.106	-0.048	-0.018	-0.018	-0.189	-0.083	0.047
Al	-0.648	0.387	0.685	0.641	0.355	0.487	0.527	0.538
Fe	-0.164	0.205	-0.016	0.183	0.330	0.174	0.061	0.332
Ca	-0.338	0.401	0.163	0.429	0.535	0.301	0.100	0.325
Na	-0.680	0.801	0.587	0.663	0.880	0.662	0.601	0.677
K	-0.682	0.727	.709	0.750	0.868	0.665	0.595	0.661
Mg	-0.387	0.403	0.165	0.242	0.344	0.296	0.135	0.413

	Hg	Ti	V	Se	Al	Fe	Ca	Na
Ti	-0.173							
V	-0.084	0.164						
Se	0.518	-0.045	-0.210					
Al	-0.162	0.779	0.182	-0.041				
Fe	0.216	-0.358	0.257	0.094	-0.164			
Ca	-0.162	-0.223	0.568	-0.039	-0.140	0.625		
Na	0.034	0.091	0.844	-0.006	0.185	0.540	0.715	
K	0.100	0.438	0.741	0.188	0.397	0.342	0.536	0.825
Mg	-0.027	-0.302	0.338	-0.105	-0.045	0.642	0.609	0.530

Table 48: Correlation coefficients (R) illustrating the co-variability of elemental concentrations through core R5.

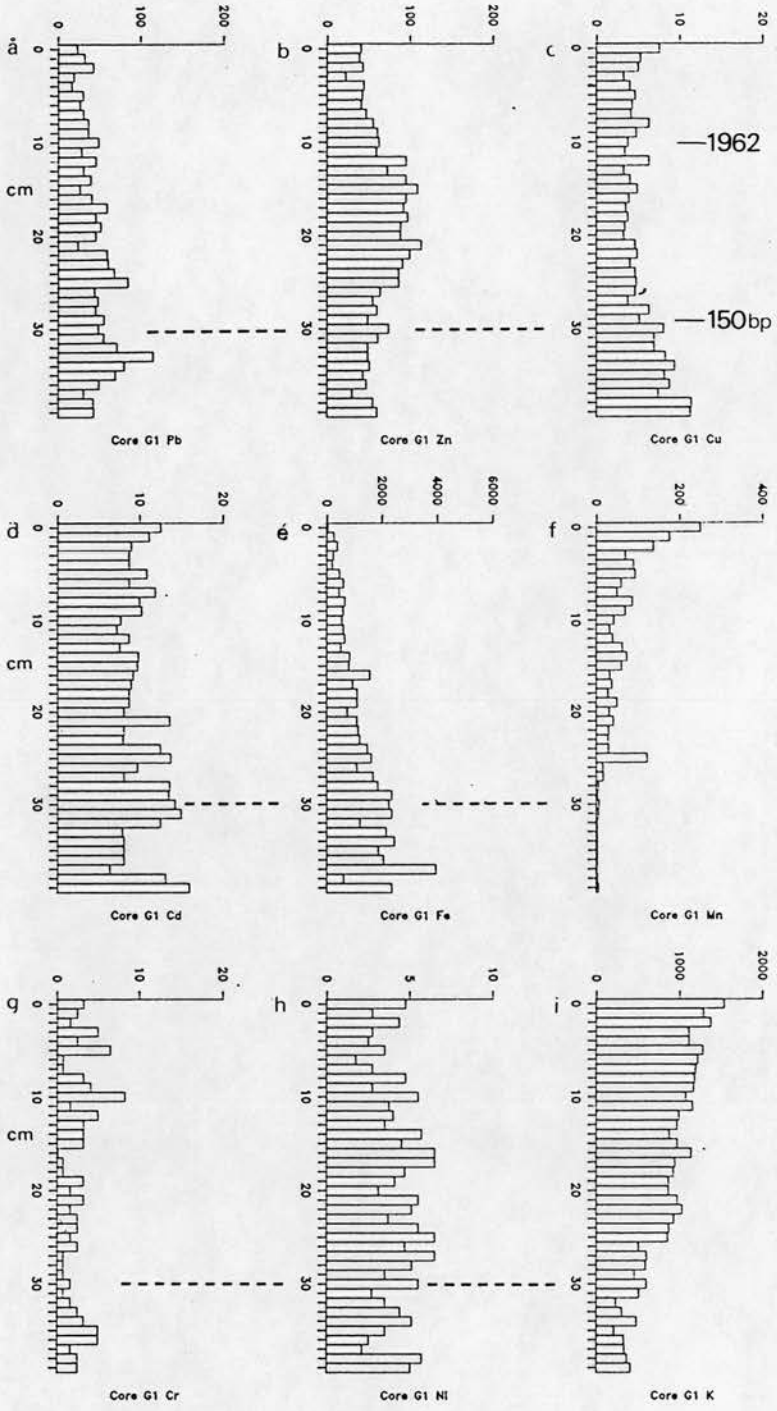

FIG 5/11: Core G1 - Total concentrations of Pb, Zn, Cu, Cd, Fe, Mn, Cr, Ni and K (µg/g dry weight) within sub-samples taken at 1cm resolution. The broken line demarks the stratigraphic level of water inundation.

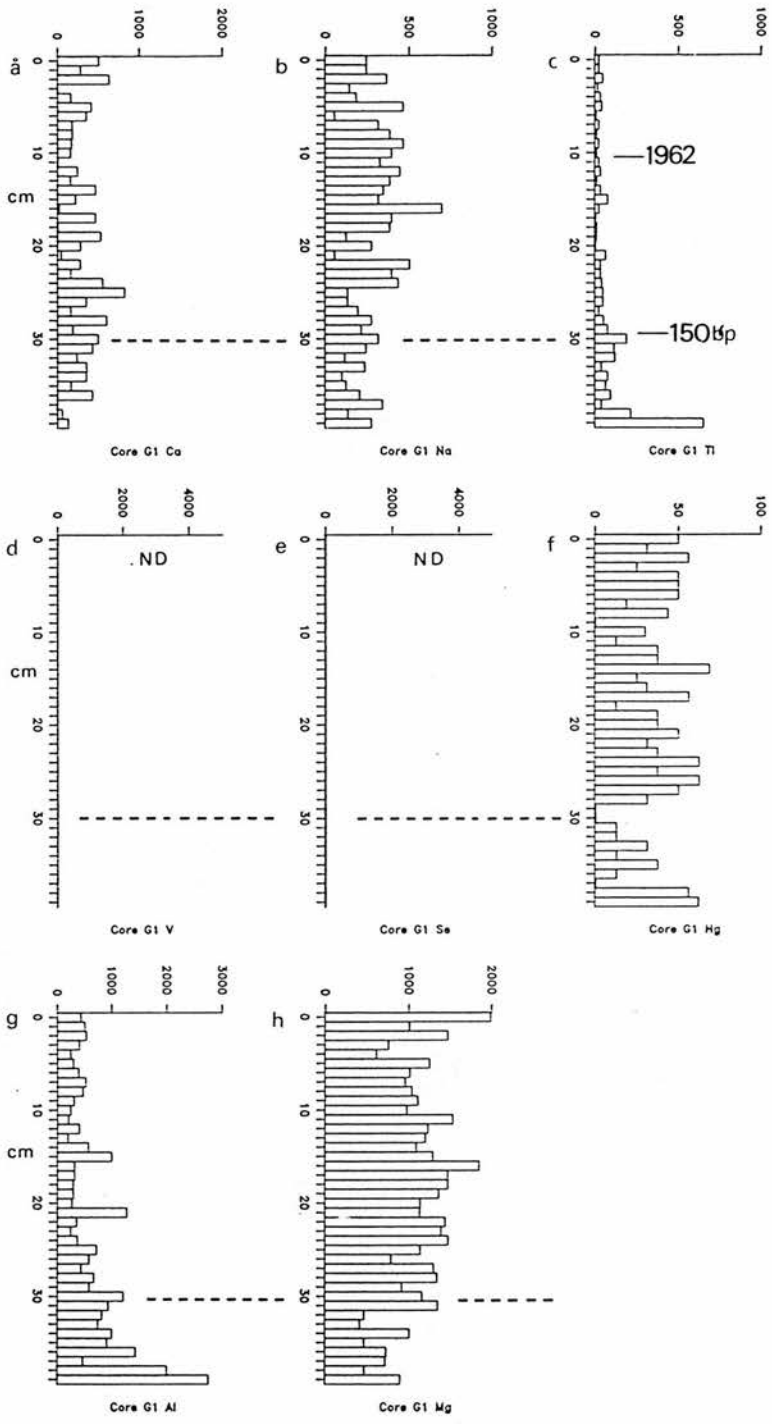

FIG 5/12: Core G1 - Total concentrations of Ca, Na, Ti, Hg, Al and Mg (µg/g dry weight) within sub-samples taken at 1cm resolution. The broken line demarks the stratigraphic level of water inundation. Note: ND signifies that data are not available.

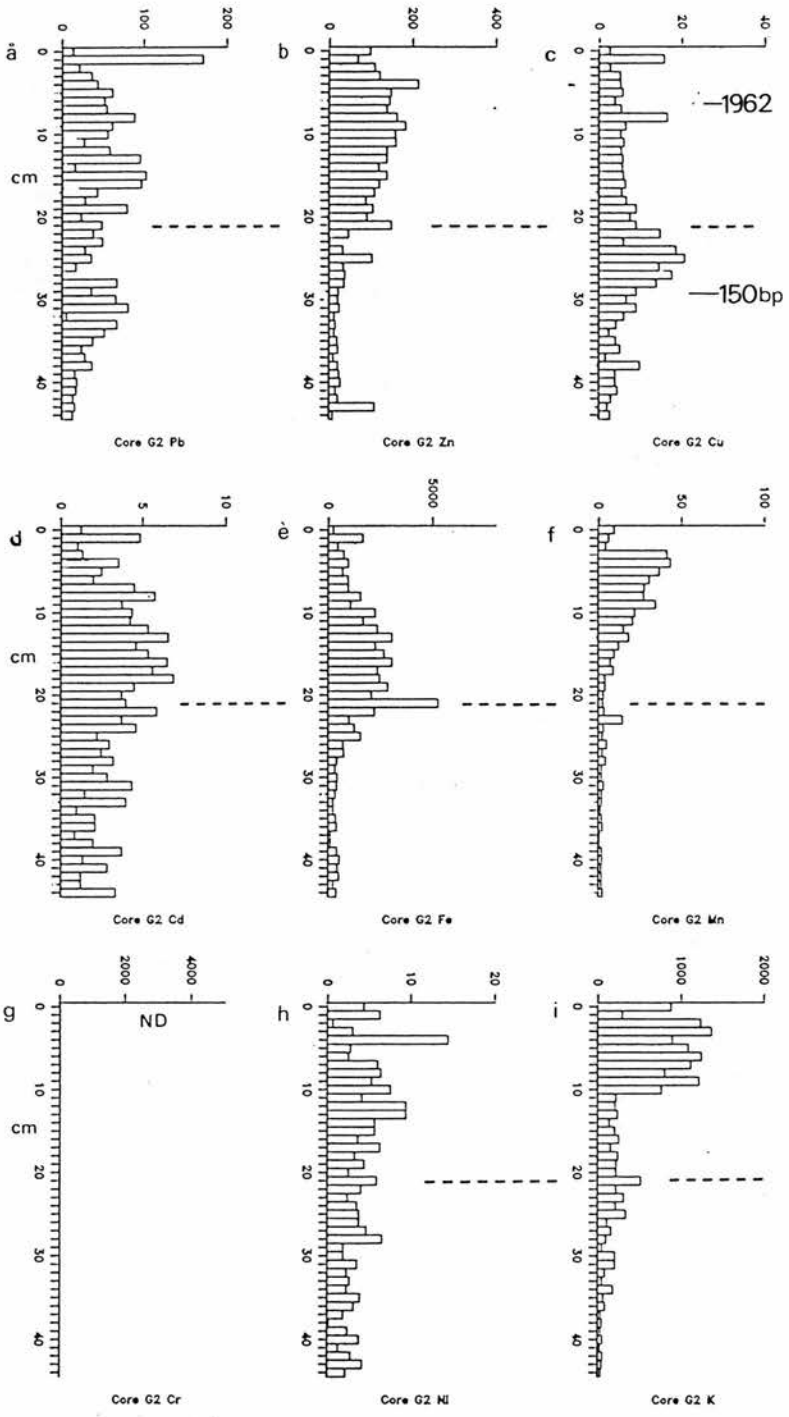

FIG 5/13: Core G2 - Total concentrations of Pb, Zn, Cu, Cd, Fe, Mn, Cr, Ni and K (µg/g dry weight) within sub-samples taken at 1cm resolution. The broken line demarks the stratigraphic level of water inundation.

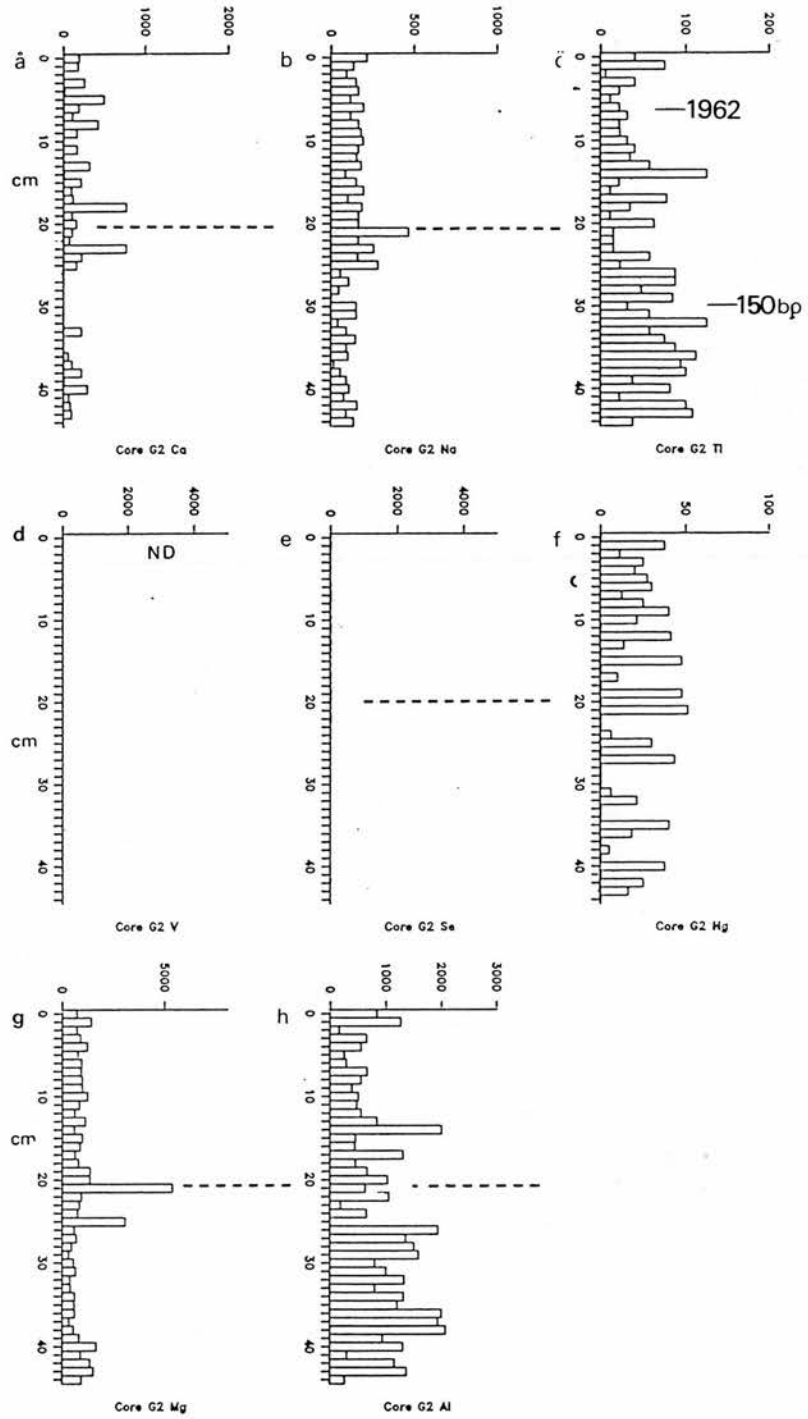

FIG 5/14: Core G2 - Total concentrations of Ca, Na, Ti, Hg, Mg and Al (µg/g dry weight) within sub-samples taken at 1cm resolution. The broken line demarks the stratigraphic level of water inundation. Note: ND signifies that data are not available.

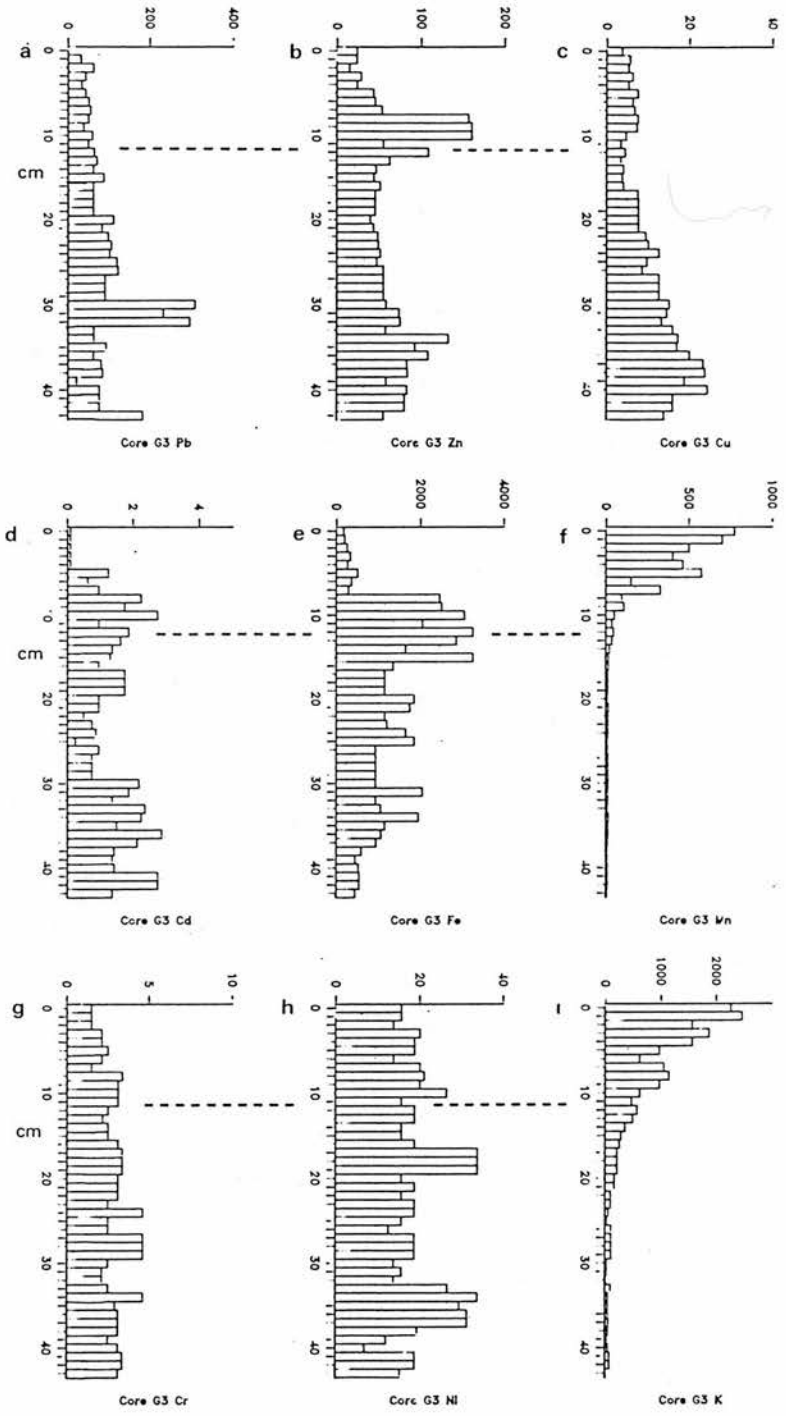

FIG 5/15: Core G3 - Total concentrations of Pb, Zn, Cu, Cd, Fe, Mn, Cr, Ni and K (µg/g dry weight) within samples taken at 1cm resolution. The broken line demarks the stratigraphic level of water inundation.

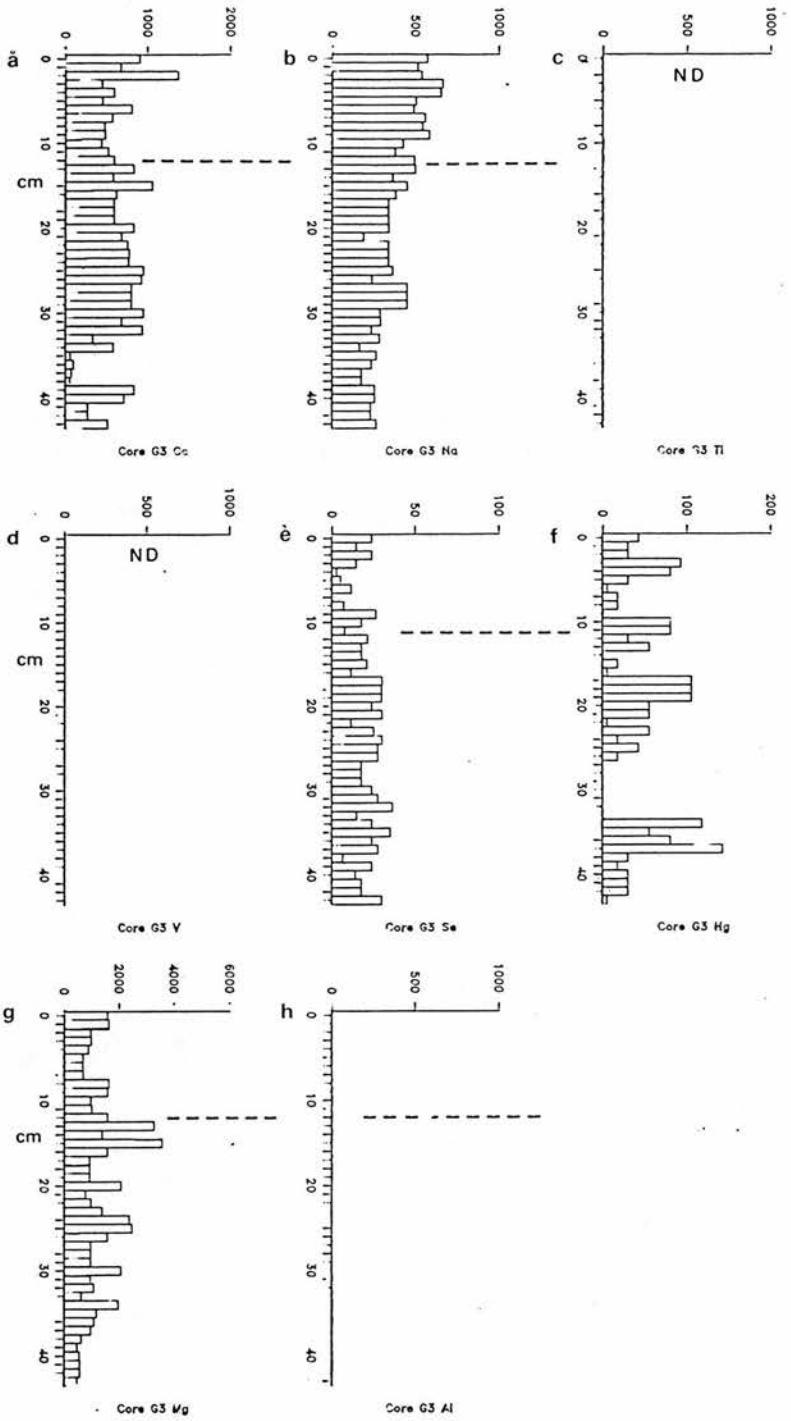

FIG 5/16: Core G3 - Total concentrations of Ca, Na, Se, Hg and Mg (µg/g dry weight) within sub-samples taken at 1cm resolution. The broken line demarks the stratigraphic level of water inundation. Note: ND signifies that data are not available.

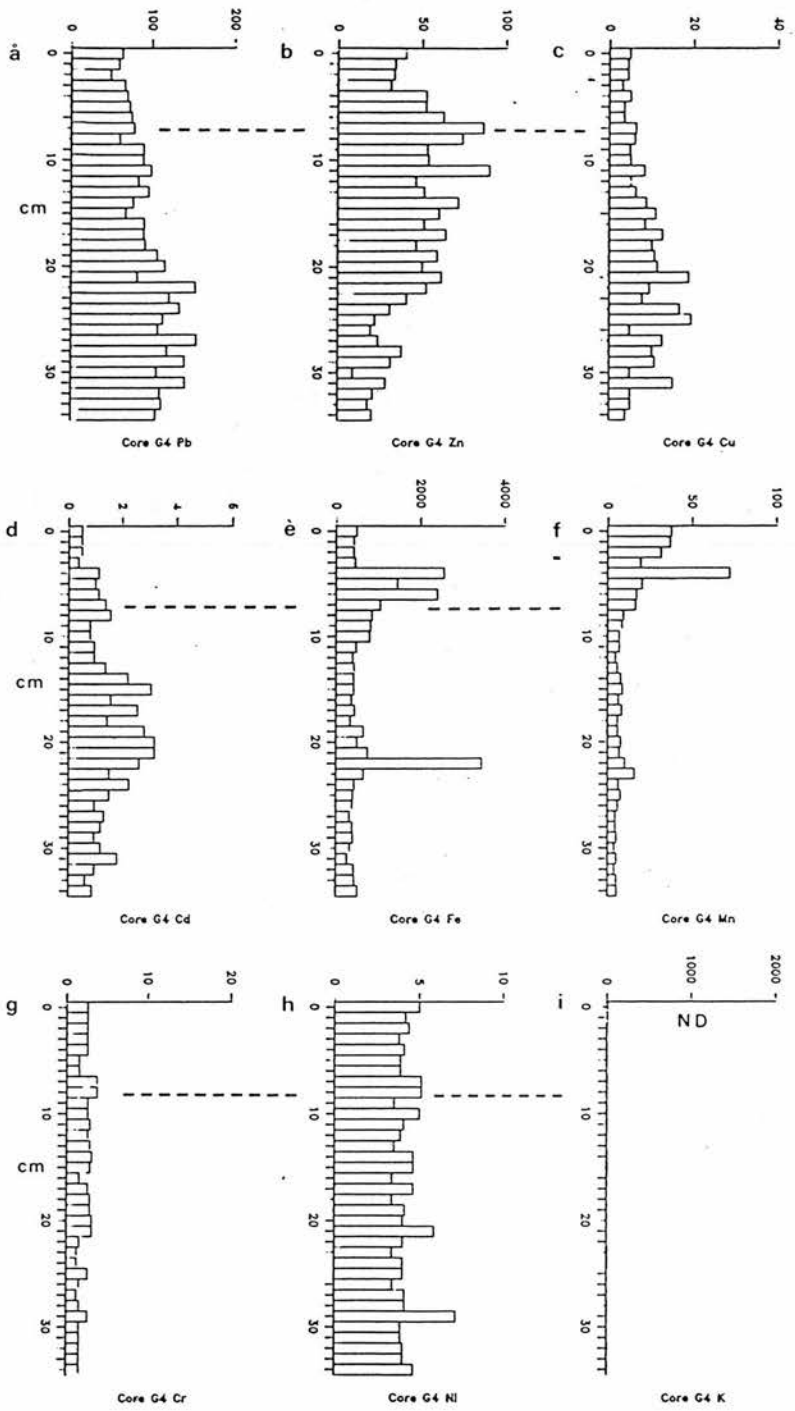

FIG 5/17: Core G4 - Total concentrations of Pb, Zn, Cu, Cd, Fe, Mn, Cr and Ni (µg/g dry weight) within sub-samples taken at 1cm resolution. The broken line demarks stratigraphic level of water inundation.

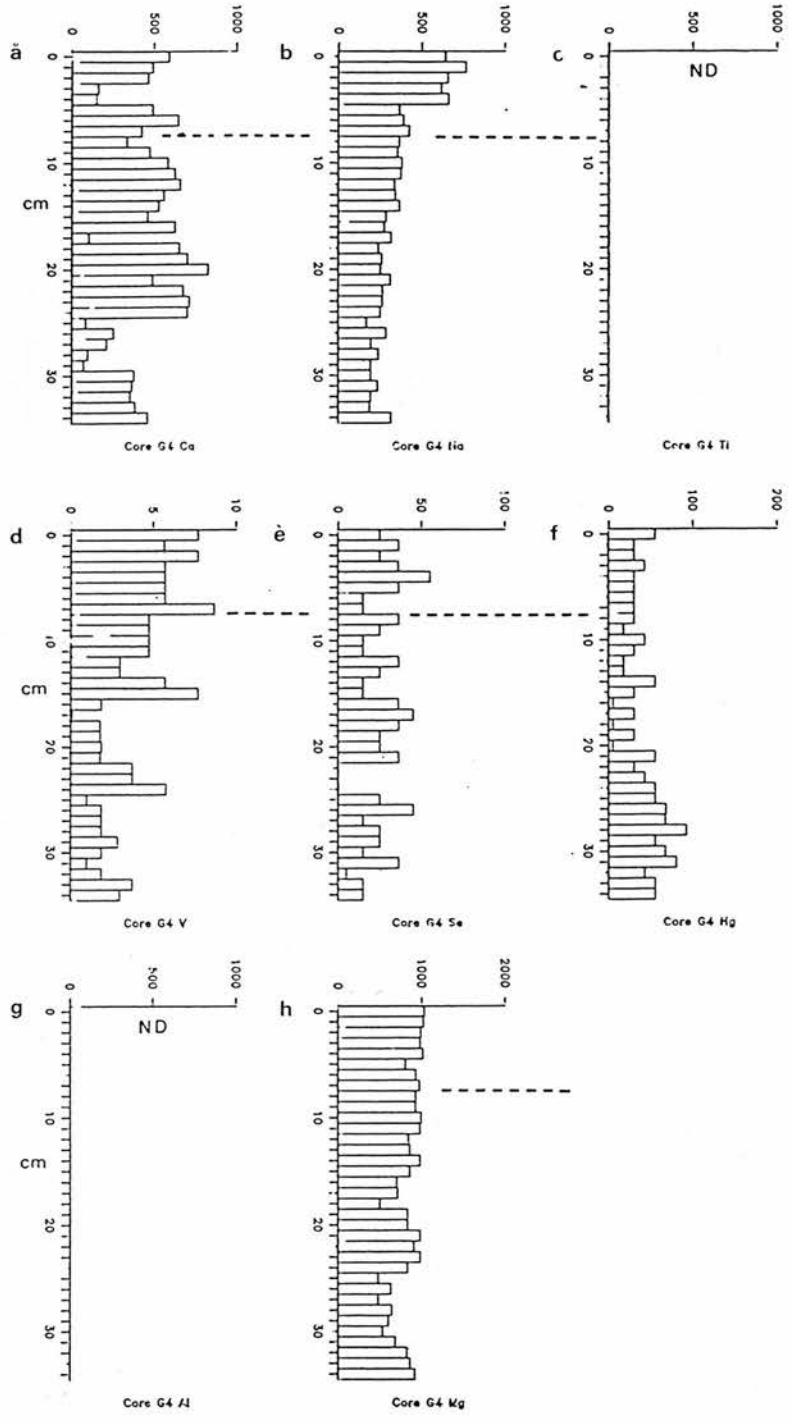

FIG 5/18: Core G4 - Total concentrations of Ca, Na, V, Se, Hg and Mg (µg/g dry weight) within sub-samples taken at 1cm resolution. The broken line demarks the stratigraphic level of water inundation. Note: ND signifies that data are not available.

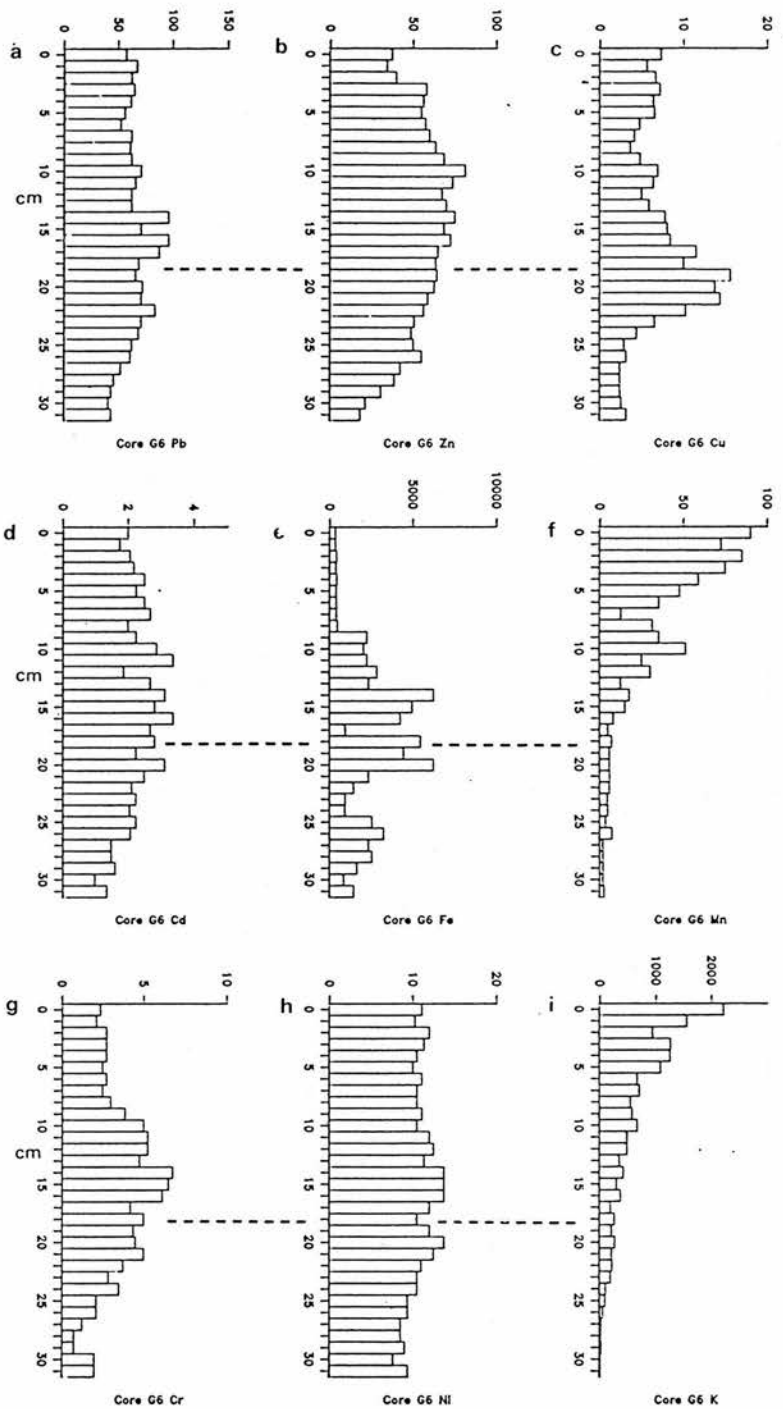

FIG 5/19: Core G6 - Total concentrations of Pb, Zn, Cu, Cd, Fe, Mn, Cr, Ni and K (µg/g dry weight) within sub-samples taken at 1cm resolution. The broken line demarks the stratigraphic level of water inundation.

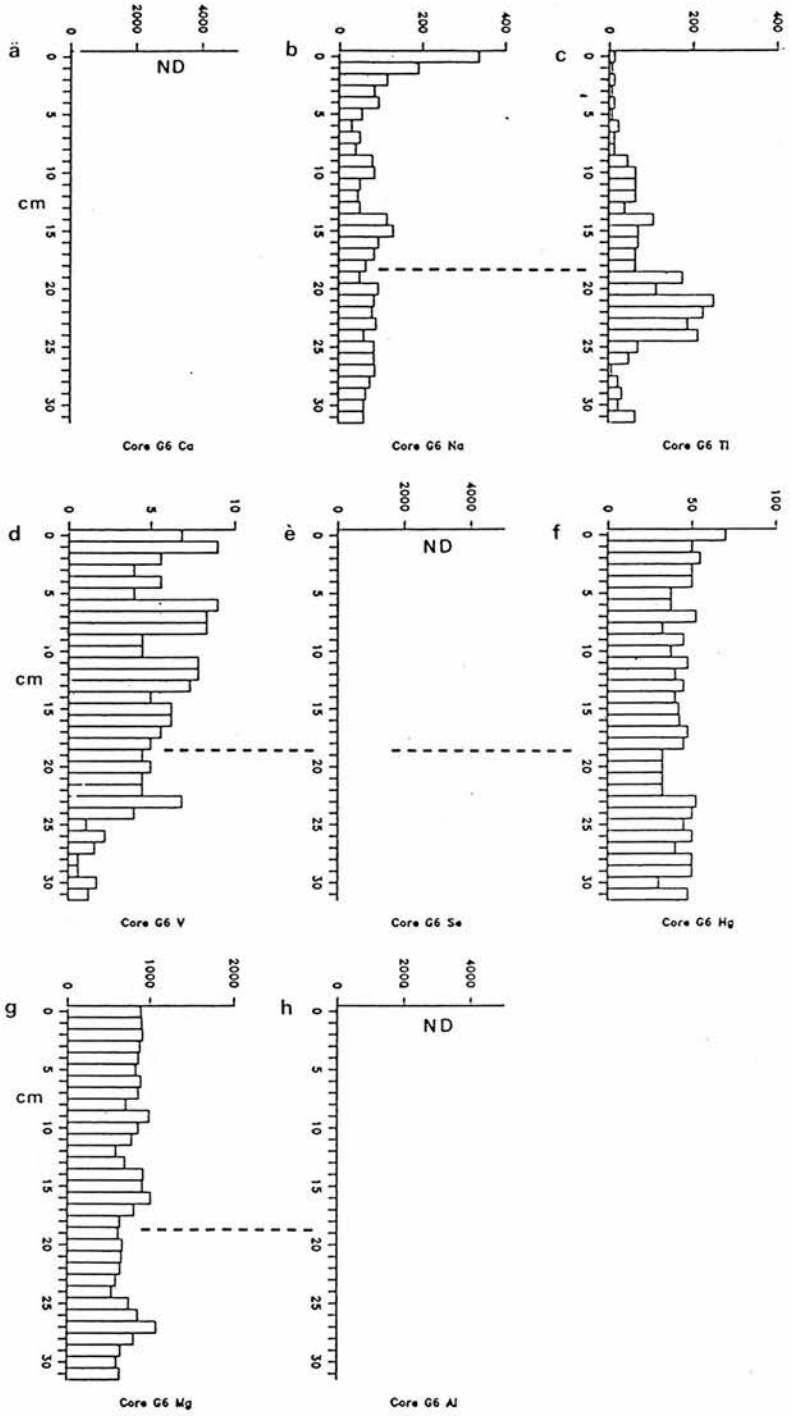

FIG 5/20: Core G6 - Total concentrations of Na, Ti, V, Hg and Mg (µg/g dry weight) within sub-samples taken at 1cm resolution. The broken line demarks the stratigraphic level of water inundation. Note: ND signifies that data are not available.

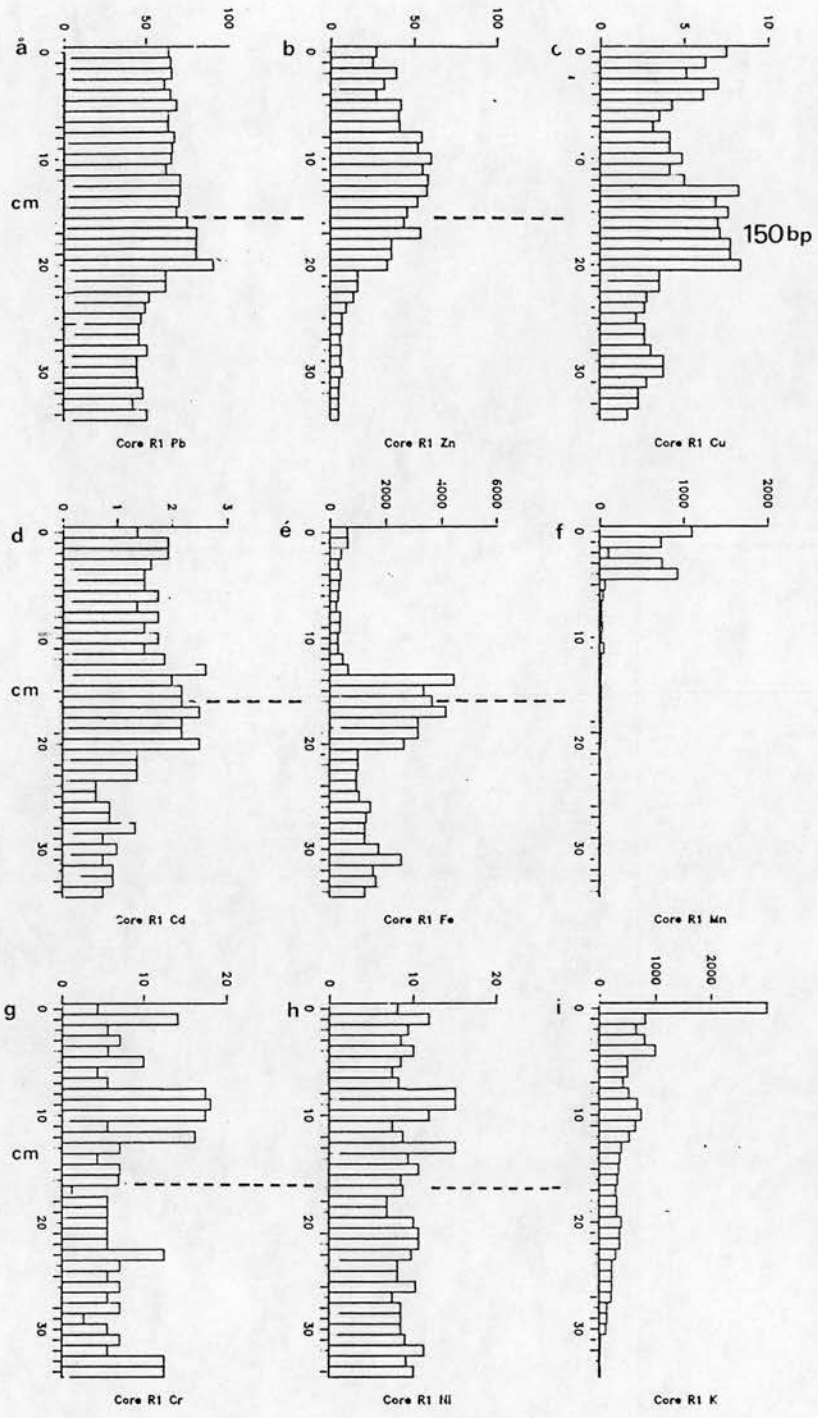

FIG 5/21: Core R1 - Total concentrations of Pb, Zn, Cu, Cd, Fe, Mn, Cr, Ni and K (µg/g dry weight) within sub-samples taken at 1cm resolution. The broken line demarks the stratigraphic level of water inundation.

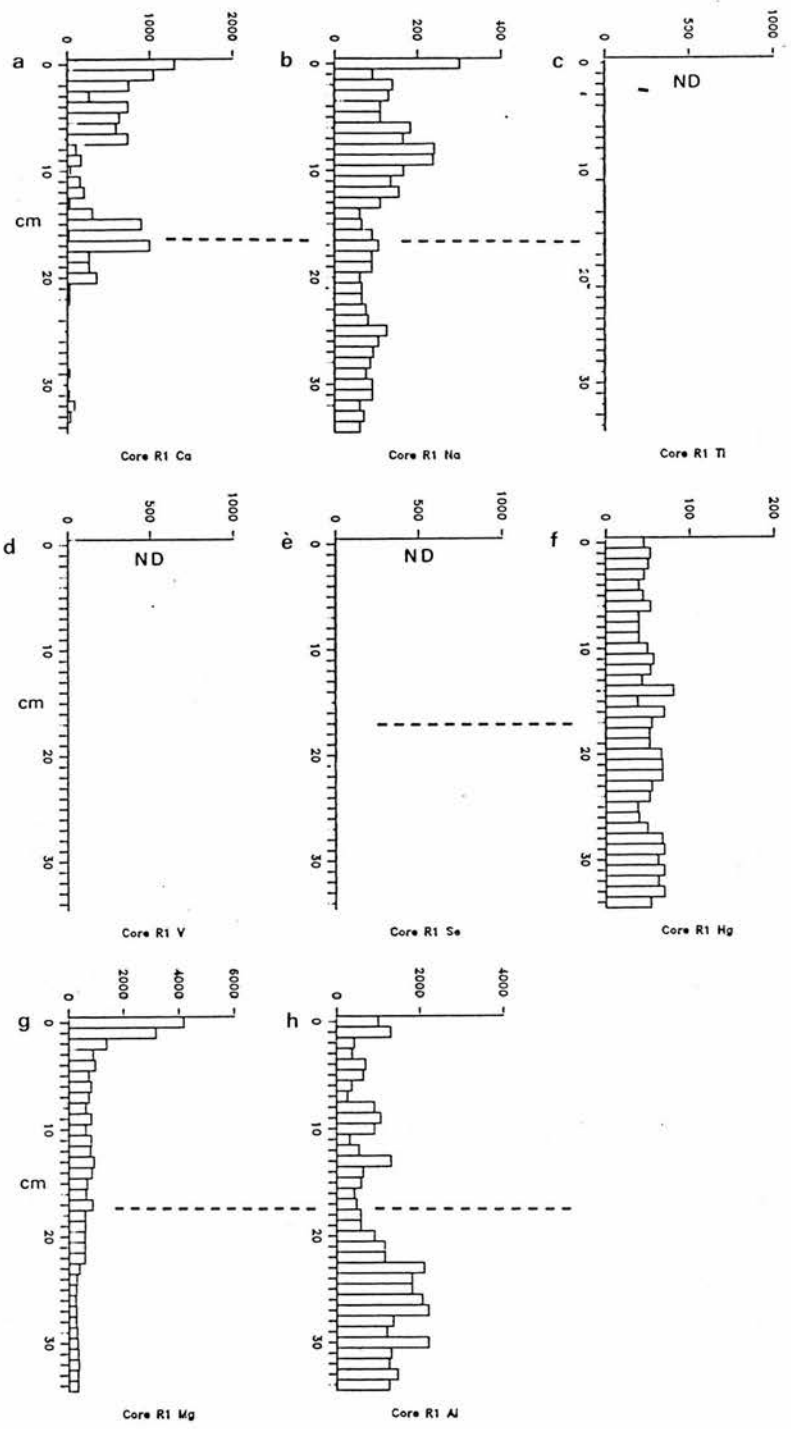

FIG 5/22: Core R1 - Total concentrations of Ca, Na, Hg, Mg and Al (µg/g dry weight) within sub-samples taken at 1cm resolution. the broken line demarks the stratigraphic level of water inundation. Note: ND signifies that data are not available.

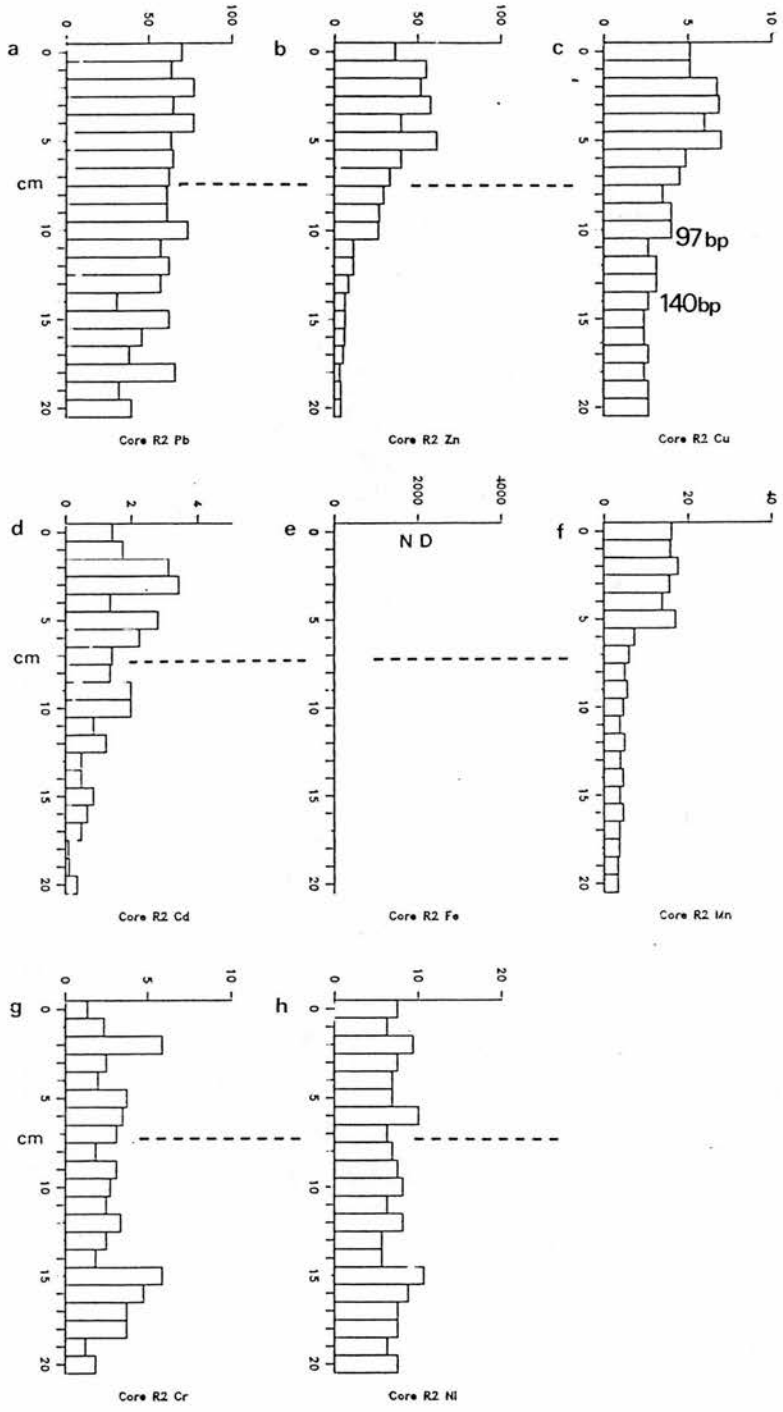

FIG 5/23: Core R2 - Total concentrations of Pb, Zn, Cu, Cd, Mn, Cr and Ni (µg/g dry weight) within sub-samples taken at 1cm resolution. The broken line demarks the stratigraphic level of water inundation. Note: ND signifies that data are not available.

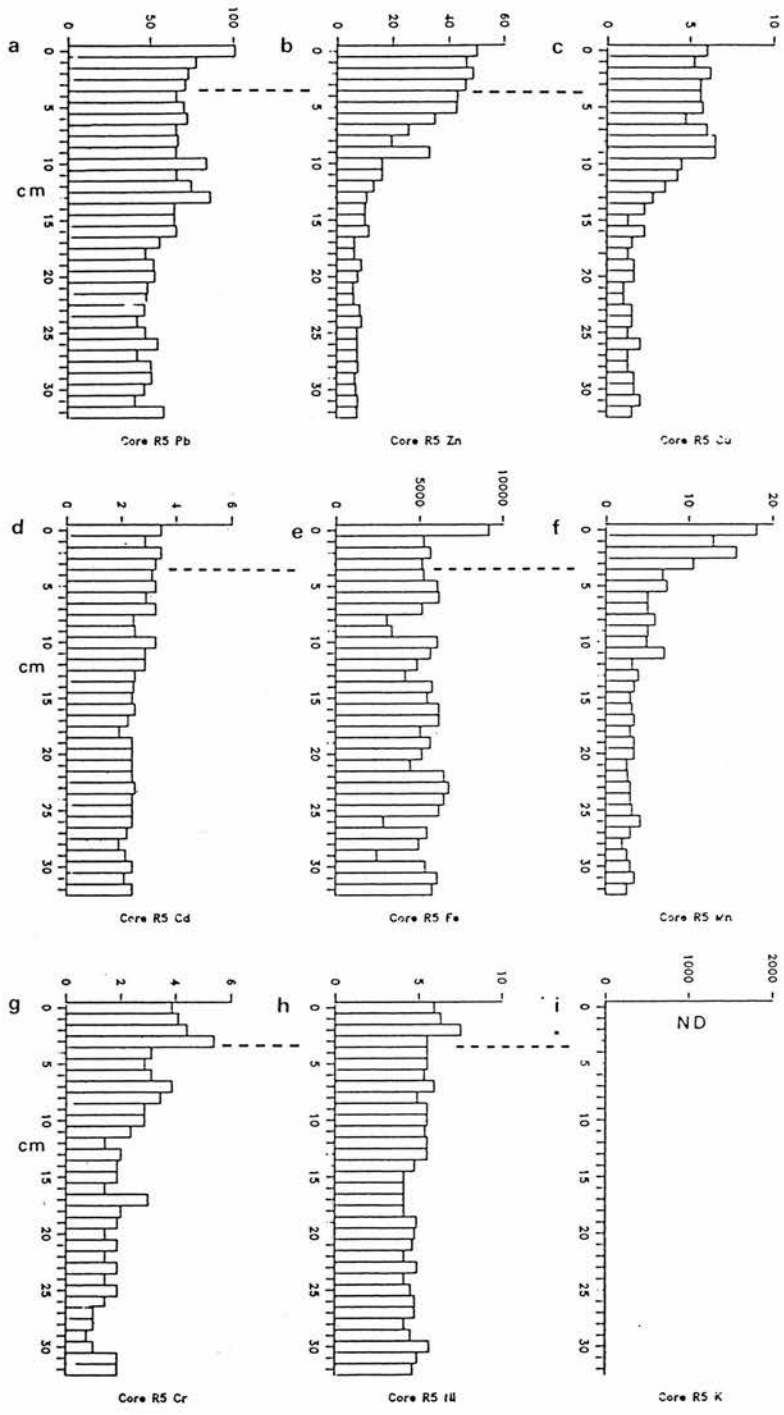

FIG 5/24: Core R5 - Total concentrations of Pb, Zn, Cu, Cd, Fe, Mn, Cr and Ni (µg/g dry weight) within sub-samples taken at 1cm resolution. The broken line demarks the stratigraphic level of water inundation.

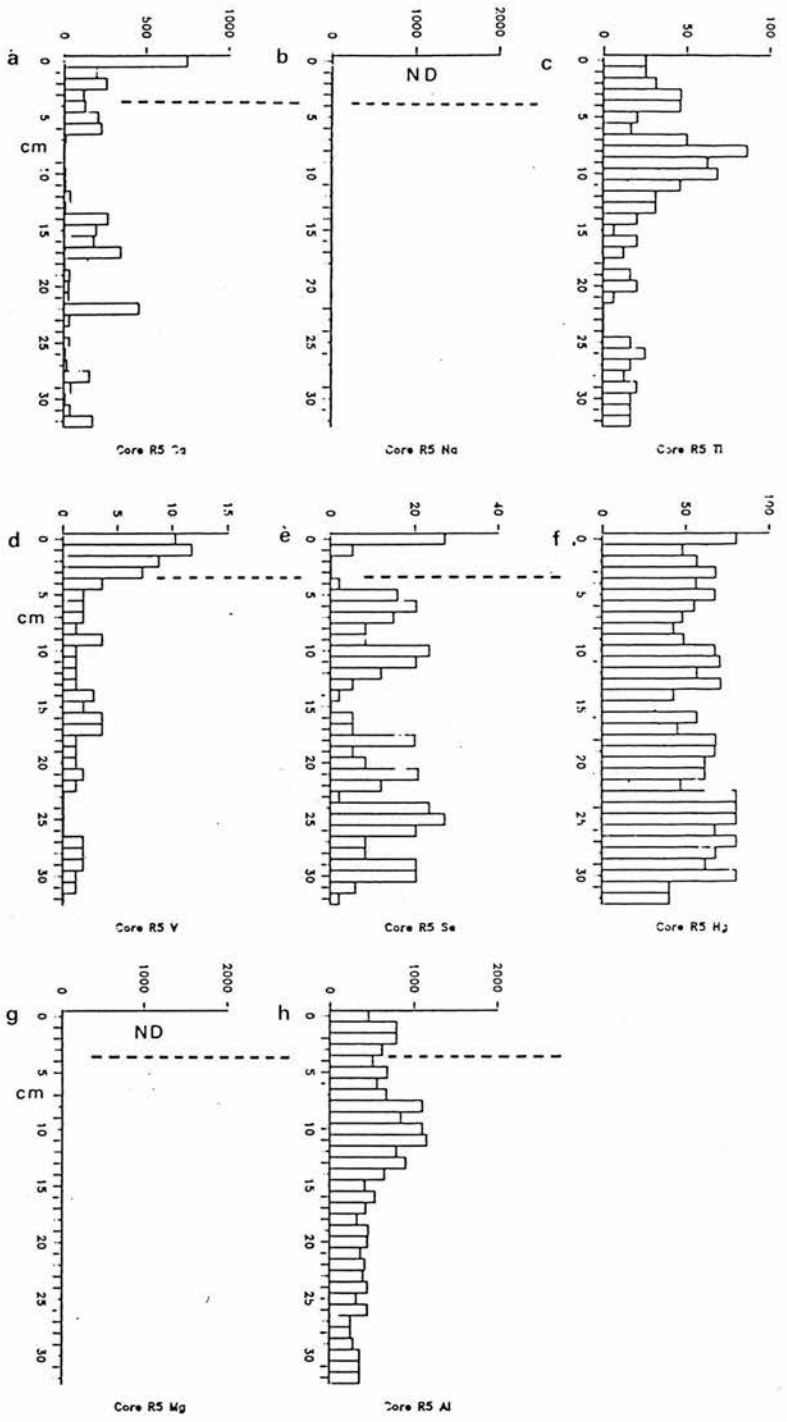

FIG 5/25: Core R5 - Total concentrations of Ca, Ti, V, Se, Hg and Al (µg/g dry weight) within sub-samples taken at 1cm resolution. The broken line demarks the stratigraphic level of water inundation. Note: ND signifies that data are not available.

With the exception of the Mn profile for core R1, the rapid depletion of Mn and K appears to coincide with the onset of inundated conditions at all coring stations. Consequently, their concentration gradients are most severe at "lawn" or submerged "pool" locations. For example, Mn concentrations decline to "background" (below 10µg/g) levels in the uppermost 10cm of cores G4, R2 and R5, in accordance with their water table levels at 8cm, 8cm and 4cm respectively (Figs 5/17f, 5/23f, 5/24f). In contrast, both Mn and K show enrichment throughout the surficial 30cm of core G1 on account of the lower water table level at this coring station (Figs 5/11f and i). These trends indicate that Mn and K are both subject to some hydrologically-influenced mobilization process in the Galloway and Beinn Chaorach peats.

The profile of Mn in core R1 is anomalous in that the elements' depletion from 970µg/g at 5cm depth to around 20µg/g downward of 7cm is unrelated to the onset of inundated conditions (Fig 5/21f). This profile is most probably a product of a rapid fall in the level of the water table immediately prior to sample collection, thus leaving a "perched" Mn profile in a state of disequilibrium with the hydrological regime.

2) The profiles of Al, Ti and Cu are separable from those of all other elements within the 0.25 - 0.5m sample cores on account of the occurrence of major enrichment anomalies at

20cm - 50cm depth. Al and Ti are also notable for their strong co-variability (R > 0.70) in all sample cores for which data are available (Tables 41 - 48). Statistical linkages between Cu and Al or Ti are less consistent, but R coefficients exceed 0.50 in cores G1, G6 and R5 (Tables 41, 45 and 48). Accordingly, the profiles of these elements can be considered to respond to similar distributional controls.

Geochronological data for the adjacent "hummock" and "lawn" cores, G1 and G2, R1 and R2, show that strata exhibiting initial Cu, Al and Ti enrichment are not temporally synchronous. In the Brishie mire cores, such discordance is particularly apparent with respect to Cu, with concentrations attaining twice the "whole core" mean of 5ug/g within peats of 200 - 250 years age in core G1 while analogous anomalies are confined to strata of below 155 years age within the lawn core, G2 (Figs 5/11c and 5/13c). At the Beinn Chaorach site, Cu concentrations rise to a maximum of 8.37µg/g in strata which accumulated prior to 200yrs BP at the "hummock" coring station R1 (Fig 5/21c), but no Cu enrichment is evident prior to 130yrs BP in core R2 (Fig 5/23c). Accordingly, the profiles of elements within this group cannot be explained solely by reference to atmospheric influx variations.

However, the stratigraphic locations at which Al, Ti and Cu anomalies occur do show consistency with respect to the

hydrological conditions prevailing at coring stations. In most cases, concentration maxima lie immediately beneath the water table. Hence, the well drained "hummock" core, G1, holds concentrations of only 5µg/g Cu, 550µg/g Al and 37µg/g Ti throughout the surficial 30cm, but concentrations increase by at least a factor of 2 within the inundated strata at 30cm - 40cm depth (Figs 5/11c, 5/12c and g). In contrast, analogous enrichment zones for Al, Ti and Cu occur downward of only 20cm in cores G2 (Figs 5/13c, 5/14c and h), G6 (Figs 5/19c, 5/20c) and R1 (Figs 5/21c, 5/22h) on account of the higher level of the water table at these coring stations. Respective Cu, Al and Ti maxima of 7µg/g, 1150µg/g and 86µg/g occur still closer to the surface at coring station R5 in accordance with the prevalence of inundated conditions downward of 4cm depth (Figs 5/24c, 5/25c and h).

3) The data presented for cores G1, G2, G3, G4, G6, R1, R2 and R5 confirm the persistence of the distributional trends shown by Pb, Zn, Cr, Cd and Fe in the 2.0m sample cores from Brishie mire and Beinn Chaorach. Peak concentrations of these elements typically occur beneath the peat surface, but in strata which overlie those holding greatest concentrations of Cu, Al and Ti. The statistical co-variability of Pb, Zn, Cr, Cd and Fe is exemplified by the data for core G2, in which R coefficients for Cd v Pb and Cd v Fe exceed 0.55 (Table 42), core G6 in which Zn v Cr, Zn v Pb and Zn v Cd coefficients exceed 0.67 (Table 45) and

in all of the Beinn Chaorach cores, in which Pb, Cd and Zn yield R coefficients of over 0.61 (Tables 46 - 48).

Geochronological data for cores G1, G2, R1 and R2 indicate that elements within the Pb, Zn, Cr, Cd and Fe group do not display temporally synchronous enrichment patterns in adjacent "hummock" and "lawn" environments. Most notably, Fe concentrations exceed their "whole core" mean of 1194µg/g by a factor of 4 within peat levels of over 200 years age at coring station G1 (Fig 5/11e) while analogous Fe anomalies are confined to strata which have accumulated since 150yrs BP at coring station G2 (Fig 5/13e). Similar variations are also apparent with respect to the Cd accumulation patterns at Beinn Chaorach, with concentrations of over 2.5µg/g being confined to more recent (post-1850) levels of the "lawn" core, R2, than in the "hummock" core, R1 (Figs 5/21d, 5/23d). Zn enrichment appears to be confined to more recent levels than the other atmophilic elements in all of the dated sample cores, but is still enhanced within older strata in the "hummock" cores, G1 and R1, than in their "lawn" counterparts, G2 and R2 (Figs 5/11b, 5/13b, 5/21b, 5/23b).

While the non-synchronous profiles of Pb, Zn, Cd, Cr and Fe within the Brishie mire, Craigherron and Beinn Chaorach peats suggest that the distributions of these elements do not solely reflect temporal variations of their atmospheric

influx, their enrichment patterns appear to relate closely to the hydrological conditions prevailing at each coring station. Specifically, these elements all appear to be subject to enrichment at, or immediately above the water table. Hence, they accumulate at greatest depth at "hummock" sites. For example, the well drained core, G1, holds Pb and Fe at mean concentrations of only 45µg/g and 840µg/g respectively throughout the uppermost 30cm of the peat column, but shows enrichment to 115µg/g Pb and 3945µg/g Fe at 30cm - 38cm depth (Figs 5/11a and e). In contrast, peak concentrations of Pb (100µg/g), Zn (50µg/g), Cd (3.4µg/g) Fe (9145µg/g) and Cr (5.3µg/g) occur within the uppermost 4cm of core R5, on account of the prevalence of inundated conditions downward of this level (Figs 5/24a, b, d, e and g). In all cores, permanently inundated strata show depletion of these elements.

4) The distribution of V within the Galloway and Beinn Chaorach peats contrasts with all previously discussed elements as enrichment patterns fail to exhibit any persistent correlation with hydrological conditions. V profiles for cores G4 and G6 show concentrations to increase progressively throughout both inundated and drained strata, from around 3µg/g at 30cm to over 8µg/g at the peat surface (Figs 5/18d and 5/20d). These profiles may, therefore, reflect temporal variations in the influx of petroleum-derived pollutants.

5) Hg, Ni and Se show no persistent enrichment patterns within the 0.25 - 0.50m cores from Brishie mire, Craigherron and Beinn Chaorach. Instead they fluctuate around their respective mean values at all stratigraphic levels. These elements cannot confidently be associated with any particular distributional control and accordingly, warrant no further consideration.

5.7.2: Elemental concentrations.

While the downcore distributions of elements in the Brishie mire, Craigherron and Beinn Chaorach peat systems are essentially analogous, the mean, peak and cumulative elemental concentration data for cores G1, G2, G3, G4, G6, R1, G2 and R5 (Tables 49 - 54) illuminate a significant distinction between the Galloway and Rannochmoor sites. Specifically, the loading of atmophilic elements to Brishie mire and Craigherron appears markedly greater than that to the Beinn Chaorach site, as signified by the higher concentrations of Pb, Zn, Cu and Cd in samples from the former. Peak Pb concentrations do not exceed 101ug/g in any sample core from Beinn Chaorach, but concentrations within the range 96µg/g - 308µg/g are observable in cores G1, G2, G3, G4 and G6. In the case of Zn, the variations between sampling sites are even more pronounced, with mean, peak and cumulative concentrations failing to exceed 29µg/g, 60µg/g and 1025µg/g respectively at Beinn Chaorach, while comparative values exceed 44µg/g (mean), 81µg/g (peak) and

2164µg/g (cumulative) in all of the Galloway sample cores. Variations between the Cu data for the Galloway and Beinn Chaorach sites are analogous to those described for Zn, with peak concentrations falling within the range 11µg/g - 24µg/g at the former and 7µg/g - 8µg/g at the latter.

Table 49: Cores G1, G2, G3, G4 and G6, mean elemental concentrations (µg/g).

	G1	G2	G3	G4	G6
Pb	46	45	87	97	64
Zn	65	78	64	44	55
Cu	5	7	10	8	6
Cd	10	3	1	1	2
Fe	1194	1209	1236	718	2126
Mn	46	11	103	12	23
Cr	2	11	2	2	3
Ni	4	4	19	4	1
K	841	355	447	260	492
Ca	286	146	633	454	250
Na	284	139	375	341	86
Ti	60	52	38	40	67
V	-	-	-	3	5
Hg	34	15	38	40	44
Mg	1108	1000	1257	828	782
Al	647	909	461	232	441

Table 50: Cores G1, G2, G3, G4 and G6, peak elemental concentrations (µg/g).

	G1	G2	G3	G4	G6
Pb	115	171	308	154	96
Zn	113	213	160	90	81
Cu	11	20	24	19	15
Cd	16	6	2	3	3
Fe	3945	5245	3245	3445	6245
Mn	249	43	775	72	90
Cr	8	21	4	3	6
Ni	6	14	33	7	13
K	1535	1365	2470	1520	2220
Ca	825	775	1345	831	850
Na	695	465	665	765	335
Ti	650	125	51	45	250
V	-	-	-	8.7	-
Se	-	-	-	-	-
Hg	68	51	142	92	70
Mg	1900	5300	1375	831	1080
Al	2750	2075	-	-	-

Table 51: Cores G1, G2, G3, G4 and G6, cumulative elemental concentrations (µg/g) after normalization against the number of samples within the respective cores.

	G1	G2	G3	G4	G6
Pb	1873	1964	3840	3395	2076
Zn	2164	3428	2871	1574	1776
Cu	221	324	462	285	210
Cd	407	127	58	50	73
Fe	47783	54440	54423	25135	68000
Mn	1862	438	4538	429	765
Cr	103	440	127	80	111
Ni	170	158	865	148	350
K	33675	20600	19860	9122	15750
Ca	11441	5694	27866	15892	8000
Na	11387	5421	16512	11966	2772
Ti	2438	2028	794	856	2163
V	-			134	159
Se	-		899	850	-
Hg	1361	1326	1712	1411	1412
Mg	44262	39350	55321	29003	25055
Al	25903	35421	54423	8120	14115

Tables 52 and 53: Cores R1, R2 and R5, mean (left) and peak (right) elemental concentrations (µg/g).

	R1	R2	R5	R1	R2	R5
Pb	61	58	61	91	77	101
Zn	29	24	17	60	61	50
Cu	4	4	3	8	7	7
Cd	1.5	1.3	2.6	2.6	3.4	3.4
Fe	1401	-	5369	4435	-	9145
Mn	114	7	5	1100	17	18
Cr	7	3	2	18	6	5.3
Ni	9	7	5	15	10	7.5
K	450	-	107	2990	-	970
Ca	290	-	123	1300	-	750
Na	123	-	56	300	-	245
Ti	95	-	24	187	-	86
V	-	-	2.58	-	-	11.8
Se	-	-	11	-	-	27
Hg	58	13	60	89	46	80
Mg	785	-	581	4180	-	750
Al	1040	-	560	2200	-	1150

Table 54: Cores R1, R2 and R5, cumulative (normalised) elemental concentrations (µg/g).

	R1	R2	R5
Pb	2167	1236	1760
Zn	1025	522	593
Cu	164	84	102
Cd	53	28	54
Fe	49045	-	177184
Mn	4016	162	153
Cr	278	63	76
Ni	336	156	166
K	15759	-	3560
Ca	10175	-	4083
Na	3697	-	1871
Ti	2085	-	824
V		-	85
Se	-	-	382
Hg	1861	291	1688
Mg	27475	-	19200
Al	36420	-	18510

5.8: Summary of bulk geochemical data:

Downcore geochemical trends in the Brishie mire, Craigherron and Beinn Chaorach peats are broadly analogous, thus indicating the influence of universally operative processes. Low resolution data for 2m cores from Brishie mire (G2M) and Beinn Chaorach (R2M) show Mn, K, Al, Cu, Ti, Cr, Pb, Zn, Cd and Fe to occur at "background" concentrations throughout strata of 60cm - 200cm depth, but to be subject to marked enrichment in the surficial 50cm of the peat column. The data derived from "high resolution" analyses of 8 shorter cores from Brishie mire, Craigherron and Beinn Chaorach all confirm that elements showing enrichment near the peat surface fall into 3 discrete groups. These are:-

1) Mn and K, which attain maximum concentrations at the peat surface and show rapid, progressive depletion with depth.

2) Al, Cu and Ti which are subject to enrichment at 20cm - 50cm below the peat surface.

3) Pb, Zn, Cd, Fe and Cr which attain maximum concentrations below the peat surface, in strata which typically overlie those displaying greatest enrichment of Cu, Al and Ti.

Geochronological data for the "paired" cores, G1 and G2, R1 and R2, suggest that strata showing initial enrichment with elements from each of the above groups are not of

temporally synchronous origin, but are consistently older in the "hummock" sample cores. The downcore profiles of Mn, K, Al, Cu, Ti, Cr, Pb, Fe, Zn and Cd cannot, therefore, be solely attributed to temporally variable atmospheric loadings to the Brishie mire, Craigherron and Beinn Chaorach sites. However, elemental distributions do show consistency with respect to the hydrological conditions prevailing at each coring station. Such trends suggest that hydrologically mediated mobilization processes promote the confinement of Mn to the drained sectors of the peat column, while Zn, Pb, Cu, Al, Ti, Cr, Cd and Fe are subject to accumulation within the zone of water table fluctuation.

Although all sampling sites are analogous in terms of their downcore geochemical constituency, distinctions are apparent between the concentrations of atmophilic elements in the Galloway and Beinn Chaorach peat systems, with Pb, Zn, Cu and Cd showing more restricted presence in the latter.

5.9: Interpretation of geochemical data.

5.9.1: Overview.

Attempts to interpret the geochemical data presented in section 5.7 are directed towards resolving two questions:-

1) What are the precise mechanisms of elemental

mobilization within the Brishie mire, Craigherron and Beinn Chaorach systems?

2) Do post-depositional processes preclude the retention of decipherable atmospheric influx chronologies?

5.9.2: Mechanisms of post-depositional alteration.

Although the distributions of elements within the Brishie mire, Craigherron and Beinn Chaorach peatlands have been characterised by reference to their relationship with hydrological conditions, additional evidence suggests that such linkages are indirect. Specifically, the data presented in Figs 5/26 and 5/27 show that the onset of inundation typically promotes the rapid depression of eH values to below -350mV. A range of elements, including Mn, Pb, Cu, Cd, Al, Ti, Fe and Mn are known to undergo valency changes and/or the formation of new, thermodynamically stable minerals upon burial in severely anoxic environments, thus promoting the formation of more or less mobile phases. Accordingly, the consistency with which particular elemental anomalies are located around the water table can most accurately be considered to reflect the operation of redox mediated processes. These processes can, in turn, be classified as involving dissolution or precipitation and their modes of operation can be illustrated by reference to the sequential Mn, Zn, Pb, Cu and Fe data for cores from Brishie mire (G5) and Beinn Chaorach (R3).

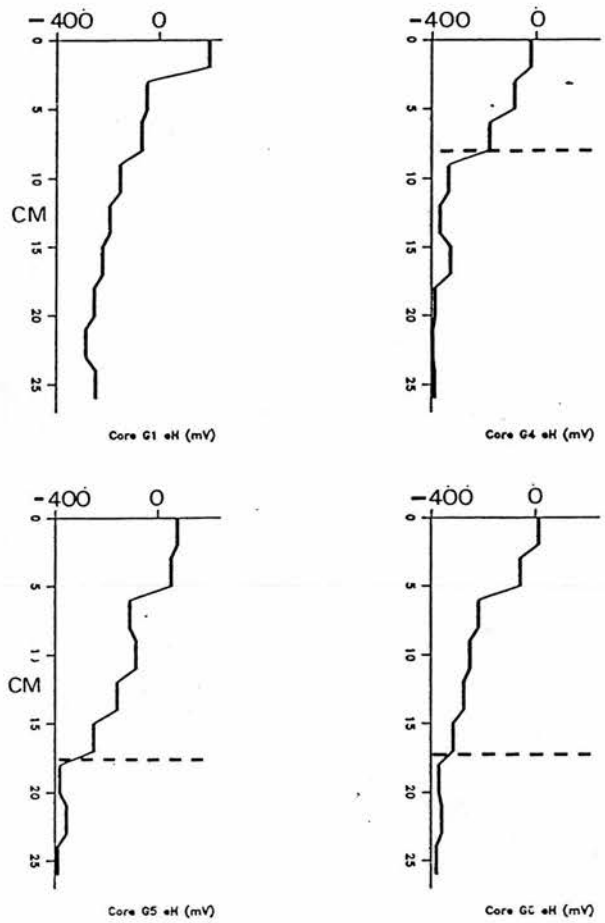

FIG 5/26: Redox gradients for cores G1, G4, G5 and G6 as defined by Pt electrode potentials. The broken line demarks the stratigraphic level of water inundation.

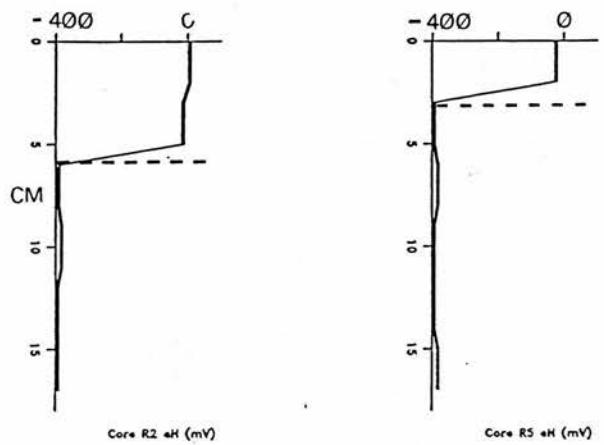

FIG 5/27: Redox gradients for cores R2 and R5 as defined by Pt electrode potentials. The broken line demarks the stratigraphic level of water inundation.

a) Dissolutionary processes.

Sequential chemical data indicate that the dissolution of hydrogenous phases exerts a major influence on the downcore distributions of Mn and Zn. In the case of Mn, data for cores G5 and R3 (Figs 5/28 - 5/29) show adsorbed, $MnCO_3$ and Mn^{4+} oxide (MnO_2) phases to constitute 65% - 90% of total concentrations within the enriched strata. These phases are inherently insoluble under oxic conditions (Krouskopf 1979, Damman 1978). Accordingly, they remain immobile upon burial in the sub-oxic, surficial 16cm of core G5 and the uppermost 4cm of core R3, but are subject to dissolution in the strongly anoxic, underlying strata. Under conditions of low pH (<5.5), $MnCO_3$ and Mn^{2+} oxides (MnO) cannot replace MnO_2 as the thermodynamically stable phase. Consequently, amorphous Mn^{2+} is produced. Mn^{2+} is highly soluble and is removed from the inundated levels of cores G5 and R3 by simple hydrological processes. The data for core R3 also indicate that, on account of the rapid removal of amorphous Mn^{2+} from the peat column, Mn enriched levels in inundated peats can almost solely be attributed to the presence of insoluble silicates, as at 25cm - 28cm depth where optically distinct Mn-rich granite fragments are present.

The data presented in Fig 5/30 illustrate the contrasts between the fractionation of Zn in the drained and inundated sectors of core G5. In the surficial 18cm, up to

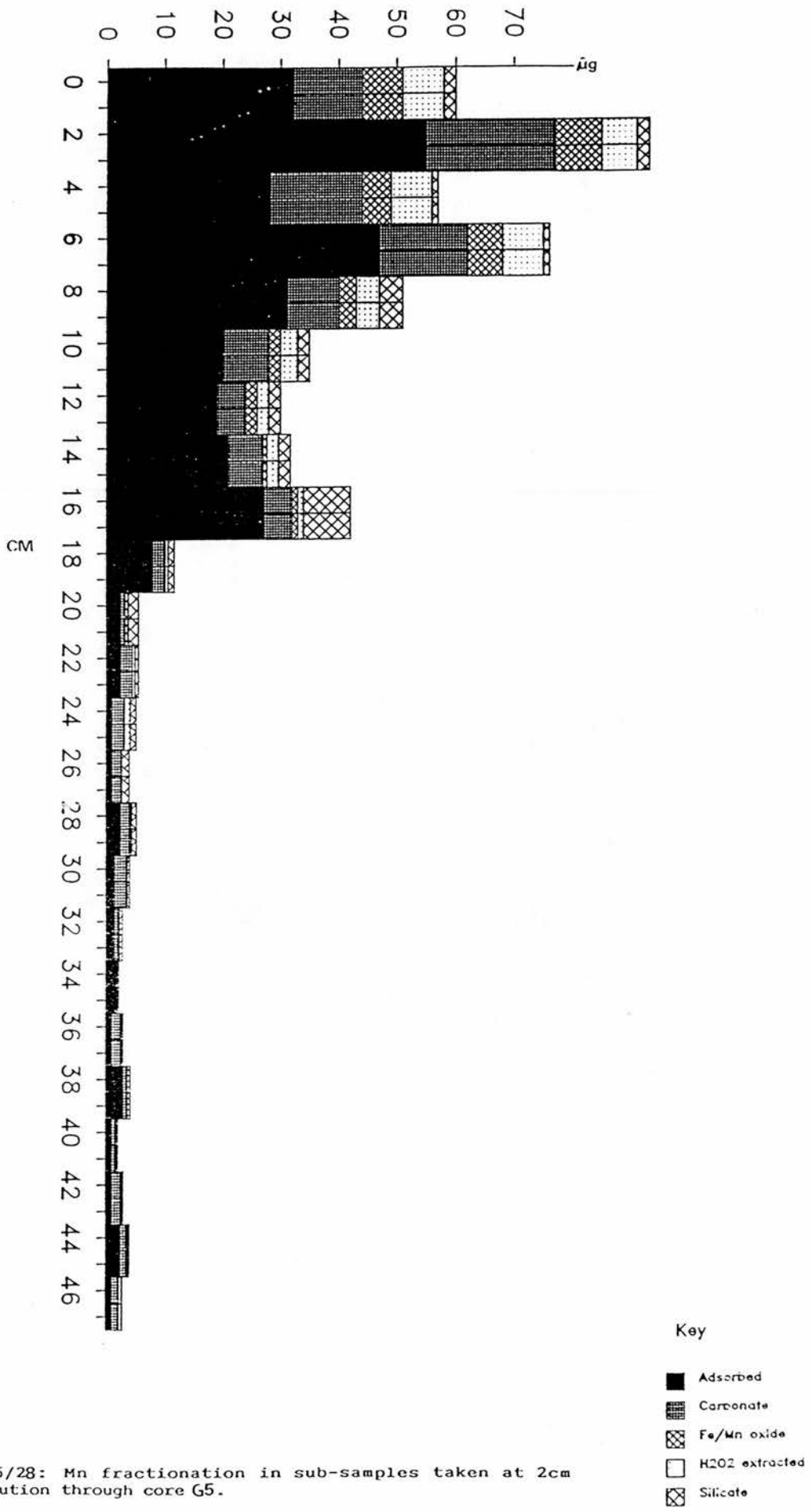

FIG 5/28: Mn fractionation in sub-samples taken at 2cm resolution through core G5.

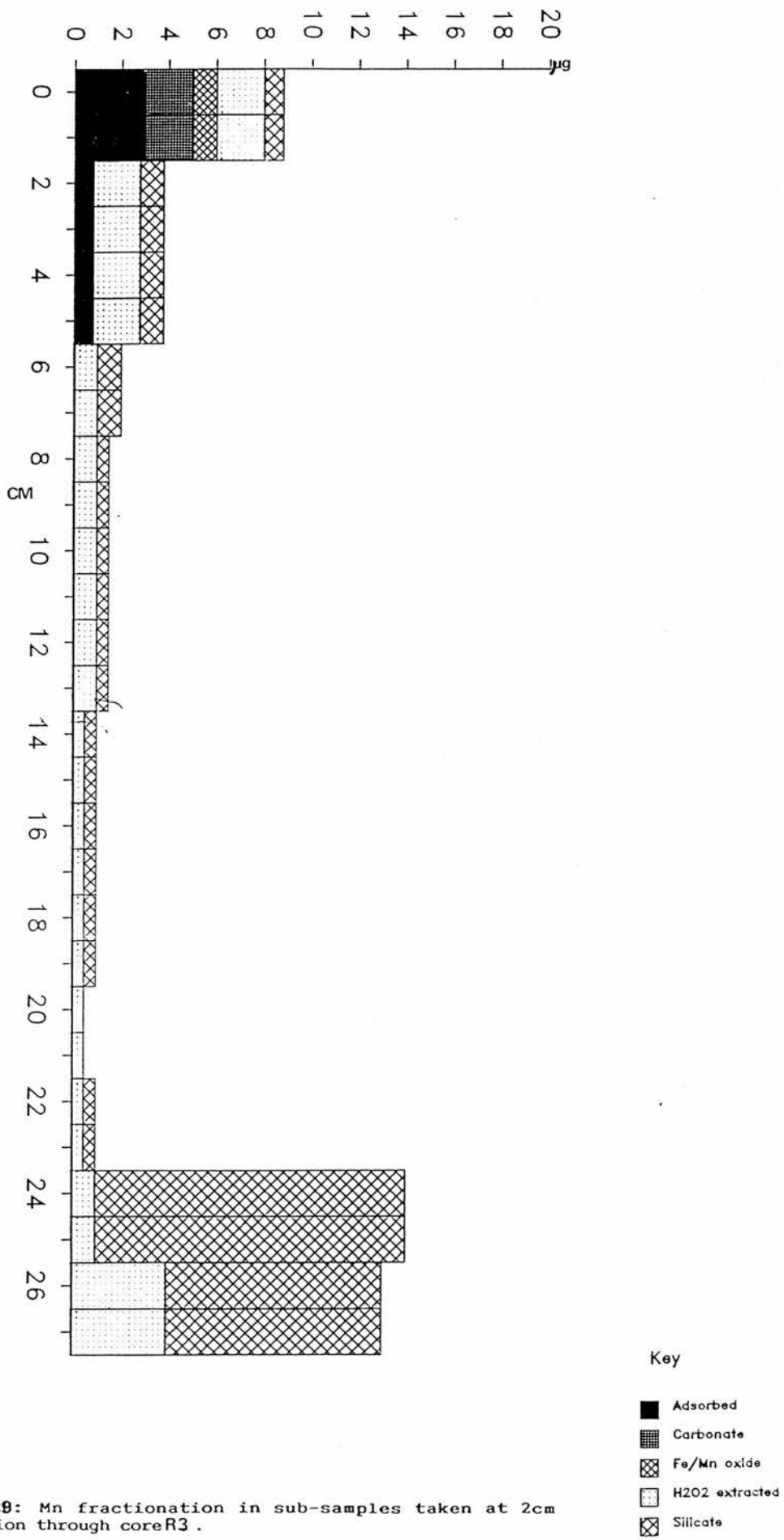

FIG 5/28: Mn fractionation in sub-samples taken at 2cm resolution through core R3 .

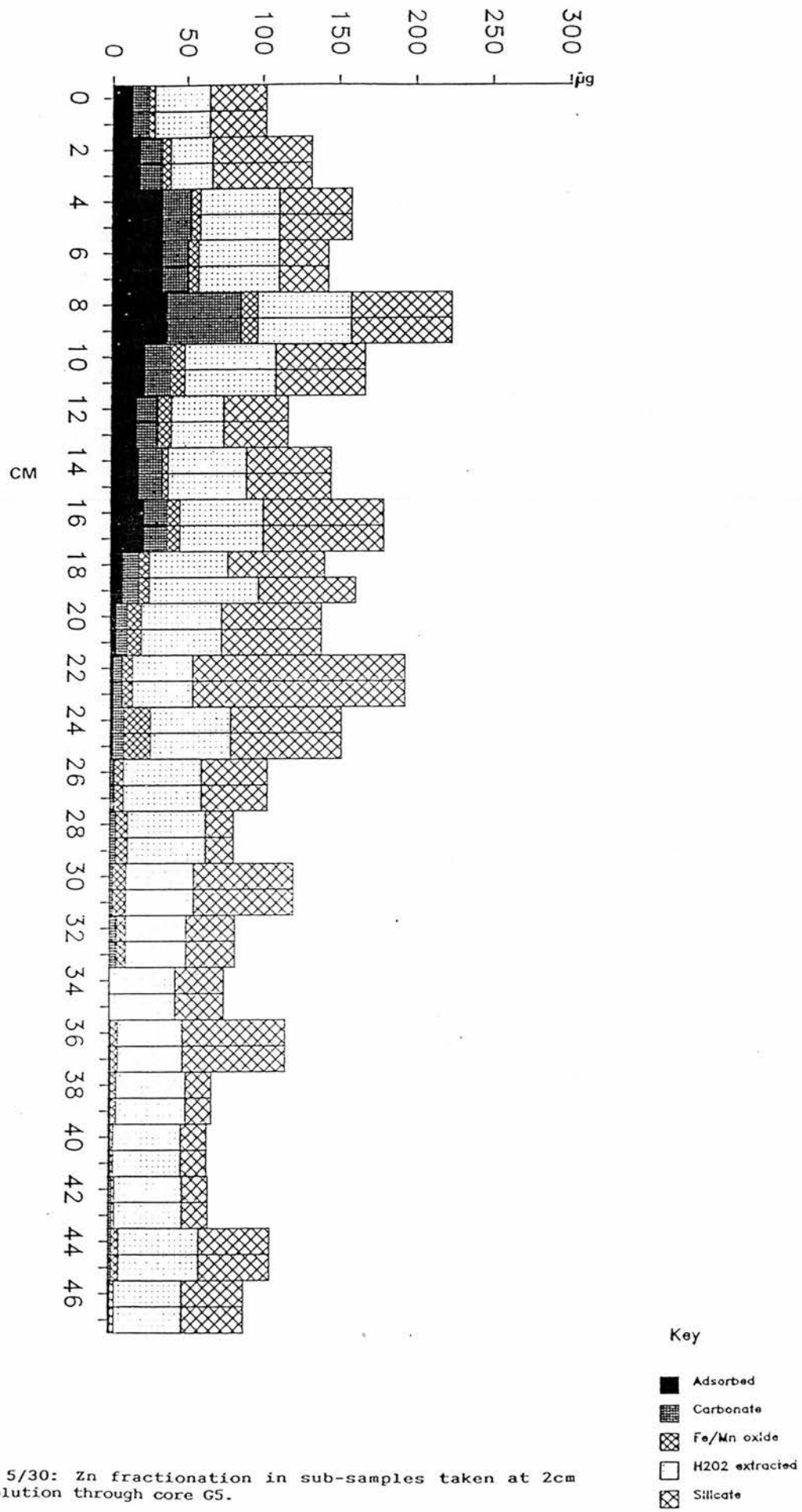

FIG 5/30: Zn fractionation in sub-samples taken at 2cm resolution through core G5.

47% of total Zn is held in adsorbed, carbonate and oxide phases, while the 19cm - 48cm levels hold over 90% in H2O2 extractable and silicate fractions. Although the increased significance of adsorbed and carbonate Zn is known to be diagnostic of atmospheric pollution in surficial sediments (Filipek et al 1979), the abrupt disappearance of these phases in the inundated levels of core G5 indicates the influence of dissolutionary processes. Hence, the enrichment of Zn above the water table appears to be a consequence of the insolubility of ZnO and ZnCO3 under oxic conditions. With reduced eH downward of 18cm depth, these phases cease to be thermodynamically stable and are replaced by aqueous Zn(OH) or Zn2+. These aqueous fractions may then be removed from the peat column in solution.

Significantly, the sequential Zn data presented in Fig 5/30 suggest that previous workers (eg Damman 1978, Gorham 1984), while acknowledging the mobility of Zn, have mis-interpreted the controlling processes. Their proposal is that Zn is subject to accumulation in the zone of water table fluctuation as a consequence of the conversion of downwardly mobile ZnSO4 to insoluble ZnS. Clearly, this is not consistent with either the low variability of H2O2 extractable Zn throughout core G5, or the characteristic enrichment of Zn above (rather than across) the water table within the Galloway and Beinn Chaorach peats.

b) Precipitation mechanisms.

Sequential Pb, Fe and Cu analyses of cores G5 and R3 confirm Dammans (1978) conclusions that these elements are enriched around the water table as a consequence of precipitation mechanisms. In the case of Pb, data for core G5 (Fig 5/31) show that while 43% - 79% of total concentrations are held in reducible phases throughout the peat column, the significance of such phases is depressed markedly in the zone of water table fluctuation (18cm - 24cm). At these levels, H2O2 extractable fractions dominate (attaining peak concentrations of 85µg/g) and signify the precipitation of slightly soluble PbSO4 as insoluble PbS on account of the sharp depression of eH values to -350mV. In addition, it is likely that enhanced H2O2 extractable Pb concentrations occur at this level as a result of increased pH (caused by SO4 reduction) which, in turn, serves to increase the efficiency of organo-metallic complexation.

Given the insolubility of PbS, the failure of Pb to be retained upon burial within the permanently inundated levels of core G5 can best be explained by reference to the observations of Damman (1978). Specifically, PbS which forms in the zone of water table fluctuation must be oxidized during dry periods. Because such transformations serve to increase the solubility of Pb (through PbSO4 production), the element can be removed from the system prior to its incorporation into the permanently anoxic strata.

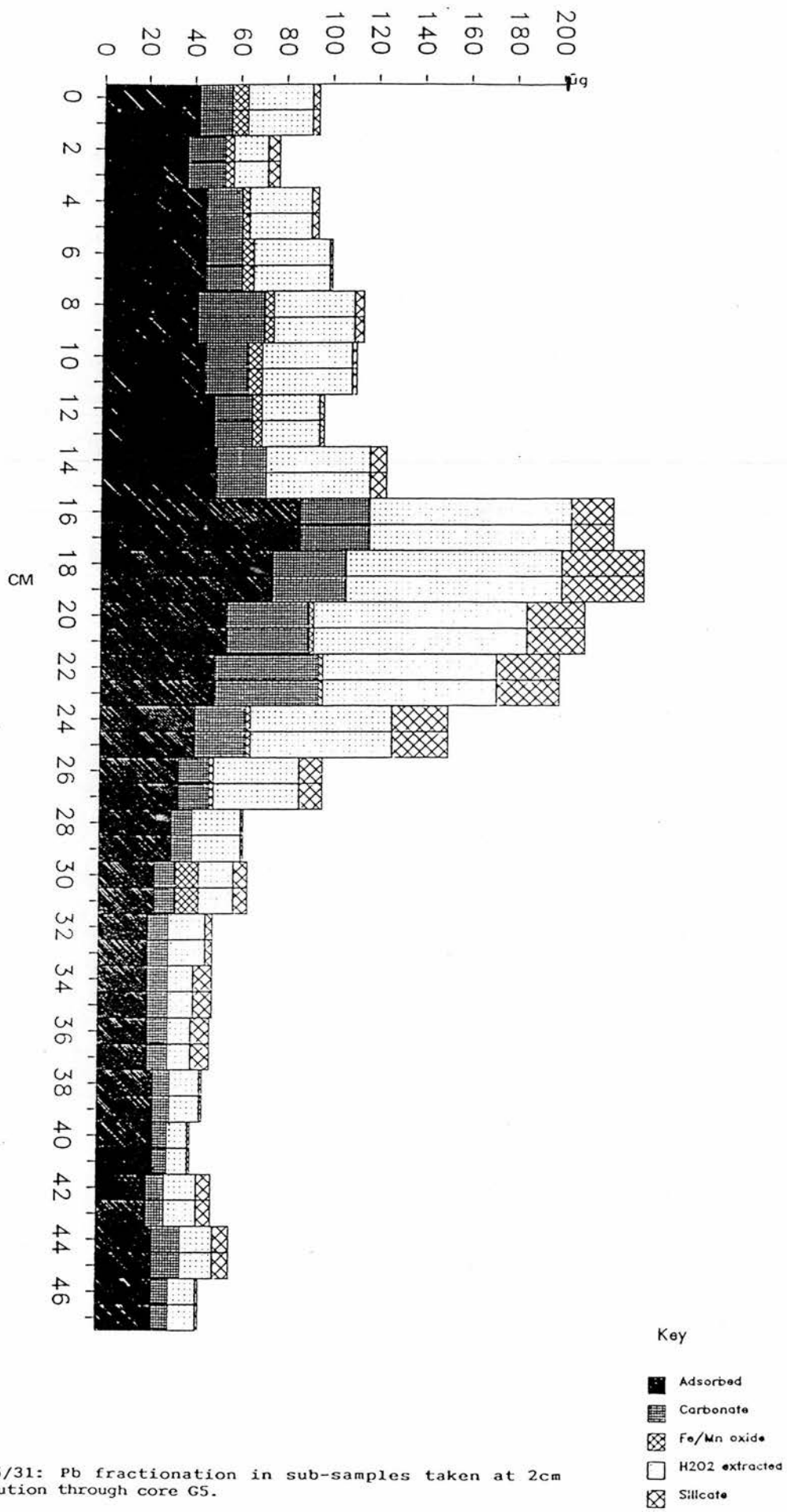

FIG 5/31: Pb fractionation in sub-samples taken at 2cm resolution through core G5.

The partitioning of Cu in sediments and peats is known to be distinctive on account of its confinement to H2O2 extractable and silicate fractions (Filipek et al 1979, Jones 1985). While the sequential Cu data for core R3 (Fig 5/32) confirm such trends, analogous processes to those described for Pb appear to promote the production of Cu anomalies in the zone of water table fluctuation. H2O2 extractable Cu concentrations increase dis-proportionately (to 4.8µg/g) at 6cm depth, signifying the precipitation of insoluble CuS at the sub-oxic/strongly anoxic boundary and increased rates of organo-metallic complexation. During prolonged dry periods, CuS will be subject to oxidation, thus forming highly soluble CuSO4. This phase may then be removed from the system and hence, precludes the accumulation of Cu in the permanently inundated strata.

The enrichment of Fe in the zone of water table fluctuation has conventionally been attributed to the precipitation of soluble Fe^{2+} from the anoxic mire waters as insoluble Fe^{3+} oxides upon contact with the aerated peat (Damman 1978). However, while the accumulation of $NH_2.OH.HCl$+HOAC extractable Fe at 11cm - 13cm depth in core R3 (Fig 5/33) confirms the operation of such processes, these strata also show 2-fold enrichment of H2O2 extractable fractions. Given the anoxic conditions prevailing, this increment to H2O2 extractable Fe is likely to result from the precipitation of immobile FeS_2, as observed by Brown (1980) in Tillingbourne peats. Should this be the case, the

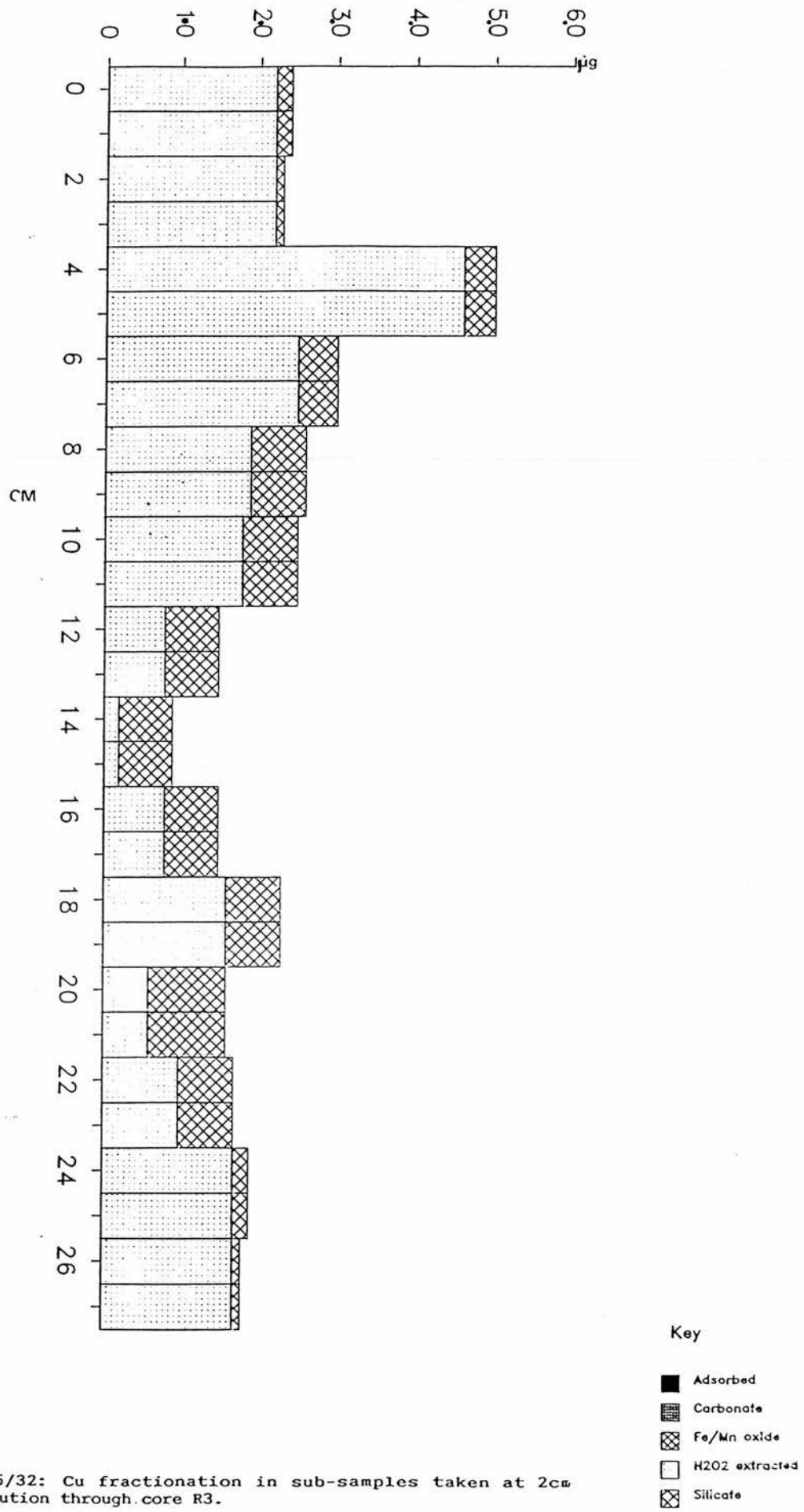

FIG 5/32: Cu fractionation in sub-samples taken at 2cm resolution through core R3.

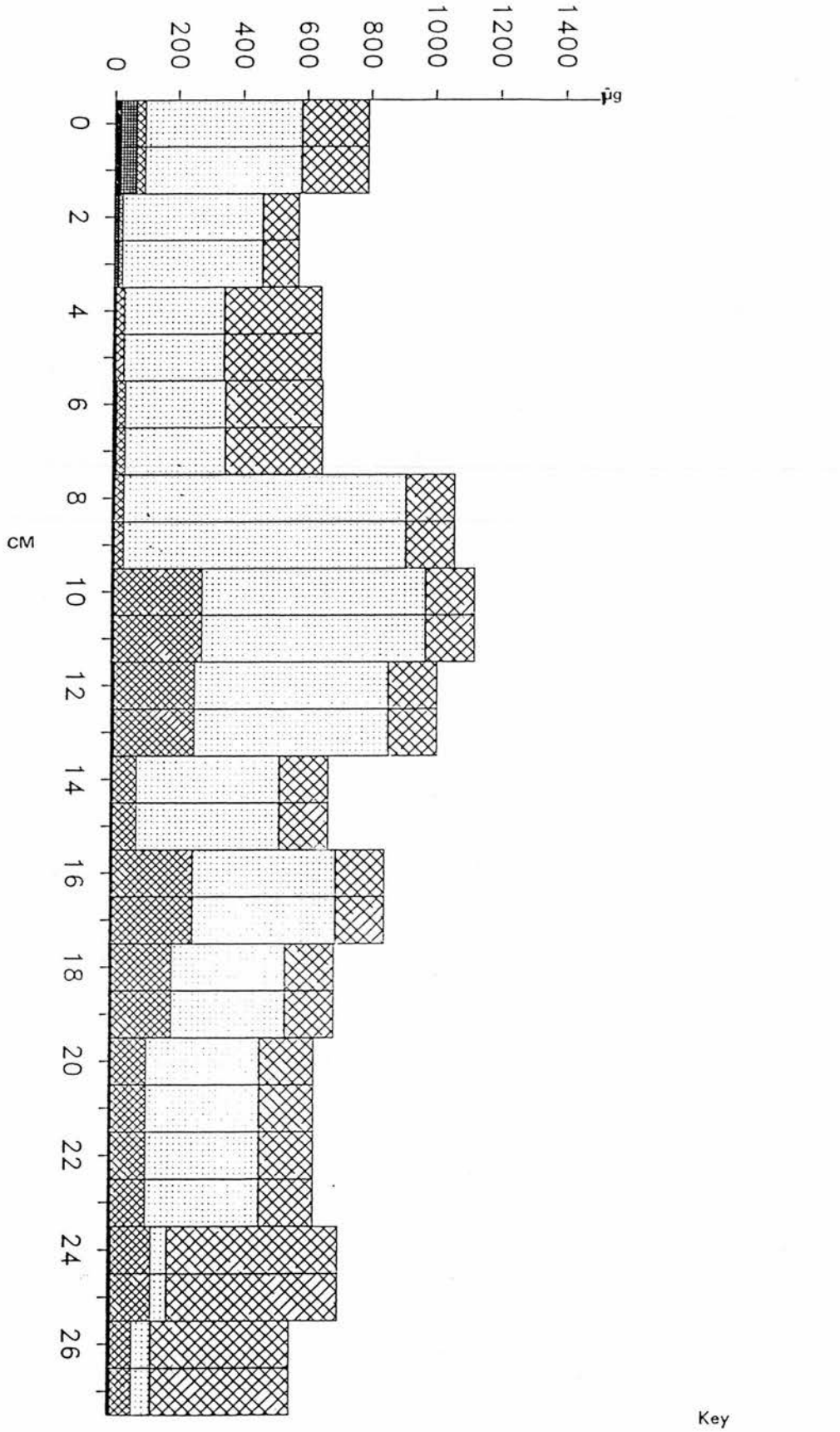

FIG 5/33: Fe fractionation in sub-samples taken at 2cm resolution through core R3.

co-existing Fe3+ oxides must be present in a state of dis-equilibrium, having formed during a prolonged dry period.

The concentrations of Cd and Cr in the sequential leachates from all G5 and R3 sub-samples fell below AAS detection limits and Al and Ti data were not collated. However, it is possible to identify the likely mechanisms of enrichment for these elements by reference to the processes identified for Pb, Cu and Fe. Ti, Cd and Cr can be assumed to precipitate as insoluble sulphides (in similar fashion to Pb) upon burial within the strongly reducing strata, thus producing anomalies in the zone of water table fluctuation. The removal of these elements prior to their incorporation into the permanently anoxic strata can be attributed to the formation of soluble metal-salts (and aqueous TiO2+) during prolonged dry periods. In contrast, Al probably accumulates in similar fashion to Fe, through the conversion of aqueous Al3+, Al(OH)4 and Al2S3 to insoluble AlSO4 at the oxic/anoxic boundary. Upon burial within the permanently anoxic strata, these Al phases will be reduced and will react with H2S to form soluble Al2S3 which may then be removed from the system.

c) Additional mobilization processes.

Despite the persistently correlated nature of Mn and K within sample cores, redox-mediated processes cannot be

cited to explain the distribution of the latter, as K is typically present either as aqueous K+ or in K-Al-silicates. However, it is likely that a major release of K+ occurs as a result of the decomposition of organic matter upon burial. Subsequently, this mobilized K may become available for uptake by active (vascular) organic matter (Malmer 1962) or may be translocated to the peat surface through the selective mechanisms of monovalent ion diffusion described by Brehm (1971).

5.9.3: Prospects for the retention of atmospheric influx chronologies.

From the sequential chemical data presented above, it is apparent that the redox regime controls elemental concentrations at and below the water table through the precipitation or dissolution of hydrogenous phases. However, such processes do not account for any variations occurring solely in the aerated, drained sectors of the Brishie mire, Craigherron and Beinn Chaorach sample cores. In addition, the persistence of Mn in lithogenous fragments at 25cm - 28cm depth in core R3 (Fig 5/29) indicates that eH conditions do not significantly influence the downcore profiles of silicate phases. Such formerly unexplained geochemical fluctuations may, therefore, plausibly reflect the influence of temporally variable atmospheric influxes.

With respect to geochemical variations in the drained,

aerated sectors of the Brishie mire, Craigherron and Beinn Chaorach peats, two sources of evidence suggest an atmospheric control. Firstly, it has been noted that the peak concentrations of atmophilic elements (Pb, Zn, Cu and Cd) within the surficial levels of the analysed Galloway sample cores are consistently higher than those in analogous stratigraphic levels of the Beinn Chaorach cores (see pages 220 - 222). Given the more remote nature of the Beinn Chaorach site, such trends are concordant with the observations of Livett (1982), Pakarinen et al (1977) and Ylirivokanen (1976), that atmospheric pollutants are retained in surficial peats, thus providing a reflection of ambient loadings. Corroberation of this relationship is provided by the low peak concentrations of Pb, Zn, Cu, Cd, Cr and V in sample cores from Glen Muich (Aberdeenshire), Glen Quoich (Invernesshire) and Loch Cluanie (Invernesshire), relative to those observed in the Beinn Chaorach cores (see Appendix 3).

Secondly, the occurrence of correlated, sub-surface concentration maxima for Pb, Zn, Cr, Cu and Cd in the Galloway and Beinn Chaorach sample cores is consistent with the documented decline in the emission of atmospheric pollutants during the past decade (Lantzy 1979, Renberg 1985) and with the relatively rapid accumulation rates of the surficial 5cm - 10cm of sample cores (see section 5.6.6). Significantly, Pb and Zn also exhibit declining

concentrations upward of 3cm in the diagenetically unaltered sediments of Loch Dee (section 3.4.1).

The differing depths at which enrichment anomalies occur in adjacent "lawn" and "hummock" peat cores may, in turn, be partially reconcilable with microtopographic variations of mass accumulation rates across the peat surface during the past 10 - 30 years. Such variations have frequently been cited in explanation of the closer proximity of SIRM peaks to the surface of "lawn" cores relative to hummocks (eg. Oldfield et al 1978, 1979, 1984) under circumstances where all peaks have been considered to be of synchronous origin.

5.9.4: Flux data.

To further examine the possibility that atmospheric "pollution chronologies" are retained in the surficial sectors of the Galloway and Beinn Chaorach peats, the Pb, Zn, Cu, Cd, Fe and Mn profiles of cores G1, G1 and R2 have been used to estimate historical influx trends (Table 55). All data are the product of the mean accumulation rate (AR cm/yr-1), the mean wet density (WD g/cm3), the mean fractional dry weight (FDW g/cm3) and the mean elemental concentrations (µg/g) of datable core sequences. Hence, for cores G1 and G2, annual flux data are presented for the pre-1840 period, 1841 - 1961 and 1962 - present. For core R2, flux data are presented for the pre-1840 period, 1841 - 1974

and 1975 - present. Flux data for strata which exceed 155 years of age have been determined by assuming their accumulation rates to approximate those of the oldest datable levels of each core.

Table 55: Mean annual elemental fluxes (µg/cm2/yr-1) at Brishie Mire and Beinn Chaorach, as recorded at coring stations G1, G2 and R2.

	FDW	AR	WD	Pb	Zn	Cu	Cd	Fe	Mn
G1 1962-1986	.03	.4	.3	.13	.19	.02	.04	1.6	.54
G1 1841-1961	.03	.15	.38	.08	.15	.01	.01	2.0	.07
G1 PRE-1840	.04	.16	.38	.15	.13	.02	.01	6.0	.01
G2 1962-1986	.03	.28	.18	.10	.26	.02	.004	1.8	.60
G2 1841-1961	.03	.20	.24	.06	.13	.01	.006	3.0	.05
G2 PRE-1840	.05	.2	.34	.12	.05	.02	.008	.99	.01
R2 1975-1986	.02	.21	.64	.25	.17	.02	.007	-	.05
R2 1841-1974	.06	.07	.86	.25	.11	.01	.005	-	.02
R2 PRE-1840	.06	.07	.86	.20	.09	.01	.004	-	.01

Upon examining the data presented in Table 55, it is notable that the pre-1840 Pb and Cu flux values for cores G1 and G2 are equal to, or in excess of their respective post-1840 flux estimates. These trends are clearly discordant with documented historical records of atmospheric Pb and Cu deposition throughout Europe (eg. Renberg 1985). Because the pre-1840 flux values have been derived from geochemical data for periodically inundated strata, they serve to confirm the distortion of atmospheric pollution chronologies which results from the precipitation of PbS and CuS at the water

table.

In contrast, the trends emerging from the flux data for the post-1840 levels of cores G1, G2 and R1 show agreement with independently established atmospheric deposition records. In particular, the data for cores G1 and G2, showing the post-1962 Pb (0.10 - 0.13µg/cm2/yr), Zn (0.19 - 0.26µg/cm2/yr) and Cu (0.02µg/cm2/yr) fluxes to have exceeded those prevailing during the 1841-1961 period by at least a factor of 1.5 are in accordance with the records deciphered from the diagenetically unaltered sediments of Loch Dee (see section 3.8 .1). In the latter study area, peak fluxes of Pb, Zn and Cu have been estimated to have prevailed during the 1967-78 period. Furthermore, the present-day Pb flux estimates for Brishie mire and Beinn Chaorach are comparable to those calculated for other remote locations. For example, Livett et al (1979) have determined the present-day Pb fluxes at Glenshieldaig and Grassington Moor to be 0.15µg/cm2/yr and 1.9µg/cm2/yr respectively. For USA sites, present day Pb fluxes have been estimated to be 0.4µg/cm2/yr-1 at Yosemite National Park (Kahl et al 1984), 1.4µg/cm2/yr-1 at Chester Morse reservoir (Schell and Barnes 1985) and 2.4µg/cm2/yr-1 within the more heavily polluted Lake Michigan basin (Robbins 1978). Accordingly, the "mass accumulation normalized" flux estimates for the upper sectors of cores G1, G2 and R2 provide strong evidence that the aerated levels of these peats have retained accurate, decipherable records of atmospheric pollutant loadings with

time.

Perhaps the most notable anomaly within the flux data presented in Table 55 is the high present-day Pb flux value for core R1, relative to the values calculated for the Brishie mire cores. This discordance between the regional trends of Pb and Zn or Cu deposition may plausibly reflect the higher loading of locally-emitted Pb at Beinn Chaorach, emanating from the major trunk road which lies 0.8km west of the sampling site. Chow and Earl (1970), Farmer (1978) and Brown (1986) have all noted the low transportation capacity of Pb following its emission from combustion engines and hence, the Brishie mire site may not be subjected to such fluxes on account of its remoteness from major routeways.

5.10: Summary and conclusions.

From the evidence presented in the preceding sections, an empirically-based model can be developed, depicting the controls upon the geochemical constituency of all analysed sample cores from Brishie mire, Craigherron and Beinn Chaorach. The model, outlined in Fig 5/34, entails the division of the peat column into three clearly defined stratigraphic sectors. In the uppermost sector comprising only aerated, drained strata, processes of elemental mobilization are severely impeded, allowing the persistence of adsorbed, carbonate and reducible oxide metal phases.

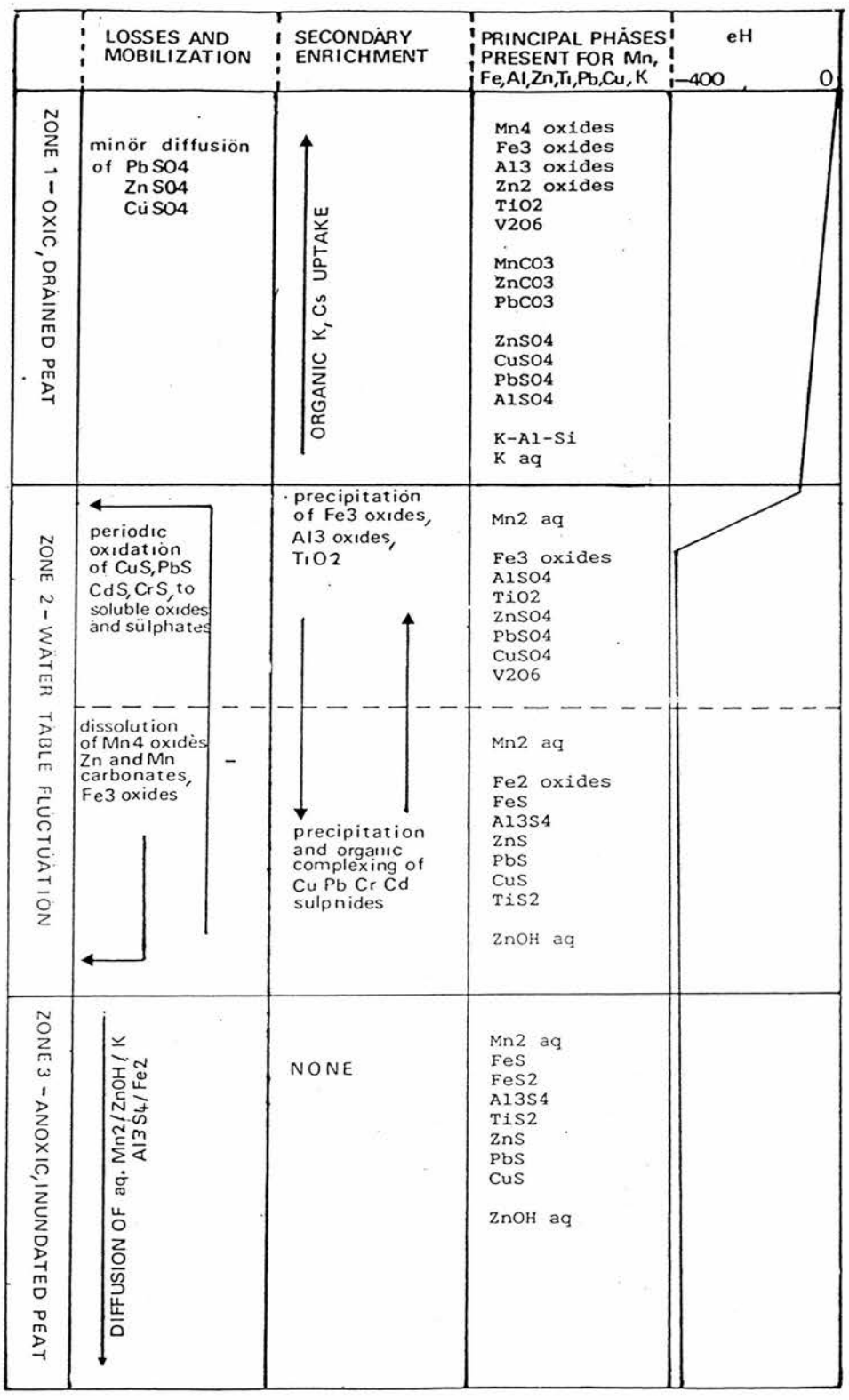

FIG 5/34: Empirically-based model of the controls on the geochemical stratigraphy of peat systems. The model depicts three distinct zones comprising the aerated or drained peat, the zone of water table-fluctuation and the permanently inundated strata. Elemental mobility is limited in the aerated sector and reducible (carbonate and oxide) metal phases can persist.

The depression of eH in the zone of water table fluctuation promotes the dissolution of reducible phases, notably Mn and Zn oxides and Mn, Zn and Pb carbonates. Cu, Pb, Cd and Cr are enriched through sulphidization. Fe and Al are enriched through oxide precipitation at the sub-oxic/strongly anoxic boundary.

All elements are subject to depletion in the permanently inundated strata.

Excepting the influence of temporally varying peat accumulation rates, elemental profiles through this sector can be considered to mirror the history of atmospheric deposition.

In the second stratigraphic sector, comprising strata which lie within the zone of water table fluctuation, periodically anoxic conditions promote the diagenetic modification of elemental accumulation patterns. Hydrogenous Mn and Zn fractions display increased solubility and are subject to removal through hydrological pathways. Fe, Al and Ti are enriched through the precipitation of authigenic oxides. Pb, Cu, Cr and Cd also precipitate as immobile sulphides.

The third geochemically distinct sector comprises permanently inundated, anoxic strata and extends from the base of the zone of water table fluctuation to the peat/bedrock interface. All strata in this zone are characterised by elemental depletion, irrespective of their geochemical constituency prior to burial. Losses are most marked with respect to Fe, Mn, Zn and Al which exhibit thermodynamic stability only in soluble or aqueous low valency phases. In instances where these elements are retained at above "background" concentrations, detrital, silicate phases are typically responsible.

The recurrent relationships between peat hydrology and

geochemistry at all of the Galloway and Beinn Chaorach sampling sites suggests that the above model has universal applicability. However, it is important to note that the stratigraphic extent of each zone will vary between sampling sites in accordance with the prevailing hydrological regime. Bearing this point in mind, the model outlined in Fig 5/34 has the following implications for past and future geochemical studies of peatlands:-

1) Previous observations that trace-element anomalies typically occur in the uppermost 20cm - 50cm of peat accumulations (Livett 1982, Livett et al 1979, Schell 1986, Pakarinen and Tolonen 1977, Ylirivokanen 1976) are wholely correct. However, assumptions that these anomalies are diagnostic of recently increased anthropogenic pollution (Livett 1982, Schell 1986) are invalid. On the basis of the empirical model (Fig 5/34), relative Zn and Mn enrichment can be expected at the surface of all peatland sites, as these elements are mobilized in all but the uppermost (oxic) geochemically distinct zone. Given the proximity of the water table (and hence the second zone of the empirical model) to the surface of most peatlands, surficial enrichment of Pb, Cu, Cd, Fe, Cr, Al and Ti can also be considered to be a natural occurrence; irrespective of the extent of atmospheric pollution.

2) The respective controls of " atmospheric deposition"

and "post depositional mobilization" on elemental profiles varies markedly with peat micro-topography. Short (c. 0.5m) sample cores from peatland "hummocks" may be characterised by oxic conditions at all levels and hence, may be entirely referable to the upper zone of the empirical model (Fig 5/34). Under such circumstances, downcore geochemical trends are largely interpetable as reflecting historical variations of atmospheric deposition.

In contrast, longer (>1.0m) sample cores or cores from "sphagnum lawn" locations typically extend into strata which are referable to zones 2 and 3 of the empirical model (Fig 5/34). In cores from submerged "pool" locations the upper, geochemically inert zone is entirely absent. Under such circumstances, post-depositional mechanisms control elemental distributions through most, or all stratigraphic levels. Livett's (1982) claim that the enrichment of trace metals at the surface of cores from water-inundated locations reflects their ability to chronicle the history of atmospheric pollutant deposition is, therefore, incorrect.

CHAPTER SIX.

Mineral magnetic studies of ombrotrophic peat cores from Galloway and Rannochmoor.

6.1: Introduction.

The data presented in the preceding chapter indicate that the total loadings of atmophilic elements to Brishie mire, Craigherron and Beinn Chaorach are directly related to the proximity of industrial complexes. However, their distributions are subject to diagenetic control within the reducing, inundated sectors of these peatlands. In the light of the known prevalence of such redox-mediated processes, the appraisal of downcore mineral magnetic trends is, in two respects, particularly critical. Firstly, no published studies to date have noted any diagenetic alteration of magnetic minerals in peatlands. Hence, their downcore concentration gradients may provide our best evidence of the history of atmospheric pollutant fluxes to the Galloway and Beinn Chaorach sites. Secondly, given the strongly acidic, reducing conditions which characterise the Brishie mire, Craigherron and Beinn Chaorach peat accumulations, it appears justifiable to scrutinise the post-depositional persistence of magnetic oxides upon burial more comprehensively than have preceding workers in this field. Bearing these points in mind, magnetic data have been collated for all of the sample cores for which geochemical

data have formerly been presented. These data are presented and interpeted in the following sections.

6.2 Rationale.

It has previously been noted that hydrocarbon combustion processes yield particulate pollutants with distinct magnetic "fingerprints" (section 2.3.1). Through their incorporation into the essentially diamagnetic matrix of ombrotrophic peats, these particulates have been found to promote conspicuous magnetic enhancement (Thompson et al 1980, Oldfield et al 1984). In a spatial context, such influences have become apparent through comparative studies of peatland sites in the UK, Scandinavia and around Sudbury, Ontario (Oldfield et al 1984, Thompson et al 1980), showing the ferrimagnetic mineral concentrations of surficial samples (as defined by SIRM and X) to vary inversely with the proximity of industrial pollutant sources (Fig 6/1). In a temporal context, Pakarinen (1977) and Oldfield et al (1981) have shown that Finnish peat profiles consistently exhibit increasing SIRM and Xlf signals in strata which have accumulated during the past 150 years. Similar trends have also been observed at Bolton Fell Moss (Oldfield et al 1978), where all analysed cores were found to exhibit initial SIRM increments (termed the "magnetic take-off") in geochronologically synchronous strata. At all locations, SIRM and X signals have been found to peak at

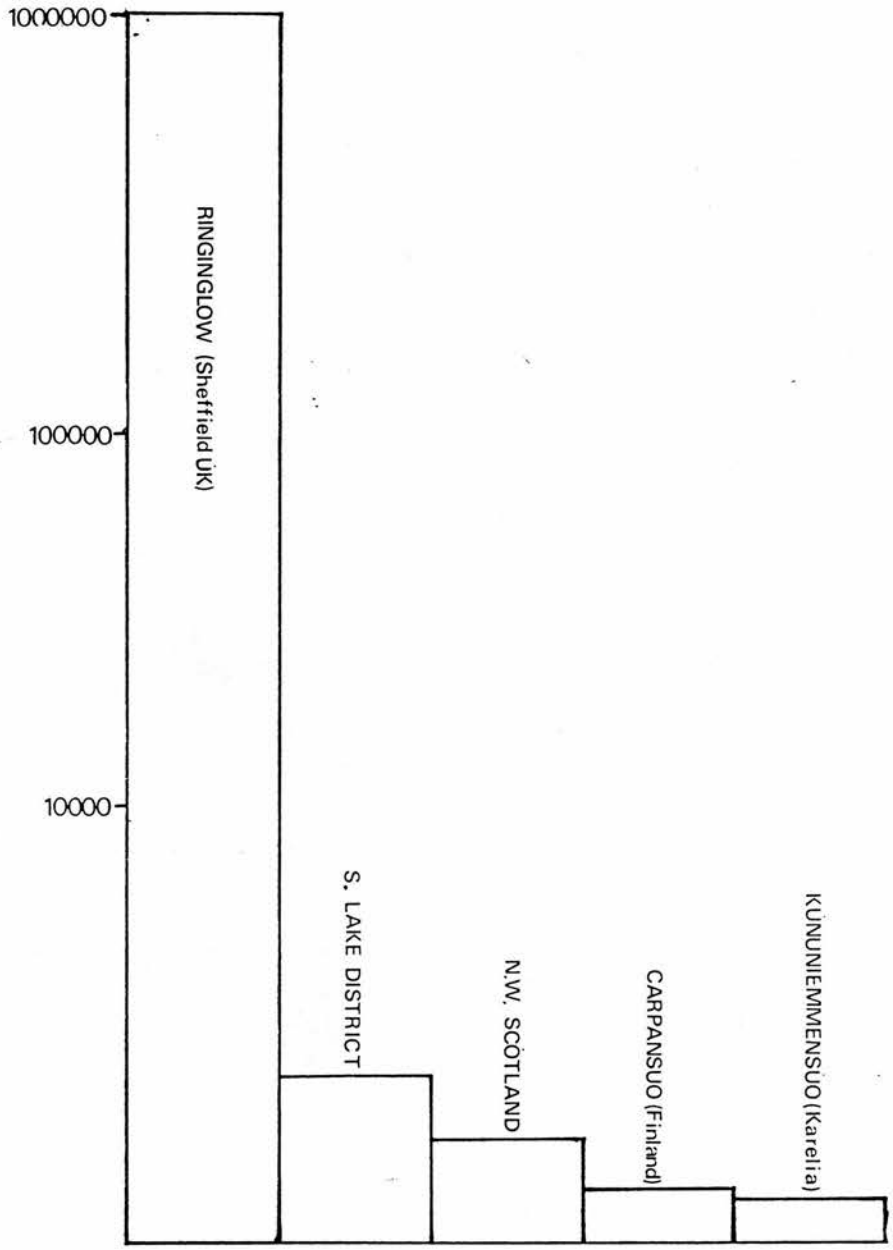

FIG 6/1: Magnetite deposition (mg/m2/yr) at UK and Scandinavian peatland sites, determined from SIRM measurements of surficial peat samples (after Thompson et al 1980). The declining deposition rates with increased distance from industrial pollutant sources are apparent from the high values obtained for Ringinglow and the extemely low values determined for Northern Scandinavian sites.

or near the present day surface of peat cores, where values typically exceed those of pre-industrial strata by two orders of magnitude. Consequently, the above-mentioned workers have all concluded that the concentration gradients of magnetic minerals in peats directly mirror the history of atmospheric particulate deposition (Oldfield et al 1978, 1979, 1983, 1984, Thompson et al 1980, Thompson 1979).

However, because magnetists have conventionally interpreted data by assuming that magnetic oxides remain in pristine condition upon burial in sediments and peats (Thompson et al 1975, Dearing 1979, Oldfield et al 1984, Levi and Banjeree 1976, Mackereth 1971), anomalies in the magnetic profiles of peat cores only appear to have been examined by reference to the "atmospheric deposition" hypothesis. Accordingly, alternative hypotheses have remained largely untested. For example, observations of the consistently low cumulative SIRM values which characterise peat cores from "pool" or "sphagnum lawn" environments when compared to those of cores from "peat hummocks" have been considered reflective of the different efficiencies with which the respective microtopographic facets filter particulates from the atmosphere (Oldfield et al 1979). This interpretation is clearly discordant with the uniform pollen catchment which occurs across peat surfaces (Bradshaw 1981, Birks and Birks 1971) and it remains to be proven that microtopographic variations in the

concentrations of magnetic mineral phases are not a product of their more rapid dissolution within the most reducing, water-indundated sectors of the peat system.

In similar fashion, downcore mineralogical anomalies have, where observed, been related to anthropogenic rather than to diagenetic processes. Most notably, high coercivity assemblages (BOCR > 50mT), indicating the presence of anti-ferromagnetic or SSD phases, have frequently been found to occur in strata which demark the "magnetic take-off" (Oldfield et al 1984, Jones 1985). Such assemblages contrast with those of the MD dominated, overlying strata and have universally been considered to reflect the deposition of particulates emanating from Bessemer combustion systems during the early post-industrial period (eg Jones 1985). Consideration has not, therefore, been given to the possibility that this downcore "hardening" of magnetic remanence may be a product of the progressive dissolution of MD structures along their domain walls upon burial, as observed by Karlin and Levi (1985) in anoxic marine sediments.

Upon examining the available geochemical literature, four sources of evidence can be cited in support of the contention that magnetic oxides may be subject to dissolution upon burial in acid, anoxic peats:-

1) Studies of reaction kinetics have shown Fe(111) oxides

to undergo both reductive and non-reductive dissolution in aqueous and sedimentary environments (Stumm and Morgan 1976, Zinder et al 1986, Krouskopf 1979). Reactions entailing no change of oxidation state analogue processes associated with Al oxides (Zinder et al 1986) and involve the detachment of an Fe centre, with the subsequent weakening of Fe-O bonds by organic chelates (Furrer and Stumm 1986). Such processes have been shown to be particularly prevalent in ligand-rich sediments due to the formation of readily soluble organo-metallic complexes (Krauskopf 1979). Accordingly, they may be widely operative in peat systems.

2) Thermodynamic data of the nature commonly used to indicate the inert behaviour of Fe3O4 under most natural environmental conditions (Watkins et al 1974, Govatt 1975) have recently been shown to have mis-represented magnetite stability fields on account of their failure to incorporate hydrous phases into calculations. From Fig 6/2, it is also apparent that the theoretical stability fields of Fe3O4 depend largely on the precise nature of the solid - solid transformations used in thermodynamic calculations. By incorporating hydrous FeOOH into formerly established phase equilibria determinations for the Fe - S - H2O system, Henshaw (1978) and Henshaw and Merrill (1980) have shown Fe3O4 dissolution/authigenesis to be plausible under the conditions occurring within the pore-waters of many anoxic sediments. Given the acid, anoxic conditions prevailing,

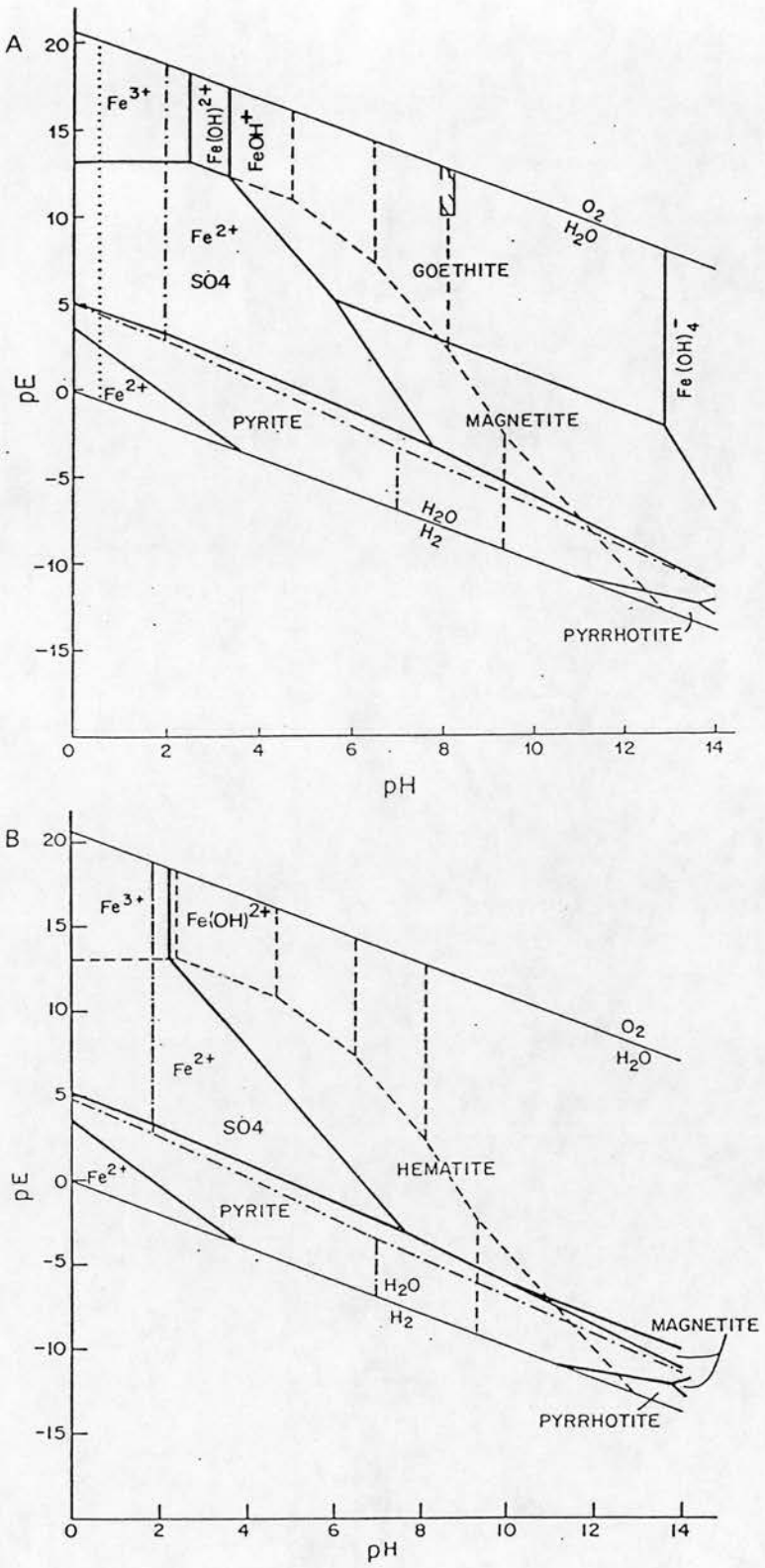

FIG 6/2: eH/pH equilibria for the Fe - S - H2O system (after Henshaw 1978) using the oxide - oxide transformation from goethite to magnetite (A) and the oxide - oxide transformation from haematite to magnetite (B). The dotted lines depict the stability fields of solution species. It is notable that calculations based on FeO(OH)/Fe3O4 transformations, rather than Fe2O3/Fe3O4 transformations, lead to the extension of the Fe3O4 stability field to low pH (5.8) and high eH (6.0). Such discrepancies cast doubt on the applicability of thermo-dynamic data for predicting Fe3O4 stability in the environment, unless all the reactive solid and aqueous phases are incorporated into calculations.

magnetite dissolution processes may, therefore, also be operative in buried peats.

3) Formerly held assumptions that processes of Fe3O4 authigenesis/dissolution are constrained in recent sedimentary systems on account of the high activation energies required (Huber 1975, Krouskopf 1979) have now been shown to be incorrect. Henshaw (1978) and James (1975) have cited kinetic catalysts in explanation of Fe3O4 formation, outwith thermodynamic stability fields, in both Jurassic and Holocene sediments. In addition, Schwertman (1972) and Yaalon (1970) have shown that kinetic constraints may simply slow down, rather than preclude magnetite dissolution processes under thermodynamically unstable conditions. On the basis of data provided by Lindsay (1979), the dissolution of magnetite may occur at kinetically controlled rates given the following pH/eH conditions: pH<4.0/eH<-106, pH<5.0/eH<-165, pH<6.0/eH<-224. Such conditions are frequently observable in ombrotrophic peats (Brown 1980) and hence their effects warrant further investigation with respect to the persistence of Fe3O4.

4) Empirical observations of the progressive dissolution of magnetite upon burial in anoxic sediments (Karlin 1984, Karlin and Levi 1983, 1985, Canfield and Berner 1987, Anderson 1986) and gleyed soils (Maher 1984), have consistently shown such processes to produce characteristic downcore SIRM and Xlf profiles which analogue those

typically observed within peat cores. Consequently, Karlin and Levi (1985) have postulated that dissolutionary processes may be directly responsible for the depletion of ferrimagnetic phases in deeply buried peats.

6.3 Methodological approach.

In the light of the above information, the downcore mineral magnetic data derived from sample cores from Brishie mire, Craigherron and Beinn Chaorach require interpretation by reference to two conflicting hypotheses. These are:

1) That, in accordance with the findings of previous workers (Oldfield et al 1978, 1979, 1983, 1984, Thompson et al 1980, Jones 1985), downcore mineral magnetic trends within peat cores from Galloway and Rannochmoor reflect the history of anthropogenic particulate deposition.

2) That, on account of the anoxic, acidic conditions prevailing in ombrotrophic peatlands, ferrimagnetic oxides are subject to dissolution upon burial with the concomitant downcore depression of SIRM and X signals.

6.4 Analytical methods.

Both the analytical sequence (Xlf > ARM > SIRM >

demagnetisation) and the instrumentation utilized for lake sediment analyses (chapter 4) have been used in the acquisition of magnetic data for sample cores from Brishie mire, Craigherron and Beinn Chaorach. These methods are described in section 2.3.6.

6.5 Results of magnetic analyses.

6.5.1 General description of downcore trends.

Figs 6/3 - 6/15 illustrate the downcore variations of SIRM and SIRM-demagnetisation in the Brishie mire cores, G1, G2, G5 and G6, the Craigherron cores, G3 and G4 and the Beinn Chaorach cores, R1, R2, R3, R4 and R5. Mass specific susceptibility (X) fluctuations within these cores are closely analogous to those displayed by SIRM, but are less sensitive to downcore variations of ferrimagnetic mineral concentration on account of the inherently weak susceptibilities of all analysed sub-samples. Consequently, the analytical "noise" component in the X1f data is unacceptably high and the results do not warrant presentation.

The downcore SIRM profiles of all analysed cores are most strongly characterised by the occurrence of values within the surficial 5cm - 30cm which exceed those of basal core samples by 2 - 3 orders of magnitude (Figs 6/3 - 6/4). With the exception of core R3, in which optically and

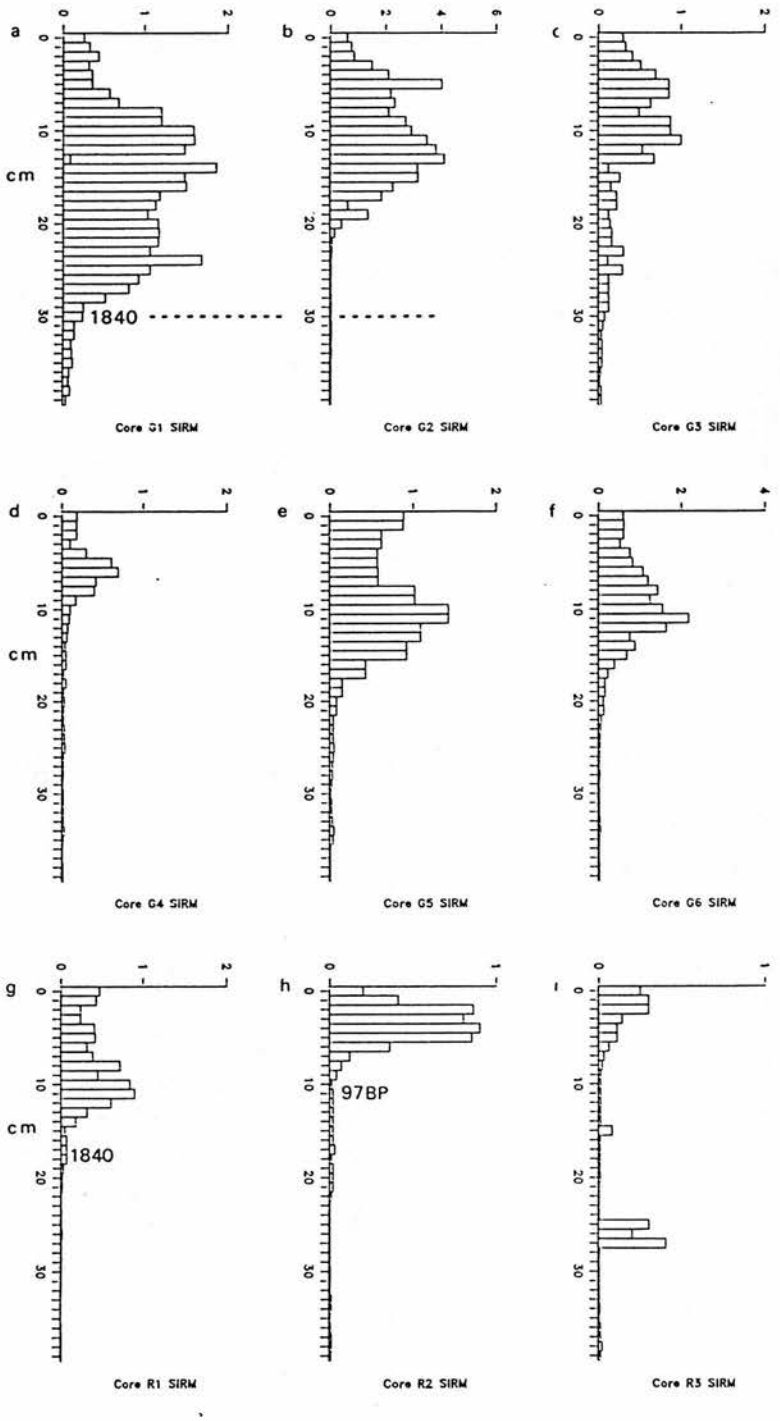

FIG 6/3: Downcore SIRM gradients through cores G1, G2, G3, G4, G5, G6, R1, R2 and R3 as determined by analyses of sub-samples at 1cm resolution. All data are expressed in mAm2/kg-1.

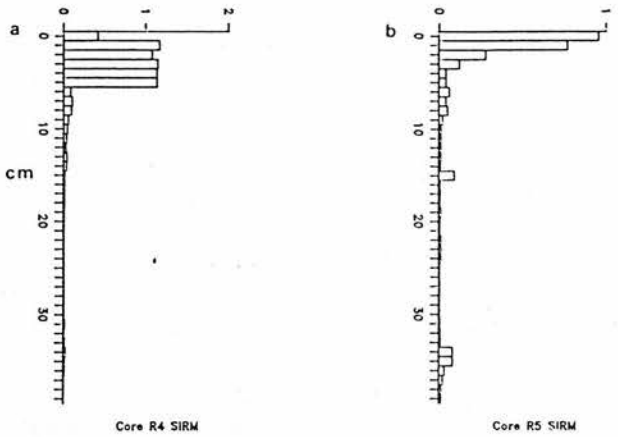

FIG 6/4: Downcore SIRM gradients through cores R4 and R5 as determined by analyses of sub-samples at 1cm resolution. All data are expressed in mAm2kg-1.

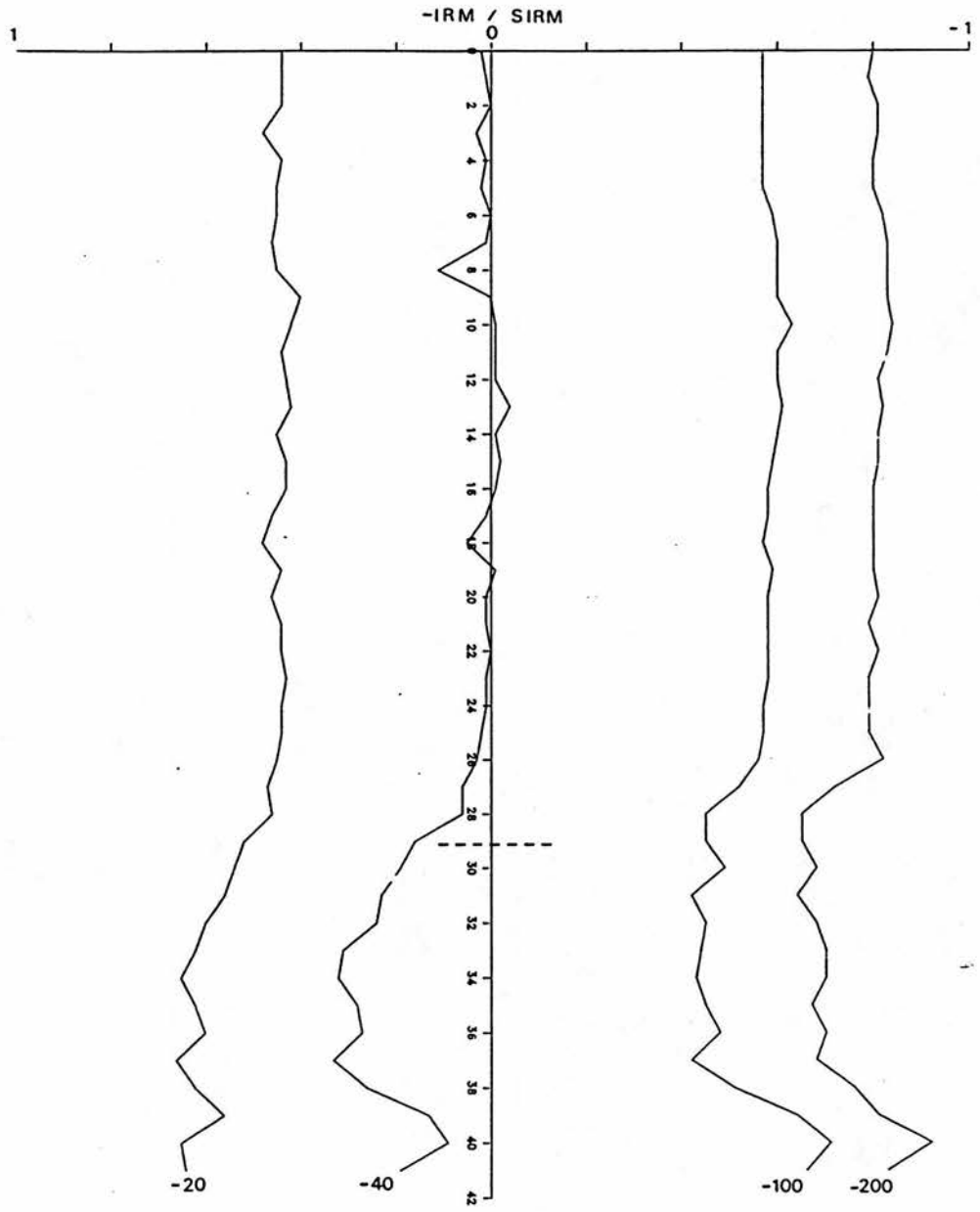

FIG 6/5: Core G1 - downcore variability of SIRM demagnetisation response, determined through the subjection of "saturated" sub-samples to reversed fields of 20mT, 40mT, 100mT and 200mT. The "magnetic take-off" is demarked by the broken line.

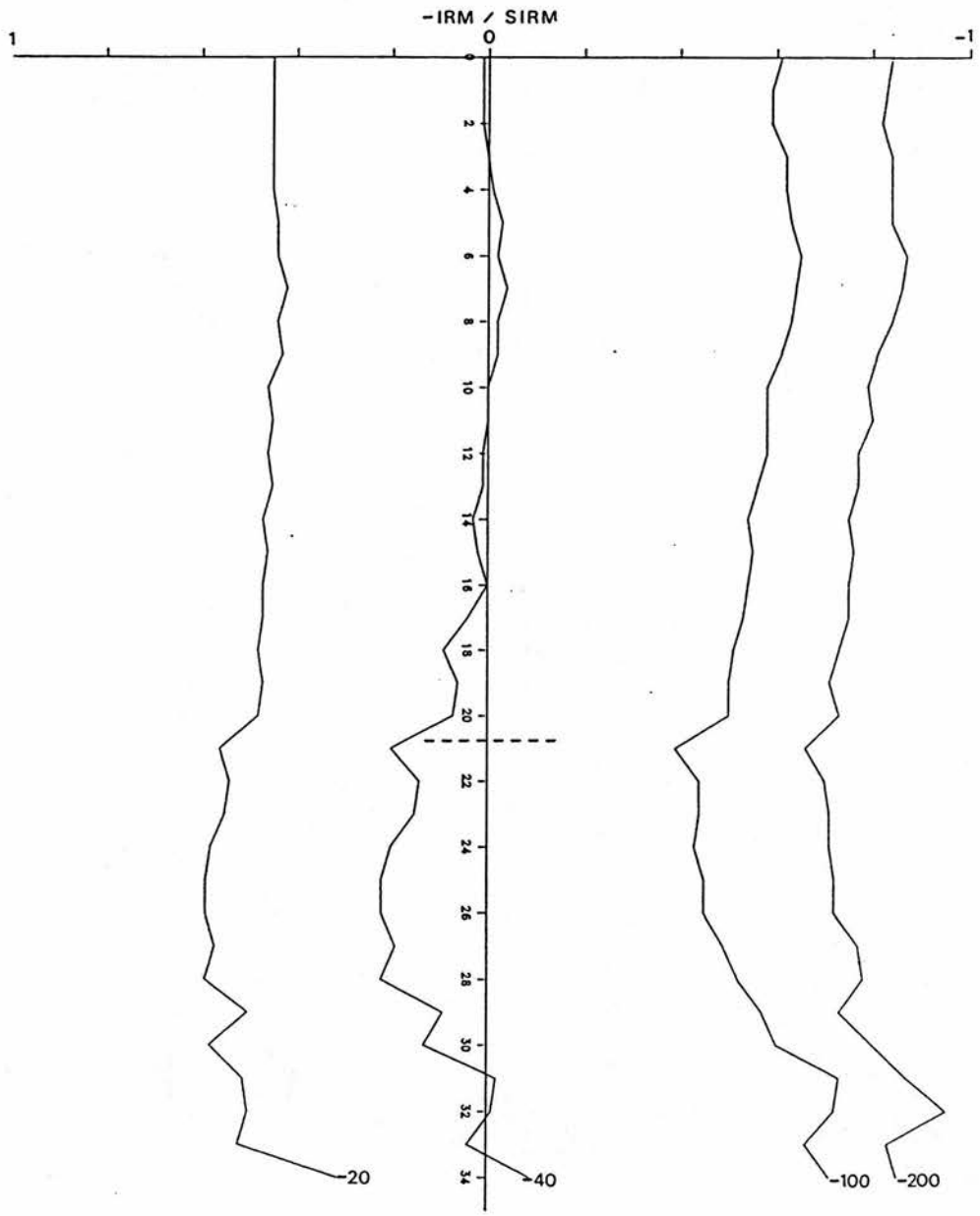

FIG 6/6: Core G2 - downcore variability of SIRM demagnetisation response, determined through the subjection of "saturated" sub-samples to reversed fields of 20mT, 40mT, 100mT and 200mT. The "magnetic take-off" is demarked by the broken line.

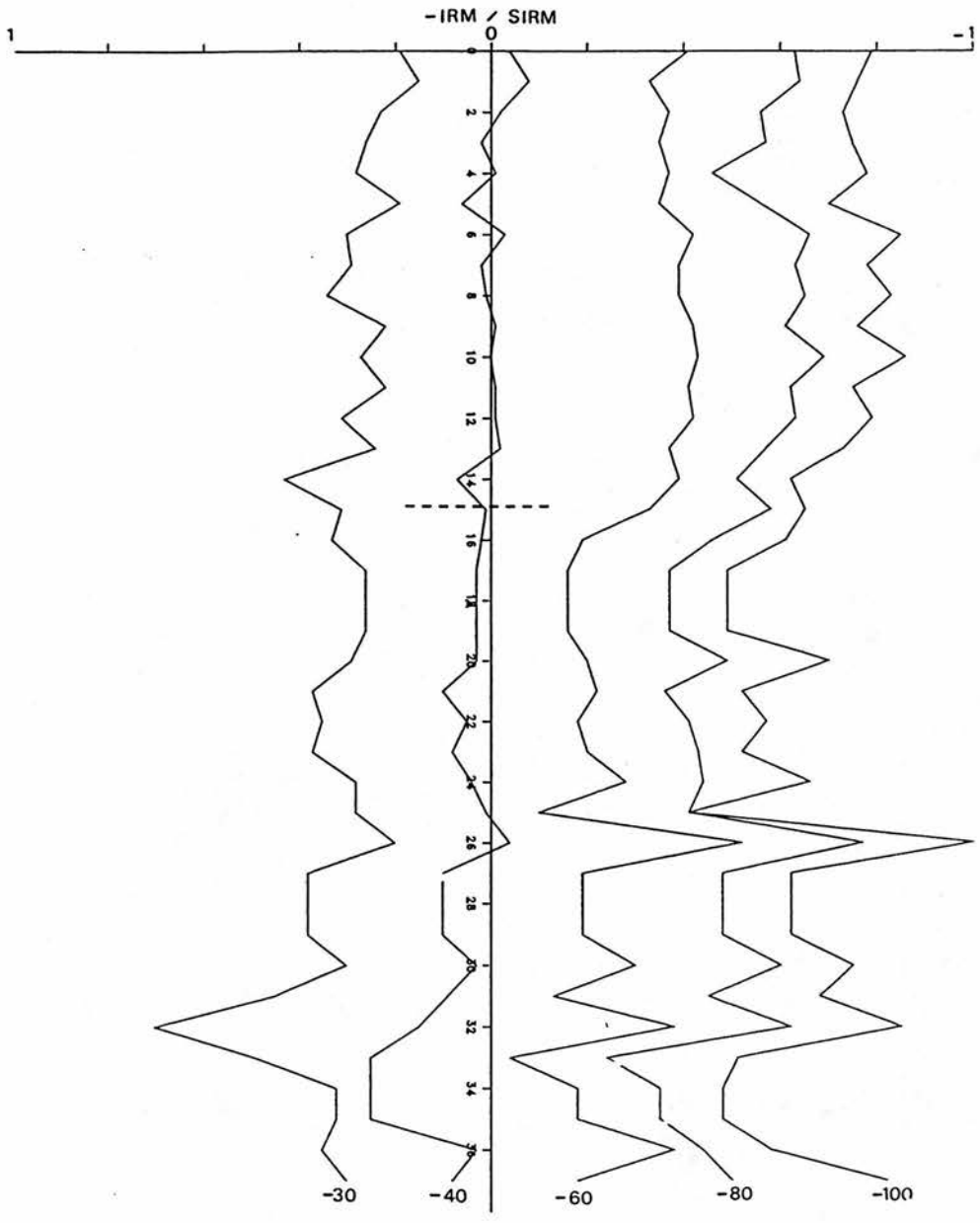

FIG 6/7: Core G3 - downcore variability of SIRM demagnetisation response, determined through the subjection of "saturated" sub-samples to reversed fields of 30mT, 40mT, 60mT, 80mT and 100mT. The "magnetic take-off" is demarked by the broken line.

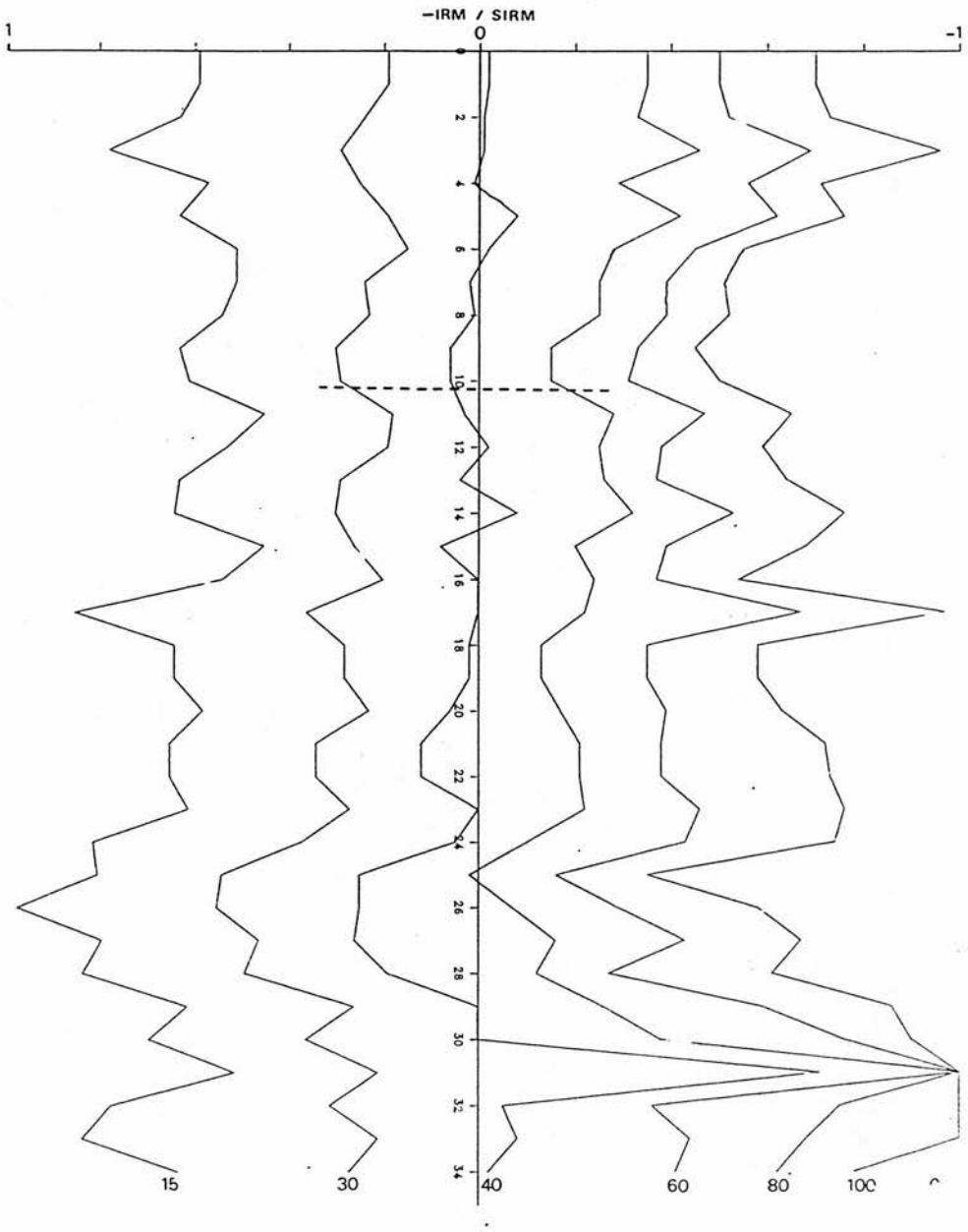

FIG 6/8: Core G4 - Downcore variability of SIRM-demagnetisation response, determined through the subjection of formerly saturated samples to reversed fields of 15mT, 30mT, 40mT, 60mT, 80mT and 100mT. The magnetic take-off is demarked by the broken line.

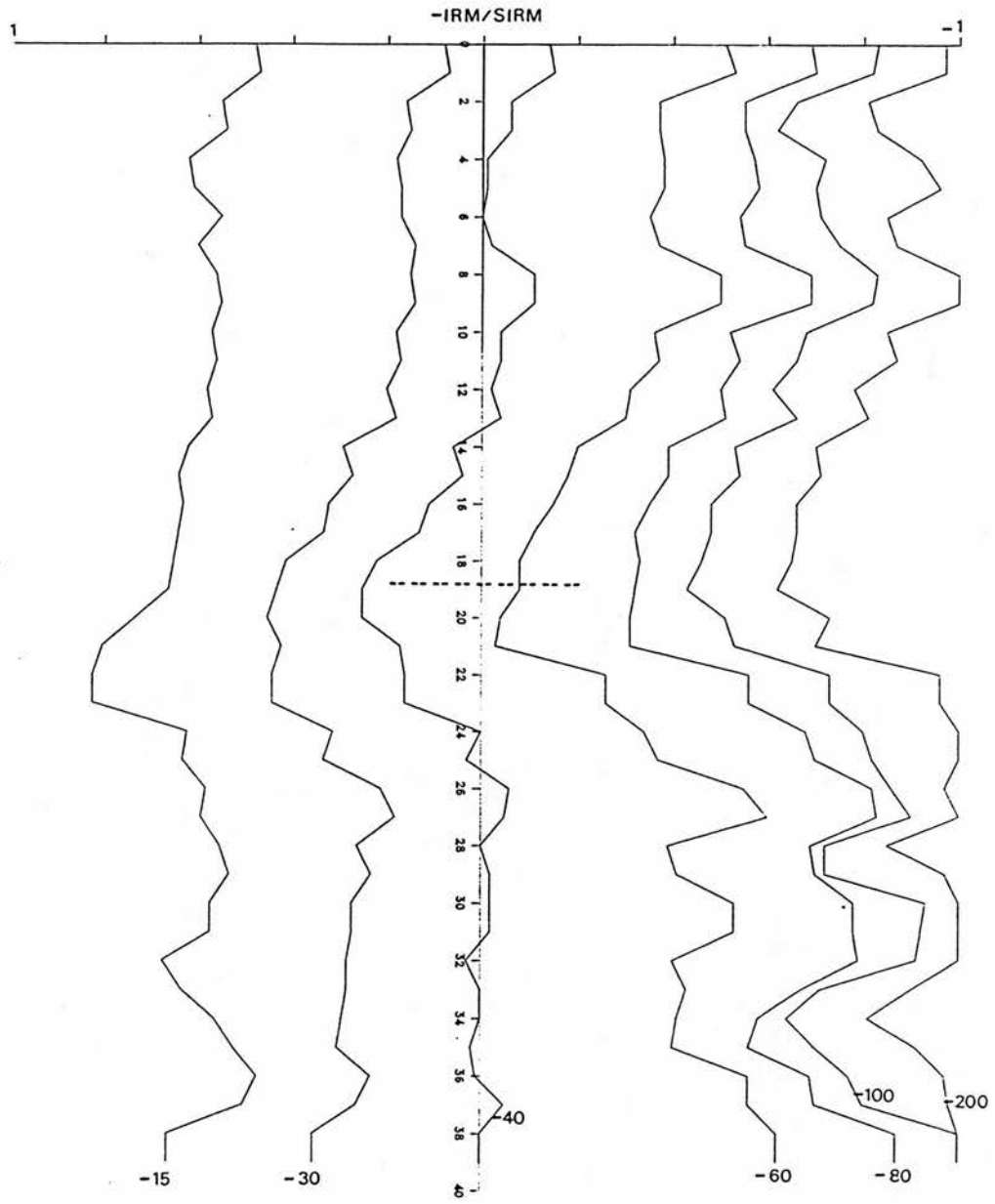

FIG 6/9: Core G5 - downcore variability of SIRM demagnetisation response, determined through the subjection of "saturated" sub-samples to reversed fields of 15mT, 30mT, 40mT, 60mT, 80mT, 100mT and 200mT. The "magnetic take-off" is demarked by the broken line.

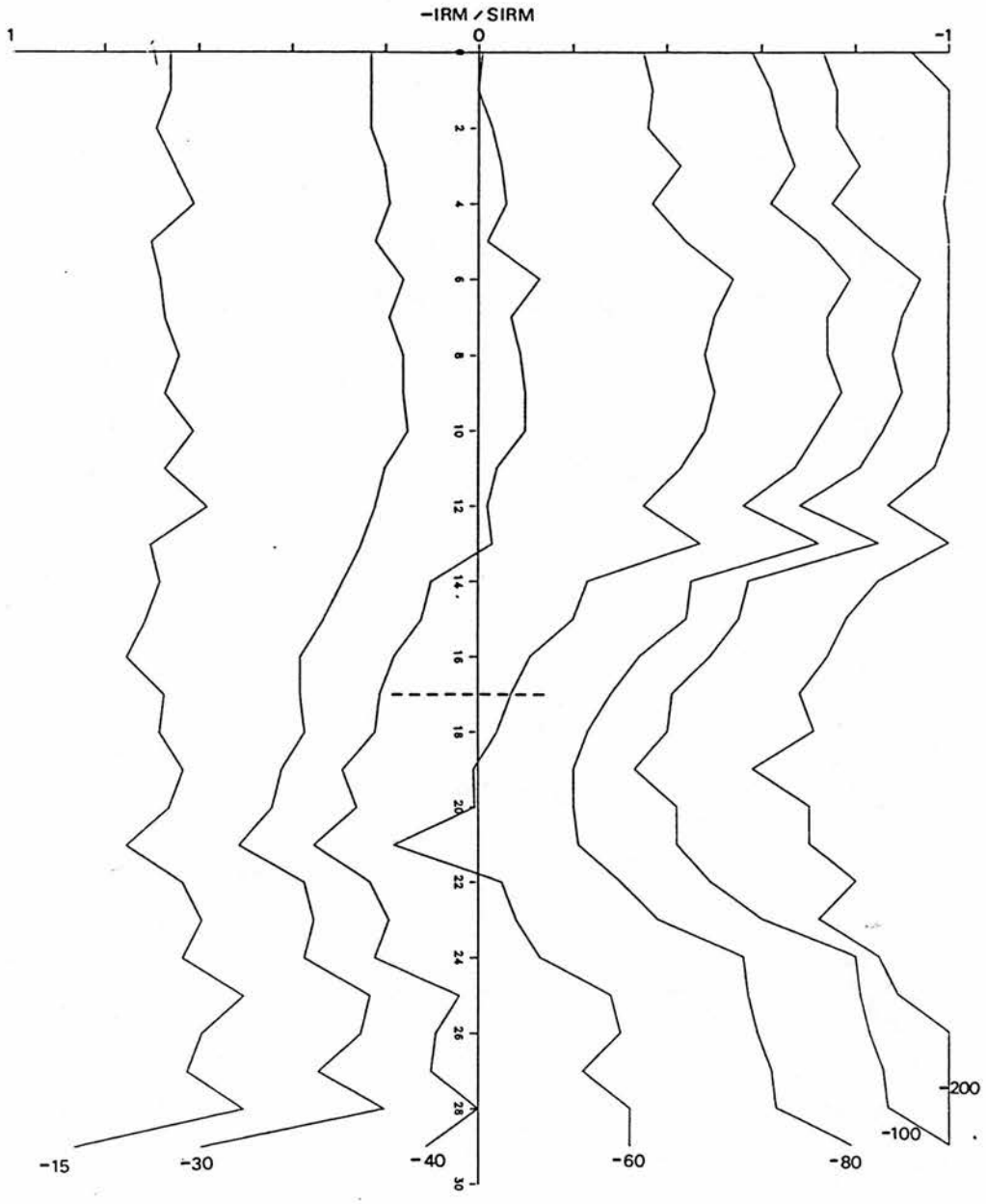

FIG 6/10: Core G6 - downcore variability of SIRM demagnetisation response, determined through the subjection of "saturated" sub-samples to reversed fields of 15mT, 30mT, 40mT, 60mT, 80mT, 100mT and 200mT. The "magnetic take-off" is demarked by the broken line.

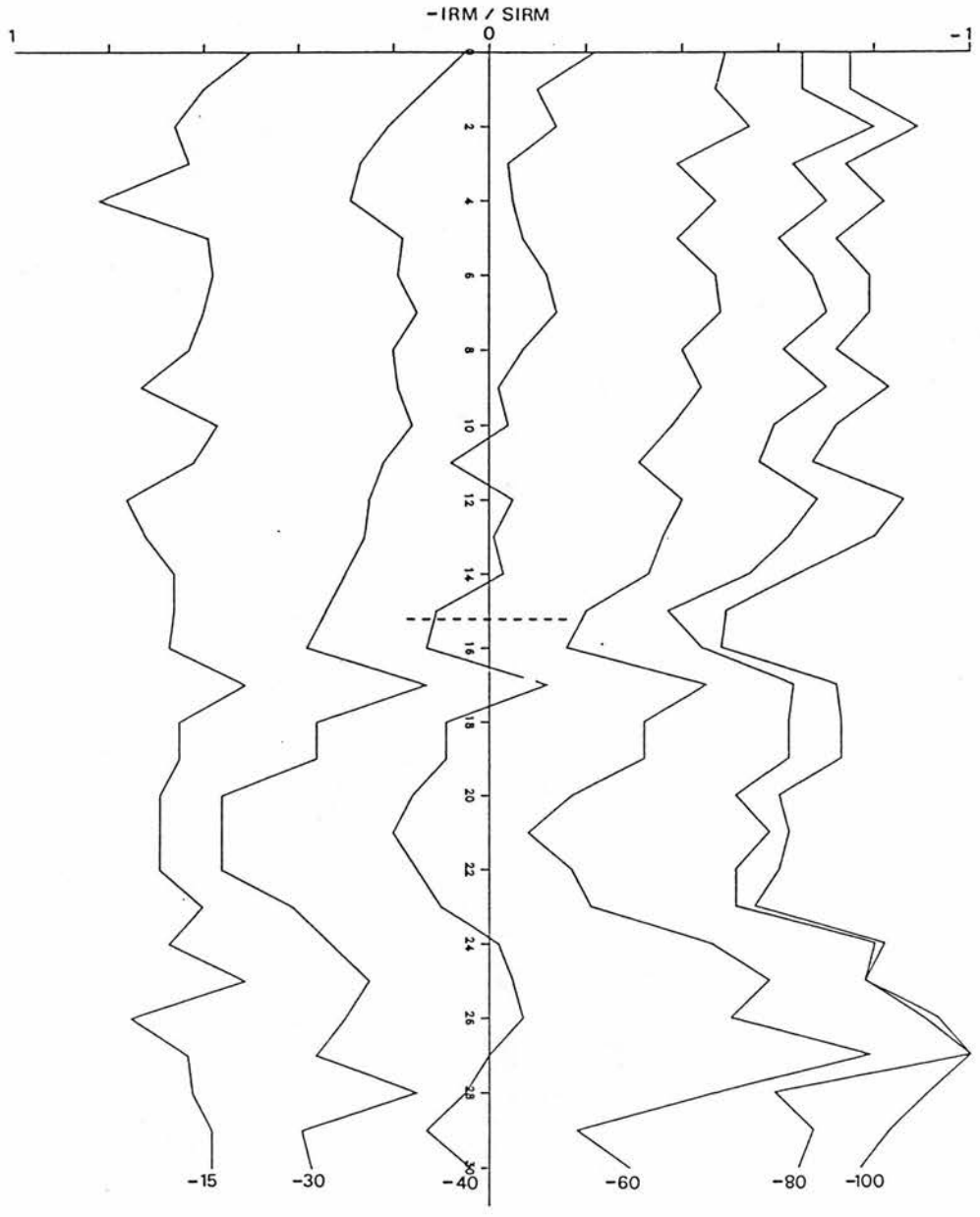

FIG 6/11: Core R1 - downcore variability of SIRM demagnetisation response, determined through the subjection of "saturated" sub-samples to reversed fields of 15mT, 30mT, 40mT, 60mT, 80mT and 100mT. The "magnetic take-off" is demarked by the broken line.

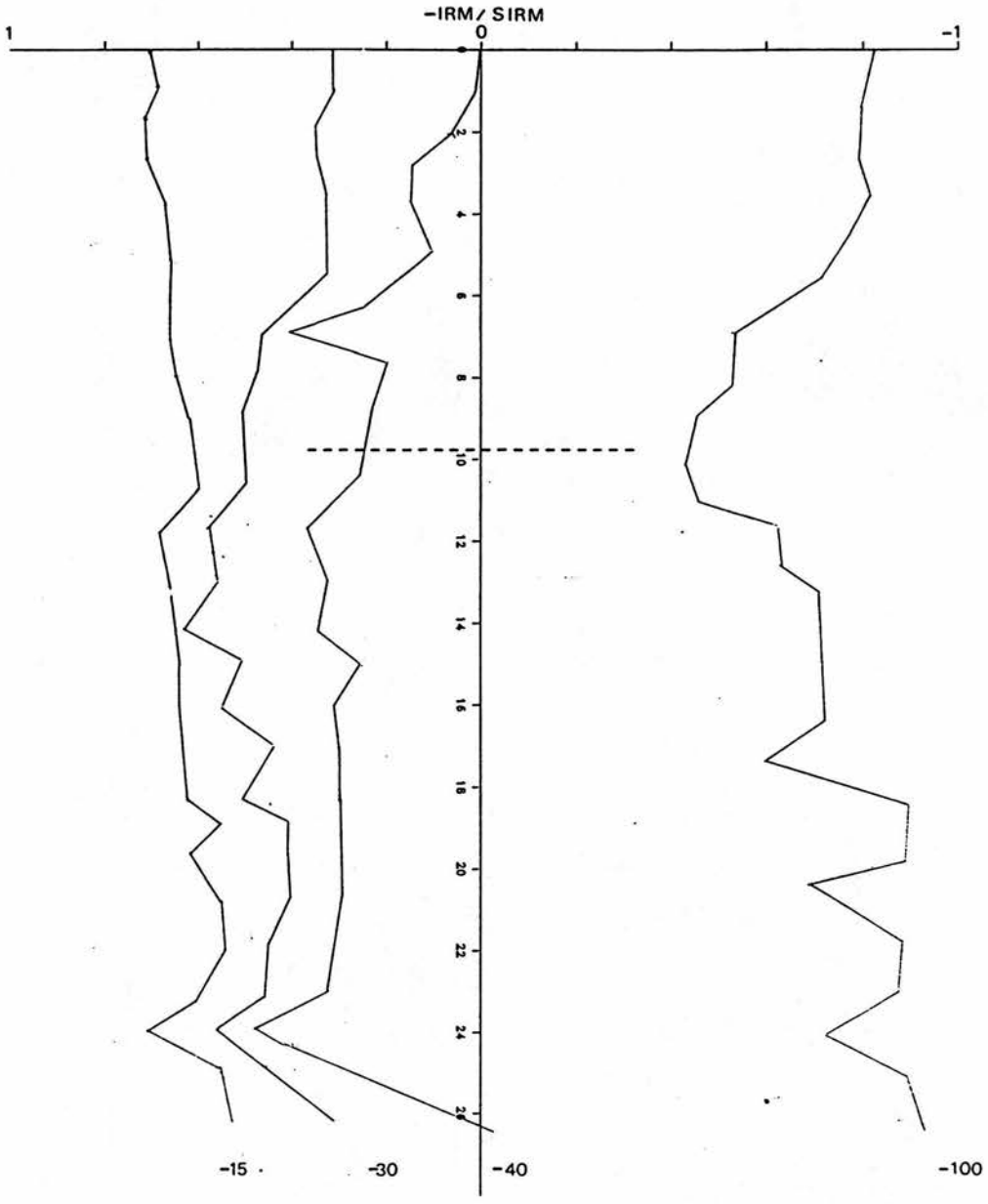

FIG 6/12: Core R2 - Downcore variability of SIRM-demagnetisation response, determined through the subjection of formerly saturated samples to reversed fields of 15mT, 30mT, 40mT and 100mT.

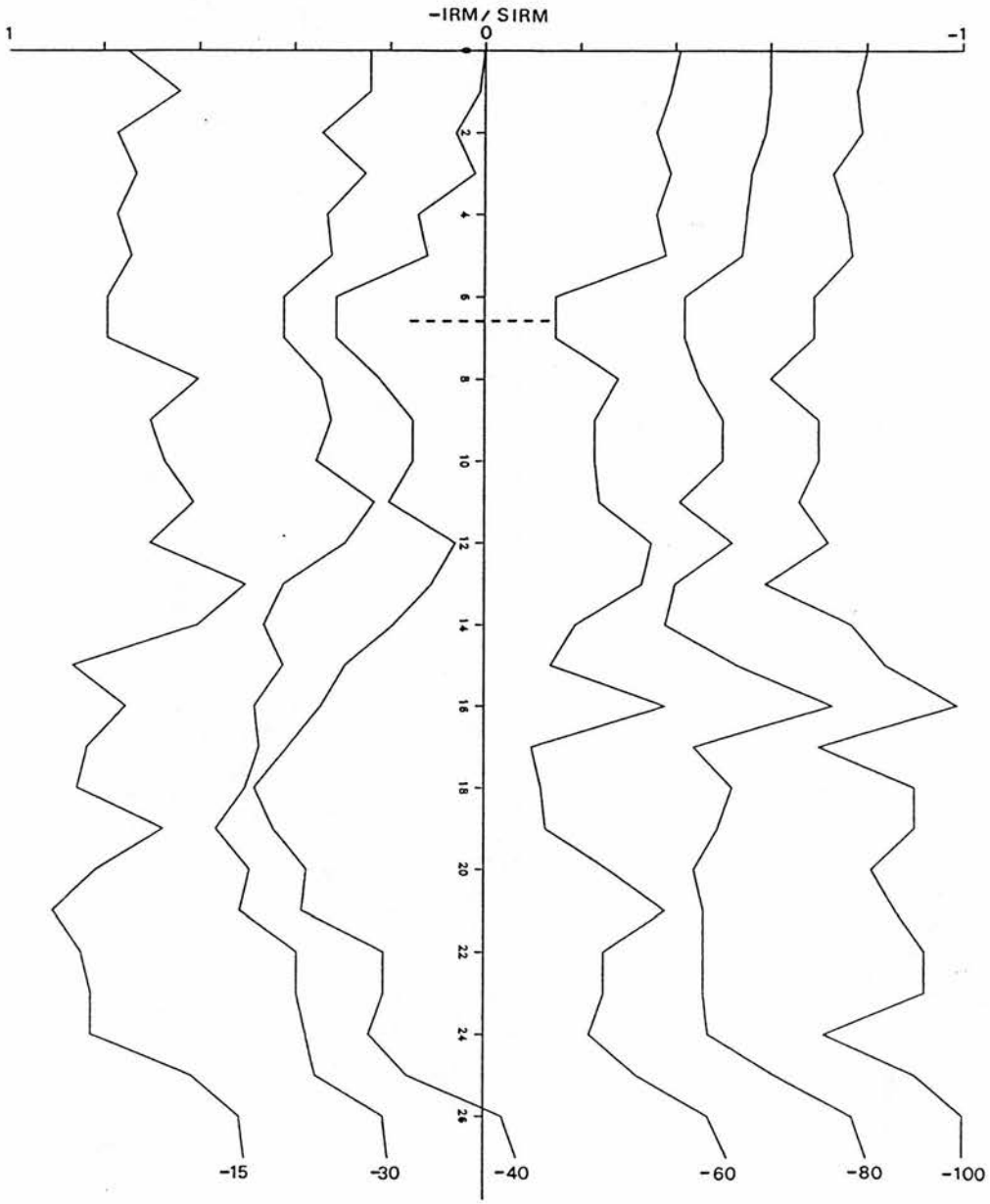

FIG 6/13: Core R3 - downcore variability of SIRM demagnetisation response, determined through the subjection of "saturated" sub-samples to reversed fields of 15mT, 30mT, 40mT, 60mT, 80mT and 100mT. The "magnetic take-off" is demarked by the broken line.

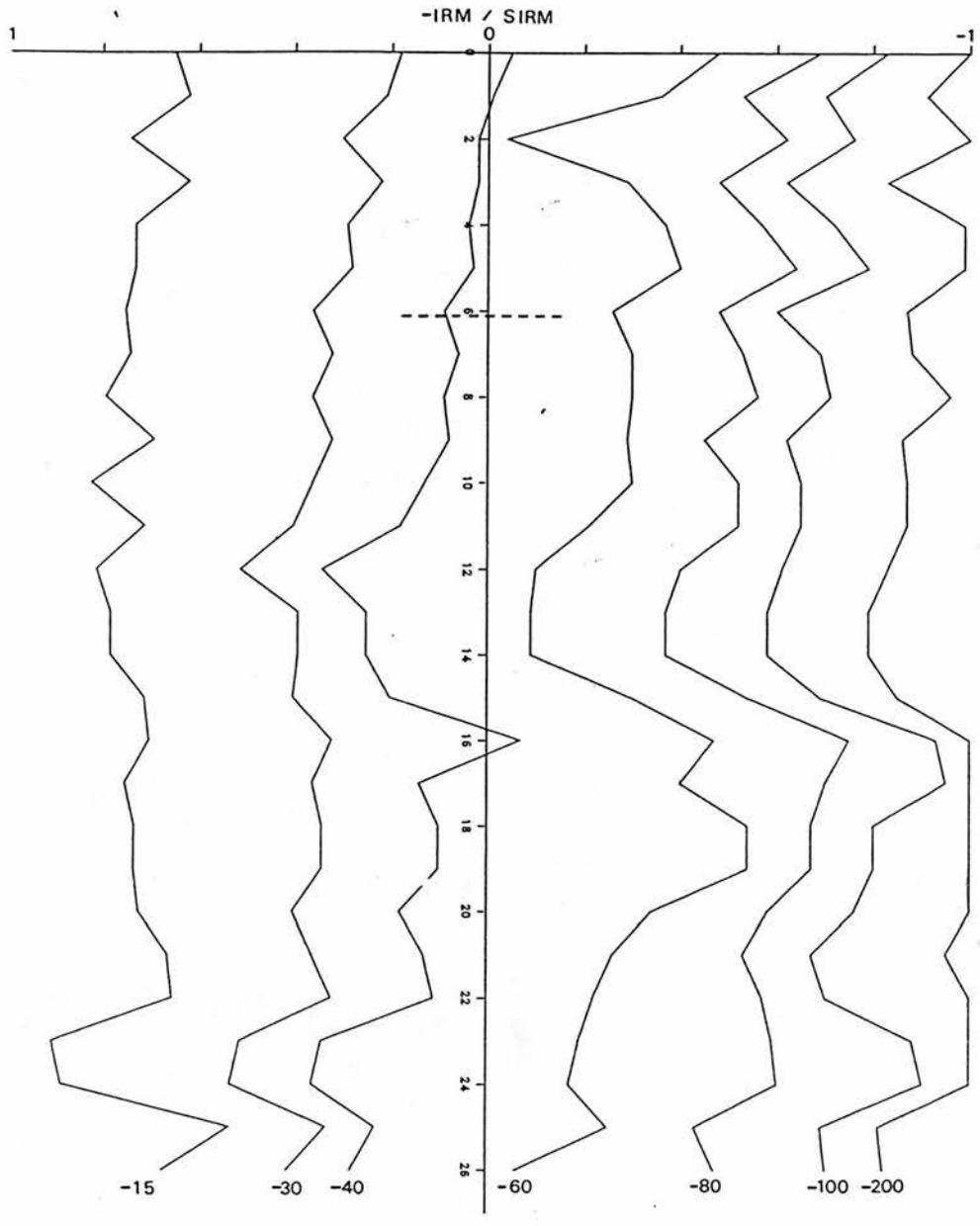

FIG 6/14: Core R4 - downcore variability of SIRM demagnetisation response, determined through the subjection of "saturated" sub-samples to reversed fields of 15mT, 30mT, 40mT, 60mT, 80mT, 100mT and 200mT. The "magnetic take-off" is demarked by the broken line.

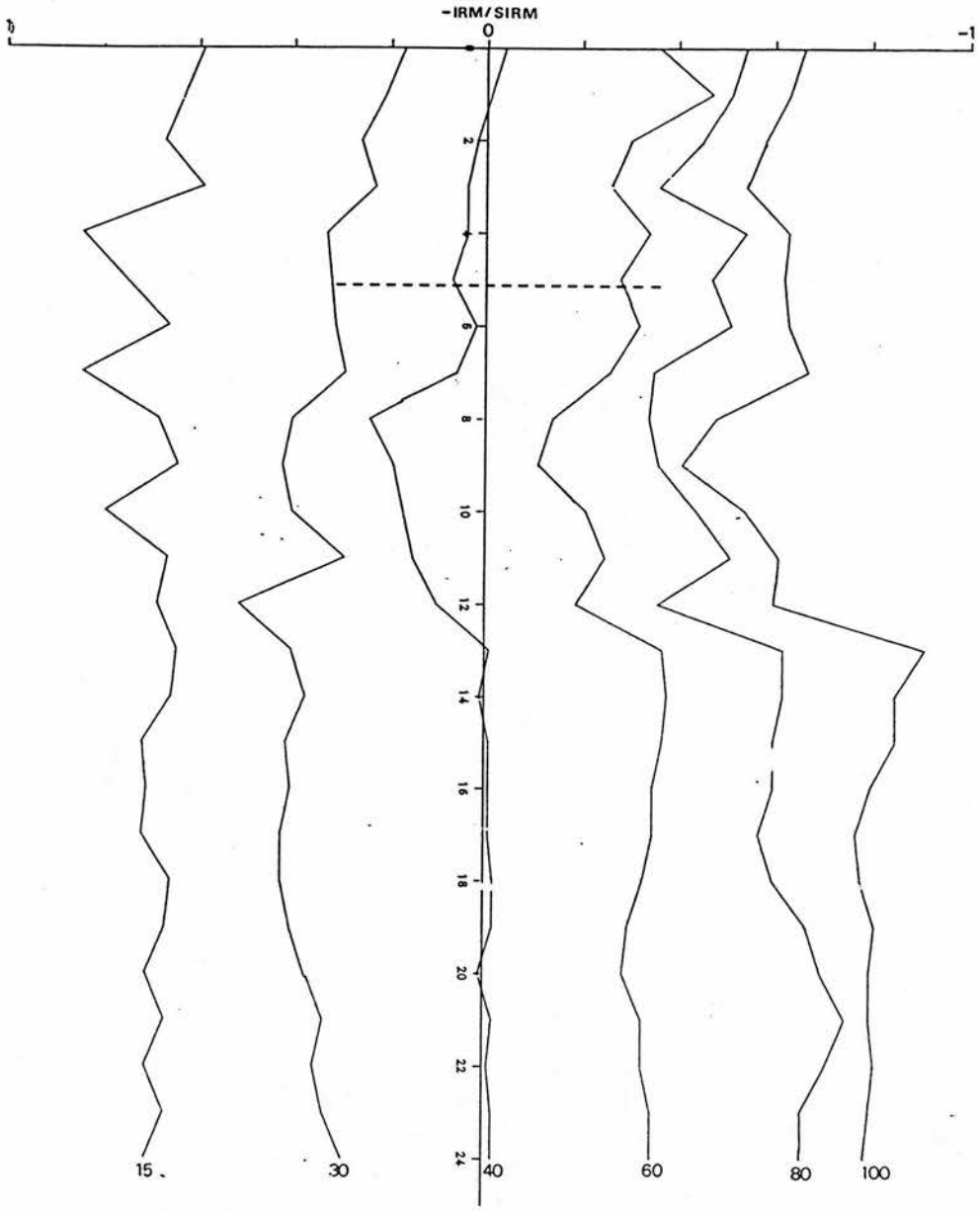

FIG 6/15: Core R5 - Downcore variability of SIRM-demagnetisation response, determined through the subjection of formerly saturated samples to reversed fields of 15mT, 30mT, 40mT, 60mT, 80mT and 100mT. The magnetic take-off is demarked by the borken line.

geochemically distinct granite fragments produce a secondary SIRM anomaly of 0.46mAm2kg-1 at 28cm depth, all SIRM profiles signify the presence of only one magnetically enhanced zone. These trends, coupled with observations of the prevalence of "noise level" SIRM signals (<0.1mAm2kg-1) throughout the 50cm - 200cm sectors of 2m cores from Brishie mire and Beinn Chaorach, confirm that ferrimagnetic enrichment is universally confined to the surficial 10cm - 30cm of peat.

Backfield-IRM profiles for the Galloway and Beinn Chaorach sample cores indicate that recurrent mineralogical or granulometric changes accompany downcore fluctuations of ferrimagnetic mineral concentration at all coring stations. On the basis of the demagnetisation data presented (Figs 6/5 - 6/15), three mineralogically distinct stratigraphic zones can be identified. Specifically:-

1) Sub-samples from the ferrimagnetically enriched, surficial sectors of sample cores consistently undergo over 60% remanence loss upon their subjection to reversed fields of 30mT and display BOCR values within the range 36 - 44mT. Such trends indicate that at least 30% of the magnetic assemblage comprises magnetites within the size range 0.07 - 0.15um. While 35 - 40% SIRM reversal is apparent following the placement of samples in a 60mT demagnetising field, further SIRM reversal is limited upon the subjection of

samples to demagnetising fields of up to 100mT. Consequently, "S" (-100mT IRM/SIRM) values fall within the range 59 - 93, signifying the presence of additional remanence-carrying components which may either be SSD ferrimagnets (<0.05um) or canted-antiferromagnets. Given that the surficial sub-samples from cores G1, G2 and G5 do not exhibit full SIRM reversal upon their subjection to a 200mT demagnetising field, haematite may be considered likely to be influential within this "magnetically hard" fraction (Figs 6/5, 6/6 and 6/9).

2) Sub-samples from strata which demark the transition between the ferrimagnetically enhanced and the weakly magnetic sectors of sample cores (ie. samples from immediately beneath the magnetic take-off) consistently show increased resistence to demagnetisation upon placement in reversed fields of 40mT - 100mT. Such behaviour is particularly conspicuous at 28cm - 40cm depth in core G1 and 18cm - 32cm depth in core G2 where BOCR values rise to over 50mT and less than 80% SIRM reversal occurs upon the subjection of samples to a 200mT demagnetising field (Figs 6/5 - 6/6). In other cores, the BOCR values of samples from this zone are not consistently distinguishable from those of samples from the overlying strata (eg Fig 6/7), but increasingly "hard" demagnetisation behaviour is again apparent with respect to their response to strong demagnetising fields. Most notably, the data presented for core G6 indicate that while samples from the surficial,

ferrimagnetically enriched strata undergo full SIRM reversal in response to placement in a 200mT demagnetising field, samples from immediately beneath the magnetic take-off (14cm - 20cm) undergo only 61 - 90% SIRM reversal (Fig 6/10). Accordingly, it can be deduced that the downcore decline of ferrimagnetic mineral concentrations towards "background" levels is universally accompanied by a shift towards an increasingly SSD magnetite and/or anti-ferromagnetically biased assemblage. However, it must be emphasised that the demagnetisation profiles for cores G3, G4, G5, G6, R1, R2 and R4 show samples from the ferrimagnetically depleted/enhanced transition to be less distinguishable from those of the overlying strata with respect to their behaviour in demagnetising fields of 15mT - 30mT. Consequently, a small MD component appears to remain present throughout the entire peat column at all sampling sites.

3) In all sample cores, the well defined zone in which SSD magnetites or antiferromagnetic phases exert a dis-proportionate influence is underlain by a zone of weakly magnetic in peat which "softer" demagnetisation behaviour prevails. Backfield IRM analyses of the 2m cores, G2M and R2M, indicate that this zone extends to the peat/bedrock interface at the Brishie mire and Beinn Chaorach sites. However, characteristic samples are identifiable downward of 40cm in core G1 (Fig 6/5), 32cm in core G2 (Fig 6/6), 22cm

in core G5 (Fig 6/9), 26cm in core G6 (Fig 6/10), 24cm in core R1 (Fig 6/11) and 16cm in core R4 (Fig 6/14). In all of these instances, samples display BOCR values of only 33 - 43mT and undergo full SIRM reversal in response to demagnetising fields of 100 - 210mT. Anti-ferromagnetic phases must, therefore, be insignificant. Although marked inconsistencies in the demagnetisation behaviour of samples from the basal sectors of cores are apparent, they can be attributed to a high analytical "noise factor", resulting from the measurement of samples which contain inherently low concentrations of remanence-carrying minerals.

In addition to the magneto-stratigraphic zonation of cores which is possible by reference to SIRM-demagnetisation data, discrete downcore changes of ferrimagnetic mineral granulometry are identifiable in cores G1, G2, G3, G4 and R1 through examination of their SIRM/ARM profiles (Fig 6/16). In all instances, these ratios decline progressively with depth, from 60 - 142 within the surficial 5cm to below 10 in strata which underlie the magnetic take-off. Given the bias displayed by ARM measurements towards dispersed, SSD

NOTE: ARM data for cores G1, G2, G3, G4 and R1 were acquired through the use of two AF demagnetisation units. These units generated similar peak AC fields (0.1T), but DC fields varied between 0.04mT and 0.1mT. To improve the comparability of data all ARM values have, therefore, been normalised against the DC field and are expressed in Fig 6/16 as SIRM/ARMX or SIRM/ARM (0.1mT DC).

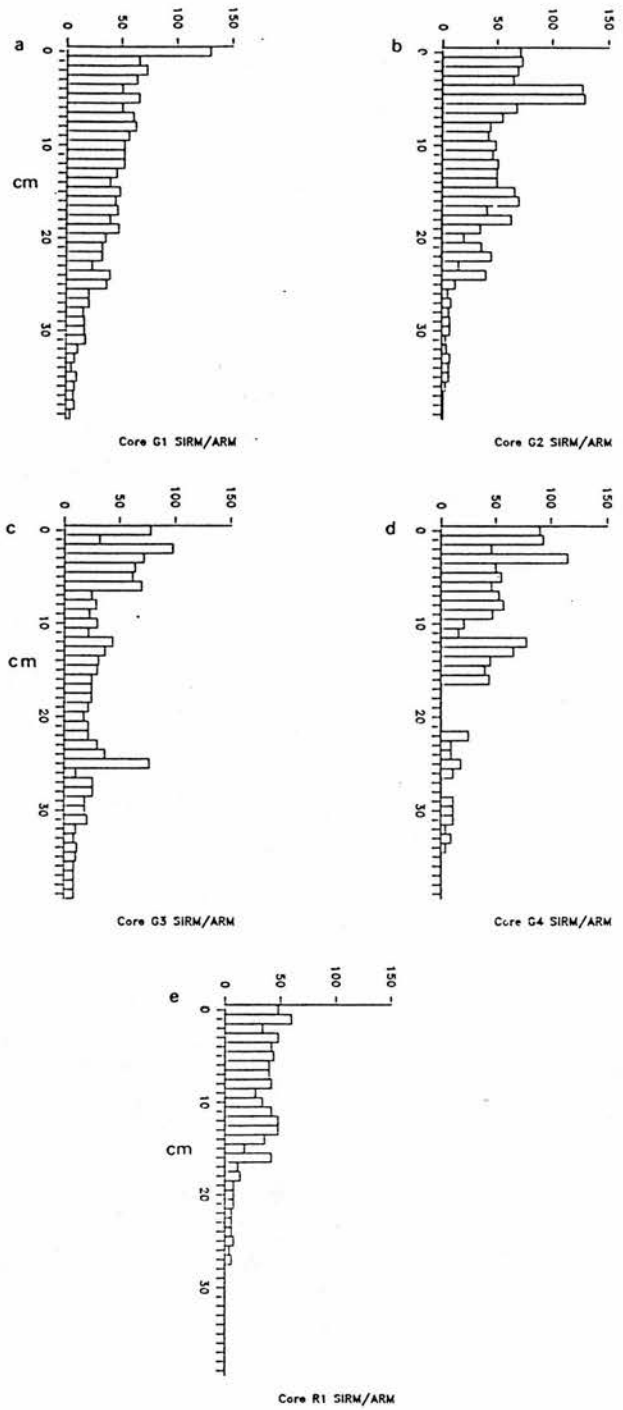

FIG 6/16: SIRM/ARM gradients through cores G1, G2, G3, G4 and R1, normalized against the DC field. For purposes of interpretation, SIRM/ARM can be considered to be directly related to ferrimagnetic grain size.

magnetites, such trends are diagnostic of a persistent downcore refinement of ferrimagnetic assemblages. On the basis of the SIRM/ARM data, it can be deduced that SSD grains of below 0.04μm form a major magnetite component downward of 30cm in core G1, 25cm in core G2, 32cm in core G3, 26cm in core G4 and 20cm in core R1.

6.5.2: Distinctions between cores.

Despite the consistency of downcore trends of ferrimagnetic mineral concentration, mineralogy and granulometry, significant distinctions can be made both between sample cores from different microtopographic facets of individual mire surfaces and between sample cores from the Galloway and Beinn Chaorach field sites.

1) The results presented for adjacent "hummock" and "lawn" cores from Brishie mire (G1 and G2), Craigherron (G3 and G4) and Beinn Chaorach (R1 and R2, R4 and R5) indicate that the depth of the "magnetic-takeoff" is subject to microtopographic control, being persistently greatest in "hummock" cores. For example, the well drained hummock core, G1, exhibits SIRM increments upward of 30cm depth, rising from background levels of around 0.015mAm2/kg-1 to a peak of 2.05mAm2/kg-1 at 15cm depth (Fig 6/3a). In contrast, ferrimagnetic enrichment is confined to the surficial 20cm of the "lawn" core, G2, with SIRM values remaining below

0.2mAm2kg-1 throughout all underlying strata (Fig 6/3b). Cores G5 and G6 were extracted from analogous micro-topographic locations to core G2. Hence they also only display SIRM increments in the uppermost 20cm (Figs 6/3e and f). At Beinn Chaorach, magnetic enhancement appears to occur within closer proximity to the peat surface at all coring stations, but microtopographic distinctions are equally conspicuous. Hence, the well drained "hummock" core, R1, holds enhanced ferrimagnetic mineral concentrations upward of 15cm depth, with peak SIRM values of 0.99mAm2kg-1 occurring at 13cm (Fig 6/3g). In contrast, the "lawn" cores, R2, R3 and R5 display background SIRM values (<0.2mAm2kg-1) downward of only 7cm depth (Figs 6/3h and i, 6/4b).

2) Excepting the paired cores, G1 and G2, the greater depths at which "magnetic take-offs" occur in hummock cores are accompanied by a tendency for cores from these facets to yield higher peak and cumulative SIRM values than their "lawn" counterparts (Table 56). These trends are consistent with the residence of ferrimagnetic minerals within hummock cores at concentrations which exceed those of proximal lawn cores by factors of 0.5 - 2.5.

Table 56: Brishie mire, Craigherron and Beinn Chaorach sample cores: peak and cumulative SIRM values (mAm2kg-1).

Core	G1	G2	G3	G4	G5	G6	R1	R2	R3	R4	R5
Peak	2.0	4.1	1.1	0.8	1.6	2.4	1.0	0.9	0.3	1.2	0.9
Cum	30	44	14	12	16	18	7	5	2	7	3

3) The data presented in Table 56, show the cumulative ferrimagnetic mineral concentrations (as defined by SIRM) in sample cores from Galloway to exceed those of the Beinn Chaorach cores by factors of 1.8 - 6. This trend persists irrespective of microtopography.

6.6: Interpretation of magnetic data.

6.6.1: Origins of magnetic minerals within sample cores.

The data presented above show the Brishie mire, Craigherron and Beinn Chaorach peatlands to be strongly characterised by the ferrimagnetic enhancement (by 2 - 3 orders of magnitude) of strata extending from the peat surface to 5cm - 30cm depth. Such observations are consistent with those of all previous workers who, in turn, have attributed downcore SIRM gradients to temporal variations in the supply of hydrocarbon-derived particulates from the atmosphere (eg. Oldfield et al 1978, 1979, Thompson et al 1980, Jones 1985). In three respects, the magnetic records deciphered from the Galloway and Beinn Chaorach peats confirm that the major source of ferrimagnets to the enriched, surficial strata is anthropogenic.

1) The low peak and cumulative SIRM values for the 5 Beinn Chaorach cores, relative to those for the 6 Galloway cores are concordant with the differing loadings of

atmophilic elements to the respective sites (section 5.7.2) and with the greater remoteness of Beinn Chaorach from major industrial complexes. Furthermore, by placing the peak and cumulative SIRM data for cores from Brishie mire, Craigherron and Beinn Chaorach alongside comparable data for cores from Ringinglow (Derbyshire), Loch Chon (Stirlingshire), Glen Muich (Aberdeenshire), Glen Quoich (Invernesshire) and Loch Cluanie (Invernesshire), a "distance-decay" pattern, analogous to that described by Thompson et al (1980) emerges (Table 57). Hence, while the

Table 57: Peak and cumulative SIRM values (mAm2kg-1) of peat cores from selected UK locations.

Core/Location	Cum SIRM	Peak SIRM
Ringinglow	46	9
G2. Brishie mire	44	4
G1. Brishie mire	30	2
Loch Chon	21	3
G3. Craigherron	14	1
G4. Craigherron	12	0.8
R1. Beinn Chaorach	7	1
M1. Glen Muich	6	1
R2. Beinn Chaorach	5	0.9
M2. Glen Muich	3	0.9
GQ. Glen Quoich	2	0.26
CL1. Loch Cluanie	2	0.18
CL2. Loch Cluanie	1	0.11

Ringinglow core yields the highest SIRM value (9mAm2kg-1) in accordance with the sites proximity to the S.Pennine industrial areas, cumulative SIRM values decline progressively northwards through south-west and central

Scotland. Lowest values prevail at the remote Aberdeenshire and Invernesshire sites, where peak and cumulative SIRMs are an order of magnitude lower than those for the Ringinglow, Brishie mire and Loch Chon cores. On the basis of this evidence it is, therefore, impossible to dispute the validity of previous claims that the magnetite concentrations of surficial peats are inversely related to the proximity of industrial pollutant sources (Thompson et al 1980, Oldfield et al 1984).

2) The predominantly anthropogenic origin of the magnetite-bearing particulates in the surficial levels of the Galloway and Beinn Chaorach peatlands is strongly signified by the chronology of downcore SIRM variations in the dated cores, G1, G2, R1 and R2 (see section 5.6.6 for the derivation of dates). In all instances, SIRM values rise above "background" levels only within strata which have accumulated since 1840 (Fig 6/3). Hence, SIRM increments show some synchroneity with the onset of increased fossil fuel combustion throughout Europe (see Fig 4/15b). By normalising the SIRM gradients of cores G1, G2 and R2 against downcore variations of mass accumulation, it is also possible to ascertain that mean annual magnetite influxes to Brishie mire and Beinn Chaorach increased progressively, from below 3mAm/m2/yr-1 prior to 1840, to over 24mAm/m2/yr-1 during the post-war period (Table 58). In interpreting these changes, it is acknowledged that the accumulation rate data

Table 58: Mean annual influxes of Fe3O4 to coring stations G1, G2 and R1, as defined by SIRM intensities.

Period and depth	FDW	WD	AR	Mean SIRM	Mean Fe3O4 flux (mAm/m2/yr-1)
			CORE G1		
1962-PD 1cm-11cm	0.03	0.4	0.3	0.668	24.0
1908-1961 12cm-20cm	0.03	0.15	0.38	1.360	23.2
1841-1907 21cm-30cm	0.03	0.12	0.38	0.976	13.3
PRE-1841 31cm-40cm	0.04	0.16	0.38	0.11	2.67
			CORE G2		
1962-PD 1cm-7cm	0.03	0.18	0.28	2.030	30.8
1895-1961 8cm-20cm	0.03	0.24	0.20	2.560	36.8
1841-1894 21cm-30cm	0.04	0.26	0.20	0.110	2.2
PRE-1840 31cm-40cm	0.05	0.26	0.20	0.040	1.04
			CORE R2		
1974-PD 1cm-3cm	0.02	0.64	0.21	0.494	32.4
1923-1973 4cm-7cm	0.03	0.08	0.09	0.784	15.8
1890-1922 8cm-11cm	0.04	0.17	0.09	0.065	1.65
1840-1889 9cm-15cm	0.06	0.86	0.09	0.025	1.16
PRE-1840 16cm-20cm	0.07	0.84	0.09	0.020	1.05

upon which flux calculations have been based are crude on account of the poor resolution of palynological and radiometric dates. However, the general trends of rapidly increasing magnetite deposition throughout the 1900 - 1960 period are closely consistent with the temporal flux records derived from the polluted sediments of Loch Dee (Table 37). Given the proximity of the Brishie mire site to Loch Dee, it is logical to assume that the analogous patterns of ferrimagnetic enrichment in the post-industrial strata at both sites reflect similar, anthropogenic influences.

3) SEM analyses of magnetic extracts from the 1cm, 4cm and 11cm levels of core G1, 1cm and 10cm levels of core G6 and the 1cm sub-sample from core R1 have illuminated the presence of spherical particulates (see Fig 6/21). The surface morphology of these spherules is variable, but all bear analogy to the hydrocarbon-derived particulates described by Raask et al (1981), Lauf (1984) and Hart (1981). Ferrimagnetic spherules have no natural terrestrial mode of origin (Riley and Chester 1971) and consequently, can be considered diagnostic of the presence of anthropogenic pollutants.

With respect to the extent to which the optically identifiable spherules control the magnetic signatures of sample cores, the inherent mineralogical characteristics of pristine fly ash samples are particularly significant.

Whitby and Cantrell (1975) have proposed a scheme whereby FeS - FeO transformations during hydrocarbon combustion exclusively produce spinel phases of MD grain size. In turn, Simons (1960) and Raask (1980) have observed the additional formation of Fe2O3 during hydrocarbon combustion, with Fe2O3/Fe3O4 ratios varying in accordance with the thermal regime and the partitioning of Fe between silicates, sulphides, sulphates, carbonates and oxides in the coal feed. Magnetic qualification of the presence of both MD magnetites and haematite phases within fly ash samples has been attained by Puffer (1980), Hansen et al (1981) and Hunt et al (1984). In the latter case, ash samples of below 1.1μm size from Hams Hall thermal plant have been shown to exhibit SIRM/ARMx ratios of 169, BOCR values of 42mT and S values of 52 - 66. Analogous data have also been acquired during the present study through magnetic analyses of graded fly ash samples from Ratcliffe thermal plant, which yielded SIRM/ARMx ratios up to 170, BOCR values of 36 - 42mT and S values of 62 - 76.

On comparing the magnetic characteristics of samples from the surficial 5cm of cores G1, G2, G3 and G4 with those of the fly ash samples described above, the affinities are striking. Notably, the peat samples yield BOCR values which fall within the 36 - 42mT range established for fly ash, while SIRM/ARMx ratios of over 100 and S values of 59 - 80 signify the predominance of MD magnetites alongside additional magnetically "hard" (ie. haematite) components.

In combination, conventional magnetic data and SEM analyses of magnetic extracts from surficial Galloway and Beinn Chaorach peats show, beyond doubt, that the deposition of hydrocarbon-derived particulates constitutes the principal cause of magnetic enhancement.

6.6.2 Persistence of magnetic oxides in the Brishie mire, Craigherron and Beinn Chaorach peatlands.

Previous mineral magnetic studies of ombrotrophic peats have been characterised by a universal acceptance of the post-depositional stability of the principal hydrocarbon-derived magnetic oxide, Fe3O4 (eg. Oldfield et al 1978, 1984, Thompson et al 1980, Jones 1986). Through the adoption of this assumption, strata demarking the "magnetic take-off have been interpreted as being temporally synchronous (Oldfield et al 1981, 1984), providing a datable horizon corresponding to the onset of accelerated fossil fuel consumption at around 1850 (Renberg 1985).

However, upon examining the "concentration dependent" magnetic data for the dated "hummock" cores G1 and R1, along with their "lawn" counterparts, G2 and R2, formerly held conceptions of the post depositional stability of Fe3O4 appear tenuous. Specifically, initial SIRM increments are not synchronous, but occur in strata which accumulated at around 150yrs BP in the "hummock" cores (Figs 6/3a and g)

and are confined to more recent levels in adjacent "lawn" cores. In core G2, SIRM values fall to background levels (<0.05mAm2Kg1)at 20cm depth, while strata which have accumulated since 150yrs BP extend to 30cm (Fig 6/3b). In core R2, the magnetic take-off is identifiable at 10cm depth, within strata which have been assigned a 210Pb age of less than 97yrs (Fig 6/3h). As a consequence of such discordance, the temporal Fe3O4 flux data acquired for stations G1 and G2 also differ unrealistically (Table 58). For example, by normalising the SIRM gradient for core G1 against downcore variations of mass accumulation, a flux estimate of 13.3mAm/m2/yr-1 has been derived for the 1841 - 1907 period. Similar normalisation of the SIRM gradient at station G2 yields a flux value of only 2.2mAm/m2/yr-1 for the period 1841 - 1894.

Such poor synchroneity between the SIRM profiles of adjacent "hummock" and "lawn" cores clearly signifies the diagenetic alteration of the magnetic mineral deposition record in the Brishie mire and Beinn Chaorach peatlands. This alteration is most extensive in the "lawn" cores, G2 and R2, entailing the complete removal of the magnetite phases deposited during the early post-industrial period. In the "hummock" cores, G1 and R1, alteration of the magnetic record is less severe, with some degree of ferrimagnetic enhancement characterising the entire post-industrial sequence.

Given the close correlation between the extent of inundation and the inclination of the downcore eH gradients at all Brishie mire, Craigherron and Beinn Chaorach coring stations (see section 5.9.2), magnetic distinctions between adjacent "hummock" and "pool" cores appear to be explicable by reference to the following hypotheses:-

1) The post-industrial stratigraphic sequences at the inundated coring stations, G2 and R2, extend into zones of severe anoxia, thus facilitating the dissolution of Fe3O4. While pH conditions are acknowledged to constitute a process control, thermodynamic data provided by Lindsay (1979) suggest that eH values must fall below -200mV within these dissolutionary zones.

2) On account of the more gentle downcore redox gradients prevailing in the "hummock" cores, G1 and R1 (Figs 5/26 - 27), conditions which are conducive to extensive Fe3O4 dissolution are confined to deeply buried strata which exceed 150 years age. These strata would have received only "background" fluxes of Fe3O4 from the atmosphere and consequently, any diagenetic alteration of their mineral assemblages is not magnetically conspicuous.

In summary, it is proposed that, in all but the most aerated facets of the Galloway and Beinn Chaorach peat systems, the "magnetic take-off" does not signify the point

during the accumulation of the peat at which anthropogenic magnetite fluxes first increased. Instead, it is considered likely that the lowermost stratigraphic location of ferrimagnetic enrichment depicts a geochemical boundary within the peat column, below which eH/pH conditions far exceed the thermodynamic stability field of Fe3O4, thus promoting dissolution.

To test the above hypothesis, it is necessary to examine the synchroneity of SIRM and eH variations within sample cores. Because only limited Pt electrode data are available, such examination has been carried out on cores from Galloway (G1, G2, G3, G4 and G6) and Beinn Chaorach (R1, R2 and R5), along with additional cores from Glen Muich and Glen Quoich, by utilizing the downcore profiles of redox-sensitive geochemical parameters. Ratios of Cu/Zn and Fe/Mn are ideal for this purpose (Mackereth 1965, 1966, Gorham and Swain 1965, Mortimer 1971, Digerfeldt 1975, Renberg 1976, Bengtsson 1979, Hirons and Thompson 1986) and are interpretable in the following manner:-

Surficial, oxic levels of the peat column are characterised by the residence of immobile Fe^{3+} and Mn^{4+} phases. Hence, these strata yield Fe/Mn ratios which are analogous to those of the allogenic flux (10 - 100). Cu and Zn also display limited mobility under oxic conditions and, in unpolluted environments, yield minimal Cu/Zn ratios. In instances where Cu/Zn ratios are not minimised at the peat

surface, distortions resulting from the deposition of Cu enriched pollutants are usually responsible. In these cases, the "natural", eH-mediated ratio can be assumed to approximate the minimum "whole core" value.

As eH values are depressed to below 50mV, Mn is subject to increased mobilization, leading to the progressive downcore enhancement of Fe/Mn ratios to a point where high Fe concentrations co-exist with "background" Mn concentrations. At the stratigraphic transition between the sub-oxic and the severely reducing levels (<-300mV) of the peat column, Fe/Mn ratios rise sharply to values of 1000 - 3000 on account of the precipitation of Fe3+ from the underlying strata (see section 5.9.2). Consequently, this transition is typically demarked by a major Fe/Mn anomaly. Similar anomalies occur within the Cu/Zn profile at the sub-oxic/strongly anoxic boundary on account of the reductive mobilization of Zn in conjunction with the precipitation of CuS. However, because Zn reduction requires lower eH values than does Mn reduction and CuS precipitates slightly further downcore than Fe3+ oxides, major Cu/Zn adjustments generally underlie the Fe/Mn peak.

In the deeply buried anoxic strata, Fe, Mn, Zn and Cu are all subject to depletion. Accordingly, Fe/Mn and Cu/Zn ratios undergo a progressive downward decline.

On examining Figs 6/17 - 6/20, in which SIRM profiles are plotted alongside Cu/Zn and Fe/Mn profiles for 11 sample cores, the persistence of magnetic - geochemical linkages is striking. In cores G1, G2, G6, R1, Muich, GQL and GQH, the depression of SIRM values towards background ($<0.05 mAm^2 kg^{-1}$) levels is fully coincident with the enhancement of Fe/Mn ratios by 2 - 3 orders of magnitude. These trends are, therefore, diagostic of the dissolution of ferrimagnetic phases upon their translocation into strata which are characterised by the prevalence of eH values of below -300mV (see footnote).

It is particularly notable that the inclination of SIRM and Fe/Mn gradients is co-variable. For example, sharp increments to Fe/Mn ratios between 29cm - 33cm in core G1, 18cm - 22cm in core G2, 13cm - 15cm in core R1, 7cm - 8cm in core GQL and 16cm - 17cm in core GQH coincide with the acute downcore depression of SIRM values. In contrast, the more progressive downward enhancement of Fe/Mn ratios in core G6 (from 350 at 14cm to around 1700 at 22cm) is accompanied by a more gradual downcore reduction of SIRM values. These trends indicate that Fe3O4 phases are subject to slow, progressive dissolution upon burial at coring station G6 as they are translocated through a

NOTE: Geochemical and direct pT electrode data for cores G1, G6, R1, R2 and R5 suggest that when Fe/Mn ratios exceed 1000, eH values are depressed to below -300mV.

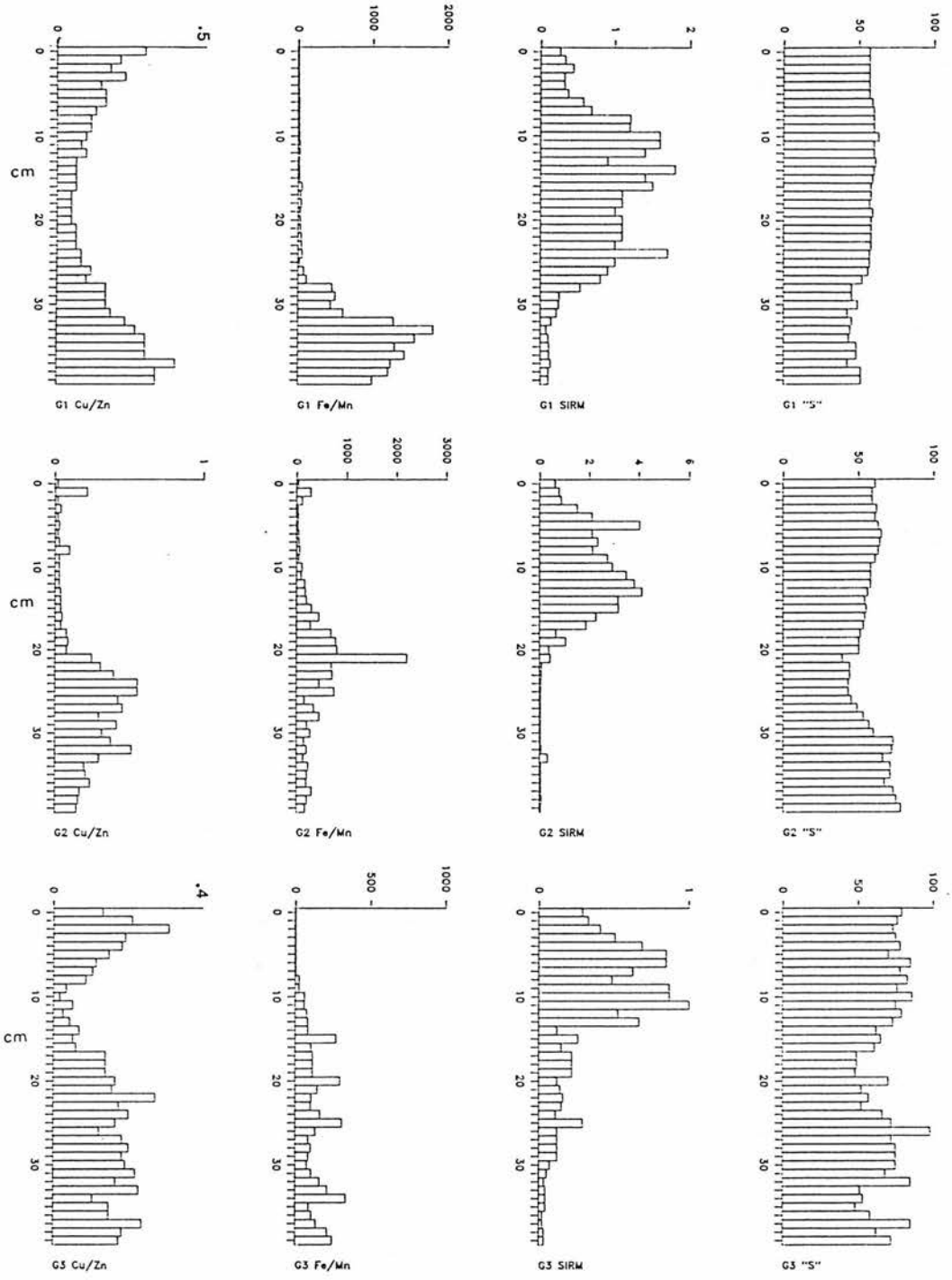

FIG 6/17: Relationships of the redox-sensitive geochemical parameters Fe/Mn and Cu/Zn with the magnetic parameters SIRM and S through cores G1, G2 and G3. SIRM data are expressed in mAm2/kg-1

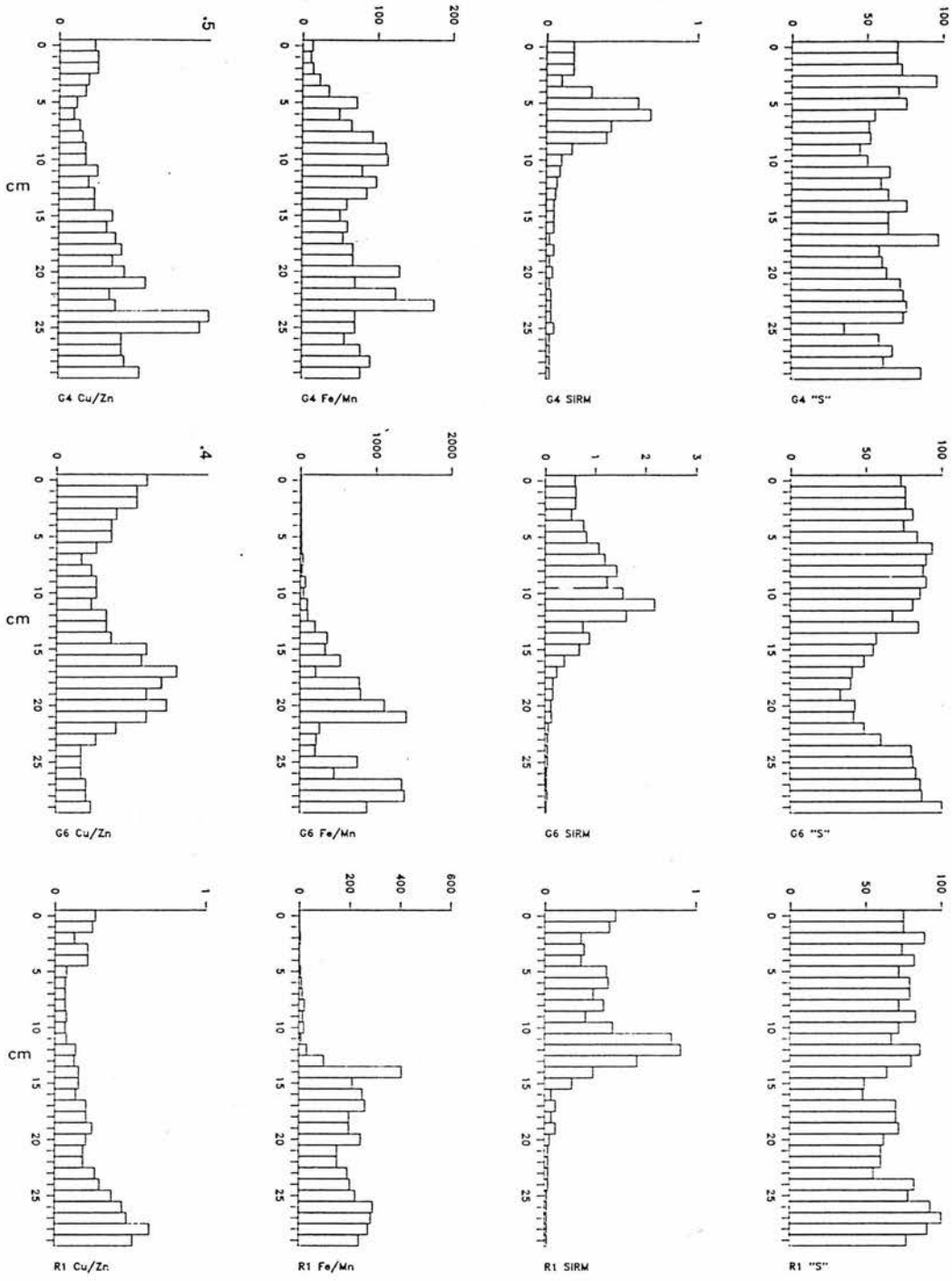

FIG 6/18: Relationships of the redox-sensitive geochemical parameters Fe/Mn and Cu/Zn with the magnetic parameters SIRM and S through cores G4, G6 and R1. SIRM data are expressed in mAm2 Kg-1.

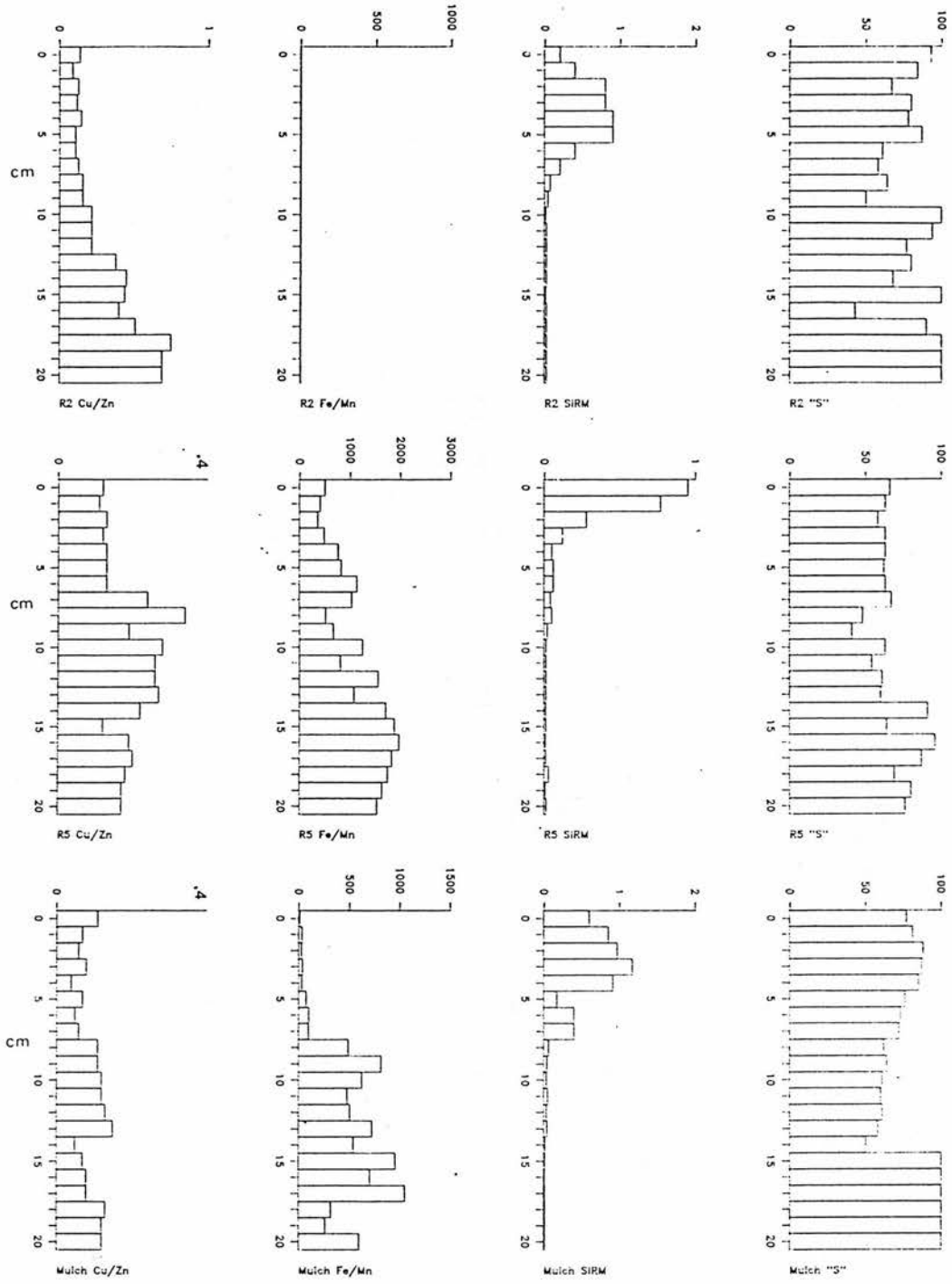

FIG 6/19: Relationships of the redox sensitive geochemical parameters Fe/Mn and Cu/Zn with the magnetic parameters SIRM and S through cores R2, R5 and Muich. SIRM data are expressed in mAm2kg-1.

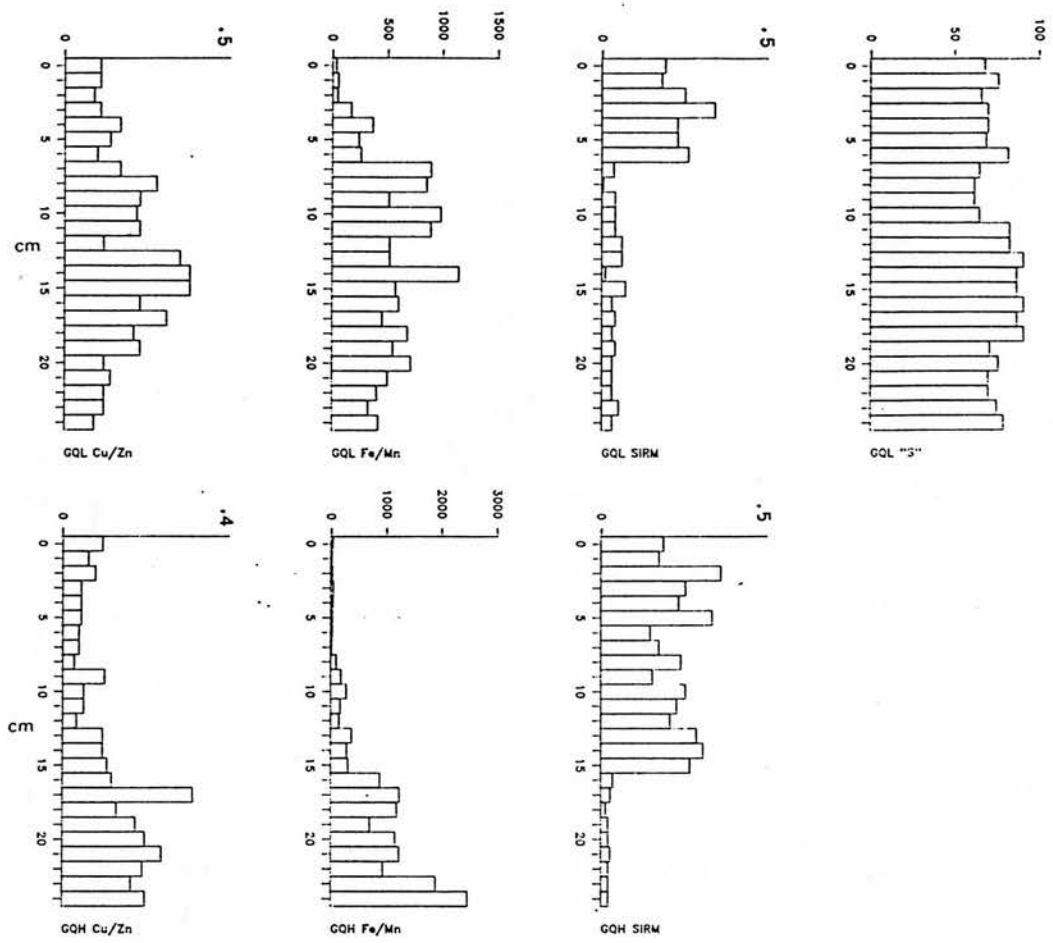

FIG 6/20: Relationships of the redox sensitive geochemical parameters Fe/Mn and Cu/Zn with the magnetic parameters SIRM and S through cores GQL and GQH (from Glenquoich). SIRM data are expressed in mAm2kg-1.

stratigraphically extensive zone in which eH/pH conditions only marginally exceed the Fe3O4 stability field. In turn, it is apparent that Fe3O4-bearing particulates undergo rapid dissolution in cores G1, G2, R1, GQL and GQH, following their translocation beneath a more sharply defined stability threshold.

Of the sample cores for which data are presented, G3 and R5 display the least clear relationships between SIRM and Fe/Mn. However, G3 is also distinctive in that Fe/Mn ratios remain below 400 throughout. Data for the previously discussed cores suggest that rapid Fe3O4 dissolution is associated with the prevalence of Fe/Mn ratios in excess of 1000. Consequently, limited magnetite persistence (SIRM > 0.1mAm2kg-1) occurs throughout most of core G3. With respect to core R5, it is noticable that Fe/Mn ratios are unusually high at the peat surface (>500). In turn, R5 is the only core which exhibits maximum SIRM values at the surface, with ferrimagnetic mineral concentrations declining rapidly with depth. Given these anomalous characteristics, it is likely that conditions are periodically sufficient for Fe3O4 dissolution throughout the core and hence, the major Fe/Mn adjustment which typically demarks the onset of dissolution is absent.

Cu/Zn ratios show less consistent inverse relationships with SIRM on account of the occurrence of Cu/Zn maxima

below the stratigraphic levels at which Fe3O4 displays initial instability. However, in instances where the transition between sub-oxic and strongly anoxic (eH < -300mV) conditions is well defined, linkages of the nature described for Fe/Mn are identifiable. Examples are provided by cores G1, G2, G3, R5, Muich, GQL and GQH, in which "magnetic take-offs" are coincident with the depression of Cu/Zn ratios by between 80% - 600%.

6.6.3: Mechanisms of Fe3O4 dissolution.

The most recently developed model relating to magnetite dissolution is that of Canfield and Berner (1987), who found the following rate law to be applicable to Long Island shelf and Mississippi delta sediments:-

$$\frac{dCmag}{dt} = -1.1 \times 10^{5} \, Cs^{0.5} \, Cmag \, Amag$$

where Cmag = the magnetite concentration, Cs = the concentration of dissolved sulphide and Amag = the magnetite surface area. This model intimates that for a given Fe3O4 and dissolved H2S concentration, dissolution is most rapid for assemblages of SP grains, followed by SSD grains and finally PSD/MD grains, with Fe3O4 "half-lives" ranging between 50 - 1000yrs.

Magnetic data derived from hemipelagic Oregon shelf

sediments (Karlin 1984), California gulf sediments (Karlin and Levi 1983, 1985) and gleyed soils (Maher 1984) also indicate the operation of granulometrically biased dissolution processes. In these instances, the downcore depression of quadrature susceptibility, rapid losses of ARM relative to IRM and decreasing MDF values have all been considered to signify a progressive coarsening of ferrimagnetic assemblages in anoxic systems.

However, Figs 6/17 - 6/20 show reductive Fe3O4 dissolution within the Galloway, Beinn Chaorach, Glen Muich and Glen Quoich peats (highlighted by 2 - 3 order increments to Fe/Mn with concomitant losses of SIRM) to be coincident with the depression of "S" ratios (IRM-100mt/SIRM). Assuming that "S" variations reflect magnetite grain size rather than varying haematite presence (Jones 1985), initial Fe3O4 diagenesis is, therefore, associated with ferrimagnetic refinement within these environments.

The discordance between the downcore "S" profiles presented in Figs 6/17 - 6/20 and conventional models of granulometrically biased Fe3O4 dissolution (Canfield and Berner 1987, Maher 1984) is explicable by reference to Karlins (1984) observations of dissolutionary activity in the California gulf basin. In these sediments, downcore increments to SIRM/ARM and MDF values, signifying the discriminatory dissolution of SSD magnetites, occur only

within strata which hold diverse assemblages of SSD and PSD/MD grains. In strata which only contain PSD/MD magnetites, dissolution operates preferentially at points of maximum structural weakness across the mineral surfaces. Consequently, MD crystals undergo progressive fragmentation and hence, tend to display magnetic properties which analogue SSD ferrimagnets. Under such circumstances, SIRM/ARM ratios become depressed and remanent stabilities increase. This latter set of conditions is closely analogous to those prevailing in the surficial levels of the Galloway and Beinn Chaorach peats, where SIRM/ARM ratios of over 60 - 150 indicate a dearth of detrital or secondary SP/SSD magnetites and the predominance of anthropogenic MD grains. Without disputing the validity of the Canfield and Berner model, a persistent, synchronous refinement of signal-carrying grains and loss of SIRM can, therefore, be reconciled with Fe3O4 dissolution in ombrotrophic peat cores.

Unfortunately, the SEM methods used by Karlin and Levi (1985) to confirm the fragmentation of large, MD magnetites during their dissolution (with the concomitant production of SSD-like assemblages) are not ideal for characterising Fe3O4 transformations in ombrotrophic peats. The problems are two-fold. Firstly, the anthropogenic magnetites which control the magnetic characteristics of recent peat deposits are typically bound within a quartz-mullite matrix. Hence, the magnetic fraction is not easily isolated. Secondly, where downcore variations in the morphology of magnetite-

bearing cenospheres do occur, it is impossible to confirm that post-depositional alteration is responsible. Because the size, oxide composition and structure of anthropogenic cenospheres is known to be controlled by the combustion temperature and the chemistry of the fuel feed (Hunt et al 1984, Raask et al 1981, Jones 1985), downcore variations could simply reflect temporal advances in combustion technology.

However, through the comparison of SEM micrographs of magnetically extracted particulates from the 2cm and 19cm levels of core G6, two distinctions are identifiable which are wholely consistent with the downcore loss of SIRM and enhancement of remanent stability through Fe3O4 dissolution.

1) Cenospheric particulates within the oxic, 2cm sub-sample have characteristic surface oxide coatings, with cubic/octahedral magnetites showing prevalence (Fig 6/21a). These oxides are absent from the surfaces of the cenospheres extracted from the 19cm sub-sample (Fig 6/21b) and may plausibly have been removed as a consequence of the translocation of particulates into a severely reducing environment.

2) Cenospheric grains from the 19cm level of core G6 typically exhibit evidence of surface fracturing (Fig 6/21b). Should the ferrimagnetic cores of these particulates

FIG 6/21: SEM micrographs of magnetic extracts taken from 2cm (A) and 19cm (B) sub-sampling levels of core G6. Cenospheres are present within the magnetic assemblages of both sub-samples, but their surface morphology differs markedly. Extracts from the 2cm level are characterised by spherules with surface oxide coatings, principally formed of magnetite (A). Spherules extracted from the 19cm level are devoid of surface oxide coatings and display evidence of surface fracturing (B).

Å

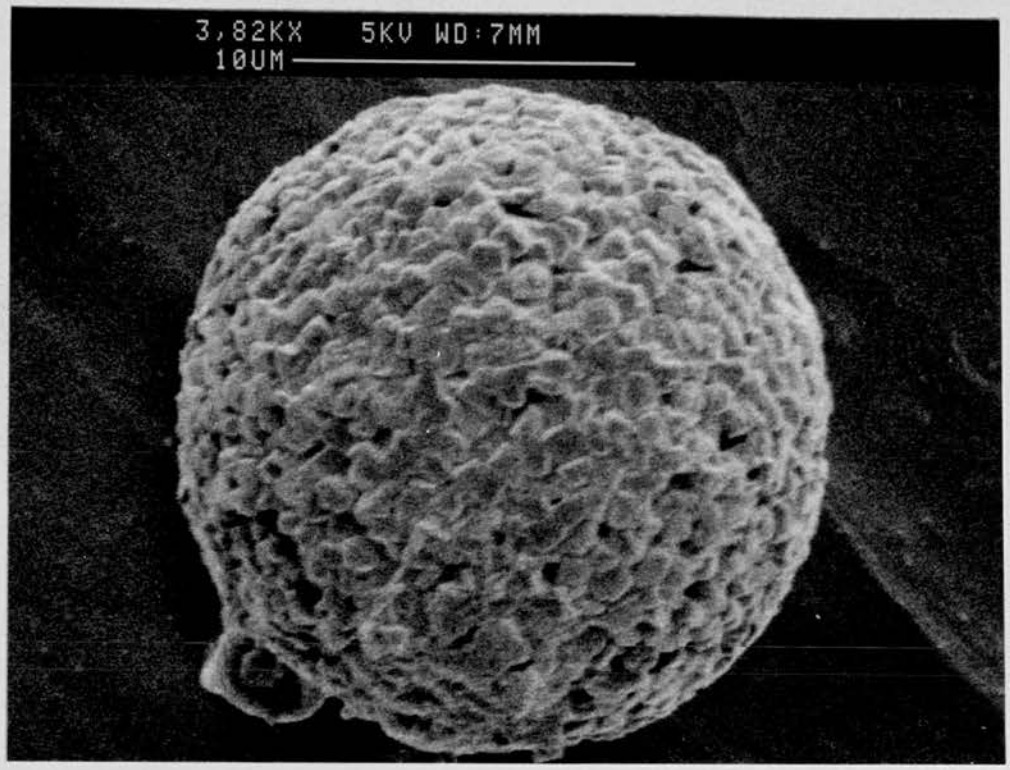

B

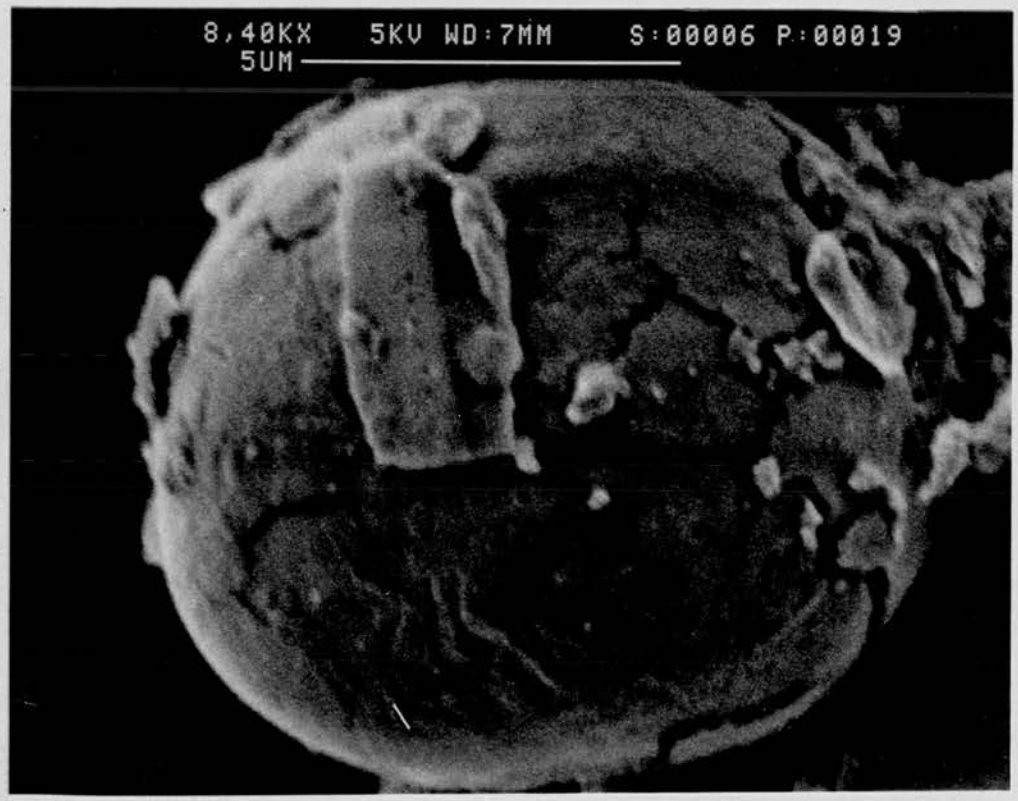

behave as inter-active MD grains when in pristine condition, fracturing and sub-division may induce the increased remanent stability occurring at 19cm depth.

6.7: Summary and conclusions.

From the evidence presented, it is possible to confirm the findings of Oldfield et al (1978, 1979, 1984), Thompson et al (1980) and Jones (1985) that the deposition of hydrocarbon-derived particulates constitutes the principal cause of magnetic enhancement within recent ombrotrophic peat sequences. However, the following facets of the interpretive framework formerly applied to downcore magnetic data require re-appraisal:-

1) Poorly synchronous SIRM increments within adjacent "hummock" and "lawn" cores, along with inversely related SIRM and Fe/Mn profiles, indicate the dissolution of anthropogenic magnetites upon burial. The "magnetic take-off" cannot, therefore, be considered to constitute a universally datable horizon corresponding to the onset of increased fossil fuel combustion during the mid-19th century.

2) The proximity to the peat surface of the stratigraphic zone in which the Fe3O4 stability field is exceeded is directly related to the level of water inundation. Accordingly, Fe3O4 dissolution occurs more rapidly upon

burial at Sphagnum "lawn" sites than at Calluna "hummock" sites. This leads to the production of anomalously low cumulative SIRM values within cores from the former. Explanatory hypotheses relating microtopographic variations of cumulative SIRM to differential particulate catchment (Oldfield et al 1979) need not, therefore, be invoked.

3) On account of the lack of small, SP/SSD magnetites which are usually subject to the most rapid dissolution, the major diagenetic control on "concentration-independent" magnetic signals involves the fragmentation of large, MD crystals upon burial. This process can fully account for the the "hardening" of magnetic remanence which typically occurs within peat strata demarking the magnetic take-off. Previous claims that such trends reflect the deposition of haematite-rich anthropogenic particulates during the early 19th century (Jones 1985) may, therefore, be incorrect.

CHAPTER SEVEN

Summary of principal observations, conclusions and wider implications.

7.1: Introduction.

The preceding chapters have outlined the controls on downcore elemental and magnetic mineral enrichment patterns through upper-Holocene deposits in the acid Loch Dee and Loch Ba catchment areas. The observations which have been made are "site-specific", but they have wide-reaching implications for the interpretation of the geochemical and magnetic stratigraphy of many other Quaternary deposits. Accordingly, the following sections serve to both summarise the findings of this study and to consider their significance in a broader perspective.

7.2: Geochemical conditions in the study basins.

A striking feature of this study is the observation of heavy metal anomalies which reflect the operation of contrasting enrichment mechanisms in the surficial sectors of sediment cores. These are:-

1) Anthropogenic enrichment: Pb, Zn and Cu exhibit progressive enrichment upward of 10cm depth in cores Dee(3), Dee(4) and Ba(2) without any concomitant variation

of sediment lithogeochemistry. This enrichment also occurs independently of downcore redox variations and cannot be equated with an exchange of metals between dissolved and solid phases. Consequently, the increased deposition of anthropogenic pollutants provides the only plausible explanation. At Loch Dee, the locus of rapidly increasing Pb, Zn and Cu accumulation dates to c.1850. Hence, the palaeo-geochemical record is wholely consistent with claims that the onset of lake acidification in Galloway (at around 1850) was synchronous with increased hydrocarbon pollutant deposition (eg. Flower and Battarbee 1983, Battarbee and Flower 1985, Jones et al 1986).

2) Natural enrichment: In common with all other analysed cores, a range of heavy metals are enriched in the post-1850 levels of core Ba(3). Yet in contrast to the Loch Dee sediments, there is strong evidence that natural mechanisms are responsible for this phenomenon. The accumulation of Pb, Zn, Cu, Co and Ni is directly coincident with a transition from anoxic to oxic sedimentary conditions upward of 3cm depth. Excepting Pb, these elements also exhibit solid-phase accumulation in association with their depletion from the interstitial pore-waters, thus suggesting a diagenetic mode of enrichment. Hydrous Fe/Mn oxides are prevalent in the oxic, surficial strata and may exert a primary influence on the constituency of sediments on account of their tendency to "scavenge" trace metals from solution (as noted by Robinson 1981, Cornwell 1983, 1986, Ballistrieri and Jones

1986, Pedersen et al 1986).

The observation of "natural" mechanisms of heavy metal enrichment in the post-1850 sediment sequence at Loch Ba has profound implications for the interpretation of geochemical anomalies in other basin sediments. In previous studies the enrichment of heavy metals in post-industrial strata has almost universally been considered to be diagnostic of cultural peturbation (eg. Aston 1973, Forstner 1976, Oullet and Jones 1983). Through the acceptance of this false premise, the historical influx of trace metals to lake catchments has typically been appraised solely by reference to "bulk" downcore geochemical profiles. From the evidence presented here, it is apparent that diagenetic and anthropogenic processes may produce "bulk" profiles which, in isolation, are indistinguishable. In the Loch Dee and Loch Ba basins the contrasting causes of heavy metal enrichment in the post-industrial strata only become conspicuous upon examining the accompanying adjustments to pore-water chemistry, geochemical fractionation and redox status.

An important implication of this study is, therefore, clear. By only referring to "bulk" geochemical profiles when appraising the controls on geochemical conditions in surficial sediments, previous workers may have incorrectly attributed natural, "diagenetic" trace metal anomalies to anthropogenic pollution. Significantly, "bulk" geochemical

profiles have frequently been interpreted in isolation during the development of temporal linkages between atmospheric deposition and lake acidification (eg. Norton et al 1981, Davis et al 1983). Should these profiles have been subject to diagenetic control, the emergent "causal" linkages may be spurious.

On the basis of the sediment-based geochemical data presented in this study, the following conclusions can be drawn:-

1) Trends of trace metal enrichment in sediments of post-industrial age can be indicative of the extent of cultural peturbation in lake basins, but cannot be considered to be diagnostic.

2) In lake sediments which comprise a two layer oxidizing-reducing system, the co-precipitation of trace elements with hydrous Fe/Mn oxides is likely upward of the anoxic/oxic threshold. Ideally, pollution chronologies should be derived from sediments in which this threshold does not occur within strata of post-industrial age. Where this is not possible, the fidelity of palaeo-geochemical records must be qualified through the provision of process-diagnostic data. In particular, it is necessary to demonstrate that enrichment anomalies are not directly equatable with the depletion of elements from sedimentary pore-waters and are not solely attributable to the accumulation of hydrogenous geochemical phases.

7.3: Magnetic mineralogy of sediments in the study basins.

This study has presented data which illustrate the operation of 3 independent mechanisms promoting ferrimagnetic enrichment in surficial lake sediments. These are:-

1) Anthropogenic processes: Sediment cores from Loch Dee exhibit progressive, 5-fold enhancement of ferrimagnetic mineral concentrations through the uppermost 8cm. Geochemical and magnetic evidence indicates that the detrital mineral influx has not varied during the accumulation period of these sediments, thus precluding any natural, allogenic enrichment mechanism. The predominant control on the magnetic properties of the surficial strata is also known to be exerted by Fe-oxides which reside in cenospheric particulates. On the basis of evidence provided by Raask et al (1981) and Riley and Chester (1971), these particulates can confidently be assigned an anthropogenic origin. From the downcore SIRM gradient through core Dee(3), the onset of increased magnetite deposition can be dated to c.1850. Throughout the post-industrial sequence, SIRM variations are also essentially co-variable with the concentrations of the atmophilic pollutant elements, Pb, Zn and Cu. Accordingly, the magnetic data derived from the Loch Dee sediments are wholely consistent with previous geochemically-based deductions, that a markedly increased hydrocarbon pollutant flux has prevailed since 1850.

2) Diagenetic processes: Up to 38% of the ferrimagnetic phases in sediments at 4cm - 16cm depth in the Loch Ba basin are sensitive to oxidation. Geochemical fractionation data also show these minerals to be H2O2-soluble. Hence they cannot be detrital or anthropogenic Fe oxides. From the evidence of Hilton et al (1986) and Karlin (1984), the above characteristics appear most consistent with the presence of the authigenic sulphide, Fe_3S_4 (greigite).

The observation of a diagenetic mechanism of ferrimagnetic enrichment in the Loch Ba sediments is important because downcore mineral magnetic variations have, to date, largely been considered to reflect the temporal influx of allogenic minerals. The results presented here indicate that Fe_3S_4 authigenesis is most prolific in surficial strata. Consequently, it must now be recognised that ferrimagnetic enrichment in sediments of post-industrial age cannot be directly equated with increased loadings of anthropogenic Fe oxides.

It is important to note that the implications of Fe_3S_4 authigenesis may not be restricted to the interpretation of ferrimagnetic anomalies in surficial sediments. At Loch Ba, Fe_3S_4 is most conspicuous in the uppermost 16cm of sediment, simply because the oxic/anoxic threshold is located in these strata. Where this threshold occurs at greater depth, bi-sulphide oxidation may yield the elemental sulphur required

for Fe3S4 precipitation. In addition, the progressive downcore monosulphide - pyrite transformations invoked to explain the limited persistence of Fe3S4 upon burial at Loch Ba, do not occur in all sediments. Berner (1971, 1981) has shown that such transformations are, in fact, entirely governed by the presence and speciation of reactive sulphur in the interstitial pore-waters.

The potential significance of the presence of Fe3S4 in deeply buried strata is two-fold. Firstly, in instances where ferrimagnetic anomalies have been used for core correlation (eg. Dearing 1979, Bloemendal et al 1979), authigenic Fe3S4 phases may promote erroneous magneto-stratigraphic linkages. Secondly, any orientation assumed by authigenic minerals will relate to the geomagnetic field prevailing at the time of their precipitation. The influence of this post-depositional remanence has largely been ignored in lake sediment-based studies of Quaternary palaeo-intensities and secular variation (eg. Mackareth 1971, Clarke and Thompson 1978, Thompson 1978, Thompson 1979, Levi and Banjeree 1976). The results obtained during these studies may, therefore, also be subject to error.

3) **Lithospheric processes:** In addition to the ferrimagnetic enrichment of the surficial Loch Ba sediments through Fe3S4 authigenesis, the concentrations of ferrimagnetic oxides also increase by factors of 2 - 5 upward of 20cm depth. These mineral phases are of PSD/MD

structure and are magnetically analogous to anthropogenic magnetites. However, SEM analyses of magnetic mineral extracts from the uppermost 1cm of sediment have shown all resident magnetites to be of octahedral morphology. Consequently, the enrichment of these strata with Fe oxides can be solely attributed to an increased detrital influx.

Sedimentological controls on downcore mineral magnetic profiles have been well appraised (eg. Dearing 1979, Bloemendal et al 1979, Thompson et al 1975, 1979, Higgitt 1982, Worsley 1983) and hence do not warrant detailed examination. However, a notable feature at Loch Ba is that temporal variations of the detrital magnetite flux occur without any concomitant variation of the supply of lithophile elements to the sediment reservoir. Conventional lithogeochemical analyses of post-industrial sediments do not, therefore, aid in distinguishing ferrimagnetic anomalies of anthropogenic and lithospheric origin.

The major conclusions to be drawn from the sediment-based magnetic data presented in this study can be summarised as follows:-

1) Ferrimagnetic anomalies in strata of post-industrial age can be indicative of anthropogenic peturbation but are not diagnostic. Lithospheric and diagenetic processes can also produce these phenomena. Accordingly, interpretations should be made by reference to evidence depicting mineral

morphology, oxidation sensitivity and geochemical speciation.

2) Coincident downcore variations of sediment geochemistry and magnetic mineralogy cannot be assumed to reflect the influence of a common process.

7.4: Geochemical conditions within peat accumulations in the study areas.

From the data acquired through the analysis of 12 sample cores from peatland sites in the Galloway and Rannochmoor regions, two trends are particularly conspicuous:-

1) The peak and cumulative concentrations of Pb, Zn, Cu, Cd and Cr are factors of 1.5 - 4 higher in sample cores from the Galloway study sites than in those from Beinn Chaorach. This trend supports the claims of Livett (1982), Livett et al (1979), Pakarinen and Tolonen (1977) and Schell (1986), that the loading of atmophilic elements to peat systems is directly related to the proximity of industrial pollutant sources.

2) The distributions of elements within sample cores are consistently related to the hydrological and redox conditions prevailing at individual coring stations. Consequently, the controls on the geochemical stratigraphy

of all cores can be explained by reference to a simple 3 sector model. In the uppermost sector, comprising freely drained strata, elemental mobility is restricted on account of the prevalence of oxic/sub-oxic conditions. Accordingly, downcore geochemical variations essentially analogue the historical influx of elements from the atmosphere.

The second sector encompasses strata which lie within the zone of water table fluctuation. The onset of water-inundated conditions induces the sharp depression of eH (to around -300mV) and the concomitant mobilization of reducible metal species. This redox change is responsible for the marked depletion of Mn and Zn. However, Fe, Al, Pb, Cu, Ti, Cr and Cd all undergo secondary enrichment through the precipitation of authigenic oxides and sulphides at the sub-oxic/strongly anoxic boundary.

The third sector comprises all permanently inundated, anoxic strata. Mn and Zn are only present at "background" concentrations in these strata on account of their inherent solubility in low valency states (hence facilitating their removal by hydrological processes). Pb, Cu, Ti, Cd and Cr are also depleted because their insoluble sulphide phases are subject to periodic oxidation and the formation of soluble sulphates whilst still within the zone of water table fluctuation. Consequently, Pb, Cu, Ti, Cd and Cr are removed from the system through hydrological pathways, prior to their translocation into the permanently

anoxic peat.

On account of its universal applicability, the above model casts considerable doubt upon the credibility of many previous interpretations of geochemical profiles through peat sequences. In the principal geochemical studies to date, Pakarinen and Tolonen (1977), Livett et al (1979), Livett (1982) and Schell (1986) have invoked industrial pollution as the major cause of Pb, Zn, Cu, Cr and Cd enrichment in surficial peats. From the evidence presented here, these trends can be explained solely by reference to naturally operative, diagenetic processes. In the case of Zn, relative enrichment is characteristic of surficial peats, simply because of its' mobility following burial within the anoxic, inundated strata. This study has also demonstrated that Pb, Cr, Cu and Cd are universally subject to diagenetic enrichment in the zone of water table fluctuation. Because this zone typically lies only 5cm - 30cm below the peat surface, the enrichment of post-industrial strata with atmophilic elements is likely, irrespective of the ambient atmospheric pollutant influx.

In the light of the above information, the following conclusions can be drawn:-

1) Existing assumptions that peat cores from inundated "lawn" and "pool" microtopography are suitable for use in deciphering the history of atmospheric pollutant deposition

(eg. Livett 1982) are invalid. These cores are characterised by the prevalence of hydrological/redox conditions which induce elemental mobilization. Consequently, downcore geochemical variations essentially reflect the influence of post-depositional processes.

2) Because elemental mobilization is associated with the onset of inundated, strongly reducing conditions in peat systems, ideal sample cores for use in the construction of pollution chronologies are those from freely drained "hummock" topography.

7.5: Magnetic mineralogy of peat accumulations in the study areas.

The data presented in this study serve to corroborate many previously documented observations regarding the controls on magnetic mineralogy in peat systems. Notably:-

1) Ferrimagnetic enrichment is restricted to the uppermost 5cm - 30cm of 16 sample cores from Galloway, Beinn Chaorach and 5 additional UK sites. In all sample cores for which geochronological data are available, the enriched strata can be assigned origins of less than 150yrs BP. SEM analyses of magnetic extracts from the surficial levels of the Brishie Mire peat accumulation indicate that the predominant magnetic phases are magnetite-bearing

cenospheres. These trends are, therefore, consistent with former claims that hydrocarbon combustion processes constitute the principal source of ferrimagnets to ombrotrophic peats (eg. Oldfield et al 1978, 1979, Thompson et al 1980, Jones 1985, Jones 1986).

2) The peak and cumulative SIRM values determined for sample cores from 8 UK sites form a persistent distance-decay pattern with respect to the proximity of industrial pollutant sources. This pattern is directly analogous to that identified by Thompson et al (1980), during the examination of geographical trends of magnetite deposition in Britain and Scandinavia.

The major discrepency between the findings of this study and all previously published research concerns the controls on mineral magnetic stratigraphy in ombrotrophic peats. The data presented here show that:-

1) Strata displaying initial ferrimagnetic enhancement (termed the magnetic take-off) within cores from adjacent "lawn" and "hummock" coring sites are not of temporally synchronous origin.

2) In most analysed cores, the stratigraphic points at which SIRM intensities fall to "background" levels are coincident with major anomalies in the profiles of the redox-sensitive elemental ratio, Fe/Mn. These trends signify

that anthropogenic magnetites are subject to rapid dissolution following their translocation into sectors of the peat column in which eH/pH conditions exceed the Fe3O4 stability field.

3) Multi-domain, anthropogenic magnetites are subject to progressive fragmentation upon burial and hence, assume SSD-like magnetic properties prior to their complete dissolution. Consequently, magnetite dissolution processes characteristically induce a downcore increase in the stability of magnetic remanence within the ferrimagnetically enriched zone.

On the basis of the above evidence, new interpretations can be placed on three of the mineral magnetic trends previously observed in ombrotrophic peats. Firstly, it is possible to refute claims that downcore SIRM gradients provide a complete, unaltered record of the history of hydrocarbon pollutant fluxes to peat systems (eg. Oldfield et al 1978, 1979, Thompson et al 1980, Jones 1986). From the evidence presented here, it is clear that this assumption is only valid in instances where the entire post-industrial sequence is characterised by oxic or sub-oxic conditions (thus precluding magnetite dissolution). Because the magnetic take-off typically depicts the lowermost level at which eH/pH conditions allow Fe3O4 persistence, assumptions that this feature can be used as a geochronological marker, dating to the onset of mass fossil fuel combustion (eg.

Oldfield et al 1984) are also invalid.

Secondly, by failing to acknowledge the influence of post-depositional processes on magnetic mineralogy, Jones (1985) has incorrectly equated the occurrence of magnetically "hard" minerals in strata demarking the magnetic take-off with the deposition of haematite-rich atmospheric pollutants. In this study, the associated downcore hardening of magnetic remanence and the depression of SIRM intensities has been shown to be wholely attributable to the dissolutionary fragmentation of multi-domain magnetites upon burial.

Finally, this study has shown that downcore redox gradients are directly controlled by peat hydrology. Because the prevalence of conditions which exceed the Fe3O4 stability field is associated with water inundation, the persistence of anthropogenic magnetites upon burial is extensively controlled by microtopography. At "hummock" coring stations, Fe3O4 may persist to depths of 30cm - 40cm on account of the low level of the water table relative to the peat surface. In contrast, conditions may be sufficiently reducing for Fe3O4 dissolution throughout the entire peat column at inundated "lawn" or "pool" coring stations. Hence, the frequent occurrence of low cumulative SIRM values in "pool" cores compared to those from "hummock" sites appears to be a predictable result of the microtopographic control on rates of Fe3O4 dissolution.

Previously, these trends have been mis-interpreted as reflecting the influence of microtopography on the efficiency of particulate catchment (eg. Oldfield et al 1979).

The principal conclusions which can be drawn from the peat-based magnetic data presented in this study are:-

1) Downcore mineral magnetic profiles through ombrotrophic peats can only be interpreted in a palaeo-environmental context, having first established that the redox regime is not conducive to Fe3O4 dissolution.

2) Because the dissolution of magnetic oxides is specific to anoxic, inundated peat strata, sample cores from raised "hummock" topography provide the most faithful records of the history of atmospheric deposition.

7.6: Future research priorities.

This study has demonstrated that a range of post-depositional processes can influence the geochemical and mineral magnetic stratigraphy of Holocene sediments and peats. Where such processes operate, they clearly detract from the utility of stratified deposits for palaeo-environmental reconstruction. The development of a methodology for identifying depositional environments which are least subject to diagenetic alteration must, therefore,

be of primary concern in future research programmes. This should entail:-

1) Characterisation of the physio-chemical conditions promoting diagenesis: Although the geochemical characteristics of Holocene sediments and peats have been evaluated independently, this study intimates that the principal controls are similar in both depositional environments. For example, elemental mobility can universally be related to chemical speciation and the prevailing eH/pH regime. The precipitation of authigenic oxides is associated with the migration of elements across an anoxic/oxic threshold in both sediments and peats. While Fe3S4 authigenesis has only been observed in sediments, this process can also be equated with specific conditions of high organic carbon, anoxia and the presence of reactive elemental sulphur. On the basis of such observations, it is possible to make the qualitative prediction that diagenetically stable environments will be oxic, inorganic and alkaline, irrespective of whether they are lacustrine sediments or ombrotrophic peats. Quantification of the environmental thresholds controlling diagenetic processes should, therefore, facilitate the rapid evaluation of the suitability of individual Holocene deposits for the provision of palaeo-environmental information.

2) Characterisation of the rate controls on magnetite dissolution. In this study, the dissolution of anthropogenic magnetites in peat systems has essentially

been attributed to the prevalence of conditions of low eH (<-300mV). The data presented suggest that multi-domain crystals are frequently destroyed within 150 years of residence in the peat system. In contrast, Canfield and Berner (1987) have established a 1000 year half-life for multi-domain magnetites in equally reducing marine sediments. Clearly, this disparity signifies that eH is not the sole "rate-contolling" influence. Characterisation the precise environmental conditions promoting rapid magnetite dissolution should, therefore, be a future research priority. Experimental assessment of the persistence of Fe3O4 under similar eH conditions, but with variable pH and dissolved sulphide presence may be of particular value in this context.

BIBLIOGRAPHY

Allegre C.J, Albarade F, Grunenfelder M and Koppel V (1974) 238U/208Pb, 235U/207Pb and 232Th/206Pb Zircon geochronology in alpine and non-alpine environments. CONT. MIN. PETROL 43: 163 - 194.

Allen S.E, Grimshaw H.M, Parkinson J.A and Quarmby C (1974). Chemical analysis of ecological materials (ed. Allen S.E), BLACKWELL, LONDON.

Allen G.C, Hocking W.H, Watson D.G, Wild R.J and Street P.J (1984). Surface studies of coke particles from residual fuel oil combustion. J. INST. ENERGY 51: 260 - 265.

Anderson N.J (1986). Diatom biostratigraphy and comparative core correlation within a small lake basin. HYDROBIOLOGIA 143: 105 - 112.

Andersson F. (1985). Properties and chemical composition of surficial sediments in the acidified Lake Gardsjon basin. In LAKE GARDSJON: AN ACID LAKE AND IT'S CATCHMENT (EDS. ANDERSSON F AND OLSSON B), ECOL. BULL, STOCKHOLM.

Aston S.R (1973). Mercury in lake sediments: a possible indicator of technological growth. NATURE 241: 450 - 451

Ballistrieri L.S and Jones W.M (1986). The surface chemistry of sediments from the Panama basin: The influence of Mn oxides on metal adsorption. GEOCHIM. ET. COSMOCHIM. ACTA 50: 2235 - 2243.

Battarbee R.W (1984). Diatom analysis and the acidification of lakes. PHIL. TRANS. R. SOC. 305: 451 - 477.

Battarbee R.W and Flower R.J (1985). Lake acidification in Galloway: a palaeoecological test of competing hypotheses. NATURE 314: 350 - 352.

Battarbee R.W and Charles D.F (1986). Diatom based pH reconstruction studies of acid lakes in Europe and North America: A synthesis. WATER, AIR AND SOIL POLLUTION 30: 347 - 354.

Baturin G.N, Kochenov A.V and Shimkus K.M (1967). Organic vs. trace metal associations in anoxic marine sediments. GEOKHIMIYA 41: 240 - 251.

Bellamy D and Reiley J (1967). Some ecological statistics of a miniature bog. OIKOS 18: 33 - 40.

Bengtsson L (1979). Chemical analysis. in PALAEOHYDROLOGICAL CHANGES IN THE TEMPERATE ZONE IN THE LAST 15000 YEARS (ED. BERGLUND E), SUB-PROJECT B, LAKES AND MIRES. IGCP PROJECT 158, LUND, SWEDEN.

Berge F (1976). Diatoms as indicators of temporal pH trends in some lakes and rivers in southern Norway. EX BEIHEFT 73 ZUR NOVA HEDWIGIA: 249 - 265.

Berner R.A (1964). An idealised model of dissolved sulphate distribution in recent sediments. GEOCHIM. ET. COSMOCHIM. ACTA 28: 1499 - 1503.

Berner R.A (1969). Migration of iron and sulphur within anaerobic sediments during early diagenesis. AM. J. SCI 267: 19 - 42.

Berner R.A (1970). Sedimentary pyrite formation. AM. J. SCI 268: 1 - 23.

Berner R.A (1981). A new geochemical classification of sedimentary environments. J. SED. PETROL 51: 359 - 365.

Bertine K.K and Goldberg E.D (1971). Fossil fuel combustion and the major sedimentary cycle. SCIENCE 173: 233 - 235.

Birks J.H.B and Birks H.H (1971). Quaternary palaeoecology. ARNOLD, LONDON.

Birks H.H (1972). Studies in the vegetational history of Scotland 2: Two pollen diagrams from the Galloway hills, Kirkudbrightshire. J. ECOL 60: 183 - 216.

Bloemendal J, Oldfield F and Thompson R (1979). Magnetic measurements used to assess sediment influx at Llyn Goddiondnon. NATURE 280: 50 - 51.

Boatman D.J (1983). The Silver Flowe National Nature Reserve, Galloway, Scotland. J. BIOGEOG 10: 163 -274.

Boatman D.J, Hulme R.D and Tomlinson R.W (1975). Monthly determinations of the concentrations of sodium, potassium, magnesium and calcium in the rain and pools of the Silver Flowe National Nature Reserve. J. ECOL 63: 903 - 912.

Boatman D.J and Tomlinson R.W (1977). The Silver Flowe: 2 Features of the vegetation and stratigraphy of Brishie Bog and their bearing on pool formation. J. ECOL 65: 531 - 546.

Braeke F.H (1981). Hydrochemistry of low pH soils in S. Norway: Peat and soil water quality. MEDOL. NOR. INST. SKOGFORSOKSVES 36 (2): 32 - 48.

Bradshaw R.H (1981). Modern pollen representation factors for woods in S.E England. J. ECOL 69: 45 - 70.

Bradshaw R.H and Thompson R (1984). The use of magnetic measurements to investigate the mineralogy of Icelandic lake sediments and to study catchment processes. BOREAS 14: 203 - 215.

Brehm K (1971). Ein Sphagnum bult als beispiel einer naturlichen lonenaustaurschersaule. BIETR. BIOL. PFANZEN 47: 287 - 312.

Broecker R (1974). Chemical oceanography. HARCOURT BRACE JOVANOVICH INC, USA.

Brown K.A (1980). The distribution of sulphur compounds in a peat bog in relation to stream-water chemistry. CERL REP. RD/L/N 150/180.

Brown K.A (1982). Sulphur in the environment: a review. ENV. POLLN. SERIES B, 3: 47 - 80.

Brown D.J.A (1986). Loch Fleet project annual proceedings. CERL CIRCULAR, LEATHERHEAD, OCT 1986.

Brugam R.B (1978). Human disturbance and the historical development of Linsley pond. ECOLOGY 59 (1): 19 - 36.

Buesseler K.O, Livingston H.D and Sholkovitz E.R (1985). 239/240Pu and excess 210Pb inventories along the shelf and slope of the north-east USA. EARTH. PLAN. SCI. LETT 76: 10 - 22.

Burns J.C, Coy J.S and Tervet D.J (1984). The Loch Dee project: a study of the ecological effects of acid precipitation and forest management in an upland catchment in south-west Scotland. FISH. MGMT 15 (NO.4): 145 - 167.

Capuzzo J.D and Anderson F.E (1973). The use of modern chromium accumulation to determine estuarine sedimentation rates. MAR. GEOL 14: 225 - 235.

Calvert S.E (1977). The geochemistry and mineralogy of nearshore sediments. in CHEMICAL OCEANOGRAPHY (EDS. RILEY J.P AND CHESTER R) VOL 6. ACADEMIC PRESS.

Canfield D.E and Berner R.A (1987). Dissolution and pyritization of magnetite in anoxic marine sediments. GEOCHIM. ET COSMOCHIM. ACTA 51: 645 - 659.

Carignan R and Nriagu J.O (1985). Trace metal deposition and mobility in the sediments of two lakes near Sudbury, Ontario. GEOCHIM. ET COSMOCHIM. ACTA 49: 1753 - 1764.

Carpenter R, Petersen M.L and Bennett J.T (1982). 210Pb derived sediment accumulation and mixing rates for the Washington continental slope. MARINE GEOL 66: 135 - 164.

Chapman S.B (1964). The ecology of Coom Rigg Moss, Northumberland. 2: Chemistry of peat profiles and the development of the bog system. J. ECOL 52: 315 - 321.

Charles D.F (1985). Relationships between surface sediment diatom assemblages and lake-water characteristics in Adirondack lakes. ECOLOGY 66: 994 - 1011.

Chow T.J and Earl J.L (1970). Lead aerosols in the atmosphere: Increasing concentrations. SCIENCE 169: 577 - 580.

Clarke R.M and Thompson R (1978). An objective method for smoothing palaeomagnetic data. GEOPHYS. J. R. ASTR. SOC 52: 205 - 213.

Cline J.T and Chambers R.L (1977). Spatial and temporal distribution of heavy metals in lake sediments near Sleeping Bear Point, Michigan. J. SED. PETROL, 47 NO 2: 716 - 727.

Clymo R.S (1963). Ion exchange in Sphagnum and its relation to bog ecology. ANN. BOT 27: 309 - 324.

Copeland R.A and Ayers J.C (1972). Trace element distribution in water, sediment, phytoplankton, zooplankton and benthos of Lake Michigan: A baseline study with calculation of concern-factors and of radioisotopes in the food webb. ENV. RES. GRP, ANN ARBOR: 271pp.

Cornwell J.C (1983). The geochemistry of Mn, Fe and P in an arctic lake. PHD THESIS, UNIVERSITY OF ALASKA.

Cornwell J.C (1986). Diagenetic trace metal profiles in Arctic lake sediments. ENV. SCI. TECH 20: 299 - 302.

Crecelius E.A, Bothner M.H and Carpenter R (1975). Geochemistries of arsenic, antimony, mercury and related elements in sediments of Puget Sound. ENV. SCI. TECH, 9 NO 4: 325 - 337.

Crozaz G (1964). Arctic snow chronology with 210Pb. J. GEOPHYS. RES, 69 (12)": 2597 - 2604.

Damman A.W.H (1978). Distribution and movement of elements in ombrotrophic peat bogs. OIKOS 30: 480 - 495.

Davis R.B, Norton S.A, Hess C.T and Braeke D.F (1983). Palaeolimnological reconstruction of the effects of the atmospheric deposition of acids and heavy metals on the chemistry and biology of lakes in New England and Norway. HYDROBIOLOGIA 103: 113 - 123.

Davis R.B, Hess C.T, Sherton S.A, Hansen D.W, Hoagland K.D and Anderson D.S (1984). 137Cs and 210Pb dating of sediments from soft-water lakes in New England, USA and Scandinavia: A failure of 137Cs dating. CHEM. GEOL 44: 151 - 185.

Davison W, Woof C and Turner D.R (1982). Handling and measurement techniques of anoxic interstitial waters. NATURE 294: 582 - 583.

Davison W, Lishman J.P and Hilton J (1985). Formation of pyrite in freshwater sediments: implications for C/S ratios. GEOCHIM. ET COSMOCHIM. ACTA 49: 1615 - 1620.

Dearing J (1979). The application of magnetic measurements to studies of particulate flux in lake watershed systems. PHD THESIS, UNIVERSITY OF LIVERPOOL, 1979.

Dearing J and Flower R.J (1982). The magnetic susceptibility of sedimenting material trapped in Lough Neagh, Northern Ireland and its erosional significance. LIMNOL. OCEANOG 27: 969 - 975.

Digerfeldt G (1975). The post-glacial development of Ranvikan bay in Lake Immeln. 3: Palaeolimnology. GEOL FOREN STOCKHOLM. FORH 97: 13 - 28.

Dillan D.J and Evans A (1982). Whole lake lead burdens in sediments of lakes in southern Ontario, Canada. HYDROBIOLOGIA 91: 131 - 137.

Dobson J.E, Peplies R.W and Rush R.M (1987). The association between Adirondack lake acidity and forest blow-down. US DEPT. OF ENERGY REP. DE ACO 5840 R21400.

Drablos D and Tollan A (1980). Ecological impacts of acid precipitation: proceedings of an international conference, Sandefjorde, Norway: SNSF PROJECT, OSLO NORWAY.

Drakeford T (1979). Land use history of Cairnsmore. NCC REP. 14, 1947, BALLOCH, SCOTLAND.

Du Reitz G.E (1949). Huvundenheter och huvudgranser i svensk myrvegetation. IBID 43: 3 - 10.

Edgington D.N and Robbins J.A (1976). Pattern of deposition of natural and fallout nuclides in the sediments of Lake Michigan and their relationship to limnological processes. in ENVIRONMENTAL BIOGEOCHEMISTRY VOL. 2 (ED NRIAGU J.O) ANN ARBOR SCIENCE, NEW YORK.

El Daoushy F, Tolonen K and Roseberg R (1982). 210Pb and moss increment dating of two Finnish Sphagnum hummocks. NATURE 296: 429 - 433.

Farmer J.G (1978). Lead deposition in lake sediments. SCI. TOT. ENV 10: 117 - 127.

Farmer J.G and Lovell M.A (1986). Natural enrichment of arsenic in Loch Lomond sediments. GEOCHIM. ET COSMOCHIM. ACTA 50: 2059 - 2067.

Faure G.F (1977). Principles of isotope geology. WILEY AND SONS, NEW YORK.

Filipek L.H and Owen R.M (1979). Geochemical associations and grain size partitioning of heavy metals in lacustrine sediments. CHEM. GEOL 26: 105 - 117.

Filipek L.H and Owen R.M (1981). Diagenetic controls of phosphorus in outer continental shelf sediments from the Gulf of Mexico. CHEM. GEOL 33: 181 - 204.

Flower R.J and Battarbee R.W (1983). Diatom evidence for the recent acidification of two Scottish lochs. NATURE 305: 130 - 133.

Forstner U (1976). Lake sediments as indicators of heavy metal pollution. NATUWISSENSCHAFTEN 63: 465 - 485.

Furrer G and Stumm W (1986). The co-ordination chemistry of weathering (1): Dissolution kinetics of Al2O3 and BeO. GEOCHIM. ET COSMOCHIM. ACTA 50: 1847 - 1860.

Galloway J.N (1979). Alteration of trace metal geochemical cycles due to the marine discharge of waste-water. GEOCHIM. ET COSMOCHIM. ACTA 43: 207 - 218.

Galloway J.N and Likens G.E (1979). Atmospheric enhancement of metal deposition in Adirondack lake sediments. LIMNOL. OCEANOG 24: 427 - 433.

Gardiner C and Reynolds S.H (1932). The Loch Doon granite area, Galloway. QT. J. GEOL SOC. LONDON 88: 1 - 34.

Goldberg E.D (1963). Geochronology with 210Pb. in PROCEEDINGS OF SYMPOSIUM ON RADIOACTIVE DATING, IAEA, VIENNA.

Goldberg E.D, Hodge V.F, Griffen J.J, Koide M and Edgington D.M (1981). Impact of fossil fuel combustion on the sediments of Lake Michigan. ENV. SCI. TECH 15 NO 4: 466 - 471.

Gordon E.G, Randle K, Goles G, Corliss J.B, Beeson M.H and Oxley S.H (1969). Instrumental activation analysis of standard rocks with high resolution gamma ray detectors. GEOCHIM. ET COSMOCHIM. ACTA 32: 369 - 396.

Goode T. (1970). Ecological studies on the Silver Flowe National Nature Reserve. PHD THESIS, UNIVERSITY OF HULL.

Gorham E and Swain D.J (1965). The influence of oxidizing and reducing conditions upon the distribution of some elements in lake sediments. LIMNOL. OCEANOG 10: 268 - 279.

Gorham E, Bayley S.E and Schindler D.W (1984). Effects of acid deposition on peatlands: a neglected field in acid rain research. CAN. J. FISH. AQUAT. SCI 41: 1256 - 1261.

Govatt G.J.S (1975). Origin of banded iron formations. in GEOCHEMISTRY OF IRON (ED. LEPP H). BENCHMARK PAPERS IN GEOLOGY 18. DOWDEN, HUTCHINSON AND ROSS INC, STROUDSBERG.

Graustein W.C and Turekian K.K (1983). Geochemical influx to Lake Washington. in PRECIPITATION SCAVENGING, DRY DEPOSITION AND RE-SUSPENSION (ED. PRUPPACHER H.A), ELSEVIER, AMSTERDAM. p1315 - 1324.

Graybeal A and Heath G.R (1984). Remobilization of transition metals in surficial pelagic sediments from the Eastern Pacific. GEOCHIM. ET COSMOCHIM. ACTA 48: 965 - 975.

Hamilton-Taylor J (1979). Enrichment of Zn, Cu and Pb in recent sediments of Lake Windermere, England. J. ENV. SCI. TECH 13 693 - 697.

Hansen L.D, Silberman D and Fisher G.L (1981). Ferrous mineral composition of power plant fly ash. ENV. SCI. TECH 15: 1057 - 1062.

Hansen G.N, Catanzaro E.J and Anderson D.H (1971) U - Pb ages for sphene in a contact metamorphic zone. EARTH. PLAN. SCI. LETTS 12: 231 - 237.

Hart R (1981). The chemistry of power station emissions. ROY. SOC. CHEM, ENERGY AND CHEMISTRY 41: 222 - 251.

Helz G.R, Setlock G.H, Cantillo A.Y and Moore W.S (1985). Processes controlling the regional distribution of 210Pb, 226Ra and anthropogenic Zn in estuarine sediments. EARTH. PLAN. SCI. LETTS 76: 23 - 34.

Henshaw P.C (1978). The interaction of trace metals and magnetic minerals with sedimentary environments. PHD THESIS, UNIVERSITY OF WASHINGTON.

Henshaw P.C and Merrill R.T (1980). Magnetic and chemical changes in marine sediments. REVS. GEOPHYS. SPACE PHYS 18: 483 - 504.

Hesslein R.H (1976). An in-situ sampler for close interval pore-water studies. LIMNOL. OCEANOG 21: 912 - 914.

Higgitt S.R (1982). A palaeoecological study of recent environmental change in the drainage basin of Lac D'Annecy (France). PHD THESIS, UNIVERSITY OF LIVERPOOL.

Higgo J.J.W (1987). Clay as a barrier to radionuclide migration. PROG. NUCLEAR ENERGY 19 NO 2: 173 - 207.

Hilton J, Lishman J.P and Chapman J.S (1986). Magnetic and chemical characterisation of a diagenetic magnetic mineral formed in the sediments of productive lakes. CHEM. GEOL 56: 325 - 333.

Hilton J, Long G.J, Chapman J.S and Lishman J.P (1986). Iron mineralogy in sediments: a Mossbauer study. GEOCHIM. ET COSMOCHIM. ACTA 50: 2147 - 2151.

Hirons K and Thompson R (1986). Palaeo-environmental application of magnetic measurements from inter-drumlin lake sediments near Dungannon, Co. Tyrone, Northern Ireland. BOREAS 15 NO 2: 118 - 135.

Howarth R.W and Teal J.M (1979). Sulphate reduction in a New England salt marsh. LIMNOL. OCEANOG 24: 999 - 1013.

Huber H (1975). The environmental control of sedimentary iron minerals. in GEOCHEMISTRY OF IRON (ED LEPP H). BENCHMARK PAPERS IN GEOLOGY, 18. DOWDEN, HUTCHINSON AND ROSS INC, STROUDSBERG.

Hunt A, Jones J.M and Oldfield F (1984). Magnetic measurements and heavy metals in atmospheric particulates of anthropogenic origin. SCI. TOT. ENV 33: 129 - 139.

Hustedt F (1937 - 39). Systematische und okologische untersuchungen uber den Diatomean flora von Java, Bali, Sumatra. ARCH. HYDROBIOL (SUPP) 15 - 16.

Hutchinson G.E (1969). Eutrophication past and present. in EUTROPHICATION: CAUSES, CONSEQUENCES, CORRECTIVES. NATL. ACAD. SCI. SYMPOSIUM.

Huttunen P and Merilainen J (1983). Interpretation of lake quality from contemporary diatom assemblages. HYDROBIOL, 103. p91 - 107.

James H.C (1975). Geochemistry of iron rich sedimentary rocks. in GEOCHEMISTRY OF IRON (ED. LEPP, H), BENCHMARK PAPERS IN GEOLOGY 18, DOWDEN, HUTCHINSON AND ROSS INC, STROUDSBERG.

Jeffries D.S and Snyder W.R (1981). Atmospheric deposition of heavy metals in central Ontario. WATER. AIR AND SOIL POLL 15: 127 - 152.

Johnson H.P, Kinoshita H and Merrill R.T (1975). Rock magnetism and palaeomagnetism of some North Pacific deep sea sediments. BULL. GEOL. SOC. AMER 86: 412 - 425.

Johnston J.H and Glasby R (1982). A mossbauer spectroscopic and X-ray diffraction study of the iron mineralogy of some sediments from the south-west Pacific ocean. MAR. CHEM 11: 437 - 448.

Jones J.M (1985). Magnetic minerals and heavy metals in ombrotrophic peats. PHD THESIS, UNIVERSITY OF LIVERPOOL.

Jones M.D.H (1986). The magnetic deposition record in some Scandinavian peat profiles. PHD THESIS, UNIVERSITY OF LIVERPOOL.

Jones B.F and Bowser C.J (1978). The mineralogy and related chemistry of lake sediments. in LAKES: CHEMISTRY, BIOLOGY, PHYSICS (ED. LERMAN A) SPRINGER, NEW YORK.

Jones V.J, Stevenson A.C and Battarbee R.W (1986). Lake acidification and the land use hypothesis: a mid-post glacial analogue. NATURE 322: 157 - 158.

Kahl J.S, Norton S.A and Williams T.S (1984). in GEOLOGICAL ASPECTS OF ACID PRECIPITATION (ED BRICKER O.P). ACID PRECIPITATION SERIES VOL 7, BUTTERWORTH, BOSTON. p23 - 25.

Karlin R (1984). Palaeomagnetism, rock magnetism and diagenesis in hemipelagic sediments from the north-east Pacific ocean and the Gulf of California. PHD THESIS, UNIVERSITY OF OREGON.

Karlin R and Levi S (1983). Diagenesis of magnetic minerals in recent hemipelagic sediments. NATURE 303: 327 - 330.

Karlin R and Levi S (1985). Geochemical and sedimentological control of the magnetic properties of hemipelagic sediments. GEOPHYS. J. ROY. ASTR. SOC 59: 1 - 55.

Kennedy J.E, Ruch R.R and Shrimp N.F (1970). Distribution of mercury in unconsolidated sediments of Lake Michigan. 3: STATE GEOL. SURV. ENVT. GEOL. NOTES, URBANA 3 NO 44.

Klein D.H, Andren A.W, Carter J.A, Emery J.F, Feldmore C, Fulkerson W, Lyon W.S, Ogle J.C, Talini Y, Hook R.I and Bolton N (1975). Pathways of 37 elements through coal fired power plant. ENV. SCI. TECH 9 NO 10: 973 - 979.

Koide M, Soutar A and Goldberg E.D (1972). Marine geochronology with 210Pb. EARTH PLAN. SCI. LETTS 14: 422 - 446.

Koide M, Bruland K.W and Goldberg E.D (1973). 228Th/232Th and 210Pb geochronologies in marine and lake sediments. GEOCHIM. ET COSMOCHIM. ACTA 37: 1171 - 1187.

Kobayashi K and Nomura M (1972). Iron sulphides in sediment cores from the Sea of Japan and their geophysical implications. EARTH PLAN. SCI. LETTS 16: 200 - 220.

Kobayashi K and Nomura M (1974). Ferromagnetic minerals in sediment cores collected from the Pacific ocean. J. GEOPHYS 40: 501 - 509.

Krauskopf K.B (1979). Introduction to geochemistry. MCGRAW HILL, KOGAKUSHA.

Krishnaswami S, Lal D, Martin J.M and Meybeck M (1971). Geochronology of lake sediments. EARTH PLAN. SCI. LETTS 11: 407 - 414.

Krishnaswami S and Lal D (1978). Radionuclide limnochronology. In LAKES: CHEMISTRY, BIOLOGY, PHYSICS (ED. LERMAN A) SPRINGER, NEW YORK.

Krug C.E and Frink C.R (1983). Acid rain on acid soil: a new perspective. SCIENCE 221: 520 - 525.

Lantzy R.J and Mackenzie F.T (1979). Atmospheric trace metals, global cycles and mans impact. GEOCHIM. ET COSMOCHIM. ACTA 43: 511 - 525.

Lee J.A and Tallis J.H (1973). Regional and historical aspects of lead pollution in Britain. NATURE 245: 216 - 218.

Levi S and Banjeree S.K (1976). On the possibility of obtaining relative palaeointensities from lake sediments. EARTH. PLAN. SCI LETTS 29: 219 - 226.

Lindsay W.L (1979). Chemical equilibria in soils. WILEY AND SONS, LONDON.

Livett E.A (1982). The interaction of heavy metals with the peat and vegetation of blanket bogs in Britain. PHD THESIS, UNIVERSITY OF MANCHESTER.

Livett E.A, Lee J.A and Tallis J.H (1979). Lead, copper and zinc analyses of British blanket peats. J. ECOL 67: 865 - 891.

Llyn D.A and Bonatti E (1965). Mobility of manganese in diagenesis of deep sea sediments. MARINE GEOL 3: 457 - 474.

Longworth G, Becker L.W, Thompson R, Oldfield F, Dearing J.A and Rummery T (1979). Mossbauer effect and magnetic studies of secondary iron oxides in soils. J. SOIL SCI 301: 93 -110.

Mackereth F.J (1965). Chemical investigations of lake sediments and their interpretation. PROC. R. SOC. LONDON B 161: 295 - 309.

Mackereth F.J (1966). Some chemical observations on post-glacial lake sediments. PHIL. TRANS. R. SOC. LONDON, SERIES B 250: 165 - 213.

Mackereth F.J (1969). A short core sampler for sub-aqueous deposits. LIMNOL. OCEANOG 14: 145 - 151.

Mackareth F.J (1971). On the variation in direction of the horizontal component of remanent magnetisation in lake sediments. EARTH PLAN. SCI. LETTS 12: 332 - 338.

Maher B.A (1984). Origins and transformations of magnetic minerals in soils. PHD THESIS, UNIVERSITY OF LIVERPOOL.

Malmer N (1958). Notes on the relation between the chemical composition of mire plants and peat. BOT. NOT 111: 274 - 288.

Malmer N (1962). Studies on mire vegetation in the archean area of S.W Gotaland (S. Sweden). 1: vegetation and habitat conditions on the Akhult mire. OP. BOT. SOC. BOT, LUND 7.1: 1 - 322.

Malmer N and Sjors H (1955). Some determinations of elementary constituents in some mire sites. BOT. NOT 108: 46 - 80.

Malo B.A (1977). Partial extraction of metal ions at the Mn-dioxide solution interface. GEOCHIM. ET COSMOCHIM. ACTA 39: 505 - 519.

McCall P.L, Robbins J.A and Matisoff G (1984). 137Cs and 210Pb transport and geochronologies in urbanised reservoirs with rapidly increasing sedimentation rates. CHEM. GEOL 44: 33 - 65.

McVean D.N and Ratcliffe D.A (1962). Plant communities in the Scottish highlands. HMSO, LONDON.

Moar N.T (1969). Late Weichselian and Flandrian pollen diagrams from south-west Scotland. NEW PHYTOL 68: 433 - 467.

Moore P and Webb G (1978). An illustrated guide to pollen analysis. HODDER AND STOUGHTON, LONDON.

Mortimer C.H (1971). Chemical exchanges between sediments and water in the Great Lakes _ speculations on probable regularatory mechanisms. LIMNOL. OCEANOG 16: 387 - 405.

Mullins C.E and Tite M.S (1973). Preisach diagrams and magnetic viscosity phenomena for soils and synthetic assemblies of iron oxide grains. J. GEOMAG. GEOELECTR 25: 213 - 229.

Mullins C.E (1977). Magnetic susceptibility of the soil and its significance to soil science. J. SOIL. SCI 28: 223 - 246.

Murozumi I, Chow T.J and Patterson C (1969). Chemical concentrations of pollutant aerosols, terrestrial dusts and sea salts in Greenland and Antarctic snow strata. GEOCHIM ET COSMOCHIM ACTA 33: 1247 - 1294

Natusch D.F, Wallace J.E and Evans C.A (1974). Toxic trace elements - preferential concentration in respirable particles. SCIENCE 183: 202 - 204.

Nature Conservancy Council (1979) Rannochmoor National Nature Reserve. NCC, BALLOCH, SCOTLAND.

Norton S.A and Hess C.T (1980). Atmospheric deposition in Norway during the past 300 years. 1: Sediment dating and chemical stratigraphy. In ECOLOGICAL IMPACTS OF ACID PRECIPITATION (EDS. DRABLOS D AND TOLLAN A) - PROCEDINGS OF AN INTERNATIONAL CONFERENCE, SANDEFJORD, NORWAY. SNSF PROJECT, OSLO.

Norton S.A, Davis R.B and Braeke D.F (1981). Responses of New England lakes to atmospheric inputs of acids and heavy metals. COMPLETION REP. USF AND WS DEPT. OF INTERIOR, PROJECT 14-16 0009-79-040 WASHINGTON.

Nriagu J.O, Kemp A.W, Wong H.K.T and Harper N (1979). Sedimentary record of heavy metal pollution in Lake Erie. GEOCHIM. ET COSMOCHIM. ACTA 43: 247 - 258.

Nriagu J.O, Wong H.K.T and Coker R.D (1982). Deposition and chemistry of pollutant metals in lakes around the smelters at Sudbury, Ontario. ENV. SCI. TECH 16: 551 - 560.

Nriagu J.O and Coker R.D (1983). Sulphur in sediments chronicles past changes in lake acidification. NATURE 303: 692 - 694.

Nygaard G (1956). Ancient and recent flora of diatoms and chrysophyceae in Lake Gribso. Studies on the humic, acid Lake Gribso. FOL. LIMNOL. SCAND 8: 32 - 94.

Ochsenbein U, Davison W, Hilton J and Haworth E.Y (1983). The geochemical record of major cations and trace elements in a productive lake. ARCH. HYDROBIOL 98: 463 - 488.

Oldfield F (1983). The role of magnetic studies in palaeohydrology. in BACKGROUND TO PALAEOHYDROLOGY (ED. GREGORY K.J), WILEY AND SONS, LONDON.

Oldfield F, Appleby P and Battarbee R.W (1978). Alternative 210Pb dating: results from the New Guinea highlands and Lough Erne. NATURE 271: 339 - 343.

Oldfield F, Thompson R and Barber K.E (1978). Changing atmospheric fallout of magnetic particulates recorded in recent ombrotrophic peat sections. SCIENCE 199: 679 - 680.

Oldfield F, Brown A and Thompson R (1979). The effect of microtopography and vegetation on the catchment of airborne particulates measured by remanent magnetism. QUAT. RES 12: 326 - 332.

Oldfield F, Appleby P, Thompson R and Huttunen P (1979). 210Pb dating of annually laminated lake sediments from Finland. NATURE 280: 53 - 55.

Oldfield F, Rummery T.A, Thompson R and Walling D.E (1979). Identification of suspended sediment sources by means of magnetic measurements: some preliminary results. WATER RESOUR. RES 15: 211 - 218.

Oldfield F, Appleby P, Cambray R.S, Eakins T.D, Barber K.E, Battarbee R.W, Pearson G.R and Williams J.M (1979). 210Pb, 137Cs and 239Pu profiles in ombrotrophic peats. OIKOS 33: 40 - 45.

Oldfield F, Thompson R and Dickson D.P.E (1981). Artificial magnetic enhancement of stream bedload: an application of superparamagnetism. PHYS. EARTH PLAN. INT 26: 107 - 124.

Oldfield F, Tolonen K and Thompson R (1981). History of particulate atmospheric pollution from magnetic measurements in dated Finnish peat profiles. AMBIO 10: 185 - 189.

Oldfield F, Barnosky C, Leopold E.B and Smith J.P (1983). Mineral magnetic studies of lake sediments. HYDROBIOLOGIA 103: 37 - 44.

Oldfield F and Appleby P (1983). The assessment of 210Pb dates from sites with varying sediment accumulation rates. HYDROBIOLOGIA 103: 29 - 35.

Oldfield F and Appleby P (1984). Empirical testing of 210Pb models for lake sediments. In LAKE SEDIMENTS AND ENVIRONMENTAL HISTORY (ED HAWORTH E) LEICESTER UNIVERSITY PRESS: 93 - 124.

Oldfield F, Bloemendal J, Barker L, Hunt A, Jones J.M, Jones M.D.H, Maxted R, Richardson N and Sahota J (1984). Magnetic measurements of atmospheric particulates in ombrotrophic peats: a review. UNIVERSITY OF LIVERPOOL, OCC. PAPER, 1984.

Oullet M and Jones H.G (1982). Palaeolimnological evidence for the long range atmospheric transport of acidic pollutants and heavy metals into the Province of Quebec, Eatern Canada. CAN. J. EARTH SCI 20: 23 - 36.

Oullet M and Jones H.G (1983). Historical changes in acid precipitation and heavy metal deposition from fossil fuel combustion plant in eastern North America as revealed by lake sediment geochemistry. WAT. SCI. TECH 15: 115 -130.

Pakarinen P and Tolonen K (1976). Studies on heavy metal concentrations in ombrotrophic peat. PROC. 5TH INT. PEAT CONGRESS, QUEBEC, VOL 2.

Pakarinen P and Tolonen K (1977). Distribution of lead in Sphagnum fuscum profiles in Finland. OIKOS 28: 69 - 73.

Pedersen T.F, Vogel J.S and Southon J.R (1986). Copper and manganese in hemipelagic sediments at 21 degrees north, East Pacific Rise: diagenetic contrasts. GEOCHIM. ET COSMOCHIM. ACTA 50: 2019 - 2031.

Pennington W (1984). Long term natural acidification of upland sites in Cumbria: evidence from post-glacial lake sediments. ANN. REP OF THE FRESHWATER BIOLOGICAL ASSOC 52: 28 - 46.

Pierson D.H, Cawse P.A, Salmon L and Cambray R.S (1973). Trace elements in the atmospheric environment. NATURE 241: 252 - 256.

Presley B.J, Brooks R.R and Kaplan I.R (1967). Manganese and related elements in the interstitial waters of marine sediments. SCIENCE 158: 906 - 910.

Presley B.J, Brooks R.R and Kappel H.M (1967). A simple squeezer for removing interstitial water from ocean sediments. J. MARINE RES 25: 355 - 357.

Presley B.J, Kolodny Y, Nissenbaum A and Kaplan I.R (1972). Early diagenesis in a reducing fjord, Saanish Inlet. 1: Trace element distributions in interstitial water and sediment. GEOCHIM. ET COSMOCHIM. ACTA 36: 1073 - 1090.

Price W.J (1972). Analytical atomic absorption spectrophotometry. SPRINGER, N.Y.

Price N.B (1977). Chemical diagenesis in sediments. in CHEMICAL OCEANOGRAPHY (EDS. RILEY J AND CHESTER R) VOL 6: 1 - 58.

Price N.B and Calvert S.E (1972). Diffusion and reaction profiles of dissolved manganese in the pore-waters of marine sediments. EARTH PLAN. SCI. LETTS 16: 245 - 260.

Puffer J.H, Russell E.W.B and Rampino M.R (1980). Distribution and origin of magnetite spherules in air, water and sediments of the Greater New York city area and North Atlantic ocean. J. SED. PETROL 50: 247 - 256.

Raask E (1980). Surface properties of pulverised coal ash and chiminey solids. POWER INDUST. RES 1: 223 - 240.

Raask E and Goetz L (1981). Characteristics of captured ash, stack solids and trace elements. J. INST. ENERGY 49: 163 - 173.

Rama M, Koide M and Goldberg E.D (1961). 210Pb in natural waters. SCIENCE 134: 98 - 99.

Rashid M.A (1974). Adsorption of metals on sedimentary and peat humic acids. CHEM. GEOL 18: 115 - 123.

Renberg I (1976). Palaeolimnological investigations of Lake Pratsjon. EARLY NORLAND 9: 113 - 161.

Renberg I (1985). Soot particle counting in recent lake sediments: an indirect dating method. in LAKE GARDSJON - AN ACID LAKE AND ITS CATCHMENT (EDS. ANDERRSON F AND OLSSON B). ECOL. BULL, STOCKHOLM.

Rickard R.T (1975). Kinetics and mechanisms of pyrite formation at low temperatures. AM. J. SCI 275: 636 - 652.

Riley J. and Chester R (1971). Introduction to marine chemistry. ACADEMIC PRESS, LONDON.

Rippey B (1982). Sediment-water interactions of Cu, Zn and Pb discharged from a domestic waste water source into a bay of Lough Neagh, Northern Ireland. ENV. POLL (B) 3: 199 - 214.

Robbins J.A (1978) Geochemical and geophysical applications of radioactive Pb. in BIOGEOCHEMISTRY OF LEAD (ED NRIAGU J.O), ELSEVIER, HOLLAND.

Robbins J.A and Edgington D.N (1973). The use of natural and fallout radionuclides to measure recent sedimentation rates in southern Lake Michigan. RAD. ENVT. RES. DIV. ANN. REP 3, JAN - DEC 1973. ARGONNE NAT. LIBRARY: ANL7690: 31 - 53.

Robbins J.A and Edgington D.N (1975). Determination of recent sedimentation rates in Lake Michigan using 210Pb and 137Cs. GEOCHIM. ET COSMOCHIM. ACTA 39: 285 - 304.

Robbins J.A, Krezoski J.R and Mozley S.C (1977). Radioactivity in sediments of the Great Lakes: post-depositional redistribution by deposit feeding organisms. EARTH PLAN. SCI. LETTS 36: 325 - 333.

Robinson G.D (1981). Adsorption of Cu, Zn and Pb near sulphide deposits by hydrous manganese-iron oxide coatings on stream alluvium. CHEM. GEOL 33: 65 - 79.

Rosenquist I (1977). Acid soil - acid water. INGENIORFORGLAGET, OSLO. 125pp.

Rosenquist I (1978). Acid precipitation and other possible sources for the acidification of lakes and rivers. SCI. TOT. ENVT 10: 39 - 49.

Rosenquist I, Jorgensen P and Rueslatten H (1980). The importance of natural H+ production for the acidity of soil and water. in ECOLOGICAL IMPACTS OF ACID PRECIPITATION (EDS. DRABLOS D AND TOLLAN A): PROCEEDINGS OF AN INTERNATIONAL CONFERENCE, SANDEFJORDE, NORWAY. SNSF PROJECT, OSLO, NORWAY.

Rosental R, Eagle G.A and Orren M.J (1986). Trace metal distribution in different chemical fractions of nearshore marine sediments. EST. COAST. SHELF. SCI 22: 303 - 324.

Rummery T.A (1981). The effects of burning on soil and sedimentary magnetism. PHD THESIS, UNIVERSITY OF LIVERPOOL.

Schell R and Barnes R.S (1985). in HANDBOOK OF ENVIRONMENTAL ISOTOPE GEOCHEMISTRY (EDS FONTES J.C AND FRITZ P), VOL B, ELSEVIER, HOLLAND.

Schell R (1986). Deposited atmospheric chemicals: a mountaintop peat bog in Pennsylvania provides a record dating to 1800. ENV. SCI. TECH 20 (9): 847 - 854.

Schwertman U and Taylor R.M (1972). The transformation of lepidocrocite to goethite. PROC. INT. CLAY CONF: 343 - 350.

Scoullos M, Oldfield F and Thompson R (1979). Magnetic monitoring of marine particulate pollution in the Elefsis Gulf, Greece. MAR. POLL. BULL 10: 288 - 291.

Shapiro J, Edmondson W.T and Allison D.E (1972). Changes in the chemical composition of sediments of Lake Washington 1958 - 1970. LIMNOL. OCEANOG 16: 437 - 451.

Sheider W.A, Jeffries D.S and Dillon P.J (1981). Bulk deposition in the Sudbury and Muskoka-Haliburton areas of Ontario during the shut-down of the Inco Ltd smelter, Sudbury. ATMOS. ENVIRON 15: 956 - 956.

Shishkina O.V and Pavlova G.A (1965). Marine iodine cycling. GEOCHEM 2: 559 - 570.

Shrimp N.F, Leland H.V and White W.A (1970). Distribution of major, minor and trace constituents in unconsolidated sediments from southern Lake Michigan. STATE GEOL. SURV. NOTES, URBANA 3 NO 32.

Sjors H (1950). On the relation between vegetation and electrolytes in northern Swedish mire waters. OIKOS 2: 241 - 256.

Skei J and Paus P.E (1979). Surface metal enrichment and partitioning of metals in a dated sediment core from a Norwegian fjord. GEOCHIM. ET COSMOCHIM. ACTA 43: 239 - 246.

Smith J.P (1986). Mineral magnetic studies on two Shropshire - Cheshire meres. PHD THESIS, UNIVERSITY OF LIVERPOOL.

Stewart J.M and Robertson R.A (1968). The chemical status of an exposed peat face. PROC. 3RD INT. PEAT. CONG, QUEBEC: 190 - 194.

Stumm W, Hohl H and Dalang F (1976). Interaction of metal ions with hydrous oxide surfaces. CROATICA CHEM. ACTA 48: 491 - 504.

Stumm W and Baccini J.J (1978). Man made chemical peturbation of lakes. in LAKES: CHEMISTRY, BIOLOGY, PHYSICS (ED. LERMAN A), SPRINGER, NEW YORK.

Stumm W and Morgan J.J (1981). Aquatic chemistry. WILEY, NEW YORK.

Swanson V.E, Frist I.C, Rader C.F and Huffman C (1966). Organic decomposition and trace metal cycling in marine sediments. US. GEOL. PROF. PARER 550C: 174 - 210.

Tamura T and Jacobs D.G (1960). Structural implications of cesuim sorption. HEALTH PHYS 2: 391 - 396.

Tessier A, Campbell P.G.C and Bissen M (1979). Sequential extraction procedure for the speciation of particulate trace metals. ANAL. CHEM 51 NO 7: 844 - 851.

Tessier A, Rapin F, Campbell P.G.C and Carignan C (1986). Potential artifacts in the determination of metal partitioning in sediments by sequential extraction procedures. ENV. SCI. TECH 20 NO 8: 836 - 840.

Thompson R (1978). European palaeomagnetic secular variation, 13000 - 0 BP. POL. ARCH. HYDROBIOL 25: 413 - 418.

Thompson R (1979). Palaeomagnetic correlation and dating. in PALAEOHYDROLOGICAL CHANGES IN THE TEMPERATE ZONE IN THE LAST 15000 YEARS (ED. BERGLUND E), SUB-PROJECT B, LAKES AND MIRES. IGCP PROJECT 158, LUND, SWEDEN.

Thompson R (1986). Modelling magnetisation data using SIMPLEX. PHYS. EARTH. PLAN. INT 42: 113 - 127.

Thompson R, Battarbee R.W, O'Sullivan P.E and Oldfield F (1975). Magnetic susceptibility of lake sediments. LIMNOL. OCEANOG 20: 687 - 698.

Thompson R, Bloemendal J, Dearing J, Oldfield F, Rummery T.A, Stober J.C and Turner G.M (1980). Environmental applications of magnetic measurements. SCIENCE 207: 482 - 486.

Thompson R and Oldfield F (1986). Environmental magnetism. ALLEN AND UNWIN, LONDON.

Thompson R and Bradshaw R (1986). The distribution of ash in Icelandic sediments and the relative importance of mixing and erosion processes. J. QUAT. SCI 1: 3 - 11.

Tolonen K and Jaakkola T (1983). History of lake acidification and air pollution studied on sediments in Finland. Ann. Bot. Fennici 20: 57 - 78.

Turekian K.K, Nozaki Y and Benninger K (1977). Geochemistry of atmospheric radon and radon products. ANN. REV. EARTH PLAN. SCI 5: 227 - 255.

Walling D.E, Peart M, Oldfield F and Thompson R (1979). Identifying suspended sediment sources by magnetic measurements on filter paper residues. NATURE 281: 110 - 113.

Warren Spring Laboratory (1983) Acid precipitation in the United Kingdom. DTI REP. ISBN 085624 323X, WARREN SPRING, STEVENAGE.

Watkins N.D, Kester D.R and Kennett J.P (1974). Palaeomagnetism of the type pliocene/pleistocene boundary section of Santa Maria de Catanzara, Italy and the problem of post-depositional precipitation of magnetic minerals. EARTH PLAN. SCI. LETTS 24: 113 - 122.

Whitby K.T and Cantrell B (1975). Atmospheric aerosols - characteristics and measurement. INT CONF ON ENVIRONMENTAL SENSING AND ASSESSMENT, LAS VEGAS, NEVADA.

Witting M (1947). Katjonbestamningan 1: Mrrvatten. BOTNOTISER, LUND: 287 - 304.

Wong H.K.T, Nriagu J.O and Coker R.D (1984). Atmospheric input of heavy metals chronicled in lake sediments of the Algonquin provincial park, Ontario. CHEM. GEOL 44: 187 - 201.

Worsley A.T (1983). A palaeoecological study of recent environmental change in the highlands of New Guinea. PHD THESIS, UNIVERSITY OF LIVERPOOL.

Yaalon D.H (1970). Palaeopedology: Origins, nature and dating of paleosols. PAPERS OF THE SYMPOSIUM ON "AGE OF PARENT MATERIALS AND SOILS". AMSTERDAM.

Ylirivokanen K (1976). Heavy metal distributions in Finnish peat bogs. PROC. 5TH. INT. PEAT. CONGRESS, QUEBEC, VOL 2.

Zinder B, Furrer G and Stumm W (1986). The co-ordination chemistry of weathering (2): Dissolution of Fe3 oxides. GEOCHIM. ET COSMOCHIM. ACTA 50: 1861 - 1869.

Zobell (1964). Studies of redox potential of marine sediments. BULL. AM. ASSOC. PETROL. GEOLOGISTS 30 (4): 477 - 513.

ADDITIONAL SOURCES.

Bock R (1979). A handbook of decomposition techniques in analytical chemistry. INT. TEXTBOOK CO, GLASGOW.

Dankers P.H.M (1978). Magnetic properties of dispersed natural iron oxides of known grain size. PHD THESIS, UNIVERSITY OF UTRECHT.

Dunlop R (1983). Determination of domain structure in igneous rocks by alternating field and other methods. EARTH PLAN SCI LETTS 63: 353 - 367.

Gupta S.K and Chen K.Y (1975). Partitioning of trace elements in selective chemical fractions of nearshore sediments. ENV. LETTS 10: 129 - 158.

Ozdemir O and Banjeree S.K (1982). A preliminary magnetic study of soil samples in western-central Minnesota. EARTH PLAN SCI LETTS 59: 393 - 403.

Stober J.C and Thompson R (1975). Palaeomagnetic secular variation in Finnish lake sediments and the carriers of remanence. EARTH PLAN SCI LETTS 37: 139 - 149.

APPENDIX 1 (a)

Wet chemical digestion method used for total elemental analyses of lake sediments.

Pre-weighed sediment samples of 1.0g mass were placed in HCl washed teflon beakers, each containing 10ml of concentrated HNO3 (ARISTAR). Samples were then heated to 90°C to facilitate the oxidation of all labile organic matter, thus precluding the danger of explosion associated with rapid oxidation by HClO4 (Allen et al 1974, Bock 1979). Subsequently, 10ml of HClO4 (ARISTAR) and 10ml of HF (60% ARISTAR) was added and the samples heated to a "white-fume" state. Digestions were considered complete when evaporation of the reagents had proceded to near-dryness and a particle free, clear or pink solution was produced. All digested sample solutions were then diluted to 25ml in 5% HCl and stored in pre-cleaned polythene containers prior to analysis by AAS.

APPENDIX 1 (b)

Wet chemical methods used in sequential analyses of lake sediments.

Sequential chemical analyses were carried out using fresh sub-samples of 2.0g mass. Considerable importance was placed on the avoidance of sample oxidation prior to analysis, so as to preclude the formation of oxide phases through the precipitation of metals held within the sediment pore-waters. The extraction of adsorbed, carbonate, oxide, non-volatile sulphide/organic and silicate metal fractions involved the following procedures.

1) Adsorbed metal fractions were removed by leaching under continual agitation with 20ml 1M. MgCl (pH 7.0) for 1 hour. Alternative reagents which are frequently used for the extraction of exchangable metals, notably NH4OAc (Allen et al 1974, Jackson 1980, Gupta and Chen 1975) and NaOAc (Chapman 1964) were not utilized on account of their tendency to attack carbonates (Tessier et al 1979).

2) Residual sediments remaining after absorbed metal extraction were leached under conditions of continuous agitation in 20ml 1M NaOAc (ph5.0) to remove carbonate phases. In all instances a leaching period of 5 hours was considered adequate.

3) Fe/Mn oxides and volatile sulphides were removed simultaneously from the residue remaining after carbonate extraction using 20ml 25% v/v HOAc in 0.4M NH2.OH.HCl. Extractions were carried out at 90° C in accordance with methods outlined by Rosental et al (1986), Filipek et al (1979), Tessier et al (1979) and Gupta and Chen (1975). Sodium dithionite/citrate methods of Fe oxide extraction were not utilized on account of the tendency for Zn contamination within dithionite and the likely precipitation of trace metals during leaching (Tessier et al 1979).

4) Organic and non-volatile sulphides were removed from the residues remaining after Fe/Mn oxide extraction through the application of 20ml 30% H2O2 (acidified to pH 2.0 with HNO3) at 90°C. Alternative oxidants (eg. HNO3, HClO4) were not utilized because of their tendency to attack silicates (Tessier et al 1979).

5) Residual silicate phases remaining after the oxidation of organic matter were digested by boiling for 4 hours in 5ml HF, 5ml HNO3 and 5ml H2SO4.

APPENDIX 2: MINERAL MAGNETISM

A2.1: Introduction.

For readers who are unfamiliar with mineral magnetic techniques, the following summary of the magnetic properties of natural materials and the relationships between magnetic parameters and mineralogy may be of assistance.

A2.2: Magnetic behaviour.

a) Diamagnetism.

Diamagnetic behaviour is characteristic of most natural materials, for example quartz (silica), carbon and water. Such behaviour is explicable through the examination of materials on an atomic scale and is the product of the balanced nature of electron and orbital spins, thus precluding the generation of any "net magnetic moment" prior to the imposition of an external field. However, during magnetization the moments attain a weak orientation in opposition to the prevailing field and consequently, negative magnetic susceptibilities may be produced. On removal from the magnetizing field, this net diamagnetic moment is immediately destroyed.

b) Paramagnetism.

The inherent magnetic properties of paramagnetic materials are dominated by thermal dis-orientation and consequently, they exhibit no spontaneous magnetization. However, when placed within a magnetizing field a weak positive alignment is attained. Because the strength of this alignment is thermally constrained, the magnetization intensity varies inversely with temperature. On removal from the magnetizing field, thermal randomization dominates once more and a remanent magnetization cannot be maintained. Accordingly, paramagnetically dominated samples exhibit susceptibilities which are dis-proportionately high with respect to their remanent magnetization values.

c) Anti-ferromagnetism and ferrimagnetism

Anti-ferromagnetic and ferrimagnetic properties are most frequently associated with the common iron oxides,

magnetite, haematite and maghemite, although such behaviour is also exhibited by certain iron sulphides (eg. pyrrhotite and greigite), chromium and manganese minerals. In contrast to paramagnets, atomic super-exchange precludes the dominance of thermal dis-orientation and a spontaneous magnetization may exist in the absence of an external magnetic field. In ferrimagnetic structures, opposed but imbalanced moments are generated, while true anti-ferromagnets display balanced, anti-parallel moments. However, antiferromagnets (eg. haematite) are commonly imperfectly structured in a manner which promotes the canted or parasitic generation of a net moment.

A2.3: Curie and Neel points.

Ferrimagnetic minerals possess a characteristic Curie point or temperature above which thermal agitation causes paramagnetic behaviour to dominate. In the case of magnetite, this point is 580°C. An analogous Neel point is operative with respect to the behaviour of antiferromagnets.

A2.4: Magnetic domains.

In addition to the variations in magnetic behaviour which derive from differences in atomic configuration, the response of minerals to magnetization is strongly controlled by their granulometry. When a large magnetic grain is magnetized, it may be energetically advantageous for it to sub-divide into discrete "domains" which then become aligned in accordance with both the field direction and with the orientation of surrounding domains. Grains which behave in this manner are termed "multidomain" (MD) grains. For most ferrimagnetic mineral species, a critical grain size is identifiable, below which the formation of domain walls ceases to be energetically advantageous. Consequently, grains falling below this threshold produce a singular alignment during magnetization and are termed "stable single domain" (SSD) phases.

Because the grain size threshold which marks the transition between SSD and MD behaviour is not well defined, grains which possess intermediate characteristics are often identifiable. These are typically described as "pseudo single domain" (PSD) grains. Critical grain size thresholds with respect to mineral domain status have been calculated by Dunlop (1981) and are summarised in Table 1.

Table 1: Relationships between mineral grain size (μm) and domain status within natural magnetic minerals (Dunlop 1981).

MINERAL	SP	SSD	PSD/MD
Magnetite	0.025	0.05	
Maghemite	0.08	0.06	
Titanomagnetite	0.08	0.20	
Haematite	0.025	1.50	

A2.5: Superparamagnetism.

SSD behaviour is only characteristic of magnetic grains which exceed a lower threshold size (around 0.03μm). Grains falling below this threshold rapidly respond to placement within a magnetizing field, but any net alignment is destroyed by thermal agitation upon removal. These "superparamagnetic" (SP) minerals are, therefore, analogous to paramagnets in that they cannot be associated with magnetic remanence. However, the magnetization intensity of SP minerals is considerably greater.

A2.6: Magnetic viscosity.

Thermal agitation commonly produces a time dependent loss of remanence following the removal of ferrimagnets from a magnetising field. This behaviour is termed "magnetic viscosity" and is primarily associated with large MD grains and those which fall on the SSD/SP boundary (Mullins and Tite 1973).

A2.7: Mineral magnetic parameters.

a) Magnetic susceptibility (X).

The initial response of a magnetic material to magnetization is both linear (ie. directly proportional to field strength) and reversible. Under such circumstances, the ratio between field strength and induced magnetization constitutes the samples "magnetic susceptibility" (Thompson 1975). Specific susceptibility (X) signals typically co-vary with magnetic mineral concentration, but show a ferrimagnetic bias of 2 - 3 orders of magnitude with respect to the X values of analogous antiferromagnetic mineral concentrations. Accordingly, this

parameter is most frequently considered to constitute a surrogate indicator of magnetite concentration.

Although X is primarily responsive to varying mineral concentration, the parameter is not fully independent of grain size influences. Most notably, Dankers (1978) and Ozdemir and Banjeree (1982) have shown that susceptibility measurements preferentially discriminate SP grains and MD minerals in the manner outlined in Fig 1.

b) Saturation isothermal remanent magnetisation (SIRM).

When the magnetising field in which a sample is placed exceeds a critical threshold strength, magnetization/field intensity ratios become non-linear and irreversible. On removal from such fields, samples containing SSD, PSD or MD minerals, therefore, retain a remanent magnetization (IRM). As the field intensity is increased, a non-linear growth of spin alignment occurs until a point is reached where further increments to the field intensity produce no additional magnetization response. This saturating field alignment (Ms) is subject to relaxation to a condition of saturation isothermal remanent magnetization (SIRM) when the sample is removed from the field.

Although SIRM intensities are ferrimagnetically biased, they are markedly more sensitive than X to granulometric variability. For example, from studying Figs 2 - 3, it is evident that MD minerals become saturated in response to the application of relatively low fields but are subject to considerable relaxation upon removal from the field. Consequently, MD minerals have low SIRM/Ms ratios in comparison to SSD dominated assemblages which saturate only in stronger (>0.1T) fields and display a lower degree of relaxation upon removal.

c) Demagnetisation parameters.

While X and SIRM are never fully independent of magnetic mineral concentration, the behaviour of materials during demagnetization is solely controlled by magnetic mineralogy and granulometry. A crude mineralogical characterisation of formerly "saturated" samples may, therefore, be made by ascertaining the strength of the reversed field required to reduce the net magnetisation to zero. This critical field constitutes the samples coercivity (BOCR).

However, because most natural samples contain a

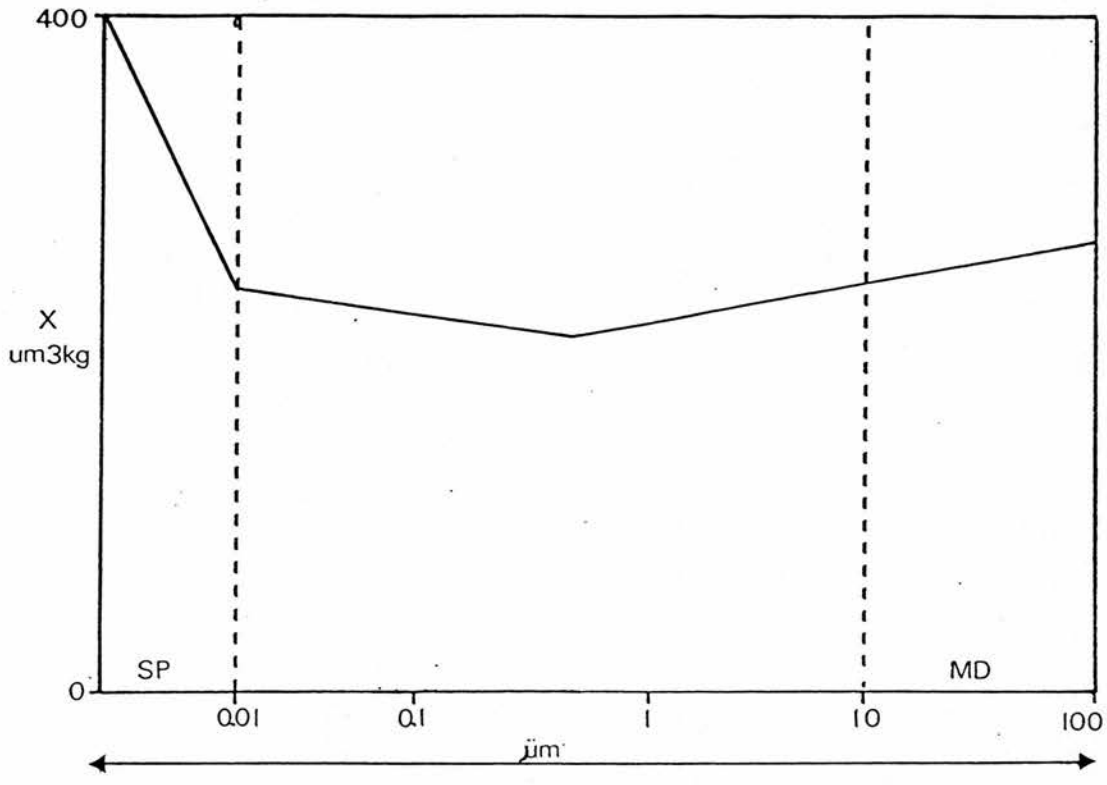

FIG 1: Idealised relationship of X with magnetite grain size.

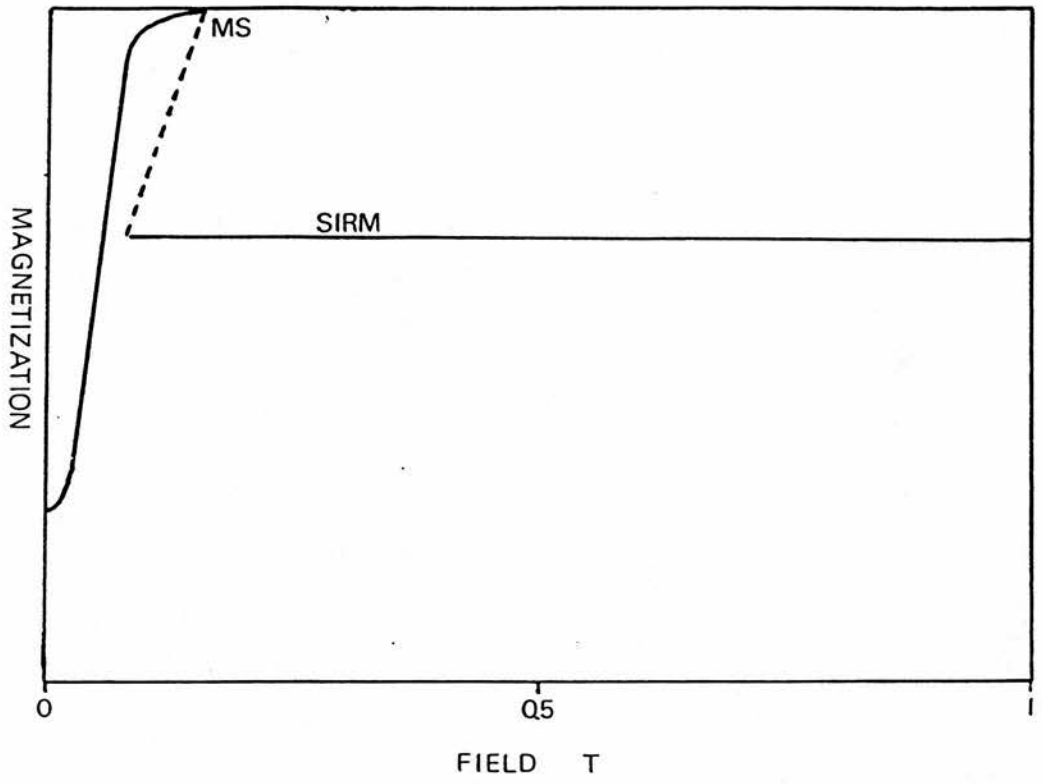

FIG 2: Idealised magnetisation curve for multi-domain magnetites of approximately 64um in size. Note that "saturation" occurs in response to a relatively low field (0.15T), but the extent of relaxation between "in-field" saturation (MS) and SIRM is large. Consequently, SIRM/MS ratios of around 0.7 prevail.

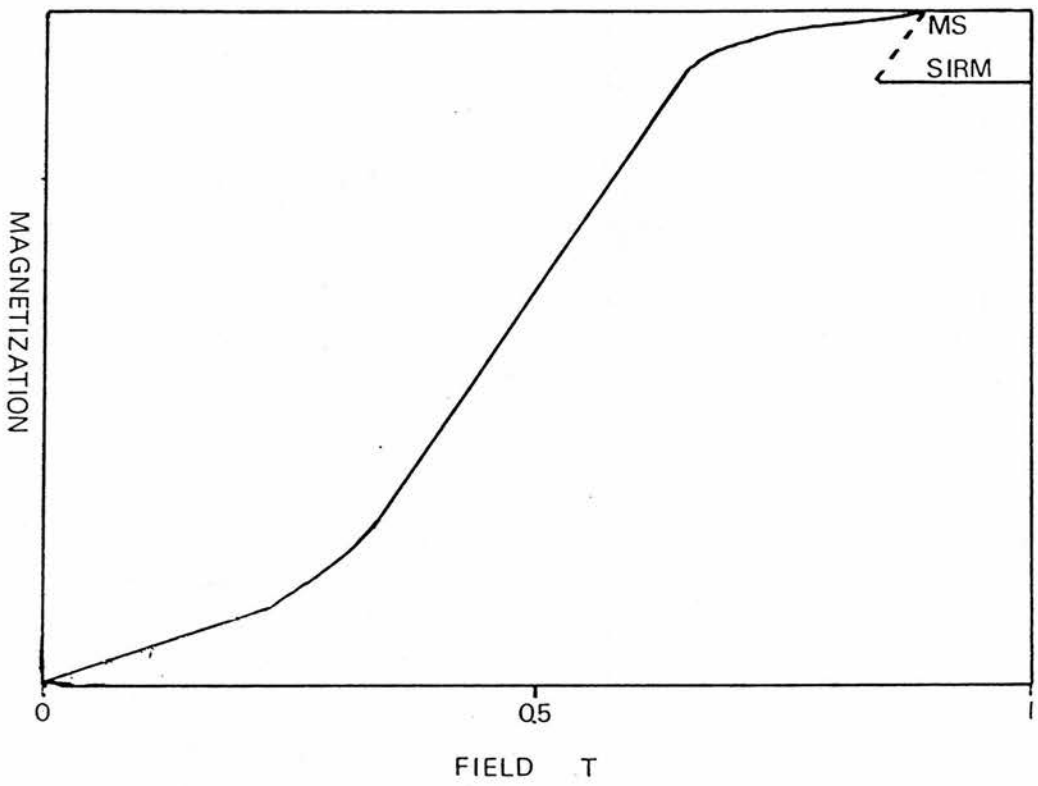

FIG 3: Idealised magnetisation curve for single domain magnetites of approximately 0.0625μm in size. Note that the initial response to magnetisation is slow and "saturation" occurs only in fields in excess of 0.8T. Relaxation upon removal from the magnetising field is limited, leading to the prevalence of SIRM/MS ratios of around 0.9.

mixed magnetic assemblage, a full mineralogical appraisal cannot usually be made from a knowledge of BO(CR) values in isolation. Consequently, techniques involving the stepwise application of increasingly reversed fields and the measurement of remanence after each stage in the demagnetization process are frequently adopted. Within this sequence, losses of remanence in response to the application of weak reversed fields (<25mT) can be used to diagnose MD magnetite presence, while any resistance to demagnetization during the subjection of samples to stronger reversed fields can be used to diagnose the presence of SSD magnetites, titanomagnetites or haematite. A range of demagnetisation parameters, for example the S ratio (IRM-0.1T/SIRM) of Stober and Thompson (1975), HIRM values (Bradshaw and Thompson 1984) and low-field/high-field demagnetisation ratios, are particulurly applicable to the appraisal of these "magnetically hard" components:-

Figs 4 - 5 provide graphic illustrations of the demagnetization curves which characterise magnetite and haematite dominated assemblages.

d) Anhysteretic remanent magnetisation (ARM).

Anhysteretic remanent magnetizations (ARM) are produced within samples during the smooth decay of a strong alternating field (0.1T) in the presence of a weak, unvarying DC field (0.05 - 0.1 mT). On account of the minerogenic bias of ARMs, they are of value for discriminating ferrimagnetic grains falling within the SSD size range (Ozdemir and Banjeree 1982). ARM susceptibility (ARMx) values may also be used to illuminate the significance of such grains within composite assemblages and simply express the ARM/DC current quotient. For reference, Fig 6 illustrates the typical relationship between ARMx and mineral granulometry.

A2.8: Interparametric ratios.

While the above parameters all demonstrate sensitivity towards specific minerogenic or granulometric phases, the use of interparametric ratios may highlight the presence of certain mineral components with increased clarity. Ratios of SIRM/X have been widely used for both granulometric and minerogenic discrimination (eg. Oldfield et al 1983, Hirons and Thompson 1986, Thompson 1986) on account of the persistence of inverse relationships between SIRM/X and magnetite grain size (Fig 7) and of the high ratios exhibited by haematite relative to magnetite. SIRM/X ratios have also been found to have utility for differentiating

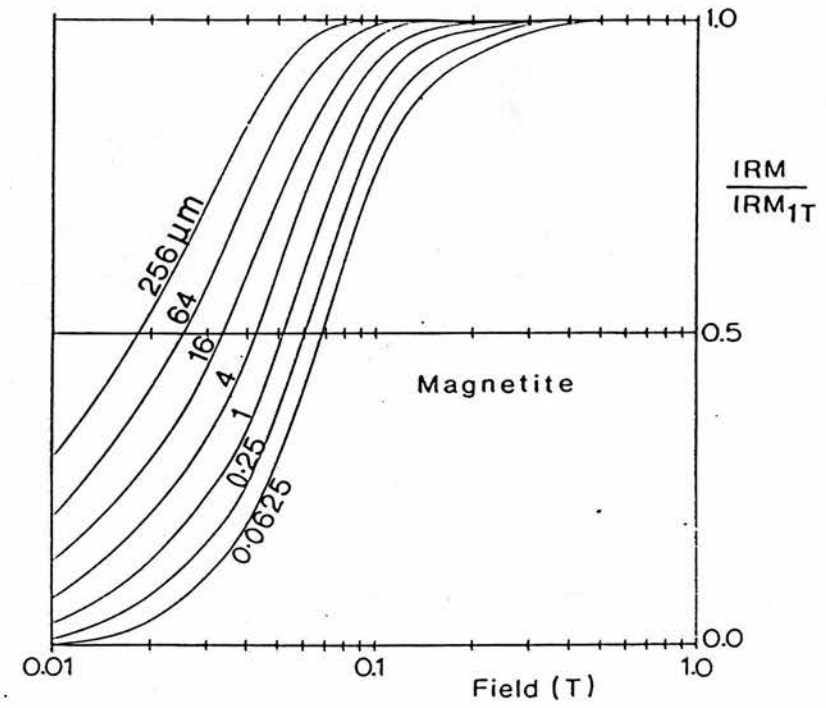

FIG 4: Demagnetisation curves for magnetite grains within the size range 0.0625 - 256um (after Thompson 1986).

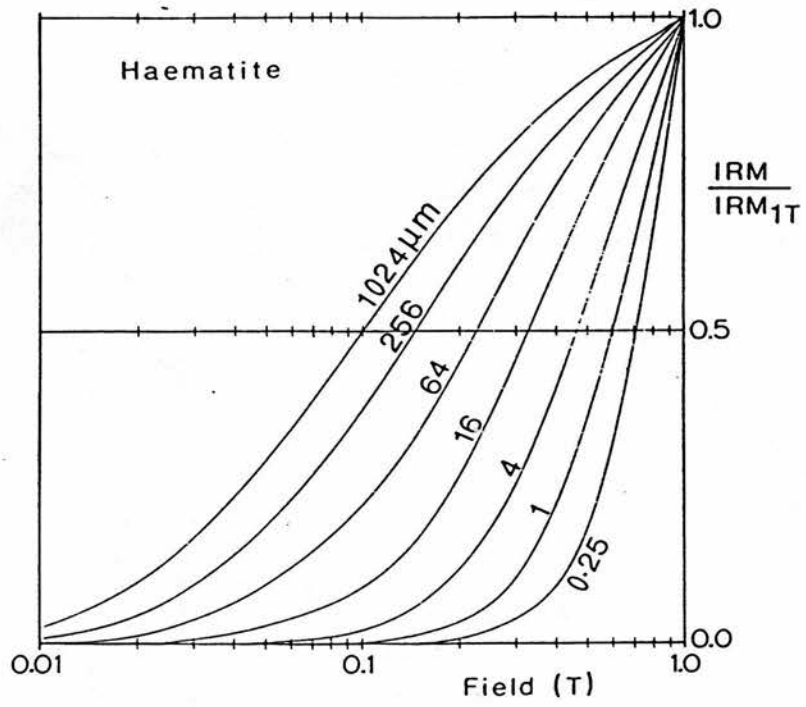

FIG 5: Demagnetisation curves for haematite grains within the size range 0.25 - 1024um (after Thompson 1986).

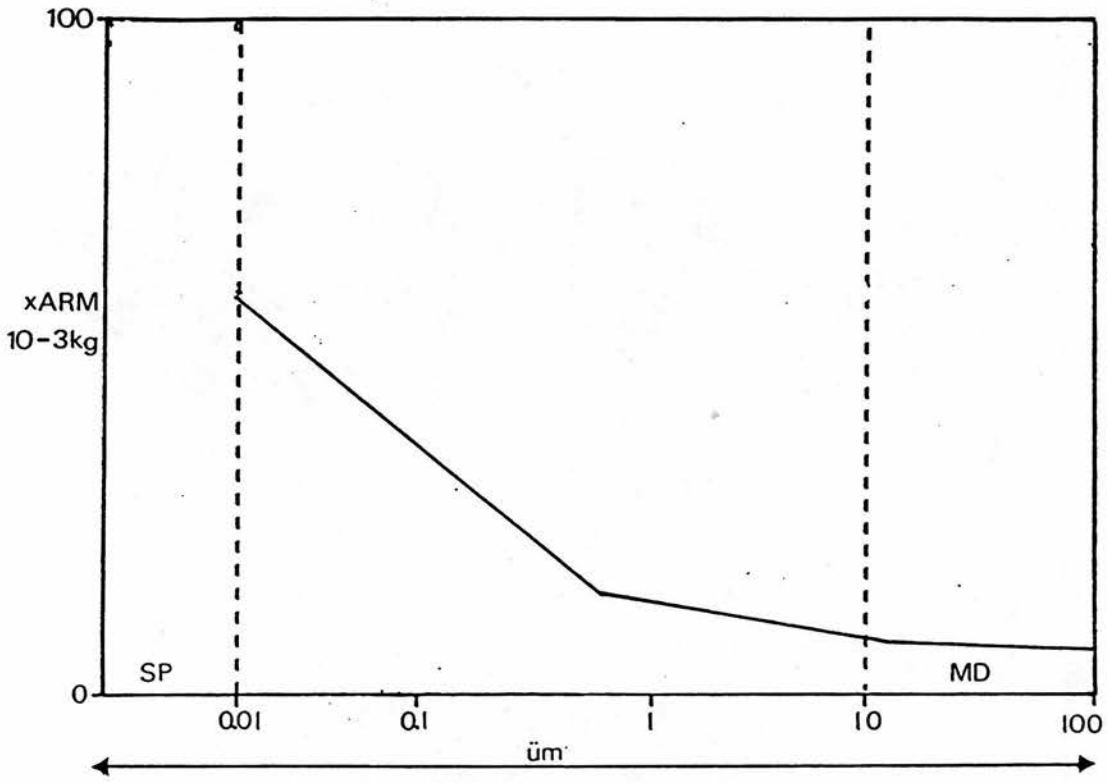

FIG 6: Idealised relationship of xARM with ferrimagnetic mineral grain size.

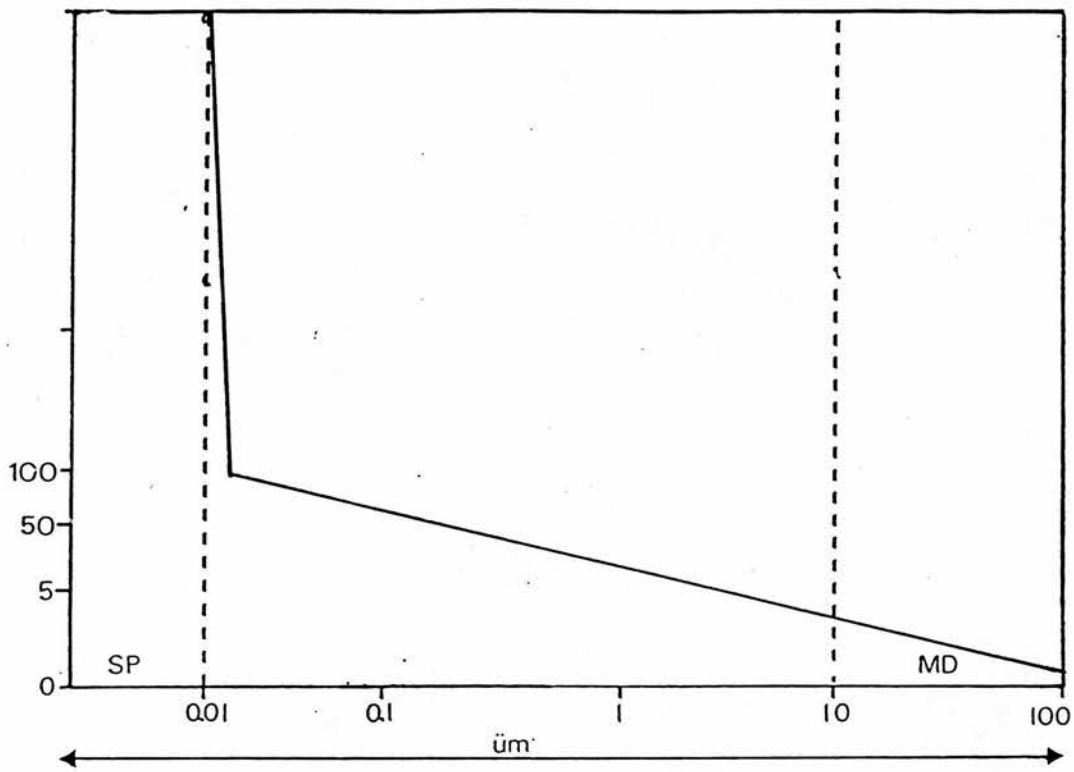

FIG 7: Idealised relationship of SIRM/X with ferrimagnetic mineral grain size (after Thompson 1986).

between ferrimagnetic oxides and sulphides, with ratios for pyrrhotite and greigite typically exceeding those of magnetite by a factor of 5 (Thompson 1986).

By using ratios of SIRM/X in conjunction with BO(CR), Thompson (1986) has shown that it is possible to distinguish between granulometrically and minerogenically controlled SIRM/X variations within sample suites. Fig 8 illustrates that for magnetite dominated assemblages, a linear pattern emerges with MD dominated samples yielding low SIRM/X ratios and BO(CR) values, while SSD assemblages yield higher SIRM/X ratios and BO(CR) values. Sulphide phases (eg. pyrrhotite) are conspicuous as they do not conform to such trends, but display dis-proportionately low coercivities (below 20mT) with respect to their SIRM/X ratios (Clarke 1983). In similar fashion, paramagnetic iron phases are conspicuous as they may produce anomalously low (below 5 kAm-1) SIRM/X ratios in high coercivity materials.

The utility of ARMx/X ratios for the determination of mineral granulometry has been outlined in detail by Ozdemir and Banjeree (1982). This ratio may be considered to be particularly useful as ARMx is sensitive to the smallest of remanence-holding ferrimagnets while X responds preferentially to MD magnetites. Consequently, it is possible to use ARMx/X for the rapid diagnosis of the predominant grain size within a given sample in accordance with the relationship illustrated in Fig 9.

When studying magnetic assemblages which contain SP minerals it is useful to determine SSD or MD mineral presence without utilizing the parameter X. SIRM may, therefore, replace X as the MD grain discriminator.

A2.9: S.I units of measurement.

PARAMETER	UNITS
Specific susceptibility (Xlf)	um3kg-1
Specific magnetization (IRM,ARM)	mAm2kg-1
Field intensity (or demagnetization)	mT
SIRM/X	kAm-1
ARM/X	kAm-1
SIRM/ARM	dimensionless

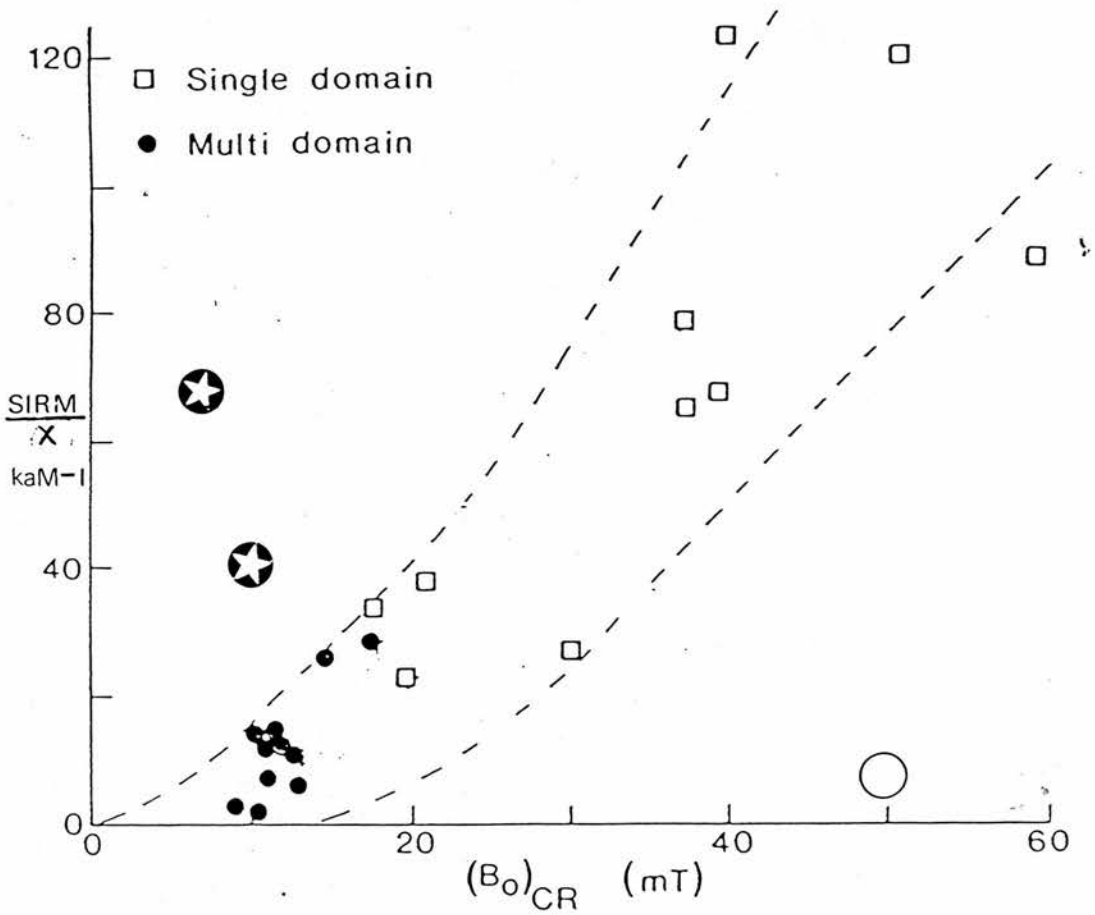

FIG 8: Relationships between SIRM/X, BOCR and magnetic mineralogy (after Thompson 1986). Magnetites form a linear, granulometrically controlled pattern, with MD grains exhibiting lowest SIRM/X and BOCR values. Samples of differing mineralogy are conspicuous as they deviate from this pattern. Samples depicted by stars are the sulphide minerals, greigite and pyrrhotite. Both yield unusually high SIRM/X ratios in low coercivity materials. The open circle depicts a paramagnetically and antiferromagneticaly dominated sample, which yields low SIRM/X ratios in high coercivity materials.

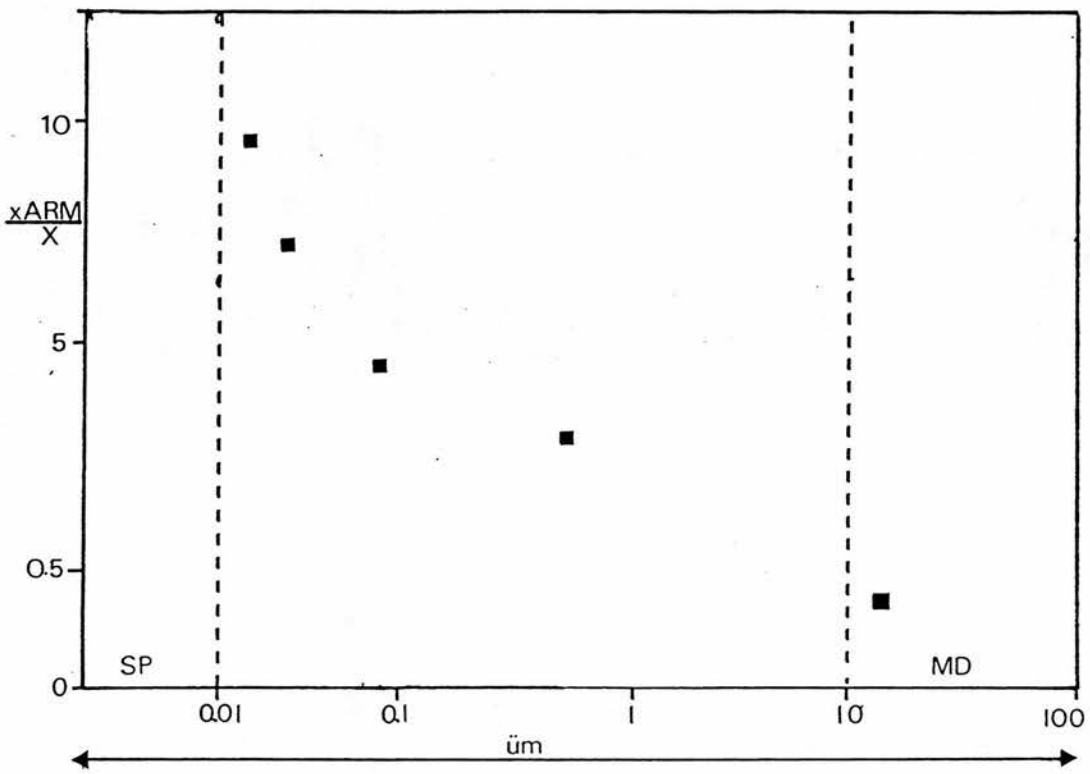

FIG 9: Empirical relationship of xARM/X with magnetite grain size (after Ozdemir and Banjeree 1982).

APPENDIX 3.

Peak (P) and cumulative (C) elemental concentrations (ug/g dry weight) in peat cores from Glen Muich, Glenquoich and Loch Cluanie, Scotland.

Site Location	Core Topography	P.Pb	C.Pb	P.Zn	C.Zn	P.Cu	C.Cu
Glen Muich	Hummock	70	640	49	295	6	71
Glen Muich	Lawn	57	725	51	270	6	104
Glenquoich	Hummock	41	475	39	320	6	77
Glenquoich	Lawn	31	510	37	180	4	42
Loch Cluanie	Hummock	33	390	29	185	7	32
Loch Cluanie	Lawn	27	310	41	165	3	31

		P.Cd	C.Cd	P.Cr	C.Cr	P.V	C.V
Glen Muich	Hummock	1	24	6	60	7	61
Glen Muich	Lawn	1	26	2	49	7	41
Glenquoich	Hummock	1	31	3	51	4	37
Glenquoich	Lawn	2	19	4	31	3	33
Loch Cluanie	Hummock	2	23	2	33	2	29
Loch Cluanie	Lawn	1	33	4	27	2	41